Orographic gradients in climate and forest cover at the Cordillera Yanachaga, Peru

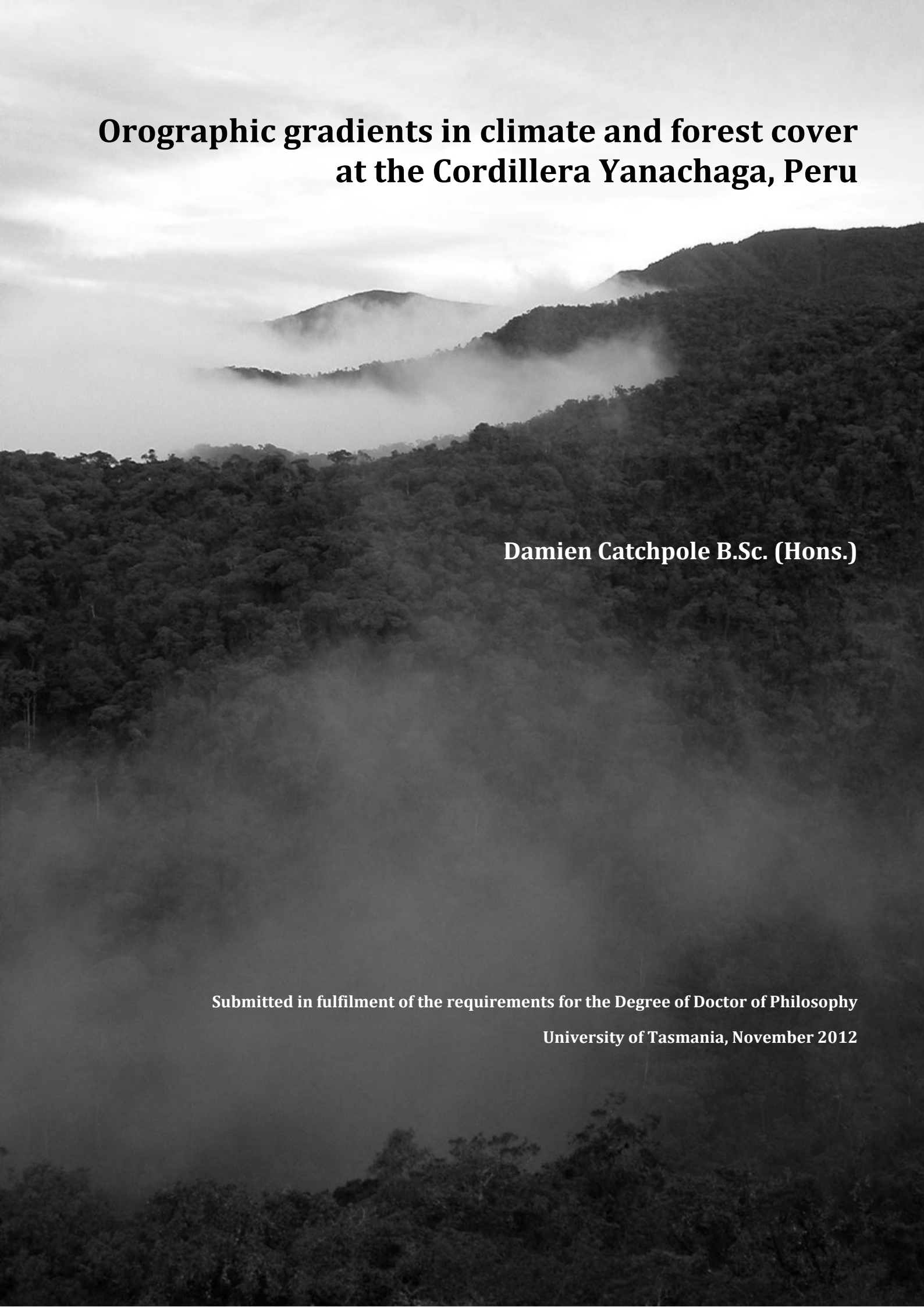

Damien Catchpole B.Sc. (Hons.)

Submitted in fulfilment of the requirements for the Degree of Doctor of Philosophy

University of Tasmania, November 2012

In memory of my dear mother-in-law Amy Chacón

12.10.1940 – 22.12.2009

Que descanses en paz

Cover illustration: photo by D.J. Catchpole, windward cloud forest of the Cordillera Yanachaga, Yanachaga-Chemillén National Park, Peru

This thesis is submitted in fulfilment of the requirements for the Degree of Doctor of Philosophy at the School of Geography and Environmental Studies, University of Tasmania (November, 2012). It contains no material which has been accepted for the award of any other Degree or Diploma in any tertiary institution, and to the best of my knowledge and belief, contains no material previously published or written by another person, except where due reference is made in the text of the thesis, nor does the thesis contain any material that infringes copyright.

This thesis may be made available for loan and limited copying and communication in accordance with the Copyright Act 1968.

Signed

Damien Catchpole

Abstract

The Cordillera Yanachaga is a semi-isolated Andean range protruding into the Peruvian Amazon that houses an important area of montane cloud forests on both windward and leeward slopes. Despite the importance of these forests for biodiversity and the provision of ecosystem services for nearby populations, their orographic variation in climate and forest ecology had not been previously described. Climatic and forest parameters were studied along an orographic gradient consisting of three sites, a windward slope forest at 2400 masl, a ridge forest on the mountain pass at 2800 masl and a leeward slope forest at 2400 masl. Common climatic measurements and visibility were recorded from canopy towers within 1-ha vegetation sampling plots, from which environmental data and taxonomic, foliage and structural characters of all stems ≥5 cm DBH were collected.

Despite its orographic location, the leeward forest received marginally less rainfall than the ridge forest and considerably more rainfall that the windward forest. The temperature variation found was attributed to altitude and an afternoon Foehn effect, while the orographic variation in PPFD was very strongly correlated to fog frequency. The ridge and windward forests showed higher canopy fog immersion (c. 75%) and a higher frequency of simultaneous rain and fog events, while the leeward forest showed less fog immersion (c. 20%) and higher rain frequency. The ridge and windward forests were affected principally by easterly air masses, while the leeward forest showed signs of localized phenomena originating from the Oxapampa valley to the west. The leeward forest displayed more climatic variation and larger parameter ranges, which were reflected in greater species richness, basal area, canopy height, foliage area and leaf size. Floristic associations within plots reflected sheltered and exposed regions. Forests at all the sites had stem densities and basal areas at the lower end of those recorded in other regions.

At the leeward site, light and moderate fog events generally displayed diurnal temperatures and PPFD more similar to clear sky events than to rain events, reflecting the warm clear upper atmosphere conditions under which they form. Dense fog events tended to mimic microclimatic conditions during rainfall events, albeit with higher PPFD.

In addition to the very strong correlation between fog frequency and PPFD, PPFD also correlated very strongly with total arboreal foliage area, suggesting as possible relationship through limitations on the development canopy substrata. While the mechanism for such a relationship remains unclear, the observations contribute to the existing theory that the effect of fog frequency on light conditions is one of the major drivers of variation in tropical montane forest productivity.

Resumen

La Cordillera Yanachaga es una cadena montañosa andina, semi-aislada por extenderse en el territorio de la amazonia peruana. Alberga un área importante de bosques montanos de niebla en sus flancos barlovento y sotavento. A pesar de la importancia de estos bosques para la biodiversidad y la provisión de servicios ecosistémicos a poblaciones cercanas, su variación orográfica en clima y ecología no han sido descritas previamente. Se estudió los parámetros climáticos y boscosos a lo largo de una gradiente orográfica que consistió en tres sitios, bosque barlovento a 2400 msnm, bosque de cresta a 2800 msnm y bosque sotavento a 2400 msnm. Se grabó mediciones climáticas estándares y visibilidad desde torres del dosel dentro de parcelas de vegetación de 1-ha, en las cuales se registraron datos ambientales y caracteres taxonómicos, de follaje y estructurales de todos los tallos ≥5 cm DAP.

A pesar de su ubicación orográfica, el bosque sotavento recibió levemente menos lluvia que el bosque de cresta y una cantidad considerablemente mayor al bosque barlovento. La variación en temperatura hallada se atribuyó a la altitud y un efecto Foehn postmeridiano, mientras la variación orográfica en radiación fotosintéticamente activa (RFA) fue altamente correlacionado a la frecuencia de neblina. Los bosques de cresta y barlovento presentaron una frecuente inmersión del dosel por neblina (c. 75%) y una mayor frecuencia de eventos de neblina y lluvia simultanea, mientras el bosque sotavento presentó menos inmersión por neblina (c. 20%) y mayor frecuencia de lluvia. Los bosques de cresta y barlovento fueron afectados principalmente por masas de aire orientales, mientras el bosque sotavento demostró señales de un fenómeno localizado originado desde el valle de Oxapampa hacia el oeste. El bosque sotavento presentó mas variación climática y mayores rangos de parámetros, lo cual fue reflejado con mayor riqueza de especies, área basal, altura del dosel, área del follaje y tamaño de hojas. Las asociaciones florísticas dentro de las parcelas reflejaron sitios protegidos y expuestos. Todos los bosques tuvieron densidades de tallos y áreas basales menores en comparación con bosques comparables de otras regiones.

En el bosque sotavento, generalmente los eventos de neblina tenue y moderada demostraron temperaturas y RFA con mayor semejanza a los eventos de cielos despejados que a los eventos de lluvia, reflejando las condiciones atmosféricas cálidas y despejadas en las que se forman. Los eventos de neblina densa demostraron similitud a las condiciones microclimáticas durante eventos de lluvia, aunque con mayor RFA.

En adición a la correlación muy fuerte entre frecuencia de neblina y RFA, RFA también tuvo una correlación fuerte con el área total del follaje arbóreo, sugiriendo una posible relación a través de limitaciones al desarrollo de substratos en el dosel. Mientras que el mecanismo para la supuesta relación no es claro, las observaciones contribuyen a la teoría existente que el efecto de la frecuencia de neblina en las condiciones de luz es uno de los factores claves para la variación en la productividad de bosque montano tropical.

Acknowledgements

This work would not have been possible without the support of many organizations and the collaboration and assistance from countless number of people, too many to be able to list all names and undertakings accurately and I apologise for any omissions.

I reserve my deepest gratitude for my wife Yoshie, not only did she help collect and process data, but she has been my pillar of support during all phases of the project and provided me with the motivation and encouragement required to continue on.

I thank all the students and colleagues who worked at the site over the 4-year field period that directly or indirectly assisted in the installation of infrastructure and data collection, including Chris Blackman, Rolando Gutierrez, Nicolai Koebernick, Yhuller Moya, Jimmy Requena, Jerry Romanski, John Switzer and Matt Taylor.

I thank Carlos Llerena of the Universidad Nacional Agraria La Molina for his friendship and institutional support over the last 10 years, without which this project may not have occurred. I also thank Michael McClain of Florida International University who provided initial opportunities in my previous projects, as well as financing for the part of the first meteorological station installed during my Honours project.

I am indebted to my supervisors Jamie Kirkpatrick, Manuel Nunez and Mick Russell for their generous support and advice, and especially for believing in me when others might not have, as well as Lorne Kriwoken, Emma Pharo and countless staff and students at the School of Geography & Environmental Studies for all their advice and assistance.

This study would not have been feasible without the local support from the Peruvian office of the Missouri Botanical Garden in Oxapampa. I am deeply grateful to Rodolfo Vasquez, Rocio Rojas and Abel Monteagudo for their support, advice, friendship and generous provision of an internet connection and a four-wheel-drive vehicle for transporting equipment, as well as their countless students, staff and botanical specialists who in one way or another have assisted in the processing and identification of the thousands of botanical samples, as well as the initial delimitation of one of the study plots. Some of these people include Edwin Becerra, Lizeth Cárdenas, Franco Mellado, Adrian Tejedor amongst others. Special thanks also go to Antonio Peña who assisted students with the collection of foliage samples from large trees.

I would like to thank Benjamin Kroll and staff of the Oxapampa office of Pronaturaleza, who generously provided the permanent use of trail bikes for accessing the sites, as well as four-wheel-drive vehicles for transporting equipment.

I would like to thank both Yanachaga-Chemillén National Park chiefs Billy Huggard and Eduardo de la Cadena for their assistance and generous provision of four-wheel-drive vehicles for transporting equipment, as well as the many Park Rangers who assisted with constructing the project infrastructure and spent many a night accompanying me in the forest.

I thank the both Instituto del Bien Común Oxapampa Project directors Percy Summers and Federico Rizo for their friendly assistance, provision of information and generous provision of four-wheel-drive vehicles for transporting equipment, as well as their many staff who were always helpful.

I thank Pedro Aguilar for his friendship, advice and general helpfulness in all matter of things. I am grateful to my lead field assistant Guido Casimiro for his friendship, support and tireless efforts in the field and laboratory during the fieldwork for this and many other associated projects. I would also like to thank the people of Oxapampa for their general friendliness, especially the 60 or so who were contracted over the project duration for the fabrication, construction and installation of field infrastructure.

I would like to thank Tony Sanford for his support and understanding in providing me with limitless time off work for the redaction of this thesis, as well as Lina Cuevas who helped with map production.

I thank two anonymous examiners for their comments and corrections of the manuscript.

Last but far from least, I deeply thank my extremely supportive family who have always provided me with encouragement, love, support and money whenever I have needed it during my adventures and in difficult times.

This work was financed by the School of Geography & Environmental Studies research funds and the University of Tasmania through an Australian Postgraduate Award scholarship. Some of the epiphyte related work not presented in the current thesis was partly funded by the American Orchid Society (USD 6,000), the South Florida Orchid Society (USD 2,000) and the San Diego County Orchid Society (USD 4,000).

Table of Contents

List of Tables and Figures

List of Tables

List of Figures

Chapter 1

Introduction

1.1 Background

The humid tropics are known for their high biodiversity. Until very recently, much of the emphasis for tropical conservation and investigation in Peru had been focussed on the Amazonian lowland forests (Gentry, 1980, Gentry, 1992a, Honorio & Reynel, 2004), which essentially vary as a function of soil and flooding characteristics and some variation in rainfall and seasonality (Gentry, 1982). Andean montane forests had until recently received less investigation, particularly in Peru (Gentry, 1992a, Honorio & Reynel, 2004), despite housing more plant species in a smaller geographical area due to the diversity of environmental gradients (Henderson *et al.*, 1991, Ibisch *et al.*, 1996, Myers *et al.*, 2000, Young *et al.*, 2002, Killeen *et al.*, 2007).

1.1.1 Environmental Gradients

Environmental gradients commonly result in the gradual change from one biological community to another. Good examples are large tropical mountains where altitudinal changes in environmental conditions over a short geographical range, contribute to changes in forest structure and species composition. Environmental lapse rates are commonly 6.5 °C/km of altitude. These temperature changes affect evaporation, growth rates, decomposition rates and a number of other environmental and biological functions. Diurnal temperature ranges are also much greater at higher elevations (Grubb & Whitmore, 1966). Rainfall can increase with altitude up to the tropical forest limit at c. 3500 meters above sea level (masl) (Juvik & Ekern, 1978), and in the cooler environment, this increases relative humidity. Wind speed commonly increases with elevation (Lawton & Campbell, 1984) and a large proportion of montane forest precipitation can be wind driven, making vegetation an important source of water and mist collection in montane areas (Cavelier *et al.*, 1996). A reduction in solar radiation from increased cloudiness affects plant photosynthesis, microbial activity and temperature. There is also an enhancement of UV-B exposure as altitude increases, especially above 2500 masl (Caldwell *et al.*, 1980). All the above equates to increasingly cooler and wetter environments with altitude on tropical mountains.

Since the pioneering work of Grubb *et al.* (1963), there have been a multitude of terminologies developed for the zonation of tropical forest along altitudinal gradients. This zonation is affected by proximity to the coast. The phenomenon of depressed tropical altitudinal limits in coastal areas known

as the 'Massenerheburg' effect (Grubb, 1971), results from the formation of cloud at much lower elevations in coastal or oceanic areas where air vapour content is high. The result is that montane cloud forest forms as low as 400 masl compared to the lower limits of continental montane cloud forest at c. 1500 masl (Bruijnzeel & Veneklaas, 1998).

Whilst much discussion in tropical montane environments has centred on windward and upslope air mass processes, another important process that inevitably affects these areas is the Foehn effect, although the name can vary in differing geographic regions (McGowan *et al.*, 2002). In the Foehn effect, air masses cooled and dried through their upslope movement along a windward slope, move downslope, causing warmer temperatures on the leeward slopes relative to the windward slopes. Foehn winds are often described as extremely warm and dry, often with high associated wind speeds. However, the Foehn effect itself can take on many forms of intensity and frequency (Seluchi *et al.*, 2003).

The environmental changes along tropical altitudinal gradients sees a change in the distributions and/or attributes of many biotic variables including; vascular plant composition and richness (Grubb *et al.*, 1963, Kirkpatrick & Hassal, 1985, Gentry, 1988a, Nakashizuka *et al.*, 1991, Kitayama, 1995, Lieberman *et al.*, 1996, Givnish, 1999, Kessler, 2001, Martin *et al.*, 2007), bryophyte composition and richness (Frahm & Gradstein, 1991, Wolf, 1993c, Wolf, 1993b, Wolf, 1993a, Kurschner & Parolly, 1998d, Hemp, 2002, Hemp, 2006), plant morphologies (Rozema *et al.*, 1997, Bruijnzeel & Veneklaas, 1998, Buot & Okitsu, 1999, van de Weg *et al.*, 2009), epiphytic characters (Gentry, 1988a, Michelsen, 1993, Wolf, 1993c, Wolf, 1994, Hietz & Hietz-Seifert, 1995, Freiberg & Freiberg, 2000, Krömer *et al.*, 2005, Werner *et al.*, 2012), forest structure and productivity (Grubb *et al.*, 1963, Tanner, 1980a, Tanner, 1980b, Ohsawa, 1991, Kitayama, 1992, Phillips *et al.*, 1994, Ohsawa, 1995a, Ohsawa, 1995b, Weaver, 2000, Kitayama & Aiba, 2002, Moser *et al.*, 2007, Gerold *et al.*, 2008, Weaver, 2010b, Häger & Dohrenbusch, 2011), carbon allocation (Darrell & James, 1999, Roderstein *et al.*, 2005, Soethe *et al.*, 2006, Leuschner *et al.*, 2007, Gibbon *et al.*, 2010, Girardin *et al.*, 2010), standing mortality rates (Matelson *et al.*, 1995), plant phenology (Primack, 1985, Wesselingh *et al.*, 1999, Kimura *et al.*, 2001), terrestrial soil characteristics (Marrs *et al.*, 1988, Cavelier & Peñuela, 1990, Wolf, 1993c, Pendry & Proctor, 1997) and animal communities (Stiles, 1981, Patterson *et al.*, 1998, Giaretta *et al.*, 1999, Richardson *et al.*, 2000). Whilst many structural, compositional and functional changes have been observed in tropical montane forest, causal processes are still widely debated.

1.1.2 Tropical Montane Forests

Tropical montane forests can be distinguished from premontane and lowland forests by higher stem densities, lower basal area and shorter canopies (Whitmore, 1989, Kappelle & Leal, 1996). Tropical montane forest is usually classified as either lower montane forest or upper montane forest. In the neotropical literature these are usually further classified as montane rain forest or cloud forest when persistent cloud presence has a strong effect on forest structure (Bruijnzeel *et al.*, 2011).

1.1.2.1 Lower Montane Forests

In the Tropical Andes, lower montane forest occurs from a lower range of c. 1200 masl, to an upper range of c. 2800 masl (Grubb & Whitmore, 1966, Homeier *et al.*, 2010). The transition from lowland forest to lower montane forest is almost always associated with a reduction in canopy height (Grubb *et al.*, 1963, Pendry & Proctor, 1997) and a reduction in leaf size (Grubb *et al.*, 1963, Buot & Okitsu, 1999). Canopy heights are commonly up to 40 m (Pendry & Proctor, 1997, Vázquez & Givnish, 1998) and tree density commonly increases from lowland forest to lower montane forest (Pendry & Proctor, 1997). Lower montane forest generally has a much lower diversity of tree species, with tree species richness and altitude nearly always inversely related (Grubb *et al.*, 1963, Gentry, 1992b). The fruiting phenologies of lower montane forest tree species in Borneo were observed to be analogous to those of the adjacent lowland forest (Kimura *et al.*, 2001), reflecting similar pollinator and frugivore distributions and hence similar seasonal effects.

Pteridophyte diversity increases from lowland forest to lower montane forest, and lower montane forest commonly has the highest pteridophyte diversity over all forest zones (Young, 1991, Kessler, 2001, Hemp, 2002, Hemp, 2006), although much of this diversity can be attributed to lower montane cloud forests (León & Young, 1996). Ground herb coverage, density and species richness can also be much higher in lower montane forest compared to lowland forest (Poulsen & Pendry, 1995), as can that for palms (Kessler, 2000). Understorey bryophyte species diversity along a Columbian transect was highest in the lower montane forest where it increased dramatically from lowland forest (Gradstein *et al.*, 1989). Epiphytic growth is higher in lower montane forest than in lowland forest (Gentry & Dodson, 1987a, Nieder *et al.*, 1999, Freiberg & Freiberg, 2000, Cardelús *et al.*, 2006) and canopy-held organic matter can form on canopy branches and trunks (Nadkarni *et al.*, 2002). These accumulations can support a high diversity of epiphytic species and often vascular epiphyte species diversity is highest in lower montane forest (Gentry & Dodson, 1987b, Gentry & Dodson, 1987a, Hietz & Hietz-Seifert, 1995, Bussmann, 2001, Kuper *et al.*, 2004, Krömer *et al.*, 2005). Epiphytic bryophytes also increase dramatically in lower montane forest in cover, phytomass and diversity, and, mark one of the most apparent changes from lowland forest (van Reenen & Gradstein, 1983, Frahm & Gradstein, 1991, Frey & Kurschner, 1991, Kurschner & Parolly, 1998d, Kurschner & Parolly, 1998e, Kurschner & Parolly, 1998a, Kurschner & Parolly, 1998b, Kurschner & Parolly, 1998c, Kurschner & Parolly, 1999).

1.1.2.2 Upper Montane Forests

Upper montane forest occurs above the lower montane forest, to an upper range of c. 3600 masl (Grubb & Whitmore, 1966) in the Andes. The majority of upper montane forest is cloud forest within its altitudinal range, although local cloudiness does not always permit cloud forest formation in the upper montane forests. The variation in climate and topography in the tropics, allows the formation of upper montane forest to altitudes of 3900 masl in some locations (Stadtmüller, 1987).

The changes from lower montane forest to upper montane forest can be gradual or distinct. Forest stature continues to decrease with upper montane forest canopies ranging from 5m to 25 m in height (Kappelle *et al.*, 1996). Upper montane forest often occurs in steep and exposed terrain. Landslide scars and tree falls maintain a broken canopy. Leaf sizes reduce and display more xeromorphic characteristics as elevation increases (Bruijnzeel & Veneklaas, 1998, Buot & Okitsu, 1999).

Vascular plant and tree species diversity continue to decline with altitude (Kappelle & Leal, 1996). Understoreys usually show a depletion of broad leaf species with elevation, these being replaced by pteridophytes and bryophytes. While pteridophytes commonly peak in diversity in lower montane forest (Young, 1991, Hemp, 2002), they may increase or decrease in diversity into upper montane forest although not substantially. On many mountains, bryophyte (mostly hepatics) density, phytomass and cover increase from the lower montane forest to upper montane forest (Gradstein *et al.*, 1989, Frahm & Gradstein, 1991, Taylor, 2008). Terrestrial forms tend to increase in abundance due to the more organic soils (Frahm & Gradstein, 1991). Understorey bryophyte species diversity along a Columbian transect decreased slightly (20%) in upper montane forest from lower montane forest (Gradstein *et al.*, 1989).

Epiphyte loads increase from lower montane forest with increasing relative humidity and cooler temperatures (lower evaporation), although vascular epiphyte diversity usually decreases in upper montane forest (Bussmann, 2001, Kuper *et al.*, 2004, Cardelús *et al.*, 2006). There is a significant increase in epiphytic bryophytes in the upper montane forest (Frahm & Gradstein, 1991). In upper montane forest, epiphytes begin to play a significant role in the water and nutrient cycling of the forest (Benzing, 1998, Clark *et al.*, 1998).

1.1.2.3 Cloud Forests

Compared to tropical montane rain forests, cloud forests are often immersed in fog that generally creates a cooler and more humid environment (Stadtmüller, 1987), and often results in peculiar forest types that can house a disproportionately large amount of locally endemic species (Lewis, 1971, Gentry, 1986, Gentry, 1992a, Leo, 1995, León & Young, 1996, Patterson *et al.*, 1998, Young *et al.*, 2002, Vásquez *et al.*, 2003, van der Werff & Consiglio, 2004). Their distribution is interspersed among lower montane forest and upper montane forest, based on local cloud immersion. Montane cloud forests therefore range in altitude between c. 1500 and 3900 masl (Weberbauer, 1945, Stadtmüller, 1987) and are often described as lower montane forest or upper montane forest in the literature. According to Leo (1995), Peruvian montane cloud forest is found within twelve Holdridge (1967) life zones.

Montane cloud forest share many features of montane rain forest, depending on the location. Relative to altitudinal equivalents, montane cloud forest commonly has a reduced canopy height and reduced Leaf Area Index (LAI), which increases atmospheric exposure in the lower canopy (Stadtmüller,

1987). The strong seasonality of fruiting in altitudinal equivalents becomes increasingly weaker in montane cloud forest and results in a larger amount of non-migratory frugivorous (Kimura *et al.*, 2001) and insectivorous populations (Long, 1995).

Montane cloud forest compositions vary significantly, but an overriding generality is a high proportion of biomass and biodiversity as epiphytes. Epiphytes in montane cloud forest play a significant role in the water and nutrient cycling of the forest (Benzing, 1998, Clark *et al.*, 1998). Veneklaas *et al.* (1990) and Kohler et al. (2007) displayed how the epiphyte masses on canopy branches can store a large amount of water in the canopy. The same functions are performed by epiphytic tank bromeliads (Richardson *et al.*, 2000). Montane cloud forest is home to by far the most diverse communities of vascular epiphytes (Gentry & Dodson, 1987a, Kuper *et al.*, 2004, Cardelús *et al.*, 2006). León and Young (1996) believe the montane cloud forest is the most diverse habitat for pteridophytes in Peru.

Elfin forests are a type of cloud forest at the extreme end of the tropical montane forest continuum and can be found at a variety of altitudes up to 3900 masl (Weberbauer, 1945). Similarly to lower or upper montane cloud forest, they have a high proportion of epiphyte biomass but are characterised by a very low (3-15 m) and open canopy structure and low tree density (Scatena, 1995). These environments are commonly found on mountain summits and mountain passes over a wide altitudinal range (Lawton, 1982), where cloud immersion and wind are most concentrated.

Elfin forest vegetation often has a very windblown or stunted appearance (Stadtmüller, 1987, Bruijnzeel & Proctor, 1995). Gnarled trunks, with a densely packed single canopy layer are a common characteristic of elfin forest trees (Lawton, 1982). Leaves are also the most xeromorphic found in tropical montane areas, similar to those of the alpine flora of some temperate regions (Turner, 1994). Woody arboreal species tend to decline in elfin forest, while tree ferns, terrestrial orchids and woody shrubs are prevalent in the waterlogged organic soils (Scatena, 1995). Non-vascular plants dominate all available space.

1.1.3 Tropical Montane Forest Structure

Some debate exists on what causes the stature reduction and morphological changes in montane forest species, and this topic has dominated the altitudinal studies in tropical montane forests. A variety of hypotheses have been proposed based on the physiology of species, nutrient limitations, water relations and solar radiation to name a few. It is likely that a wide range of environmental variables is responsible and that these will vary in influence between sites. The following is a summary of evidence from a range of studies concerned with the changes in forest stature and species morphology in tropical montane forest.

Many studies claimed the physical and structural reductions observed in montane forest are indirectly related to climate, and, that nutrient availability is the limiting factor. Many have postulated that mineralisation and nitrification may control growth (Marrs *et al.*, 1988, Bruijnzeel & Veneklaas,

1998, Waide *et al.*, 1998). Marrs et al. (1988) supported less nitrification in Costa Rica as a plant growth limiting factor, while others supported understorey light to be the limiting factor for a montane cloud forest tree, not nitrogen (Anten *et al.*, 1996). Nitrogen in leaf and litter has been found at lower concentrations in upper montane forest compared to lower montane forest (Vera *et al.*, 1999, Wesselingh *et al.*, 1999) though van de Weg et al. (2009) found that montane forest leaves were not nitrogen limited on a Peruvian lowland-montane gradient. The low LAI and foliar nutrient content of montane cloud forest relative to lower montane rain forest was responsible for lowering forest floor litterfall inputs in Jamaica (Tanner *et al.*, 1998). Toxic phenols have also been recorded in montane cloud forest litter, believed to be a result of a plant response to UV-B exposure (Bruijnzeel *et al.*, 1993, Bruijnzeel & Proctor, 1995). Precipitation is higher within lower montane forest than lowland forest leading to seasonally saturated soils with less microbial activity (Cavelier *et al.*, 2000). The wet upper montane forest environment lowers decomposition rates and hence the organic content of soils is enhanced (Tanner *et al.*, 1998), while increased soil wetness also inhibits respiration (Silver, 1998).

In montane forest, steep slopes and high leaching often result in shallow soils with little horizon development. Combined with low soil nitrogen, lower decomposition rates, low sunlight, and high aluminium and organic carbon, montane soils are generally associated with low rates of primary productivity (Marrs *et al.*, 1988, Bruijnzeel & Veneklaas, 1998, Tanner *et al.*, 1998). Soils within lower montane forest upslope from lowland forest may have a difference in soil structure and texture as a result of erosion processes. Kirkby et al. (1997) found that upper slopes had reduced profiles from sediment transport to lower slopes. They also found that upper slopes showed chemical and physical changes compared to lower slopes, resulting in increased leaching and a loss of fine particles. As texture is known to affect nutrient storage (Silver *et al.*, 2000), and physical downslope processes could also affect the distribution of nutrients, especially in high slope areas. Regardless of the importance of nutrient levels to forest processes, it is a general consensus that nutrient inputs/availability decrease with altitude (Vitousek, 1998).

Physiological differences in hydraulic architecture between lowland forest and lower montane forest species was believed to be attributed to growth differences through reduced transpiration rates (Cavelier *et al.*, 2000). This was apparently disproved by Zotz et al. (1998) who found no differences in transpiration but that water use efficiency increased with elevation. Bruijnzeel and Proctor (1995) concluded from a review of physiological studies that the waterlogging of soils was responsible for the majority of physiological responses observed in montane cloud forest plants. They stressed that leaf transpiration rates required a greater deal of study and that it was unclear if species physiology was directly responsible for lower canopy heights.

Recently reported is the shift in aboveground/belowground carbon allocation patterns, where Leuschner et al. (2007) described a ten-fold shift

in the ratio to a markedly higher belowground allocation in upper montane forests compared to lower montane at the expense of aboveground growth, similar to that reported by Kitayama & Aiba (2002). Ultimately the reasons for this change were linked to LAI, temperatures, waterlogging and soil conditions as suggested in many of the studies mentioned above, though the above-belowground ratio change appears crucial to explaining the processes behind the observed reduced height and above ground biomass at so many sites. This ratio was confirmed in a comprehensive study over a larger gradient, yet lower net primary productivity was reported in montane forests, while above- and belowground productivity partitioning was the same as lowland and premontane forests (Girardin *et al.*, 2010).

A noticeable difference between lowland and montane areas is the increase in relative relief. Some tropical montane forests occupy very steep slopes, while there is almost always variation between ridge, slope and ravine type topographies. Takyu et al. (2002, 2003), Weaver (2000, 2010a) and Homeier et al. (2010) found that species composition and forest structure changes within montane forest as a result of topographical changes. In the study by Takyu et al. (2002), this effect was more influential where nutrient pool sizes were larger, while Cox et al. (2002) found topography affected elements associated with geochemical processes. Bellingham and Tanner (2000) found in Jamaica that tree mortality rates were also affected by topography, while Schwarzkopf et al. (2010) found that aspect was related to differing LAI and Werner et al. (2012) found variation in epiphytic biomass.

An example of physical processes acting upon montane forest morphologies may be the elfin forests, usually restricted to the peaks and ridges on mountains. Lawton (1982) believed that the gnarled trunks and densely packed single canopy of elfin forest trees is an adaptive response to wind. Contrary to Lawton, Fetcher et al. (2000) found little evidence, except for increased survivorship, for the influence of wind on growth. However, there is no way to compare the amount of wind between the sites of these two studies. In another elfin forest, Dupuy et al. (1993) believed their evidence was sufficient to show that gnarling/stunting was partly due to trees rolling over in the wind and continuing to grow.

Contrary to the beneficial photosynthetically active radiation (400-700 nm), the Ultraviolet-B radiation (UV-B) waveband (290-315 nm) is detrimental to most organisms. UV-B can inhibit photosynthesis in plants. This has been shown to alter growth patterns, compound production and fruiting and flowering cycles (Caldwell, 1981, Day *et al.*, 1992, Sullivan *et al.*, 1992, Ziska *et al.*, 1992, Rozema *et al.*, 1997, Bruijnzeel & Veneklaas, 1998, Sampson & Cane, 1999). It becomes detrimental to plant growth generally above 2500 masl due to the reduction in both aerosol optical thickness and the attenuation of Rayleigh scattering (Caldwell *et al.*, 1980, Caldwell, 1981). Due to a 40-70% scattering of UV-B flux, foliage angle has no effect on exposure levels (Caldwell *et al.*, 1980).

Flenley (1992, 1995), following the hypothesis constructed by the late Francis Merton, believed cloud immersion-UV-B dynamics significantly

influence mountain top vegetation and that the effects of ultra-violet radiation distribution extend to the distribution of plant species, plant morphologies and forest limits. Other studies have supported this hypothesis (Caldwell *et al.*, 1980, Day *et al.*, 1992, Sullivan *et al.*, 1992, Ziska *et al.*, 1992, Wolf, 1993b, Rozema *et al.*, 1997). In montane cloud forest, polyphenols have been found in fresh leaf litter (Bruijnzeel *et al.*, 1993, Bruijnzeel & Proctor, 1995). These compounds, known to be produced by some plants in defence of UV-B (Rozema *et al.*, 1997, Nomura *et al.*, 2001), may interfere with cell growth and uptake of nutrients (Bruijnzeel & Proctor, 1995). Polyphenols are also known to slow decomposition processes (Kuiters, 1990).

Whilst possibly excluding many species from higher elevations, UV-B may also contribute to the small thick leaves and gnarled and stunted growth commonly observed in montane cloud forest species (Leigh, 1975, Stadtmüller, 1987, Flenley, 1992, Dupuy *et al.*, 1993, Bruijnzeel & Proctor, 1995, Velez *et al.*, 1998). Some studies have noted thick cuticle growth on leaves, twisted stem growth and reduced growth heights from UV-B exposure (Sullivan *et al.*, 1992, Rozema *et al.*, 1997). While spectrum measurements were not made, Bader et al. (2007) suggested that very high radiation resulted in the failure of non-shaded seedling transplants above the current treeline in Ecuador.

1.1.4 Cloud Forest Distribution

Andean montane cloud forests are found in areas subject to orographic rain and cloud formation phenomena, resulting in a complex of forest types along altitudinal and/or topographic gradients, many of which present both windward and leeward slopes that in other landscapes have been shown to present differing vegetation (Kappelle *et al.*, 1995, Häger & Dohrenbusch, 2011).

Forest structures are known to change sharply in areas where the base of a cloud band forms at regular altitudes (Stadtmüller, 1987, Merlin & Juvik, 1995). Cloud immersion lowers temperatures and solar exposure (Stadtmüller, 1987, Obregon *et al.*, 2011). It increases humidity and can contribute to large increases in water inputs through cloud water deposition (Cavelier & Goldstein, 1989), where wind driven fog particles are precipitated onto vegetation on contact. The presence of frequent fog in montane cloud forest permits the great abundance of epiphyte communities that harness this atmospheric moisture.

In many montane cloud forest areas, orographic cloud formation dominates the microclimatic conditions in forests. In the Andean montane forests, diurnal atmospheric cooling and warming cause daily fluctuations in cloud height (Gordon *et al.*, 1994). This spatial and temporal variation influences environmental lapse rates and the distribution of all manner of parameters that influence the composition of plant communities (Brass, 1964, Grubb & Whitmore, 1966, Flenley, 1992, Bruijnzeel & Veneklaas, 1998).

The principal effect of high rates of cloud immersion in montane cloud forest is a reduction in the seasonality of hydrological cycles. Many montane cloud forests commonly receive moisture inputs through cloud water deposition

during seasons in which rainfall is absent (Stadtmüller & Agudelo, 1990, Juvik & Nullet, 1995, Holder, 2003), whilst in others evaporation is at least significantly reduced. This reduces water stress for plants, often causing permanent waterlogging (Bruijnzeel & Proctor, 1995), and in areas with seasonal rainfall, montane cloud forest can host a completely different flora to the adjacent forest (Vitousek, 1998). Sharp montane cloud forest boundaries are often formed as result of the topographic channelling of orographic cloud, which can create islands of montane cloud forest vegetation even in arid areas (Sugden, 1982a). However, most cloud forests in humid areas still rely on rainfall as the overwhelming hydrological input, thus the most important effects of fog on cloud forests are more likely to be microclimatic that affect plant physiology as opposed to hydrologic (Eugster *et al.*, 2006).

While our understanding of tropical montane cloud forest climate gradients has increased dramatically in recent years through numerous studies along large altitudinal gradients, much less has been described of changes in cloud forest environments and characteristics across orographic gradients, and no such studies have been published in southern neotropical latitudes.

1.2 Research Aims

1.2.1 Montane Forest Classification

The first of the overlying aims of this study was to determine the fog frequency of three montane forest types along an orographic gradient. Despite the considerable increase in cloud forest meteorological databases, classifications of cloud forest have mostly focussed on physical and biological attributes such as rainfall, canopy structure and height, bryophyte density and botanical morphology (Frahm & Gradstein, 1991, Scatena *et al.*, 2010, Bruijnzeel *et al.*, 2011), while descriptions of their intrinsic climate environment, '… frequently covered in cloud or mist' (Stadtmüller, 1987), have been cursory.

Numerous studies have directly investigated the occurrence or properties of canopy level cloud, mist or fog (the term fog is used here on in) in tropical montane cloud forests, some being visual estimates of occurrence (Sugden, 1982a, Gordon *et al.*, 1994, Bendix *et al.*, 2008), a growing number based on remote sensing techniques (Bendix *et al.*, 2006, Nair *et al.*, 2008, Welch *et al.*, 2008), while the vast majority have focussed on determining the contribution of fog to forest water balances through the use of physical fog collectors with often limited if any diurnal data resolution (Bruijnzeel, 2001, DeLay & Giambelluca, 2010, Bruijnzeel *et al.*, 2011), especially in the older literature. Simple fog frequency statistics are not published for the majority of well-studied cloud forest sites. These data could be used to further classify cloud forests by the characteristics of their diurnal and seasonal fog frequencies, just as precipitation is often used with other factors to characterise tropical rain forests (Holdridge *et al.*, 1971).

This lack of published data on the temporal fog environment is likely to change with the recent advent of relatively affordable and automated

visibility sensors, which provide the opportunity to produce simple and comparable statistics such as annual, monthly and diurnal fog frequencies and densities such as those produced by Obregon et al. (2011) and Eugster et al. (2006). While the determination of the hydrological budgets of cloud forest areas with these sensors alone may have some limitations, they can provide information on the duration and effects of fog that are likely more relevant to some ecological processes than interception measurements alone, as many cloud forests still depend on rainfall for hydrological inputs (Eugster *et al.*, 2006).

The addition of such measurements should help to discern some of the difficulties in forest classification, especially the determination between lower montane rain forests and lower montane cloud forests using current forest structure based classifiers (sensu Bruijnzeel *et al.*, 2011). In order to compare fog frequencies with the results of the most common montane forest classifiers, I recorded 10-minute fog frequency at three distinct montane forest sites, as well as other common biological, morphological and structural traits used to classify montane rain and cloud forests.

1.2.2 Orographic Variation

The second of the overlying aims of this study was to investigate variations in climate and cloud forest characteristics over an orographic gradient. Tropical windward slopes are usually more humid than their leeward counterparts, which often results in differing microclimates, forest composition and stand structure (Weaver *et al.*, 1986, Dupuy *et al.*, 1993, Kappelle *et al.*, 1995, Martin *et al.*, 2007, Häger & Dohrenbusch, 2010). Forest structure affects many ecological aspects of forests (Nadkarni *et al.*, 2008). In cloud forests interception is especially affected (Ataroff, 2002, Brauman *et al.*, 2010). Variation in tropical montane cloud forest composition and structure has been widely observed in altitudinal forest zonation studies (Gentry, 1988a, Heaney & Proctor, 1990, Nakashizuka *et al.*, 1991, Ohsawa, 1991, Kitayama, 1992, Kappelle *et al.*, 1995, Lieberman *et al.*, 1996, Pendry & Proctor, 1996, Pendry & Proctor, 1997, Vázquez & Givnish, 1998, Aiba & Kitayama, 1999, Buot & Okitsu, 1999, Givnish, 1999, Kitayama & Aiba, 2002, Takyu *et al.*, 2002, Hemp, 2006, Leuschner *et al.*, 2007, Martin *et al.*, 2007, Gerold *et al.*, 2008, Homeier *et al.*, 2010, Martin *et al.*, 2010). However, fewer studies have investigated compositional and structural changes along the orographic gradients of tropical montane cloud forest, which often create distinctive biophysical conditions regardless of altitude (Grubb, 1977, Stadtmüller, 1987, Bruijnzeel & Veneklaas, 1998, Häger & Dohrenbusch, 2011). To date in the neotropics, only a few forest structure and composition studies have been undertaken on orographic gradients of tropical montane cloud forest. These have been in the Caribbean and Pacific slopes of certain ranges in Costa Rica (Kappelle *et al.*, 1995, Häger & Dohrenbusch, 2010) and Puerto Rico (Weaver, 2000, Weaver, 2010b), and in some Columbian cloud forests on the Caribbean rim (Sugden, 1982a, Sugden, 1982b, Dupuy *et al.*, 1993). A larger number of studies (that include higher elevation continental cloud forests) have inadvertently studied forest structure and composition at either a leeward or windward cloud forest, some of which include ridge sites for comparison (Madsen & Ollgaard, 1994, Homeier *et al.*, 2010), although often

the term ridge forest is used in the microtopographic sense (exposed ridge on any scale in any part of the terrain), not the orographic sense (exposed ridge along the divide between leeward and windward slopes). Distribution patterns of biodiversity across orographic gradients have not been addressed in southern Neotropical latitudes. Furthermore, while the species diversity of the montane cloud forests of Central Peru appear to be very high (Vásquez *et al.*, 2005), the floristic composition has only been previously described by general botanical collections (Gentry, 1980, Gentry, 1988b, Gentry, 1992a, Vásquez *et al.*, 2005).

In order to investigate the variation of climate and forest characters across an orographic gradient, I recorded the climate and performed a detailed forest inventory at three forests with distinct orographic locations.

1.2.3 Fog Environment

The third overlying aim of this study was to investigate the interrelations of fog with microclimatic parameters. While the presence of cloud, fog or mist is the inherent characteristic of cloud forests, very few studies have reported the climatic conditions prevalent during fog formation or how canopy level fog events affect the behaviour of other climatic parameters commonly linked to ecological theory such as temperature, moisture and radiation (Bruijnzeel & Veneklaas, 1998, Eugster *et al.*, 2006).

The presence of canopy level fog is generally thought to be associated with reductions in temperature and radiation, and increases in humidity, contributing significantly to well-described ecological effects that affect cloud forest hydrology through increased interception and cloud forest taxa through waterlogging, reduced drought stress and productivity and photosynthetic adaptations amongst others (Pendry & Proctor, 1996, Clark *et al.*, 1998, Tausz *et al.*, 2001, Leon-Vargas *et al.*, 2006, Holder, 2007, Kohler *et al.*, 2007, Leuschner *et al.*, 2007, Häger & Dohrenbusch, 2011). As argued by Eugster et al. (2006), most tropical cloud forests still depend on rainfall for the vast majority of their hydrological balance, and as such the influence of fog may be more defining in terms of its microclimatological effects on plant physiology and soil dynamics.

In addition, while many tropical montane cloud forests sites are clearly affected by orographically formed fog, the processes leading to fog formation and the resulting microclimates at some sites such as leeward cloud forest for example might be more complex than generally assumed. Furthermore, cloud forests differ greatly in composition and structure from rain forests, and whilst it is accepted that fog events help bridge the gap between humid rain events in comparison with the often prolonged dry periods in rain forests, there appears to be even less published on how fog events differ from rain events in their effects on microclimate.

Eugster et al. (2006) presented the most detailed study to date on fog occurrence and microclimatic parameters from a tropical cloud montane forest in Puerto Rico. They found a 48 % reduction in photosynthetically active photon flux density (PPFD) during dense fog events. Obregon et al. (2011) also presented a detailed study on fog occurrence at a tropical cloud

forest, albeit at one of the rare lowland cloud forests sites, where orographic processes could obviously not explain a high fog frequency that resulted from *in situ* temperature and rainfall dynamics. Thus our knowledge on spatial and temporal fog formation and the incurring microclimatic effects is still mostly inferential.

In order to investigate the effect of fog on microclimate and the conditions associated with fog occurrence, a 5-year microclimatic database with visibility measurements was analysed from a leeward montane forest, ideally suited to the task due its large variation in climatic conditions.

1.3 Objectives and Structure

In order to fulfil the above mentioned interrelated overlying research aims, three principal objectives were set out and are addressed in separate analytical chapters that include specific objectives, methodologies, results and discussions. A general site description pertinent to all following chapters is presented below in the current chapter.

Chapter 2 addresses temporal and spatial climate dynamics over an orographic gradient comprised of three distinct forest types at a tropical montane cloud forest area in Central Peru. The principal objective of this chapter was to describe the changes in climate with altitude and orographic location between a windward, ridge and leeward tropical montane forest and evaluate the orographic influence on the *in situ* microclimatic regime.

Chapter 3 addresses the patterns of species distribution, forest composition and structure and the relationships with environmental variables along the same orographic gradient studied in chapter 2. The principal objective of this chapter was to describe the changes in families and species of shrubs and trees (stems ≥5 cm DBH) among the sites, determine floristic sub-communities at each site and analyse the similarity of communities and relationships to biophysical variables between sites and to compare forest structures and leaf morphologies.

Chapter 4 addresses the microclimatic dynamics of a 5-year climatic database that included visibility measurements at a leeward tropical montane forest. The principal objective of this study was to quantify the duration of rainfall, fog and rain-fog free weather events, and compare at various temporal scales the statistics for temperature, humidity, wind and photosynthetic photon flux density (PPFD) during each weather event type.

The concluding Chapter 5 synthesizes the results of each analytical chapter to address the relationships between climate and forest structure within the scope of the overlying research aims.

1.4 Study Area

1.4.1 Location

The Cordillera Yanachaga is a semi-isolated range located between the Amazonian Plain to the east and the Andean Cordillera to the west (Figure

1.4.1.1). The cordillera lies approximately 80 km west of the true Amazonian plain, separated by a series of low foothills, yet is the first major range that Amazonian air masses encounter along their western trajectory (Figure 1.4.1.2). The cordillera was protected with the formation of the 120,000 ha Yanachaga-Chemillén National Park in 1986 for its cultural and biophysical aspects. The park houses an important area of tropical montane cloud forest on its eastern and western slopes from approximately 2000 to 3400 masl (INRENA, 2005).

Whilst previously only botanically prospected, in recent years the National Park has been the location for an increasing number of scientific studies, many of which focussed on the areas denominated as cloud forest. However, the distribution, composition and ecology of the different forest types within the cloud forest zones are still mostly undescribed (Vásquez *et al.*, 2005). The present study is one of the numerous works in recent years within the San Alberto Valley of the national park, which is a leeward valley on the western flank of the Cordillera Yanachaga, which begins at a mountain pass known as Abra Esperanza that gives way to the windward Danubio Azul watershed on the eastern flank (Figure 1.4.1.3). The present study was undertaken in order to characterize the aspects of the climate, forest structure, floristic composition and deduce ecological relationships particular to the leeward, ridge and windward cloud forests in this area.

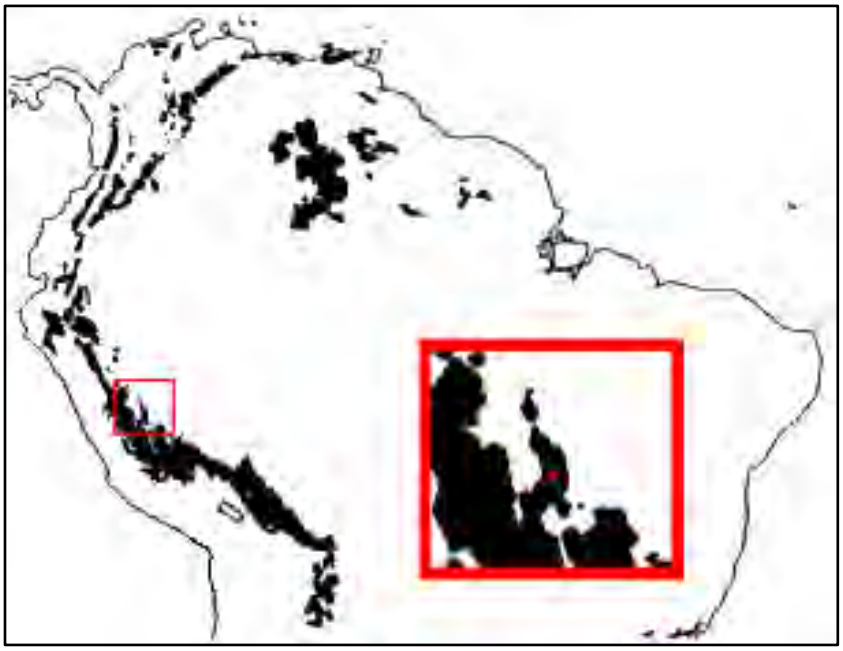

Figure 1.4.1.1: Location of the study area within the continental distribution of neotropical montane forest.

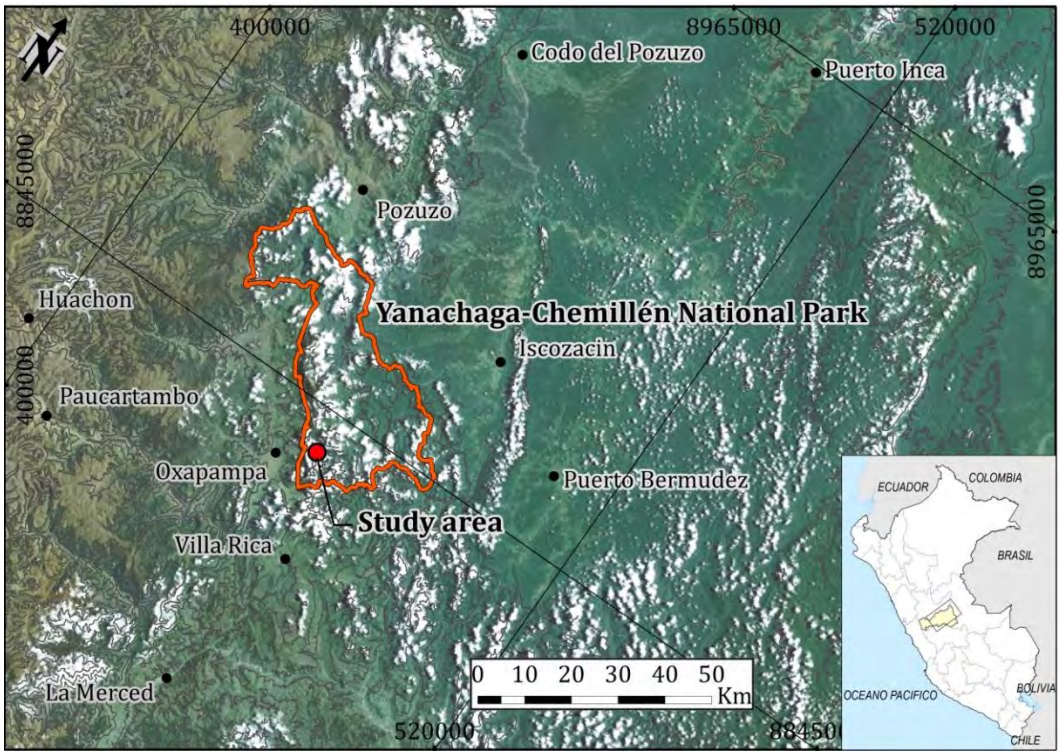

Figure 1.4.1.2: Location of the Yanachaga-Chemillén National Park in Central Peru.

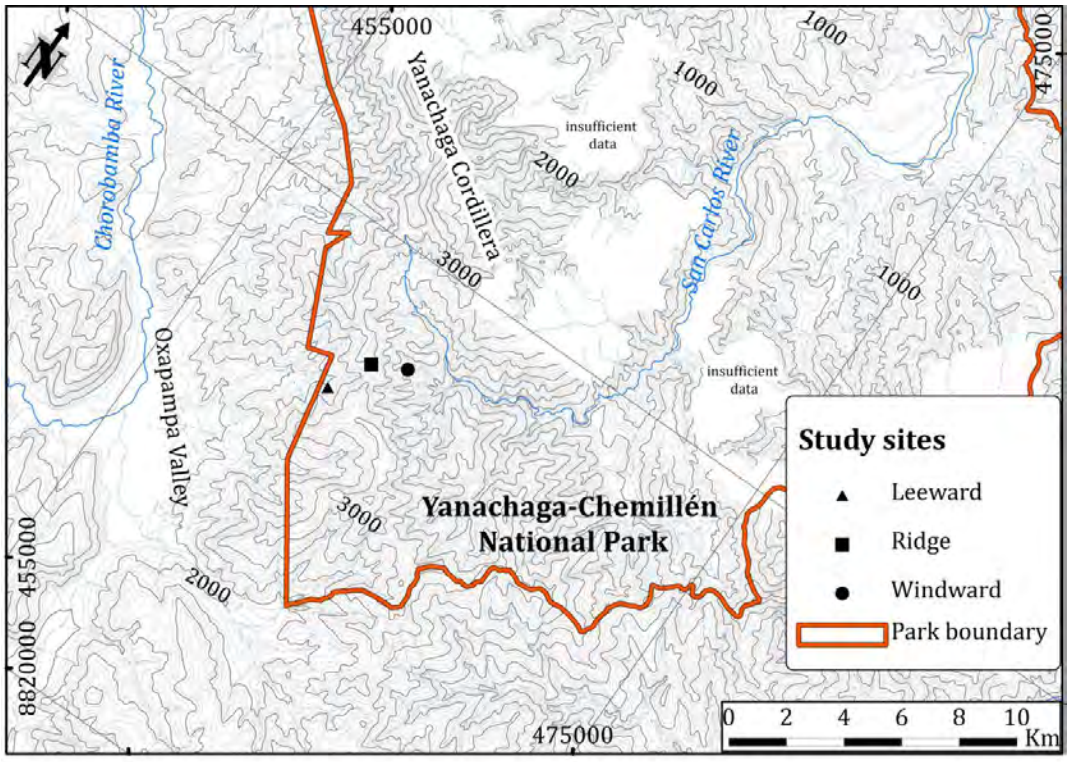

Figure 1.4.1.3: Location of the three study sites.

1.4.2 Regional Climate

Meteorological data has been collected at Oxapampa at the base of the San Alberto Valley at an altitude of 1830 m since 1983, at a distance 5 km from the leeward forest site, from which data was collected from 2003 to 2011.

Rainfall at Oxapampa has an average of 1450 mm (1984 – 2011) and has never exceeded more than 2000 mm/yr, while with an average of 3247 mm (2003 – 2011) the leeward forest site receives twice the rainfall as Oxapampa (Figure 1.4.2.1). A noteworthy event at the leeward forest sites highlighting the type of hydrological regime was a the recording of c. 2000 mm over a 7 day period during February 2011, which included three days in a four day period with >350 mm/day. The average annual temperatures are 16.35 °C and 13.47 °C at Oxapampa and the leeward forest respectively. The sites show a difference of approximately 3 – 4 °C, showing an average temperature lapse rate of 4.79 °C/km on the leeward slope. Oxapampa has shown a steady temperature rise over the last 25 years (Figure 1.4.2.2) that equates to an increase of roughly 0.08 °C/yr, which is probably a result of both regional trends in climate (Malhi & Wright, 2004) and the recent complete deforestation of the Oxapampa Valley that on accounts once housed arguably the largest volumetric stand of *Podocarpus montanus* forest in the Peruvian Andes.

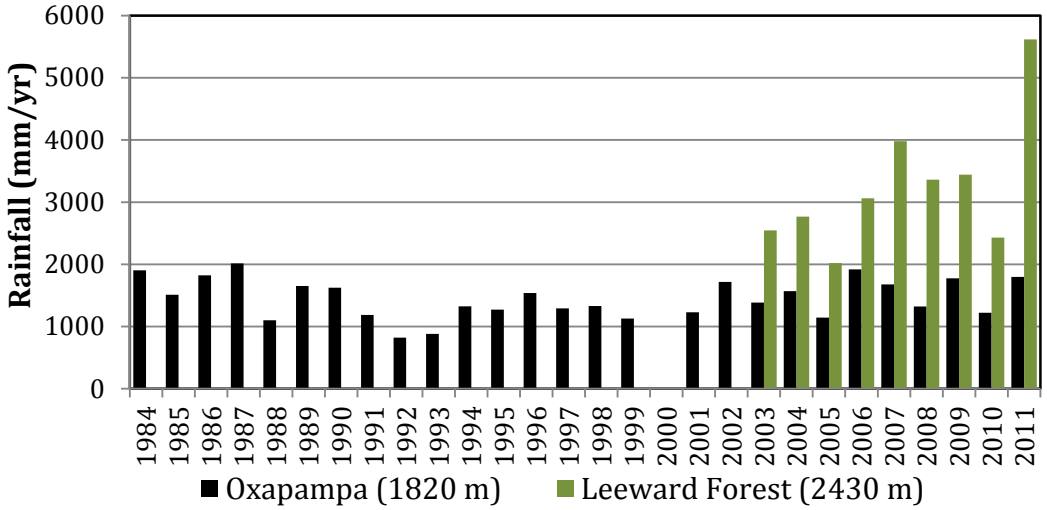

Figure 1.4.2.1: Annual rainfall record from Oxapampa and the leeward forest site. Data from Oxapampa is uncalibrated and received an instrumentation overhaul in 2000 (data missing).

The seasonal climate can be typified by a 7-month wet season from October until April (Oxapampa rainfall >100 mm/mon; leeward forest rainfall >200 mm) and a 5-month dry season from May until September (Figure 1.4.2.3).

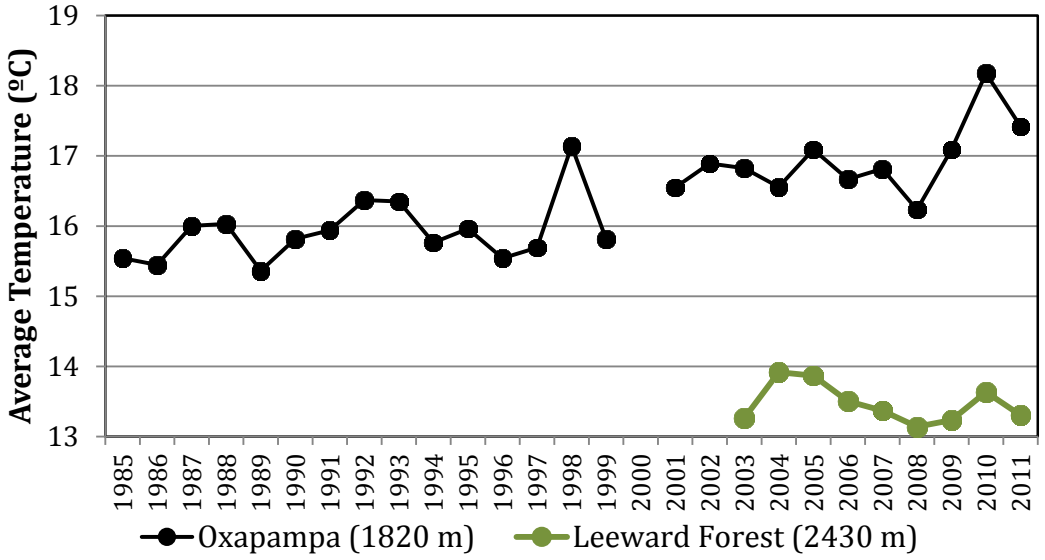

Figure 1.4.2.2: Annual temperature record from Oxapampa and the leeward forest site. Data from Oxapampa is uncalibrated and received an instrumentation overhaul in 2000 (data missing).

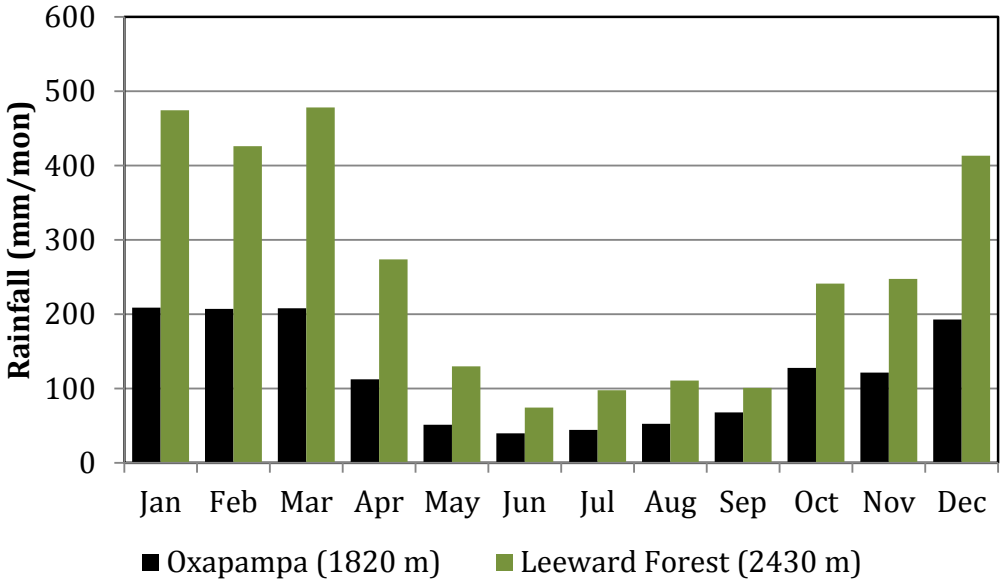

Figure 1.4.2.3: Average Monthly rainfall from Oxapampa and the leeward forest site.

1.4.3 Forest Types

The leeward montane forest at c. 2400 masl is located at a site known as "El Cedro" (after the locally dominant emergent *Cedrela montana*) in what could be described as a sheltered valley location. Soils are deep, organic and well-drained eutric cambisols on an underlying geology of Mesozoic sediments. The forest has a relatively tall slightly broken canopy (15 – 25 m) and the c.

26° slope has a WSW aspect. The understorey has a c. 15 cm organic layer covered principally (c. 40%) by leaf litter, receives c. 12% of above canopy PPFD and is situated in acidic soils (pH 4.4) with high organics, low macronutrients and an average bulk density of 0.46 g/cm^3 (Taylor, 2008). The site is well known for its extraordinarily speciose epiphytic flora, with an unprecedented 195 species of vascular epiphytes (Catchpole & Kirkpatrick, 2010) and 110 species of non-vascular epiphytes (Romanski *et al.*, 2011) each being recorded from single trees within the study area, for which the current list of vascular epiphytes recorded is at c. 225 species (unpublished data, D. Catchpole). Gómez (1999) found 154 tree species in a 1-ha study plot adjacent to that of the present study, in which 204 species (per ha) of understorey herbs were found, principally of the Piperaceae, Urticaceae, Asteraceae and Melastomataceae (Taylor, 2008). Gomez-Peralta et al. (2008) classified the site as a lower montane rain forest due to an apparent lack of cloud water interception after conducting an interception study during what turned out to be a known drought period (Zeng *et al.*, 2008), although as is often the case at this altitude the forest has elements of both lower montane rain and cloud forests. The site can be topographically classified as a slope forest whose arboreal strata is characterized by genera such as *Guarea, Alchornea, Weinmannia*, *Myrsine*, *Nectandra*, *Palicorea, Podocarpus, Ficus, Clusia* and *Miconia*, whilst being visibly dominated throughout the understorey by the tree fern genera *Alsophila* and *Cyathea*.

The ridge forest at c. 2800 masl is located just above the lowest point on the exposed mountain pass known as “Abra Esperanza”. Similar to the leeward site, soils are deep, organic and well-drained eutric cambisols on an underlying geology of Mesozoic sediments. The forest has a relatively short and open canopy (5 – 20 m) and the c. 16° slope has a SSW aspect. The understorey has a c. 60 cm organic layer covered principally by bryophytes (c. 35%) and leaf litter (c. 30%), receives c. 28% of above canopy PPFD and is situated in highly acidic soils (pH 3.4) with very high organics, low macronutrients and an average bulk density of 0.16 g/cm^3 (Taylor, 2008). This forest has much lower vascular epiphyte species richness than the leeward site with c. 45 species being recorded from the study plot (unpublished data, D. Catchpole), and also shows a lower number of understorey herbs with 140 species principally of the Asteraceae, Melastomataceae, Rubiaceae and Poaceae (Taylor, 2008). Gomez-Peralta et al. (2008) classified the site as an upper montane cloud forest cloud with large cloud water interception rates despite conducting an interception study during a known drought period (Zeng *et al.*, 2008). The site can be topographically classified as a slope forest whose arboreal strata are characterized by genera such as *Weinmannia*, *Myrsine*, *Podocarpus, Hedyosmum, Licaria, Clusia* and *Miconia*.

The windward forest at c. 2400 masl is located at a site denominated as “Danubio Azul” in what could be described as an exposed ridge location. Soils are variable, including shallow clays in a debris flow area and deep, organic and well-drained eutric cambisols on an underlying geology of Mesozoic sediments. The forest has a relatively short and broken canopy (10 – 18 m) and the c. 32° slope has a SE aspect. The understorey has a c. 50 cm organic

layer covered principally by leaf litter (c. 40%), receives a highly variable yet similar percentage of above canopy PPFD as the ridge forest and is situated in highly acidic soils (pH 3.7) with very high organics, low macronutrients (with the exception of high levels of K) and an average bulk density of 0.20 g/cm^3 (Taylor, 2008). This forest has lower vascular epiphyte species richness than the leeward site with c. 110 species being recorded from the study plot (unpublished data, D. Catchpole), and also shows the lowest number of understorey herbs with 113 species principally of the Melastomataceae, Clusiaceae, Ericaceae, Urticaceae and Lauraceae, with a large abundance of bamboos and grasses (Taylor, 2008). The site can be topographically classified as a slope forest whose arboreal strata is characterized by genera such as *Weinmannia*, *Cyathea*, *Myrcia*, *Podocarpus, Nectandra, Myrsine, Clusia* and *Miconia,* whilst being dominated throughout the understorey by the *Cyathea* tree ferns.

Chapter 2

Variation in Climate along an Orographic Gradient in Peruvian Montane Forest

2.1 Objectives

In order to fill the gaps in knowledge identified previously (Chapter 1.2.1 & 1.2.2), this chapter documents the temporal and spatial patterns of temperature, humidity, radiation, rainfall wind and fog across a windward to leeward gradient in montane forest. Thus, the aim of the present chapter is to investigate how climate changes with altitude and orographic location between a windward, ridge and leeward tropical montane forest site.

In order to detect any similarities or localized phenomena, the principal objectives were to:

- Determine differences between sites in temperature, relative humidity, radiation, rainfall, wind and fog regimes on annual, seasonal, monthly and hourly timescales;
- Analyse the relationships between climatic parameters;
- Determine the amount of time each site was subjected to humid (rain/fog) events.

2.2 Materials & Methods

2.2.1 Site Description

The climatic data was obtained from three sites within the pristine area tropical montane forest within the Yanachaga-Chemillén National Park, which is located in the Selva Central region of eastern Peru (Figure 1.4.1.1). Sites were selected at leeward, ridge and windward locations for the installation of above canopy meteorological stations. Both leeward and windward sites had an altitude of 2400 masl, and were both less than 2 km from the ridge site at 2800 masl (Figure 2.2.1.1). Each site was a distinct forest type with a different canopy structure from the other sites (see Chapter 1.4.3).

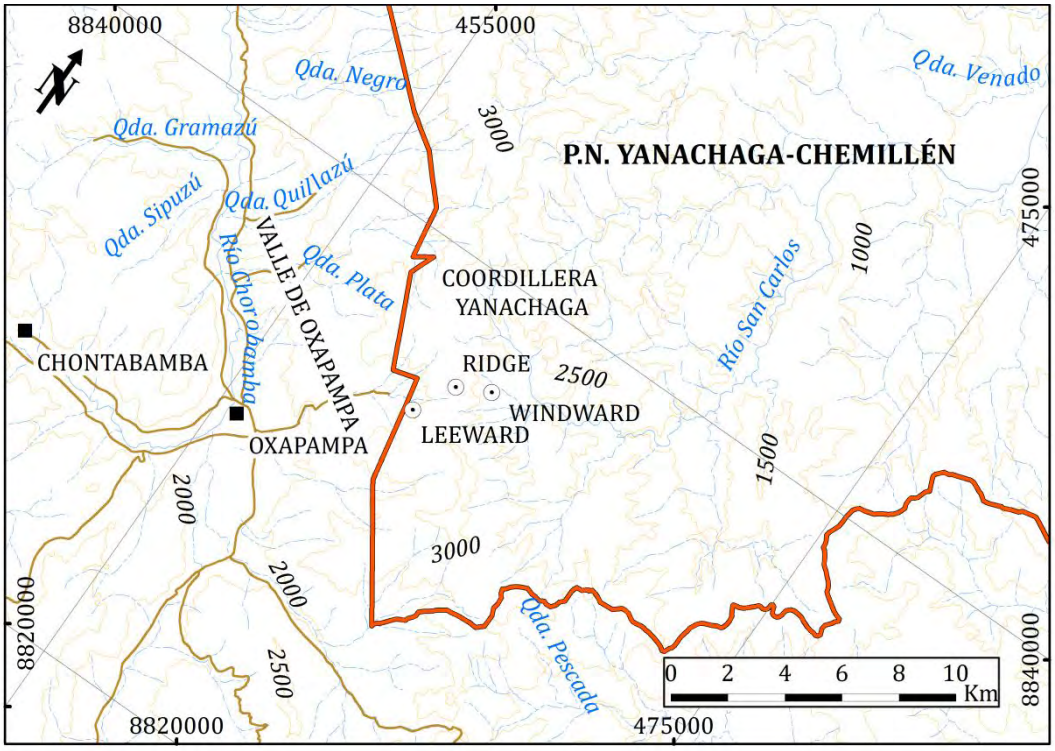

Figure 2.2.1.1: Location of study area and meteorological stations

2.2.2 Measurements

To record the atmospheric conditions, a canopy mast was constructed in each forest such that meteorological observations could be obtained from a height of c. 5 – 10 m above the canopy surface. The 40 m (leeward), 18 m (ridge) and 20 m (windward) masts were constructed of galvanised metal tube in a triangular design and anchored in 3.375 m^3 cement bases and gyred on all three angles with galvanised steel cable to form a rigid platform for the installation of instruments at the top of each the mast above each forest canopy (Figure 2.2.2.1, Figure 2.2.2.2, Figure 2.2.2.3). The remote stations were powered by 60 W solar panels and a 95 Ahr sealed AGM battery, which supplied constant power to a Campbell Scientific CR10X datalogger, which controlled and recorded data from all tower sensors at 10 sec intervals to produce an array of 10 min data outputs from all sensors (see Table 2.2.2.1).

All instruments were temporarily installed at one location (Oxapampa, Peru – 1860 masl) for two weeks in order to compare all sensors outputs prior to installation[1]. In order to check for sensor drift, field calibrations were performed with mobile temperature, humidity and radiation sensors installed amongst each instrument array for a 4-day period at 6-monthly intervals. No significant measurement drift was detected from a particular sensor in comparison with the others. Therefore, the synchronized data from the 2007-2008 periods was used as recorded. All sensor outputs were

[1] One of the LiCor quantum sensors was found to have slight linear variation from the other sensors which was corrected with an adjustment coefficient added to the datalogger program.

averaged or totalized for each 10-min period, with absolute maximum and minimum values also being recorded where pertinent.

Figure 2.2.2.1: The 40 m leeward forest canopy mast.

Figure 2.2.2.2: The 18 m ridge forest canopy mast.

Figure 2.2.2.3: The 20 m windward forest canopy mast.

Table 2.2.2.1: Instruments of each meteorological station

Instrument	Raw Output Description
Optical Sensors OFSMk2	Average visibility (0 – 5000 m) over a 1-min period
R.M. Young 81000	2D & 3D wind speed (m/s), direction (degrees) and elevation (+/- degrees) at 10-sec intervals
LiCor LI-190SB	Photosynthetically Active Photon Flux Density ($\mu mol/m^2/sec$) at 10-sec intervals
Vaisala HMP50-L	Temperature (ºC) and relative humidity (%) at 10-sec intervals
Hydrological Services TB-4	Rainfall (0.254 mm amounts) at 10-sec intervals
Campbell Scientific CR10X	Datalogger used for sensor programming and data storage

2.2.3 Representativity of Evaluation Period

Meteorological data was collected at the leeward site from 2003 to 2011. Synchronous data was collected from all sites from January 2007 through to December 2008 for all parameters except visibility, which was only collected from all sites in 2008. However, it should be noted that the windward site

visibility dataset does not cover all of 2008 due to datalogger problems during that period and only runs from January to September 2008.

In order to contextualize the climatic conditions occurring during the time in which the comparative dataset was collected, and given that annual averages can mask marked seasonal differences in a bimodal hydrological regime, seasonal climatic statistics are presented for every dry (May – September) and wet (October – April) season in the meteorological record from 2003 till 2011 at the leeward site. The leeward site had an annual rainfall of 3307 mm with an annual average temperature of 13.53 ºC. Figure 2.2.3.1 shows that the evaluation period (2007 & 2008) was close to typical for the longer period, albeit being slightly wetter, although not by any means as wet as that recorded in 2010/2011 (5254 mm). Temperature during the evaluation period was mostly around and sometimes slightly below the average.

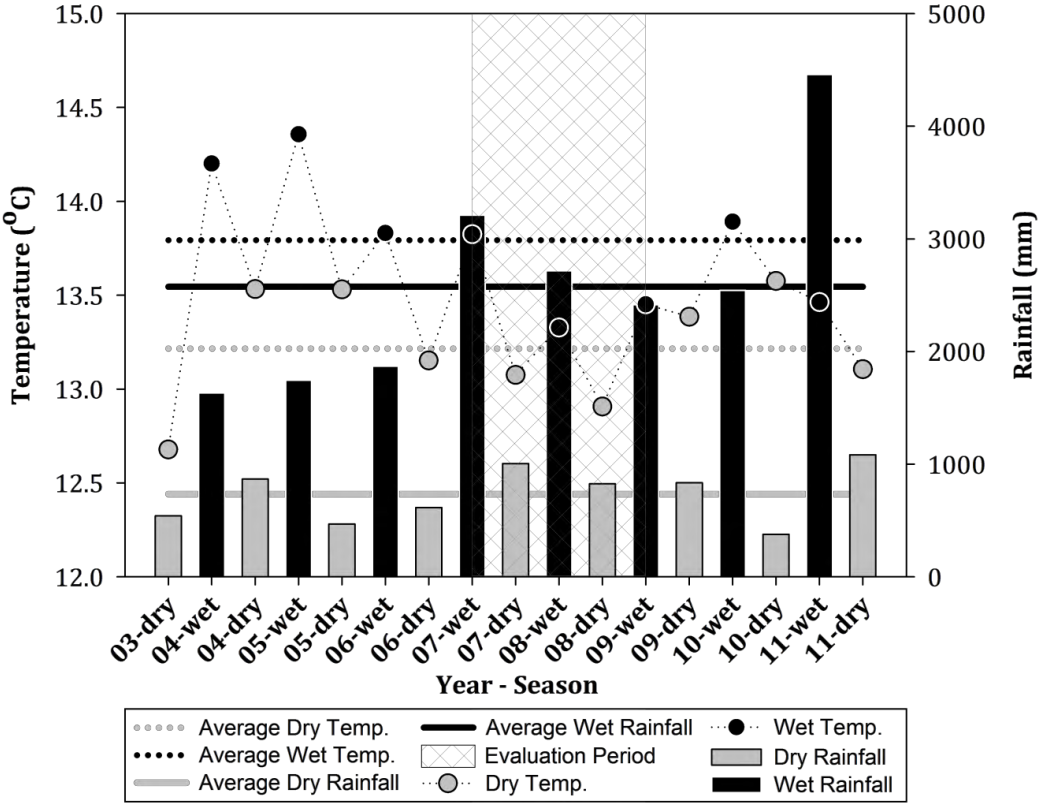

Figure 2.2.3.1: Total rainfall and average temperature per season at the leeward site compared to the 2003 – 2011 averages. Dry season = April – September; wet season = October – March, with current evaluation period indicated within the hatched box.

Thus, the atmospheric conditions during the evaluation period were slightly wetter than average, but the values were not extreme in terms of the variability within the 8-year meteorological record. Furthermore, the well described historic Amazonian 2005 and 2010 dry season droughts (Xavier *et al.*, 2010, Marengo *et al.*, 2011) can be observed in the dry season rainfall (and consequently temperature) data, highlighting the lack of extremes during the evaluation period. Zeng *et al.* (2008) show how the 2005 drought

was actually the end result of a long regional drought that began in 2002 that affected both wet and dry season rainfall, in which case the first three years of the dataset are likely to be slightly anomalous, thus increasing the likelihood that the evaluation period is actually representative of longer-term averages.

2.2.4 Data Production

Saturation vapour pressure (e_s) was estimated with 10-min average temperature and relative humidity using the following formula following Lawrence (2005):

$$e_s = C_a * 10.0 \exp (7.5 * T_c / (237.7 + T_c))$$

where C_a is the pressure coefficient corrected for altitude, T_c is temperature in degrees Celsius.

C_a was calculated using the following formula following Lawrence (2005):

$$C_a = (P_i / P_s) * C_s$$

where P_i is the atmospheric pressure at the i^{th} site, P_s is the atmospheric pressure at sea level and C_s is the pressure coefficient at sea level (6.11), which produced the pressure coefficients of 4.316777 (leeward), 4.087515 (ridge) and 4.344002 (windward).

The actual vapour pressure (e) of the air was estimated with 10-min average relative humidity using the following formula following Lawrence (2005):

$$e = (RH * e_s) / 100$$

where RH is relative humidity expressed as a percentage.

Calm periods for wind speed are considered as wind speeds < 0.5 m/sec.

In order to compare with data for other cloud forests presented by Jarvis & Mulligan (2011), the seasonality of the rainfall at each site was calculated using the Markham Seasonality Index (Markham, 1970), which expresses the ratio of average monthly rainfall totals compared to the average annual rainfall total. This method uses vectorial quantities, where magnitude represents the monthly rainfall total (mm) and direction of arc represents calendar month (015° for January, 044° for February, 074° for March, etc.). The vector is traced and the vector resultant gives an index of seasonal rainfall concentration, where large values represent high seasonality (1 = total annual rainfall in just one month) and low values represent low seasonality (0 = monthly rainfall equal in all months). See Figure 3 in Markham (1970) for an example.

Most statistics and plots were produced using Minitab® Version 16.1.1. and SigmaPlot Version 11.0.0.77, while some simple plots were produced using Microsoft Excel 2010 Version 14.0.6106.5005.

Prior to the generation and presentation of wind statistics, 10-min wind data was filtered for erroneous values occasionally caused by fog and rain droplets that result in abnormally high wind speeds and/or an error value registered in the sensor and data output[2]. Moreover, every case of abnormally high wind speeds for a 10-min period was accompanied by an error value. Thus, for 10-minute periods with non-zero error values, the data for wind speed, elevation and direction were eliminated from the dataset. Filtered 10-min wind data covered c. 85% of the evaluation period across all sites.

All 10-minute datasets were converted into equivalent hourly datasets in order to model their distribution in polar plots using the software WRPLOT View Version 7.0.0. Hourly categories were recorded from 00 to 23 hr categories, with 00 hr representing the six 10-minute data series from 00:00 to 00:50 hr etc.

Throughout the analysis, data and results are often categorized or discussed either generally or specifically for both diurnal and nocturnal periods; these refer to data periods between 0600 - 1700 h and 1800 - 0500 h respectively.

For the presentation of PPFD statistics, each 10-min average $\mu mol.sec^{-1}.m^{-2}$ value was first converted to a total $mol.min^{-10}.m^{-2}$ value, and then summed to produce a total $mol.hr^{-1}.m^{-2}$ value.

For the presentation of fog statistics, 10-min average visibility values (0 – 5000 m) were first filtered to the 1000 m threshold for the international classification of fog (Roach, 1994) and averaged into 1-hr fog visibility values, then categorized into fog density groups following Eugster et al (2006) and Obregon *et al.* (2011), where:

Dense fog = (visibility ≤ 200 m)

Moderate fog = (visibility >200 m to 500 m)

Light fog = (visibility > 500 m to < 1000 m)

The frequency of (a.) fog, (b.) rain and (c.) synchronous fog and rain events was determined over different temporal scales.

Pearson Correlation tests were performed between and among climatic parameters to clarify relationships within and between sites using data categorized into four datasets analysed based on season and time of day (1. wet season nocturnal; 2. wet season diurnal; 3. dry season nocturnal; 4. dry season diurnal). These databases were checked for normality with Anderson-Darling normality test using Minitab® Version 16.1.1 and probability plots and test results are presented in Appendix O. Whilst a high level of autocorrelation is to be expected among many climatic parameters, the comparison of correlation strength serves to clarify linkages among air

[2] For each 4-sec data grab, the R.M. Young 81000 microprocessor records an error value (0 = error free; 1 = error detected), which were averaged to determine the percentage of errors out of the 150 data grabs in each 10-min period.

masses and identify changes in air mass linkages along the orographic gradient, especially in regard to the effects of fog on other climatic parameters.

For the purposes of reporting Pearson Correlation test results between and among climatic parameters, statistically significant correlations ($P < 0.05$) between and among climatic parameters are described in the text as follows:

Very strong correlation = ($r \geq \pm 0.8$)

Strong correlation = ($r \geq \pm 0.6$ to $< \pm 0.8$)

Moderate correlation = ($r \geq \pm 0.4$ to $< \pm 0.6$)

Weak correlation = ($r \geq \pm 0.2$ to $< \pm 0.4$)

Poor correlation = ($r < \pm 0.2$)

2.3 Results

2.3.1 Temperature

2.3.1.1 General Statistics

The difference in annual average temperature between the ridge and lower forests was 2.55 ºC and 2.34 ºC between the leeward and windward forests respectively, and monthly statistics show a highly stable temperature regime, with monthly averages at all forests ranging by only c. 1.5 ºC throughout the entire year (Table 2.3.1.1).

Moreover, the range of monthly absolute minimum and maximum temperatures was only in the order of c. 4 ºC and c. 3 ºC respectively. The annual range between absolute minimum and maximum temperatures was 14.5, 14.7 and 14.5 ºC for the leeward, ridge and windward forests respectively.

The low monthly temperature variability can be appreciated in the monthly proportional distribution of average hourly temperature (Figure 2.3.1.1), which shows a larger proportion of cooler temperatures at all forests in July, with a larger proportion of warmest temperatures in at the beginning and end of the wet season.

2.3.1.2 Seasonal and Daily Trends

The effects of topographic shading and/or diurnal fog regimes can be seen in the daily distribution of hourly temperature (Figure 2.3.1.2 A - F), with slightly differing heating and cooling regimes of the leeward compared to the ridge and windward forests. Figure 2.3.1.2 shows how the westerly aspect leeward forest displayed the relatively warmer afternoon temperatures in both seasons (A & D), while both the easterly aspect windward forest and the ridge forest displayed relatively warmer morning temperatures in the dry season (E & F), with a more evenly balanced diurnal temperature regime during the wet season (B & C). It can be observed that the most notable

seasonal temperature differences at all forests are the lower dry season nocturnal temperatures at all forests, a reflection of the greater nocturnal cloud cover during the wet season. Despite the leeward forest being the warmest site on average, the windward forest displayed warmer nocturnal temperatures (post 2100 h) in both seasons. This warmth is likely to be a reflection of differences in calmness and humidity (fog). The notable equality of seasonal diurnal temperatures may be important ecologically.

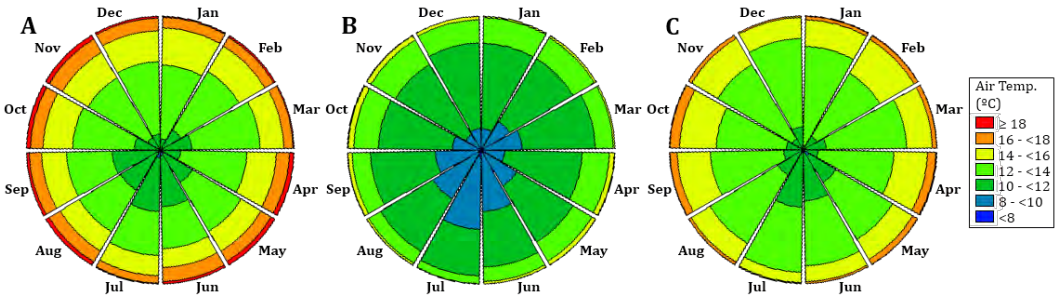

Figure 2.3.1.1: Monthly distribution (radial scale 100%) of average hourly temperatures (°C) at the leeward (A), ridge (B) and windward (C) forests during 2007 and 2008.

Table 2.3.1.1: Monthly absolute minimum, average and absolute maximum temperature (°C/hr) for all forests and terrestrial lapse rates for the leeward and windward slopes (°C/km) during 2007 and 2008.

Month	Absolute Minimum			Average			Absolute Maximum			Lapse Rate	
	Lee	Ridge	Wind	Lee	Ridge	Wind	Lee	Ridge	Wind	Lee	Wind
Jan	10.6	8.0	11.1	13.7	11.1	13.5	19.1	15.0	19.2	6.6	6.1
Feb	8.9	6.3	10.0	13.3	10.8	13.4	20.5	17.8	19.4	6.4	6.5
Mar	9.7	7.3	10.4	13.2	10.7	13.2	19.9	16.1	19.0	6.3	6.2
Apr	9.3	7.7	9.9	13.6	11.1	13.4	20.9	17.4	20.8	6.2	5.8
May	7.4	3.4	6.5	13.1	10.6	12.7	20.2	16.8	21.0	6.4	5.3
Jun	8.0	5.9	8.5	12.7	10.2	12.3	19.2	16.5	17.6	6.4	5.4
Jul	7.6	6.0	7.4	12.4	9.7	12.1	19.3	15.2	17.4	6.7	6.0
Aug	8.6	6.6	8.7	13.0	10.3	12.8	21.9	16.5	18.3	6.8	6.2
Sep	9.1	6.9	8.8	13.1	10.7	13.4	20.1	17.5	18.4	5.9	6.8
Oct	9.8	7.1	10.3	13.5	11.0	13.5	20.5	17.4	19.1	6.2	6.2
Nov	9.7	7.9	10.4	13.8	11.3	13.3	20.8	18.1	17.9	6.5	5.2
Dec	9.2	7.3	9.2	13.6	11.0	12.9	19.7	16.2	17.5	6.5	4.8
Range	3.2	4.6	4.6	1.5	1.6	1.4	2.8	3.1	3.6	0.9	2.0
Annual	7.4	3.4	6.5	13.3	10.7	13.0	21.9	18.1	21.0	6.4	5.9

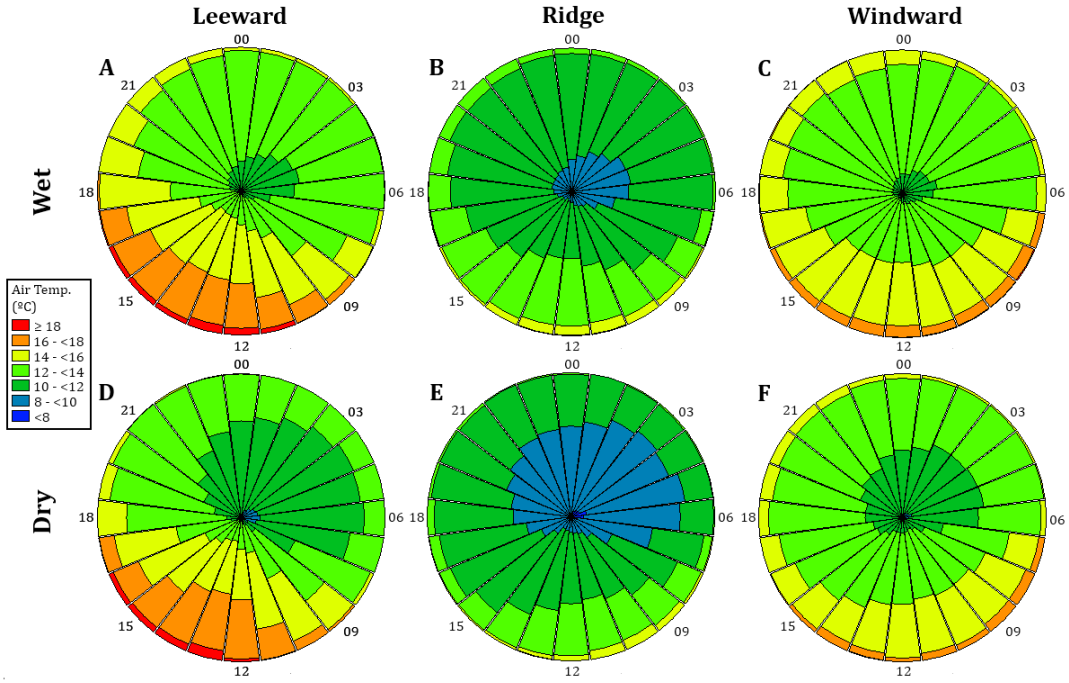

Figure 2.3.1.2: Hourly distribution (radial scale 100%) of average temperature (ºC/hr) for wet and dry season periods at all forests during 2007 and 2008.

2.3.1.3 Lapse Rates

The difference in annual average temperature between forests results in a different terrestrial lapse rate for each slope; 6.4 and 5.9 ºC/km on the leeward and windward slopes respectively, well within the typical terrestrial lapse rates recorded globally between 5 and 8 ºC/km (Strahler & Strahler, 1987) and very close to the global mean of 6.5 ºC/km (Wolfe, 1964). However simple terrestrial lapse rates do not often provide a good description of the spatial temperature structure. Figure 2.3.1.3 shows the difference in the hourly distribution of the lapse rate, with the leeward forest showing far greater variation from the average lapse rate both diurnally and nocturnally, while the windward forest displays near average lapse rates throughout most of the day in both seasons, with the only slight exception being the early morning as the sunrise warms the entire windward slope. The maximum lapse rate recorded at the leeward forest (1500 h) is in the order of 2.5 times the average, while for a very few early morning (0700 – 0800 h) instances the lapse rate is inverted which is simply explained by topographic shading.

This difference in lapse rates between slopes in Figure 2.3.1.3 indicated a Foehn effect on the leeward slope, which can be clearly observed during the afternoon hours, especially in the dry season, when between 1300 h and 1500 h the Foehn effect is the norm (Figure 2.3.1.4).

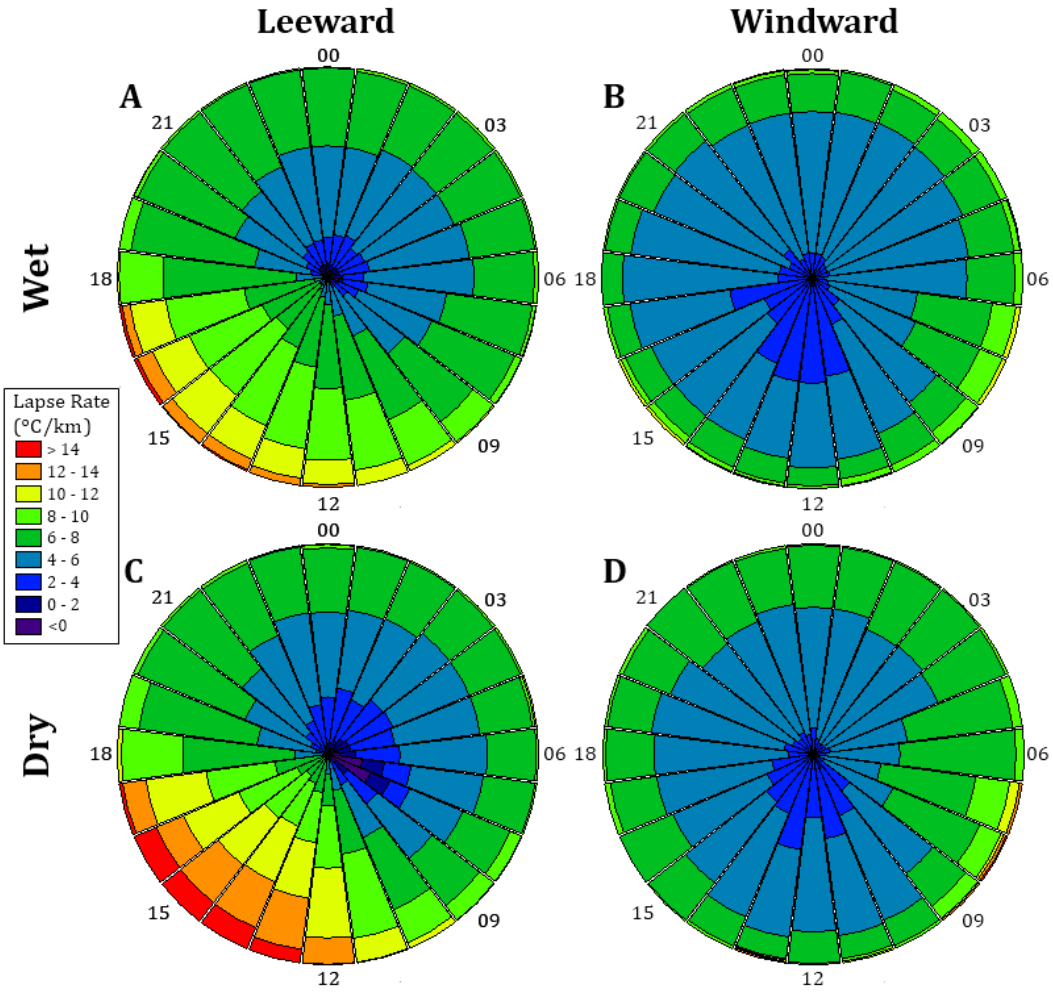

Figure 2.3.1.3: Hourly distribution (radial scale 100%) of average temperature lapse rate (°C/km) per season on the leeward and windward slopes during 2007 and 2008.

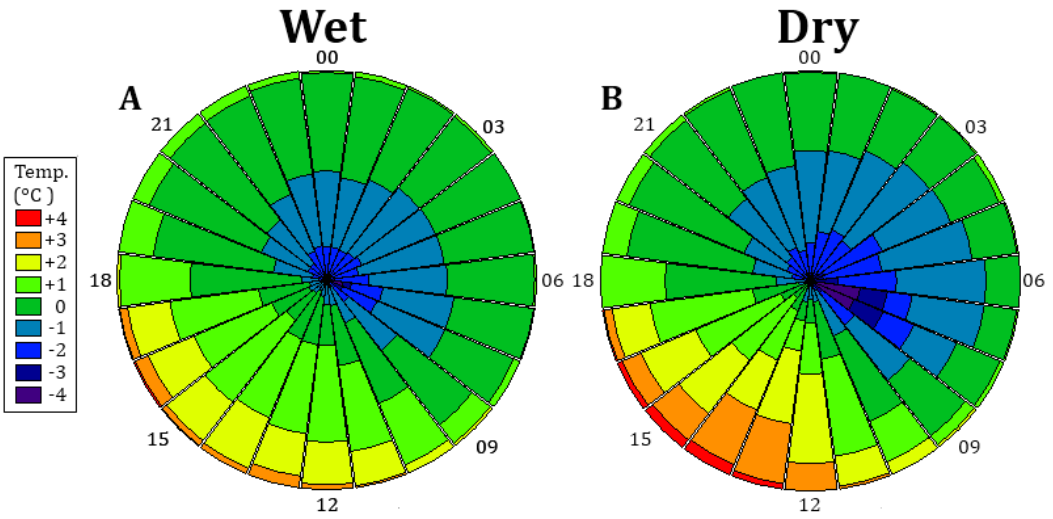

Figure 2.3.1.4: Hourly distribution (radial scale 100%) of temperature (°C) difference between leeward and windward sites (leeward minus windward) per season during 2007 and 2008.

2.3.1.4 Correlations

During the wet season, the ridge forest 1-hr diurnal (0600 h – 1700 h) average temperatures were very strongly correlated with those of the leeward forest (r = 0. 85, P < 0.001), with a strong correlation with those of the windward forest (r = 0. 75, P < 0.001), while the latter two forests showed a strong but lower correlation (Table 2.3.1.2). During the same period the nocturnal temperatures showed the same trend but with slightly lower correlation scores.

During the dry season, the windward forest had very strong temperature correlations with the ridge forest both diurnally and nocturnally, while the temperature correlations between the leeward and windward forests remained the weakest. In contrary to the wet season, temperature correlations between the leeward forest and other forests were greater during nocturnal hours.

In terms of diurnal temperature correlations with other *in situ* parameters (see Appendix A), during the wet season leeward temperatures were strongly correlated to PPFD and moderately correlated to vapour pressure and wind speed (Appendix Table 1). Ridge temperatures were strongly correlated to PPFD and vapour pressure, and moderately correlated to visibility. Windward temperatures were only strongly correlated to PPFD, and moderately correlated to vapour pressure.

Dry season diurnal *in situ* temperature correlations were strong at the leeward forest with PPFD and vapour pressure, with moderate correlation with wind speed (Appendix Table 2). The ridge temperatures were again strongly correlated to PPFD and vapour pressure, while windward temperatures were strongly correlated to PPFD, and moderately correlated to vapour pressure.

Table 2.3.1.2: Statistically significant (P < 0.05) Pearson's Correlation scores (r) between all forests for hourly average temperatures during the 2007-2008 period.

Period		Wet		Dry	
		Lee	Ridge	Lee	Ridge
Diurnal	Ridge	0.85	-----	0.69	-----
(0600 - 1700 h)	Wind	0.62	0.75	0.53	0.81
Nocturnal	Ridge	0.72	-----	0.72	-----
(1800 - 0500 h)	Wind	0.53	0.70	0.64	0.80

In terms of nocturnal temperature correlations with other *in situ* parameters, during the wet season (Appendix Table 1 & Appendix Table 3) temperatures showed a notable reduction in correlations with other parameters, with leeward temperatures only being moderately correlated to vapour pressure, while ridge and windward temperatures showed no correlations.

Dry season diurnal *in situ* temperature correlations (Appendix Table 4) showed the same lack of correlation, again with leeward temperatures only being moderately correlated to vapour pressure, and now with ridge temperatures now being moderately correlated to visibility, with windward temperatures again showing no correlations.

In terms of *ex situ* temperature correlations of note, during all periods the leeward temperatures were better (and strongly) correlated with the vapour pressure recorded at the ridge and windward forests (in order of correlation strength) than that recorded *in situ* (Appendix A), which highlights the relationship between the general atmospheric conditions and the orographic cloud formation processes (Foehn effect) that prevail on the windward slopes, of which the ridge forest (being a mountain pass) is the ultimate indicator. In all cases, the ridge vapour pressure correlations were actually the strongest of all leeward temperature correlations with other parameters, indicating the variability of vapour pressure changes from ridge to leeward.

2.3.2 Vapour Pressure

2.3.2.1 General Statistics

The difference in annual average vapour pressure between the ridge and lower forests was 1.25 and 1.47 mb at the leeward and windward forests respectively. As would be expected, the dynamic of the monthly distribution of vapour pressure was identical at all forests, with variation in the actual vapour pressure between the leeward and windward forests (Figure 2.3.2.1), which indicates a loss of water content in the air mass during the orographic transition.

2.3.2.2 Seasonal and Daily Trends

The daily distribution of hourly vapour pressure in both seasons shows an identical increment of vapour pressure during diurnal hours, that mostly decreases in the afternoon towards a daily minimum at 0500 – 0600 h at all forests (Figure 2.3.2.2). This indicates a diurnal pulse of increasingly humid air, which tends to confirm the diurnal activity of the Foehn effect. It can be observed that the only seasonal differences were the amplitude of vapour pressure regimes.

2.3.2.3 Correlations

Over all the periods during the evaluation period, the 1-hr average vapour pressure values of all forests were very strongly correlated, with only those of the diurnal wet season period between leeward and windward forest showing a weaker correlation albeit still strong (Table 2.3.2.2). Correlations were slightly lower during diurnal hours of both seasons, with the only exception being those between the ridge and the windward forest during the dry season that remained practically the same. Similarly, correlations between the leeward and ridge forests were slightly weaker during diurnal periods compared to nocturnal periods. This also tends to emphasize the greater action of the Foehn effect during the day.

In terms of correlations between vapour pressure and other *in situ* parameters (see Appendix A), all forests showed strong to moderate correlations with temperature during diurnal hours of both seasons (Appendix Table 1 & Appendix Table 2), while during nocturnal periods of both seasons only the leeward forest showed correlations with temperature (Appendix Table 3 & Appendix Table 4).

In terms of correlations with *ex situ* parameters of note, as previously mentioned the ridge and windward vapour pressures were actually better correlated with temperature at the leeward forest than *in situ* temperature during all periods. Similarly, albeit with a lower strength of correlation, the ridge and windward vapour pressures were also better correlated with PPFD at the leeward forest than *in situ* PPFD. This was not surprising as the leeward forest has the clearer skies and thus PPFD values more closely aligned with differing general atmospheric patterns.

Table 2.3.2.1: Monthly absolute minimum, average and absolute maximum vapour pressure (mb/hr) for all forests during 2007 and 2008.

Month	Absolute Minimum			Average			Absolute Maximum		
	Lee	Ridge	Wind	Lee	Ridge	Wind	Lee	Ridge	Wind
Jan	8.31	6.89	8.30	10.31	8.88	10.57	12.23	10.83	12.39
Feb	7.76	6.48	7.80	9.98	8.61	10.24	12.16	11.18	12.57
Mar	7.69	6.03	6.58	9.73	8.42	9.87	11.44	10.24	11.77
Apr	7.48	6.13	7.19	9.93	8.60	10.09	11.98	10.54	12.11
May	5.82	2.82	5.33	9.56	8.26	9.72	12.01	10.12	11.72
Jun	5.44	4.02	5.58	9.03	7.93	9.31	11.19	9.61	11.00
Jul	5.91	5.20	5.41	8.95	7.83	9.27	11.25	9.71	11.09
Aug	6.27	4.58	5.30	9.10	7.99	9.46	10.81	9.70	11.43
Sep	6.27	4.86	5.56	8.88	7.81	9.12	11.11	9.96	11.30
Oct	6.12	5.18	6.25	9.48	8.25	9.60	11.55	10.39	11.72
Nov	7.82	6.19	7.27	9.97	8.71	10.12	11.93	10.50	12.08
Dec	8.04	6.21	7.32	9.92	8.58	10.09	11.65	10.27	11.74
Annual	5.44	2.82	5.30	9.57	8.32	9.79	12.23	11.18	12.57

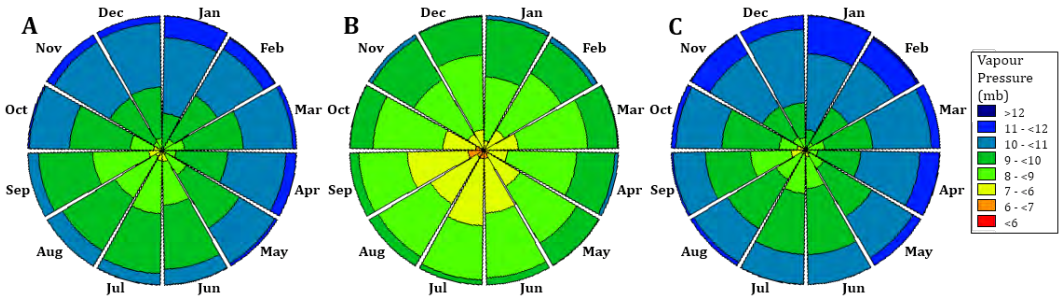

Figure 2.3.2.1: Monthly distribution (radial scale 100%) of average hourly vapour pressure (mb) at the leeward (A), ridge (B) and windward (C) forests during 2007 and 2008.

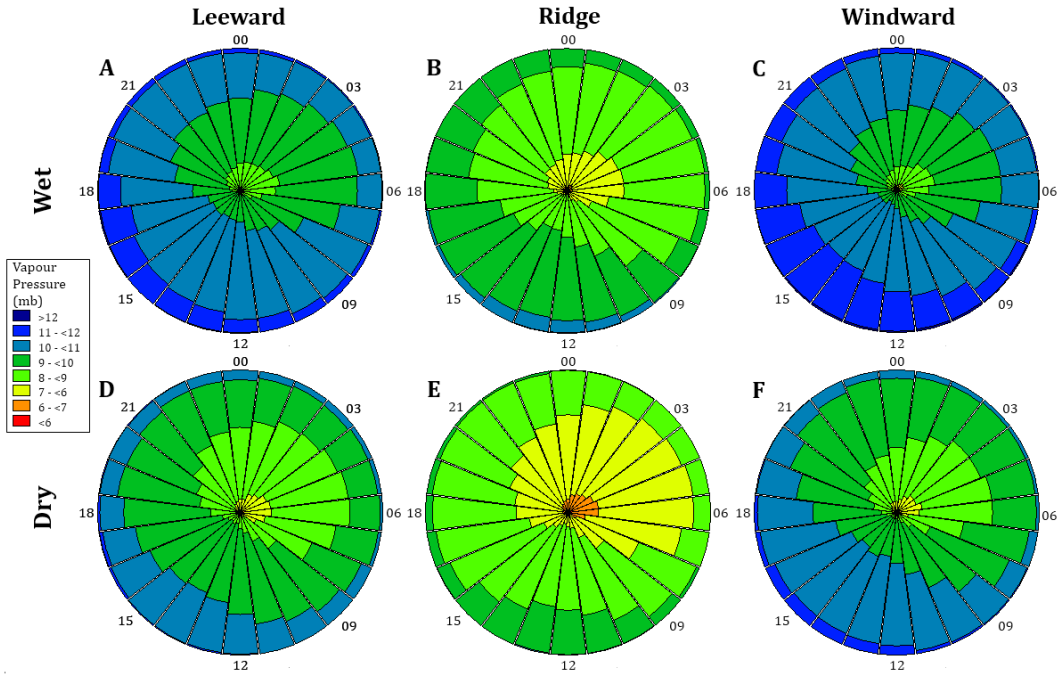

Figure 2.3.2.2: Hourly distribution (radial scale 100%) of average vapour pressure (mb) for wet and dry season periods at all forests during 2007 and 2008.

Table 2.3.2.2: Statistically significant ($P < 0.05$) Pearson's Correlation scores (r) between all forests for hourly average vapour pressure during the 2007-2008 period.

Period		Wet		Dry	
		Lee	Ridge	Lee	Ridge
Diurnal	Ridge	0.83	-----	0.83	-----
(0600 - 1700 h)	Wind	0.75	0.82	0.80	0.87
Nocturnal	Ridge	0.91	-----	0.90	-----
(1800 - 0500 h)	Wind	0.81	0.84	0.83	0.86

2.3.3 Photosynthetically Active Photon Flux Density

2.3.3.1 General Statistics

The average daily PPFD at the leeward forest was approximately 20-30% greater than the ridge forest during the warmer months, with that difference increasing during the winter months (Table 2.3.3.1). The windward forest showed very similar trends to the ridge forest during summer and autumn months, while a divergence can be observed from August through to the end of the year, where the windward forest received a fifth more PPFD than the ridge forest (Figure 2.3.3.1). While minimum daily PPFD figures were similar, the large and consistent difference in monthly maximum daily PPFD in all months between the leeward and other forests highlights the large differences in transmission.

2.3.3.2 Seasonal and Daily Trends

The seasonal distribution of hourly PPFD (Figure 2.3.3.2) highlights the very low variation in PPFD between the ridge and windward forests despite the difference in altitude, whereas the leeward forest shows important increases in the consistency of greater intensity PPFD during both seasons, especially the dry season.

During both seasons, the ridge and windward forests receive slightly greater relative contributions of PPFD in the hours proceeding and up till noon, while the leeward forest receives a relatively greater proportion of contributions from noon onwards. These dynamics cannot be solely attributed to topographic shading as all forests receive unobstructed sunlight between 0900 and 1500 hr.

2.3.3.3 Correlations

As was to be expected, over the entire evaluation period, the ridge forest 1-hr PPFD totals were very strongly correlated with those of the windward forest, with slightly weaker correlations with the leeward forest (Table 2.3.3.2). The latter two forests showed weaker correlations, albeit still strong.

In terms of correlations between PPFD and other *in situ* parameters (Appendix A), the strong correlations with temperature at all forests in both has been previously mentioned (Appendix Table 1 & Appendix Table 2). Other moderate correlations are observed with visibility and vapour pressure at the ridge forest during the wet season, while at the windward forest, PPFD was moderately correlated with wind direction, speed and elevation during the dry season, indicating certain wind associations with certain air mass conditions.

Table 2.3.3.1: Monthly minimum, average and maximum daily photosynthetically active photon flux density (mol.day^{-1}.m^{-2}) for all forests during 2007 and 2008.

Month	Minimum			Average			Maximum		
	Lee	Ridge	Wind	Lee	Ridge	Wind	Lee	Ridge	Wind
Jan	3.7	2.6	5.3	20.4	15.6	14.6	42.4	32.8	23.3
Feb	3.3	2.4	4.7	18.4	13.8	12.9	37.1	28.1	30.9
Mar	4.9	4.0	4.2	18.0	13.5	14.0	37.5	23.1	28.8
Apr	6.8	5.9	5.2	20.8	14.6	15.4	36.8	28.3	29.9
May	3.6	2.4	2.8	21.5	13.7	14.7	37.4	27.0	28.2
Jun	8.5	5.9	6.6	25.6	15.0	15.8	36.2	25.1	25.9
Jul	7.0	6.5	6.0	22.3	12.1	13.1	36.5	22.3	24.5
Aug	4.7	2.9	3.0	24.6	12.4	15.1	42.0	27.2	27.8
Sep	11.6	5.0	4.6	23.2	14.1	17.4	39.9	29.0	29.9
Oct	11.8	6.1	8.5	22.1	13.9	18.9	44.2	29.3	33.5
Nov	7.1	4.4	7.1	21.4	13.4	15.3	39.3	24.7	26.8
Dec	3.0	2.3	5.9	18.7	12.1	15.2	41.1	32.2	34.0
Annual	3.0	2.3	2.8	21.4	13.7	15.2	44.2	32.8	34.0

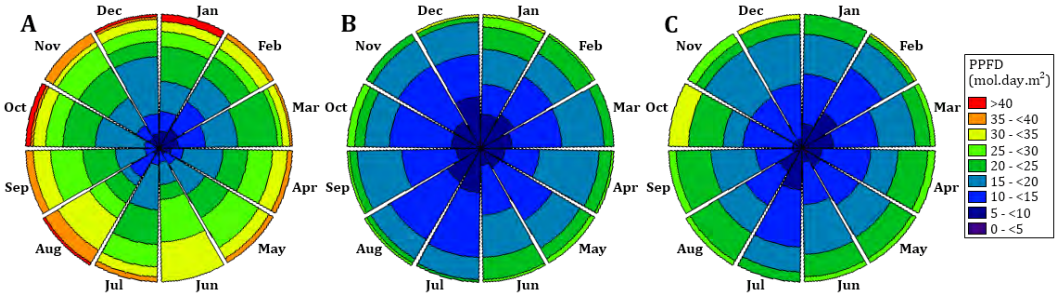

Figure 2.3.3.1: Monthly distribution (radial scale 100%) of total daily photosynthetically active photon flux density (mol.day^{-1}.m^{-2}) at the leeward (A), ridge (B) and windward (C) forests during 2007 and 2008.

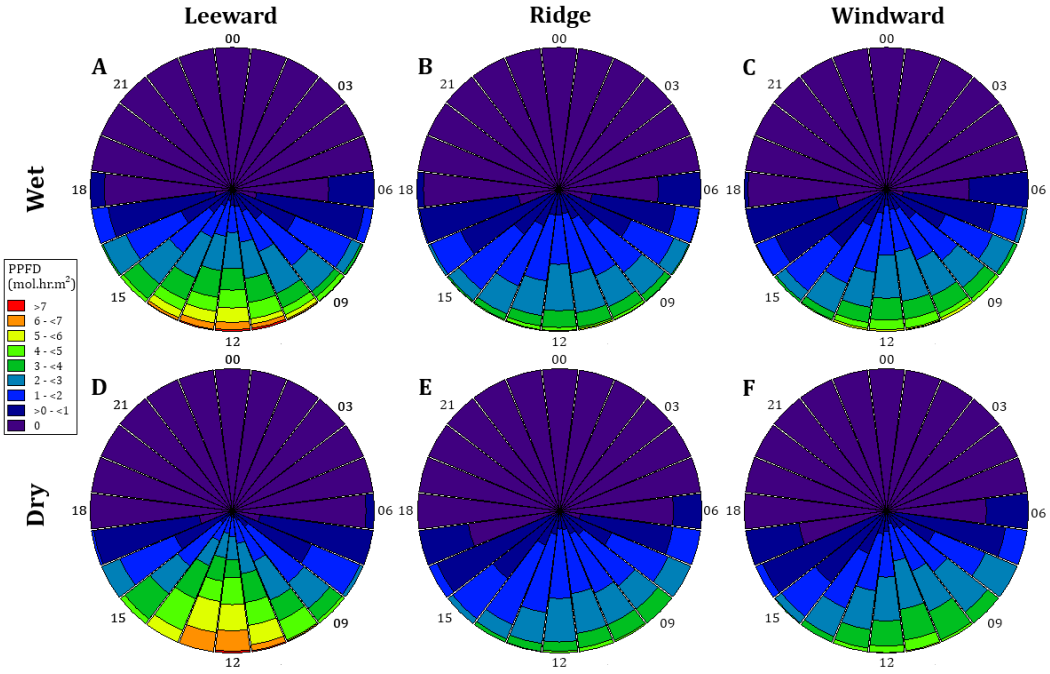

Figure 2.3.3.2: Hourly distribution (radial scale 100%) of total photosynthetically active photon flux density (mol.hr^{-1}.m^{-2}) for wet and dry season periods at all forests during 2007 and 2008.

Table 2.3.3.2: Statistically significant (P < 0.05) Pearson's Correlation scores (r) between all forests for hourly total photosynthetically active photon flux density (mol.hr^{-1}.m^{-2}) during the 2007-2008 period.

Period		Wet		Dry	
		Lee	Ridge	Lee	Ridge
Diurnal	Ridge	0.81	-----	0.71	-----
(0600 - 1700 h)	Wind	0.69	0.84	0.68	0.86

In terms of PPFD correlations with *ex situ* parameters of note, the leeward PPFD was actually better (albeit moderately) correlated with vapour pressure at the ridge forest than *in situ* vapour pressure during both seasons. In addition, PPFD at all forests in both seasons was better correlated (albeit sometimes weakly) with windward wind direction, speed and elevation, again indicating certain prevailing wind associations with certain air mass conditions that are subject to less turbulent affectation at the windward forest than the others.

2.3.4 Rainfall

2.3.4.1 General Statistics

The rainfall statistics show that the windward forest receives considerably less, just over half that of the ridge forest, while the leeward forest received an amount only slightly less than the ridge forest (Table 2.3.4.1). Both these latter forests received more than 100 mm/day on several occasions during the evaluation period, which appears to be a common occurrence in the local climate (see Chapter 1.4.2). These differences in the distribution of rainfall intensity can be seen appreciated in Figure 2.3.4.1. The apparent similarity in amount of rainless days at the leeward and windward forests, despite the large difference in annual rainfall, is noteworthy. June is clearly the driest month and the 5-month dry season can be clearly observed, during which less than half the rainfall can be observed in comparison with any of the seven wet months.

Table 2.3.4.1: Monthly average total rainfall (mm), and average and maximum 24-hour rainfall (mm/day) for all forests during 2007 and 2008.

Month	Monthly Average			24h Average			24h Maximum		
	Lee	Ridge	Wind	Lee	Ridge	Wind	Lee	Ridge	Wind
Jan	714.5	771.2	324.9	23.0	24.9	10.5	109.7	144.5	71.4
Feb	515.2	543.7	271.4	18.1	19.1	9.5	99.3	123.2	52.6
Mar	572.3	561.9	276.5	18.5	18.1	8.9	94.0	80.5	51.3
Apr	331.7	343.3	201.9	11.1	11.4	6.7	66.3	75.4	61.2
May	131.3	177.7	108.3	4.2	5.7	3.5	56.9	61.0	33.0
Jun	64.1	85.1	48.3	2.1	2.8	1.6	26.4	30.2	27.4
Jul	115.6	173.5	75.9	3.7	5.6	2.4	61.5	61.7	38.4
Aug	145.8	154.2	112.4	4.7	5.0	3.6	85.9	98.5	82.8
Sep	126.2	164.1	112.0	4.2	5.5	3.7	31.8	40.9	37.6
Oct	300.7	244.6	183.6	9.7	7.9	5.9	48.8	45.2	36.6
Nov	316.9	371.1	267.6	10.6	12.4	8.9	50.3	56.9	44.7
Dec	335.8	479.3	178.8	10.8	15.5	5.8	60.5	56.1	20.9
Range	650.4	686.1	276.6	20.9	22.1	8.9	83.3	114.3	61.9
Annual	3670.1	4069.7	2161.6	10.1	11.2	5.9	109.7	144.5	82.8

The Markham Seasonality Index scores were 0.41, 0.39 and 0.31 for the leeward, ridge and windward forests respectively.

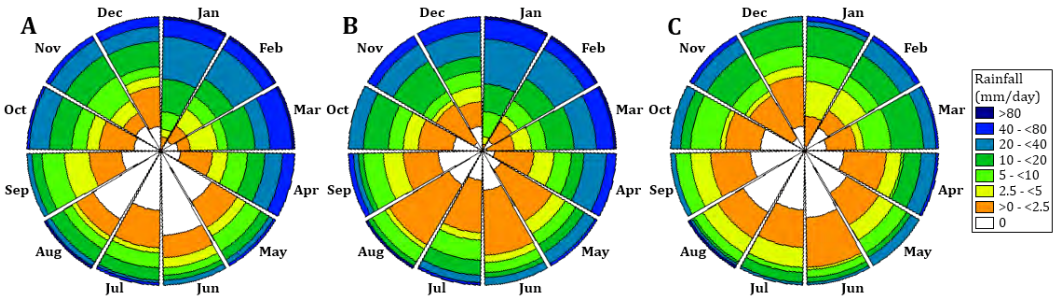

Figure 2.3.4.1: Monthly distribution (radial scale 100%) of 24-hour rainfall (mm/day) at the leeward (A), ridge (B) and windward (C) forests during 2007 and 2008.

2.3.4.2 Seasonal and Daily Trends

The distribution of hourly rainfall during the wet season (Figure 2.3.4.2 A, B & C) shows a slight trend towards lower rainfall in the early evening, with more gentle events in the middle of the day. The most intense rainfall events occur most frequently around noon, as well as in the hours proceeding midnight, although the strength of the trend is marginal.

Dry season rainfall (Figure 2.3.4.2 D, E & F) shows a slight trend towards more frequent afternoon and early evening rainfall events, although this trend is barely noticeable.

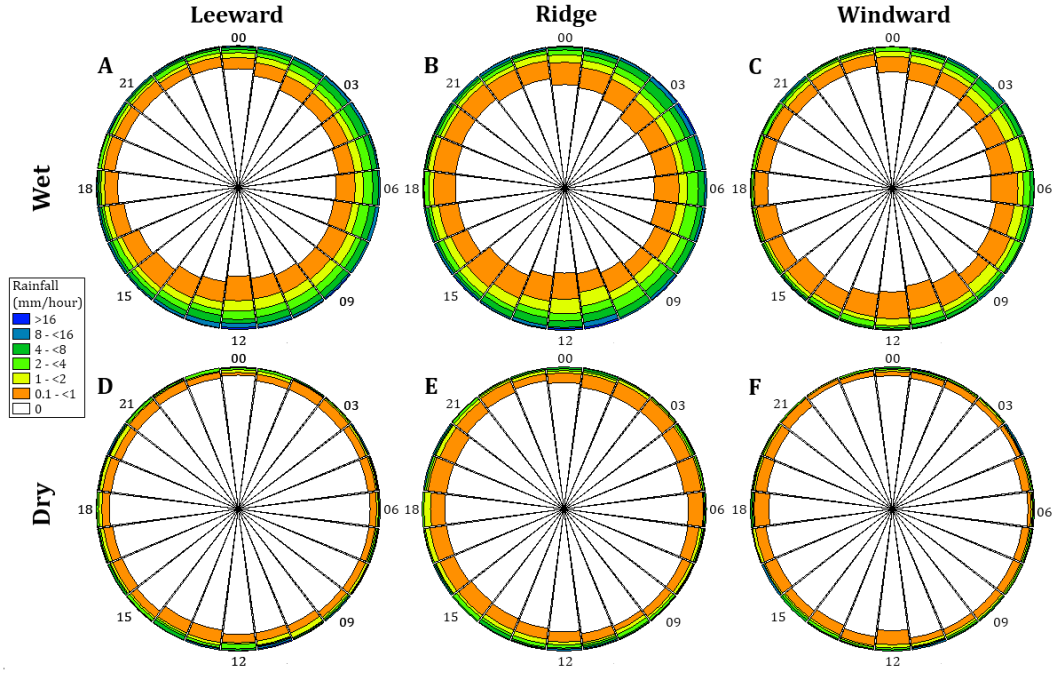

Figure 2.3.4.2: Hourly distribution (radial scale 100%) of rainfall (mm/hr) for wet and dry season periods at all forests during 2007 and 2008.

2.3.4.3 Correlations

Over the entire evaluation period, the ridge forest 1-hr rainfall totals were very strongly correlated with those of the leeward forest, and stronger than those with windward forest with the exception of diurnal dry season periods where both forests recorded the strongest correlations with the ridge forest (Table 2.3.4.2). Correlations between the leeward and windward forests rainfall were moderate to strong. Wet season correlations were mostly stronger during nocturnal periods, while dry season correlations showed the opposite trend.

In terms of both *in situ* and *ex situ* correlations with other parameters, there was no correlation with any parameter at or between any forest (Appendix A).

Table 2.3.4.2: Statistically significant ($P < 0.05$) Pearson's Correlation scores (r) between all forests for hourly total rainfall during the 2007-2008 period.

Period		Wet		Dry	
		Lee	Ridge	Lee	Ridge
Diurnal	Ridge	0.81	-----	0.90	-----
(0600 - 1700 h)	Wind	0.55	0.70	0.71	0.91
Nocturnal	Ridge	0.89	-----	0.87	-----
(1800 - 0500 h)	Wind	0.64	0.70	0.62	0.81

2.3.5 Wind

2.3.5.1 General Statistics

The ridge forest was significantly windier than the other forests, as shown by the average and absolute maximum wind speeds, as well as the percentage of calm periods as was to be expected due to its mountain pass location (Table 2.3.5.1). The leeward and ridge forests were windiest in September, October and November, while the windward forest peaked in November and December. The leeward forest had the greatest percentage of calm periods, while the ridge forest practically always showed some air movement. However in terms of patterns, there did not appear to be an obviously defined windy or calm period in general. The general air flow pattern up the windward slope and down the leeward slope is evidenced by the positive and negative wind elevation angles respectively.

Figure 2.3.5.1 shows how the wind conditions of the forests coincides with their topographic position, with a clearly ENE prevailing wind direction.

Table 2.3.5.1: Monthly average and maximum wind speed (m/s), percentage of calm period (%) and wind elevation angle (±°) for all forests during 2007and 2008.

Month	Average			Maximum			Calms			Elevation		
	Lee	Ridge	Wind	Lee	Ridge	Wind	Lee	Ridge	Wind	Lee	Ridge	Wind
Jan	1.41	2.67	1.88	5.65	9.92	4.12	7.50	1.02	0.94	-5.60	1.30	10.00
Feb	1.46	2.69	1.73	6.47	7.70	5.25	5.03	0.22	0.90	-6.37	0.92	4.64
Mar	1.48	2.84	1.73	5.10	8.51	4.44	5.24	0.07	2.29	-6.86	1.60	5.22
Apr	1.53	2.77	1.89	6.25	9.26	4.25	4.67	0.57	2.50	-7.54	1.21	6.84
May	1.54	2.67	1.73	6.60	9.24	4.20	5.21	0.14	3.51	-7.95	0.30	6.54
Jun	1.69	2.61	1.85	5.88	7.63	4.82	3.78	0.70	6.37	-9.14	0.03	3.18
Jul	1.62	2.72	1.74	5.24	8.44	4.49	5.13	0.34	2.69	-9.28	-0.06	5.16
Aug	1.72	2.79	1.63	5.69	7.70	5.05	2.67	0.40	4.04	-4.90	0.54	3.47
Sep	1.89	2.97	1.85	5.52	8.33	4.84	1.11	0.00	1.67	-3.16	0.78	1.43
Oct	1.80	2.99	1.84	5.40	9.67	4.35	2.00	0.20	2.82	-4.20	-1.23	4.71
Nov	1.79	3.24	2.03	6.63	8.72	5.04	2.23	0.14	3.94	-4.75	-1.02	3.28
Dec	1.64	2.75	2.08	6.39	9.03	5.18	4.04	0.63	6.46	-4.89	-1.62	4.64
Annual	1.63	2.81	1.83	6.63	9.92	5.25	4.05	2.07	3.18	-6.22	0.23	4.93

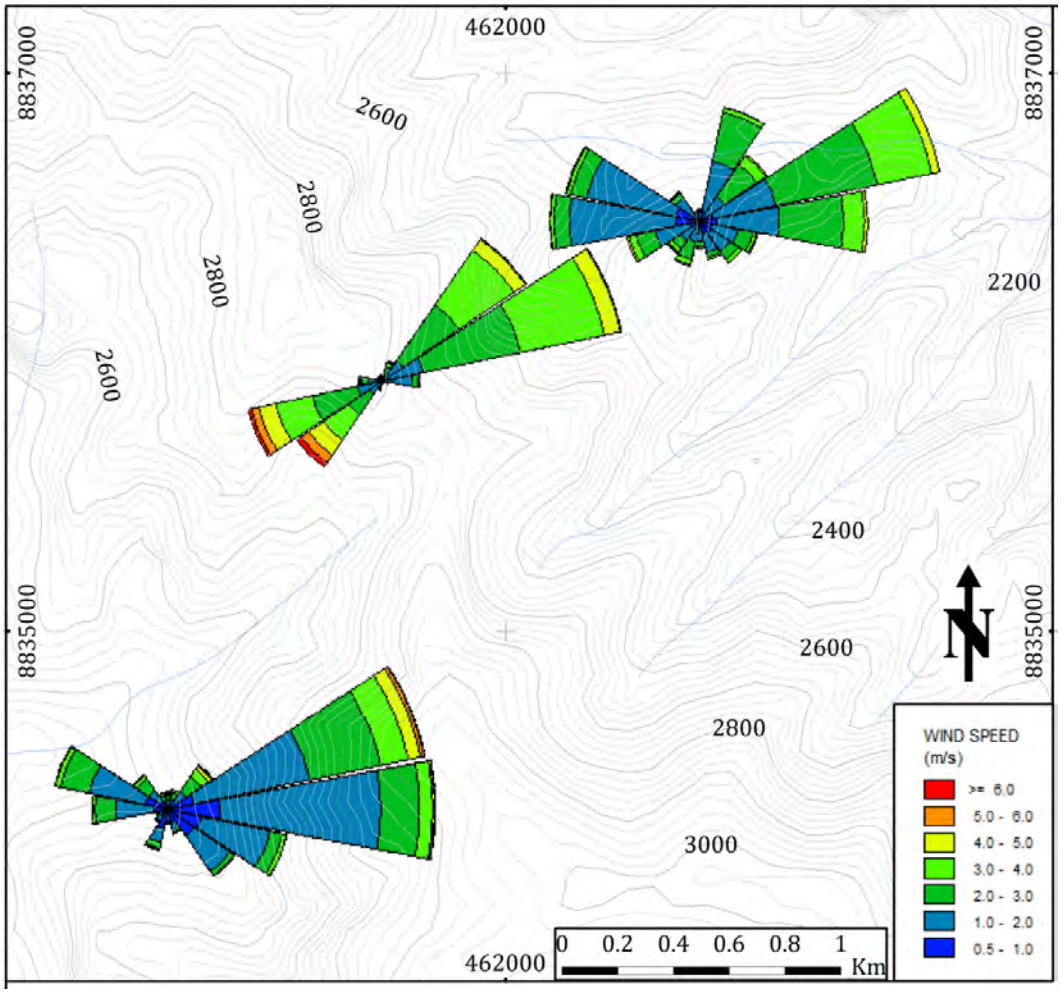

Figure 2.3.5.1: Annual windrose for all forests in relation to their topographic location.

2.3.5.2 Seasonal and Daily Trends

The predominant diurnal wind direction showed an ENE direction, with a frequency greater than 50% (Figure 2.3.5.2 A - F), although the leeward forest shows an important amount of westerly winds during the wet season, indicating affectation by two wind systems, these being the regional ENE flow, and a localized westerly flow associated with the large Oxapampa valley. In addition, although of low frequency, the strongest diurnal winds at the ridge forest showed a WSW direction (Figure 2.3.5.2 B). There was a slight increase in diurnal wind frequency during the dry season, but the proportion of wind speed and direction remained mostly unchanged as compared to the wet season.

The nocturnal winds indicate a shutdown of the diurnal ENE regime, with evidence at the leeward and windward forests of downslope nocturnal slope winds on either side of the ridgeline (both showing mostly light winds from the direction of the ridgeline) that usually only develop in relatively dry and cool conditions, while the ridge forest shows a large increase in winds with WSW direction in comparison with the diurnal conditions (Figure 2.3.5.2 G - L).

Similarly to diurnal winds, the seasonal difference in relation to nocturnal winds is a slight increase in frequency without change to the regime of speed and direction.

The distribution of diurnal wind elevation angle showed little seasonal variation, indicating the expected patterns of elevation angle from the opposing westerly and easterly directions (Figure 2.3.5.3 A - F). The leeward forest (and the ridge forest to a lesser extent) data shows what appears a separate distribution of high negative elevation angle events, which is explained by the down forcing caused by turbulent rainfall events. These events are evenly distributed among east and westerly direction at the ridge forest, indicating the increased turbulence caused by the

The nocturnal wind elevation data at the leeward forest show much less noise, showing the dominance of the easterly downslope winds, especially in the dry season (Figure 2.3.5.3 G & J). Interestingly, the high negative elevation winds associated with turbulent rainfall events were all from the westerly direction.

The windward forest also showed a dominance of downslope (easterly) winds during the dry season nocturnal hours, again indicating the shutdown of the diurnal ENE regional flow in favour of nocturnal slope winds due to cooling (Figure 2.3.5.3 I & L).

The ridge forest nocturnal wind elevation angles showed a few distinct distributions related to differing conditions (Figure 2.3.5.3 H & K). Again the high negative angle events related to turbulence from rainfall from eastern winds is present, although in the wet season there is a group of events with much greater wind speed also related to rainfall, but from the westerly direction. Secondly, a group of very high positive angle events from the

westerly direction can be observed in both seasons, which showed lower temperature, much higher humidity and greater fog presence than the rest of the dataset (data not shown).

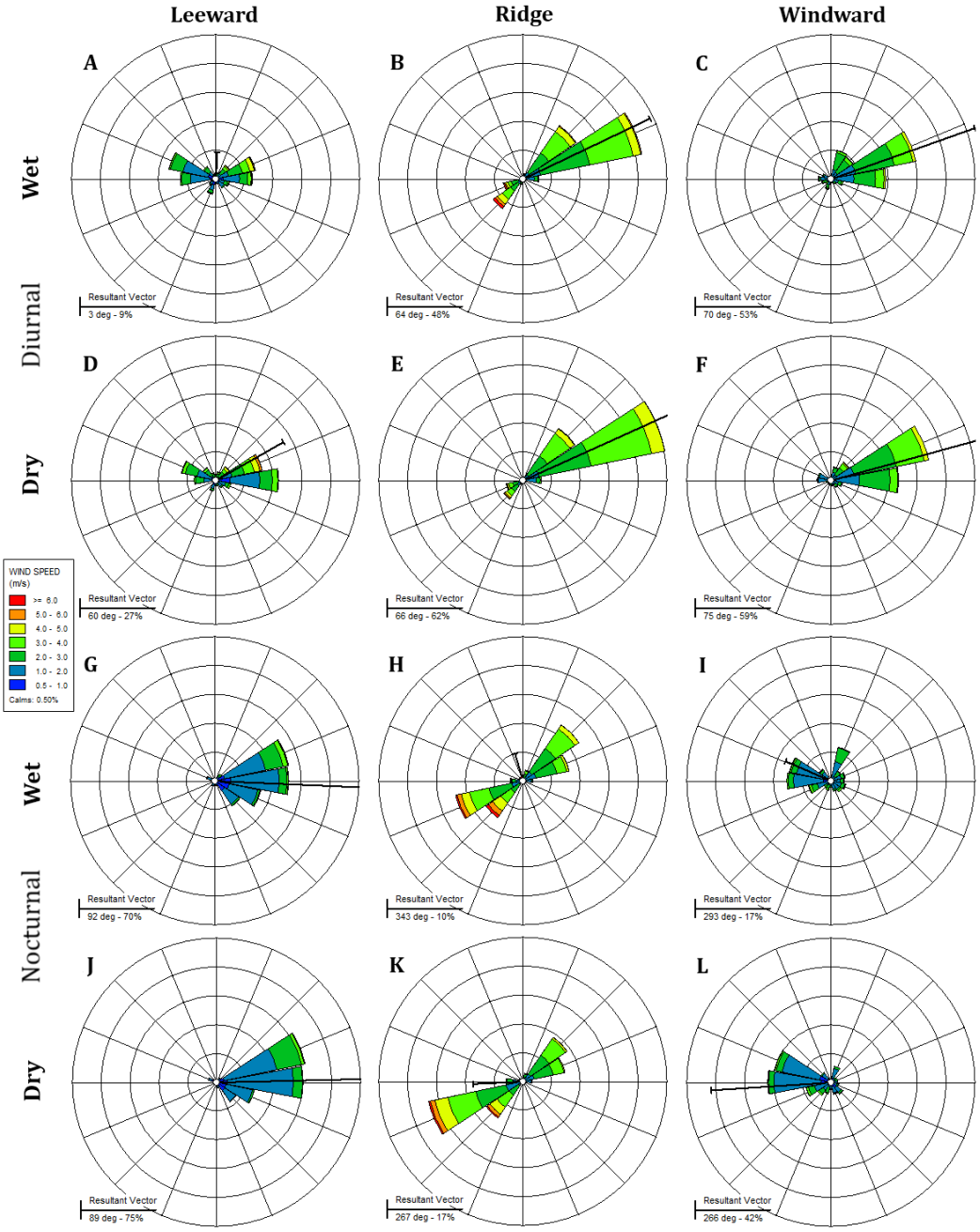

Figure 2.3.5.2: Seasonal windroses (radial scale 50%) for diurnal and nocturnal periods during the wet and dry seasons at all forests during 2007 and 2008.

2.3.5.3 Correlations

Given the differing topographic locations and the turbulent caused by the general ruggedness of the terrain, it was not surprising that mostly poor and

some weak correlations could be found in the wind parameters between the forests (Table 2.3.5.2). Notwithstanding, of note was the consistent albeit weak correlations for most parameters in most periods between the ridge and windward forests. Diurnal wind speed was the only parameter to show weak correlations among all forests, while leeward-ridge and leeward-windward correlations with all other parameters were almost exclusively poor.

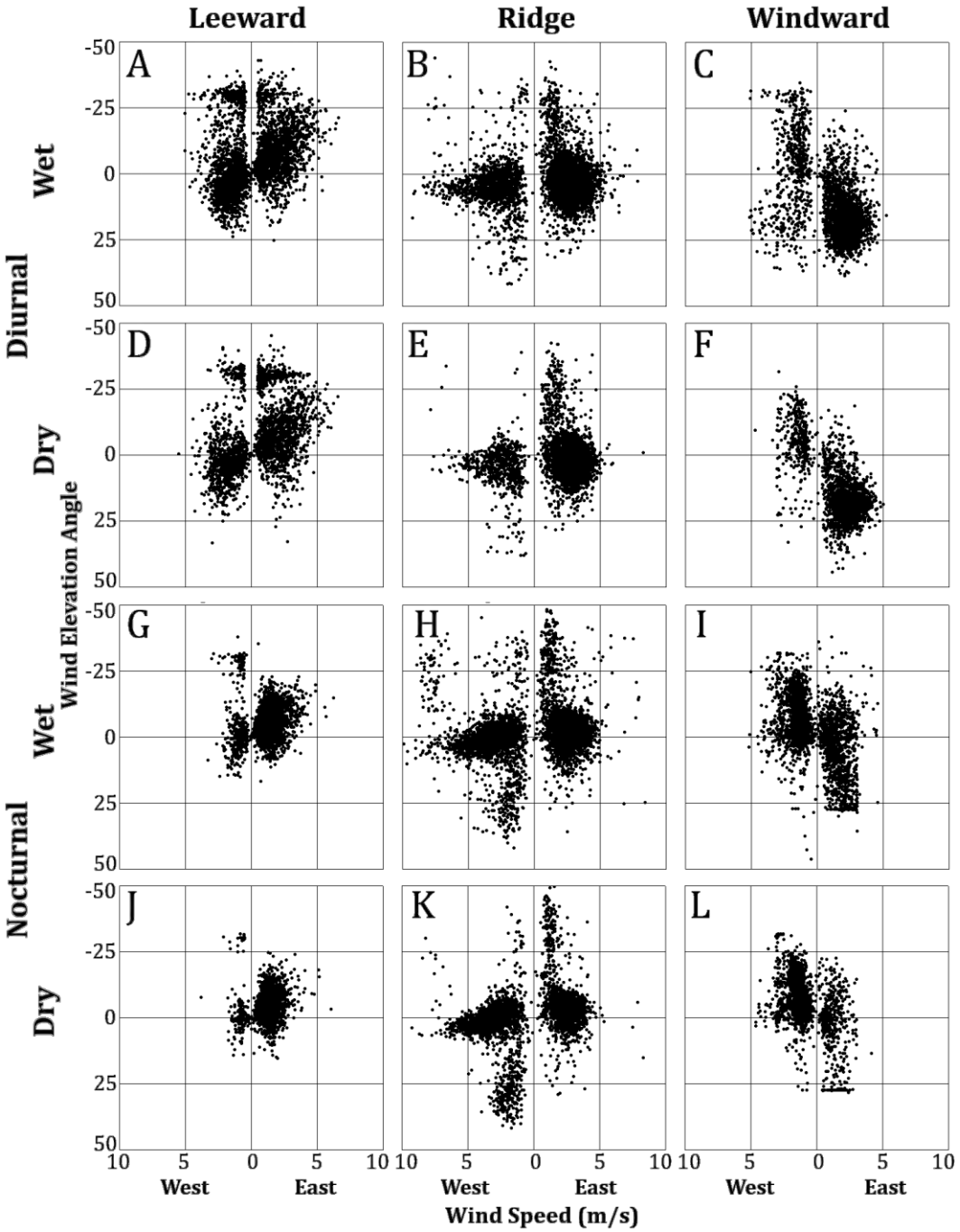

Figure 2.3.5.3: Seasonal scatterplots of wind elevation angle versus both westerly (right half of each figure) and easterly (left half of each figure) wind speeds (m/s) for diurnal and nocturnal periods of all forests during 2007 and 2008.

Table 2.3.5.2: Statistically significant ($P < 0.05$) Pearson's Correlation scores (r) between all forests for hourly average wind direction, speed and elevation during the 2007-2008 period.

Parameter	Period		Wet		Dry	
			Lee	Ridge	Lee	Ridge
Wind Direction	Diurnal	Ridge	0.14	-----	0.07	-----
	(0600 - 1700 h)	Wind	-0.03	0.35	-0.12	0.27
	Noctural	Ridge	0.02	-----	0.05	-----
	(1800 - 0500 h)	Wind	-0.08	0.24	-0.08	0.13
Wind Speed	Diurnal	Ridge	0.27	-----	0.42	-----
	(0600 - 1700 h)	Wind	0.35	0.34	0.30	0.34
	Noctural	Ridge	0.21	-----	0.19	-----
	(1800 - 0500 h)	Wind	0.09	0.35	0.08	0.30
Wind Elevation	Diurnal	Ridge	0.09	-----	0.15	-----
	(0600 - 1700 h)	Wind	0.16	0.27	0.09	0.33
	Noctural	Ridge	0.04	-----	-0.07	-----
	(1800 - 0500 h)	Wind	0.05	0.28	-	0.18

In terms of *in situ* correlations with other parameters, of note was the strong (dry season) and moderate (wet season) correlations in both diurnal and nocturnal conditions between windward wind elevation and direction, while no other forest showed the same pattern (Appendix A). This highlights the simplicity of the windward wind regime despite the complex terrain. In addition, during both seasons the PPFD of all forests was better correlated to the wind parameters of the windward forest pattern (Appendix Table 1 & Appendix Table 2), highlighting the general relationship between the constant windward wind conditions and general weather conditions. Furthermore, the same can also be said for the diurnal correlations between windward wind parameters and those of temperature and vapour pressure, although the general strength of correlation and improvement on *in situ* correlations is weaker.

2.3.6 Fog

2.3.6.1 General Statistics

There was a large difference in cloudiness between the leeward forest and the windward and ridge forests, the latter two being enveloped in cloud for a much greater proportion of the year (Table 2.3.6.1). This is without doubt the general Foehn effect on the orographic flow of moist Amazonian air from the east. However, despite the general congruence of monthly fluctuations in other parameters, the fog statistics show that fog frequency does not have an even monthly distribution amongst the forests, with the leeward forest being its foggiest in December, the ridge forest in February and the windward forest in August. Due to the stable wind regime, the greater fog frequency at the windward forest compared to the ridge forest for some periods is most likely indicative that the orographic cloud base is at times below the ridge forest (especially nocturnally). However the reasons for the varying fog

frequency fluctuations at the leeward forest are more complex, because as seen through the wind dynamics (and personal observation), the leeward forest is affected by several weather conditions, the regional foehn effected ENE flow, as well as the localized effects of the adjacent *Oxapampa* valley. Such differences are notable, for example between the December and January fog distribution between the leeward and ridge forests (Figure 2.3.6.1).

The vast majority of visibility readings at all forests were categorized as light fog, decreasing through moderate to dense fog, with the only exception being the slightly greater frequency of dense than moderate fog at the leeward forest in December.

Looking at the moist summer months (Figure 2.3.6.1), the leeward forest does not show any marked increase in fog frequency as the other forests do, indicating that the majority of moisture laden air reaching the ridge forests is precipitated at the leeward forest as rain as it makes the sharp descent down the leeward slope (see Figure 2.3.4.1).

Table 2.3.6.1: Monthly frequency (%) of Dense, Moderate and Light Fog classes and Total Fog Frequency (%) for all forests during 2008.

Month	Dense Fog			Moderate Fog			Light Fog			Fog Frequency		
	Lee	Ridge	Wind	Lee	Ridge	Wind	Lee	Ridge	Wind	Lee	Ridge	Wind
Jan	0.0	9.7	2.4	0.1	21.9	6.5	12.9	52.3	59.8	13.0	83.9	68.7
Feb	0.4	6.5	1.4	1.3	23.1	7.8	22.4	59.3	64.8	24.1	88.9	74.0
Mar	0.3	0.9	1.1	1.1	8.2	1.5	17.5	67.6	36.7	18.8	76.7	39.2
Apr	0.0	2.9	1.7	1.5	8.6	18.1	19.3	69.4	66.8	20.8	81.0	86.5
May	0.0	0.3	0.5	0.0	1.9	5.4	9.1	61.7	75.4	9.1	63.8	81.3
Jun	0.0	0.3	0.1	1.3	4.3	0.4	12.8	69.3	29.3	14.0	73.9	29.9
Jul	0.4	1.2	0.3	2.0	19.0	1.2	15.9	65.5	35.9	18.3	85.6	37.4
Aug	0.8	0.5	1.5	1.7	12.0	23.9	20.6	66.4	63.8	23.1	78.9	89.2
Sep	0.4	0.4	5.0	0.8	7.9	3.9	15.4	68.8	62.5	16.7	77.1	71.4
Oct	0.7	0.9	n/a	2.2	5.6	n/a	27.2	68.1	n/a	30.0	74.7	n/a
Nov	1.7	0.4	n/a	2.4	10.4	n/a	26.3	54.2	n/a	30.3	65.0	n/a
Dec	5.6	0.8	n/a	5.4	5.6	n/a	29.2	52.0	n/a	40.2	58.5	n/a
Jan-Sep	0.3	2.5	1.6	1.1	11.9	7.6	16.2	64.5	55.0	17.6	78.9	64.2
Annual	0.9	2.1	-	1.6	10.7	-	19.0	62.9	-	21.5	75.7	-

2.3.6.2 Seasonal and Daily Trends

While the leeward forest shows a moderate increase in fog frequency from the dry to wet season, there was little seasonal variation in the hourly distribution of fog events, with a greater frequency occurring during diurnal hours (Figure 2.3.6.2 A & D). The denser fog events at the leeward forest during the wet season, albeit of low frequency, tend to occur between 0700 h and 0900 h, near dusk, and around midnight, many of which are likely to be unrelated to the ENE orographic flow, especially in the case of the early morning events that commonly occur as the nocturnal fog bank forming in

the Oxapampa valley bottom begins to lift and dissipate after sunrise (personal observation).

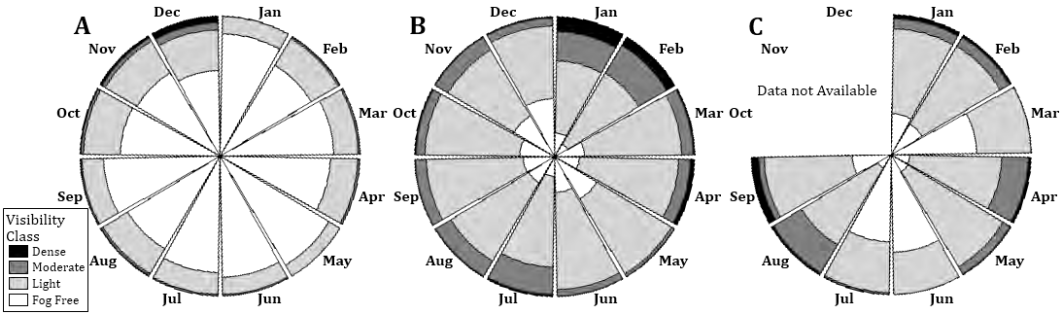

Figure 2.3.6.1: Monthly distribution (radial scale 100%) of hourly visibility class frequencies (%) at all forests during 2008.

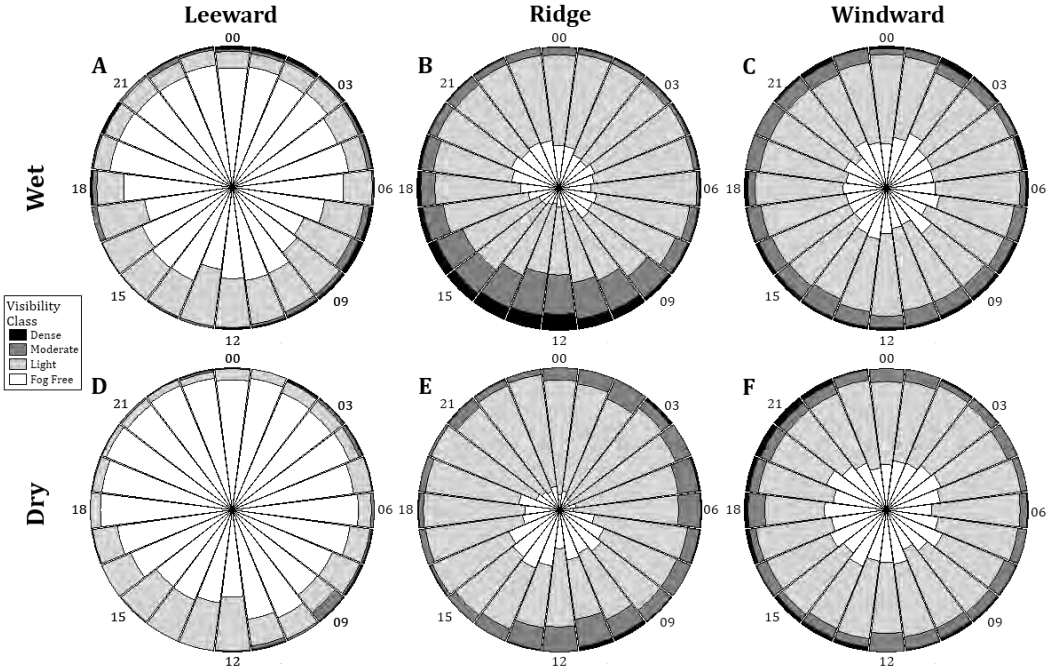

Figure 2.3.6.2: Hourly distribution (radial scale 100%) of visibility classes for wet and dry season periods at all forests during 2008.

The ridge forest does show considerable seasonal variation in the hourly distribution, with a high frequency of denser fog during the diurnal wet season hours with lighter fog and most of the clear periods during the evening, whereas in the dry season nights appear foggier and most clear periods occur during the day (Figure 2.3.6.2 B & C). Although in general, in comparison with the other forests, it can be said that the ridge forest exhibits near complete fog immersion during most of the year.

The windward forest showed little seasonal or diurnal variation, with only a slight reduction in frequency during the dry season (Figure 2.3.6.2 C & F).

2.3.6.3 Correlations

None of the visibility data showed even a moderate correlation among forests, highlighting the highly variable and complex nature of the data (Table 2.3.6.2). However in terms of correlations with other *in situ* parameters (Appendix A), the ridge forest visibility showed some moderate correlations with *in situ* temperature, PPFD and vapour pressure during diurnal wet season hours (Appendix Table 1). Diurnal dry season visibility correlations were weak at best (Appendix Table 2), the leeward forest visibility showed moderate correlation with in situ wind direction during nocturnal wet season hours (Appendix Table 3), while both the leeward and ridge forest visibility showed moderate correlation with in situ temperature during the nocturnal dry season hours (Appendix Table 4) as previously mentioned.

In terms of *ex situ* parameter correlations, only the ridge visibility during the diurnal wet season period was found to have moderate and better correlations than *in situ* counterparts for leeward temperature and windward vapour pressure (Appendix Table 1).

Table 2.3.6.2: Statistically significant ($P < 0.05$) Pearson's Correlation scores (r) between all forests for hourly average visibility during 2008.

Parameter	Period		Annual		Wet		Dry	
			Lee	Ridge	Lee	Ridge	Lee	Ridge
Visibility	Diurnal	Ridge	-0.10	-----	-0.21	-----	0.01	-----
	(0600 - 1700 h)	Wind	-0.04	0.24	-0.06	-0.04	-0.06	0.06
	Noctural	Ridge	-0.04	-----	-0.11	-----	0.08	-----
	(1800 - 0500 h)	Wind	0.05	0.16	0.07	-0.07	-0.02	-0.03

2.3.7 Humid Events

2.3.7.1 General Statistics

The humid event frequencies show the differences between the leeward forest and the ridge and windward forests in terms of moisture regimes (Table 2.3.7.1). The combination of data in this format resolves the disparities shown in the previous section in terms of fog regimes, where the leeward forest displayed a relatively low fog frequency during some of the wettest months (Figure 2.3.6.1). With the addition of rainfall events, it can be observed how the apparently lacking fog frequency at the leeward forest from January through April is compensated by the large number of lone rain events (Figure 2.3.7.1). During these months, the ridge and leeward forests show a much higher proportion of combined rain and fog events (that resulted in very high apparent fog frequency), while the leeward forest showed a much lower proportion of the combined event in most months, vice versa showing the highest proportion of lone rain events (Table 2.3.7.1). Comparing the total fog frequency (Table 2.3.6.1) and the total humid event frequency (Table 2.3.7.1) of all forests, it can be observed how the humid event total of the ridge and windward forests is slightly increased (~5 - 7%

proportional increase respectively) over the fog frequency, while the leeward forest shows an important increase (~35% proportional increase).

2.3.7.2 Seasonal and Daily Trends

In comparison with the fog frequency trends, the diurnal and nocturnal humid event trends at the leeward forest show no real change in the hourly distribution, although both wet season late nocturnal hours (0100 h – 0500 h) and dry season early nocturnal hours (1900 h – 2300 h) now appear more bolstered in terms of their importance to the humidity regime (Figure 2.3.7.2 A & D). The ridge forest wet season humid events show a shift from a diurnally centred increase in fog density (0900 h – 1600 h, Figure 2.3.7.2 B) to a more humid late nocturnal - early diurnal (0200 h – 1300 h) regime (Figure 2.3.7.2 B), while the dry season distribution tends to describe the diurnal periods from 0900 h to 1700 h as the most humid (Figure 2.3.7.2 D). The windward forest humid events show a similar pattern to the fog frequency pattern (Figure 2.3.7.2 C &F).

Table 2.3.7.1: Monthly Fog, Fog & Rain and Rain event frequency (%) and total humid event frequency (%) statistics for all forests during the 2008 period.

Month	Lone Fog			Fog & Rain			Lone Rain			Total Humid Events		
	Lee	Ridge	Wind	Lee	Ridge	Wind	Lee	Ridge	Wind	Lee	Ridge	Wind
Jan	8.5	45.0	49.5	4.6	38.8	19.2	31.7	7.8	7.7	44.8	91.7	76.3
Feb	12.2	57.5	56.8	11.9	31.5	17.2	21.8	5.2	5.3	46.0	94.1	79.3
Mar	12.0	55.4	31.6	6.9	21.4	7.7	15.3	4.0	10.1	34.1	80.8	49.3
Apr	13.9	57.8	71.0	6.9	23.2	15.6	14.6	5.0	3.6	35.4	86.0	90.1
May	8.1	52.4	71.8	1.1	11.4	9.5	9.0	3.9	2.3	18.1	67.7	83.6
Jun	11.5	63.3	26.0	2.5	10.6	3.9	9.6	5.4	7.9	23.6	79.3	37.8
Jul	15.7	79.7	35.5	2.6	5.9	1.9	3.6	0.3	4.0	21.9	85.9	41.4
Aug	17.7	71.4	80.0	5.4	7.5	9.3	4.8	2.7	0.0	28.0	81.6	89.2
Sep	12.5	69.4	62.6	4.2	7.6	8.8	4.6	1.1	2.5	21.3	78.2	73.9
Oct	17.7	56.9	-	12.2	17.9	-	8.7	3.1	-	38.7	77.8	-
Nov	20.4	52.6	-	9.9	12.4	-	6.8	4.3	-	37.1	69.3	-
Dec	25.9	45.4	-	14.2	13.0	-	5.8	7.0	-	46.0	65.5	-
Jan-Sep	12.5	61.3	53.8	5.1	17.5	10.3	12.8	3.9	4.8	30.4	82.8	69.0
Annual	14.7	58.9	-	6.9	16.8	-	11.4	4.1	-	32.9	79.8	-

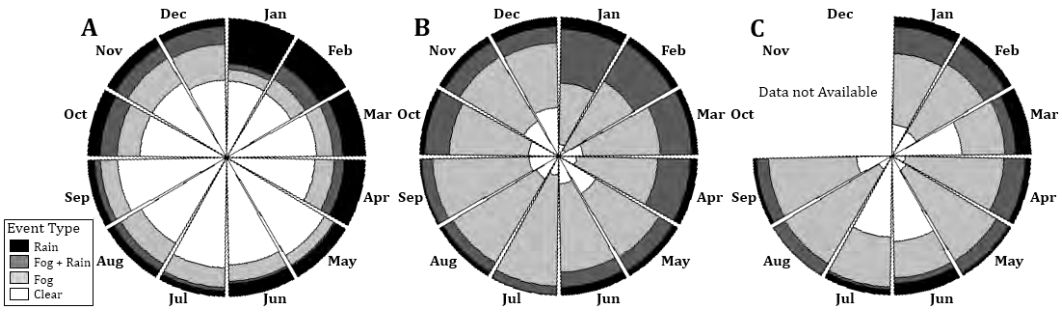

Figure 2.3.7.1: Monthly distribution (radial scale 100%) of hourly humid event type frequencies (%) at all forests during 2008.

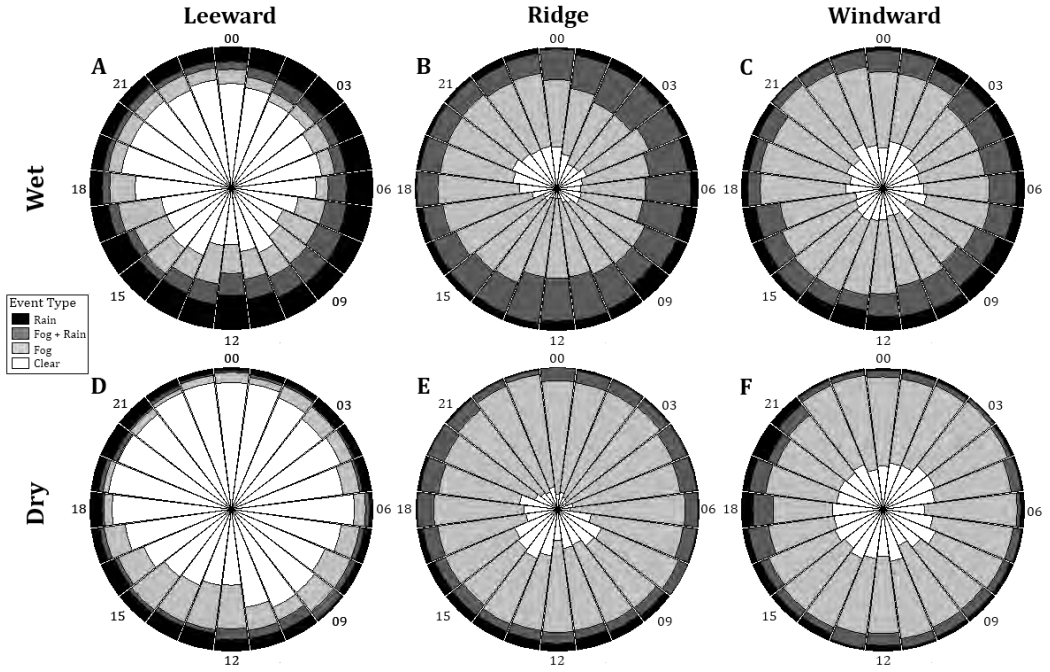

Figure 2.3.7.2: Hourly distribution (radial scale 100%) of humid event type for wet and dry season periods at all forests during 2008.

2.4 Discussion

The orographic location of each forest and the resulting exposure to the predominantly easterly flow of Amazonian air masses was evident in the climatic statistics. Despite the closeness and similarity in altitude, the leeward and windward forests showed slight differences in most of the variables studied, and large differences others, a function of their exposure to the predominant air masses, while both these forests differed markedly from the higher ridge forest.

2.4.1 General Comparisons

The average temperature and rainfall for the three forests fell within the range of other cloud forest sites (Figure 2.4.1.1).

The seasonality index calculated from monthly rainfall averages (Markham, 1970), places the forests of the present study at the higher end of rainfall seasonality for the cloud forest sites described by Jarvis & Mulligan (2011), although their listing has a very broad geographical and altitudinal range (Figure 2.4.1.2). The average lapse rates calculated for each slope are slightly higher than the 5.7°C/km calculated by Kappelle *et al.* (1995) on windward Costa Rican slope, while Martin *et al*. (2010) reported a large drop in the windward lapse rate within the cloud base range from 6.2°C/km to 3.1°C/km, which then returned to 4.2°C/km above the cloud base for what remained of the slope.

Despite the closeness of the sites and relatively small altitudinal variation, the leeward site showed much higher incoming radiation than the other sites,

probably due to the increased cloud immersion at the ridge and windward forests. However on the windward slope, the decrease in PPFD was similar to that found on a Bolivian transect (Gerold *et al.*, 2008)

The greater wind speed at the ridge forest was to be expected, as it has been recorded at other cloud forest sites (Cavelier & Mejia, 1990), although comparatively the wind speeds at the forests of the present study were mild compared to those reported in cloud forest areas in the Caribbean (Cavelier & Mejia, 1990, Eugster *et al.*, 2006).

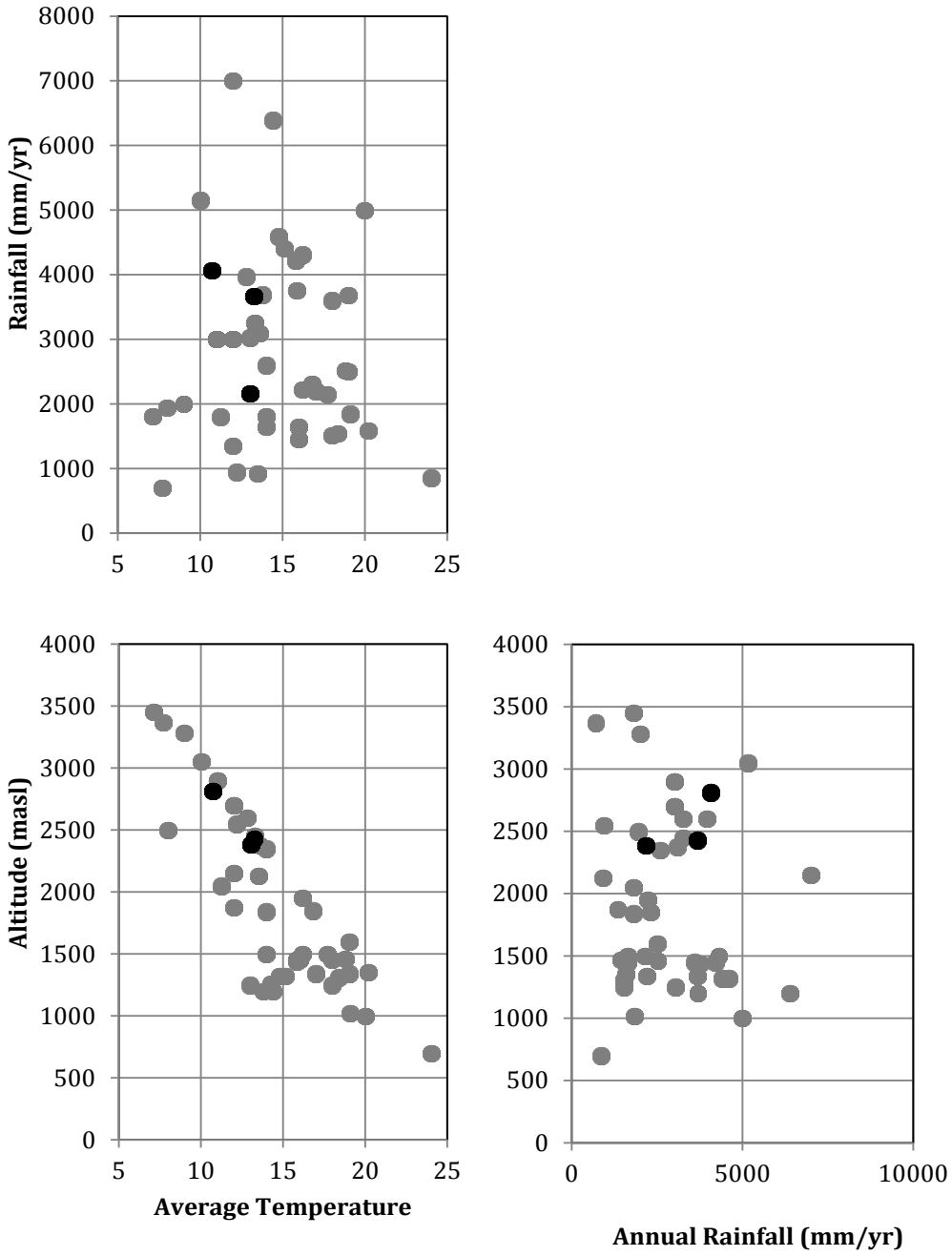

Figure 2.4.1.1: Relationships between temperature, rainfall and altitude at the present (black circles) and other known neotropical cloud forest sites (see Appendix B).

In a Thai lower montane forest, Tanaka *et al*. (2011) found that fog was recorded for 6.32 % of a 3-year period, or 2.87 % lone fog, 3.46 % fog and rain, and 3.73 % lone rain, approximately a quarter of the fog frequency recorded at the leeward forest, with a much larger proportion as synchronous fog and rain. The ridge and windward fog frequencies were similar to those reported in elfin cloud forest in Puerto Rico (Eugster *et al.*, 2006), but greater fog frequency than the 30% reported by Martin *et al*. (2007, 2010) in a Dominican cloud forest and 28% and 48% at two cloud forest sites in Venezuela by Gordon *et al*. (1994), while the leeward forest was similar to the drier of those two latter cloud forests. Also similar to this study, Gordon *et al*. (1994) found a minimal drop in seasonal fog frequency, from two sites reporting 30 and 51% in the wet season to 26 and 44% in the dry season. Generally, the leeward and ridge forest fog frequencies show similarities to the altitudinal distribution of fog frequencies on an Ecuadorian leeward slope described by Bendix (2008).

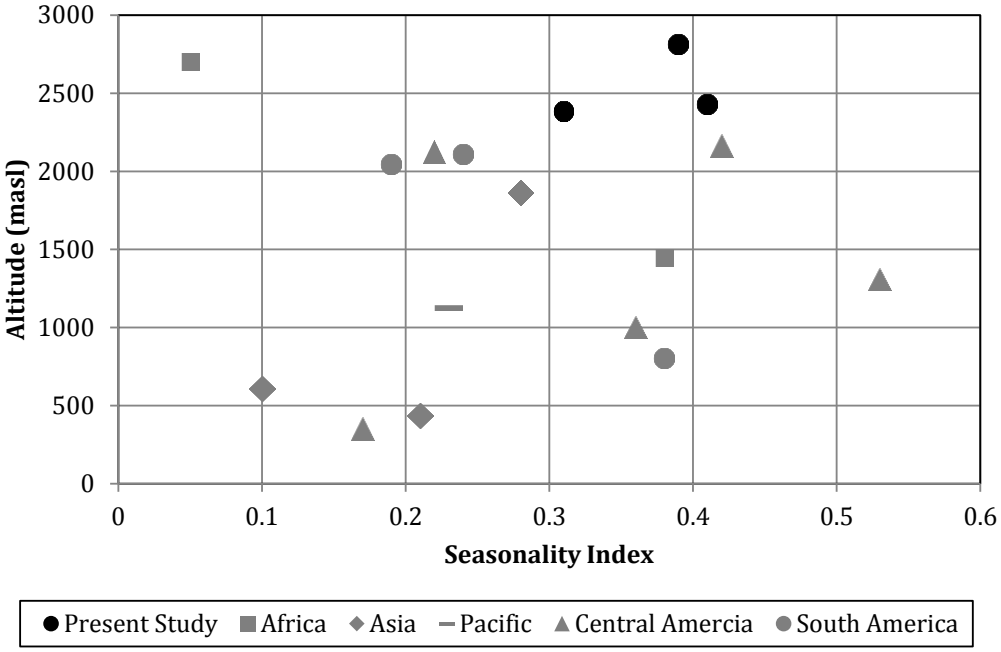

Figure 2.4.1.2: Seasonality Index of the present study forests and other cloud forest sites listed in Jarvis & Mulligan (2011).

2.4.2 Site Characteristics

The vast majority of visibility readings ≤1000 m were categorized as light fog (Table 2.3.6.1), despite the visual observation of "dense" fog at the sites with a high frequency (pers. obs. D. Catchpole). This may be a result of the sensor itself, highlighting the need for a comparative study of the different visibility sensors on the market in tropical conditions at different altitudes, as in this case, the averaging function of the sensor microprocessor will mask many dense fog events, and the infrared backscatter technique of the visibility sensor used in the present study might be affected by atmospheric pressure and thus is not ideal for comparison between sites at significantly different altitudes. If this is the case, fog frequency may indeed be higher or fog may be

denser at all sites, though this aspect of the data has not been explored and visibility measurements from other high altitude sites do not exist for comparison. In addition to what vapour pressure, rainfall and fog alone can indicate, the humid event regimes provide an indication of conditions relevant to moisture dependent plants such as epiphytes common in cloud forests. While the ridge and windward forests showed much greater (threefold) fog frequencies than the leeward forest, the much greater rain frequency at the leeward forest reduces the differences in humid conditions, although differences were still twofold.

Despite the relatively high rainfall seasonality index, the forests are thermally stable. The thermal stability of the forests is due in part to the tropical mid-altitude location, as well as the austral summer wet season of the Amazonian climate system. Land surfaces within the tropical mid-altitudinal belt (1500 – 3000 masl) are naturally protected from the diurnal air temperature extremities experienced above and below them year round because of the increase in air density in the lower troposphere. The wet tropical summer charges the air masses flowing from the Atlantic with humidity, which increase cloud formation and thus provides buffering from increased radiation through reduced transmission of solar energy. The relatively dry winters help to increase the heat balance during the cooler period through reduced cloudiness that allows a less unobstructed transmission. This mix of factors creates the conditions for one of the more stable thermal regimes found in the earth's humid terrestrial environments.

What little seasonal thermal variation does exist at the surface is essentially limited to the variation in nocturnal temperatures (Figure 2.3.1.2). While the nocturnal maximum temperatures show little seasonal variation, the nocturnal minimum temperatures are lower during the dry season, albeit slightly. The lack of diurnal variation through the seasons is due to the relatively small difference in seasonal radiation due to the closeness to the equator. The top of atmosphere seasonal radiation differences are masked at the ridge and windward forest by the effect of constant cloud immersion (Figure 2.3.7.2) on transmission during the periods of higher solar energy, resulting in the uniform seasonal PPFD distribution (see Figure 2.3.3.2). The slight differences in diurnal heating between the leeward and windward forest, in which the leeward forest shows greater heating in the afternoon (Figure 2.3.1.2), are principally explained by the frequency of rain and fog free periods (Figure 2.3.7.2).

The rainfall statistics showed that the windward forest receives considerably less rainfall, in contrary to other orographic studies that show greater windward rainfall (Weaver, 2000, Sherman *et al.*, 2005). When compared to the leeward forest, this was partly a result of lower rainfall intensity as the rainless periods were not markedly different (Figure 2.3.4.2). This lower windward rainfall, in conjunction with the fog data, indicates that the orographically lifted easterly air masses reach their maximum condensation point above the altitude of the windward site. Given the steepness of the windward slope, the most plausible explanation for the higher leeward precipitation is that air masses continue to rise after passing the ridgeline

before descending. During this continued ascent, raindrops continue to form and fall in greater intensity on the leeward slope, at least to the distance of the leeward site, while at some point further down the leeward slope the rain shadow begins to form, resulting in the much lower rainfall observed at the bottom of the slope in Oxapampa.

All these data indicate that the windward forest site lies just below the altitudinal belt of maximum discharge of orographic precipitation, and that the leeward forest site is located above the point on the leeward slope where the rain shadow effect begins, despite being nearly 2 km from the ridge. Whilst this phenomenon might occur at similar sites, it is likely to be highly site dependent. The predominant wind direction was clearly ENE (Figure 2.3.5.1), which was observed at all forests at some time or another, especially during diurnal hours at the ridge and windward forests. However, there appear to be two localised phenomena affecting the leeward and windward forests. The first is that the nocturnal data indicate the presence of very light downslope winds, which occur in non-turbulent nocturnal conditions as radiation is released from the forest during nocturnal cooling. This was evidenced in the data by the recording of light nocturnal downslope breezes in opposite directions at both forests, both coming from the direction of the higher landmasses above. The second phenomenon was the presence of westerly winds in the morning at the leeward forest coupled with increased fog frequency and density. This is a result of the early morning rise of the cloud base from the adjacent deforested leeward valley, which is usually immersed in low lying cloud during the night during relatively clear and dry conditions. It is likely that as radiation heats the low lying air mass in the early morning (see Figure 2.4.2.1), the rising air mass collides with the overlying ENE air mass, causing it to disperse to either side of the valley, creating, at this location, westerly winds and causing the passing of the cloud mass by the leeward forest 600 m above.

Figure 2.4.2.1: The Oxapampa Valley immersed in cloud at 0730 h, 26/06/2005. The upper cloud level is at 2200 masl with a cloud base thickness of approximately 200 m. Photo taken at WSW orientation from the ridge forest at 2800 masl.

Chapter 3

Variation in Composition and Canopy Structure on a Windward to Leeward Peruvian Montane Gradient

3.1 Objectives

In order to fill the gaps in knowledge identified previously (Chapter 1.2.2), this chapter addresses the orographic variation in forest attributes at three distinct forest types (see Chapter 1 for site descriptions) by presenting analyses of spatial patterns in floristic composition, forest structure and leaf morphology across a windward to leeward gradient. In addition to the gaps previously identified, the leeward forest 400 masl downslope and c. 2 km downwind of the ridge forest, have been shown to receive much higher rainfall than the similarly situated windward forest (Chapter 2) contrary to general orographic theory.

The aim of this chapter was to investigate how orography changes the composition, structure and leaf morphology of the forests in the study area, for which the principal objectives were to:

- Determine the similarity in floristic composition and diversity among forests;
- Determine the structural similarity among forests;
- Determine and compare the predominant leaf types and sizes among forests; and
- Determine the relationships between floristic composition, forest structure and biophysical parameters within and among forests.

3.2 Materials & Methods

3.2.1 Study Area

The floristic data was obtained from the same three sites mentioned previously (Chapter 1.4.3) within a pristine area of tropical montane forest of the Yanachaga-Chemillén National Park. Figure 3.2.1.1 shows the location of the 1-ha sampling plots installed at each of the leeward, ridge and windward forest locations (see Appendix C).

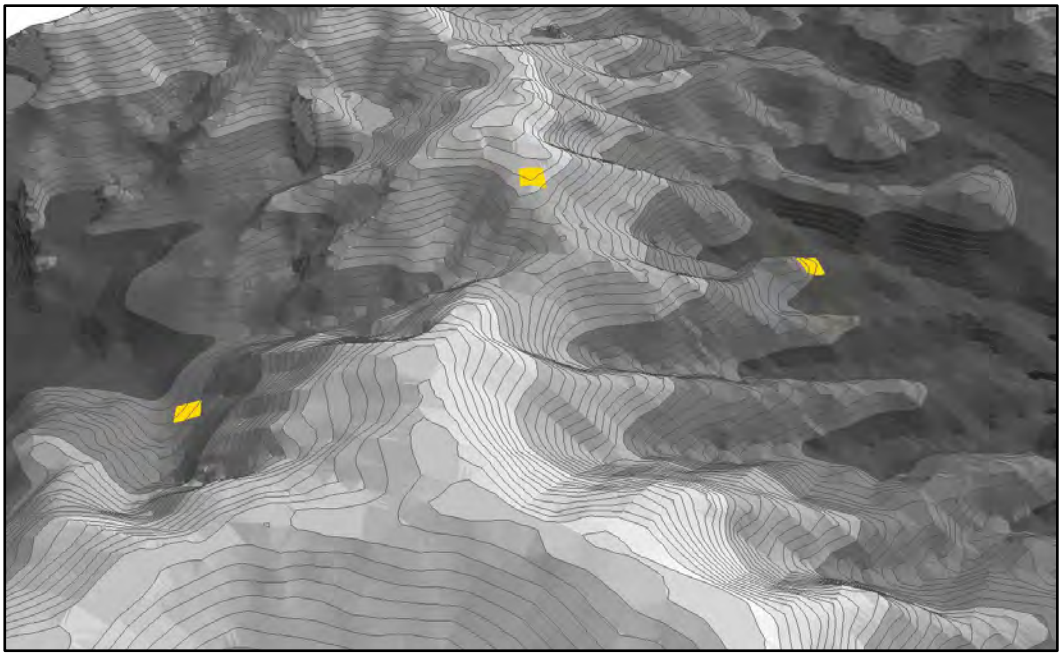

Figure 3.2.1.1: Location of the 1-ha sampling plots at the leeward (left), ridge (centre) and windward (right) forests.

3.2.2 Vegetation Sampling

Each of the three 100 m x 100 m sampling plots were gridded into 25 equal subplots (20m x 20 m), the corners of which were permanently marked with 1.5 m metal stakes with PVC sheaths. Despite the forest canopies, a series of GPS measurements from along the plot borders, from the tops of certain tree canopies and from the top of the meteorological towers, provided enough information to precisely georeference the plots. In order to perform high resolution stem mapping in the understorey without the constant use of measuring tapes (due to the limitations of GPS below the canopy), the subplots were further gridded into 5 m x 5 m areas, all of which were then delimited with white synthetic cord and colour coded flagging tape on corners and intervals such that one's location could be visually ascertained from anywhere within the plot with minimal error (< 1 m).

All stems ≥5 cm DBH rooted within each plot were surveyed using RAINFOR protocols (Phillips & Baker, 2002) at the leeward site during 2006/2007 by Requena Rojas (2007)[3] and the ridge and windward sites during 2007/2008 by Gutierrez Centeno & Moya Hinojosa (2008)[4], who performed the work under the daily instruction and supervision of the author and with the assistance of a professional botanical sample collector (Antonio Peña) and additional field assistants. For every stem ≥5 cm DBH the following records were taken:

[3] Basic species diversity data at an early stage of species identification was presented for the leeward forest site in a Peruvian (Spanish) undergraduate thesis by Requena Rojas (2007).
[4] Basic species diversity data at an early stage of species identification were presented individually for each of the ridge and windward sites in Peruvian (Spanish) undergraduate theses by Gutierrez Centeno & Moya Hinojosa (2008).

- each stem was given a unique field code and marked with an aluminium nail and tag;
- a vegetative sample was collected for later laboratory species identification/confirmation and sample cross-referencing;
- the X and Y coordinates of the stem within the subplot were recorded on a field map by visual reference to the above-mentioned cord and flagging tape 5 m x 5 m marking system (error < 1m);
- the DBH was recorded in centimetres according to RAINFOR protocols (Phillips & Baker, 2002) using a metal diametric tape measure;
- the stem height (ground to canopy top) was recorded in metres using a marked PVC tube ruler for stems up to 6 metres high, or a digital rangefinder for taller stems;
- the diameter of the crown area was recorded in meters at the equidistant point between the longest and shortest diameter using a digital rangefinder;
- the angle of stem incline was recorded using a clinometer (where 90° represented a perfectly straight stem and 0° represented a horizontally lying stem); and
- the cardinal direction of the stem incline was recorded with a magnetic compass.

Specimens of every individual were collected and identified to species or morphospecies in a local herbarium (HOXA, Missouri Botanical Garden – Peru), where a specimen of each distinct species from each plot was deposited. Species identification was performed initially by Jimmy Requena Rojas, Rolando Gutierrez Centeno and Yhuller Moya Hinojosa under the supervision of the author and with guidance and revision by specialized botanists of the Missouri Botanical Garden, including Abel Monteagudo and Rodolfo Vasquez amongst many others.

3.2.3 Analysis

In order to facilitate comparison with a large number of studies, many of the analyses are presented for both the ≥5 cm DBH and ≥10 cm DBH datasets. This also permits an evaluation of the benefits of both data collection scales for certain forest attributes.

3.2.3.1 Composition

Diversity statistics were performed using PC-ORD Version 6.07, general statistics and graphs were produced using Minitab® Version 16.1.1, while other plots were produced using Microsoft Excel 2010 Version 14.0.6106.5005 and SigmaPlot Version 11.0.0.77.

Alpha diversity was reported with the Shannon Index (H') (Shannon, 1948) and the Simpson's Index (D) (Simpson, 1949) using the following formulae:

$$H' = -\sum_{i=1}^{n} P_i \log P_i$$

$$D = 1 - \sum_{i=1}^{n} P_i^2$$

where P_i is the importance probability in species i, H' is the Shannon Diversity Index and D is the Simpson's Index. P is relative to subplot richness/abundance totals (Greig-Smith, 1983).

Species-area curves and associated statistics were generated using PC-ORD Version 6.07 with a Sørenson distance measure. Species richness estimates were provided by first- (Palmer, 1990) and second-order (Palmer, 1991) jackknife estimations. While these estimators are known to be susceptible to overestimation in heterogeneous distributions with many rare species (Palmer, 1995), they still serve to provide insight into differences between communities.

3.2.3.2 Structural Characteristics

Structural parameters used during the analysis are shown in Table 3.2.3.1. Basal area was calculated from DBH measurements, while the crown area of each stem was calculated as a 2-dimensional circular plane based on the field-measured crown diameter. To reduce the error of this simplistic representation of crown area for cases of non-circular crowns, the diameter of the crown area was field-measured at the equidistant point between the longest and shortest diameter (per Chapter 3.2.2).

At varying scales throughout the analyses, the crown areas were summed to represent total arboreal foliage areas, which may exceed the ground surface area represented due to multi-layering of the canopy. However imprecise, this parameter is intended as an indicator of productivity, which with quicker recovery rates than basal area, is likely to be less susceptible to being affected by within plot mortality events and thus maintain a relatively less dynamic equilibrium compared to basal area.

For the presentation of distributions and comparison of data, stem data were often separated into 5-cm diameter class intervals, 1-m stem height class intervals and 2-m crown diameters class intervals. Given that high stem incline can be a part of normal growth in montane forest on steep slopes, measured stem inclinations were grouped into erect (90 - 60°) and inclined (< 60°) following Madsen & Ollgaard (1994).

The average canopy height of each forest plot was calculated as the average of the maximum stem heights in each of the 25 sub-plots.

The best regression slope fit between crown radius (m) and DBH (cm) was calculated with Minitab® Version 16.1.1.

3.2.3.3 Leaf Characteristics

Collected specimens were inspected to determine average leaf size according to the Raunkiaer classification system (Raunkiaer, 1934) modified by Webb (1959). A number of representative leaves (5 – 20) per species were scanned on a flatbed scanner and leaf images were measured using the software ImageJ Version 1.45 to determine average leaf size. Following Buot & Okitsu (1999), leaflets of compound leafs were compared with simple leaves. Species were also classified according to the presence of a "drip-tip" and the

presence of a compound leaf, which were converted to proportion of foliage present on the basis of the total arboreal foliage area per species.

3.2.3.4 Species Associations

In order to investigate the relationship between biophysical variables and the floristic composition (DBH ≥10 cm), analyses were performed using the cluster analysis, Non-metric Multidimensional Scaling (NMS), joint plot, matrix correlation species association and indicator species functions of the software PC-ORD Version 6.07.

Prior to performing the analyses, species represented by one individual in a single 20 m x 20 m sub-plot in a single 100 m x 100 m plot were removed from the DBH ≥10 cm quantitative database that left a total of 136 species. No further modification or transformation of the databases was performed or deemed necessary for the particular analyses that followed.

For each of the three forest databases, a separate cluster analysis was performed using the Ward Linkage Method and Euclidean distance measure. Cluster groups in each forest type were assigned from the dendrograms using a cutoff of 50% similarity. The NMS ordination technique used the method developed by Mather (1976) and Kruskal (1964) with a Sørenson distance measure. A separate NMS ordination was performed for each forest type, initially run for 250 iterations from a random starting configuration with the real data and dimensionality was assessed with a Monte Carlo test with 250 iterations of randomised data. A second ordination was run with the ideal dimensionality and starting point and 1000 iterations. To overlay the NMS results, a joint plot analysis was performed using an r^2 threshold of 0.4 in all cases and Pearson's correlation scores were determined between species-environmental variables and ordination axes using the Correlation with Matrix function of the same PC-ORD software. The Plexus Values function was used to calculate pairwise presence-absence standardized chi-square distance statistics to determine direct species associations (Goodall, 1978), while the Indicator Species Analysis function was used to determine the definitive species of the cluster groups (Dufrene & Legendre, 1997).

Understorey biophysical variables were collected by Taylor (2008) and included data collected from two 2 m x 2 m plots within each of the 25 sub-plots per plot. These and other variables used in the joint plot of the NMS analyses are summarized in Table 3.2.3.1.

One-way ANOVA tests were performed with Minitab® Version 16.1.1 to determine differences in each biophysical variable among sub-plots according to the cluster groups identified. Each biophysical variable database was checked for normality with an Anderson-Darling normality test using Minitab® Version 16.1.1.

Table 3.2.3.1: Summary of sub-plot biophysical variables used in NMS analyses and their average values for all sites with SD values in parenthesis.

Parameter	Code	Leeward	Ridge	Windward
Floristic Parameters (DBH 10cm)				
Stem density (# stems)	SD	22.8 (6.4)	16.2 (6.3)	24.7 (8.4)
Species richness (# species)	SP	16.3 (4.7)	9.7 (3.2)	10.8 (3.8)
Total basal area (m^2)	BA	1.4 (0.6)	0.6 (0.3)	0.6 (0.2)
Total arboreal foliage area (m^2)	CA	593 (197)	340 (117)	406 (161)
Average basal area (m^2)	BAm	0.033 (0.016)	0.013 (0.006)	0.01 (0.006)
Average crown area (m^2)	CAm	9.2 (1.3)	7.8 (1)	7.4 (1.1)
Average stem height (m)	SH	14.1 (4.2)	7.7 (4.1)	6.6 (4)
Average stem inclination (^{o})	SI	77.5 (4)	62.3 (4.2)	59.1 (8.8)
Ground slope (^{o})	SL	26 (10)	16.1 (8.6)	32 (10.6)
Environmental Parameters (Taylor, 2008) [5]				
Visible sky fraction (%)	VS	5.9 (2.2)	14 (5.5)	13.4 (6.4)
PPFD ($\mu mol.sec^{-1}.m^{-2}$)	Mol	2438 (1073)	5767 (2412)	5096 (2461)
LAI Index	Lai	3.5 (0.7)	2.3 (0.5)	2.5 (0.8)
LAI Deviation Index	LaiD	3.7 (0.6)	3.2 (0.7)	3.3 (0.7)
Course woody debris cover (%)	WD	23.7 (14.1)	17.8 (10.4)	19.4 (11.6)
Exposed soil cover (%)	ES	26 (17)	7.6 (7.5)	5.7 (5.4)
Leaf litter cover (%)	Li	46.2 (18.3)	42 (12.4)	56 (10.9)
Bryophyte cover (%)	Br	7.2 (5.7)	62 (15.5)	15.9 (16)
A horizon bulk density (g/cm^3)	BD	0.46 (0.29)	0.16 (0.06)	0.21 (0.16)
Root mat height (cm)	RmH	15 (5.6)	63.9 (16.5)	52.7 (16.3)
A horizon pH	MpH	5.1 (0.9)	4.3 (0.3)	4.2 (0.3)
O horizon pH	OpH	4.4 (0.7)	3.4 (0.2)	3.6 (0.2)
O horizon elect. cond. ($dS \cdot m^{-1}$)	CE	0.2 (0.1)	0.2 (0.1)	0.2 (0.1)
O horizon organics (%)[6]	OM	26.4 (9.7)	50.2 (12.7)	53.1 (16)
O horizon P (ppm) [7]	P	15.9 (14.9)	18.8 (18.3)	4.1 (1.1)
O horizon K (ppm) [8]	K	223 (109)	321 (132)	287 (117)
O horizon Al+3 (me/100 g) [9]	Al3	1.2 (0.8)	4.4 (1.1)	5.1 (1.1)

3.3 Results

3.3.1 Composition & Diversity

A total of 247 and 190 species were recorded in the ≥5 cm and ≥10 cm diameter classes of the study respectively, distributed among 89 and 76

[5] All soil analyses were conducted at the Soil, Plant, Water and Fertilizer Analysis Laboratory, Department of Soils, Faculty of Agronomy, Universidad Nacional Agraria La Molina in Lima, Peru
[6] Analyses conducted using the Walkey & Black method
[7] Analyses conducted using the CIC method
[8] Analyses conducted using the modified Olsen method
[9] Analyses conducted using the Yuan method

genera and 47 and 40 families (see Appendix D). Over 50% of the species, genera and families recorded were present at the leeward forest (Figure 3.3.1.1), which also presented the highest family, genus and species richness in both diameter classes (Table 3.3.1.1), while the windward forest presented slightly greater general richness than the ridge forest, with the same trend applying to sub-plot species richness.

In both diameter classes, the species richness of sub-plots was significantly higher at the leeward site (P = 0.001). The leeward forest showed the greater diversity index scores in both diameter classes, followed by the ridge and windward forests (Table 3.3.1.1). The Podocarpaceae, the only gymnosperm family, was best represented at the windward forest, while the Cyatheaceae was the only pteridophyte family and best represented at the leeward forest (Table 3.3.1.1). While the leeward forest had the largest number of species with very low abundance or sub-plot frequency (Table 3.3.1.1), the proportions were similar among forests (Figure 3.3.1.2).

Table 3.3.1.1: General floristic and structural statistics from the leeward, ridge and windward forest 1-ha plots.

	DBH ≥5cm			DBH ≥10cm		
Description	Lee	Ridge	Wind	Lee	Ridge	Wind
Species/ha	136	74	81	109	51	59
Genera/ha	61	37	44	56	28	35
Families/ha	34	27	28	31	22	23
Angiosperm N sp.	130	71	76	103	48	54
Gymnosperm N sp.	1	2	3	1	2	3
Pteridophytes N sp.	5	1	2	5	1	2
Aver. species/400m^2	26.5	21.0	22.1	16.3	9.7	10.8
Live stem density/ha	1013	1187	1344	542	390	507
Dead stem density/ha	38	24	378	28	16	111
Shannon's H'	4.29	3.61	3.55	4.10	3.22	3.16
Simpson's D	0.98	0.96	0.95	0.97	0.94	0.91
Species with abun. =1	30	16	20	34	14	14
Species with abun. =2	17	8	4	18	7	10
Species with freq. =1	36	19	21	37	17	16
Species with freq. =2	14	10	9	18	10	12
Basal area (m^2/ha)	33.9	15.3	15.4	32.0	12.2	11.2
Arboreal foliage area (m^2/ha)	14822	8506	10138	11850	6377	7234
Aver. stem height (m/ind)	9.16	7.65	7.13	11.96	9.78	8.47
Max. stem height (m)	-	-	-	32	20.9	17.6
Aver. stem incline (°/ind)	76.8	62.6	58.7	77.8	66.4	63.3
Aver. DBH (cm/ind)	15.2	10.4	9.6	22.1	17.5	14.4

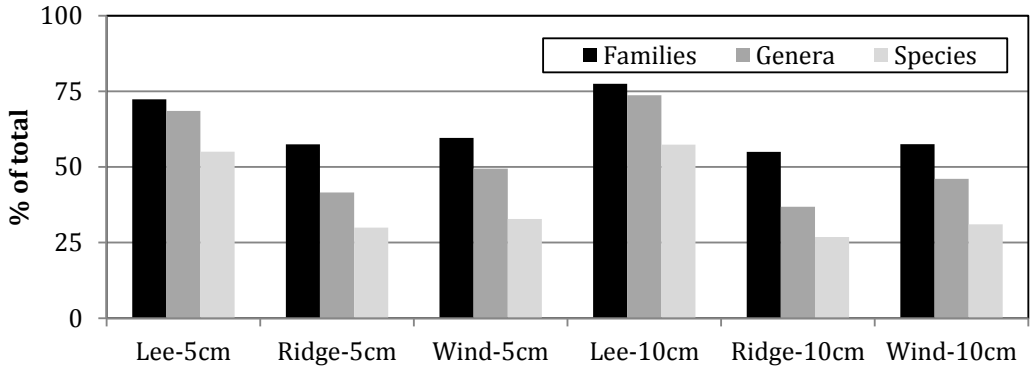

Figure 3.3.1.1: Proportion of total number of families, genera and species at the leeward, ridge and windward sites for both ≥ 5cm and ≥ 10cm diameter classes.

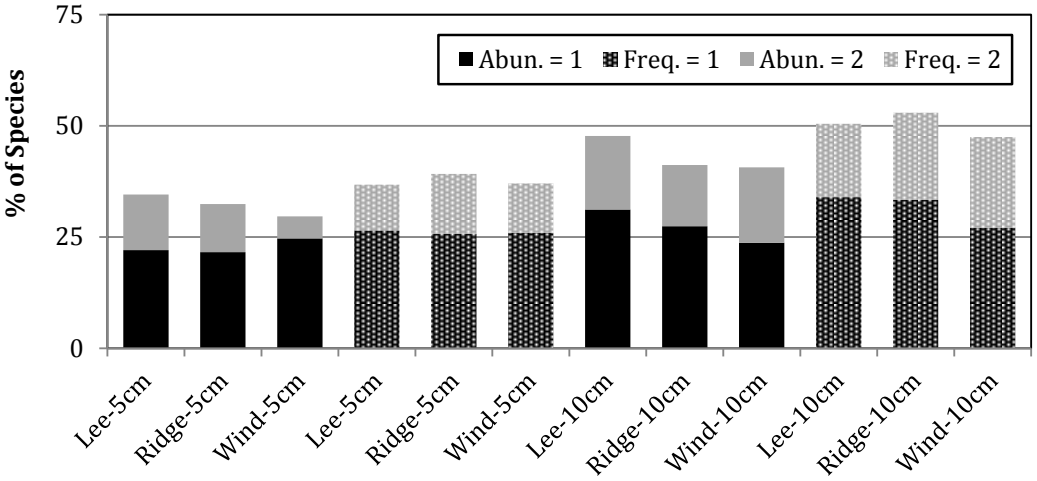

Figure 3.3.1.2: Proportion of species with an abundance of 1 or 2 and sub-plot frequency of 1 or 2 in each 1-ha plot at the leeward, ridge and windward sites for both ≥ 5cm and ≥ 10cm diameter classes.

The species-area curve for the leeward forest (≥ 10cm class) shows some flattening (Figure 3.3.1.3), although the 109 species recorded is much lower than the 144 and 162 predicted species of the first and second-order the Jackknife estimates respectively (32 and 48% increase). The species-area curve for the ridge forest also shows some flattening (Figure 3.3.1.4), and in a similar fashion to the leeward forest, the 51 species recorded is much lower than the 67 and 74 predicted species of the first and second-order the Jackknife estimates respectively (31 and 45% increase). The windward forest species-area curve shows a similar trend to the other forests, although the 59 species recorded was slightly closer to the 74 and 78 predicted species of the first and second-order the Jackknife estimates respectively (25 and 32% increase) compared to the other forests.

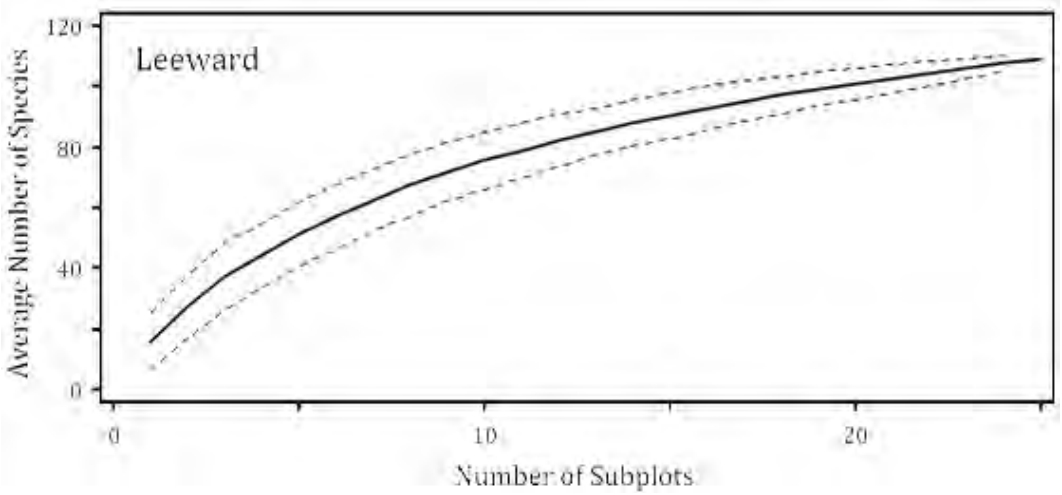

Figure 3.3.1.3: Species-area curve for the ≥ 10cm diameter class of the leeward forest 1-ha plot.

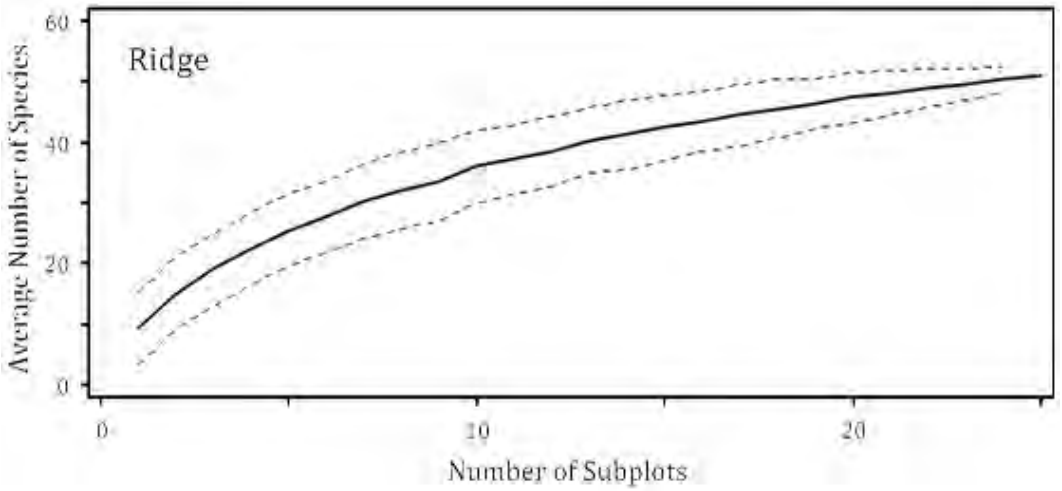

Figure 3.3.1.4: Species-area curve for the ≥ 10cm diameter class of the ridge forest 1-ha plot.

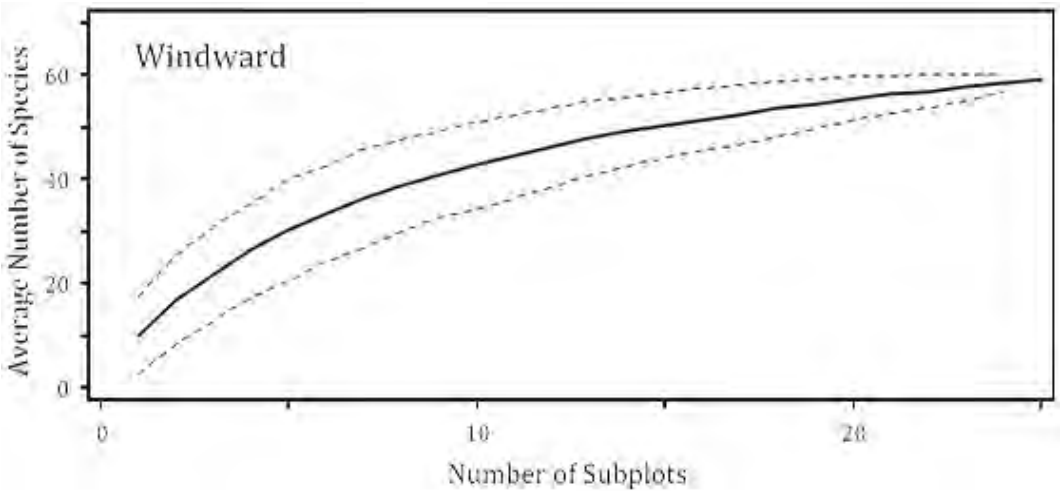

Figure 3.3.1.5: Species-area curve for the ≥ 10cm diameter class of the windward forest 1-ha plot.

From here on in, compositional results are reported only for the ≥ 5 cm diameter class. The Melastomataceae was the dominant family (relative abundance ≥ 20%) at the leeward and ridge forests, the Clusiaceae dominated at the windward forest (relative abundance 17%), while the Cyatheaceae and the Chloranthaceae were sub-dominant (relative abundance ≥ 10%) at the leeward and ridge forests respectively (Appendix E). Other highly abundant (relative abundance ≥ 5%) families included Rubiaceae, Euphorbiaceae and Meliaceae at the leeward forest, Mysinaceae and Clusiaceae at the ridge forest, Araliaceae and Cyatheaceae at the ridge forest and Lauraceae and Cunoniaceae at all forests. The relative importance of families (IVI) largely reflected the abundance trends (Appendix F).

In terms of highly abundant genera (relative abundance ≥ 5%), *Weinmannia* figured at all forests, *Miconia* dominated at the leeward and ridge forests, *Clusia* dominated at the windward forest and also figured at the ridge forest, *Cyathea* figured at the leeward and windward forests, while the leeward forest also presented *Alsophila*, the ridge forest *Myrsine* and *Hedyosmum*, and the ridge forest *Schefflera* and *Freziera* (Appendix E).

The leeward forest did not show any clear domination in abundance by any one species, presenting four species that can be classified as dominant (4 – 5 % relative abundance), the ridge forest was co-dominated by *Miconia aprica* and *Hedyosmum dombeyanum*, while the windward forest dominant was *Clusia schultesii* (Appendix E).

The relative importance of species (IVI) largely reflected the abundance trends, with only mostly just rearrangement of the order of the most abundant species with no significant inclusion (Appendix F).

Of the 247 species recorded, 85 % (209 spp.) were only recorded from one of the forests, 13 % (33 spp.) occurred at two forests and only 2 % (5 spp.) occurred at all three forests. The greatest overlap of species occurred between the ridge and windward forests with 25 shared species, followed by the leeward and windward forests with 13 shared species, while the leeward and ridge forests showing the least amount of overlap with only nine shared species (Appendix G).

3.3.2 Structural Characteristics

A total of 3544 live stems of ≥ 5 cm DBH and 1439 live stems ≥ 10 cm DBH were recorded in the study. The windward site presented the highest stem density in the ≥ 5 cm diameter class, the leeward site presented the highest density in the ≥ 10 cm class, while the windward site presented a vastly higher proportion of standing dead stems in the ≥5 cm and ≥10 cm diameter classes (21.9%, 17.9% respectively), followed by the leeward (3.6%, 4.9%) and ridge (2.0%, 3.9%) forests (Table 3.3.1.1).

The average canopy height was highest at the leeward forest (23.4 m, SD 4.4), followed by the ridge (15.8 m, SD 3.2) and windward (12.9 m, SD 2.7) forests.

The total arboreal foliage and basal areas again reflect a large difference between the leeward forest and the relatively similar ridge and windward

forests, the latter two showing much lower and near identical basal areas in both diameter classes (Figure 3.3.2.1). In the ≥5 cm diameter class, basal area was significantly higher at the leeward site ($P > 0.001$), while stem height, stem incline and crown diameter were significantly different at all sites ($P > 0.001$). In the ≥10 cm class, basal area, stem height, stem incline and crown diameter were all significantly different at all sites ($P > 0.001$).

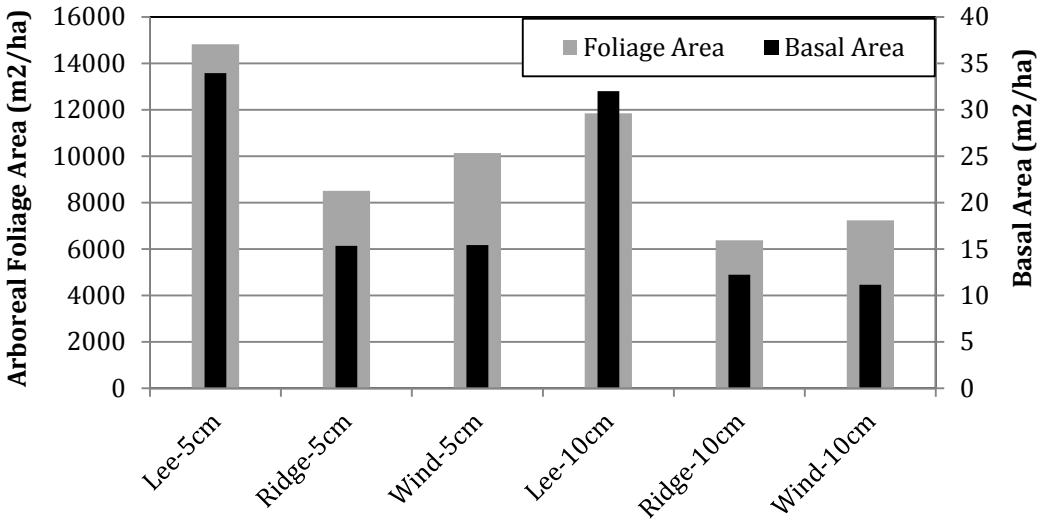

Figure 3.3.2.1: Arboreal foliage and basal area at the leeward, ridge and windward sites for both DBH ≥ 5cm and DBH ≥ 10cm classes.

These differences in total basal area mentioned above were obviously reflected in the distribution of stem diameters, where both the ridge and windward sites presented a high concentration of the narrowest diameter class, whereas the leeward forest showed a greater proportion of the large diameter classes and interestingly did not show the typical high frequency in the lowest class (Figure 3.3.2.2). This trend was also shown for the distribution of height classes, where again the ridge and windward forest sites show a similar pattern distinct to that of the taller leeward site, which also showed a bimodal distribution indicating to some degree a second understorey canopy level (Table 3.3.1.1, Figure 3.3.2.3). The distribution of crown diameters also showed this distinction between the leeward and other forests, of note is the lower frequency of the smaller crown diameter classes in the leeward forest, an indication of the lower light availability of a relatively closed canopy (Figure 3.3.2.4).

The leeward forest presented a relatively closed canopy in terms of montane forest on a slope, albeit still broken, as shown by the plotted crown diameters (Figure 3.3.2.5), the ridge forest presented a very open canopy (Figure 3.3.2.6), while the windward forest presented a broken canopy, with a wide range of density within the plot (Figure 3.3.2.7).

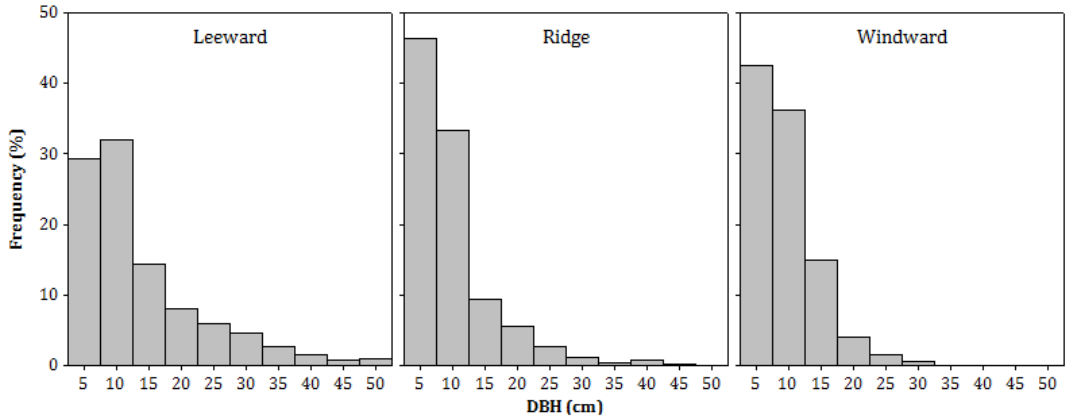

Figure 3.3.2.2: Distribution of diameter classes of 5-cm intervals at the leeward, ridge and windward forest plots.

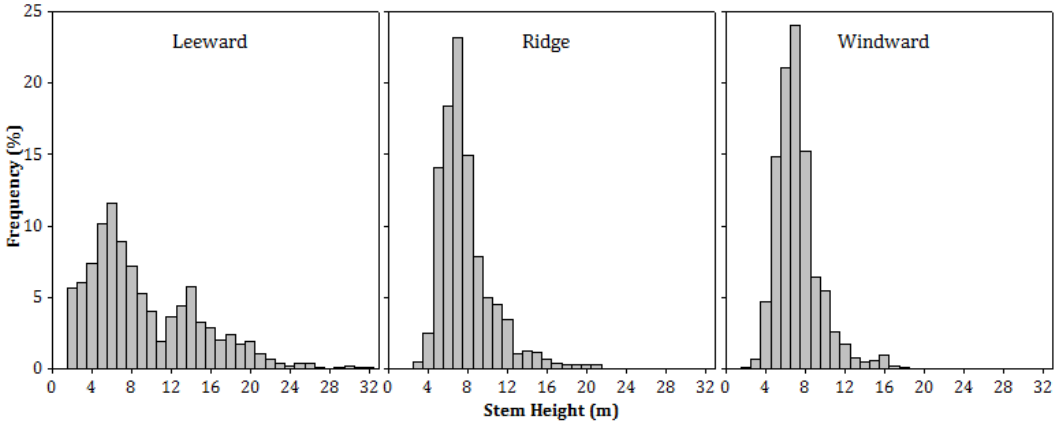

Figure 3.3.2.3: Distribution of height classes of 1-m intervals at the leeward, ridge and windward forest plots.

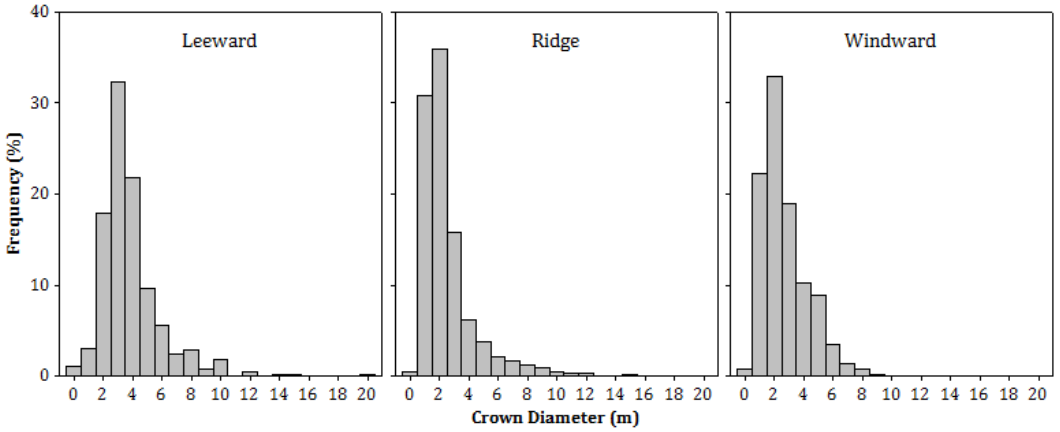

Figure 3.3.2.4: Distribution of crown diameter classes of 2-m intervals at the leeward, ridge and windward forest plots.

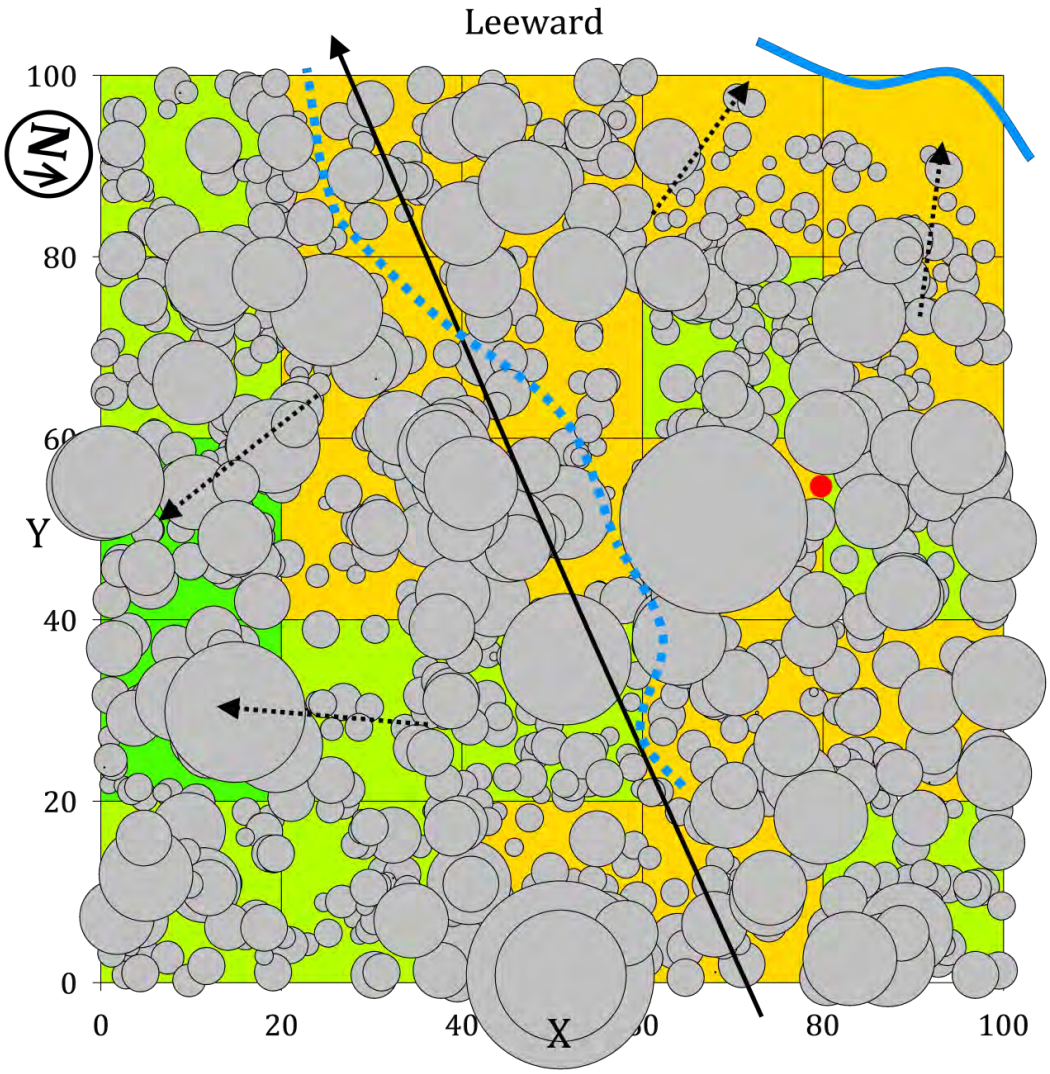

Figure 3.3.2.5: Distribution of physical features and crown diameters (m) in the leeward forest sub-plots categorized by cluster group. Positions of crowns are vertical from base of stem and does not account for stem height/incline. Orange represents cluster group 1, lime green represents cluster group 2 and green represents cluster group 3. Solid black line indicates direction of slope descent. Dotted black lines indicate direction of descent of micro-topographic features. Solid blue line indicates stream. Doted blue line indicates streamlet initiating from spring within plot. Red dot indicates canopy tower. Maximum and minimum altitude are 2447m (X100:Y0) and 2414m (X0:Y100).

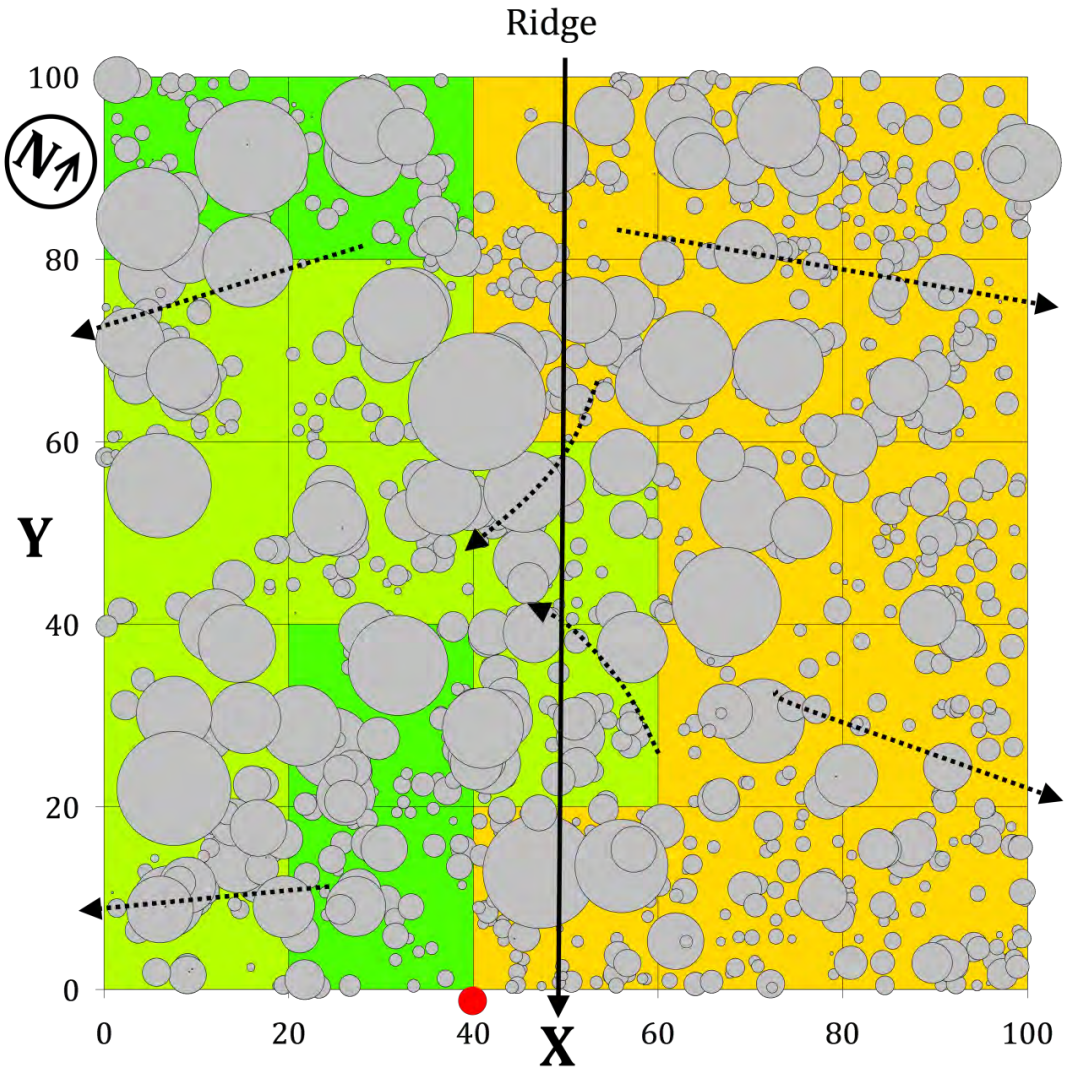

Figure 3.3.2.6: Distribution of physical features and crown diameters (m) in the ridge forest sub-plots categorized by cluster group. Positions of crowns are vertical from base of stem and does not account for stem height/incline. Orange represents cluster group 6, lime green represents cluster group 4 and green represents cluster group 5. Solid black line indicates direction of slope descent. Dotted black lines indicate direction of descent of micro-topographic features. Red dot indicates canopy tower. Maximum and minimum altitudes are 2834m (X48:Y100) and 2797m to the east (X100:Y0) and 2804m to the west (X0:Y0).

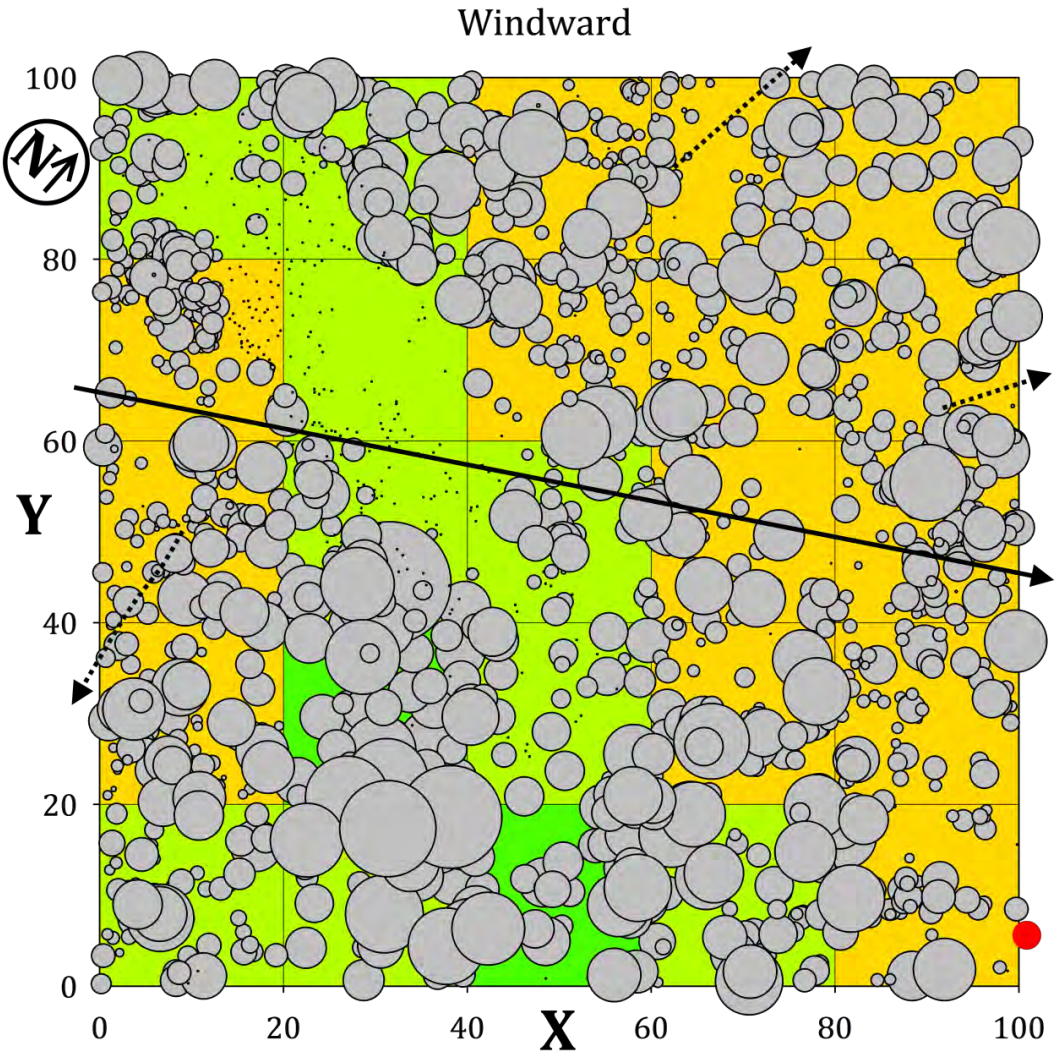

Figure 3.3.2.7: Distribution of physical features and crown diameters (m) in the windward forest sub-plots categorized by cluster group. Positions of crowns are vertical from base of stem and does not account for stem height/incline. Orange represents cluster group 9, lime green represents cluster group 7 and green represents cluster group 8. Solid black line indicates direction of slope descent. Dotted black lines indicate direction of descent of micro-topographic features. Red dot indicates canopy tower. Maximum and minimum altitudes are 2427m (X05:Y100) and 2380m (X100:Y0).

The distribution of arboreal foliage in the canopy shows that as opposed to the more open and broken canopies of the ridge and windward sites, the leeward site distribution of arboreal foliage shows a bimodal distribution, indicating an understorey canopy level at around 8 m, distinct from that of the upper canopy at 16 to 20 m (Figure 3.3.2.8).

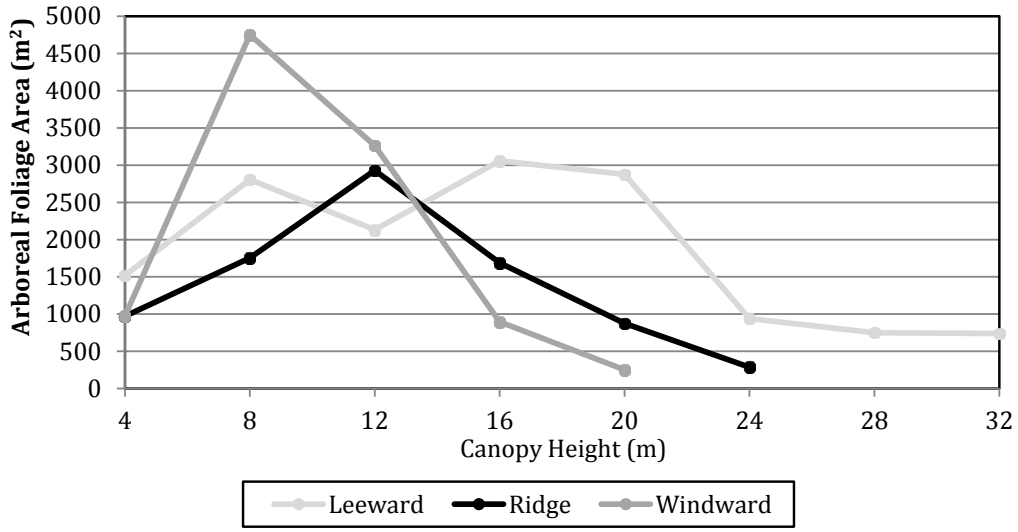

Figure 3.3.2.8: Total arboreal foliage area at 4-m canopy height intervals at the leeward, ridge and windward forest plots.

The patterns of stem inclination reflected the slope and orientation characteristics of each plot, with the ridge forest showing the broadest distribution in inclination direction, while both the ridge and windward forests showing a greater proportion of highly inclining stems (Figure 3.3.2.9). The leeward forest presented the lowest amount (5.96 %) of inclined (< 60°) stems, while the ridge (20.71 %) and windward (27.08 %) forests showed a much greater incidence.

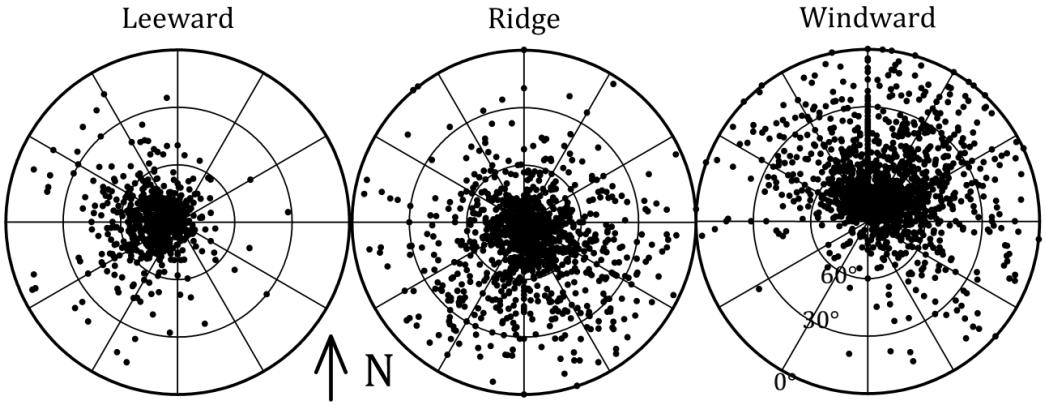

Figure 3.3.2.9: Distribution of stem incline angle and direction at all sites.

The best fit for the crown radius (CR) and DBH relationship for all stems ≥5 cm DBH for all forests was described by the cubic model (Figure 3.3.2.10, Figure 3.3.2.11 & Figure 3.3.2.12), followed by the quadratic and linear

models. The average CR-DBH ratio decreases with increasing DBH class (Table 3.3.2.1), although there was no acceptable fit for the CR-DBH ratio and DBH relationship for any of the forests (Figure 3.3.2.13, Figure 3.3.2.14 & Figure 3.3.2.15). These data indicate that significant crown foliage areas develop before significant basal areas, and furthermore that the small stems in the leeward forest appear to have a larger foliage area than those in the ridge and windward forests.

Table 3.3.2.1: Average CR-DBH ratio (SD) per DBH class from the leeward, ridge and windward forest 1-ha plots.

DBH Class (cm)	Leeward	Ridge	Windward
10	0.20 (0.07)	0.13 (0.05)	0.14 (0.06)
20	0.14 (0.05)	0.11 (0.05)	0.14 (0.05)
30	0.11 (0.04)	0.12 (0.04)	0.12 (0.03)
40	0.10 (0.03)	0.11 (0.03)	0.09 (0.04)
50	0.10 (0.03)	0.11 (0.02)	-
60	0.07 (0.02)	0.07 (0.02)	0.09 (-)
70	0.05 (0.02)	0.09 (0.04)	-
80	0.06 (0.01)	-	-
90	0.08 (-)	-	-
100	0.05 (-)	-	-
110	0.04 (-)	-	-
120	0.09 (-)	-	-
130	0.01 (-)	-	-
140	0.07 (-)	-	-

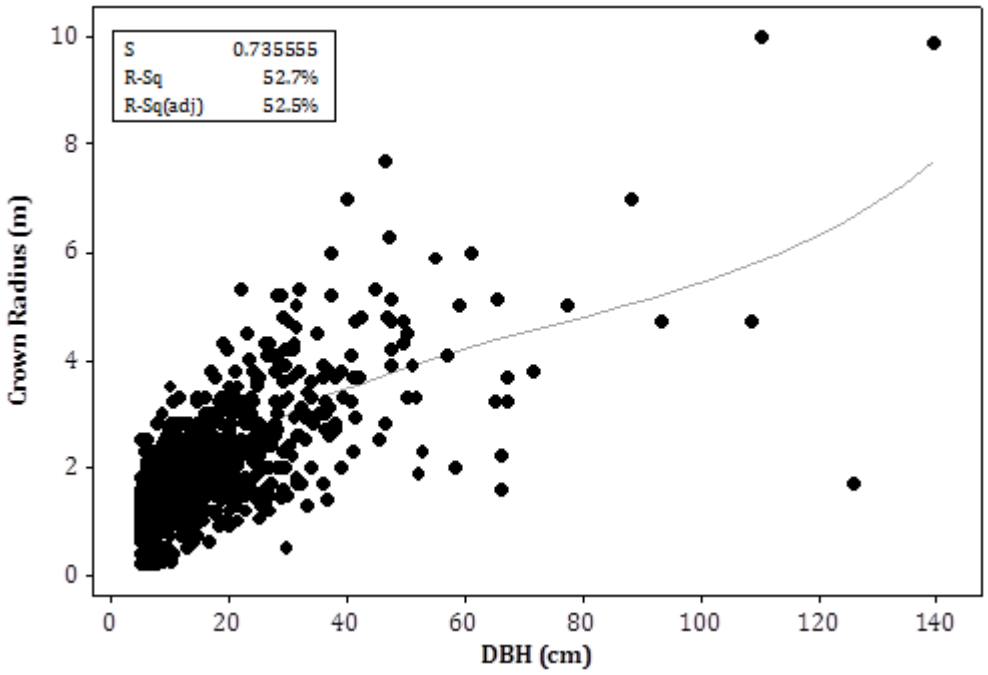

Figure 3.3.2.10: Relationship between DBH and crown radius (Cubic model) at the leeward forest plot.

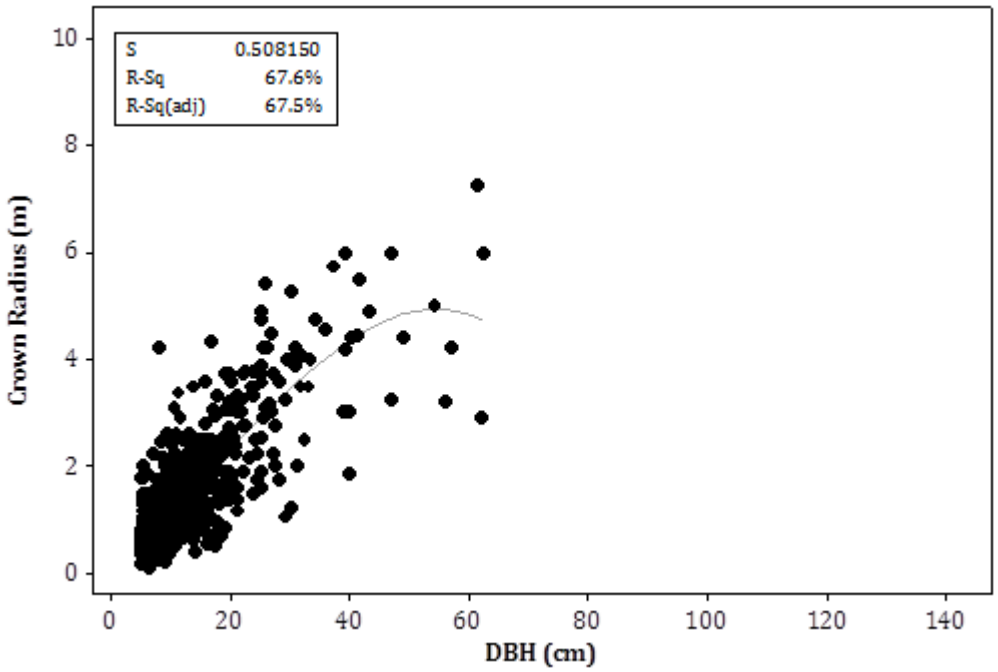

Figure 3.3.2.11: Relationship between DBH and crown radius (Cubic model) at the ridge forest plot.

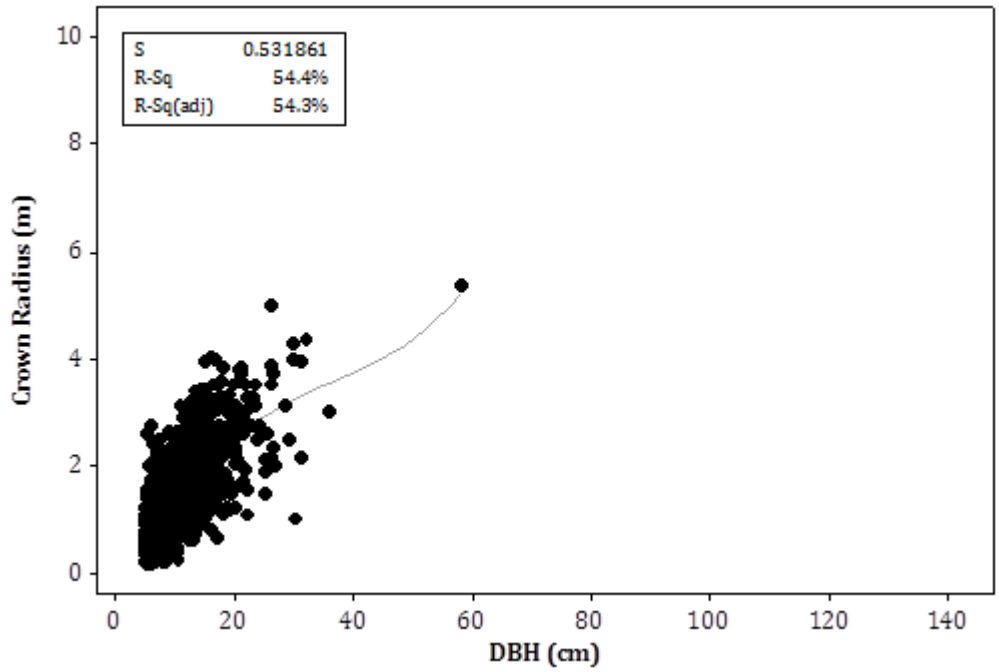

Figure 3.3.2.12: Relationship between DBH and crown radius (Cubic model) at the windward forest plot.

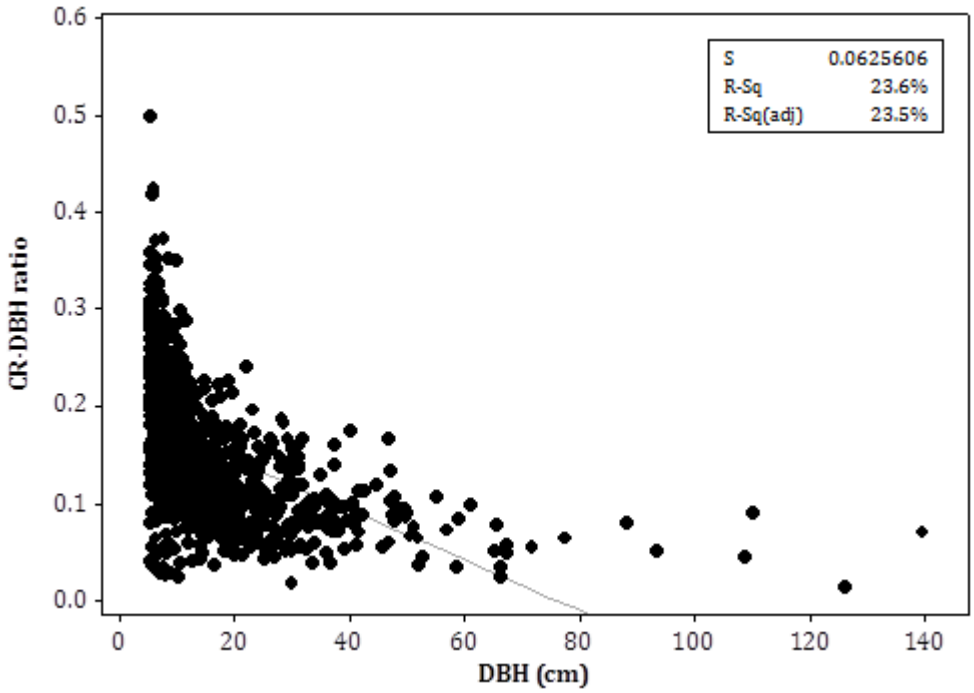

Figure 3.3.2.13: Relationship between DBH and the CR-DBH ratio (linear model) at the leeward forest plot.

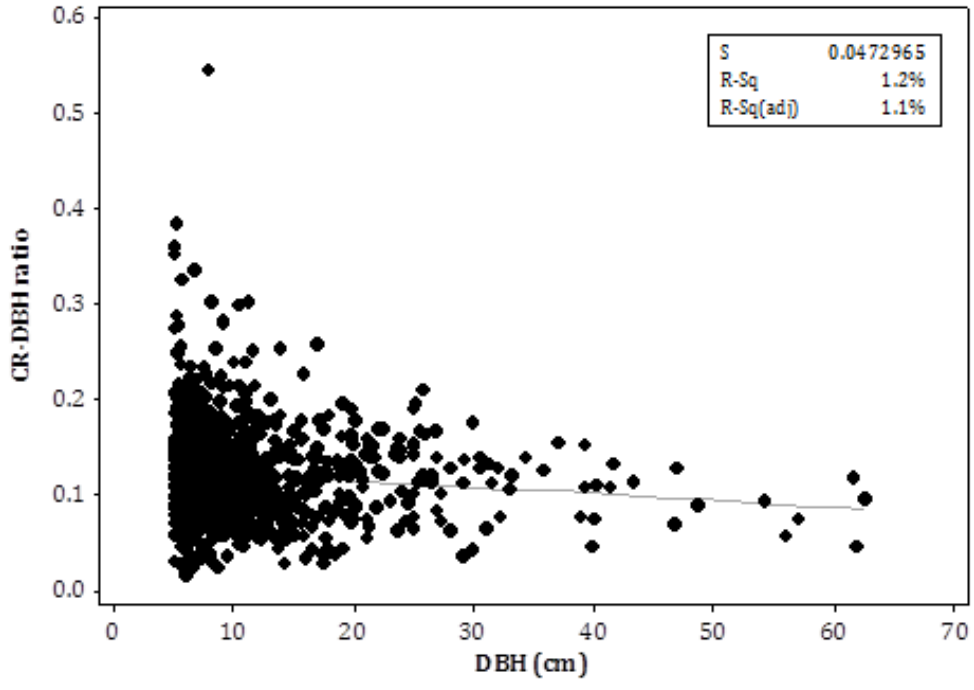

Figure 3.3.2.14: Relationship between DBH and the CR-DBH ratio (linear model) at the ridge forest plot.

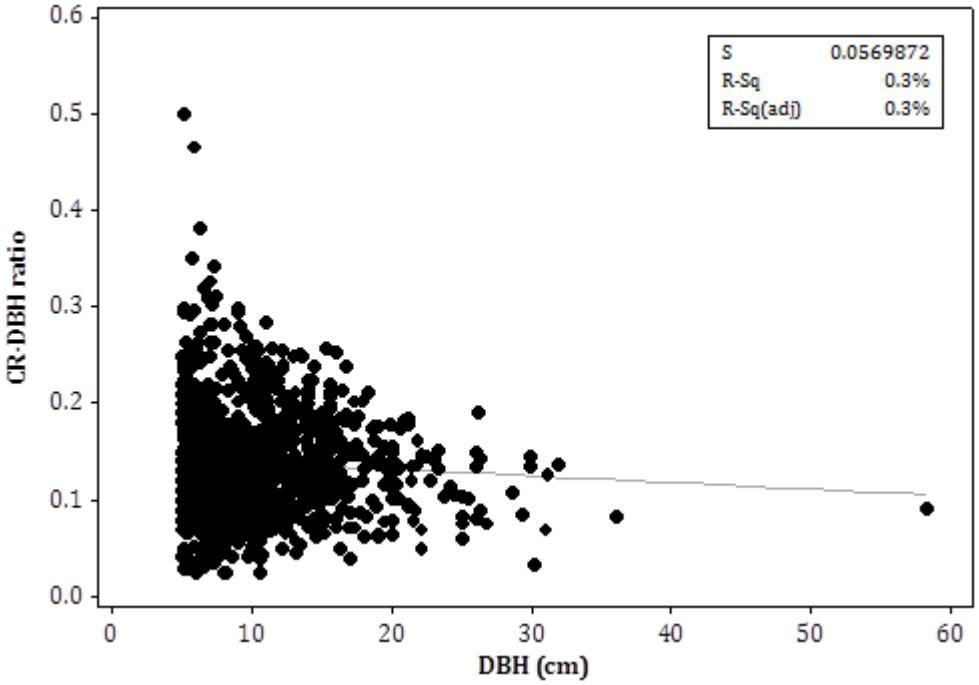

Figure 3.3.2.15: Relationship between DBH and the CR-DBH ratio (linear model) at the windward forest plot.

3.3.3 Leaf Characteristics

In the ≥ 5 cm diameter class, the ridge forest showed a higher proportion of species with leaf drip-tips, followed by the windward and leeward forests, while in the ≥ 10 cm class, the leeward site showed a higher proportion (Figure 3.3.3.1). In terms of the proportion of total arboreal foliage, the importance of leaf drip-tips was reduced in the ridge and windward plots compared to the proportion of species exhibiting this trait (Figure 3.3.3.1).

The windward forest presented a slightly greater proportion of species with compound leaves in all diameter classes, and the ridge forest showed the least, but considered as a proportion of the arboreal foliage present, compound leaves formed a more important proportion of the leeward forest canopy than at the other forests (Figure 3.3.3.1).

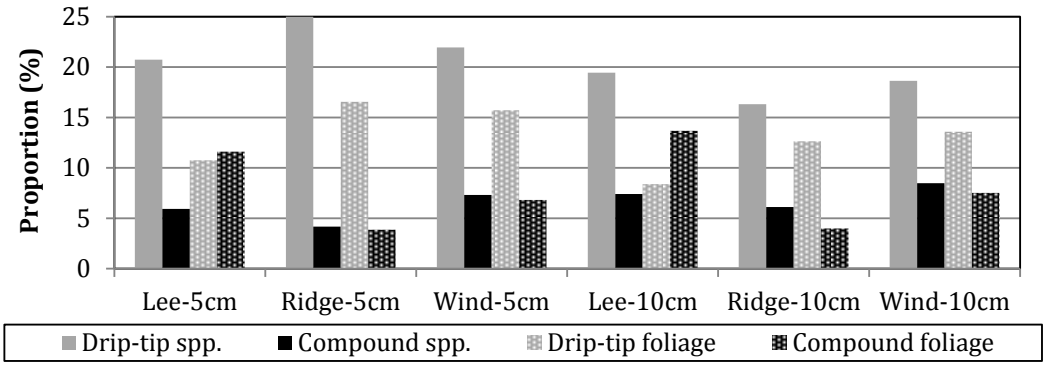

Figure 3.3.3.1: Proportion of species and arboreal foliage with leaf drip-tips and compound leaves at the leeward, ridge and windward sites for both ≥ 5cm and ≥ 10cm diameter classes.

The leeward forest presented a larger number of species with mesophyllous leaves, while the ridge and windward forests had a larger number of species with notophyllous leaves (Figure 3.3.3.2). This trend carried through to the proportion of arboreal foliage at the leeward and windward forests, yet the ridge forest canopy arboreal foliage was dominated by microphyllous leaf types, with the leeward and windward forests showing an increase in the importance of fern fronds (Figure 3.3.3.3). As such, about half the ridge site arboreal foliage was microphyllous or smaller, while this proportion was vastly less at the leeward and windward sites.

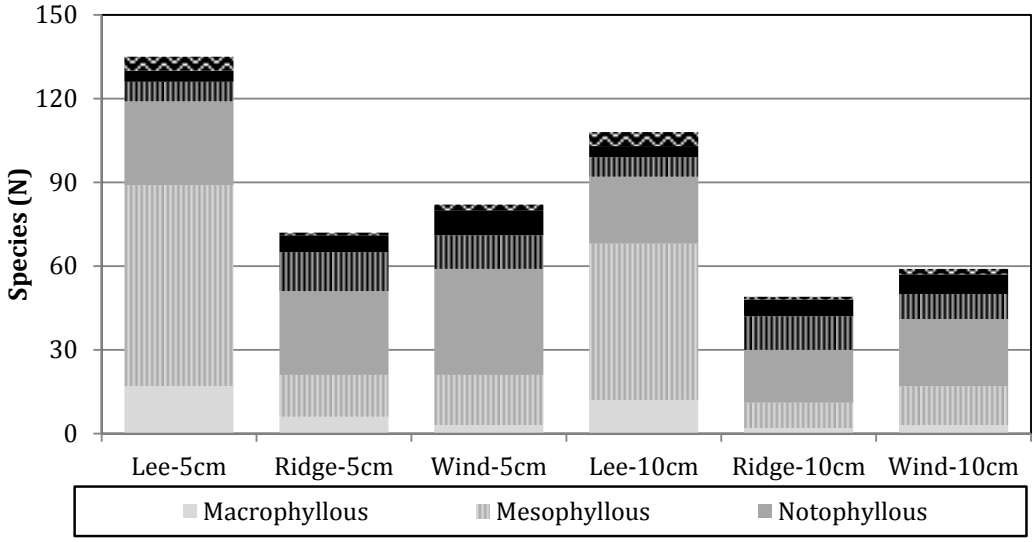

Figure 3.3.3.2: Distribution of leaf size classes among the species present at the leeward, ridge and windward sites for both ≥ 5cm and ≥ 10cm diameter classes.

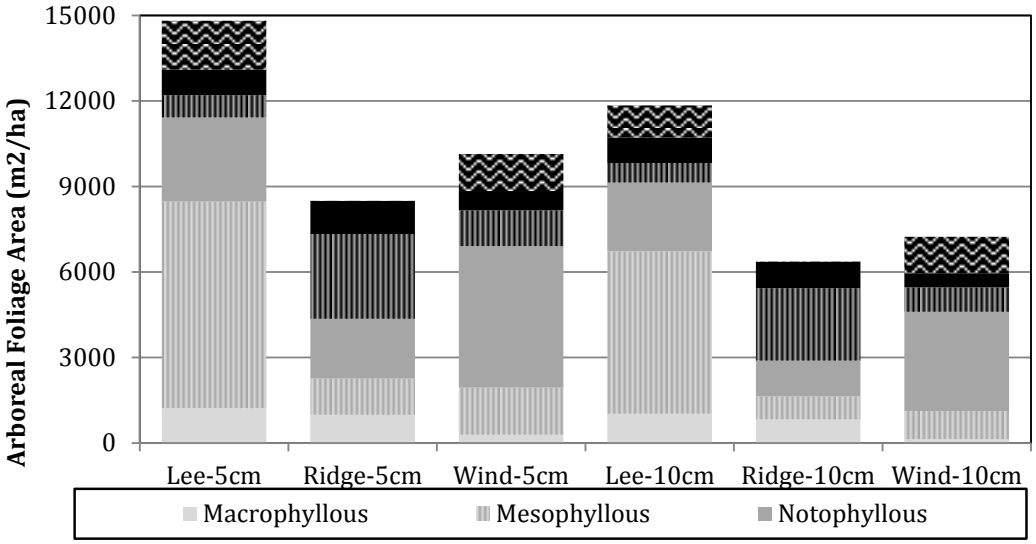

Figure 3.3.3.3: Distribution of leaf size classes among the total arboreal foliage area present at the leeward, ridge and windward sites for both ≥ 5cm and ≥ 10cm diameter classes.

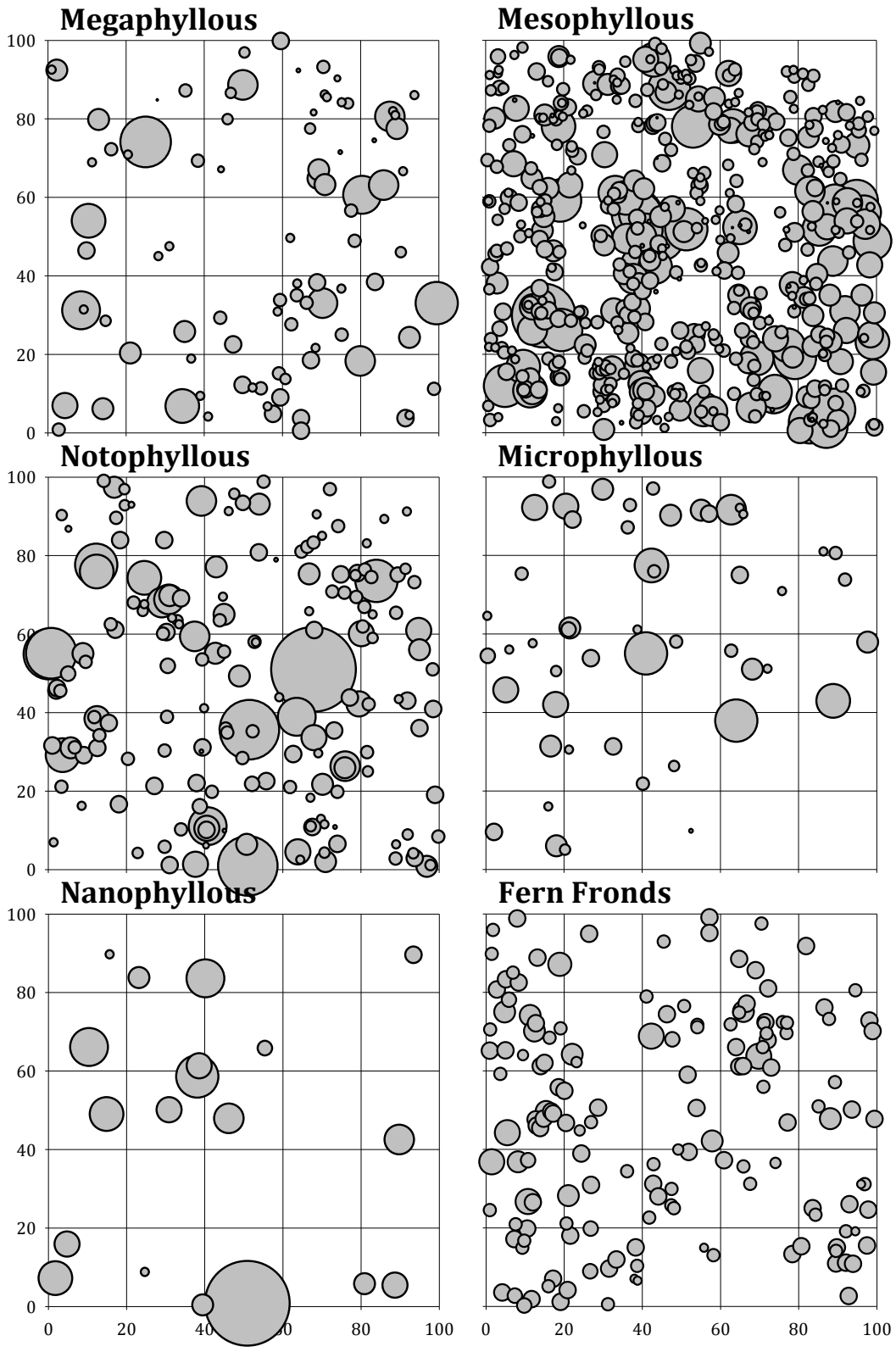

Figure 3.3.3.4: Dispersion of crowns per leaf size class at the leeward forest. Circles indicating crowns are to scale.

The dispersion of leaf sizes at the leeward forest shows a good distribution of the dominant mesophyllous species over the entire in the plot, with fern fronds common in areas free of other tree crowns trend (Figure 3.3.3.4).

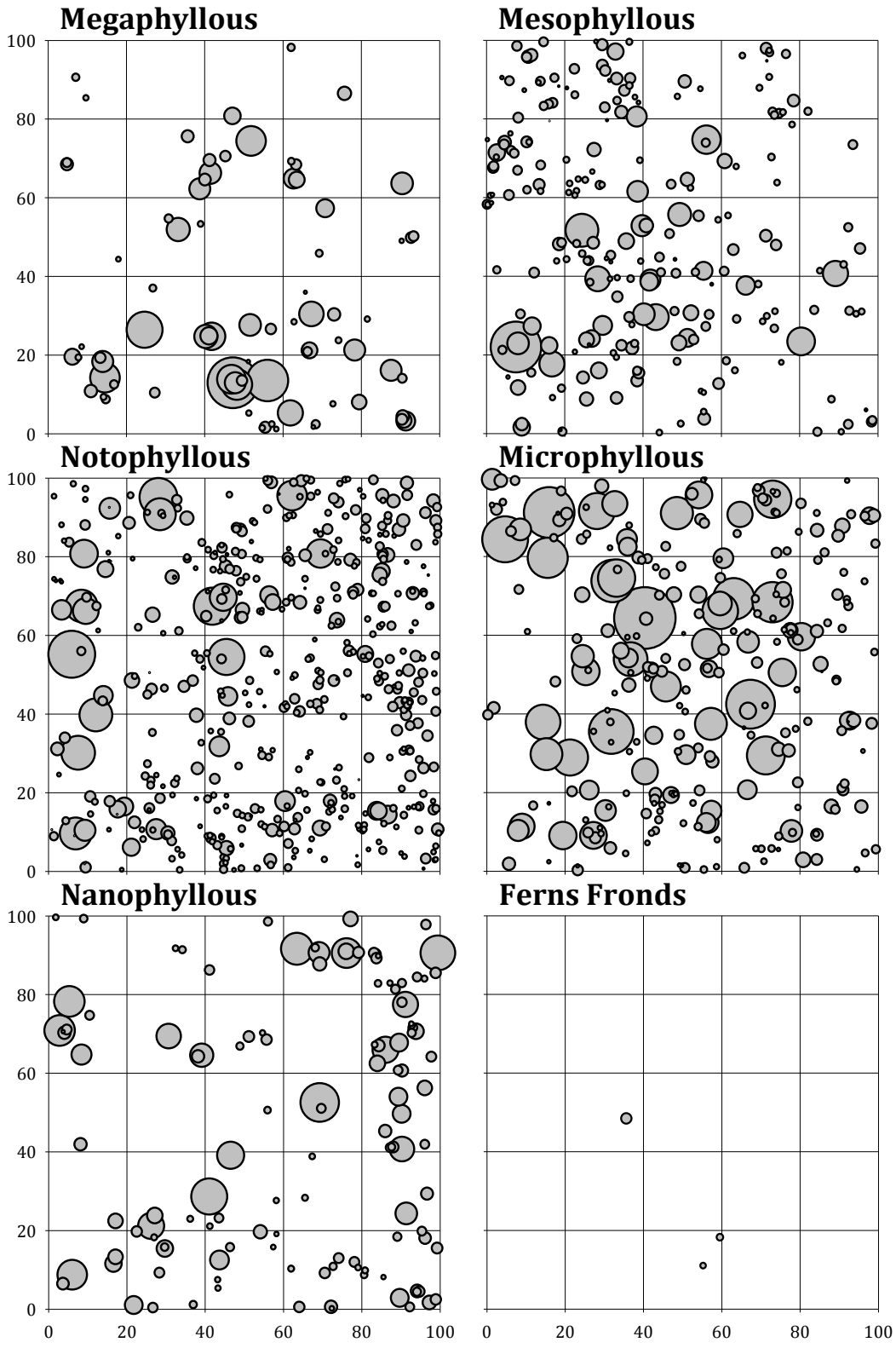

Figure 3.3.3.5: Dispersion of crowns per leaf size class at the ridge forest. Circles indicating crowns are to scale.

At the ridge forest, the large notophyllous crowns appeared in the more sheltered areas, while on the exposed side of the ridge, the majority of larger crowns were micro- and nanophyllous (Figure 3.3.3.5).

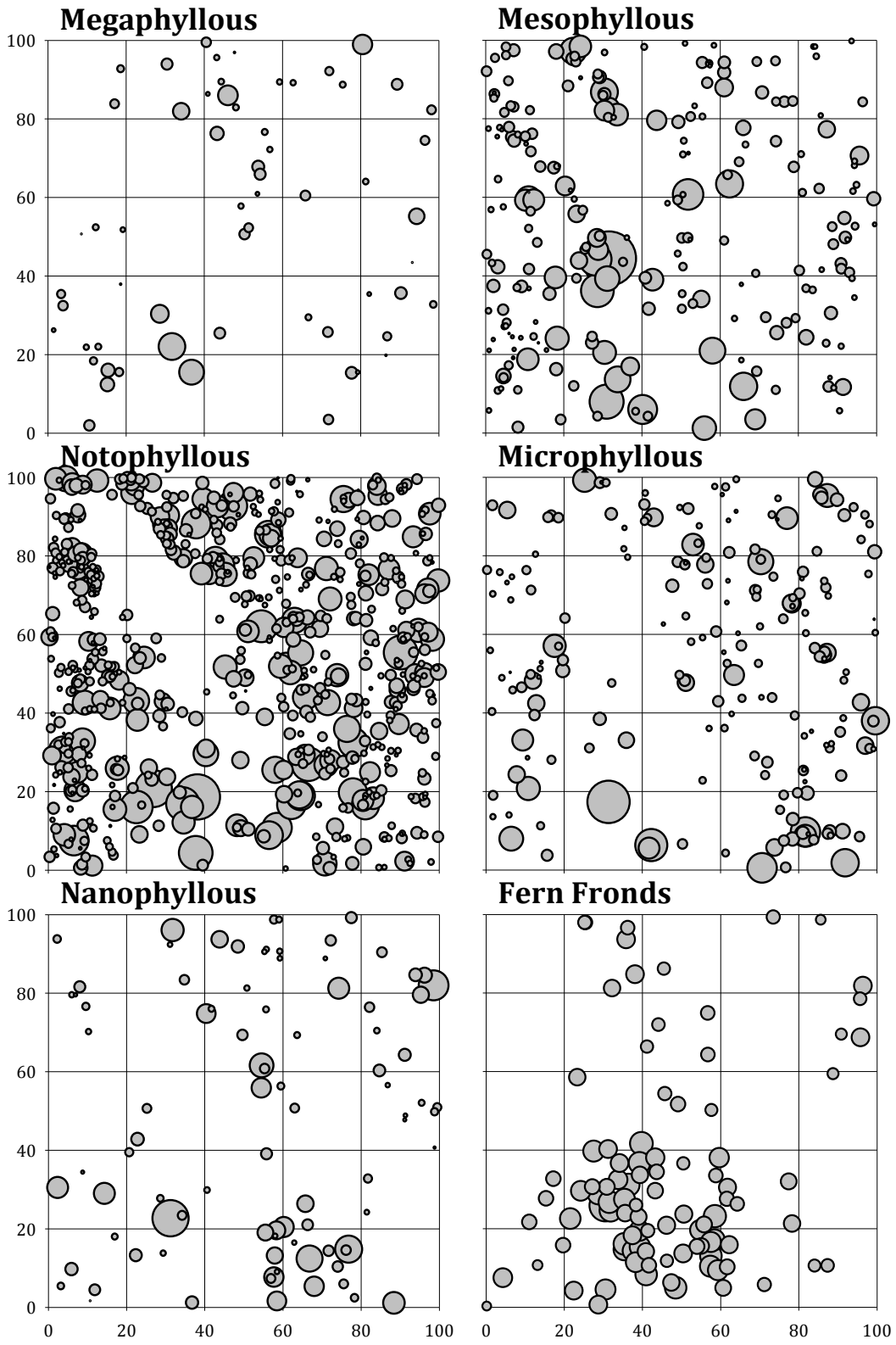

Figure 3.3.3.6: Dispersion of crowns per leaf size class at the windward forest. Circles indicating crowns are to scale.

At the windward site, the most notable feature was the clustered nature of the ferns and the lack of megaphyllous crowns (Figure 3.3.3.6).

Though sampling of leaf sizes was not adequate for statistical tests, a number of species clearly showed different leaf sizes in different forests. *Gordonia fruticosa* was notophyllous at the leeward forest and microphyllous at the windward forest, *Meliosma frondosa* was megaphyllous at the leeward forest and mesophyllous at the other forests, *Myrsine andina* was notophyllous at the windward forest and microphyllous at the ridge forest, while *Myrsine coriacea* was notophyllous at the leeward forest and microphyllous at the ridge and windward forests.

3.3.4 Community Associations

3.3.4.1 Leeward Forest

The cluster analyses for the leeward forest showed three clusters with the dendrogram truncated at a low level of remaining information (low similarity). Group 1 comprised of nine subplots, Group 2 comprised of 14 subplots, while the associated Group 3 was comprised of just two sub-plots (Figure 3.3.4.2). The tree ferns *Cyathea* sp. 3 followed by *Alsophila* sp. 1 were the most abundant group 1 species, the former being absent in high abundance in group 2, while *Guarea kunthiana* was the most abundant species of both groups 2 and 3, which with *Weinmannia lecheriana*, was absent from group 1 (Table 3.3.4.1). The group 3 also houses the majority of *Perrottetia* sp. 1 individuals. Perhaps a mayor difference between groups 1 and 2 is the different abundance of the Cyatheaceae.

The indicator species analysis showed that the large cluster groups 1 and 2 were heterogeneous clusters, with only the presence of *Alsophila* sp. 1 being moderately likely (60.0% probability) to be predictive of group 1, group 2 had no statistically significant indicator species, while the small group 3 had *Persea* sp. 1 (100% probability), *Cecropia* sp. 1 (95.5% probability) and *Perrottetia* sp. 1 (91% probability) as very strong indicator species (Appendix I).

The NMS ordination of all sub-plots resulted in a 3-dimensional result, in which the the cluster group 1 and (the closer related) both groups 2 and 3 were separated on the second axis (Figure 3.3.4.1). Of the 18 species that showed at least a moderate correlation ($r \geq 0.4$) with an ordination axis (see Appendix J), only *Guarea kunthiana* (group 2 & 3) showed moderate correlations with two axes (axis 2, r -0.47; axis 3, r 0.58), while the strongest correlations were between *Cecropia* sp. 2 (group 2) and axis 1 (r 0.77) and between *Cyathea* sp. 2 (group 1) and axis 2 (r -0.68). Three pairs of species showed high pairwise association (0.8), but they were all pairs of species with sub-plot frequencies of two and three, thus do not warrant further mention. The joint plot showed a strong vector for O layer Al^{+3} content (Figure 3.3.4.1), also on the second axis, thus coinciding with the floristic dissimilarity between cluster group 1 and both groups 2 and 3. This variable was strongly correlated to axis 2 (r 0.64), whilst other moderate correlations with axes were found for four other soil parameters, LAI and stem incline (see Appendix K). The physical layout of the cluster grouped sub-plots at the leeward forest has some trends that may explain some of differences between the two large cluster groups, with the group 2 subplots on the

southern side occupying the areas most protected from windthrow and the two neighbouring group 3 subplots are located in one of the steepest and most protected sections of the 1-ha plot (Figure 3.3.2.5), which appeared to maintain a very high level of humidity due to shading and southern aspect (pers. obs. D. Catchpole).

Table 3.3.4.1: Relative abundance (ra) of abundant species (ra ≥ 2%) per cluster group within the leeward forest plot.

№	Group 1	ra	Group 2	ra	Group 3	ra
1	*Cyathea* sp. 3	12.9	*Guarea kunthiana*	7.0	*Guarea kunthiana*	15.0
2	*Alsophila* sp. 1	9.8	*Cecropia* sp. 2	6.7	*Perrottetia* sp. 1	11.7
3	dead	4.9	dead	6.0	*Weinmannia lechleriana*	8.3
4	*Miconia adinantha*	4.9	*Alsophila* sp. 1	5.6	*Cyathea* sp. 3	6.7
5	*Nectandra cissiflora*	3.6	*Weinmannia lechleriana*	4.9	*Cecropia* sp. 1	5.0
6	*Alchornea grandis*	3.1	*Alchornea grandis*	4.2	*Cyathea pallescens*	3.3
7	*Miconia banggi*	3.1	*Miconia adinantha*	3.9	*Eugenia* sp. 5	3.3
8	*Myrsine pellucida*	2.7	*Myrsine pellucida*	3.2	*Guettarda* sp. 2	3.3
9	*Eugenia* sp. 4	2.2	*Miconia banggi*	2.5	*Hedyosmum anisodorum*	3.3
10	*Myrsine coriacea*	2.2	*Weinmannia* sp. 2	2.5	*Miconia adinantha*	3.3
11			*Cyathea* sp. 2	2.1	*Miconia banggi*	3.3
12			*Topobea multiflora*	2.1	*Nectandra reticulata*	3.3
13					*Persea* sp. 1	3.3

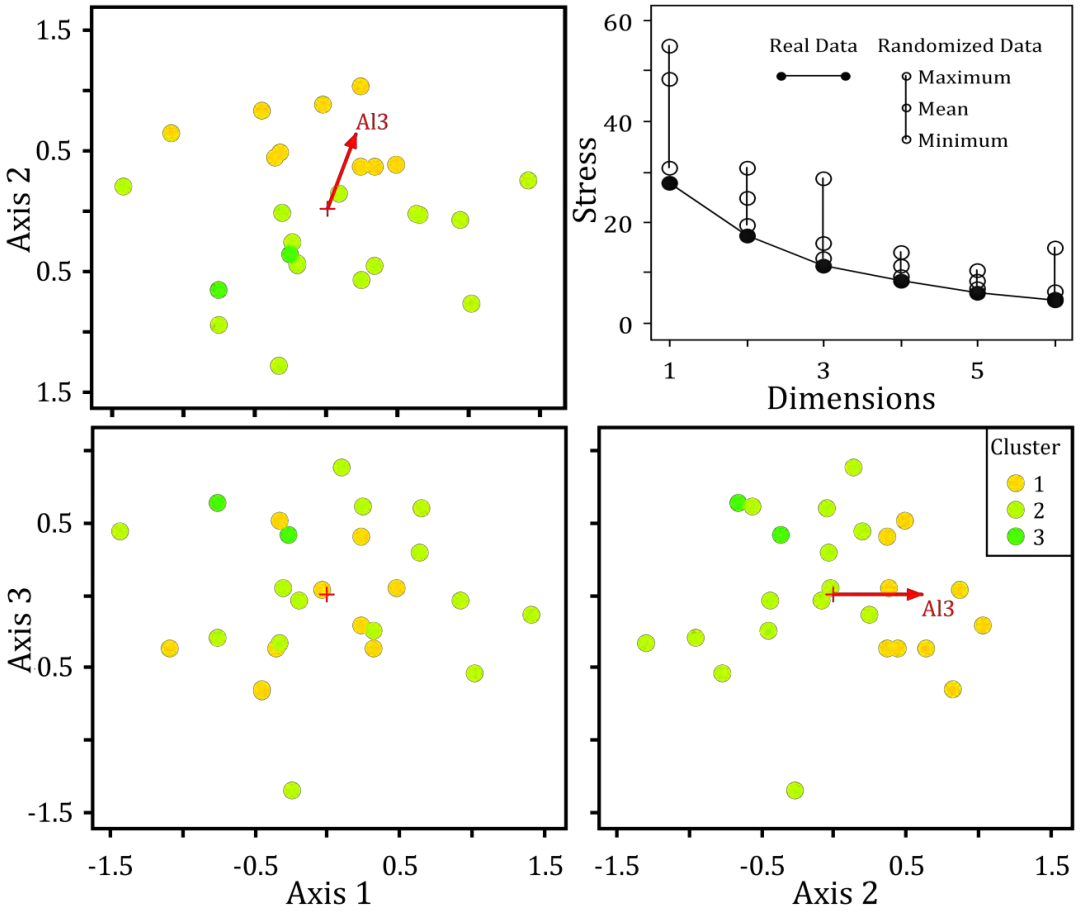

Figure 3.3.4.1: NMS ordination results and joint plot of leeward forest sub-plots for the ≥ 10cm diameter class. See text for joint plot codes.

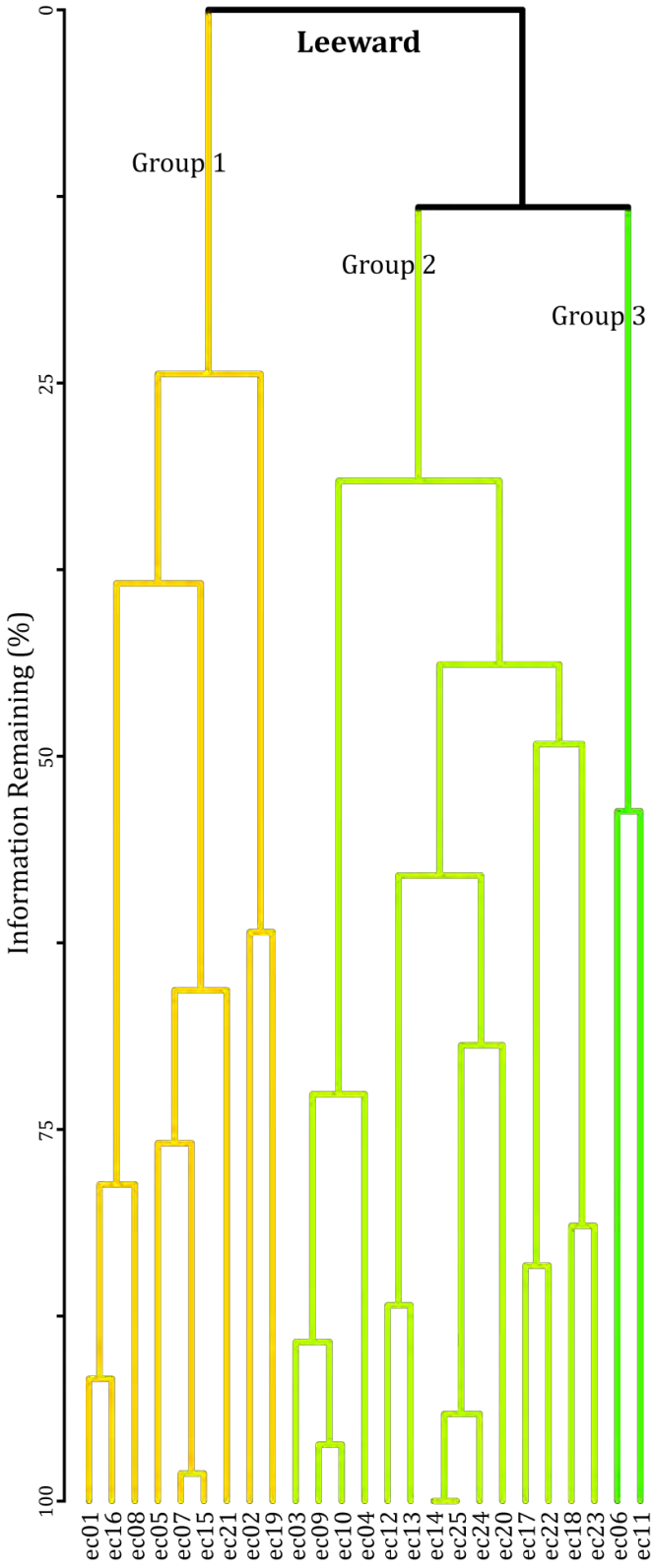

Figure 3.3.4.2: Dendrogram for the cluster analysis of 25 sub-plots for the ≥ 10 cm diameter class at the leeward forest.

The one-way ANOVAs on biophysical variables of the cluster group sub-plots found that group 2 showed significantly lower ≥5cm DBH stem density than groups 1 and 3 (P = 0.006), group 3 had significantly higher arboreal foliage

area in both diameter classes than group 2 (P = 0.043), group 3 slope, bryophyte cover and A horizon pH were significantly higher than that of groups 1 and 2 (P = 0.047, P = 0.001, P = 0.004 respectively).

3.3.4.2 Ridge Forest

The cluster analyses for the ridge forest showed three clusters with the dendrogram truncated at a low level of remaining information (low similarity). Group 4 comprised of eight subplots, the associated Group 5 was comprised of four subplots, while Group 3 was comprised of 13 sub-plots (Figure 3.3.4.4).

Miconia aprica followed by *Weinmannia balbisiana* were the most abundant species in both groups 4 and 5, highlighting their similarity, while *Myrsine andina* was the most abundant species of group 6, which was present in the other groups but with much lower abundance (Table 3.3.4.2). There was a large reduction of *Miconia aprica* abundance, in group 6, while absences of note include that of *Hedyosmum lechleri* in group 4, *Podocarpus* spp. from group 5 and *Podocarpus oleifolius* was restricted to group 6.

The indicator species analysis reflected a large amount of overlap among the groups, with only the presence of *Myrsine andina* being moderately likely (65.6% probability) to be predictive of group 6, and group 4 had no statistically significant indicator species (see Appendix I). Moreover, *M. andina* along with other indicators of moderate likelihood were also present among the abundant species of other groups. The NMS ordination of all sub-plots resulted in a 3-dimensional result, in which the cluster group 6 and both (closer related) groups 4 and 5 were separated on the first axis (Figure 3.3.4.3).

Of the 16 species that showed at least a moderate correlation ($r \geq 0.4$) with an ordination axis (see Appendix J), only *Weinmannia microphylla* (group 4 & 5) showed moderate correlations with two axes (axis 1, r -0.45; axis 2, r -0.57), while the strongest axis correlations were shown by *Myrsine andina* (Axis 1, r 0.7) and *Clusia elliptica* (axis 1, r -0.61). Only two pairs of species showed high pairwise association (0.8), but they were all pairs of species with abundances of two and three, thus do not warrant further mention.

The joint plot ($r2 \geq 0.4$) showed strong and opposing vectors for bryophyte ground cover and leaf litter ground coverage (Figure 3.3.4.3), also on the first axis, thus coinciding with the floristic dissimilarity between cluster group 6 and both groups 4 and 5. These were the only strongly correlated factors (axis 1, r 0.67, -0.63 respectively), while eight of the 26 biophysical variables showed a moderate correlation (r 0.4 to <0.6) with one or more axes including average basal and crown area, stem height and incline, visible sky fraction, slope, P and K (Appendix K). As opposed to the leeward forest, the physical distribution of the cluster grouped sub-plots at the ridge forest was strongly related to the position on the ridge, clearly defining an east-west transition of species distribution (Figure 3.3.2.6).

Table 3.3.4.2: Relative abundance (ra) of abundant species (ra ≥ 2%) per cluster group for the ≥ 10 cm diameter class within the ridge forest plot.

Group 4	ra	Group 5	ra	Group 6	ra
Miconia aprica	15.4	*Miconia aprica*	25.0	*Myrsine andina*	14.8
Weinmannia balbisiana	9.4	*W. balbisiana*	17.5	*W. balbisiana*	11.5
Clusia elliptica	7.7	*Hedyosmum lechleri*	11.3	*Clusia alata*	8.6
W. microphylla	6.8	*Clusia elliptica*	5.0	*Hedyosmum lechleri*	8.6
Schefflera angulata	6.0	dead	5.0	*Freziera* sp. 4	6.2
Clusia alata	5.1	*Miconia* sp. 1	5.0	*Schefflera angulata*	5.3
Gordonia sp. 1	5.1	*Freziera* sp. 4	3.8	*Miconia aprica*	4.3
dead	4.3	*Myrsine andina*	3.8	*Miconia saltuensis*	3.8
Myrsine andina	3.4	*W. microphylla*	3.8	*Podocarpus oleifolius*	3.8
Podocarpus magnifolius	3.4	*Miconia saltuensis*	2.5	dead	3.3
Miconia lasiostyla	2.6			*Ilex hualgayoca*	3.3
Miconia sp. 1	2.6			*Hedyosmum dombeyanum*	2.9
Myrsine coriacea	2.6			*Podocarpus magnifolius*	2.9
Nectandra sp. 1	2.6			*Clusia elliptica*	2.4
Nordenstamia cajamarcensis	2.6			*W. pinnata*	2.4
W. aff. *auriculata*	2.6				

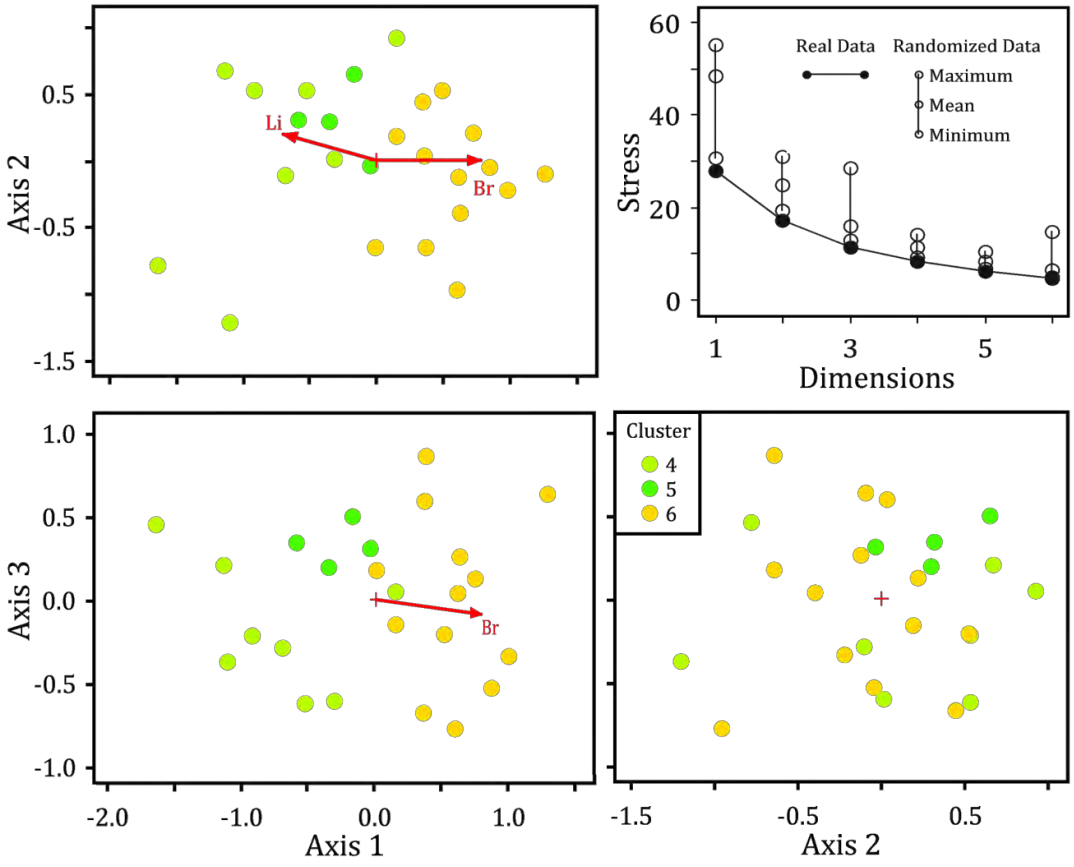

Figure 3.3.4.3: NMS ordination results and joint plot of ridge forest sub-plots for the ≥ 10cm diameter class. See text for joint plot codes.

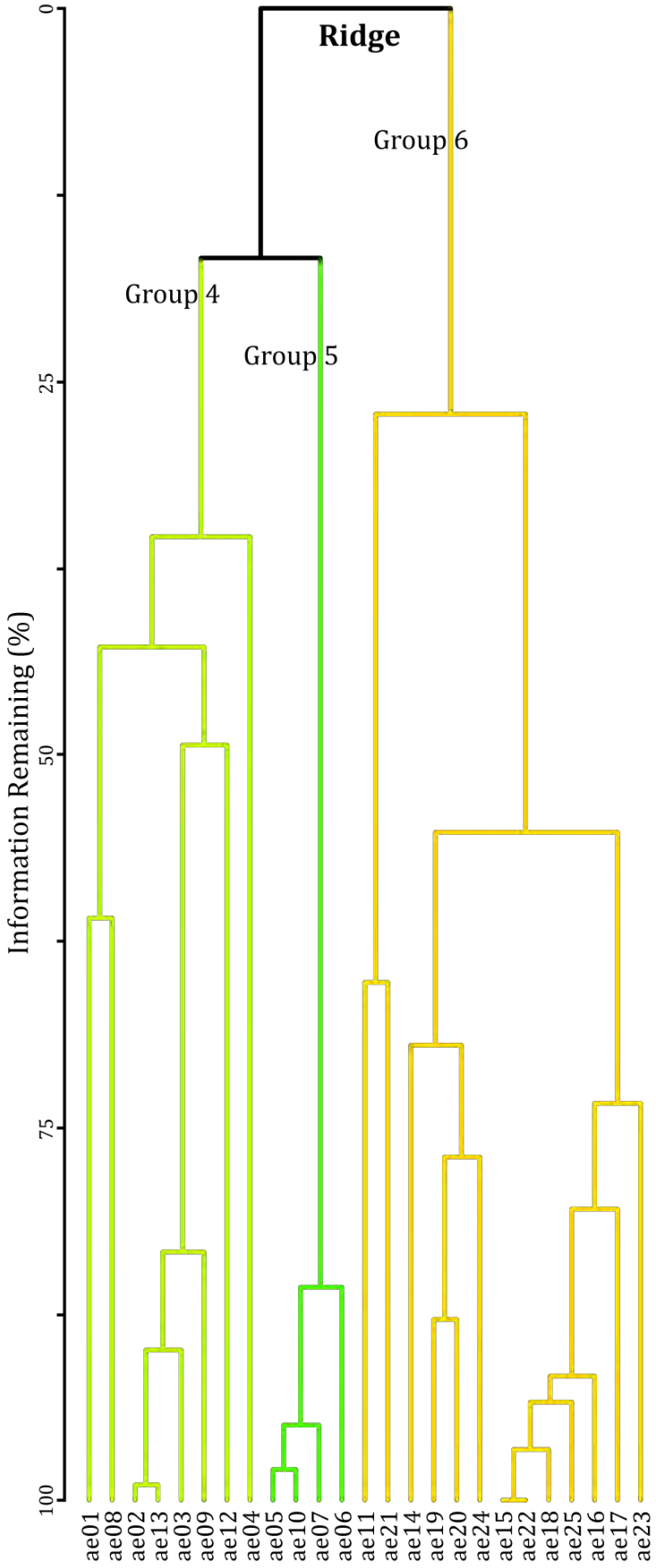

Figure 3.3.4.4: Dendrogram for the cluster analysis of 25 sub-plots for the ≥ 10 cm diameter class at the ridge forest.

The one-way ANOVAs on biophysical variables of the cluster group sub-plots found that group 4 sub-plots showed significantly lower ≥5cm DBH stem density, higher average basal area, average crown area and average stem height in both diameter classes, higher maximum stem height, higher leaf litter cover, lower bryophyte cover, than group 6 ($P < 0.022$).

3.3.4.3 Windward Forest

The cluster analyses for the windward forest showed three clusters with the dendrogram truncated at a low level of remaining information (low similarity). Group 7 comprised of nine subplots, the associated Group 8 was comprised of two subplots, while Group 9 was comprised of 14 sub-plots (Figure 3.3.4.6). *Cyathea caracasana* was the most abundant species in both groups 7 and 8, and second most abundant in group 9 though much less abundant than the other groups, while *Clusia schultesii* was the most abundant species of group 9, which showed much lower abundance in group 7 and was not abundant in group 8 (Table 3.3.4.3). All groups showed a high abundance of standing dead individuals. *Freziera* spp. were only abundant in group 7, *Schefflera pedicellata* and *Weinmannia auriculata* were only abundant in group 9, while aside from *Cyathea caracasana* and *Weinmannia pinnata* that were abundant at all sites, the group 8 abundant species were not abundant at any other sites.

The indicator species analysis revealed five species likely (63 to 87.5% probability) to be predictive of group 8, *Clusia schultesii* was the highest indicator species for group 9 (82.1%), while no indicator species were revealed for group 7 (Appendix I).

The NMS ordination of all sub-plots resulted in a 2-dimensional result, in which the cluster group 9 and both (closer related) groups 7 and 8 were separated on the first axis (Figure 3.3.4.5). Of the 16 species that showed at least a moderate correlation ($r \geq 0.4$) with an ordination axis (see Appendix J), six species showed correlations with both axes. *Clusia schultesii* showed a strong correlation with axis 1 (r 0.77), as did *Cyathea caracasana* (axis 1, r 0.69) and *Freziera* sp. 1 with axis 2 (r -0.62). Only two pairs of species showed high pairwise association (0.8), but similar to results for the previous sites, they were all pairs of species with abundances of two and three, thus do not warrant further mention.

The joint plot ($r^2 \geq 0.4$) showed vectors for the majority of structural parameters, with slope coinciding with the axis one trend to separate group 9 from groups 7 and 8, while the average crown area vector indicated toward group 8 (Figure 3.3.4.5). These variables, along with stem density, species richness, total crown area, average basal area and stem height, were all strongly correlated with one or two axes, while nine other variables showed moderate correlations (r 0.4 to <0.6) with axes including total basal, stem incline, visible sky fraction, below canopy radiation, coarse woody debris cover, rootmat height, O-layer pH, OM, P, K and soil bulfk density (see Appendix K). Similar to the ridge forest, the physical distribution of the cluster grouped sub-plots at the windward forest appeared strongly related to the microtopography, with group 9 representing communities on steeper

and more exposed areas (Figure 3.3.2.7). The location of the two neighbouring group 8 sub-plots is the most heavily wooded area of the plot.

The one-way ANOVAs on biophysical variables of the cluster group sub-plots found that group 8 sub-plots showed significantly higher ≥10cm DBH stem density and total stem length, higher ≥5 cm DBH average height and less inclined stems in both diameter classes than group 9 ($P < 0.015$), group 8 showed significantly higher average crown area in both diameter classes and higher ≥10cm DBH average height than group 7 and 9 ($P < 0.021$), group 9 showed significantly lower maximum height and higher slope angles than groups 7 and 8 ($P = 0.005$), while group 7 showed significantly higher course woody debris cover and lower O horizon K than group 9 ($P = 0.009$).

Table 3.3.4.3: Relative abundance (ra) of abundant species (ra ≥ 2%) per cluster group within the windward forest plot.

№	Group 7	ra	Group 8	ra	Group 9	ra
1	dead	32.5	*Cyathea caracasana*	39.7	*Clusia schultesii*	31.4
2	*Cyathea caracasana*	15.8	dead	14.1	dead	7.8
3	*Freziera* sp. 1	7.3	*Weinmannia pubescens*	6.4	*Cyathea caracasana*	6.5
4	*Clusia schultesii*	3.8	*Weinmannia pinnata*	5.1	*Myrcia* sp. 1	5.9
5	*Freziera* sp. 2	3.4	*Clethra revoluta*	3.8	*Schefflera pedicellata*	5.9
6	*Ilex teratopis*	3.0	*Beilschmiedia latifolia*	2.6	*Weinmannia auriculata*	5.2
7	*Weinmannia pinnata*	3.0	*Cyathea delgadii*	2.6	*Ocotea arnottiana*	4.9
8	*Ruagea pubescens*	2.1	*Hyeronima* sp. 1	2.6	*Gordonia fruticosa*	3.3
9	*Ternstroemia* sp. 1	2.1			*Schefflera* sp. 1	2.6
10					*Ternstroemia* sp. 1	2.6
11					*Weinmannia pinnata*	2.6

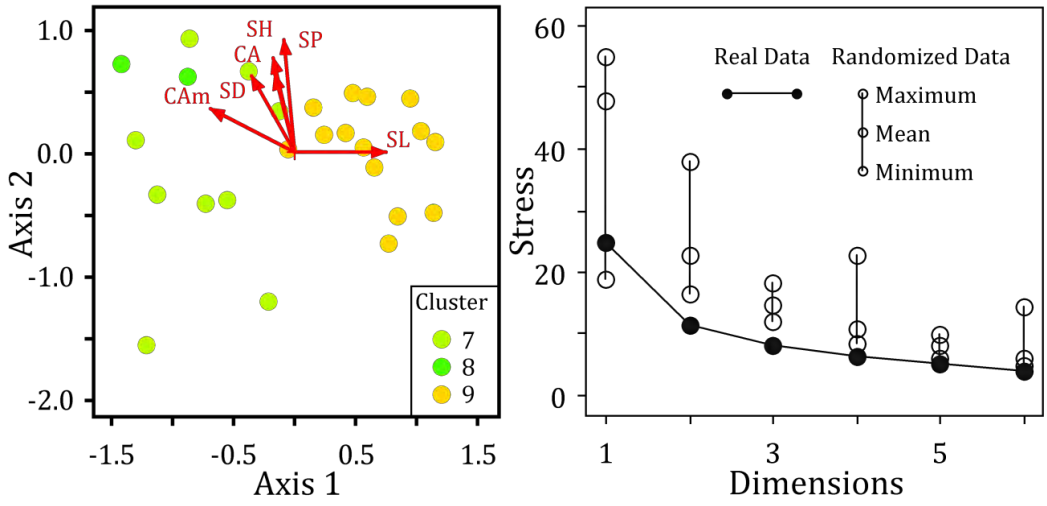

Figure 3.3.4.5: NMS ordination results and joint plot of windward forest sub-plots for the ≥ 10cm diameter class. See text for joint plot codes.

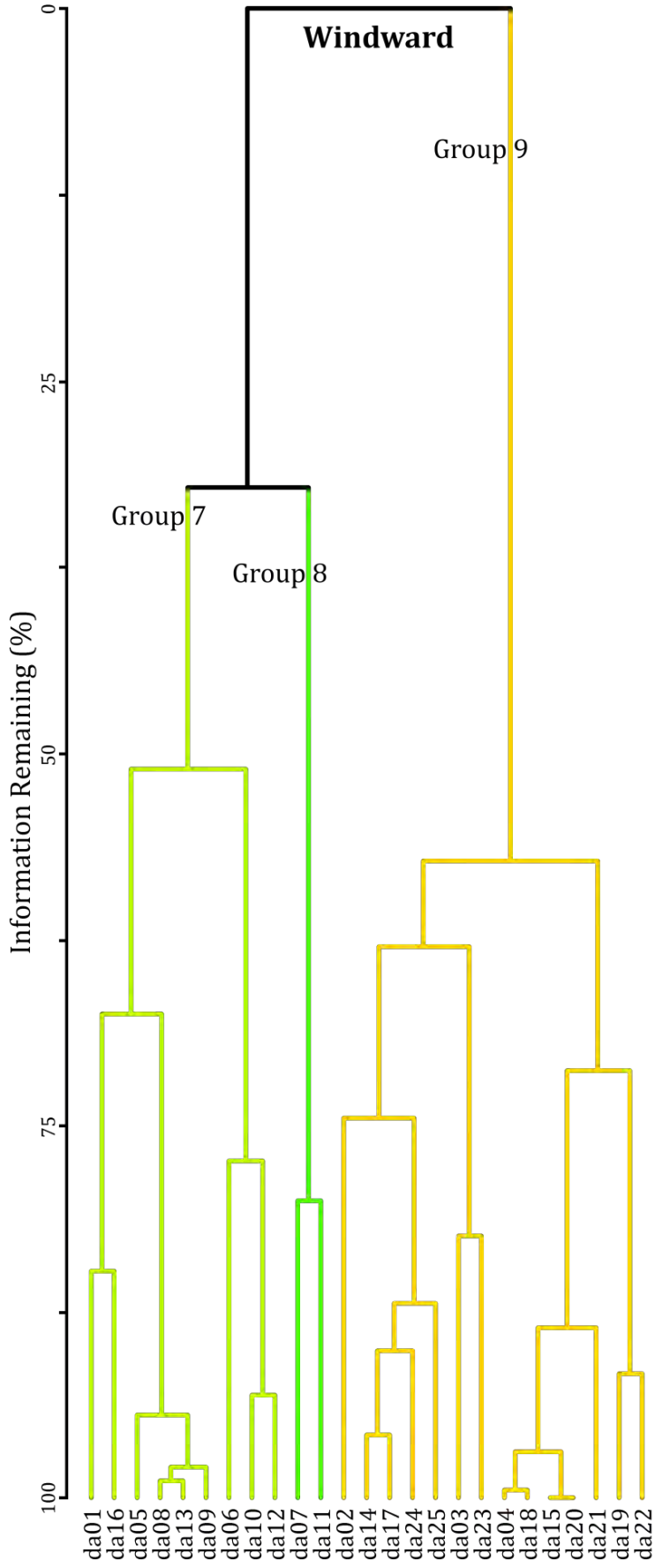

Figure 3.3.4.6: Dendrogram for the cluster analysis of 25 sub-plots for the ≥ 10 cm diameter class at the windward forest.

3.3.4.4 Forest Associations

The NMS ordination of all sub-plots resulted in a very strong 2-dimensional result, reflecting the very high species turnover between sites as the sub-plots from all sites were clearly separated into distinct groups according to forest plot (Figure 3.3.4.7). The ridge forest cluster groups identified per leeward and windward side of the ridge line were divided along the same vector that divides the leeward and windward forests. Likewise, the ridge and windward forest cluster groups identified as being associated with sheltered topographies (green colour) were also to some degree split along the same vertical vector, while the leeward and windward 'sheltered' groups also showed more affinity than the more 'exposed' groups.

The joint plot vectors demonstrated the differences in structural (stem incline, basal area) and soil (O layer pH, Al^{+3} and root mat height) characteristics between the leeward forest and the other forests, while the ridge forest showed the greater bryophyte coverage (Figure 3.3.4.7) as described by Taylor (2008). Given the distinctive compositions, it was not surprising that most biophysical parameters showed a moderate to very strong correlation ($r \geq 0.4$) with the ordination axes, reflecting the differences between forests of the soil parameters shown by Taylor (2008).

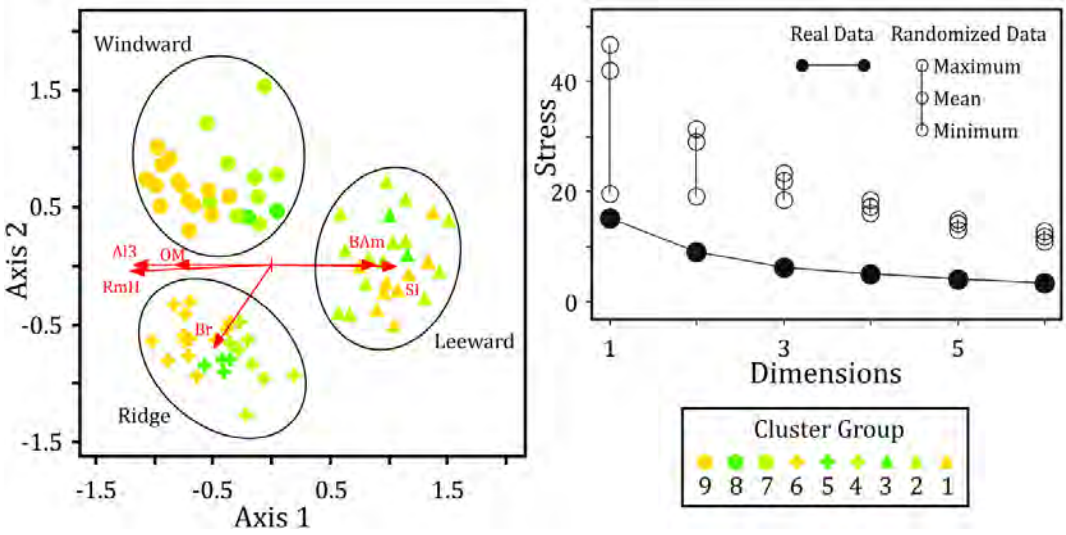

Figure 3.3.4.7: NMS ordination results, scree plot and joint plot of leeward, ridge and windward site sub-plots for the ≥ 10cm diameter class. See text for joint plot variable codes.

The dominance-abundance curves for all forests were well fitted to a lognormal distribution (R^2 = 0.98 – 0.99) that describes dominance by few species, with many species of intermediate abundances and an important proportion of rare species (Figure 3.3.4.8).

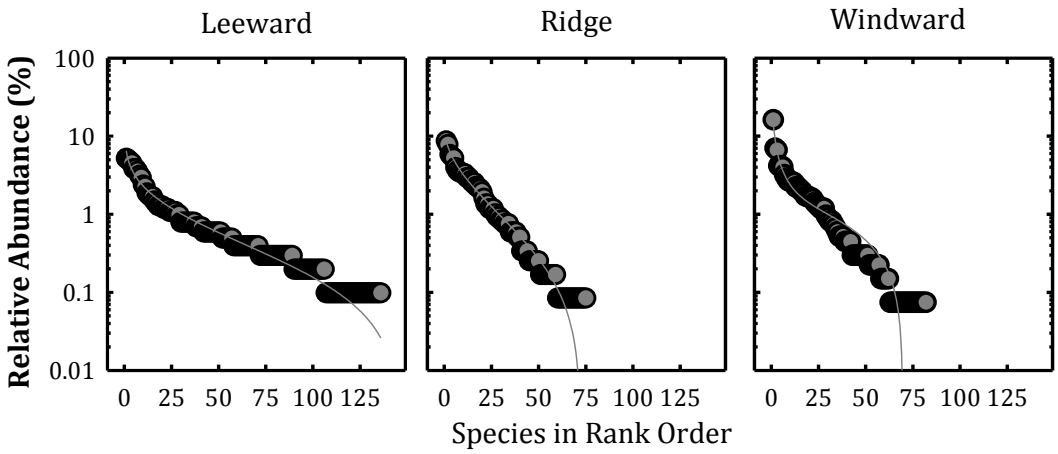

Figure 3.3.4.8: Dominance-Abundance curves for the woody species ≥ 5 cm DBH of all forests.

3.3.5 Species Dispersion

Very few of the species described recorded at the leeward forest plot showed clear signs of recruitment from a particular nearby mature individual within the plot, while various appeared to show tree fall gap colonization (Appendix L). At the ridge forest plot, a good proportion of the species showed preference for a particular part of the plot, with many species showing a highly clumped distribution (Appendix M). At the windward forest plot, many of the species showed a clumped distribution with preferences for certain areas of the plot (Appendix N), while all the Friziera spp. were clearly associated with the edges of the debris slide identified with the plot (Appendix Figure 49).

3.4 Discussion

3.4.1 Composition & Diversity

Gómez (1999) surveyed a 1-ha plot (≥ 10 cm DBH) just 300 m from the leeward forest plot at an altitude of 2450-2500 m with slightly steeper and variable topography and found a third more species (154 spp.) than the leeward plot survey in the present study, although it must be taken into account that his 1-ha plot was determined from a flat-plain projection, and given the extremely steep and variable terrain, the area of soil surface sampled was indeed much greater than the plot delimited in this study using RAINFOR protocols (Phillips & Baker, 2002). Nonetheless, combining both ≥ 10 cm class lists provides a total of 192 species, only 67 of which occur in both plots. However, the comparative confidence is limited as only ~20 % (32 spp.) of the species listed by Gómez (1999) were completely identified. Even so, with a very conservative comparison of both species lists at the family level, it would appear that at least 170 species of ≥ 10 cm DBH exist within the total area of both plots. This suggests a high rate of species turnover within the same forest type.

The distribution of relative abundances between the two surveys was similar, although within the 10 most abundant species of each survey there are a few species that do not occur in both plots. Notable, yet not floristically definitive,

was the absence of the large emergent species *Cedrela montana* (after which the area is named) and *Prumnopytis harmsiana* from the Gómez (1999) plot, while *Prumnopitys montana* was absent in the plot from this study.

The family and species richness of the cloud forests in the present study was higher than that found at an Ecuadorian upper montane forest (Valencia & Jørgensen, 1992), Costa Rican montane forests at 2600 m (Heaney & Proctor, 1990, Lieberman *et al.*, 1996) and an Ecuadorian leeward forest at 2900 m (Madsen & Ollgaard, 1994), although their ridge forest at 2700 m showed a near identical family and species richness as the ridge and windward forests of the present study.

When compared to the smaller plot statistics commonly reported (400 m^2), the ridge and windward forests were comparable to four Ecuadorian montane cloud forests with very similar altitude, annual temperature and rainfall, while the leeward forest showed a similar species richness to sites at much lower elevations at the same transect (Homeier *et al.*, 2010) and those of leeward cloud forest plots in Costa Rica (Häger & Dohrenbusch, 2010).

The H' scores for all forests were relatively high, higher than upper montane cloud forests in Sierra Nevada de Mérida, Venezuela (Ramírez *et al.*, 2009) and Southern Brazil (Scheer *et al.*, 2011), yet similar those from two large altitudinal transects (Kappelle *et al.*, 1995) and a lleward-windward transect in Costa Rica and several Bornean lower montane cloud forests (Pendry & Proctor, 1997, Takyu *et al.*, 2002).

In the windward to leeward cloud forest transect in Costa Rica, Häger & Dohrenbusch (2010) found equal species richness at lower leeward and windward forest, both of which had higher species richness than the ridge cloud forest, highest generic richness at the ridge forest, while the lowest family, genus and species richness was found at their leeward cloud forest. The present study reveals a very different distribution of richness, though their study recorded highest rainfall on the windward slope compared to the much lower windward rainfall recorded in this study. Madsen & Ollgaard (1994) also reported a higher species richness in a ridge forest compared to their leeward slope forest, although the plots were relatively distant and their leeward site was 200 masl higher than the ridge forest. However, comparing less comparable windward and leeward lower montane forests at c. 500 m in Puerto Rico, Weaver (2000) found the leeward slopes to be more species rich, and similar to the finding here, Takyu *et al.* (2002) in Borneo and Homeier *et al.* (2010) in Ecuador also found a decrease in species diversity from slope to ridge topography.

The cloud forests from the Cordillera Yanachaga do not present any taxonomic surprises, presenting a range of species, genera and families typical of an Andean flora (Gentry, 1992a), though the species richness appears quite high for montane cloud forest (Figure 3.4.1.1), especially the ridge site when compared to other upper montane cloud forests.

Combining the species list with that of the understorey herb data collected from the plot by Taylor (2008) and the vascular epiphyte data collected from

the largest trees in the plot (unpublished data, D. Catchpole), reveals a total of 485 vascular species in the leeward forest plot, with roughly half the amount of species at the other forest plots (Table 3.4.1.1). This places the leeward forest plot among the most species rich forests ever surveyed, not including the 110 species of non-vascular epiphytes recorded within the plot on a single tree by Romanski et al. (2011).

Table 3.4.1.1: Vascular plant species richness from the leeward, ridge and windward forest 1-ha plots.

Vascular component	Leeward	Ridge	Windward
Shrub and tree species (≥5 cm DBH)	136	74	81
Additional herb species from Taylor (2008)	124	88	65
Epiphyte species estimate (unpubl. data, D. Catchpole)	225	45	110
Total vascular plant species	485	207	256

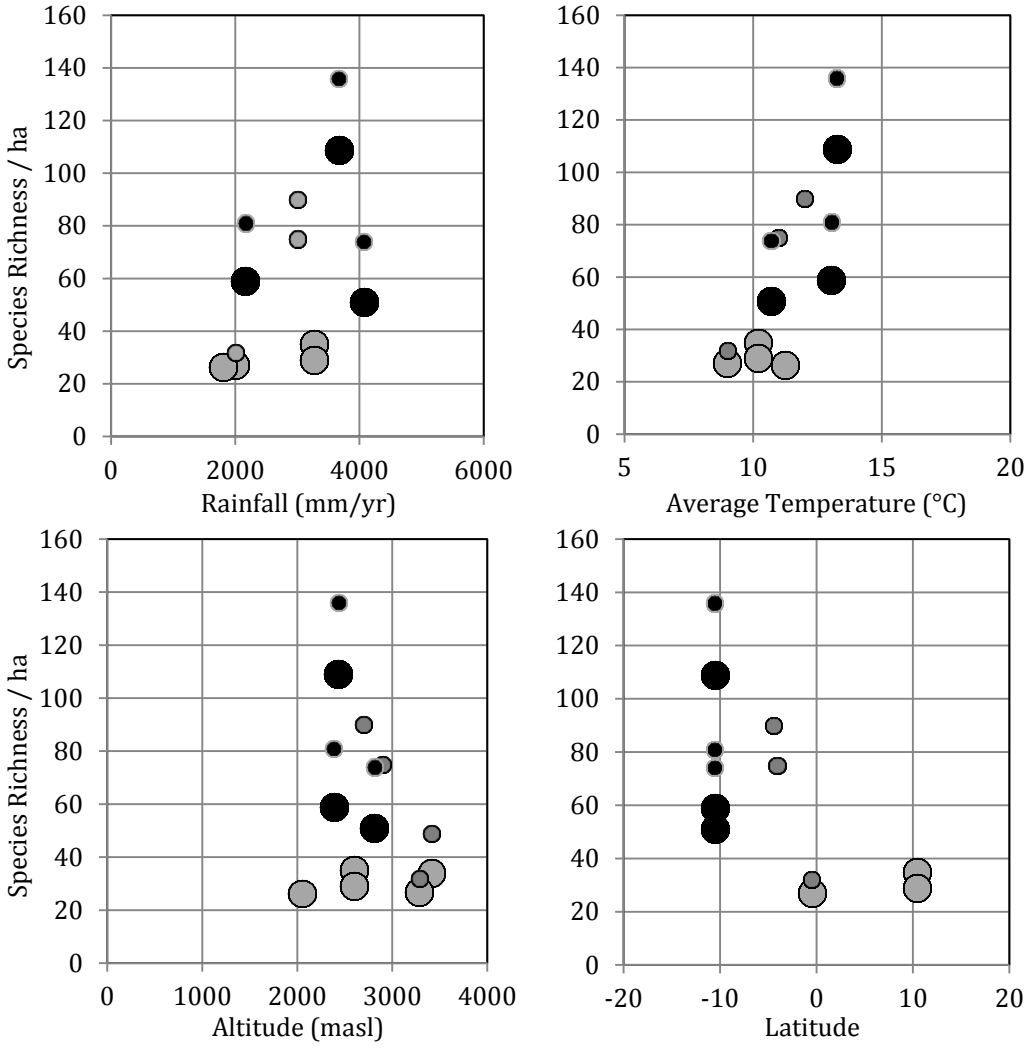

Figure 3.4.1.1: Distribution of species richness from known neotropical cloud forest sites according to annual rainfall, average temperature, altitude and latitude. Large and small circles indicate ≥10 cm and ≥5 cm DBH data, while black and grey circles indicate data from this and other studies respectively.

3.4.2 Forest Structure

3.4.2.1 Basal Area

Basal areas in the present study were much less than that recorded in a northern Peruvian cloud forest at ca. 2700 m (≥ 7.5 cm DBH 45.27 m^2/ha, Ledo et al. (2009)), Venezuelan montane cloud forests at 1320 and 1400 m (≥ 10 cm DBH 51.6 m^2/ha, Hernández (2012)), a Venezuelan montane cloud forest at 2320 m (≥ 10 cm DBH 48.7 m^2/ha, Rollet (1984)), Venezuelan montane cloud forests at 2220 and 2588 m (≥ 10 cm DBH 48.7 and 166 m^2/ha, Schwarzkopf (2010)), Costa Rican montane forest from 2380 - 2710 m (≥ 10 cm DBH ≥ 41.3 m^2/ha, Heaney (1990), Oosterhoorn *et al.* (2000)) and an Ecuadorian ridge cloud forest at 2700 (≥ 5 cm DBH 44 m^2/ha, Madsen (1994)).

The leeward forest in the present study was similar to Dominican upper montane cloud forests at 1900–2200 m (≥ 10 cm DBH 26.3 m^2/ha, Martin (2007)), an Ecuadorian upper montane forest (≥ 5 cm DBH 25.7 m^2/ha, Valencia (1992)), Bornean lower montane cloud forest at 850 m (≥ 10 cm DBH 37.5 m^2/ha, Pendry (1997)) and 1860 m (≥ 5 cm DBH 34.7 m^2/ha, Takyu, 2002 #175}), a Mexican cloud forest at 1340 m (≥ 5 cm DBH 35.2 m^2/ha, Williams-Linera (2002)) and a Venezuelan montane cloud forest at 2320 m (≥ 10 cm DBH 38.3 m^2/ha, Schwarzkopf (2010)).

The ridge and windward forests in the present study were the same as an Ecuadorian non-ridge cloud forest at 2900 (≥ 5 cm DBH 15.3 m^2/ha, Madsen (1994)), and less than those forests mentioned above and an upper montane bolivian forest (≥ 10 cm DHB 19.4 m^2/ha, Araujo-Murakami (2005)). The physiographically similar montane forest plots of Homeier *et al.* (2010) showed much lower basal areas than any of the plots here.

The greater basal area of the leeward forest compared to the windward forest was similar to that described in a windward-leeward transition in Colombia (Dupuy *et al.*, 1993) and Costa Rica (Häger & Dohrenbusch, 2010), although basal areas from the latter plots were much greater than the present study, with the leeward forest of the present study showing similar basal areas to the shortest stature and lowest basal area windward site in that study (≥ 5 cm DBH 33 m^2/ha). Takyu *et al.* (2002) also found a decrease in basal area from slope to ridge topography, while in Ecuador, a leeward slope forest showed lower basal area than a ridge forest, although the latter was lower in altitude (Madsen & Ollgaard, 1994).

From accounts in the comparable literature available from known cloud forest sites with sufficient site data, the basal areas of the cloud forests do not appear to be dependent on any annual temperature, rainfall or altitude, while all similarly low basal areas come from the group of continental cloud forests in the southern hemisphere (Figure 3.4.2.1), placing the data from this study well within the normal limits of that group.

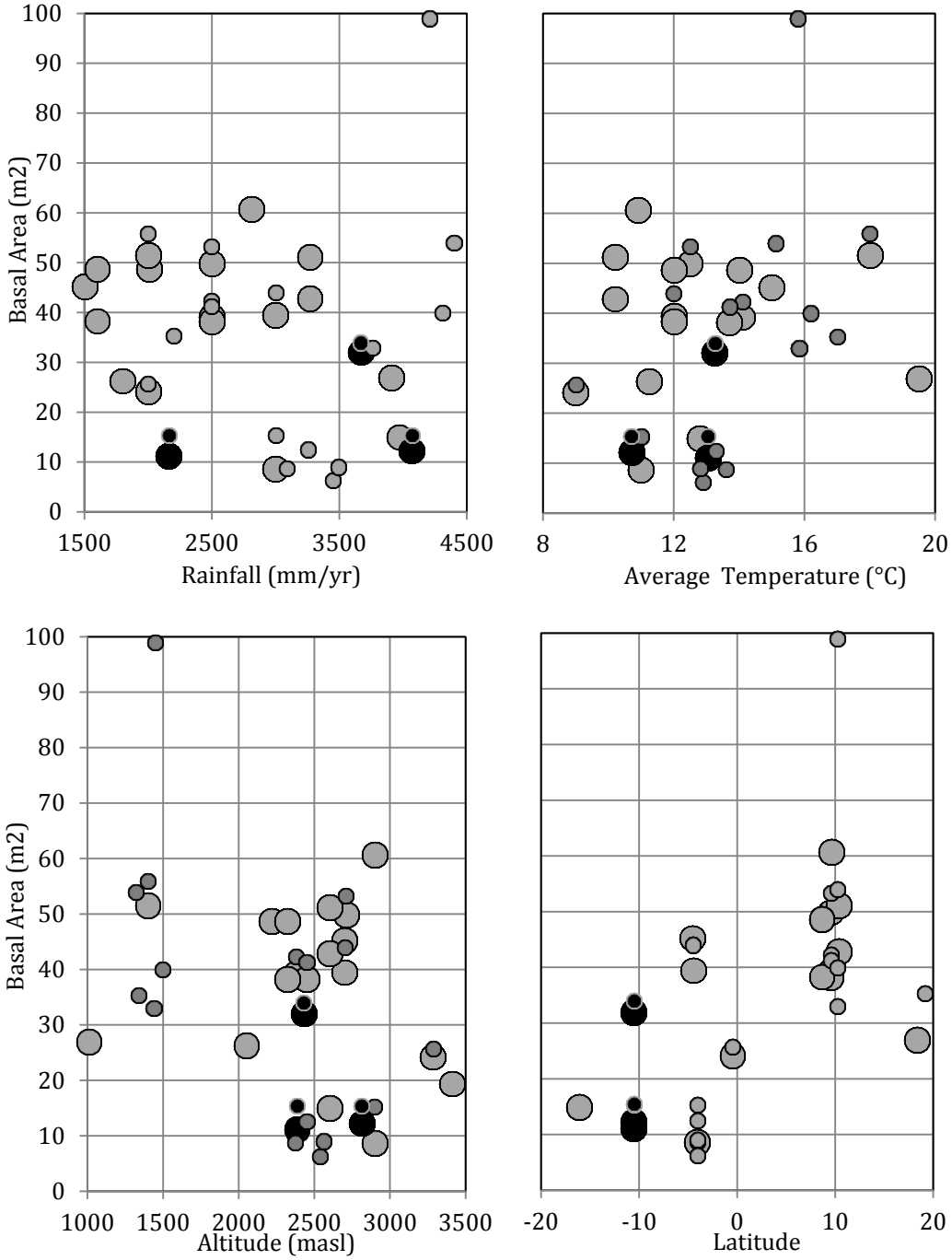

Figure 3.4.2.1: Distribution of basal area from known neotropical cloud forest sites according to annual rainfall, average temperature, altitude and latitude. Large and small circles indicate ≥10 cm and ≥5 cm DBH data, while black and grey circles indicate data from this and other studies respectively.

3.4.2.2 Stem Density

The stem density of the ridge forest was very similar to that found in an upper montane *Quercus* forest at 2900 m in Costa Rica (≥ 5 cm DBH 1197 stems/ha, Kappelle (1996)), while the windward forest was very similar to a Mexican cloud forest at 1340 m (≥ 5 cm DBH 1370/ stems/ha Williams-Linera (2002)). An Ecuadorian ridge cloud forest at 2700 showed a

comparable density in the ≥ 10 cm diameter class (478 stems/ha) to the windward forest, however the density of the 5 cm class in the same plot (2090 stems/ha) was much higher (Madsen & Ollgaard, 1994). Other forests with stem densities similar to those of the present study include an Ecuadorian upper montane forest at 3300 m (≥ 5 cm DBH 1058 stems/ha, Valencia (1992)), an Ecuadorian lower montane cloud forest at 1710 m (≥ 10 cm DBH 494 stems/ha, Grubb (1963)), more Ecuadorian montane forests between 2350 and 2560 (≥ 5 cm DBH 1075-1250 stems/ha, Homeier (2010)) and various Costa Rican cloud forests (Heaney & Proctor, 1990, Oosterhoorn, 2000).

However in varying diameter classes, the stem densities of a series of mid-elevation Venezuelan cloud forests (≥ 10 cm DBH 814 stems/ha, Hernández (2012)), Bornean lower montane cloud forests at 850 m (≥ 10 cm DBH 798 stems/ha, Pendry (1997)) and at 1860 m (≥ 5 cm DBH 4100 stems/ha, Takyu (2002)), a Venezuelan montane cloud forest at 2320 m (≥ 10 cm DBH 859 stems/ha, Rollet (1984)), a Puerto Rican cloud forest (≥ 10 cm DBH 687 stems/ha, Gould (2006)) and a Dominican cloud forests (≥ 10 cm DBH 810 stems/ha, Martin (2010)) all showed a much greater values than any of the forests studied here.

The much greater density of standing dead stems at the windward site is attributed to a region of the plot that had recently (within ca. 10 years) suffered a landslide, in which a distinct understorey community has developed (Taylor, 2008). On investigation, the buried previous rootmat could be observed at ca. 30 – 70 cm below the surface of the present mineral soil (pers. obs. D. Catchpole), although the area and depth of the debris flow was not mapped. The event appears to have suffocated the existing root mat and caused the mortality of the majority of individuals with established root systems in this area. A total of seven subplots were affected, in which 51.1 % of standing stems ≥5 cm DBH were dead, while in the other non-affected areas the same statistic was 6.1%, which is still higher than that recorded in the same diameter class at the leeward (3.6%) and ridge (2.0%) forests. The impact on the windward forest plot of this event might also suggest that a representative live stem density for the windward forests may indeed be higher, however, statistics of live stem density and basal area have not been adjusted, as this appears to be a common phenomenon affecting the dynamics of these forests, with a similar buried root mat being previously reported near the leeward forest plot by Catchpole (2002).

The greater stem density in the windward forest compared to the leeward forest has also been previously reported in Costa Rica (Häger & Dohrenbusch, 2010) and Colombia (Dupuy *et al.*, 1993), and Takyu *et al.* (2002) and Madsen & Ollgaard (1994) also found an increase in stem density from slope to ridge topography. However, this does not coincide with the higher density of the steeper windward plot compared to the ridge plot, which was also found in within plot dynamics by Valencia & Jørgensen (1992) in Ecuador.

In less comparable windward and leeward lower montane forests at c. 500 m in Puerto Rico, Weaver (2000) found that stem density was similar in the ≥ 2 cm DBH class, but in the ≥ 4 cm class (Weaver, 2010a) stem density was higher at the leeward forest. However, the more comparable leeward and windward cloud forest in the same area agreed with the present study and showed a much great stem density in the windward cloud forests (Weaver, 2010b).

From accounts in the comparable literature available from known cloud forest sites with sufficient site data, the stem density of the cloud forests do not appear to be dependent on any of annual temperature, rainfall, altitude or latitude (Figure 3.4.2.2), placing the data from the present study at the lower end of stem density recorded for cloud forests.

The differing order of stem densities among two diameter classes of the forests of the present study (leeward forest lowest in ≥5 cm and highest in ≥10 cm) demonstrate the different structures within each forest. This is explained by the higher understorey density of the windward and ridge forests due to the higher canopy openness and less developed canopy stature compared to the leeward site, where a higher canopy has developed that limits understorey development, as seen in the distribution of diameter and height classes (Figure 3.3.2.2, Figure 3.3.2.3). These patterns may indicate a different state of flux at the time of sampling, where as opposed to the growing nature of the windward and ridge forests, the leeward forest may be in a temporary state of declining recruitment after having previously reached a maximum period. The state of flux may be the reason why the lowest diameter class had a lower frequency than the second lowest class in the leeward forest, which to the author's knowledge has not been recorded in the literature. A feasible explanation for such a phenomenon lies within the climatic record. The leeward forest inventory was performed in 2007, after what was shown to be an unusually dry period in the region that began in 2002 and culminated in the well documented 2005 Amazonian drought (Zeng *et al.*, 2008). While rainfall records at the site from 2003 onwards show some of the lowest rainfall on record, it is unlikely this negatively affected the arboreal community; moreover it is possible that as a result of the prevailing drier atmospheric conditions, cloud cover and fog immersion were heavily reduced at the leeward site, and the increased PPFD observed during this period (data not shown) may have initiated a pronounced growth spurt in the existing vegetation, which may have negatively affected the cohort of recently recruited stems and new recruitment in general. This is partly supported by the work of Gomez-Peralta *et al*. (2008), who performed a cloud-water interception study at both the leeward and ridge site during 2003 and 2004 (when PPFD was highest on record), and essentially concluded there was no evidence of cloud water interception at the leeward site, thus classifying the leeward site as a rain forest, which contrasts with the cloud immersion (visibility) data collected at the site from 2006 – 2011 that indeed shows significant periods of cloud immersion (see Chapter 2.3.6.1). While these conditions may have affected the leeward site, it is likely that insolation remained low at the windward and ridge site, as Gomez-Peralta *et al*. (2008) still recorded significant cloud interception at the ridge

site during this period, which suggests a scenario where orographic processes were still in play, though the reduced moisture content of the air masses may have prevented the moisture from carrying as far as the leeward forest site as it did during the measured period as of 2006.

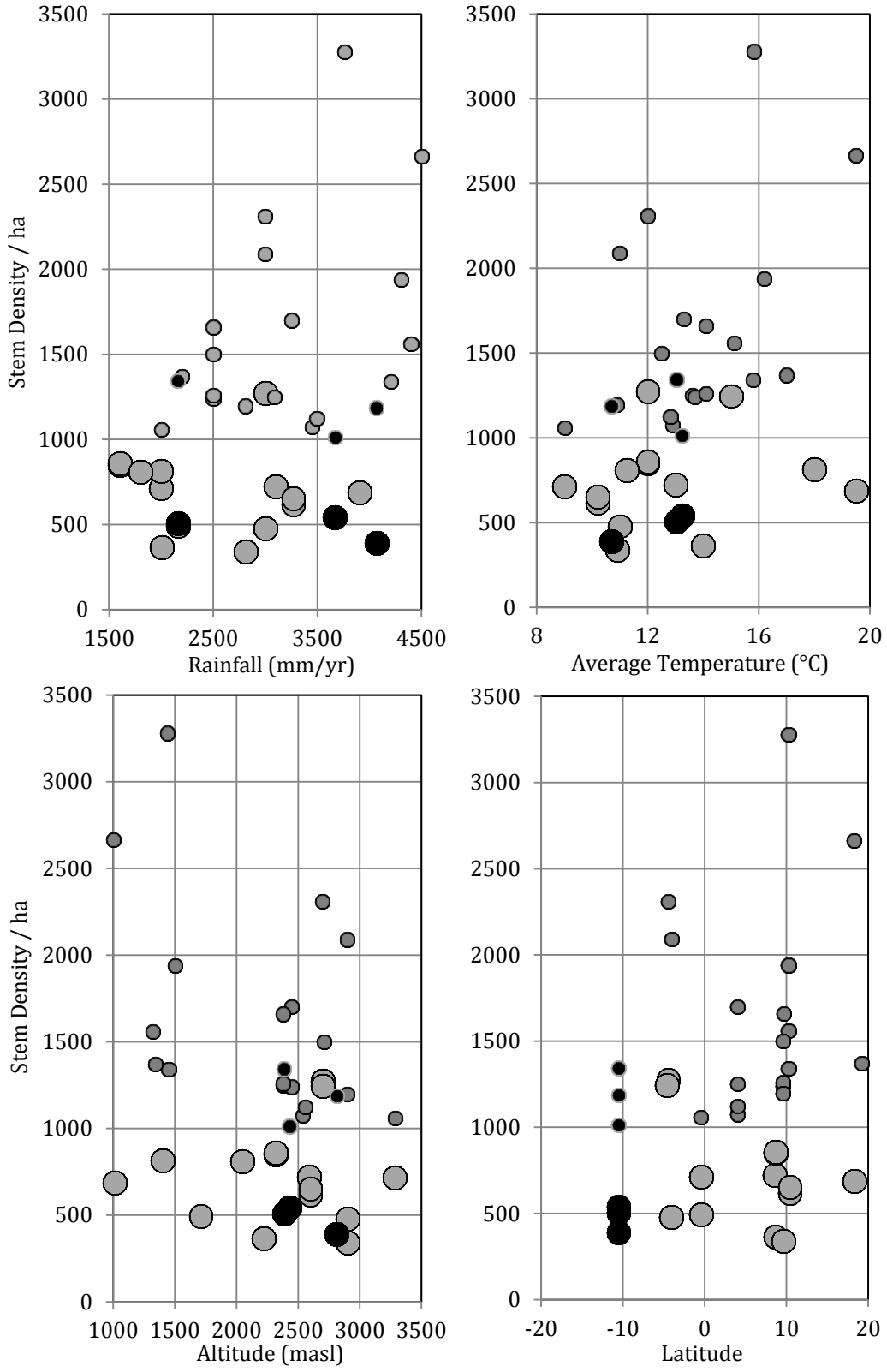

Figure 3.4.2.2: Distribution of stem density from known neotropical cloud

forest sites according to annual rainfall, average temperature, altitude and latitude. Large and small circles indicate ≥10 cm and ≥5 cm DBH data, while black and grey circles indicate data from this and other studies respectively.

3.4.2.3 Canopy Stature

The greater canopy height of the leeward compared to the windward forest was similar to that described in a windward-leeward transition in Costa Rica (Häger & Dohrenbusch, 2010) and Colombia (Sugden, 1982a), while canopy heights were slightly taller than Ecuadorian ridge and leeward cloud forests at 2700 and 2900 respectively (Madsen & Ollgaard, 1994). The ridge and windward forests showed a similar canopy height to an upper montane Bolivian forest (Araujo-Murakami *et al.*, 2005) and an Ecuadorian cloud forest at 2400 (Homeier *et al.*, 2010).

Despite being of slightly higher average height, the ridge forest showed a very similar distribution of height classes to an upper montane forest surveyed by Valencia & Jørgensen (1992). In the less comparable windward and leeward lower montane forests at c. 500 m in Puerto Rico, stem height was much greater at the leeward forest in both the ≥ 2 cm (Weaver, 2000) and ≥ 4 cm diameter class (Weaver, 2010a), as well as in the more comparable cloud forests at 1000 m in the same area (Weaver, 2010b).

In Colombia, Dupuy *et al.* (1993) found that the leeward slopes actually showed the larger number of inclined live trees (survivors of tree fall), which they attributed to the temporary reversal of trade winds for part of the year where the leeward slopes were converted into windward slopes, while similar to the present study, Madsen & Ollgaard (1994) reported a higher amount of inclined stems in an Ecuadorian ridge forest compared to their Ecuadorian leeward forest, although these values (44.1 % vs. 31.9 %) were much higher than those recorded in the present study.

From accounts in the comparable literature available from known cloud forest sites with sufficient site data, the heights of the cloud forests do not appear to be dependent on any annual temperature, rainfall, altitude or latitude (Figure 3.4.2.2), placing the data from the present study in the normal range of average stem height and canopy height recorded for cloud forests.

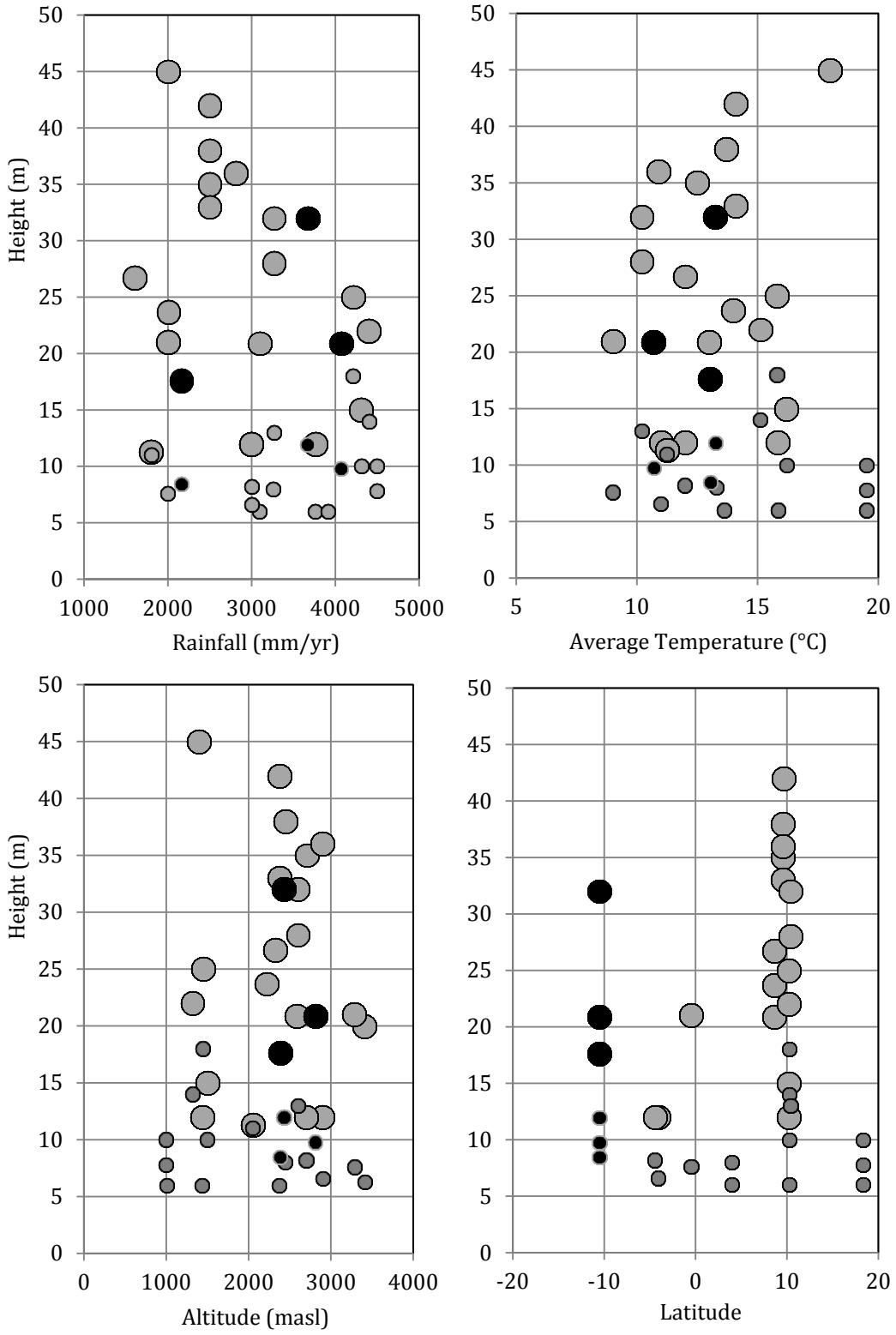

Figure 3.4.2.3: Distribution of stem and canopy heights from known neotropical cloud forest sites according to annual rainfall, average temperature, altitude and latitude. Large and small circles indicate canopy height and average ≥10 cm DBH stem height data, while black and grey circles indicate data from this and other studies respectively.

3.4.3 Leaf Morphology

3.4.3.1 Leaf Size

The decrease in leaf size with altitude (temperature) in tropical areas is well known (Grubb *et al.*, 1963, Leigh, 1975, Buot & Okitsu, 1999), and while the data shows a clear reduction in leaf size at the ridge site, the larger leaf size of the leeward forest compared to the windward forest reflects the microclimatic differences between the sites.

The leaf size distribution of species reported in an upper montane *Quercus* forest at 2900 m in Costa Rica (Kappelle *et al.*, 1996) slightly resembles the upper montane ridge site in this study, while none of the sites showed a similar distribution to any of the 10 sites (2000 – 2700m) studied at Mt. Pulog in the Philippines (Buot & Okitsu, 1999), although these forests are compositionally distinct compared to most neotropical montane forests. The leaf size distribution among species found in the Ecuadorian lower montane cloud forest studied by Grubb *et al.* (1963) also has little resemblance to that of the forest in the present study, while the windward and ridge forest leaf size distribution among species bare much resemblance to an upper montane cloud forest in Costa Rica (Kappelle & Leal, 1996).

3.4.3.2 Leaf Type

Sugden (1982a) noted a complete lack of leaf drip-tips in the cloud forest of Serranía de Macuira in Colombia, while Kappelle & Leal (1996) recorded a dominance of species with some form of leaf drip-tip in varios cloud forests in Costa Rica. Even in the upper montane ridge forest, the proportion of species with leaf drip-tips (25%) was relatively high and not indicative of the rareness or absence supposedly indicative of this forest type (Frahm & Gradstein, 1991, Bruijnzeel *et al.*, 2011). This may be a feature of Peruvian montane cloud forests, although there are no other leaf morphology studies from other areas of Peru.

The percentage of species with compound leaves was lower than the 10% reported in an upper montane *Quercus* forest at 2900 m in Costa Rica (Kappelle *et al.*, 1996), or the 9% reported by Grubb *et al*. (1963), while Madsen & Ollgaard (1994) reported a lower 4% of species and a higher 13.5% of relative species abundance, and a higher 10% of species and 10.2% of relative species abundance in an Ecuadorian leeward and ridge cloud forest respectively. Compound leaves were only important in this study at the leeward forest when considered as a percentage of the arboreal foliage present.

Chapter 4

The Climate Environment of a Peruvian Lower Montane Forest

4.1 Objectives

In order to fill the gaps in knowledge identified previously (Chapter 1.2.3), this chapter addresses the fog environment at a montane forest types by presenting analyses of the microclimatic variation under differing weather conditions.

The aim of this chapter was to investigate how fog events differ from other weather conditions through the quantification of the duration of rainfall, canopy fog immersion and rain-fog free weather events, and the quantification of the background conditions peculiar to each weather event type. In order to complete this aim, the principal objectives of this chapter were to:

- Determine the duration of periods when the forest was subject to rainfall, fog immersion, overcast and clear sky weather conditions; and
- Determine the seasonal variation in temperature, vapour pressure, PPFD and wind regimes under each of rainfall, fog immersion, overcast and clear sky weather conditions.

4.2 Materials & Methods

4.2.1 Climatic Measurements

The climatic data were obtained from a pristine area of lower montane leeward forest within the Yanachaga-Chemillén National Park described in Chapter 1.4.2 and 1.4.3.

The atmospheric conditions above the forest canopy were recorded at the top of the 40 m canopy tower described in Chapter 2.2.2 (see Figure 2.2.2.1) using the instruments described in Table 2.2.2.1.

4.2.2 Data Processing

The data used for this study were collected over a 5-year period from July 2006 through to June 2011. Throughout the analysis, data are presented by seasons. There is a wet season from October - April and a dry season from May – September (see Chapter 1.4.2).

4.3 Weather Event Classification

In order to describe the fog environment in comparison to other weather events, valid 10-min data were required to be categorized to resemble climatically distinct and meaningful weather events, which included periods of differing rainfall intensity, periods of differing fog density and periods of differing cloudiness. This required several hierarchical sub-categorizations and assumptions based upon the instrument limitations and the importance of the effects of each weather event. For simultaneous rain and fog, rainfall events were given first priority over fog, based on the theoretical assumption that rainfall has a greater effect on air mass properties than any concurrent fog. From the remaining data fog events were extracted using visibility data, after which PPFD was used to define cloudiness events.

4.3.1 Visibility Measurements during Rainfall Events

Whilst simultaneous rainfall and fog is a common occurrence, the deciphering of simultaneous precipitation and low visibility measurements in the 10-minute database as a proxy for fog requires some considerations.

There are three possible scenarios to describe this common fog and rain episode. Firstly, simultaneous fog and rainfall is a common occurrence at this site, especially at the initiation of rainfall events, where rainfall from upper level cloud arrives at the canopy that is already immersed in fog, although typically the fog dissipates after prolonged rainfall (pers. obs. D. Catchpole.). Secondly, many rainfall events in this area are preceded by fog events, thus while not simultaneous in real-time, the first rainfall recording will coincide with a low visibility record in the same 10-min period.

Thirdly, rain drops tends to affect visibility sensor readings (Obregon *et al.*, 2011), especially with heavier rain. Low visibility was recorded during 28.5% of 10-min periods with rainfall recorded. While there was no relationship between low visibility measures (<1000 m) and rainfall intensity (Figure 4.3.1.1), the trend of increasing frequency of low visibility records with increasing rainfall intensity (Figure 4.3.1.2) suggests an expected effect of raindrops on the infrared refraction measured by the visibility sensor. Periods of simultaneous low visibility and rainfall are therefore considered as rainfall events.

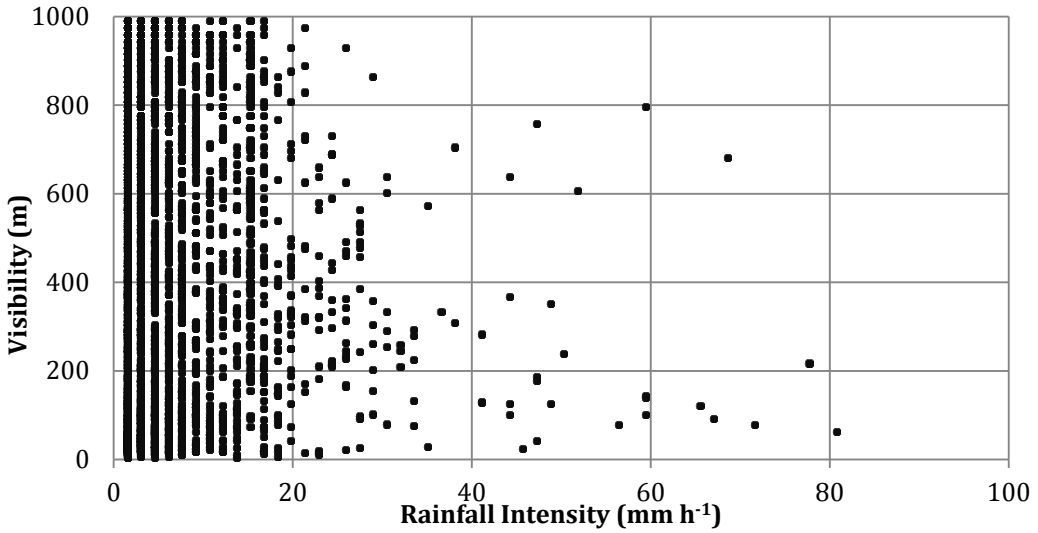

Figure 4.3.1.1: Distribution of 3569 simultaneous 10-minute low visibility and rainfall measurements from July 2006 through to June 2011

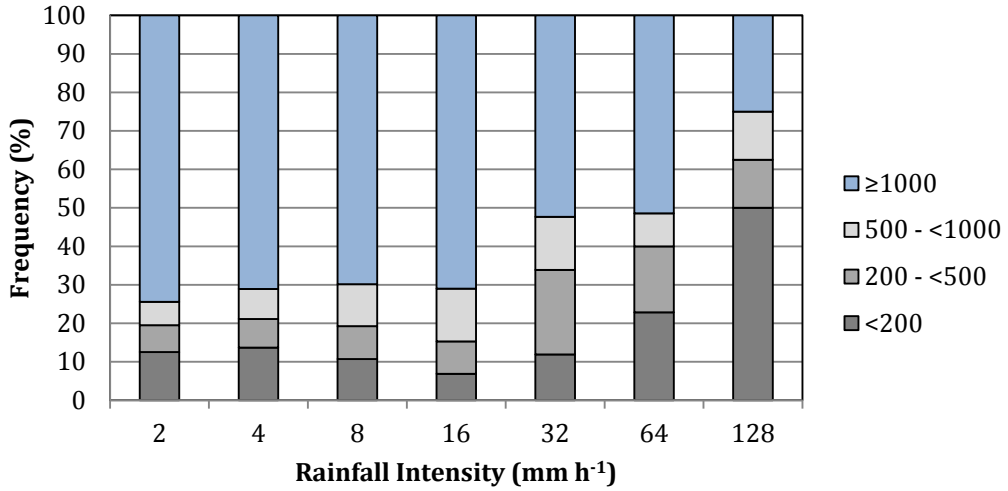

Figure 4.3.1.2: Frequency of low visibility records in rainfall intensity categories.

4.3.2 Rainfall Events

The 10-min data periods with rainfall records were divided into two groups based arbitrarily on the distribution of rainfall intensity (RI) calculated from 10-min totals. The spike in the RI distribution (Figure 4.3.2.1), representing the large amount of values just above 16 mm/hr, most likely represents the minimum RI for stratiform storm front events. As such, the first criterion for Heavy Rain (HR) was RI >15 mm/hr derived from 10-min totals. However, as that this might exclude very heavy yet short-lived rain events (that might have an equally strong and lasting effect on other parameters), data periods with RI >15 mm/hr were classified as HR when RI >0.75 mm/min (45

mm/hr)[10]. All remaining data periods were classified as Light Rain (LR) as shown in Table 4.3.2.1. While much lower RI threshold values are common in the general literature, the thresholds in the current study are designed to classify 10-minute data periods. Had the study analysed 1-hour data periods, a distribution-based threshold for the same dataset would be much lower.

Table 4.3.2.1: Weather Event Category Criteria

Weather Event	Code	Defining Measure	Value	Time of Day	Dependent Criteria
Heavy Rain	HR	RI	>15mm/hr or >0.75mm/min	any	-
Light Rain	LR	RI	≤15mm/hr or ≤0.75mm/min	any	-
Dense Fog	DF	VI	0 - 200 m	any	RI=0
Moderate Fog	MF	VI	>200 - 500 m	any	RI=0
Light Fog	LF	VI	>500 - <1000 m	any	RI=0
Clear Nocturnal	CN	VI	≥1000 m	1800-0650	RI=0
Strong Cloudiness	SC	ST	<0.425	0700-1750	RI=0/VI=≥1000
Weak Cloudiness	WC	ST	≥0.425	0700-1750	RI=0/VI=≥1000

Note: RI = rainfall intensity; VI = visibility; ST = solar transmission.

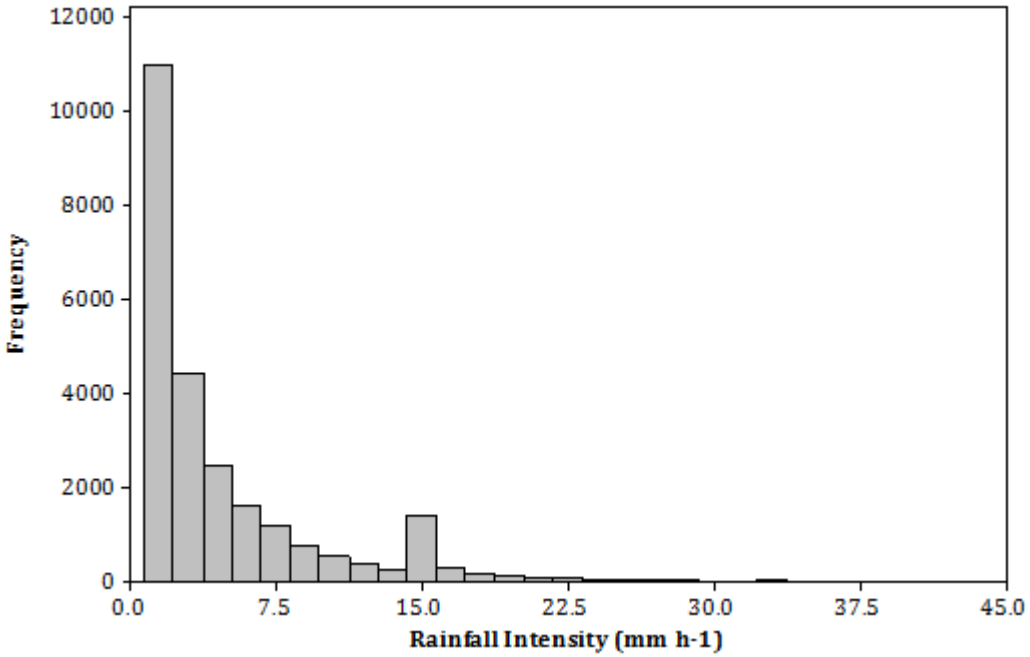

Figure 4.3.2.1: Frequency of rainfall intensity from 10-min total rainfall records

4.3.3 Fog Events

Visibility records of <1000 m were considered as a proxy for the presence of fog (Roach, 1994) within the short (2 m) range of the OFS. The distribution of low visibility distinguishes a higher relative frequency of very low visibility records. However, when taken into account the resolution limitation of the

[10] It should be noted that the sensor resolution (0.254 mm) prevents using a lower HR threshold at the 1-min scale.

visibility sensor (1-minute average), and the extreme temporal variability in fog properties, many low visibility records are likely to be lost by the averaging function of the OFS microprocessor, thus masking the typical densities of possibly different fog types that may occur.

Nonetheless, for the purposes of this study, the visibility (V) thresholds for fog density classification were adopted from those used by both Eugster et al. (2006) that define dense fog as V ≥200 m, and Obregon *et al.* (2011) (based on Eldridge (1971)) that define moderate fog as V = 200 to 500 m and light fog as as V = >500 to 1000 m (Table 4.3.2.1).

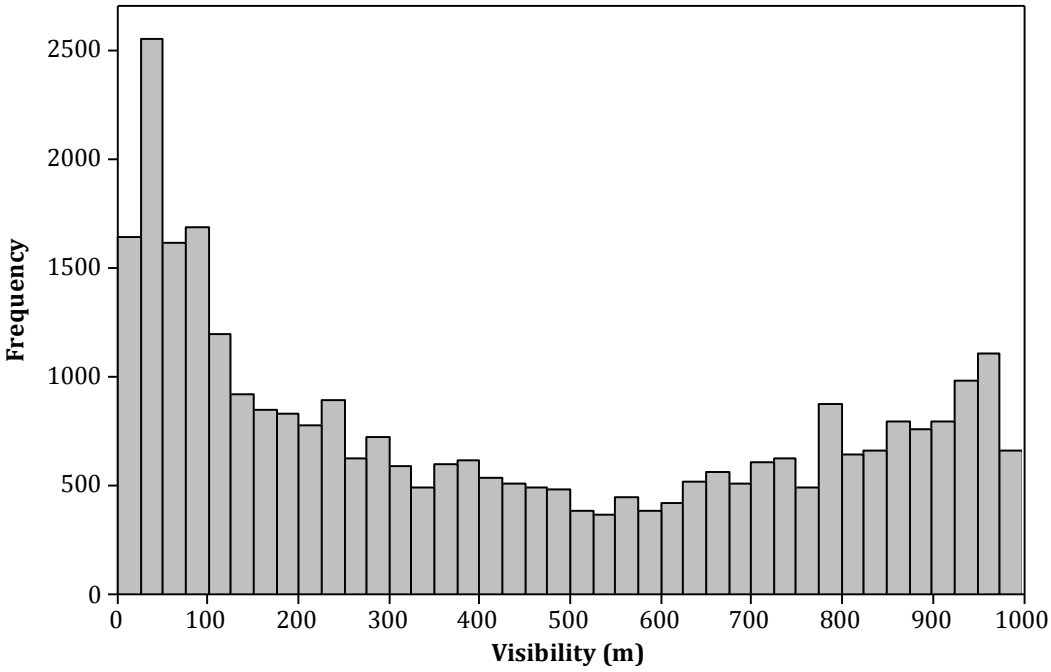

Figure 4.3.3.1: Frequency of low visibility records

4.3.4 Rain and Fog Free Events

Given the vast differences in microclimatic conditions caused by the presence of absence of overlying cloud, remaining data periods were classified into three further weather event categories. All nocturnal data periods free of rain and low visibility records from 1800 h to 0650 h were classified as Clear Nocturnal (CN), while diurnal data periods from 0700 h to 1750 h were subjected to analysis of PPFD records to determine solar transmission rates and create the weather event categories of Strong Cloudiness (SC) and Weak Cloudiness (WC) based on solar transmission (Table 4.3.2.1).

Solar transmission (ST) was calculated using the following equation.

$$ST = PPFD_{itds} / PPFD^{toa}_{tds}$$

where $PPFD_i$ = recorded PPFD (µmol m^{-2} s^{-1}); t = time of day; d = day of year; s = site; and $PPFD^{toa}$ = modelled PPFD at top of atmosphere.

$PPFD^{toa}$ was calculated using the following equation from Guenther *et al.* (2006).

$$PPFD_{toa} = 3000 + 99 * \cos(2 * 3.14 * (d - 10)/365)$$

To allow for local topography, latitude, altitude and time of day, $PPFD^{toa}{}_{tds}$ was modelled using the solar model of the HemiView canopy analysis program Version 2.1 (Delta-T Devices Ltd., 2001). To account for the site specific topographical shading, a vertical hemispherical image was taken at the LI-190SB location at the top of the tower with a NIKON 4500 Coolpix digital camera and a NIKON FC-E8 fisheye lens adapter. The image was analysed by the HemiView solar model using the site specific geographic coordinates and altitude, the lens specific equation coefficients, a transmissivity of 1, a diffuse proportion of 0.52 previously calculated for the site by Catchpole (2004) and very similar to proportions derived from measured Amazonian diffuse radiation (Butt *et al.*, 2010), and an external solar flux ($PPFD^{toa}$) specific to each day of year. The solar model used the Uniform Overcast Sky setting (Steven & Unsworth, 1980). The manufacturers specifications of lens distortion used by HemiView had been previously shown to be sufficient (Frazer *et al.*, 2001) and were used without modification. The model was run for each day of the year with 10-min outputs.

The ST threshold for the classification of local cloudiness was based arbitrarily on interpretations of ST distributions derived from both 1-minute absolute maximum and 10-minute average PPFD values. To account for local atmospheric conditions, such as aerosol loading and humidity, the ST derived from absolute maximum PPFD values were taken as a proxy for local clear sky conditions, which at this site can occur at any time of day year-round (pers. obs. D. Catchpole). Figure 4.3.4.1 shows how midday absolute maximum ST rates range between 60 and 80%, indicating that clear sky conditions would be possible with even lower ST. The data fits the assumption of peak atmospheric humidity during the peak of the wet season (January/February), creating a trend of increasing ST under clear skies towards the peak of the dry season (August). The overall distribution of 1-minute absolute maximum ST (Figure 4.3.4.2) shows a bimodal distribution (also evident in the average data), the peaks of which are assumed to represent overcast and clear conditions. As a result, the midpoint of ST = 0.425 was determined as the threshold between two rain and fog free diurnal categories, Strong Cloudiness (SC) and Weak Cloudiness (WC), as shown in Table 4.3.2.1.

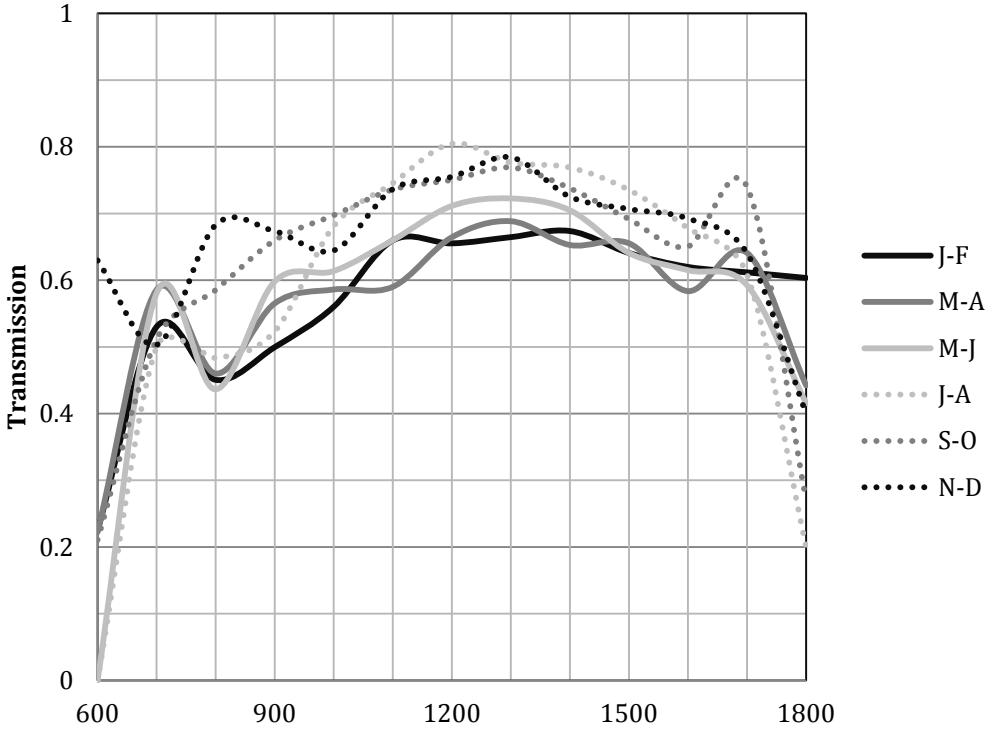

Figure 4.3.4.1: Bimonthly hourly absolute maximum transmission rates

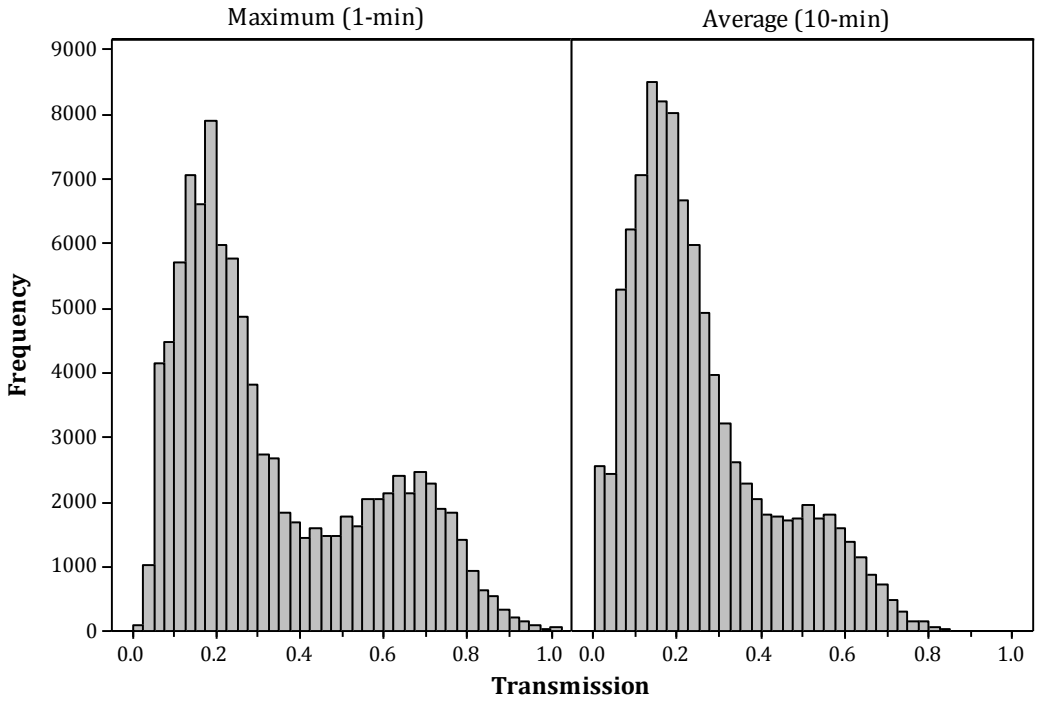

Figure 4.3.4.2: Distribution of absolute maximum and average transmission values

4.3.5 Weather Event Frequency

The weather event category data from the 5-year dataset was divided into wet and dry season datasets and averaged at 3-hour intervals, where 00:00 h = 22:40 – 01:30, 03:00 h = 01:40 – 04:30 etc.

The distribution of weather event frequencies shows the expected high frequency of rainfall and fog event categories in the wet season, while the rain events are much lower in frequency during the dry season (Figure 4.3.5.1).

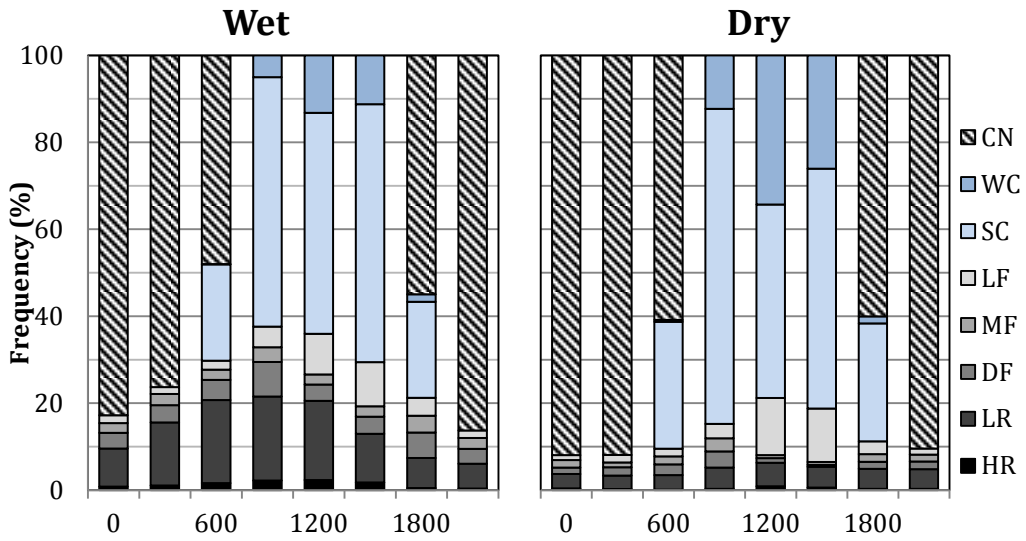

Figure 4.3.5.1: Distribution of weather event categories at 3-hour intervals.

4.4 Results

4.4.1 Air

Weather event type had little effect on nocturnal temperatures (Table 4.4.1.2), while diurnal temperatures in the wet season were lowest under light rainfall, followed by heavy rain and dense fog, and highest under weak cloudiness and light fog (Table 4.4.1.1, Table 4.4.1.2, Figure 4.4.1.1). Dry season trends were similar, yet diurnal trends for heavy rain during the dry season show that early morning (06:00 h) heavy rain events are associated with increased temperatures, while the continuance of these events to midmorning (09:00 h) is associated with lower temperatures, indicating a reduction of temperature by the heavy rain at this time. This indicates that light fog generally forms during warmer weather periods.

Table 4.4.1.1: Diurnal climatic averages for each weather event during the wet (upper table) and dry (lower table) season

Diurnal Event	Temperature (°C)	Vapour Pressure (mb)	PPFD (µmol.m^{-2}.s^{-1})	Wind Speed (m/s)	Wind Elevation (±°)
Wet season					
Heavy Rain	13.1	9.92	157	0.50	-6.3
Light Rain	12.9	9.75	218	0.54	-3.2
Dense Fog	13.4	10.19	329	0.68	-2.1
Moderate Fog	13.9	10.18	414	0.49	-6.0
Light Fog	15.0	10.22	646	0.51	-8.0
Strong Cloudiness	14.5	10.03	424	0.61	-5.6
Weak Cloudiness	16.0	10.20	1131	1.14	-6.2
Dry Season					
Heavy Rain	13.0	9.82	153	0.46	0.7
Light Rain	12.4	9.45	223	0.56	-3.1
Dense Fog	12.6	9.76	330	0.62	-13.8
Moderate Fog	13.7	9.90	485	0.58	-10.0
Light Fog	15.0	9.79	735	0.61	-12.7
Strong Cloudiness	13.9	9.50	382	0.58	-6.2
Weak Cloudiness	15.4	9.55	981	1.01	-12.9

Table 4.4.1.2: Nocturnal climatic averages for each weather event during the wet (upper table) and dry (lower table) season.

Nocturnal Event	Temperature (°C)	Vapour Pressure (mb)	Wind Speed (m/s)	Wind Elevation (±°)
Wet season				
Heavy Rain	12.7	9.82	0.38	-4.3
Light Rain	12.4	9.61	0.39	-2.3
Dense Fog	12.6	9.86	0.24	0.9
Moderate Fog	12.7	9.77	0.25	1.0
Light Fog	12.6	9.72	0.27	0.2
Clear Nocturnal	12.7	9.41	0.48	-1.4
Dry Season				
Heavy Rain	12.0	9.48	0.23	-4.6
Light Rain	11.8	9.31	0.46	-3.0
Dense Fog	11.7	9.43	0.21	-6.9
Moderate Fog	11.8	9.48	0.18	-4.9
Light Fog	11.8	9.32	0.23	-5.6
Clear Nocturnal	12.0	8.94	0.40	3.0

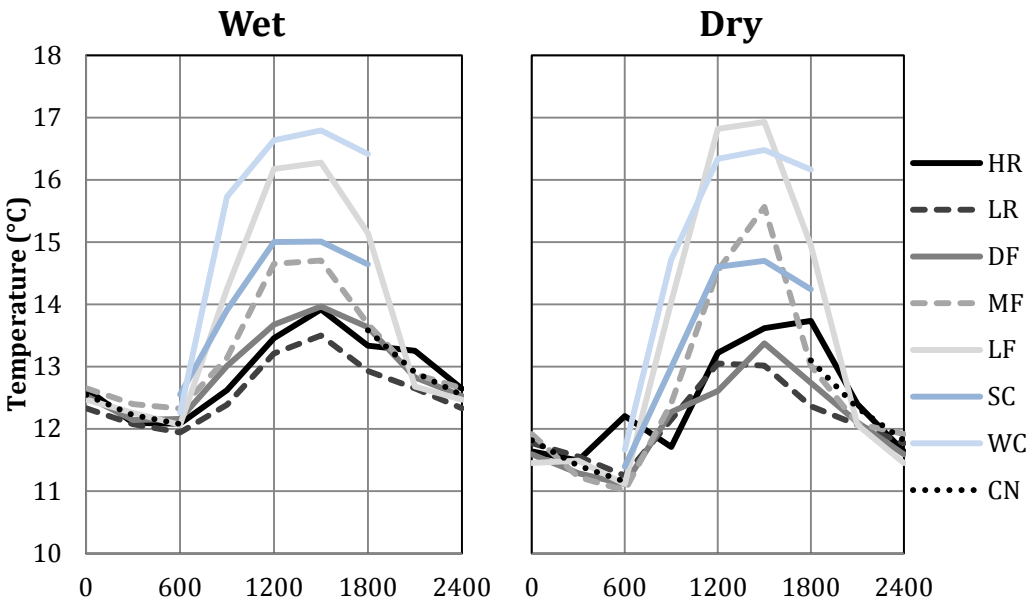

Figure 4.4.1.1: Average 3-hourly temperature during weather event categories per season.

During the wet season, vapour pressure was highest during weak cloudiness and fog events during the diurnal hours, with rain events occurring at the lowest diurnal vapour pressure, while clear nocturnal events showed the lowest nocturnal vapour pressure (Table 4.4.1.1, Table 4.4.1.2, Figure 4.4.1.2). During the dry season, light and moderate fog events mostly had the highest diurnal vapour pressure, with the exception of the strong association of early morning (06:00 h) heavy rainfall and relatively high vapour pressure for that period.

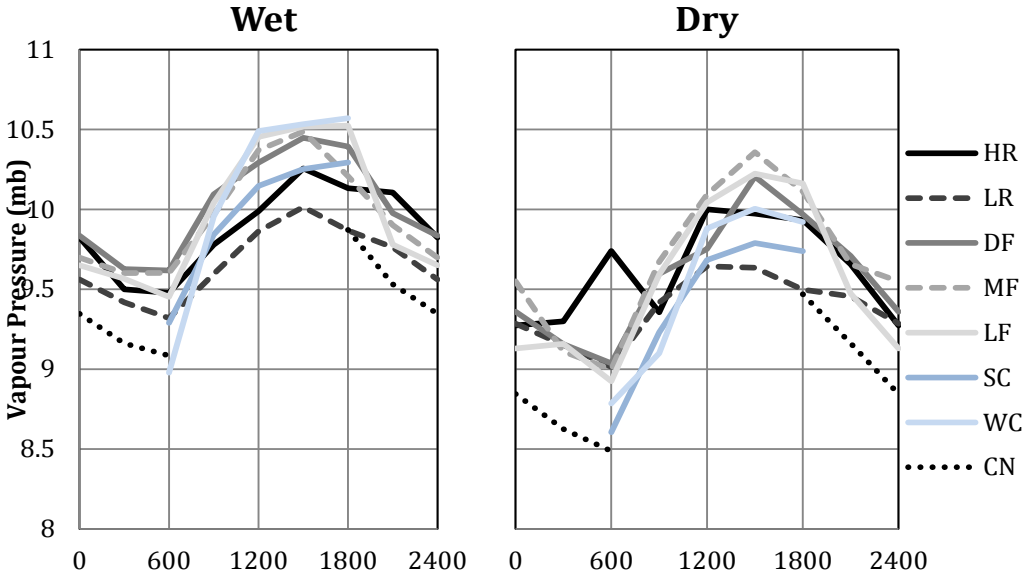

Figure 4.4.1.2: Average 3-hourly vapour pressure during weather event categories per season.

4.4.2 Light

The pattern of PPFD in both seasons showed higher midday radiation during light and moderate fog events than that of strong cloudiness (Figure 4.4.2.1), indicating that many of the light and moderate fog events occurred during periods of low cloudiness, whereas PPFD during dense fog was lower than but similar to that during strong cloudiness (Table 4.4.1.1, Table 4.4.1.2). Transmission results reflected those of the highly related PPFD (Figure 4.4.2.2), and reinforced the finding that fog events have a much lesser effect on radiation than rain events.

Compared to wet season weak cloudiness PPFD, heavy rain events showed the greatest PPFD attenuation, while the least was shown by light fog events (Figure 4.4.2.3), while dry season trends were similar (Figure 4.4.2.4). The percentage attenuation in PPDF during rain events and strong cloudiness events compared to weak cloudiness events was similar in the wet and dry season (c. 5% dry season increase), the attenuation in PPDF during light rain and dense fog events increased slightly in the dry season (c. 15%), while the light and moderate fog events had the largest increase into the dry season (c. 25%) (Table 4.4.2.1).

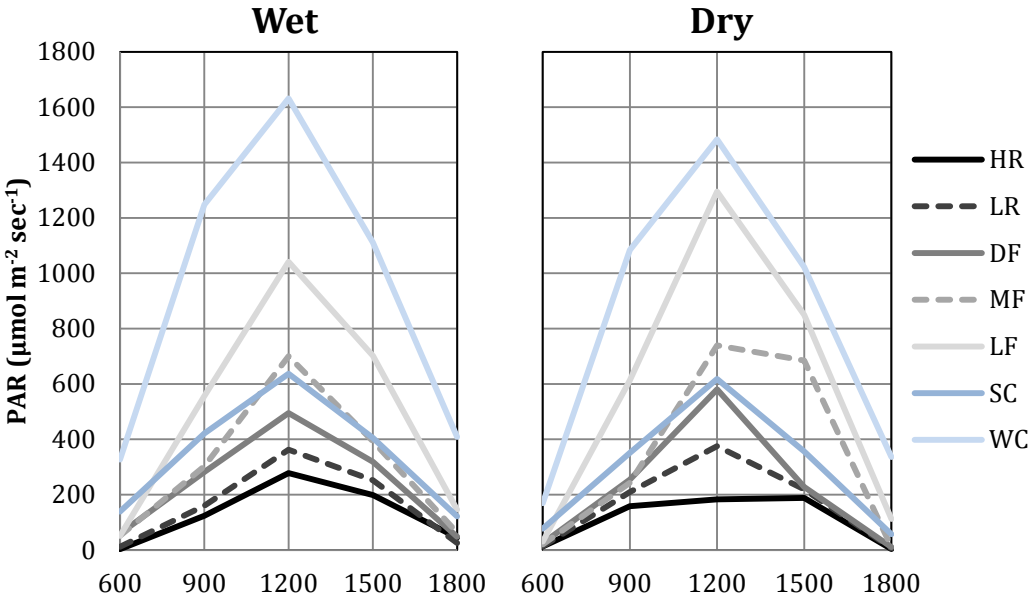

Figure 4.4.2.1: Average 3-hourly PPFD during weather event categories per season.

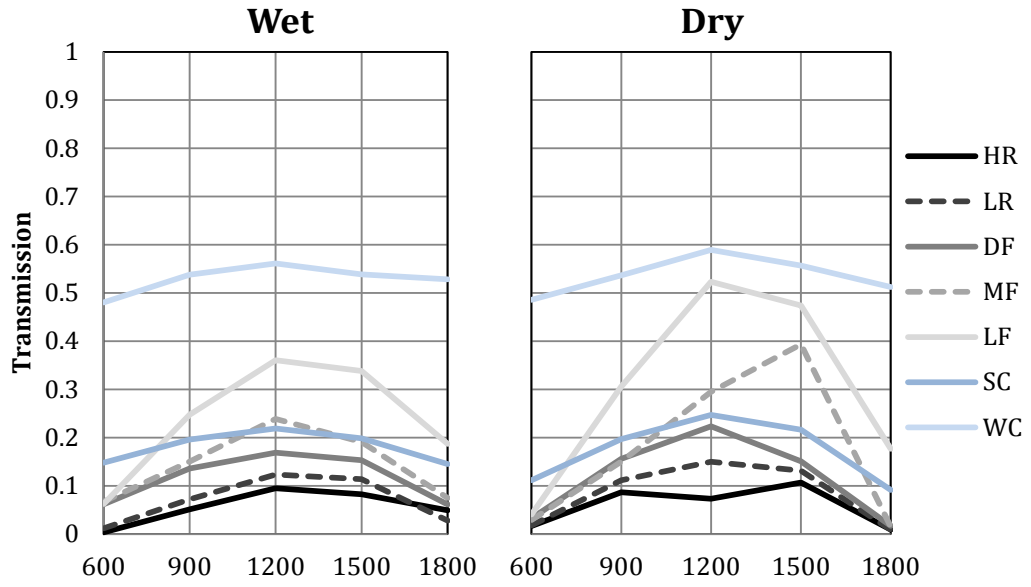

Figure 4.4.2.2: Average 3-hourly solar transmission during weather event categories per season

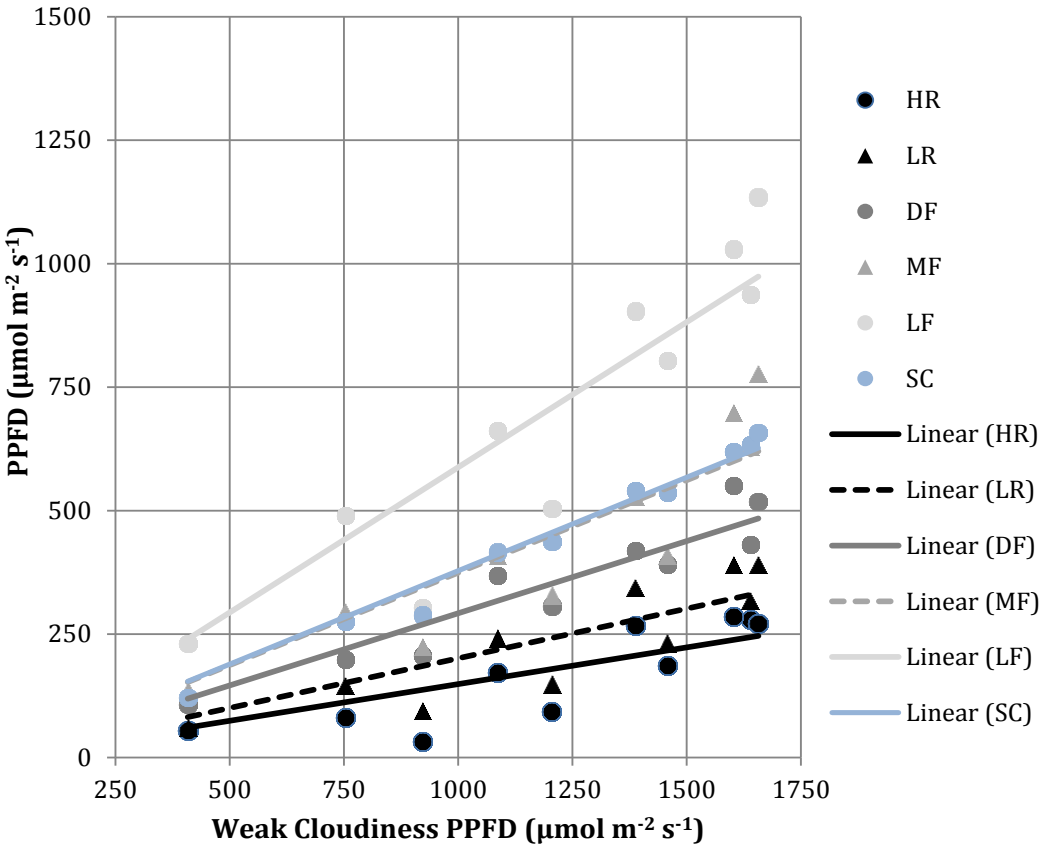

Figure 4.4.2.3: Wet season PPFD under different weather events compared to corresponding values under clear sky (weak cloudiness). Data compared are hourly averages from 08:00 h to 17:00 h. Linear relationships are shown in

Table 4.4.2.1.

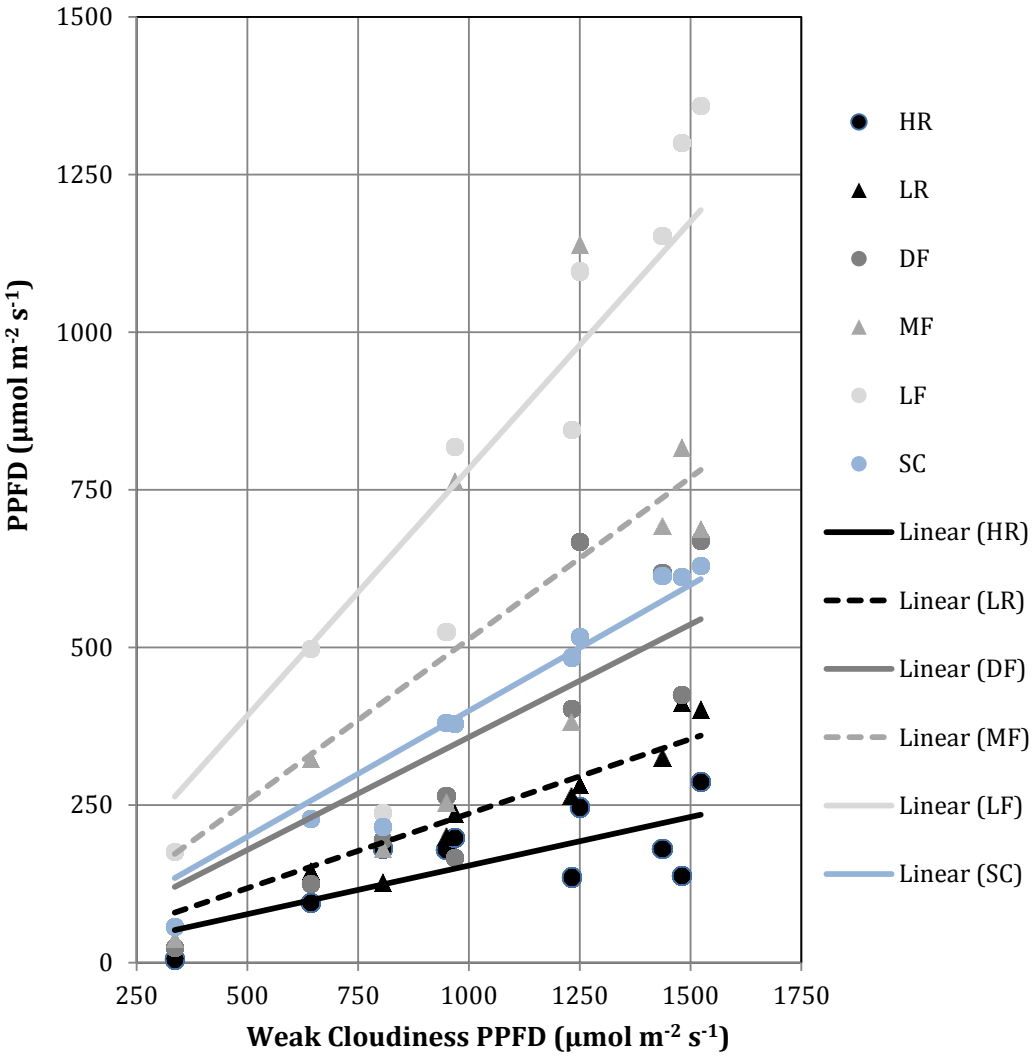

Figure 4.4.2.4: Dry season PPFD under different weather events compared to corresponding values under clear sky (weak cloudiness). Data compared are hourly averages from 08:00 h to 17:00 h. Linear relationships are shown in

Table 4.4.2.1.

Table 4.4.2.1: Intercept and R^2 values for the 1:1 relationships in PPFD between weak cloudiness and other weather events.

Description	HR	LR	DF	MF	LF	SC
Wet Season y intercept	14.9	20.1	29.2	37.4	58.8	37.8
Wet Season R^2	0.69	0.74	0.89	0.79	0.83	0.98
Dry Season y intercept	15.4	23.7	35.8	51.3	78.4	40.0
Dry Season R^2	0.51	0.89	0.69	0.51	0.82	0.94
Dry Season Proportional Increase (%)	3.38	14.97	18.31	27.05	24.99	5.31

4.4.3 Wind

During the wet season, nocturnal fog events generally occurred during the periods of lowest wind speed, the same being mostly true during the dry season except that heavy rainfall also showed similar low wind speeds during the early evening and at 03:00 h (Table 4.4.1.2, Figure 4.4.3.1). Diurnal trends showed the much higher early morning (06:00 h) wind speeds in the wet season under weak cloudiness, higher midday wind speeds during moderate fog than all other events obviously except weak cloudiness, while during the dry season diurnal hours showed that rain events tended to occur in less turbulent conditions than fog events (Table 4.4.1.1).

The wet season wind inclination data indicate that nocturnal fog events are more associated with upslope winds from the lower valley than the downslope winds from the general windward direction, while heavy rain was associated with downslope winds from the windward direction (Table 4.4.1.2, Figure 4.4.3.2). Diurnally, in the early to mid-morning during the wet season, dense fog was the only event strongly associated with upslope winds from the valley bottom, with some light rain events obviously being associated to ascending winds as well given the similar albeit negative (downslope) average. In the late afternoon in the wet season, all events were associated with the windward downslope winds. During the dry season, the association of diurnal events with downslope winds was much stronger than in the wet season (Table 4.4.1.1), with the exception of midday dense fog and heavy rain (Figure 4.4.3.2). Clear nocturnal conditions were also strongly associated with upslope winds from the valley bottom during the dry season.

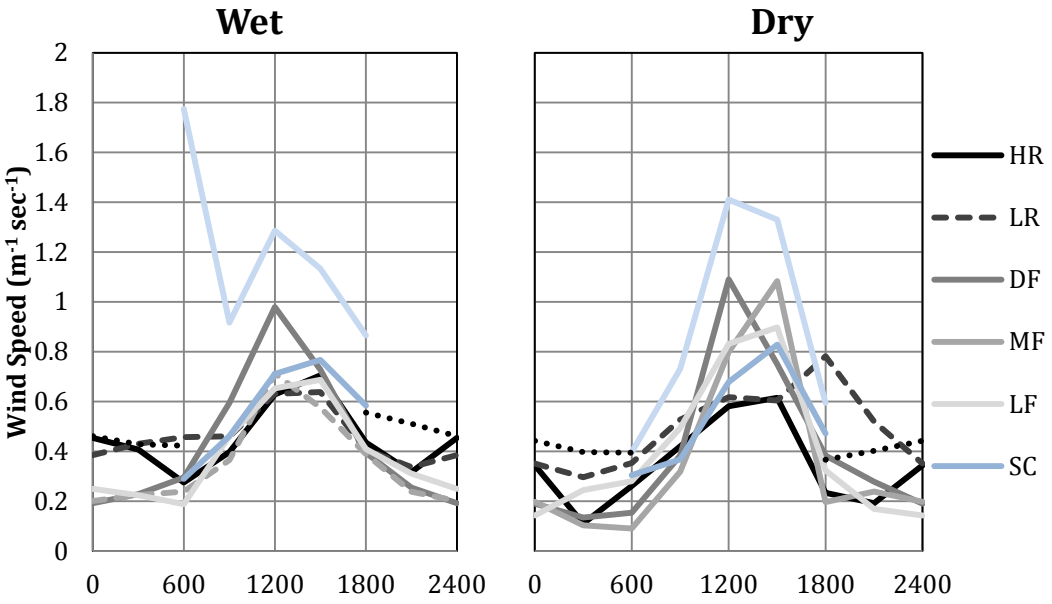

Figure 4.4.3.1: Average 3-hourly wind speed during weather event categories per season

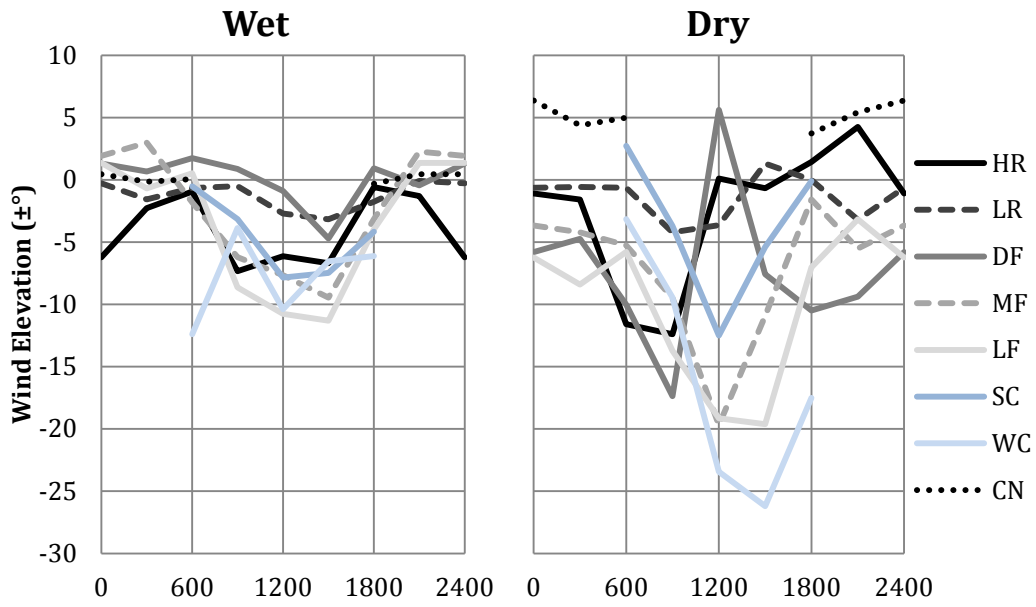

Figure 4.4.3.2: Median 3-hourly wind elevation during weather event categories per season. Positive angles indicate upslope winds, negative angles indicate downslope winds.

4.5 Discussion

The PPFD attenuation during dense fog (to 29.2 – 35.8 % of clear sky PPFD) was much lower than the 42% recorded in a Puerto Rican montane cloud forest by Eugster et al. (2006) or the attenuation to 66.3% of global radiation recorded in a French Guianan lowland cloud forest by Obregon et al. (2011)[11]. Obregon et al. (2011) also reported attenuation to 79.8% of global radiation during light and moderate fog events, higher than the attenuation in PPFD recorded in the present study with the exception of light fog events in the dry season. This may be a result of the longer observation period of the present study, although here PPFD reductions are not compared to perfectly cloudless periods as in the above mentioned studies, but long periods of weak cloudiness that no doubt produces a relatively lower clear sky PPFD baseline for comparison. This implies that PPFD attenuations due to fog are higher in this high altitude environment.

The diurnal weather event average temperature and vapour pressure suggest that light and moderate fog tend to occur during relatively warm weather periods that coincide with the arriving air masses holding the most moisture, as indicated by the generally higher vapour pressure (especially during diurnal hours) of the fog events, and is also supported by the strong positive correlation between temperature and vapour pressure (see Chapter 2.3.2). Furthermore, the weather event averages for PPFD and transmission indicates that light and moderate fog also tends to occur frequently during

[11] Eugster et al. (2006) found that fog caused attenuation of PPFD and net short-wave radiation were very similar.

periods when upper atmosphere cloudiness is low. Combined, these two patterns suggest that the evaporative buffering effect of light and moderate fog events is less than that provided under overcast conditions, mostly as a result of the conditions in which they are most prevalent. On the other hand, diurnal dense fog events generally show a similar albeit slightly lower vapour pressure to the other fog events, while average temperature is very similar to the rain events, with similar albeit slightly higher PPFD and transmission. This indicates that while diurnal dense fog events occur in similar conditions to the light and moderate fog events, the evaporative buffering of the diurnal dense fog events is similar to the rain events and stronger than that of overcast (strong cloudiness) events.

As would be expected, diurnal weak cloudiness was associated with the strongest wind speeds, though of particular interest was the wet season association of weak cloudiness with very strong early morning (06:00 h) downslope winds, an association which was not present during the dry season. This may be explained by a local circulation pattern caused by topographic shading. As this part of the leeward slope is the only small percentage of the surface area in the local topography that remains cool and shaded during the early morning, the strong downslope winds in the clear conditions during this period may form as a compensatory response to what can be assumed to be a large amount of thermal upwelling above the surrounding irradiated surfaces, while the disappearance of this association during the following 3-hour period is associated with the largest increase in 3-hourly temperature (c. 3.5° C) within the local context.

Nocturnally, the effect of weather rain and fog events was much lower compared to diurnal patterns. None of the weather events showed any influence on temperature, while vapour pressure was lower under all fog and rain events compared to the clear nocturnal events, while differences in nocturnal wind speeds were also marginal, all of which averaged to calm conditions (<0.5 m/s). Despite this, to a certain extent it can be said that the drier clear nocturnal events generally had higher wind speeds and fog events usually had the lowest nocturnal wind speeds, while the major differences between nocturnal weather events was found in the wind elevations that indicate changes in the provenance of the air masses themselves. The wind elevations showed some relatively large seasonal differences between and among the weather events, where nocturnal clear events shifted from a median balanced between upslope and downslope in the wet season to a strongly upslope median in the dry season, while conversely, fog events shifted from an wet season upslope association to a dry season association with downslope winds, indicating that nocturnal dry season fog events are associated with nocturnal downslope winds, which are only active during the dry season.

Chapter 5

Synthesis

5.1 Research Aims

5.1.1 Cloud Forest Classification

The first of the overlying aims of this study was to record fog frequencies from the three montane forests and compare with the determination of forest types from the most common biological, morphological and structural traits used to classify tropical montane forests into different types of rain and cloud forests.

Bruijnzeel et al. (2011) presented a summary of key structural characters used to define the different types of tropical montane forest (see Table 5.1.1.1). The lack of percentile ranges for most of these characters and the lack of distinction in many characters between lower montane rain and cloud forests leaves many open to interpretation. Regardless, a logical forest type definition was able to be determined for each character based on the ranges described and the known distribution of attributes from the literature.

Due to the lack of indication on whether leaf character abundance should be determined from the proportion of species present or an abundance based calculation, leaf character abundance was determined as both a proportion of the total species present and a proportion of the total arboreal foliage area. It was found that using abundances derived from the proportion of species present did not result in definitions in congruence with those listed by Bruijnzeel et al. (2011) and only abundances derived from total arboreal foliage area were used, although both are reported for reference (Table 5.1.1.1).

Table 5.1.1.1 shows the description of each character for each of the three forests in the present study and the resulting definition of forest type per character. The leeward characters were all within the range of both lower montane rain and cloud forests, while the ridge and windward forest characters ranged from lower montane rain forest to upper montane cloud forest, with no sites showing characters typical of lowland rain forest or sub-alpine cloud forest. It should be noted that leaf drip-tip abundance did not coincide with the abundances listed in Bruijnzeel et al. (2011), with the upper most ridge forest showing the greatest abundances (in the range of lowland forests when taken as a proportion of species present), closely followed by the windward forest. If further studies show that high Andean cloud forests show the same high leaf drip-tip abundances, it is

recommended that this character not be used for generalized cloud forest classification. Other characters of the forests studied tended to show congruence with the abundances listed in Bruijnzeel et al. (2011).

Bruijnzeel et al. (2011) did not design their summarized set of forest defining characters as a quantitative tool for forest definition, nor are the characters weighted or adequately defined for such a purpose. Nonetheless, given that each forest exhibited character traits associated to different forest types, the exercise of determining the percentage of attributes associated with each forest type per forest was deemed as useful tool to help define the forest type for each forest, despite the lack of weighting.

Table 5.1.1.1: Characterization of three forests according to parameters defined by Bruijnzeel et al. (2011) to determine tropical montane forest types (upper table) and resulting forest classifications with fog and rain frequencies (lower table).

Characteristic	Leeward Forest	Type*	Ridge Forest	Type*	Windward Forest	Type*
Canopy height	23.4 m	LMCF	15.8 m	UMCF	12.9 m	UMCF
Emergent tree height	32 m	LMRF	21 m	UMCF	18 m	UMCF
Compound leaves (% of spp.)	Occasional (5.9)	LMCF	Occasional (4.2)	LMCF	Occasional (7.3)	LMCF
Compound leaves (% of fol.)	Frequent (11.6)	LMRF	Occasional (3.9)	LMCF	Occasional (6.8)	LMCF
Principal leaf size class (% of spp.)	Mesophyllous (53.3)	LMRF	Notophyllous (41.1)	LMCF	Notophyllous (46.3)	LMCF
Principal leaf size class (% of fol.)	Mesophyllous (48.9)	LMRF	Microphyllous (35.0)	UMCF	Notophyllous (49.0)	LMCF
Leaf drip-tips (% of spp.)	Frequent (20.7)	LMRF	Abundant (25.0)	LRF	Frequent (21.0)	LMRF
Leaf drip-tips (% of fol.)	Occasional (10.7)	LMCF	Frequent (16.5)	LMRF	Frequent (15.7)	LMRF
Butresses	Rare	LMCF	Absent	UMCF	Absent	UMCF
Cauliflory	Rare	LMCF	Rare	LMCF	Rare	LMCF
Big woody climbers	Rare	LMCF	Absent	UMCF	Rare	LMCF
Bole climbers	Frequent	LMCF	Frequent	LMCF	Frequent	LMCF
Vascular epiphytes	Abundant	LMRF	Frequent	UMCF	Abundant	LMCF
Non-vascular epiphytes	Abundant	LMCF	Very Abundant	UMCF	Abundant	LMCF
LMRF attributes**	36%		9%		9%	
LMCF attributes**	64%		27%		64%	
UMCF attributes**	0%		64%		27%	
Classification	LMCF		UMCF		LMCF	
Fog Freq.	21.6%		75.7%		61.6%	
Rain Freq.	18.3%		20.9%		14.9%	
Fog + Rain Freq.	32.9%		79.8%		66.5%	

* Tropical montane forest type classification according to Bruijnzeel et al. (2011)
** Percentage of structural characteristics listed in Bruijnzeel et al. (2011) attributed to the forest type despite the lack of weighting. The characteristics in italics (% of spp. data) are not included in the percentage calculations.

The majority of leeward and windward forest characters indicated a lower montane cloud forest (64% each), although the remaining leeward characters indicated lower montane rain forest, while most remaining windward characters indicated upper montane cloud forest (Table 5.1.1.1). The majority of ridge forest characters indicated upper montane cloud forest (64%), while most remaining characters indicated lower montane cloud forest.

While the leeward and windward forests can be both classified as lower montane cloud forest, both forests still show vast differences in forest structure (see Chapter 3.3.2) and climate (see Chapter 2.3). While the leeward forest still shows a greater frequency of fog events than rain events (albeit similar), arguably justifying a cloud forests classification, the windward forest showed much greater fog frequency. Thus, at least in the Peruvian setting, it appears pertinent that these cloud forests be further sub-classified as leeward lower montane cloud forest and windward lower montane cloud forest, where the former accepts an amount of lower montane rain forest attributes and the latter accepts an amount of upper montane cloud forest attributes.

5.1.2 Orographic Variation

The second of the overlying aims of this study was to investigate the variation of climate and forest characters across an orographic gradient through the recording of climate and forest parameters at three sites with a distinct orographic location.

Chapter 2.3 showed a number of subtle climatic differences along the orographic gradient. The windward forest showed lower seasonality in rainfall than the ridge and leeward forests, although this was result of the lack of the very high wet season rainfall recorded at the other forests. The much higher rainfall at the leeward forest was an unexpected result, partly due to the fact that the windward site had not been accessed (for any purpose) prior to this study.

The ridge forest displayed the expected difference in air parameters due to its higher and mountain pass location, while the windward and leeward forests showed a similar temperature regime based on altitude, with only a slight increase in average temperature at the leeward site. However, the analysis of hourly lapse rates and leeward-windward temperature differences clearly showed the presence of a Foehn effect that was strongest in the afternoon, and more pronounced during the dry season.

There was a large difference in total PPFD among the sites that was very strongly correlated (r = -0.998, P = 0.043) to the frequency of the fog events that obstruct it indicated by a strong linear regression (Figure 5.1.2.1), an effect already well described (Cavelier & Mejia, 1990, Reinhardt *et al.*, 2008, Mildenberger *et al.*, 2009, Letts *et al.*, 2010). Humid event frequency resulted in a similar correlation, while rain event frequency showed no relation at all. This fog induced difference in PPFD between forests also correlated very strongly with the large difference in measured total arboreal foliage area (only when using data from stems ≥5 cm DBH), with the leeward and

windward forests resulting in exactly the same PPFD-foliage ratio, which was slightly higher than that for the ridge forest (Table 5.1.2.1). Even with the slightly lower ridge forest PPFD-foliage ratio, the 1:1 relationship among all sites was quite strong ($R^2 = 0.96$), while the linear regression was very strong (Figure 5.1.2.1) with a resulting very strong correlation ($r = 0.998$, $P = 0.042$). Aside from the myriad of factors that might influence arboreal foliage area across different ecosystems, within this localised ecosystem a different foliage distribution at the ridge site should be expected due to the differences in topography, wind, temperature and soils that might affect growth strategies and canopy structure in general.

This PPFD-foliage area relationship is based on just three samples, the likes of which are not available in the literature for comparison, yet there are a number of reasons why these similar PPFD-foliage ratios may or may not represent a real ecophysiological relationship. However these should be preceded by a brief discussion of foliage areas and disturbance regimes.

The foliage area of trees is determined by species specific genetics (structural architecture) and physical abrasion with adjacent tree crowns during wind events in the competition for space in the light environment (Zimmerman & Brown, 1971, Kramer & Kozlowski, 1979). The total arboreal foliage area of each plot likely represents an equilibrium with more dynamism than plot basal area at the 1-ha scale, since the expansion rate of foliage area is faster than stem thickening in initial growth stages, as has been shown in Chapter 3.2.2 through the relationship between crown radius and DBH and the distribution of their ratios. Plot basal area and arboreal foliage area ratios were not alike, and were much higher in the relatively thin windward forest plot (Table 5.1.2.1), where only a single tree > 40cm DBH was recorded, compared to the larger number at the ridge (13) and leeward (46) forest plots. Thus at a 1-ha plot scale, foliage area should be a better predictor of biophysical conditions than other structural characters due to its faster response to disturbance.

In terms of local disturbance regimes, as was described in Chapter 3.4.2.2, the windward site had recently (c. 5 to 10 years ago) suffered a debris flow in a localized part of the plot that resulted in a large amount of standing dead individuals, resulting in a congregation of small live stems along its perimeter. Had the plot not included this area, live basal area might indeed have been higher and reduced the basal area-arboreal foliage ratios towards those calculated for the leeward and ridge forest. Despite the slower basal area recovery, the period since the event has likely been sufficient for the plot arboreal foliage area to return to equilibrium. On the other hand, all the forest plots had similarly steep topography with recent treefall gaps, and evidence of debris flows (through buried organic layers) have also been revealed in soil studies at the leeward site (Catchpole, 2002), while Taylor (2008) recorded higher coarse woody debris in the leeward plot understorey (lowest in the ridge plot). However, the percentage of standing dead stems was slightly higher at the windward plot (excluding the landslide affected sub-plots) than that recorded in the other plots (see Chapter 3.4.2), which

along with the reduced DBH range, does tend to indicate that the windward forest has a stronger disturbance regime.

Canopy photosynthesis has been shown to be limited by PPFD in cloud forests (Reinhardt & Smith, 2008, Mildenberger *et al.*, 2009), yet the question remains as to whether the photosynthetic activity of canopies should be necessarily related to its physical size. While the leeward forest plot showed a much higher degree of canopy layering, as also seen through an arboreal foliage area c. 1.5 times greater than the plot area, there were also lower stem density, and as such a key parameter to understanding the foliage area results was that the leeward average crown area was double that of the other sites (Table 5.1.2.1).

A number of studies have argued that the leaves with reduced specific leaf areas (and increased longevity) seen in cloud forests is a response to PPFD limitation (Williams *et al.*, 1989, Letts *et al.*, 2010), which in turn have been shown to have reduced maximum photosynthetic rates (Shipley *et al.*, 2006). However, there is a scarcity of photosynthetic studies that actually determine species specific foliage areas of the species studied. In the present study there were no relationships whatsoever between any of the foliage area or stem statistics and the leaf size classes recorded (analysis not presented), thus ruling out a hypothesis of smaller leaf class induced smaller foliage area.

It is well known however, that PPFD is heavily attenuated within the canopy, which might give rise to PPFD limitations to canopy layering. If above canopy PPFD is predominantly below the maximum photosynthetic rates of the species present, as seen in other cloud forests (Letts & Mulligan, 2005, Letts *et al.*, 2010), it is plausible that as above canopy PPFD is reduced, within canopy PPFD levels further restrict foliage development, such that total foliage areas decrease with PPFD. The scope of the present study did not encompass such questions, yet canopy layering would appear an important element in understanding the PPFD-foliage area relationship. While more plot data with a better spread along the local PPFD gradient would be needed to be more conclusive, the data from this study do indicate greater canopy layering at the leeward plot, least at the ridge plot with slightly more layering at the windward site, showing a similar direction to the trend in Figure 5.1.2.1. Despite the fact that the ridge forest showed a total foliage area less than the plot area, indicating canopy gaps, all the forest plots showed a large amount of canopy gaps as seen in the projected crown area figures (Chapter 3.3.2), this being the nature of montane forest on steep slopes, leading to much of the stem density being clumped and providing opportunity for canopy layering.

While it remains uncertain whether these relationships will hold up across other orographic landscapes, they will nonetheless contribute to understanding the cause of variation in some elements of tropical montane forest structure. The findings also highlight the usefulness in undertaking forest inventories from the ≥5 cm diameter class, which in this case included a very important additional proportion (20 to 29%) of arboreal foliage when compared to the typical ≥10 cm diameter inventory total.

Table 5.1.2.1: PPFD, basal area and arboreal foliage area and their ratios at each forest site.

Description	Leeward	Ridge	Windward
PPFD (mol.year^{-1}.m^{-2})	7710	4926	5472
Basal area (m^{-2}.ha^{-1})	33.95	15.34	15.44
Arboreal foliage area (m^{-2}.ha^{-1})	14822	8506	10138
Average crown area (m^{-2})	14.64	7.17	7.54
Basal:Foliage ratio	1:437	1:554	1:657
PPFD:Basal ratio	1:44	1:31	1:28
PPFD:Foliage ratio	1:1.9	1:1.7	1:1.9

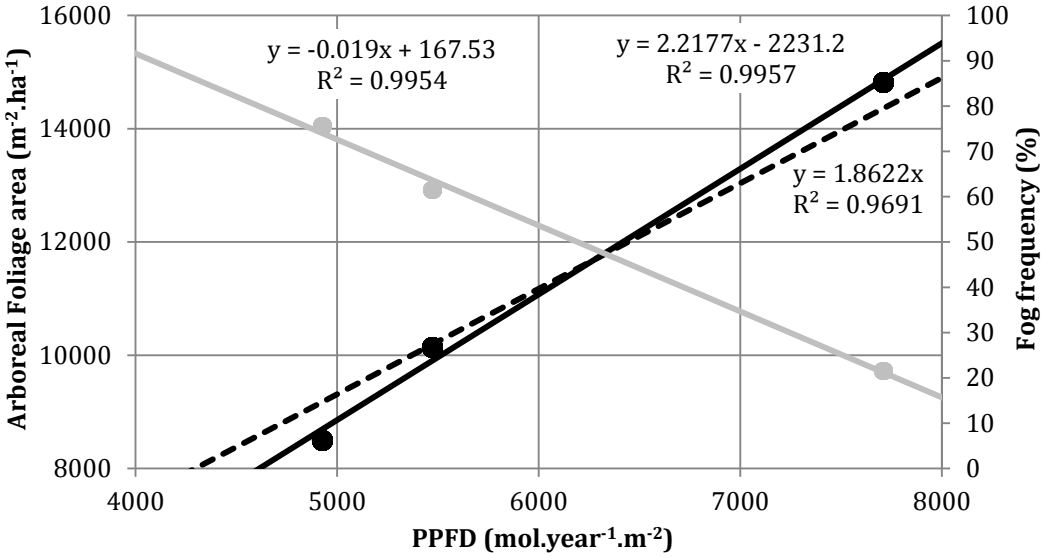

Figure 5.1.2.1: The relationship between PPFD and both total arboreal foliage area (black) and fog frequency (grey) across the orographic gradient. Solid lines indicate the linear regressions while the broken line represents the 1:1 relationship.

No other forest parameter was so well explained by a single climatic parameter as ≥5 cm DBH arboreal foliage area, which suggests that this rarely measured and laborious parameter may be equally useful for understanding certain dynamics of tropical montane gradients as other structural parameters such as stem density, height or girth. As the ultimate driver for total photosynthetic activity, if arboreal foliage area is limited so strictly by PPFD in montane forests, its measurement at other sites should contribute to further understanding limits on productivity and allocation patterns.

This precise relationship between arboreal foliage area and PPFD (or PPFD and fog frequency) over an tropical montane orographic or altitudinal gradient has not been reported in the literature, likely as a result of the rareness of ≥5 cm DBH 1-ha forest inventories, the scarcity of ground measured arboreal foliage area estimations from any plot studies, as well as the lack of both from sites with canopy level instrumentation (that includes visibility measurements) at the exact same location. Furthermore, and just as

this study has shown, variation can be large in climatic parameters over short distances in the complex orographic and topographic gradients presented by tropical montane areas. The ultimate driver of the PPFD-foliage relationship was fog frequency, which intuitively varies more over orographic and topographic gradients than any other. Studies in cloud forest areas using climatic data collected even just a kilometre away may not precisely represent the light environment of a particular study site in order to accurately derive such relationships.

Whatever the causes, biophysical conditions at the leeward forest appear ideal for the optimum expression of floristic diversity. The 136 species recorded in the present study is very high for a montane forest at this altitude. Gómez (1999) found an even higher 154 tree species (in the ≥10 cm class) in an adjacent plot, in which an unprecedented 195 species of vascular epiphytes were found in a single tree (Catchpole & Kirkpatrick, 2010). Within this plot, Taylor (Taylor, 2008) also found a very high 204 species of understorey herbs, Romanski et al. (Romanski *et al.*, 2011) found an unprecedented 110 species of non-vascular epiphytes in a single tree and c. 225 species of vascular epiphytes have been recorded on the largest trees (unpublished data, D. Catchpole). The vascular species recorded at the windward and ridge forest plots in this and other studies is still relatively high, yet only half to less than half of the leeward richness respectively.

5.1.3 Fog Environment

The third overlying aim of this study was to investigate the effect of fog on microclimate and the conditions associated with fog occurrence from a montane forest area.

Chapter 4.4.2 showed how in both the wet and dry seasons, both fog and rain events showed large attenuation of PPFD. PPFD measurements during fog periods were generally higher than that during rainfall events, suggesting that much of the fog occurrence coincides with a relatively clear upper atmosphere, whereas it is intuitive that nearly all significant rain events should occur while the upper atmosphere shows strong cloudiness, thus furthering any PPFD attenuation from the rain drops themselves. Indeed light fog PPFD was much higher on average than that of strong cloudiness, with moderate fog PPFD also being similar (wet season) or higher (dry season), confirming the association with weak cloudiness. The importance of fog event PPFD attenuation was highlighted in Chapter 0, where the frequency of fog events was very strongly correlated with the total PPFD of each forest, while the frequency of rain events showed no correlation whatsoever. The fact that fog frequency appears to explain all the variation in PPFD on this orographic gradient should not be surprising. Other events with attenuating effects such as rain events, should be almost completely linked to upper atmosphere cloudiness, which in turn should be equal for all sites due to their close proximity.

The assumed association of the less dense fog events with weak cloudiness and rain events with strong cloudiness suggests fog and rain events reduce

temperatures by 1 to 2 °C on average during the warmer wet season, while this effect is reduced by half during the cooler dry season. Despite the association of clear nocturnal conditions with cooler temperatures, there was a lack of nocturnal temperature differences among any weather events. While fog events reduce diurnal wet season temperatures, in this relatively stable and cool climate the ecosystemic importance this effect is probably nominal compared to the significance of other effects.

Both fog and rain events were important for increasing nocturnal relative humidity above clear nocturnal events. Diurnally rain and dense and moderate fog events increased diurnal relative humidity to levels above those of strong and weak cloudiness, while light fog increased diurnal relative humidity to levels similar to those of strong cloudiness, though this is still important as light fog events appear to occur frequently during periods of weak cloudiness. Thus the effect of fog events on relative humidity can be considered important for reducing the evaporative potential.

5.2 Conclusions

The three forests investigated in the present study can be considered lower and upper montane cloud forests as all forests receive canopy level fog for a greater period of time than rain events, though the lower montane cloud forests require further sub-classification into leeward and windward lower montane cloud forests to give justice to their distinct climatic and structural differences.

The orographic gradient produced a less speciose and structurally inferior windward forest compared to the highly speciose multilayered leeward forest, while the ridge forest at the mountain pass was the least speciose, yet structurally similar to the windward forest. The most important orographic effects on climate were the increased leeward rainfall compared to the windward slope, while there was a strong orographic gradient in fog frequency, with the ridge and windward forests receiving much greater canopy level fog than the leeward forest. Given that upper atmospheric conditions are the same for all three forests, this meant fog frequency explained all variation in PPFD among the sites. PPFD in turn appeared to control the production of arboreal foliage in each canopy, as the total arboreal foliage area of the forests was the exact proportion to the amount of PPFD received, though the mechanism is unclear. Fog events showed important effects on microclimate. Fog caused large PPFD attenuation and reduced diurnal temperatures, yet light and moderate fogs are associated with higher vapour pressures reflecting the prevailing upper atmosphere conditions conducive to canopy-level fog formation.

Bibliography

Aiba, S. & Kitayama, K. (1999) Structure, composition and species diversity in an altitude-substrate matrix of rain forest tree communities on Mount Kinabalu, Borneo. *Plant Ecology,* 140**,** 139-157.

Anten, N.P.R., Hernandez, R. & Medina, E.M. (1996) The photosynthetic capacity and leaf nitrogen concentration as related to light regime in shade leaves of a montane tropical forest tree, *Tetrorchidium rubrivenium*. ***Functional Ecology,*** **10,** 491-500.

Araujo-Murakami, A., Jørgensen, P.M., Maldonado, C. & Paniagua-Zambrana, N. (2005) Composición florística y estructura del bosque de ceja de monte en Yungas, sector de Tambo Quemado- Pelechuco, Bolivia. *Ecología en Bolivia,* 40**,** 325-338.

Arriaga, L. (2000) Types and causes of tree mortality in a tropical montane cloud forest of Tamaulipas, Mexico. *Journal of Tropical Ecology,* 16**,** 623-636.

Ataroff, M. (2002) Precipitation and interception in forest ecosystems of the Venezuelan Andes. *Ecotropicos,* 15**,** 195-202.

Bader, M.Y., Geloof, I.v. & Rietkerk, M. (2007) High solar radiation hinders tree regeneration above the alpine treeline in northern Ecuador. *Plant Ecology,* 191**,** 33-45.

Bascopé, S.F. & Jørgensen, P.M. (2005) Caracterización de un bosque montano húmedo: Yungas, La Paz. *Ecología en Bolivia,* 40**,** 356-379.

Bautista-Cruz, A. & del Castillo, R.F. (2005) Soil changes during secondary succession in a tropical montane cloud forest area. *Soil Science Society of America Journal,* 69**,** 906-914.

Bellingham, P.J. & Tanner, E.V.J. (2000) The influence of topography on tree growth, mortality, and recruitment in a tropical montane forest. *Biotropica,* 32**,** 378-384.

Bendix, J., Rollenbeck, R., Gottlicher, D. & Cermak, J. (2006) Cloud occurrence and cloud properties in Ecuador. *Climate Research,* 30**,** 133-147.

Bendix, J., Rollenbeck, R., Goettlicher, D., Naubss, T. & Fabian, P. (2008) Seasonality and diurnal pattern of very low clouds in a deeply incised valley of the eastern tropical Andes (South Ecuador) as observed by a cost-effective WebCam system. *Meteorological Applications,* 15**,** 281-291.

Benzing, D.H. (1998) Vulnerabilities of tropical forests to climate change: the significance of resident epiphytes. *Climatic Change,* 39**,** 519-540.

Brass, L.J. (1964) Results of the Archbold Expeditions No. 86. Summary of the sixth Archbold Expedition to New Guinea (1959). *Bulletin of the American Museum of Natural History,* 127**,** 145-216.

Brauman, K.A., Freyberg, D.L. & Daily, G.C. (2010) Forest structure influences on rainfall partitioning and cloud interception: A comparison of native forest sites in Kona, Hawai'i. *Agricultural and Forest Meteorology,* 150**,** 265-275.

Bruijnzeel, L.A. (2001) Hydrology of tropical montane cloud forests: A reassessment. *Land Use and Water Resources Research,* 1**,** 1.1-1.18.

Bruijnzeel, L.A. & Proctor, J. (1995) Hydrology and biogeochemistry of tropical montane cloud forests: what do we really know? *Tropical Montane Cloud Forests: Proceedings of an International Symposium* (eds Hamilton, L.S., Juvik, J.O. & Scatena, F.N.), pp. 38-78. Springer Verlag, New York.

Bruijnzeel, L.A. & Veneklaas, E.J. (1998) Climatic conditions and tropical montane forest productivity: the fog has not lifted yet. *Ecology,* 79**,** 3-9.

Bruijnzeel, L.A., Mulligan, M. & Scatena, F.N. (2011) Hydrometeorology of tropical montane cloud forests: emerging patterns. *Hydrological Processes,* 25**,** 465-498.

Bruijnzeel, L.A., Waterloo, M.J., Proctor, J., Kuiters, A.T. & Kotterink, B. (1993) Hydrological Observations in Montane Rain-Forests on Gunung Silam, Sabah, Malaysia, with Special Reference to the Massenerhebung Effect. *Journal of Ecology,* 81**,** 145-167.

Buot, I.E. & Okitsu, S. (1999) Leaf size zonation pattern of woody species along an altitudinal gradient on Mt. Pulog, Philippines. *Plant Ecology,* 145**,** 197-208.

Bussmann, R.W. (2001) Epiphyte diversity in a tropical Andean forest - Reserva Biologica San Francisco, Zamora-Chinchipe, Ecuador. *Ecotropica,* 7**,** 43-59.

Butt, N., New, M., Malhi, Y., Lôla da Costa, A.C., Oliveira, P. & Silva-Espejo, J.E. (2010) Diffuse radiation and cloud fraction relationships in two contrasting Amazonian rainforest sites. *Agricultural and Forest Meteorology,* 150**,** 361-368.

Caldwell, M.M. (1981) Plant response to solar ultraviolet radiation. *Physiological Plant Ecology* (eds Lange, O.L., Nobel, P.S., Osmond, C.B. & Ziegler, H.), pp. 169-197. Springer, Berlin.

Caldwell, M.M., Robberecht, R. & Billings, W.D. (1980) A steep latitudinal gradient of solar ultraviolet-B radiation in the arctic-alpine life zone. *Ecology,* 61**,** 600-611.

Cardelús, C.L., Colwell, R.K. & Watkins, J.E. (2006) Vascular epiphyte distribution patterns: explaining the mid-elevation richness peak. *Journal of Ecology,* 94**,** 144-156.

Catchpole, D.J. (2002) *Riparian-upland Transitions of Fine Root Biomass Within Primary and Secondary Lower Montane Tropical Forest at Cordillera Yanachaga, Peru*. Internship Report, Western Washington University.

Catchpole, D.J. (2004) *The ecology of vascular epiphytes on a Ficus L. host (Moraceae) in a Peruvian cloud forest*. Unpublished Honours Thesis, University of Tasmania, Hobart, Australia.

Catchpole, D.J. & Kirkpatrick, J.B. (2010) The outstandingly speciose vascular epiphytic flora of a single strangler fig (*Ficus crassiuscula*) in a Peruvian montane cloud forest. *Tropical Montane Cloud Forests: Science for Conservation and Management* (eds Bruijnzeel, L.A., Scatena, F.N. & Hamilton, L.S.), pp. 142-146. Cambridge University Press, Cambridge, UK.

Cavelier, J. & Goldstein, G. (1989) Mist and fog interception in elfin forests in Columbia and Venezuela. *Journal of Tropical Ecology,* 5**,** 309-322.

Cavelier, J. & Mejia, C.A. (1990) Climatic factors and tree stature in the elfin cloud forest of Serrania de Macuira, Colombia. *Agricultural and Forest Meteorology,* 53**,** 105-123.

Cavelier, J. & Peñuela, M.C. (1990) Soil respiration in the cloud forest and dry deciduous forest of Serrania de Macuira, Colombia. *Biotropica,* 22**,** 346-352.

Cavelier, J., Solis, D. & Jaramillo, M.A. (1996) Fog interception in montane forest across the Central Cordillera of Panama. *Journal of Tropical Ecology,* 12**,** 357-369.

Cavelier, J., Tanner, E. & Santamaria, J. (2000) Effect of water, temperature and fertilizers on soil nitrogen net transformations and tree growth in an elfin cloud forest of Colombia. *Journal of Tropical Ecology,* 16.

Cavelier, J., Jaramillo, M., Solis, D. & de Leon, D. (1997) Water balance and nutrient inputs in bulk precipitation in tropical montane cloud forest in Panama. *Journal of Hydrology,* 193**,** 83-96.

Clark, K.L., Nadkarni, N.M. & Gholz, H.L. (1998) Growth, net production, litter decomposition, and net nitrogen accumulation by epiphytic bryophytes in a tropical montane forest. *Biotropica,* 30**,** 12-23.

Clark, K.L., Lawton, R.O. & Butler, P.R. (2000) The Physical Environment. *Monteverde: Ecology and Conservation of a Tropical Cloud Forest* (eds Nadkarni, N. & Wheelwright, N.T.), pp. 18-38. Oxford University Press, Oxford.

Cox, S.B., Willig, M.R. & Scatena, F.N. (2002) Variation in nutrient characteristics of surface soils from the Luquillo Experimental Forest of Puerto Rico: A multivariate perspective. *Plant and Soil,* 247**,** 189-198.

Darrell, A.H. & James, H.F. (1999) Forest Productivity and Efficiency of Resource Use Across a Chronosequence of Tropical Montane Soils. *Ecosystems,* 2**,** 242-254.

Day, T.A., Vogelmann, T.C. & Delucia, E.H. (1992) Are some plant life forms more effective than others in screening out Ultraviolet-B radiation. *Oecologia,* 92**,** 513-519.

DeLay, J.K. & Giambelluca, T.W. (2010) History of fog and cloud water interception research in Hawai'i. *Tropical Montane Cloud Forests: Science for Conservation and Management* (eds Bruijnzeel, L.A., Scatena, F.N. & Hamilton, L.S.), pp. 332-341. Cambridge University Press, Cambridge, UK.

Delta-T Devices Ltd. (2001). Hemiview canopy analysis program. Cambridge, UK.

Dufrene, M. & Legendre, P. (1997) Species assemblages and indicator species: the need for a flexible asymmetrical approach. *Ecological Monographs* 67**,** 345-366.

Dupuy, J.M., Santamaria, M. & Cavelier, J. (1993) Estructura del bosque enano nublado de la Serrania-De-Macuira, Colombia, en laderas de barlovento y sotavento. *Biotropica,* 25**,** 340-344.

Eldridge, R.G. (1971) The Relationship Between Visibility and Liquid Water Content in Fog. *Journal of the Atmospheric Sciences,* 28**,** 1183-1186.

Eugster, W., Burkard, R., Holwerda, F., Scatena, F.N. & Bruijnzeel, L.A.S. (2006) Characteristics of fog and fogwater fluxes in a Puerto Rican elfin cloud forest. *Agricultural and Forest Meteorology,* 139**,** 288-306.

Fetcher, N., Cordero, R.A. and Voltzow, J. (2000) Lack of ecotypic differentiation: Plant response to elevation, population origin, and wind in the Luquillo Mountains, Puerto Rico. *Biotropica,* 32**,** 225-234.

Flenley, J.R. (1992) UV-B insolation and the altitudinal forest limit. *Nature and dynamics of forest-savanna boundaries* (eds Furley, P.A., Proctor, J. & Ratter, J.A.), pp. 273-282. Chapman & Hall, London.

Flenley, J.R. (1995) Cloud forest, the Massenerhebung effect and ultraviolet insolation. *Tropical Montane Cloud Forests: Proceedings of an International Symposium* (eds Hamilton, L.S., Juvik, J.O. & Scatena, F.N.), pp. 150-155. Springer Verlag, New York.

Frahm, J.P. & Gradstein, S.R. (1991) An altitudinal zonation of tropical rain-forests using bryophytes. *Journal of Biogeography,* 18**,** 669-678.

Frazer, G.W., Fournier, R.A., Trofymow, J.A. & Hall, R.J. (2001) A comparison of digital and film fisheye photography for analysis of forest canopy structure and gap light transmission. *Agricultural and Forest Meteorology,* 109**,** 249-263.

Freiberg, M. & Freiberg, E. (2000) Epiphyte diversity and biomass in the canopy of lowland and montane forests in Ecuador. *Journal of Tropical Ecology,* 16**,** 673-688.

Frey, W. & Kurschner, H. (1991) Life strategies of epiphytic bryophytes in a lowland and mountain rain-forest of Mount Kinabalu (Sabah, Northern Borneo). *Nova Hedwigia,* 53**,** 307-330.

Gentry, A.H. (1980) The Flora of Peru: A conspectus. *Fieldiana: Botany,* 5**,** 1-11.

Gentry, A.H. (1982) Patterns of neotropical plant species diversity. *Evolutionary Biology,* 15**,** 1-84.

Gentry, A.H. (1986) Endemism in tropical versus temperate plant communities. *Conservation Biology: the science of scarcity and diversity* (ed Soulé, M.E.), pp. 1532-1581. Sinauer Associates, Sunderland, Massachusetts.

Gentry, A.H. (1988a) Changes in plant community diversity and floristic composition on environmental and geographic gradients. *Annals of the Missouri Botanical Garden,* 75**,** 1-34.

Gentry, A.H. (1988b) Tree species richness in upper Amazonian forests. *Proceedings of the National Academy of Sciences, USA,* 85**,** 156-159.

Gentry, A.H. (1992a) Diversity and floristic composition of Andean forests of Peru and adjacent countries: implications for their conservation. *Memorias del Museo de Historia Natural U.N.M.S.M. (Lima),* 21**,** 11-29.

Gentry, A.H. (1992b) Tropical forest biodiversity: distributional patterns and their conservation significance. *Oikos,* 63**,** 19-28.

Gentry, A.H. & Dodson, C.H. (1987a) Diversity and biogeography of neotropical vascular epiphytes. *Annals of the Missouri Botanical Garden,* 74**,** 205-233.

Gentry, A.H. & Dodson, C. (1987b) Contribution of non-trees to species richness of a tropical rain forest. *Biotropica,* 19**,** 149-156.

Gerold, G., Schawe, M. & Bach, K. (2008) Hydrometeorologic, Pedologic and Vegetation Patterns along an Elevational Transect in the Montane Forest of the Bolivian Yungas. *Die Erde,* 139**,** 141-168.

Giaretta, A.A., Facure, K.G., Sawaya, R.J., Meyer, J.H.D. & Chemin, N. (1999) Diversity and abundance of titter frogs in a montane forest of southeastern Brazil: seasonal and altitudinal changes. *Biotropica,* 31**,** 669-674.

Gibbon, A., Silman, M.R., Malhi, Y., Fisher, J.B., Meir, P., Zimmermann, M., Dargie, G.C., Farfan, W.R. & Garcia, K.C. (2010) Ecosystem Carbon Storage Across the Grassland-Forest Transition in the High Andes of Manu National Park, Peru. *Ecosystems,* 13**,** 1097-1111.

Girardin, C.A.J., Malhi, Y., Aragao, L., Mamani, M., Huasco, W.H., Durand, L., Feeley, K.J., Rapp, J., Silva-Espejo, J.E., Silman, M., Salinas, N. & Whittaker, R.J. (2010) Net primary productivity allocation and cycling of carbon along a tropical forest elevational transect in the Peruvian Andes. *Global Change Biology,* 16**,** 3176-3192.

Givnish, T.J. (1999) On the causes of gradients in tropical tree diversity. *Journal of Ecology,* 87**,** 193-210.

Gomez-Peralta, D., Oberbauer, S.F., McClain, M.E. & Philippi, T.E. (2008) Rainfall and cloud-water interception in tropical montane forests in the eastern Andes of Central Peru. *Forest Ecology and Management,* 255**,** 1315-1325.

Gómez, D. (1999) *Composición florística en el bosque ribereño de la cuenca alta San Alberto, Oxapampa, Perú*. Undergraduate Thesis, Universidad Nacional Agraria La Molina, Lima, Peru.

Goodall, D.W. (1978) Sample similarity and species correlation

Ordination of Plant Communities (ed Whittaker, R.H.), pp. 99-149 Junk, The Hague.

Gordon, C.A., Herrera, R. & Hutchinson, T.C. (1994) Studies of fog events at 2 cloud forests near Caracas, Venezuela. I. Frequency and duration of fog. *Atmospheric Environment,* 28**,** 317-322.

Gould, W.A., González, G. & Carrero Rivera, G. (2006) Structure and composition of vegetation along an elevational gradient in Puerto Rico. *Journal of Vegetation Science,* 17**,** 563-574.

Gradstein, S.R., van Reenen, G.B.A. & Griffin, D. (1989) Species richness and origin of the bryophyte flora of the Columbian Andes. *Acta Botanica Neerlandica,* 38**,** 439-448.

Greig-Smith, P. (1983) *Quantitative Plant Ecology.* Blackwell Scientific Publications, Oxford.

Grubb, P.J. (1971) Interpretation of the 'Massenerhebung' Effect on Tropical Mountains. *Nature,* 229**,** 44-45.

Grubb, P.J. (1977) Control of forest growth and distribution on wet tropical mountains: with special reference to mineral nutrition. *Annual Review of Ecology and Systematics,* 8**,** 83–107.

Grubb, P.J. & Whitmore, T.C. (1966) A comparison on montane and lowland rainforest in Ecuador: II. The climate and its effects on the distribution and physiognomy of the forests. *Journal of Ecology,* 54**,** 303-333.

Grubb, P.J., Lloyd, J.R., Pennington, T.D. & Whitmore, T.C. (1963) A comparison of montane and lowland rain forest in Ecuador: I. The

forest structure, physiognomy, and floristics. *Journal of Ecology,* 51**,** 567-601.

Guenther, A., Karl, T., Harley, P., Wiedinmyer, C., Palmer, P.I. & Geron, C. (2006) Estimates of global terrestrial isoprene emissions using MEGAN (Model of Emissions of Gases and Aerosols from Nature). *Atmospheric Chemistry and Physics,* 6**,** 3181-3210.

Gutierrez Centeno, R. & Moya Hinojosa, Y.L. (2008) *Estructura y composición florística de dos bosques montanos en el Parque Nacional Yanachaga-Chemillén, Pasco*. Unpublished Undergraduate Thesis, Universidad Nacional del Centro del Perú, Huancayo, Peru.

Häger, A. & Dohrenbusch, A. (2010) Structure and dynamics of tropical montane cloud forests under contrasting biophysical conditions in north-western Costa Rica. *Tropical Montane Cloud Forests: Science for Conservation and Management* (eds Bruijnzeel, L.A., Scatena, F.N. & Hamilton, L.S.), pp. 208-216. Cambridge University Press, Cambridge, UK.

Häger, A. & Dohrenbusch, A. (2011) Hydrometeorology and structure of tropical montane cloud forests under contrasting biophysical conditions in north-western Costa Rica. *Hydrological Processes,* 25**,** 392-401.

Heaney, A. & Proctor, J. (1990) Preliminary studies on forest structure and floristics on Volcán Barva, Costa Rica. *Journal of Tropical Ecology,* 6**,** 307-320.

Hemp, A. (2002) Ecology of the pteridophytes on the southern slopes of Mt. Kilimanjaro - I. Altitudinal distribution. *Plant Ecology,* 159**,** 211-239.

Hemp, A. (2006) Continuum or zonation? Altitudinal gradients in the forest vegetation of Mt. Kilimanjaro. *Plant Ecology,* 184**,** 27-42.

Henderson, A., Churchill, S.P. & Luteyn, J. (1991) Neotropical plant diversity. *Nature,* 351**,** 21-22.

Hernández, L., Dezzeo, N., Sanoja, E., Salazar, L. & Castellanos, H. (2012) Changes in structure and composition of evergreen forests on an altitudinal gradient in the Venezuelan Guayana Shield. *International Journal of Tropical Biology,* 60**,** 11-33.

Hietz, P. & Hietz-Seifert, U. (1995) Composition and ecology of vascular epiphyte communities along an altitudinal gradient in central Veracruz, Mexico. *Journal of Vegetation Science,* 6**,** 487-498.

Holder, C.D. (2003) Fog precipitation in the Sierra de las Minas Biosphere Reserve, Guatemala. *Hydrological Processes,* 17**,** 2001-2010.

Holder, C.D. (2007) Leaf Water Repellency as an Adaptation to Tropical Montane Cloud Forest Environments. *Biotropica,* 39**,** 767-770.

Holdridge, L.R. (1967) *Life zone ecology.* Tropical Science Center, San José, Costa Rica.

Holdridge, L.R., Grenke, W.C., Hatheway, W.H., Liang, T. & Tosi Jr, J.A. (1971) *Forest environments in tropical life zones.* Pergamon Press, New York.

Homeier, J., Breckle, S.-W., Günter, S., Rollenbeck, R.T. & Leuschner, C. (2010) Tree Diversity, Forest Structure and Productivity along Altitudinal and Topographical Gradients in a Species-Rich Ecuadorian Montane Rain Forest. *Biotropica,* 42**,** 140-148.

Honorio, E. & Reynel, C. (2004) *Vacíos en la colección de la flora de los Bosques Húmedos del Perú.* Herbario de la Facultad de Ciencias Forestales, Universidad Nacional Agraria La Molina, Lima, Peru.

Ibisch, P., Boegner, A., Nieder, J. & Barthlott, W. (1996) How diverse are neotropical epiphytes ? An analysis based on the "Catalogue of flowering plants and gymnosperms of Peru". *Ecotropica,* 2**,** 13-28.

INRENA (2005). Plan Maestro 2005 - 2009 del Parque Nacional Yanachaga-Chemillén. Instituto Nacional de Recursos Naturales, Lima, Peru.

Jarvis, A. & Mulligan, M. (2011) The climate of cloud forests. *Hydrological Processes,* 25**,** 327-343.

Juvik, J.O. & Ekern, P.C. (1978). A climatology of mountian fog on Mauna loa, Hawai'i Island. *Technical Report No. 118*. Water Resources Research Centre, University of Hawaii, Honolulu, Hawaii.

Juvik, J.O. & Nullet, D. (1995) Relationships between rainfall, cloud-water interception, and canopy throughfall in a Hawaiian montane forest. *Tropical Montane Cloud Forests: Proceedings of an International Symposium* (eds Hamilton, L.S., Juvik, J.O. & Scatena, F.N.), pp. 165-182. Springer Verlag, New York.

Kappelle, M. & Leal, M.E. (1996) Changes in leaf morphology and foliar nutrient status along a successional gradient in a Costa Rican upper montane *Quercus* forest. *Biotropica,* 28**,** 331-344.

Kappelle, M., van Uffelen, J.G. & Cleef, A.M. (1995) Altitudinal zonation of montane *Quercus* forests along 2 transects in Chirripo National-Park, Costa-Rica. *Vegetatio,* 119**,** 119-153.

Kappelle, M., Geuze, T., Leal, M.E. & Cleef, A.M. (1996) Successional age and forest structure in a Costa Rican upper montane *Quercus* forest. *Journal of Tropical Ecology,* 12**,** 681-698.

Kessler, M. (2000) Upslope-Directed Mass Effect in Palms along an Andean Elevational Gradient: A Cause for High Diversity at Mid-Elevations? *Biotropica,* 32**,** 756-759.

Kessler, M. (2001) Pteridophyte species richness in Andean forests in Bolivia. *Biodiversity and Conservation,* 10**,** 1473-1495.

Killeen, T.J., Douglas, M., Consiglio, T., Jorgensen, P.M. & Mejia, J. (2007) Dry spots and wet spots in the Andean hotspot. *Journal of Biogeography,* 34**,** 1357-1373.

Kimura, K., Yumoto, T. & Kikuzawa, K. (2001) Fruiting phenology of fleshy-fruited plants and seasonal dynamics of frugivorous birds in four vegetation zones on Mt. Kinabalu, Borneo. *Journal of Tropical Ecology,* 17**,** 833-858.

Kirkby, C.A., Smythe, L.J., Cox, J.W. & Chittleborough, D.J. (1997) Phosphorus movement down a toposequence from a landscape with texture contrast soils. *Australian Journal of Soil Research,* 35**,** 399-417.

Kirkpatrick, J.B. & Hassal, D.C. (1985) The vegetation and flora along an altitudinal transect through tropical forest at Mt. Korobaba, Fiji. *New Zealand Journal of Botany,* 23**,** 33-46.

Kitayama, K. (1992) An altitudinal transect study of the vegetation on Mount Kinabalu, Borneo. *Vegetatio,* 102**,** 149-171.

Kitayama, K. (1995) Biophysical conditions of the montane cloud forest of Mount Kinabalu, Sabah, Malaysia. *Tropical Montane Cloud Forests* (eds

Hamilton, L.S., Juvik, J.O. & Scatena, F.N.), pp. 183-197. Springer Verlag, New York.

Kitayama, K. & Aiba, S.I. (2002) Ecosystem structure and productivity of tropical rain forests along altitudinal gradients with contrasting soil phosphorus pools on Mount Kinabalu, Borneo. *Journal of Ecology,* 90**,** 37-51.

Kohler, L., Tobon, C., Frumau, K.F.A. & Bruijnzeel, L.A. (2007) Biomass and water storage dynamics of epiphytes in old-growth and secondary montane cloud forest stands in Costa Rica. *Plant Ecology,* 193**,** 171-184.

Kramer, P.J. & Kozlowski, T.T. (1979) *Physiology of woody plants.* Academic Press, Orlando, FL.

Krömer, T., Kessler, M., Gradstein, S.R. & Acebey, A. (2005) Diversity patterns of vascular epiphytes along an elevational gradient in the Andes. *Journal of Biogeography,* 32**,** 1799-1809.

Kruskal, J.B. (1964) Nonmetric multidimensional scaling: a numerical method. *Psychometrika,* 29**,** 115-129.

Kuiters, A.T. (1990) Role of phenolic substances from decomposing forest litter in plant-soil interactions. *Acta Botanica Neerlandica,* 39**,** 329-348.

Kuper, W., Kreft, H., Nieder, J., Koster, N. & Barthlott, W. (2004) Large-scale diversity patterns of vascular epiphytes in Neotropical montane rain forests. *J Biogeography,* 31**,** 1477-1487.

Kurschner, H. & Parolly, G. (1998a) Syntaxonomy of trunk-epiphytic bryophyte communities of tropical rain forests - A first pantropical approach. *Phytocoenologia,* 28**,** 357-425.

Kurschner, H. & Parolly, G. (1998b) Life strategies of epiphytic bryophytes in the rainforests along the eastern Andean slopes and the Amazonian lowlands of northern Peru. *Nova Hedwigia,* 67**,** 1-22.

Kurschner, H. & Parolly, G. (1998c) Stem epiphytic moss communities on the Andean border and in the lowlands of Amazonia in northern Peru. *Nova Hedwigia,* 66.

Kurschner, H. & Parolly, G. (1998d) Canopy epiphytic moss vegetation in the eastern Andes and the Amazonian lowlands of northern Peru. *Nova Hedwigia,* 66**,** 1-87.

Kurschner, H. & Parolly, G. (1998e) Life forms and adaptations for water conduction and water storage of the epiphytic bryophytes of northern Peru (Amazonian Lowlands, Cordillera Oriental, Cordillera Central). *Nova Hedwigia,* 67**,** 349-379.

Kurschner, H. & Parolly, G. (1999) Pantropical epiphytic rain forest bryophyte communities - coeno-syntaxonomy and floristic-historical implications. *Phytocoenologia,* 29**,** 1-52.

Lawrence, M.G. (2005) The relationship between relative humidity and the dewpoint temperature in moist air - A simple conversion and applications. *Bulletin of the American Meteorological Society,* 86**,** 225-+.

Lawton, R.O. (1982) Wind stress and elfin stature in a montane rain forest tree: an adaptive explanation. *American Journal of Botany,* 69**,** 1124-1230.

Lawton, R.O. & Campbell, J. (1984) Climate and vegetation of a neotropical montane forest. *Bulletin of the Ecological Society of America,* 65**,** 59.

Ledo, A., Montes, F. & Condes, S. (2009) Species dynamics in a montane cloud forest: Identifying factors involved in changes in tree diversity and functional characteristics. *Forest Ecology and Management,* 2585**,** S75-S84.

Leigh, J.E.G. (1975) Structure and climate in tropical rain forest. *Annual Review in Ecology and Systematics,* 6**,** 67-86.

Leo, M. (1995) The importance of tropical montane cloud forest for preserving vertebrate endemism in Peru: the Rio Abiseco National Park as a case study. *Tropical Montane Cloud Forests: Proceedings of an international symposium* (eds Hamilton, L.S., Juvik, J.O. & Scatena, F.N.), pp. 198-205. Springer Verlag, New York.

Leon-Vargas, Y., Engwald, S. & Proctor, M.C.F. (2006) Microclimate, light adaptation and desiccation tolerance of epiphytic bryophytes in two Venezuelan cloud forests. *Journal of Biogeography,* 33**,** 901-913.

León, B. & Young, K.R. (1996) Distribution of pteridophyte diversity and endemism in Peru. *Pteridology in perspective* (eds Camus, J.M., Gibby, M. & Johns, R.H.), pp. 77-91. Royal Botanic Gardens, Kew.

Letts, M.G. & Mulligan, M. (2005) The impact of light quality and leaf wetness on photosynthesis in north-west Andean tropical montane cloud forest. *Journal of Tropical Ecology,* 21**,** 549-557.

Letts, M.G., Mulligan, M., Rincón-Romero, M.E. & Bruijnzeel, L.A. (2010) Environmental controls on photosynthetic rates of lower montane cloud forest vegetation in south-western Colombia. *Tropical Montane Cloud Forests: Science for COnservation and Management* (eds Bruijnzeel, L.A., Scatena, F.N. & Hamilton, L.S.), pp. 465-478. Cambridge University Press.

Leuschner, C., Moser, G., Bertsch, C., Röderstein, M. & Hertel, D. (2007) Large altitudinal increase in tree root/shoot ratio in tropical mountain forests of Ecuador. *Basic and Applied Ecology,* 8**,** 219-230.

Lewis, W.H. (1971) High floristic endemism in low cloud forests of Panama. *Biotropica,* 3**,** 78-80.

Lieberman, D., Lieberman, M., Peralta, R. & Hartshorn, G.S. (1996) Tropical forest structure and composition on a large-scale altitudinal gradient in Costa Rica. *Journal of Ecology,* 84**,** 137-152.

Long, A.J. (1995) The importance of tropical montane cloud forests for endemic and threatened birds. *Tropical Montane Cloud Forests* (eds Hamilton, L.S., Juvik, J.O. & Scatena, F.N.), pp. 79-106. Springer Verlag, New York.

Madsen, J.E. & Ollgaard, B. (1994) Floristic Composition, Structure, and Dynamics of an Upper Montane Rain-Forest in Southern Ecuador. *Nordic Journal of Botany,* 14**,** 403-423.

Malhi, Y. & Wright, J. (2004) Spatial patterns and recent trends in the climate of tropical rainforest regions. *Philosophical Transactions of the Royal Society of London Series B-Biological Sciences,* 359**,** 311-329.

Marengo, J.A., Tomasella, J., Alves, L.M., Soares, W.R. & Rodriguez, D.A. (2011) The drought of 2010 in the context of historical droughts in the Amazon region. *Geophysical Research Letters,* 38**,** 5.

Markham, C.G. (1970) Seasonality of Precipitation in the United States. *Annals of the Association of American Geographers,* 60**,** 593-597.

Marrs, R.H., Proctor, J., Heaney, A. & Mountford, M.D. (1988) Changes in soil nitrogen-mineralization and nitrification along an altitudinal transect in tropical rain forest in Costa Rica. *Journal of Ecology,* 76**,** 466-482.

Martin, P.H., Sherman, R.E. & Fahey, T.J. (2007) Tropical montane forest ecotones: climate gradients, natural disturbance, and vegetation zonation in the Cordillera Central, Dominican Republic. *Journal of Biogeography,* 34**,** 1792-1806.

Martin, P.H., Fahey, T.J. & Sherman, R.E. (2010) Vegetation Zonation in a Neotropical Montane Forest: Environment, Disturbance and Ecotones. *Biotropica,* 43**,** 533-543.

Matelson, T.J., Nadkarni, N.M. & Solano, R. (1995) Tree damage and annual mortality in a montane forest in Monteverde, Costa Rica. *Biotropica,* 27**,** 441-447.

Mather, P.M. (1976) *Computational methods of multivariate analysis in physical geography.* J. Wiley & Sons, London.

McGowan, H.A., Sturman, A.P., Kossmann, M. & Zawar-Reza, P. (2002) Observations of foehn onset in the Southern Alps, New Zealand. *Meteorology and Atmospheric Physics,* 79**,** 215-230.

Meier, W. (2011) Los bosques nublados de la Cordillera de la Costa en Venezuela. *BioLlania Edición Esp.,* 10**,** 106-121.

Merlin, M.D. & Juvik, J.O. (1995) Montane cloud forest in the tropical Pacific: some aspects of their floristics, biogeography, ecology, and conservation. *Tropical Montane Cloud Forests* (eds Hamilton, L.S., Juvik, J.O. & Scatena, F.N.), pp. 234-253. Springer Verlag, New York.

Michelsen, A. (1993) The mycorrhizal status of vascular epiphytes in Bale Mountains National Park, Ethiopia. *Mycorrhiza,* 4**,** 11-15.

Mildenberger, K., Beiderwieden, E., Hsia, Y.J. & Klemm, O. (2009) CO2 and water vapor fluxes above a subtropical mountain cloud forest-The effect of light conditions and fog. *Agricultural and Forest Meteorology,* 149**,** 1730-1736.

Monedero, C. (1998) Quantitative analysis of the arboreal structure in a tropical cloud forest: Ramal interior of the Cordillera de la Costa, Loma de Hierro (Estado Aragua), Venezuela. *Forest biodiversity in North, Central and South America, and the Caribbean: research and monitoring* (eds Dallmeier, F. & Comiskey, J.A.), pp. 427-447. UNESCO, Paris.

Moser, G., Hertel, D. & Leuschner, C. (2007) Altitudinal change in LAI and stand leaf biomass in tropical montane forests: a transect shady in Ecuador and a pan-tropical meta-analysis. *Ecosystems,* 10**,** 924-935.

Myers, N., Mittermeier, R.A., Mittermeier, C.G., da Fonseca, G.A.B. & Kent, J. (2000) Biodiversity hotspots for conservation priorities. *Nature,* 403**,** 853-858.

Nadkarni, N.M. & Matelson, T.J. (1992) Biomass and nutrient dynamics of epiphytic litterfall in a neotropical montane forest, Costa-Rica. *Biotropica,* 24**,** 24-30.

Nadkarni, N.M., McIntosh, A.C.S. & Cushing, J.B. (2008) A framework to categorize forest structure concepts. *Forest Ecology and Management,* 256**,** 872-882.

Nadkarni, N.M., Schaefer, D., Matelson, T.J. & Solano, R. (2002) Comparison of arboreal and terrestrial soil characteristics in a lower montane forest, Monteverde, Costa Rica. *Pedobiologia,* 46**,** 24-33.

Nair, U.S., Asefi, S., Welch, R.M., Ray, D.K., Lawton, R.O., Manoharan, V.S., Mulligan, M., Sever, T.L., Irwin, D. & Pounds, J.A. (2008) Biogeography of tropical montane cloud forests. Part II: Mapping of orographic cloud immersion. *Journal of Applied Meteorology and Climatology,* 47**,** 2183-2197.

Nakashizuka, T., Yusop, Z. & Rahim Nik, A. (1991) Altitudinal zonation of forest communities in Selangor, Peninsular Malaysia. *Journal of Tropical Forest Science,* 4**,** 233-244.

Nieder, J., Engwald, S. & Barthlott, W. (1999) Patterns of neotropical epiphyte diversity. *Selbyana,* 20**,** 66-75.

Nomura, M., Kaji, A., He, Z., Ma, W.-Y., Miyamoto, K.-i., Yang, C.S. & Dong, Z. (2001) Inhibitory Mechanisms of Tea Polyphenols on the Ultraviolet B-activated Phosphatidylinositol 3-Kinase-dependent Pathway. *J. Biol. Chem.,* 276**,** 46624-46631.

Obregon, A., Gehrig-Downie, C., Gradstein, S.R., Rollenbeck, R. & Bendix, J. (2011) Canopy level fog occurrence in a tropical lowland forest of French Guiana as a prerequisite for high epiphyte diversity. *Agricultural and Forest Meteorology,* 151**,** 290-300.

Ohsawa, M. (1991) Structural comparison of tropical montane rain-forests along latitudinal and altitudinal gradients in south and east Asia. *Vegetatio,* 97**,** 1-10.

Ohsawa, M. (1995a) Latitudinal comparison of altitudinal changes in forest structure, leaf-type, and species richness in humid monsoon Asia. *Vegetatio,* 121**,** 3-10.

Ohsawa, M. (1995b) The montane cloud forest and its gradational changes in Southeast Asia. *Tropical Montane Cloud Forests* (eds Hamilton, L.S., Juvik, J.O. & Scatena, F.N.), pp. 254-265. Springer Verlag, New York.

Oosterhoorn, M.a.K., M. (2000) Vegetation structure and composition along an interior-edge-exterior gradient in a Costa Rican montane cloud forest. *Forest Ecology and Management,* 126**,** 291-307.

Palmer, M.W. (1990) The estimation of species richness by extrapolation. *Ecology,* 71**,** 1195-1198.

Palmer, M.W. (1991) Estimating species richness: the second-order jackknife reconsidered. *Ecology,* 72**,** 1512-1513.

Palmer, M.W. (1995) How should one count species? *Natural Areas Journal* 15**,** 124-135.

Patterson, B.D., Stotz, D.F., Solari, S., Fitzpatrick, J.W. & Pacheco, V. (1998) Contrasting patterns of elevational zonation for birds and mammals in the Andes of southeastern Peru. *Journal Of Biogeography,* 25**,** 593-607.

Pendry, C.A. & Proctor, J. (1996) The causes of altitudinal zonation of rain forests on Bukit Belalong, Brunei. *Journal of Ecology,* 84**,** 407-418.

Pendry, C.A. & Proctor, J. (1997) Altitudinal zonation of rain forest on Bukit Belalong, Brunei: soils, forest structure and floristics. *Journal of Tropical Ecology,* 13.

Phillips, O.L. & Baker, T.R. (2002) *Field Manual for plot establishment and remeasurement (RAINFOR).*

Phillips, O.L., Hall, P., Gentry, A.H., Sawyer, S.A. & Vázquez, R. (1994) Dynamics and species richness of tropical forests. *Proceedings of the National Academy of Sciences, USA,* 91**,** 2805-2809.

Poulsen, A.D. & Pendry, C.A. (1995) Inventories of ground herbs at 3 altitudes on Bukit-Belalong, Brunei, Borneo. *Biodiversity and Conservation,* 4**,** 745-757.

Primack, R.B. (1985) Longevity of individual flowers. *Annual Review of Ecology and Systematics,* 16**,** 15-37.

Ramírez, L., Llambí, L.D., Schwarzkopf, T., Gámez, L.E. & Márquez, N.J. (2009) Vegetation structure along the forest – páramo transition belt in the Sierra Nevada de Mérida: implications for understanding treeline dynamics. *Ecotrópicos,* 22**,** 83-98.

Raunkiaer, C. (1934) *The Life Forms of Plants and Statistical Plant Geography.* Clarendon Press, Oxford.

Reinhardt, K. & Smith, W.K. (2008) Impacts of cloud immersion on microclimate, photosynthesis and water relations of Abies fraseri (Pursh.) Poiret in a temperate mountain cloud forest. *Oecologia,* 158**,** 229-238.

Reinhardt, K., Smith, W.K. & Carter, G.A. (2008) Clouds and cloud immersion alter photosynthetic light quality in a temperate mountain cloud forest. *Botany-Botanique,* 88**,** 462-470.

Requena Rojas, E.J. (2007) *Estimación de las emisiones de isopreno y monoterpenos generadas por la vegetación en una parcela ubicada en el Parque Nacional Yanachaga-Chemillén – Oxapampa, Pasco (Perú).* Unpublished Undergraduate Thesis, Universidad Nacional del Centro del Perú, Huancayo, Peru.

Richardson, B.A., Richardson, M.J., Scatena, F.N. & McDowell, W.H. (2000) Effects of nutrient availability and other elevational changes on bromeliad populations and their invertebrate communities in a humid tropical forest in Puerto Rico. *Journal of Tropical Ecology,* 16**,** 167-188.

Roach, W.T. (1994) Back to Basics: Fog: Part 1 - Definitions and basic physics. *Weather,* 49**,** 411-415.

Roderstein, M., Hertel, D. & Leuschner, C. (2005) Above- and below-ground litter production in three tropical montane forests in southern Ecuador. *Journal of Tropical Ecology,* 21**,** 483-492.

Rollet, B. (1984) Études sur une forêt d'altitude des Andes Vénézuéliennes. *Revue Bios Forêts Des Tropique,* 205**,** 3–23.

Romanski, J., Pharo, E.J. & Kirkpatrick, J.B. (2011) Epiphytic bryophytes and habitat variation in montane rainforest, Peru. *Bryologist,* 114**,** 720-731.

Rozema, J., Chardonnens, A., Tosserams, M., Hafkenscheid, R. & Bruijnzeel, S. (1997) Leaf thickness and UV-B absorbing pigments of plants in relation to an elevational gradient along the Blue Mountains, Jamaica. *Plant Ecology,* 128**,** 150-159.

Sampson, B.J. & Cane, J.H. (1999) Impact of enhanced ultraviolet-B radiation on flower, pollen, and nectar production. *American Journal Of Botany,* 86**,** 108-114.

Scatena, F.N. (1995) The management of Luquillo elfin cloud forest ecosystems: irreversible decisions in a nonsubstitutable ecosystem. *Tropical Montane Cloud Forests* (eds Hamilton, L.S., Juvik, J.O. & Scatena, F.N.), pp. 296-308. Springer Verlag, New York.

Scatena, F.N., Bruijnzeel, L.A., Bubb, P. & Das, S. (2010) Setting the stage. *Tropical Montane Cloud Forests: Science for Conservation and Management* (eds Bruijnzeel, L.A., Scatena, F.N. & Hamilton, L.S.), pp. 3-13. Cambridge University Press, Cambridge, UK.

Scheer, M.B., Mocochinski, A.Y. & Roderjan, C.V. (2011) Tree component structure of tropical upper montane rain forests in Southern Brazil. *Acta Botanica Brasilica,* 25**,** 735-750.

Schwarzkopf, T., Riha, S.J., Fahey, T.J. & Degloria, S. (2010) Are cloud forest tree structure and environment related in the Venezuelan Andes? *Austral Ecology,* 36**,** 280-289.

Seluchi, M.E., Norte, F.A., Satyamurty, P. & Chou, S.C. (2003) Analysis of three situations of the Foehn effect over the Andes (zonda wind) using the Eta-CPTEC regional model. *Weather and Forecasting,* 18**,** 481-501.

Shannon, C.E. (1948) The mathematical theory of communication. *Bell System Technical Journal* 27**,** 379–423 & 623–656.

Sherman, R.E., Martin, P.H. & Fahey, T.J. (2005) Vegetation-environment relationships in forest ecosystems of the Cordillera Central, Dominican Republic. *Journal of the Torrey Botanical Society,* 132**,** 293-310.

Shipley, B., Lechowicz, M.J., Wright, I. & Reich, P.B. (2006) Fundamental trade-offs generating the worldwide leaf economics spectrum. *Ecology,* 87**,** 535-541.

Silver, W.L. (1998) The potential effects of elevated CO2 and climate change on tropical forest soils and biogeochemical cycling. *Climatic Change,* 39**,** 337-361.

Silver, W.L., Neff, J., McGroddy, M., Veldkamp, E., Keller, M. & Cosme, R. (2000) Effects of soil texture on belowground carbon and nutrient storage in a lowland Amazonian forest ecosystem. *Ecosystems,* 3**,** 193-209.

Simpson, E.H. (1949) Measurement of diversity. *Nature,* 163**,** 688.

Soethe, N., Lehmann, J. & Engels, C. (2006) The vertical pattern of rooting and nutrient uptake at different altitudes of a south ecuadorian montane forest. *Plant and Soil,* 286**,** 287-299.

Stadtmüller, T. (1987) *Cloud forests in the humid tropics. A bibliographic review.* The United Nations University, Tokyo.

Stadtmüller, T. & Agudelo, N. (1990) Amount and variability of cloud moisture input in a tropical cloud forest. *International Association of Hydrological Sciences Publication,* 193**,** 25-32.

Steven, M.D. & Unsworth, M.H. (1980) The angular distribution and interception of diffuse solar radiation below overcast skies. *Quarterly Journal of the Royal Meteorological Society,* 106**,** 57-61.

Stiles, G.F. (1981) Geographical aspects of bird-flower coevolution, with particular reference to Central America. *Annals of the Missouri Botanic Garden,* 68**,** 323-351.

Strahler, A.N. & Strahler, A.H. (1987) *Modern Physical Geography.* John Wiley & Sons Inc., New York, USA.

Sugden, A.M. (1982a) The vegetation of the Serranía de Macuira, Guajira, Colombia - a contrast of arid lowlands and an isolated cloud forest. *Journal of the Arnold Arboretum,* 63**,** 1-30.

Sugden, A.M. (1982b) The ecological, geographic, and taxonomic relationships of the flora of an isolated Colombian cloud forest, with some implications for island biogeography. *Journal of the Arnold Arboretum,* 63**,** 31-61.

Sugden, A.M. (1986) The montane vegetation and flora of Margarita Island, Venezuela. *Journal of the Arnold Arboretum,* 67**,** 187-232.

Sullivan, J.H., Teramura, A.H. & Ziska, L.H. (1992) Variation in UV-B sensitivity in plants from a 3,000-m elevational gradient in Hawaii. *American Journal of Botany,* 79**,** 737-743.

Takyu, M., Aiba, S.I. & Kitayama, K. (2002) Effects of topography on tropical lower montane forests under different geological conditions on Mount Kinabalu, Borneo. *Plant Ecology,* 159**,** 35-49.

Takyu, M., Aiba, S.I. & Kitayama, K. (2003) Changes in biomass, productivity and decomposition along topographical gradients under different geological conditions in tropical lower montane forests on Mount Kinabalu, Borneo. *Oecologia,* 134**,** 397-404.

Tanaka, N., Kuraji, K., Tantasirin, C., Takizawa, H., Tangtham, N. & Suzuki, M. (2011) Relationships between rainfall, fog and throughfall at a hill evergreen forest site in northern Thailand. *Hydrological Processes,* 25**,** 384-391.

Tanner, E.V.J. (1980a) Studies on the biomass and productivity in a series of montane rain forests in Jamaica. *Ecology,* 68**,** 573-588.

Tanner, E.V.J. (1980b) Litterfall in montane rain forests of Jamaica and its relation to climate. *Ecology,* 68**,** 833-848.

Tanner, E.V.J., Vitousek, P.M. & Cuevas, E. (1998) Experimental investigation of nutrient limitation of forest growth on wet tropical mountains. *Ecology,* 79**,** 10-22.

Tanner, E.V.J., Kapos, V., Freskos, S., Healey, J.R. & Theobald, A.M. (1990) Nitrogen and Phosphorus Fertilization of Jamaican Montane Forest Trees. *Journal of Tropical Ecology,* 6**,** 231-238.

Tausz, M., Heitz, P. & Briones, O. (2001) The significance of carotenoids and tocopherols in photoprotection of seven epiphytic fern species of a Mexican cloud forest. *Australian Journal of Plant Physiology,* 28**,** 775-783.

Taylor, M. (2008) *The ecology of understorey vegetation in a Peruvian cloudforest*. Unpublished Honours Thesis, University of Tasmania, Hobart, Australia.

Turner, I.M. (1994) Sclerophylly - Primarily Protective. *Functional Ecology,* 8**,** 669-675.

Valencia, R. & Jørgensen, P.M. (1992) A quantitative inventory of a humid montane forest on volcan Pasochoa, Ecuador. *Nordic Journal of Botany,* 12**,** 239-247.

van de Weg, M.J., Meir, P., Grace, J. & Atkin, O.K. (2009) Altitudinal variation in leaf mass per unit area, leaf tissue density and foliar nitrogen and

phosphorus content along an Amazon-Andes gradient in Peru. *Plant Ecology & Diversity,* 2**,** 243-U7.

van der Werff, H. & Consiglio, T. (2004) Distribution and conservation significance of endemic species of flowering plants in Peru. *Biodiversity and Conservation,* 13**,** 1699-1713.

van Reenen, G.B.A. & Gradstein, S.R. (1983) A transect analysis of the bryophyte vegetation along a gradient on the Sierra Nevada de Santa Marta, Columbia. *Acta Botanica Neerlandica,* 32**,** 163-175.

Vásquez, R., Ibisch, P.L. & Gerkmann, B. (2003) Diversity of Bolivian Orchidaceae - a challenge for taxonomic, floristic and conservation research. *Organisms Diversity & Evolution,* 3**,** 93-102.

Vásquez, R., Rojas, R., Monteagudo, A., Meza, K., Van der Werff, H., Ortiz-Gentry, R. & Catchpole, D.J. (2005) Flora Vascular de la selva central del Perú: Una aproximación de la composición florística de tres Áreas Naturales Protegidas. *Arnaldoa,* 12 112-125.

Vázquez, J.A. & Givnish, T.J. (1998) Altitudinal gradients in tropical forest composition, structure, and diversity in the Sierra de Manantlan. *Journal of Ecology,* 86**,** 999-1020.

Velez, V., Cavelier, J. & Devia, B. (1998) Ecological traits of the tropical treeline species Polylepis quadrijuga (Rosaceae) in the Andes of Colombia. *Journal of Tropical Ecology,* 14**,** 771-787.

Veneklaas, E.J. & van Ek, R. (1990) Rainfall interception in two tropical montane rain forests, Colombia. *Hydrological Processes,* 4**,** 311-326.

Veneklaas, E.J., Zagt, R.J., van Leerdam, A., Vanek, R., Broekhoven, A.J. & van Genderen, M. (1990) Hydrological properties of the epiphyte mass of a montane tropical rain-forest, Colombia. *Vegetatio,* 89**,** 183-192.

Vera, M., Cavelier, J. & Santamaria, J. (1999) Tree leaf nitrogen and phosphorus reabsorption in a montane forest of the central Andes, Colombia. *Revista De Biologia Tropical,* 47**,** 33-43.

Vitousek, P.M. (1998) Special Feature - The structure and functioning of montane tropical forests: control by climate, soils and disturbance. *Ecology,* 79**,** 1-2.

Waide, R.B., Zimmerman, J.K. & Scatena, F.N. (1998) Controls of primary productivity: lessons from the Luquillo Mountains in Puerto Rico. *Ecology,* 79**,** 31-37.

Weaver, P.L. (2000) Environmental gradients affect forest structure in Puerto Rico's Luquillo Mountains. *Interciencia,* 25**,** 254-259.

Weaver, P.L. (2010a) Forest structure and composition in the lower montane rain forest of the Luquillo Mountains, Puerto Rico. *Interciencia,* 35**,** 640-646.

Weaver, P.L. (2010b) Tree species distribution and forest structure along environmental gradients in the dwarf forest of the Luquillo Mountains of Puerto Rico. *Bois et forêts des tropiques,* 306**,** 33-44.

Weaver, P.L., Medina, E., Pool, D., Dugger, K., Gonzales-Liboy, J. & Cuevas, E. (1986) Ecological observations in the dwarf cloud forest of the Luquillo Mountains in Puerto Rico. *Biotropica,* 18**,** 79-85.

Webb, L.J. (1959) A physiognomic classification of Australian rain forests. *Journal of Ecology,* 47**,** 551-570.

Weberbauer, A. (1945). El mundo vegetal de los andes peruanos. Ministerio de Agricultura, Lima.

Welch, R.M., Asefi, S., Zeng, J., Nair, U.S., Han, Q., Lawton, R.O., Ray, D.K. & Manoharan, V.S. (2008) Biogeography of Tropical Montane Cloud Forests. Part I: Remote Sensing of Cloud-Base Heights. *Journal of Applied Meteorology and Climatology,* 47**,** 960-975.

Werner, F.A., Homeier, J., Oesker, M. & Boy, J. (2012) Epiphytic biomass of a tropical montane forest varies with topography. *Journal of Tropical Ecology,* 28**,** 23-31.

Wesselingh, R.A., Witteveldt, M., Morissette, J. & den Nijs, H.C.M. (1999) Reproductive ecology of understory species in a tropical montane forest in Costa Rica. *Biotropica,* 31**,** 637-645.

Whitmore, T.C. (1989) Tropical forest nutrients, where do we stand? A tour de horizon. *Mineral nutrients in tropical forest and savanna ecosystems* (ed Proctor, J.), pp. 1-13. Blackwell Scientific Press, Oxford, UK.

Wilcke, W., Yasin, S., Valarezo, C. & Zech, W. (2001) Change in water quality during the passage through a tropical montane rain forest in Ecuador. *Biogeochemistry,* 55**,** 45-72.

Williams-Linera, G. (2002) Tree species richness complementarity, disturbance and fragmentation in a Mexican tropical montane cloud forest. *Biodiversity and Conservation,* 11**,** 1825-1843.

Williams, K., Field, C.B. & Mooney, H.A. (1989) Relationships among leaf construction cost, leaf longevity, and light environment in rain-forest plants of the genus *Piper*. *American Naturalist,* 133**,** 198-211.

Wolf, J.H.D. (1993a) Epiphyte communities of tropical montane rain forest in the Northern Andes. I. Lower Montane communites. *Phytocoenologia,* 22**,** 1-52.

Wolf, J.H.D. (1993b) Epiphyte communities of tropical montane rain forest in the Northern Andes. II. Upper Montane communites. *Phytocoenologia,* 22**,** 53-103.

Wolf, J.H.D. (1993c) Diversity patterns and biomass of epiphytic bryophytes and lichens along an altitudinal gradient in the Northern Andes. *Annals of The Missouri Botanical Garden,* 80**,** 928-960.

Wolf, J.H.D. (1994) Factors controlling the distribution of vascular and nonvascular epiphytes in the northern Andes. *Vegetatio,* 112**,** 15-28.

Wolfe, J.A. (1964) *An Analysis of Present-Day Terrestrial Lapse Rates in the Western Conterminous United States and Their Significance to Paleoaltitudianal Estimates.* U.S. Geological Survey, Denver, USA.

Xavier, L., Becker, M., Cazenave, A., Longuevergne, L., Llovel, W. & Rotunno, O.C. (2010) Interannual variability in water storage over 2003-2008 in the Amazon Basin from GRACE space gravimetry, in situ river level and precipitation data. *Remote Sensing of Environment,* 114**,** 1629-1637.

Young, K.R. (1991) Floristic diversity on the eastern slopes of the Peruvian Andes. *Candollea,* 46**,** 125-143.

Young, K.R., Ulloa, C.U., Luteyn, J.L. & Knapp, S. (2002) Plant evolution and endemism in Andean South America: An introduction. *Botanical Review,* 68**,** 4-21.

Zeng, N., Yoon, J.H., Marengo, J.A., Subramaniam, A., Nobre, C.A., Mariotti, A. & Neelin, J.D. (2008) Causes and impacts of the 2005 Amazon drought. *Environmental Research Letters,* 3**,** 9.

Zimmerman, M.H. & Brown, C.L. (1971) *Trees: structure and function.* Springer-Verlag, New York.

Ziska, L.H., Teramura, A.H. & Sullivan, J.H. (1992) Physiological sensitivity of plants along an elevational gradient to UV-B radiation. *American Journal of Botany,* 79**,** 863-871.

Zotz, G., Tyree, M.T., Patino, S. & Carlton, M.R. (1998) Hydraulic architecture and water use of selected species from a lower montane forest in Panama. *Trees-Structure And Function,* 12**,** 302-309.

Appendices

Appendix A: Pearson's Correlation scores among climatic variables

Appendix Table 1: Pearson's Correlation scores (*r*) between all sites and hourly diurnal measurements (0600 – 1700 h) during the 2007-2008 wet season (October – April) periods. Only significant *r* scores (P < 0.05) are shown.

	1AT	2AT	3AT	1PA	2PA	3PA	1RA	2RA	3RA	1VP	2VP	3VP	1WD	2WD	3WD	1WS	2WS	3WS	1VI	2VI	3VI	1WE	2WE
2AT	0.85																						
3AT	0.62	0.75																					
1PA	0.69	0.61	0.44																				
2PA	0.57	0.65	0.55	0.81																			
3PA	0.48	0.57	0.64	0.69	0.84																		
1RA	-0.23	-0.21	-0.19	-0.21	-0.21	-0.14																	
2RA	-0.24	-0.24	-0.23	-0.22	-0.24	-0.17	0.81																
3RA	-0.19	-0.20	-0.25	-0.16	-0.18	-0.19	0.55	0.70															
1VP	0.57	0.49	0.25	0.30	0.22	0.13			-0.04														
2VP	0.78	0.71	0.42	0.55	0.47	0.36	-0.11	-0.13	-0.11	0.83													
3VP	0.64	0.54	0.46	0.38	0.30	0.27	-0.03	-0.05	-0.11	0.75	0.82												
1WD	-0.07		0.07		0.18	0.20				0.11													
2WD	-0.32	-0.26	-0.10	-0.26	-0.19	-0.13	0.06			-0.17	-0.31	-0.21	0.14										
3WD	-0.34	-0.31	-0.19	-0.27	-0.23	-0.21				-0.34	-0.37	-0.38		0.35									
1WS	0.40	0.29	0.12	0.37	0.24	0.15	-0.06	-0.06		0.18	0.35	0.23	-0.23	-0.28	-0.23								
2WS	0.12		0.05	0.15	0.14	0.09				-0.09		-0.05	-0.14	0.07	0.10	0.27							
3WS	0.38	0.36	0.19	0.41	0.37	0.39		0.05		0.19	0.34	0.25		-0.10	-0.21	0.35	0.34						
1VI	0.17	0.13	0.11	0.13	0.11	0.09	-0.11	-0.10	-0.12	-0.18			-0.09	-0.08			0.07						
2VI	-0.49	-0.50	-0.33	-0.39	-0.42	-0.30	0.06	0.13	0.07	-0.28	-0.46	-0.40	0.11	0.16		-0.09	-0.06	-0.15	-0.18				
3VI	-0.08	-0.11		-0.06	-0.07		0.09	0.08		-0.08	-0.09		0.10							0.13			
1WE	-0.17	-0.04		-0.14	0.04					0.04	-0.09	-0.11	0.40	0.11	-0.04	-0.09				0.12			
2WE	0.05	0.11	0.04	0.14	0.18	0.15	0.06	0.11	0.07		0.08		0.11	0.08			0.12	0.16	0.06	-0.14		0.09	
3WE	0.30	0.35	0.21	0.28	0.31	0.26			-0.05	0.32	0.36	0.34	0.12	-0.17	-0.53	0.22		0.28		0.21		0.16	0.27

Very strong correlation (*r* > 0.8)	Strong correlation (r > 0.6 - 0.8)	Moderate correlation (r > 0.4 - 0.6)	Weak correlation (r > 0.2 - 0.4)	Poor correlation (r < 0.2)

Notes: 1 = leeward site; 2 = ridge site; 3 = windward site; AT = air temperature; PA = photosynthetically active photon flux density; RA = Rainfall; VP = vapour pressure; WD = wind direction; WS wind speed; VI = visibility; WE = wind elevation.

Appendix Table 2: Pearson's Correlation scores (r) between all sites and hourly diurnal measurements (0600 – 1700 h) during the 2007-2008 dry season (May – September) periods. Only significant r scores (P < 0.05) are shown.

	1AT	2AT	3AT	1PA	2PA	3PA	1RA	2RA	3RA	1VP	2VP	3VP	1WD	2WD	3WD	1WS	2WS	3WS	1VI	2VI	1VI	1WE	2WE
2AT	0.69																						
3AT	0.53	0.81																					
1PA	0.72	0.55	0.37																				
2PA	0.45	0.69	0.54	0.71																			
3PA	0.44	0.65	0.63	0.68	0.86																		
1RA	-0.11	-0.12	-0.13	-0.12	-0.12	-0.10																	
2RA	-0.12	-0.14	-0.17	-0.13	-0.14	-0.14	0.90																
3RA	-0.08	-0.10	-0.15	-0.10	-0.11	-0.12	0.71	0.91															
1VP	0.62	0.35	0.19	0.32	0.10	0.10																	
2VP	0.74	0.63	0.44	0.52	0.40	0.39	-0.05	-0.04	-0.04	0.83													
3VP	0.71	0.52	0.40	0.40	0.22	0.24				0.80	0.87												
1WD		0.13	0.10	0.04	0.21	0.21				0.13	0.08	0.06											
2WD	-0.34	-0.17	-0.10	-0.29	-0.18	-0.16				-0.14	-0.24	-0.20	0.07										
3WD	-0.38	-0.38	-0.25	-0.43	-0.44	-0.43				-0.27	-0.40	-0.35	-0.12	0.27									
1WS	0.40	0.19	0.10	0.33	0.13	0.09				0.19	0.28	0.24	-0.14	-0.27	-0.26								
2WS	0.31	0.13	0.15	0.28	0.17	0.12				0.06	0.14	0.13	-0.12	-0.12	-0.07	0.42							
3WS	0.51	0.53	0.38	0.59	0.55	0.63				0.22	0.44	0.31	0.12	-0.17	-0.35	0.30	0.34						
1VI				-0.06			-0.20	-0.14	-0.07	-0.19		-0.05				-0.12							
2VI	-0.06	-0.20	-0.12	-0.14	-0.19	-0.18				0.10		0.06	0.14				-0.08		0.06				
3VI			-0.10							-0.14	-0.10	-0.12											
1WE	-0.09	0.07	0.11	-0.15	0.06	0.06						-0.10	0.41	0.07	-0.07	0.07	0.07	0.09		0.09			
2WE	0.07	0.23	0.23	0.16	0.25	0.29					0.13	0.07	0.06	0.13	-0.25	0.13	0.18	0.31	-0.07	-0.10	-0.06	0.15	
3WE	0.32	0.40	0.31	0.41	0.49	0.47				0.24	0.37	0.33	0.15	-0.17	-0.72	0.19		0.32				0.09	0.33

Very strong correlation (r > 0.8)	Strong correlation (r > 0.6 - 0.8)	Moderate correlation (r > 0.4 - 0.6)	Weak correlation (r > 0.2 - 0.4)	Poor correlation (r < 0.2)

Notes: 1 = leeward site; 2 = ridge site; 3 = windward site; AT = air temperature; PA = photosynthetically active photon flux density; RA = Rainfall; VP = vapour pressure; WD = wind direction; WS wind speed; VI = visibility; WE = wind elevation.

Appendix Table 3: Pearson's Correlation scores (r) between all sites and hourly nocturnal measurements (1800 – 0500 h) during the 2007-2008 wet season (October – April) periods. Only significant r scores (P < 0.05) are shown.

	1AT	2AT	3AT	1RA	2RA	3RA	1VP	2VP	3VP	1WD	2WD	3WD	1WS	2WS	3WS	1VI	2VI	1VI	1WE	2WE
2AT	0.72																			
3AT	0.53	0.70																		
1RA	-0.06	-0.12	-0.14																	
2RA		-0.10	-0.14	0.89																
3RA	-0.07	-0.13	-0.16	0.64	0.70															
1VP	0.67	0.30	0.15	0.11	0.12	0.06														
2VP	0.74	0.33	0.18	0.05	0.07		0.91													
3VP	0.64	0.26	0.21	0.07	0.07	0.07	0.81	0.84												
1WD		-0.06	-0.07	0.13	0.14	0.07	0.29	0.15	0.18											
2WD	-0.08	-0.04		-0.04	-0.08	-0.08	0.04		-0.09											
3WD	-0.17	-0.05	0.08	-0.16	-0.17	-0.15	-0.26	-0.22	-0.27	-0.08	0.24									
1WS	0.07	0.16	0.16				-0.33	-0.19	-0.21	-0.28	-0.13									
2WS			0.07				-0.15	-0.11	-0.17	-0.06	0.23	0.04	0.21							
3WS	0.11			0.06	0.09	0.06	0.12	0.12	0.11	0.04	0.14	-0.05	0.09	0.35						
1VI	0.06	0.12	0.08	-0.12			-0.29	-0.10	-0.09	-0.40	-0.08			0.17						
2VI	0.05	0.20	-0.09	-0.12	-0.08		-0.10	-0.10	-0.22		0.07			0.08						
3VI		-0.13											-0.17				0.14			
1WE		0.13		-0.04			0.08			0.13			-0.18	-0.05	-0.10	0.17				
2WE			-0.05	0.07	0.10	0.08	0.08	0.07	0.06	0.11	0.22	-0.05		0.09	0.16				0.04	
3WE	0.22	0.11	-0.05	0.15	0.17	0.14	0.31	0.26	0.31	0.11	-0.05	-0.57			0.06				0.05	0.28

Very strong correlation (*r* > 0.8)	Strong correlation (r > 0.6 - 0.8)	Moderate correlation (r > 0.4 - 0.6)	Weak correlation (r > 0.2 - 0.4)	Poor correlation (r < 0.2)

Notes: 1 = leeward site; 2 = ridge site; 3 = windward site; AT = air temperature; RA = Rainfall; VP = vapour pressure; WD = wind direction; WS wind speed; VI = visibility; WE = wind elevation.

Appendix Table 4: Pearson's Correlation scores (r) between all sites and hourly nocturnal measurements (1800 – 0500 h) during the 2007-2008 dry season (May – September) periods. Only significant r scores (P < 0.05) are shown.

	1AT	2AT	3AT	1RA	2RA	3RA	1VP	2VP	3VP	1WD	2WD	3WD	1WS	2WS	3WS	1VI	2VI	1VI	1WE	2WE
2AT	0.72																			
3AT	0.64	0.80																		
1RA		-0.05	-0.07																	
2RA		-0.04	-0.06	0.87																
3RA		-0.04	-0.06	0.62	0.81															
1VP	0.68	0.30	0.18	0.12	0.12	0.09														
2VP	0.73	0.33	0.27	0.06	0.07	0.04	0.90													
3VP	0.70	0.31	0.18	0.09	0.10	0.07	0.83	0.86												
1WD		-0.06	-0.18	0.09	0.06	0.08	0.32	0.19	0.19											
2WD				-0.04	-0.08		0.12	0.11		0.05										
3WD	-0.11		0.09	-0.13	-0.14	-0.13	-0.21	-0.18	-0.20	-0.08	0.13									
1WS		0.18	0.27				-0.39	-0.27	-0.25	-0.37	-0.10	0.05								
2WS	0.06	0.11	0.17	-0.04		-0.04	-0.12	-0.04	-0.10	-0.10	0.18		0.19							
3WS	0.12	0.11	0.11	0.07	0.06		0.13	0.11	0.10		0.11	0.09	0.08	0.30						
1VI	0.10	0.15	0.15	-0.15		-0.06	-0.15				-0.06			0.11						
2VI	0.44	0.57	0.37				0.25	0.24	0.20		0.06					0.10				
3VI	-0.19	-0.18	-0.22				-0.13	-0.15	-0.11								-0.13			
1WE				-0.05					-0.05	0.17	-0.06		-0.19	-0.06	-0.07					
2WE		-0.07	-0.08	0.06			0.11	0.10		0.15	0.39	-0.07		0.12	0.18	-0.05			-0.07	
3WE	0.12		-0.17	0.13	0.13	0.10	0.28	0.25	0.29	0.13		-0.52	-0.09		-0.13					0.18

Very strong correlation (r > 0.8)	Strong correlation (r > 0.6 - 0.8)	Moderate correlation (r > 0.4 - 0.6)	Weak correlation (r > 0.2 - 0.4)	Poor correlation (r < 0.2)

Notes: 1 = leeward site; 2 = ridge site; 3 = windward site; AT = air temperature; RA = Rainfall; VP = vapour pressure; WD = wind direction; WS wind speed; VI = visibility; WE = wind elevation.

Appendix B: Climatic variables from known neotropical cloud forests

Appendix Table 5: Forest type, location, altitude, annual rainfall and average temperature of known neotropical cloud forest research sites.

Site	Forest	Lat	Long	Alt.	Rain	Tem	Source
Tamaulipas, Mex.	LMCF	23.1	-99.3	1250	3026	13.0	(Arriaga, 2000)
Xalapa, Mex.	LMCF	19.7	-96.9	1840	1806	14.0	(Williams-Linera, 2002)
Xalapa, Mex.	LMCF	19.6	-96.9	1470	1451	16.0	(Williams-Linera, 2002)
Xalapa, Mex.	LMCF	19.6	-97.0	1875	1350	12.0	(Williams-Linera, 2002)
Xalapa, Mex.	LMCF	19.5	-97.0	1450	1650	16.0	(Williams-Linera, 2002)
Xalapa, Mex.	LMCF	19.5	-96.9	1250	1517	18.0	(Williams-Linera, 2002)
Xalapa, Mex.	LMCF	19.5	-97.0	1500	1650	14.0	(Williams-Linera, 2002)
Xalapa, Mex.	LMCF	19.2	-97.0	1340	2200	17.0	(Williams-Linera, 2002)
Luquillo, PR	UMCF	18.3	-65.8	1000	5000	20.0	(Scatena, 1995)
Blue, Jam.	LMCF	18.0	-76.6	1600	2500	19.0	(Tanner *et al.*, 1990)
El Rincon, Mex.	UMCF	17.4	-96.3	1309	1540	18.4	(Bautista-Cruz & del Castillo, 2005)
Macuira, Col.	MCF	12.2	-71.4	700	853	24.0	(Sugden, 1986)
El Ávila, Ven.	MCF	10.5	-66.9	2129	925	13.5	(Meier, 2011)
Ran. Grande, Ven.	MCF	10.4	-67.5	1020	1842	19.1	(Meier, 2011)
Volcán Barva, CR	UMCF	10.4	-84.0	2600	3268	-	(Heaney & Proctor, 1990)
Monteverde, CR	LMCF	10.3	-84.8	1500	2150	17.7	(Nadkarni & Matelson, 1992)
Monteverde, CR	LMCF	10.3	-84.8	1200	6390	14.4	(Häger & Dohrenbusch, 2010)
Monteverde, CR	LMCF	10.3	-84.8	1200	3690	13.8	(Häger & Dohrenbusch, 2010)
Monteverde, CR	LMCF	10.3	-84.8	1320	4400	15.1	(Häger & Dohrenbusch, 2010)
Monteverde, CR	LMCF	10.3	-84.8	1320	4590	14.8	(Häger & Dohrenbusch, 2010)
Monteverde, CR	LMCF	10.3	-84.8	1440	3760	15.8	(Häger & Dohrenbusch, 2010)
Monteverde, CR	LMCF	10.3	-84.8	1450	4210	15.8	(Häger & Dohrenbusch, 2010)
Monteverde, CR	LMCF	10.3	-84.8	1460	2519	18.8	(Clark *et al.*, 2000)
Monteverde, CR	LMCF	10.3	-84.8	1500	4310	16.2	(Häger & Dohrenbusch, 2010)
Hierro, Ven.	MCF	10.2	-67.2	1355	1588	20.2	(Monedero, 1998)
Fortuna, Pan.	LMCF	8.7	-82.2	1340	3678	19.0	(Cavelier *et al.*, 1997)
La Mucuy, Ven.	UMCF	8.6	-71.0	2350	2600	14.0	(Ataroff, 2002)
Mérida, Ven.	LMCF	8.6	-71.2	3452	1811	7.1	(Ramírez *et al.*, 2009)
Pereira, Col.	LMCF	4.8	-75.5	2550	945	12.2	(Veneklaas & van Ek, 1990)
Pereira, Col.	UMCF	4.8	-75.5	3370	705	7.7	(Veneklaas & van Ek, 1990)
San Francisco,	LMCF	4.0	-79.1	1950	2220	16.2	(Wilcke *et al.*, 2001)

Site	Forest	Lat	Long	Alt.	Rain	Tem	Source
Ec.							
San Francisco, Ec.	LMCF	4.0	-79.1	2375	3089	13.6	(Homeier *et al.*, 2010)
San Francisco, Ec.	LMCF	4.0	-79.1	2450	3254	13.3	(Homeier *et al.*, 2010)
Tambito, Col.	LMCF	2.5	-77.0	1450	3600	18.0	(Letts *et al.*, 2010)
Tambito, Col.	LMCF	2.5	-77.0	2150	7000	12.0	(Letts *et al.*, 2010)
Pasochoa, Col.	-	-0.5	-78.7	3285	2000	9.0	(Valencia & Jørgensen, 1992)
Loja, Ec.	LMCF	-4.1	-79.2	2900	3000	11.0	(Madsen & Ollgaard, 1994)
Zamora, Ec.	UMCF	-4.5	-79.2	2700	3000	12.0	(Madsen & Ollgaard, 1994)
Yanachaga, Peru	LMCF	-10.5	-75.4	2385	2161	13.0	Present Study
Yanachaga, Peru	LMCF	-10.5	-75.4	2430	3670	13.3	Present Study
Yanachaga, Peru	UMCF	-10.5	-75.4	2812	4069	10.7	Present Study
Cotapata, Bolivia	LMF	-16.2	-68.9	1850	2310	16.8	(Gerold *et al.*, 2008)
Cotapata, Bolivia	UMCF	-16.2	-68.9	2600	3970	12.8	(Gerold *et al.*, 2008)
Cotapata, Bolivia	UMCF	-16.2	-68.9	3050	5150	10.0	(Gerold *et al.*, 2008)

Appendix C: View of 1-ha plots

Appendix Figure 1: View of lower south-western corner of the leeward sampling plot from within.

Appendix Figure 2: View of lower southern border of the ridge sampling plot from outside.

Appendix Figure 3: View of upper western border of the ridge sampling plot from within.

Appendix D: Forest species data

Appendix Table 6: Abundance (Ab.), average DBH, average stem incline (Incl.), average stem height (Hei.), total basal area (BA) and total crown area (CA) of all woody species ≥5 cm DBH of each species in the 1-ha forest plot where they occurred.

Taxon	Forest	Ab.	DBH	Incl.	Hei.	Cro.	BA	CA
Actinidiaceae								
Saurauia biserrata	Leeward	11	9.1	70.7	5.8	2.5	0.077	65.5
Adoxaceae								
Sambucus sp. 1	Leeward	1	9.8	67.0	5.0	4.0	0.008	12.6
Anacardiaceae								
Mauria heterophylla	Leeward	1	29.8	51.0	10.0	1.0	0.070	0.8
Annonaceae								
Guatteria sp. 1	Windward	3	9.5	52.0	7.3	2.5	0.022	19.2
Guatteria sp. 2	Windward	1	7.8	72.0	5.6	2.1	0.005	3.5
Guatteria sp. 3	Windward	1	5.4	80.0	3.7	0.7	0.002	0.4
Aquifoliaceae								
Ilex hualgayoca	Ridge	14	12.0	65.0	6.3	2.0	0.219	51.3
Ilex laurina	Windward	4	9.7	51.3	6.6	2.0	0.032	14.5
Ilex sp. 1	Windward	16	9.3	65.1	8.7	2.1	0.134	88.9
Ilex sp. 2	Windward	2	13.5	50.5	11.4	1.7	0.031	4.5
Ilex sp. 3	Ridge	11	9.4	67.3	6.8	2.0	0.086	44.4
Ilex teratopis	Windward	14	10.6	46.1	7.8	2.7	0.138	101.2
Araliaceae								
Dendropanax cuneatus	Leeward	1	14.2	90.0	13.0	3.0	0.016	7.1
Dendropanax sp. 1	Leeward	4	31.7	76.3	16.3	6.5	0.342	141.4
Oreopanax iodophyllus	Leeward	6	9.0	71.8	7.8	2.8	0.043	39.9
Oreopanax platanifolius	Leeward	1	19.0	58.0	11.0	3.0	0.028	7.1
Oreopanax sp. 1	Leeward	11	12.8	78.1	9.9	2.9	0.209	82.7
Oreopanax sp. 2	Leeward	1	26.0	80.0	17.0	5.0	0.053	19.6
Oreopanax sp. 3	Leeward	3	6.7	79.3	8.0	2.0	0.011	9.4
Schefflera angulata	Ridge	35	14.2	62.3	9.3	3.0	0.860	399.6
Schefflera angulata	Windward	3	11.9	58.0	6.6	2.7	0.042	20.3
Schefflera microcephala	Windward	2	13.7	30.5	9.4	4.3	0.029	39.7
Schefflera pedicellata	Windward	94	8.7	69.6	6.8	2.5	0.638	590.1
Schefflera sp. 1	Windward	23	9.4	58.7	5.8	3.2	0.181	221.6
Arecaceae								
Geonoma weberbaueri	Ridge	2	11.1	83.5	7.8	2.7	0.019	11.1
Asteraceae								
Baccharis brachylaenoides	Ridge	14	7.6	49.0	6.8	1.7	0.071	36.9
Nordenstamia cajamarcensis	Ridge	32	7.4	57.0	6.1	1.8	0.147	93.4
Brunelliaceae								
Brunellia weberbaueri	Windward	1	5.8	90.0	6.2	1.7	0.003	2.3
Buxaceae								
Styloceras cf. *brokawii*	Leeward	6	9.3	67.3	5.3	2.6	0.048	34.8
Celastraceae								
Maytenus macrocarpa	Leeward	12	25.4	72.8	12.6	3.9	0.815	161.0
Perrottetia sp. 1	Leeward	21	15.5	68.2	8.5	3.8	0.589	245.8
Chloranthaceae								
Hedyosmum angustifolium	Ridge	19	6.7	59.7	6.4	1.5	0.074	36.6
Hedyosmum anisodorum	Leeward	8	12.4	67.6	7.9	3.4	0.122	76.6

Taxon	Forest	Ab.	DBH	Incl.	Hei.	Cro.	BA	CA
Hedyosmum dombeyanum	Ridge	93	6.9	55.6	6.6	1.6	0.374	200.0
Hedyosmum dombeyanum	Windward	34	6.5	37.3	6.1	1.8	0.122	111.6
Hedyosmum lechleri	Ridge	69	9.7	62.8	7.0	2.0	0.577	273.5
Hedyosmum sp. 1	Ridge	41	6.7	43.7	5.7	1.5	0.153	82.9
Hedyosmum sp. 2	Ridge	1	6.8	73.0	7.2	1.5	0.004	1.8
Hedyosmum sp. 2	Windward	16	6.5	46.1	6.1	1.4	0.054	26.7
Clethraceae								
Clethra pedicellaris	Leeward	3	19.3	83.0	14.0	5.0	0.091	60.5
Clethra revoluta	Ridge	4	16.0	81.5	10.7	3.8	0.149	99.7
Clethra revoluta	Windward	19	9.9	65.1	8.8	2.9	0.163	163.9
Clusiaceae								
Clusia alata	Leeward	2	7.6	70.0	12.5	4.5	0.010	41.6
Clusia alata	Ridge	39	13.5	71.1	8.1	3.9	0.695	581.4
Clusia cf. *elliptica*	Leeward	5	22.3	80.6	12.8	5.9	0.228	167.5
Clusia ducuoides	Leeward	4	19.3	75.3	11.0	3.0	0.137	39.3
Clusia ducuoides	Windward	28	9.1	22.5	7.2	2.6	0.206	181.6
Clusia elliptica	Ridge	41	13.1	61.9	9.2	3.8	0.733	603.9
Clusia schultesii	Windward	217	11.1	63.0	6.7	3.1	2.625	2110.4
Clusia sp. 1	Leeward	2	18.4	80.0	14.0	6.5	0.053	66.8
Clusia sp. 1	Windward	11	6.6	38.2	5.8	2.5	0.040	62.0
Clusia sphaerocarpa	Ridge	6	9.3	60.5	8.5	3.1	0.053	65.1
Clusia thurifera	Windward	35	7.5	53.8	6.6	2.3	0.170	188.3
Cunoniaceae								
Weinmannia aff. *auriculata*	Ridge	4	15.0	78.3	10.7	4.5	0.083	82.3
Weinmannia auriculata	Ridge	2	19.7	79.5	8.9	3.4	0.070	18.7
Weinmannia auriculata	Windward	56	9.5	53.7	7.3	2.3	0.460	282.4
Weinmannia balbisiana	Ridge	65	21.5	73.0	11.6	5.1	3.359	1896.3
Weinmannia cf. *microphylla*	Leeward	1	32.6	90.0	19.0	6.0	0.083	28.3
Weinmannia cochensis	Ridge	1	10.7	50.0	6.4	3.3	0.009	8.6
Weinmannia cochensis	Windward	1	21.6	69.0	11.5	3.9	0.037	11.9
Weinmannia haenkeana	Windward	1	10.5	68.0	11.1	3.1	0.009	7.5
Weinmannia lechleriana	Leeward	39	14.3	80.7	10.2	3.8	0.920	553.1
Weinmannia microphylla	Ridge	32	11.8	58.5	7.4	3.0	0.459	283.2
Weinmannia microphylla	Windward	1	5.2	90.0	4.7	1.4	0.002	1.5
Weinmannia pinnata	Ridge	9	10.0	83.4	8.5	2.1	0.073	36.0
Weinmannia pinnata	Windward	54	10.3	60.5	7.9	2.5	0.644	382.8
Weinmannia pubescens	Leeward	7	30.3	72.7	14.6	5.6	0.723	212.8
Weinmannia pubescens	Windward	9	10.6	80.9	10.5	3.4	0.086	94.2
Weinmannia sp. 1	Windward	1	6.6	18.0	5.2	1.8	0.003	2.5
Weinmannia sp. 2	Leeward	10	26.6	81.9	17.5	6.4	0.659	342.6
Cyatheaceae								
Alsophila sp. 1	Leeward	53	11.4	82.0	3.3	3.4	0.560	504.4
Cyathea caracasana	Windward	89	13.5	75.1	6.0	4.1	1.371	1201.9
Cyathea delgadii	Windward	8	14.2	70.8	6.5	3.9	0.138	97.2
Cyathea pallescens	Leeward	7	14.2	86.0	4.4	5.4	0.117	162.0
Cyathea pallescens	Ridge	3	14.8	63.0	6.2	1.8	0.052	8.5
Cyathea sp. 2	Leeward	39	8.0	82.6	3.3	3.6	0.225	409.8
Cyathea sp. 3	Leeward	49	11.8	80.4	3.8	3.8	0.568	588.1
Cyathea sp. 4	Leeward	5	9.5	67.8	3.7	3.5	0.037	48.9
Ericaceae								
Cavendishia bracteata	Ridge	6	5.9	25.0	8.0		0.017	0.0
Cavendishia bracteata	Windward	1	5.4				0.002	0.0

Taxon	Forest	Ab.	DBH	Incl.	Hei.	Cro.	BA	CA
Ericaceae (cont.)								
Cavendishia nobilis	Ridge	4	5.5				0.009	0.0
Disterigma ovatum	Windward	1	5.8				0.003	0.0
Gaultheria glomerata	Windward	6	5.3	12.5	6.0	2.1	0.013	21.9
Thibaudia floribunda	Ridge	1	9.5	35.0	7.9	2.1	0.007	3.5
Escalloniaceae								
Escallonia paniculata	Windward	1	5.2	65.0	6.3	3.1	0.002	7.5
Euphorbiaceae								
Actinostemun sp. 1	Windward	1	13.9	75.0	16.1	5.3	0.015	22.1
Alchornea grandis	Leeward	30	21.5	75.9	11.4	4.2	1.588	497.4
Alchornea sp. 1	Leeward	13	15.6	85.2	9.4	3.6	0.591	199.9
Alchornea sp. 1	Windward	4	9.8	66.0	8.0	3.7	0.036	49.7
Croton sp. 1	Leeward	7	30.6	83.1	19.4	7.3	0.597	311.8
Croton sp. 2	Leeward	1	18.6	96.0	16.0	7.0	0.027	38.5
Hyeronima andina	Leeward	3	10.5	84.7	8.7	3.0	0.028	22.8
Hyeronima duquei	Leeward	2	6.5	89.0	7.0	2.5	0.007	9.8
Hyeronima scabra	Ridge	25	6.9	56.3	6.5	1.6	0.098	59.5
Hyeronima scabra	Windward	4	16.4	58.8	9.9	3.7	0.099	45.8
Hyeronima sp. 1	Windward	25	7.8	46.0	7.2	1.9	0.129	92.9
Sapium sp. 1	Leeward	2	10.3	80.5	9.5	2.5	0.017	10.2
Fabaceae								
Inga sp. 1	Leeward	1	26.3	83.0	19.0	6.0	0.054	28.3
Icacinaceae								
Citronella sp. 1	Leeward	4	13.7	86.0	8.8	2.6	0.069	22.2
Citronella sp. 2	Leeward	3	18.3	77.3	10.0	3.3	0.097	26.7
Lauraceae								
Beilschmiedia aff. *latifolia*	Leeward	4	21.3	71.0	10.8	2.6	0.160	25.3
Beilschmiedia aff. *tovarensis*	Leeward	3	25.0	88.3	13.7	3.3	0.149	26.7
Beilschmiedia latifolia	Windward	7	14.9	69.9	10.4	4.7	0.155	144.0
Beilschmiedia sp. 1	Leeward	6	16.2	82.8	10.3	3.7	0.142	84.8
Beilschmiedia sp. 2	Leeward	6	7.7	72.8	5.7	2.0	0.035	22.9
Cinnamomum triplinerve	Windward	1	20.8	84.0	17.6	7.6	0.034	45.4
Endlicheria sp. 1	Windward	4	6.4	33.8	6.6	1.4	0.013	7.2
Licaria applanata	Ridge	2	6.5	45.5	4.9	0.8	0.007	1.0
Licaria cannella	Ridge	1	7.2	-5.0	5.9	0.9	0.004	0.6
Licaria subsessilis	Ridge	47	6.9	65.3	6.4	1.5	0.190	103.7
Licaria subsessilis	Windward	7	6.6	56.1	6.6	1.7	0.026	28.4
Nectandra cissiflora	Leeward	19	16.0	74.1	10.6	3.3	0.724	210.9
Nectandra purpurea	Windward	35	8.6	64.8	7.2	2.0	0.253	135.8
Nectandra reticulata	Leeward	6	35.0	85.0	16.2	5.5	1.101	179.9
Nectandra sp. 1	Ridge	10	10.1	64.2	8.5	2.1	0.095	47.1
Nectandra sp. 1	Windward	17	8.3	69.8	6.7	1.6	0.109	45.6
Ocotea arnottiana	Windward	27	11.4	56.7	6.5	2.7	0.314	195.4
Ocotea calophylla	Windward	7	13.1	64.3	10.9	4.0	0.140	134.5
Ocotea sp. 1	Ridge	4	6.8	63.8	6.9	1.4	0.015	7.3
Ocotea sp. 1	Windward	3	8.5	75.7	10.0	2.5	0.018	15.4
Ocotea sp. 2 sp. nov.	Leeward	2	37.8	72.0	17.5	6.5	0.251	69.9
Ocotea sp. 3	Leeward	1	27.0	78.0	16.0	5.0	0.057	19.6
Persea areolatocostae	Windward	3	17.9	52.0	11.6	5.7	0.086	92.3
Persea sp. 1	Leeward	4	12.2	83.8	11.5	3.5	0.051	51.8
Persea sp. 2	Leeward	3	9.3	84.7	8.0	3.3	0.022	29.5

Taxon	Forest	Ab.	DBH	Incl.	Hei.	Cro.	BA	CA
Loranthaceae								
Gaiadendrum punctatum	Ridge	1	18.8	70.0	12.0	4.5	0.028	15.9
Gaiadendrum punctatum	Windward	3	6.8	31.0	5.2	1.3	0.012	4.4
Melastomataceae								
Axinaea lanceolata	Leeward	8	12.5	82.1	9.3	3.4	0.148	76.6
Axinaea weberbaueri	Leeward	4	18.5	89.3	15.5	5.8	0.115	110.7
Blakea aff. *repens*	Leeward	1	15.5	90.0	14.0	4.0	0.019	12.6
Blakea cf. *latifolia*	Leeward	1	22.5	60.0	6.0	4.0	0.040	12.6
Graffenrieda emarginata	Windward	22	8.0	45.0	6.3	1.8	0.123	79.3
Graffenrieda sp. 1	Leeward	2	6.0	90.0	8.0	4.0	0.006	26.7
Miconia adinantha	Leeward	36	19.6	83.5	13.2	5.2	1.479	918.3
Miconia aff. *amnicola*	Leeward	4	11.9	72.0	7.3	3.3	0.048	35.3
Miconia aff. *pavoniana*	Leeward	11	10.4	85.5	10.4	3.5	0.110	119.6
Miconia aff. *schunkei*	Leeward	4	7.5	70.0	6.5	2.6	0.018	26.1
Miconia agregata	Ridge	2	6.7	2.0	6.6	1.8	0.007	5.2
Miconia aprica	Ridge	103	10.6	75.6	8.2	2.6	1.160	691.2
Miconia banggi	Leeward	51	9.3	75.2	8.3	3.4	0.392	540.2
Miconia barbeyana	Leeward	10	15.0	80.2	12.3	4.7	0.214	207.7
Miconia brachyanthera	Leeward	5	8.2	72.6	6.6	3.2	0.034	48.7
Miconia brachyanthera	Windward	1	6.8	33.0	5.0	1.0	0.004	0.8
Miconia bracteolata	Ridge	3	6.1	59.7	5.3	2.3	0.009	13.1
Miconia calvescens	Leeward	8	7.8	80.3	6.3	3.3	0.040	68.7
Miconia carpishana	Leeward	2	17.5	77.0	11.0	6.0	0.049	62.8
Miconia carpishana	Ridge	35	7.7	59.5	7.0	2.0	0.251	209.2
Miconia carpishana	Windward	1	7.7	-15.0	7.8	1.5	0.005	1.8
Miconia cf. *paradisica*	Leeward	2	5.9	67.0	6.0	3.0	0.006	14.1
Miconia coelestis	Leeward	14	9.3	79.5	8.4	3.4	0.119	159.0
Miconia coelestis	Ridge	9	9.0	47.4	6.4	2.5	0.062	44.9
Miconia filamentosa	Leeward	2	5.8	82.0	5.0	3.3	0.005	17.5
Miconia lasiostyla	Leeward	11	6.7	76.2	6.5	3.0	0.043	82.1
Miconia lasiostyla	Ridge	16	8.0	38.3	6.5	2.3	0.087	78.8
Miconia media subsp. *borealis*	Ridge	26	7.7	61.7	7.0	2.3	0.129	114.8
Miconia micropetala	Windward	10	6.0	36.7	5.7	1.8	0.029	28.1
Miconia molinopampana	Ridge	1	5.5	70.0	6.8	1.2	0.002	1.1
Miconia neriifolia	Windward	11	6.8	22.1	6.6	2.2	0.045	53.7
Miconia nigricans	Ridge	1	5.5	80.0	5.7	2.6	0.002	5.3
Miconia polychaeta	Ridge	3	9.7	77.7	8.5	2.4	0.024	13.6
Miconia reflexipila	Leeward	1	6.2	57.0	4.0	3.0	0.003	7.1
Miconia saltuensis	Ridge	39	8.6	56.6	6.9	1.9	0.263	132.6
Miconia sp. 1	Ridge	7	16.2	78.3	10.3	4.5	0.154	131.7
Miconia sp. 2	Ridge	16	8.4	62.3	6.4	2.1	0.107	66.3
Miconia sp. 3	Ridge	1	6.5	60.0	7.2	1.1	0.003	1.0
Miconia sp. 4	Windward	1	6.6	5.0	7.2	4.2	0.003	13.9
Miconia sp. 5	Leeward	2	16.6	77.5	9.0	4.0	0.057	26.7
Miconia subandicola	Windward	36	8.2	34.1	6.5	2.2	0.205	162.3
Miconia terera	Leeward	13	6.6	66.2	6.2	3.1	0.049	100.5
Miconia terera	Windward	1	6.2	80.0	5.9	3.1	0.003	7.5
Miconia theizans	Leeward	6	6.9	73.0	5.7	2.9	0.027	41.4
Miconia tomentosa	Leeward	4	7.3	80.0	7.5	3.5	0.017	39.3
Miconia weberbaueri	Leeward	6	16.7	81.2	11.7	4.0	0.167	91.1
Topobea multiflora	Leeward	8	37.2	69.0	14.4	7.4	1.107	407.6

Taxon	Forest	Ab.	DBH	Incl.	Hei.	Cro.	BA	CA
Meliaceae								
Cedrela montana	Leeward	4	62.6	78.5	19.3	10.3	2.159	487.7
Guarea kunthiana	Leeward	46	19.2	73.2	10.0	3.5	1.888	597.0
Ruagea glabra	Leeward	2	14.9	70.0	9.0	2.5	0.044	10.2
Ruagea pubescens	Leeward	5	40.7	62.4	8.6	3.7	1.372	56.0
Ruagea pubescens	Windward	6	18.2	59.0	12.5	6.1	0.176	193.3
Monimiaceae								
Mollinedia tomentosa	Leeward	3	7.6	76.3	6.0	2.3	0.015	13.4
Moraceae								
Ficus aff. *cuatrecasana*	Leeward	12	13.3	70.8	7.5	3.7	0.298	270.8
Ficus americana	Leeward	3	56.2	75.7	24.3	10.0	0.904	260.8
Ficus cf. *maxima*	Leeward	1	47.3	90.0	17.0	8.0	0.176	50.3
Ficus gigantosyce	Leeward	8	39.3	81.9	20.8	5.8	1.253	242.9
Ficus sp. 1	Leeward	1	9.0	68.0	5.0	2.0	0.006	3.1
Ficus tonduzzi	Leeward	1	14.2	90.0	12.0	5.0	0.016	19.6
Morus insignis	Leeward	3	13.8	80.0	12.0	2.7	0.047	20.4
Myricaceae								
Morella pubescens	Ridge	1	11.5	74.0	7.2	3.6	0.010	10.2
Morella pubescens	Windward	4	22.0	61.3	10.4	4.9	0.290	111.0
Myrsinaceae								
Ardia aff. *weberbaueri*	Leeward	1	8.0	84.0	4.0	3.0	0.005	7.1
Geissanthus peruvianus	Ridge	3	8.9	46.7	7.0	1.3	0.020	4.7
Myrsine andina	Ridge	62	11.9	69.3	8.9	2.7	0.790	457.6
Myrsine andina	Windward	39	6.6	40.9	7.2	1.9	0.144	130.0
Myrsine coriacea	Leeward	12	14.2	80.2	12.0	3.7	0.241	136.1
Myrsine coriacea	Ridge	30	8.0	65.8	8.2	2.2	0.183	153.7
Myrsine coriacea	Windward	1	7.5	35.0	6.3	1.9	0.004	2.8
Myrsine latifolia	Leeward	4	14.7	84.5	10.5	3.6	0.077	45.0
Myrsine pellucida	Leeward	17	17.6	77.4	14.2	3.6	0.461	190.5
Myrtaceae								
Eugenia florida	Leeward	1	16.9	90.0	17.0	5.0	0.022	19.6
Eugenia lambertiana	Leeward	17	11.5	78.4	7.5	3.0	0.272	151.8
Eugenia muricata	Leeward	13	14.0	83.6	9.7	4.5	0.286	258.8
Eugenia pubescens	Leeward	7	15.4	83.9	12.3	3.7	0.182	93.9
Eugenia riparia	Leeward	3	8.7	90.0	8.0	1.7	0.019	7.1
Myrcia fallax	Ridge	3	8.6	52.3	4.7	1.0	0.019	2.6
Myrcia sp. 1	Leeward	3	26.4	86.7	16.3	5.3	0.225	99.0
Myrcia sp. 1	Windward	43	11.5	56.9	7.3	3.0	0.548	427.1
Myrcia sp. 2	Leeward	2	7.4	90.0	6.0	1.5	0.009	3.9
Myrcia sp. 5	Leeward	1	9.2	90.0	8.0	3.0	0.007	7.1
Myrciantes sp. 1	Leeward	1	31.5	88.0	22.0	5.0	0.078	19.6
Myrciantes sp. 2	Leeward	3	18.8	84.3	15.7	4.7	0.118	64.4
Odoxaceae								
Viburnum hallii	Ridge	9	6.4	41.6	7.1	1.7	0.029	23.4
Pentaphylacaceae								
Freziera alata	Windward	6	14.6	79.0	12.9	4.8	0.104	124.1
Freziera cyanocantha	Windward	56	9.0	58.1	8.1	3.1	0.397	480.9
Freziera incana	Windward	21	10.1	74.7	10.6	3.8	0.184	353.4
Freziera uncinata	Ridge	43	9.8	61.7	6.8	2.8	0.436	355.8
Piperaceae								
Piper apodum	Leeward	6	6.1	63.8	4.6	2.8	0.018	38.9
Piper roqueanum	Leeward	3	6.6	68.3	5.0	1.7	0.010	7.1

Taxon	Forest	Ab.	DBH	Incl.	Hei.	Cro.	BA	CA
Piper sp. 1	Ridge	1	5.0	26.0	7.0	1.2	0.002	1.1
Podocarpaceae								
Podocarpus magnifolius	Ridge	27	15.8	63.0	8.6	2.8	0.996	255.0
Podocarpus magnifolius	Windward	6	7.6	35.8	6.4	1.7	0.029	14.6
Podocarpus oleifolius	Ridge	12	19.1	70.8	9.4	4.4	0.470	218.0
Podocarpus oleifolius	Windward	13	10.7	63.5	7.9	3.0	0.136	120.7
Podocarpus sp. 1	Windward	4	13.8	31.3	7.6	3.4	0.086	45.0
Prumnopytis harmsiana	Leeward	1	110.0	84.0	26.0	20.0	0.950	314.2
Proteaceae								
Oreocallis grandiflora	Windward	4	8.8	12.3	8.0	2.4	0.028	19.7
Panopsis sp. 1	Windward	22	8.4	44.8	5.8	1.9	0.130	76.2
Panopsis sp. 2	Windward	4	6.9	1.8	5.5	1.2	0.015	4.8
Rosaceae								
Hesperosmeles ferruginea	Windward	1	17.4	60.0	11.3	5.1	0.024	20.4
Prunus amplifolia	Ridge	1	9.7	34.0	8.1	1.2	0.007	1.1
Prunus sp. 1	Ridge	1	6.3	42.0	5.6	1.8	0.003	2.5
Prunus sp. 2	Ridge	2	17.0	73.0	13.7	5.8	0.055	74.3
Rubiaceae								
Cinchona calisaya	Ridge	11	6.9	61.5	7.3	1.7	0.044	27.6
Cinchona calisaya	Windward	1	11.2	45.0	7.0	2.0	0.010	3.1
Cinchona hirsuta	Windward	30	7.9	50.7	6.5	1.8	0.150	92.9
Elaeagia utilis	Leeward	4	31.8	65.0	13.5	6.5	0.409	141.4
Faramea oblongifolia	Ridge	2	9.0	44.0	8.8	1.4	0.013	3.3
Faramea sp. 1	Leeward	3	10.7	64.3	4.3	2.2	0.030	11.2
Faramea sp. 1	Windward	2	5.7	10.5	5.5	1.0	0.005	1.5
Guettarda ochreata	Leeward	8	7.5	85.8	6.8	2.6	0.036	42.6
Guettarda sp. 1	Windward	1	10.0	70.0	9.8	3.0	0.008	7.1
Guettarda sp. 2	Leeward	2	51.0	75.0	19.5	12.0	0.411	226.2
Palicourea cf. *apicata*	Leeward	1	9.3	56.0	6.0	2.5	0.007	4.9
Palicourea cf. *lineata*	Leeward	24	7.0	63.7	4.8	2.5	0.099	123.9
Palicourea cf. *obovata*	Leeward	18	6.7	65.8	4.6	2.7	0.069	106.8
Palicourea coriacea	Leeward	1	9.0	72.0	7.0	3.0	0.006	7.1
Palicourea jaramilloi	Ridge	7	6.3	44.9	5.8	1.2	0.023	8.6
Palicourea sp. 1	Ridge	1	10.6	80.0	7.7	3.1	0.009	7.5
Posoqueria cf. *latifolia*	Leeward	4	10.4	88.5	10.0	1.9	0.036	12.8
Posoqueria coriacea	Leeward	5	28.6	77.4	13.6	4.1	0.449	83.4
Psychotria falcata	Leeward	1	10.0	20.0	5.0	2.0	0.008	3.1
Psychotria falcata	Ridge	14	6.0	57.4	6.2	1.2	0.041	17.9
Psychotria falcata	Windward	2	6.0	43.5	5.1	1.9	0.006	5.9
Psychotria heteropsychotria	Leeward	3	6.9	82.3	5.7	2.2	0.012	11.2
Psychotria tinctoria	Leeward	1	4.5	45.0	4.0	3.0	0.002	7.1
Rudgea sp. 1	Ridge	1	16.5	25.0	8.2	2.2	0.021	3.8
Rudgea sp. 2	Ridge	2	9.7	53.5	8.1	1.1	0.015	1.8
Sabiaceae								
Meliosma frondosa	Leeward	6	5.9	73.5	4.0	1.8	0.017	20.6
Meliosma frondosa	Ridge	3	7.3	69.7	7.1	1.1	0.013	3.0
Meliosma frondosa	Windward	4	5.7	47.3	6.2	0.8	0.010	2.2
Salicaceae								
Casearia mariquitensis	Leeward	3	13.7	69.7	9.0	1.7	0.047	10.2
Sapindaceae								
Allophylus pilosus	Leeward	8	9.9	76.0	8.6	2.7	0.081	56.0
Cupania americana	Leeward	3	22.4	78.3	13.7	6.2	0.135	111.7

Taxon	Forest	Ab.	DBH	Incl.	Hei.	Cro.	BA	CA
Sapotaceae								
Pouteria sp. 1	Leeward	1	7.2	70.0	6.0	2.5	0.004	4.9
Pouteria sp. 2	Leeward	1	11.0	83.0	11.0	2.0	0.010	3.1
Cestrum conglomeratum	Leeward	1	9.3	56.0	6.0	3.0	0.007	7.1
Cestrum microcalyx	Ridge	1	6.7	68.0	6.3	1.1	0.004	1.0
Cestrum sp. 2	Leeward	1	7.8	60.0	4.0	3.0	0.005	7.1
Solanum asperolanatum	Ridge	1	5.9	76.0	5.8	0.6	0.003	0.3
Solanum maturecalvans	Leeward	3	9.9	84.7	8.0	4.5	0.027	52.8
Solanum sessile	Leeward	2	5.3	83.0	4.3	1.8	0.004	4.9
Solanum trachycyphum	Leeward	5	8.3	69.0	7.3	2.7	0.028	34.3
Staphyleaceae								
Turpinia occidentalis	Leeward	15	9.1	89.4	7.5	3.1	0.109	131.6
Styracaceae								
Styrax cordatus	Leeward	6	20.4	79.5	12.8	2.8	0.214	37.9
Styrax vilcabambae	Windward	16	8.1	42.6	7.2	1.7	0.097	43.1
Symplocaceae								
Symplocos andicola	Ridge	2	12.8	78.5	9.3	3.1	0.028	18.4
Symplocos apiciflora	Leeward	2	42.8	72.5	16.0	1.8	0.372	9.6
Symplocos coriacea	Ridge	7	8.8	69.1	6.0	1.6	0.057	16.5
Symplocos fuliginosa	Leeward	6	10.8	83.2	9.0	3.1	0.069	50.5
Symplocos quitensis	Ridge	10	9.3	75.1	7.1	2.3	0.085	50.9
Symplocos quitensis	Windward	18	7.1	67.3	6.9	2.3	0.081	92.6
Symplocos sp. 1	Ridge	7	7.4	54.4	8.8	2.0	0.031	24.6
Theaceae								
Gordonia fruticosa	Leeward	2	5.3	61.0	5.0	2.5	0.004	10.2
Gordonia fruticosa	Windward	30	8.8	42.8	7.1	2.1	0.212	126.6
Gordonia sp. 1	Leeward	1	66.0	75.0	23.0	3.0	0.342	7.1
Gordonia sp. 1	Ridge	23	10.1	57.1	7.3	1.8	0.243	97.9
Gordonia sp. 1	Windward	3	16.6	70.0	12.3	2.8	0.066	20.8
Ternstroemia quinquepartida	Leeward	2	9.7	60.0	6.5	2.0	0.017	6.3
Ternstroemia sp. 1	Windward	23	9.9	73.6	7.9	2.7	0.191	149.4
Urticaceae								
Cecropia sp. 1	Leeward	4	26.0	73.3	17.0	7.8	0.232	230.1
Cecropia sp. 2	Leeward	32	17.2	75.4	12.8	3.8	1.032	469.7

Appendix E: Forest taxon relative abundance

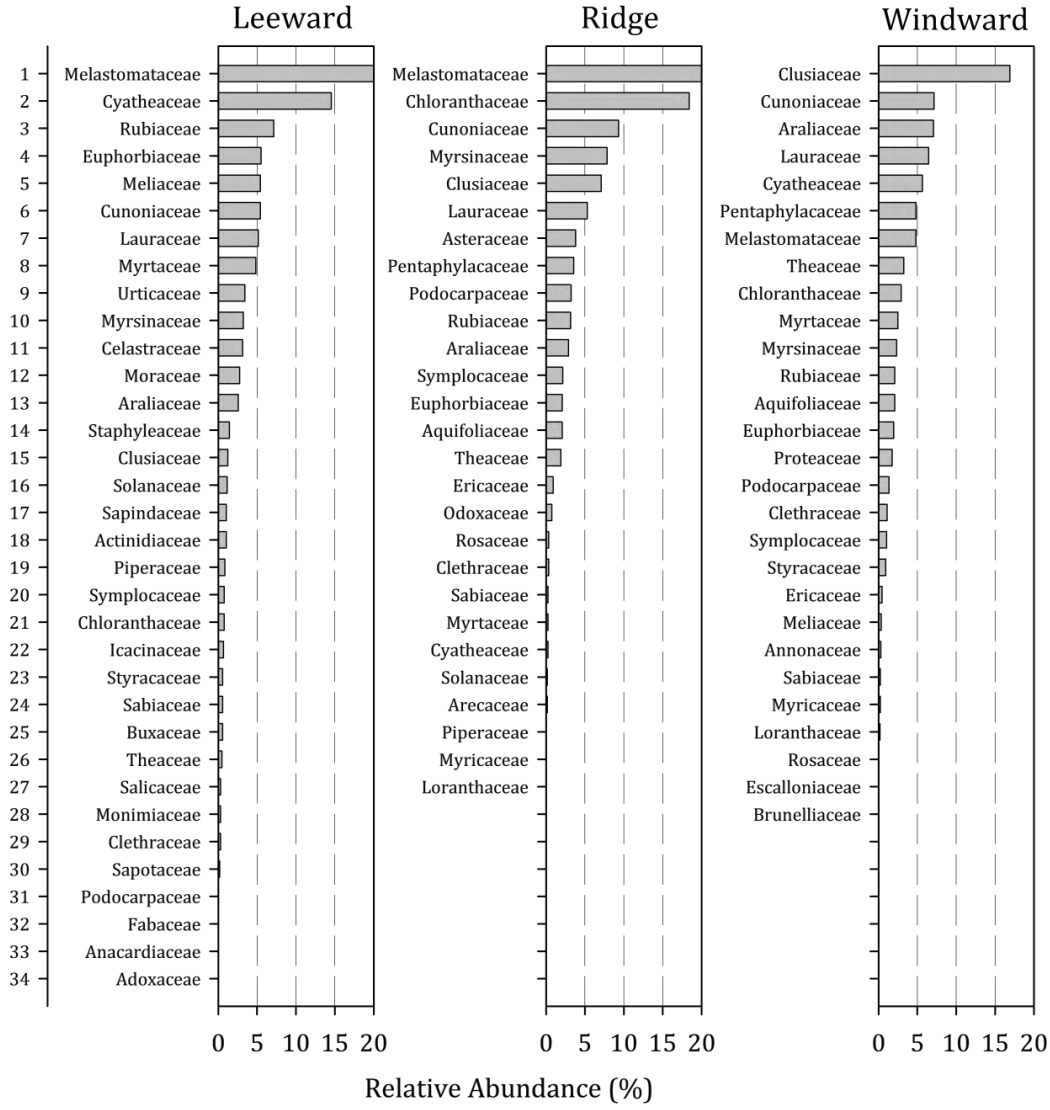

Appendix Figure 4: Relative Abundance of woody families of DBH ≥ 5cm occurring at each site.

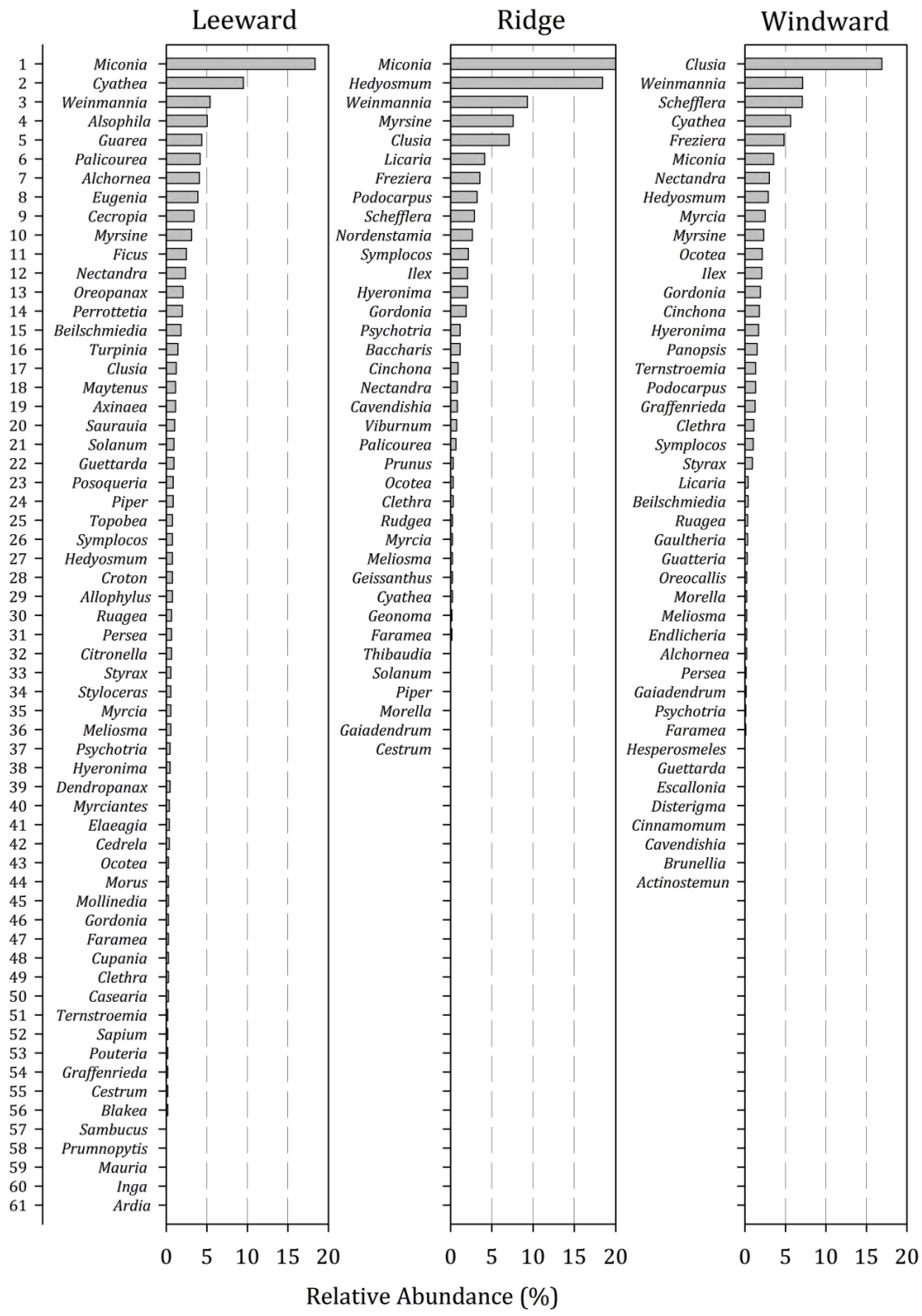

Appendix Figure 5: Relative Abundance of woody genera of DBH ≥ 5cm occurring at each site.

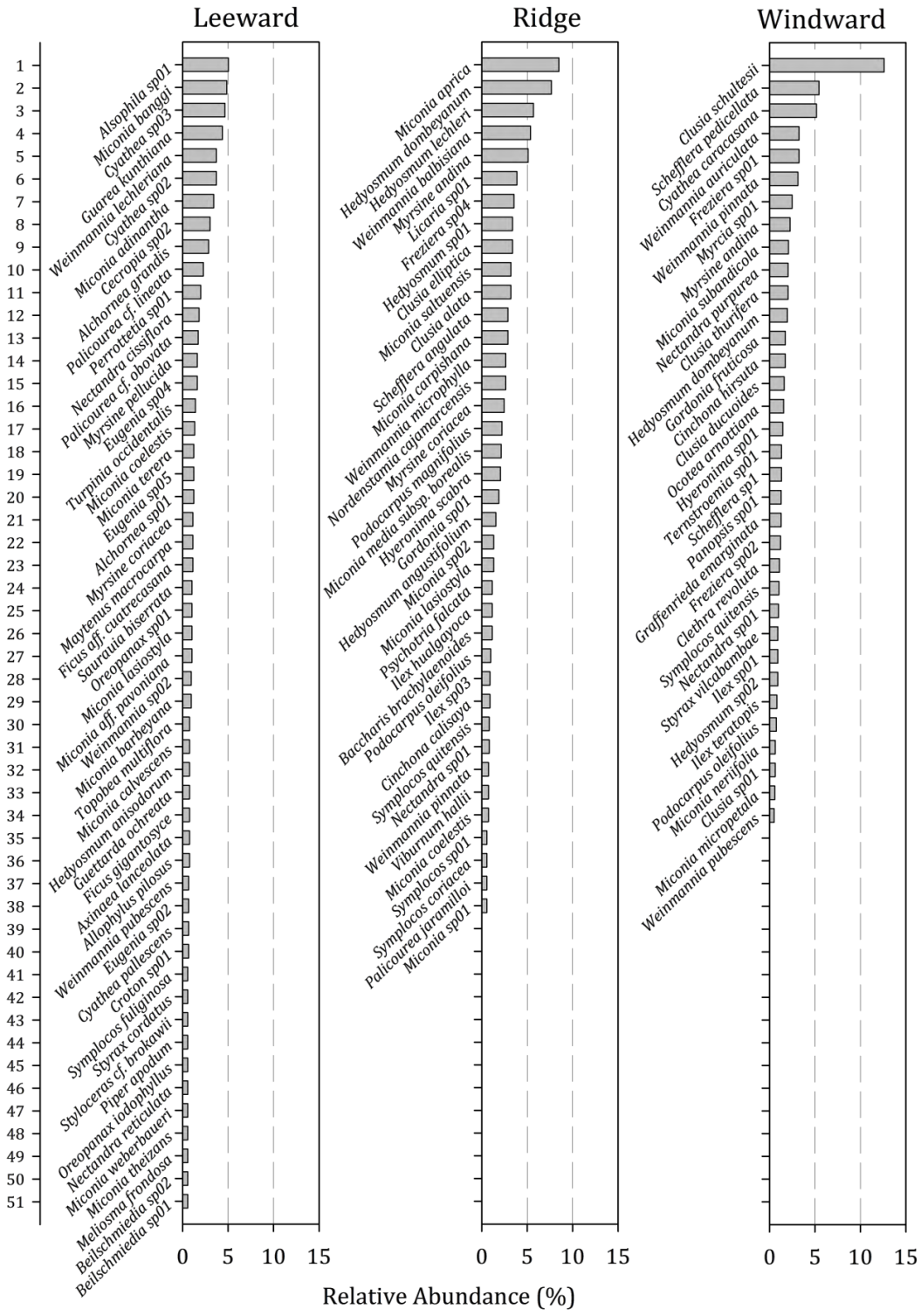

Appendix Figure 6: Relative abundance of woody species of DBH ≥ 5cm occurring at each site. Only species with a relative abundance of ≥ 5% are shown.

Appendix F: Forest taxon IVI scores

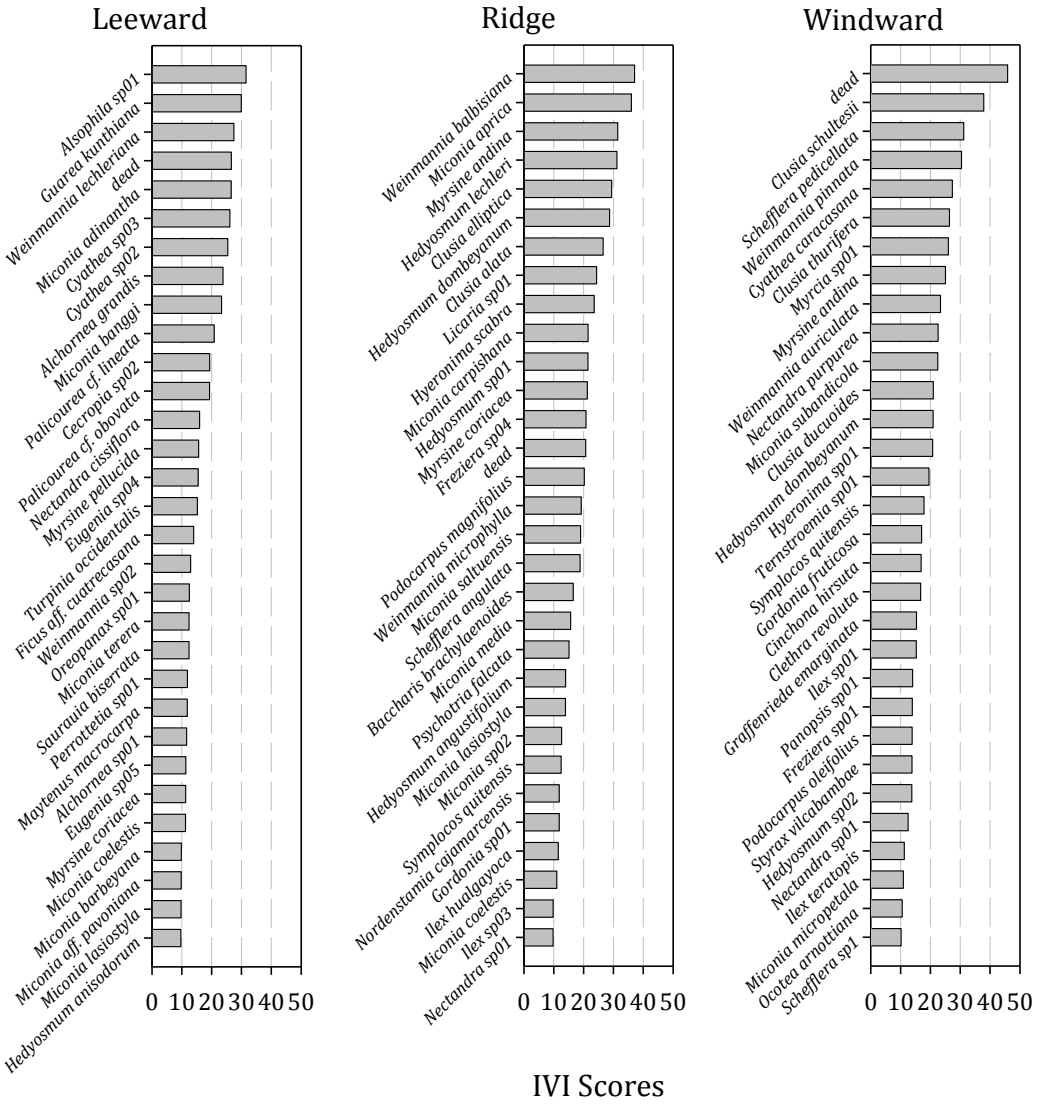

Appendix Figure 7: Importance Value Index (IVI) scores of woody species of ≥ 5cm DBH occurring at each site. Only the first 30 species in order of importance are shown.

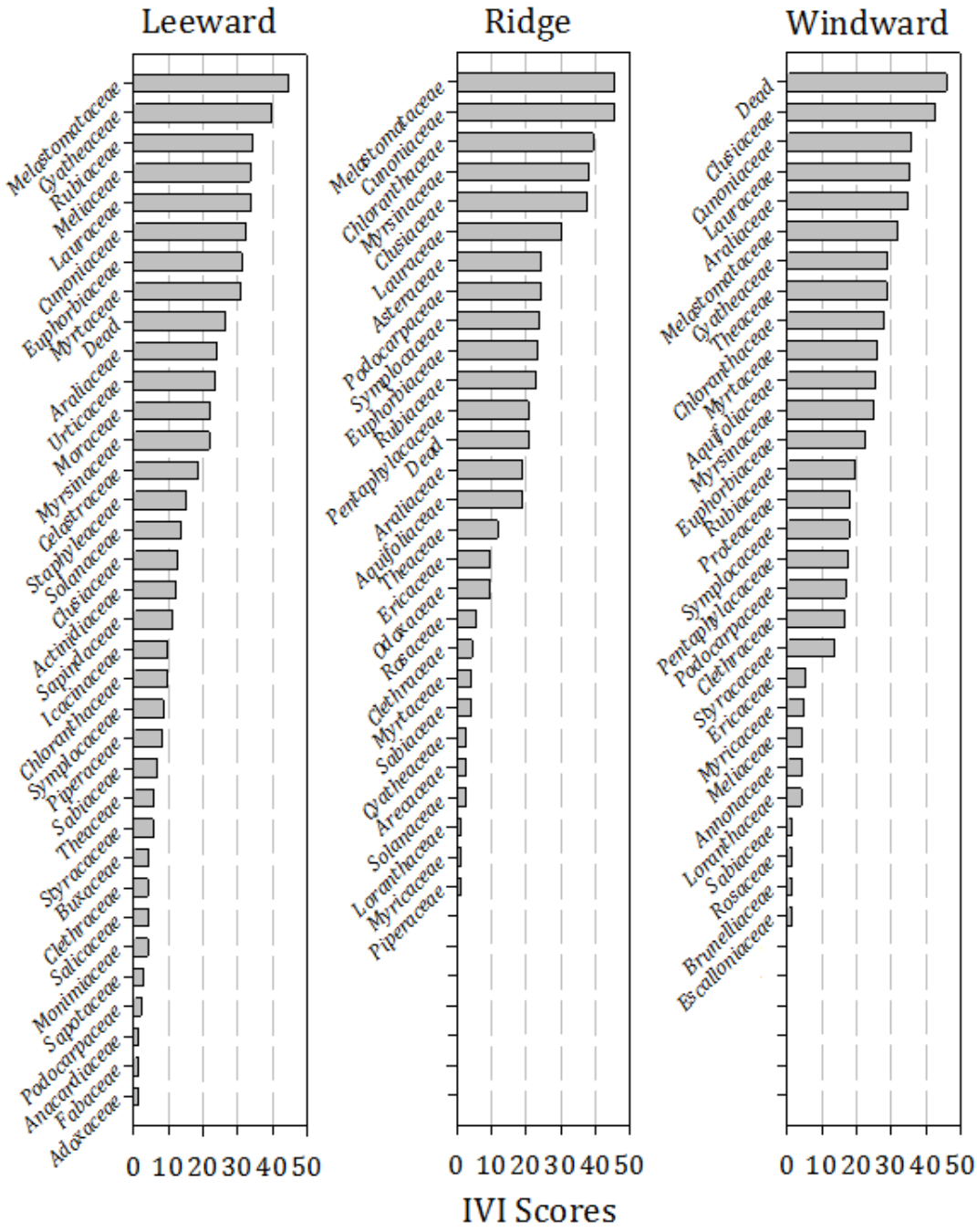

Appendix Figure 8: Importance Value Index (IVI) scores of woody families of ≥ 5cm DBH occurring at each site.

Appendix G: Overlapping species

Appendix Table 7: Woody species of DBH ≥ 5cm occurring at two or all sites.

Species	Leeward	Ridge	Windward
Alchornea sp. 1	X		X
Cavendishia bracteata		X	X
Cinchona calisaya		X	X
Clethra revoluta		X	X
Clusia alata	X	X	
Clusia ducuoides	X		X
Clusia sp. 1	X		X
Cyathea pallescens	X	X	
Faramea sp. 1	X		X
Gaiadendrum punctatum		X	X
Gordonia fruticosa	X		X
Gordonia sp. 1	X	X	X
Hedyosmum dombeyanum		X	X
Hedyosmum sp. 2		X	X
Hyeronima scabra		X	X
Licaria sp. 1		X	X
Meliosma frondosa	X	X	X
Miconia brachyanthera	X		X
Miconia carpishana	X	X	X
Miconia coelestis	X	X	
Miconia lasiostyla	X	X	
Miconia terera	X		X
Morella pubescens		X	X
Myrsine andina		X	X
Myrsine coriacea	X	X	X
Nectandra sp. 1		X	X
Ocotea sp. 1		X	X
Podocarpus magnifolius		X	X
Podocarpus oleifolius		X	X
Psychotria falcata	X	X	X
Ruagea pubescens	X		X
Schefflera angulata		X	X
Symplocos quitensis		X	X
Weinmannia auriculata		X	X
Weinmannia cochensis		X	X
Weinmannia microphylla		X	X
Weinmannia pinnata		X	X
Weinmannia pubescens	X		X

Appendix H: Forest structure parameters from known neotropical cloud forests

Appendix Table 8: Basal areas and physical data from known cloud forest sites.

Site	Forest	Lat	Long	≥5cm	≥10cm	Alt.	Rain	Temp.	Source
Xalapa,Mexico	LMCF	19.2	-97	35.3	-	1340	2200	17	(Williams-Linera, 2002)
Luquillo, Puerto Rico	UMCF	18.3	-65.8	-	27	1010	3908	19.5	(Gould *et al.*, 2006)
Volcán Barva, Costa Rica	-	10.4	-84	-	42.9	2600	3268	10.2	(Lieberman *et al.*, 1996)
Volcán Barva, Costa Rica	UMCF	10.4	-84	-	51.2	2600	3268	10.2	(Heaney & Proctor, 1990)
Monteverde, Costa Rica	LMCF	10.3	-84.8	54	-	1320	4400	15.1	(Häger & Dohrenbusch, 2010)
Monteverde, Costa Rica	LMCF	10.3	-84.8	33	-	1440	3760	15.8	(Häger & Dohrenbusch, 2010)
Monteverde, Costa Rica	LMCF	10.3	-84.8	99	-	1450	4210	15.8	(Häger & Dohrenbusch, 2010)
Monteverde, Costa Rica	LMCF	10.3	-84.8	40	-	1500	4310	16.2	(Häger & Dohrenbusch, 2010)
Talamanca, Costa Rica	UMCF	9.59	-83.7	-	60.7	2900	2812	10.9	(Kappelle *et al.*, 1996)
Alto Roble	LMCF	9.56	-83.9	42.3	39.2	2380	2500	14.1	(Oosterhoorn, 2000)
Providencia	LMCF	9.56	-83.8	41.3	38.2	2450	2500	13.7	(Oosterhoorn, 2000)
San Gerardo, Costa Rica	LMCF	9.54	-83.8	53.3	49.9	2710	2500	12.5	(Oosterhoorn, 2000)
La Carbonera, Venezuela	LMCF	8.65	-71.4	-	38.3	2321	1600	12	(Schwarzkopf *et al.*, 2010)
La Carbonera, Venezuela	LMCF	8.65	-71.4	-	48.7	2321	1600	12	(Rollet, 1984)
Monte Zerpa, Venezuela	LMCF	8.63	-71.2	-	48.7	2219	2008	14	(Schwarzkopf *et al.*, 2010)
La Mucuy, Venezuela	LMCF	8.61	-71	-	166	2588	3100	13	(Schwarzkopf *et al.*, 2010)
Pasochoa Volcano, Ecuador	-	-0.48	-78.7	25.7	24.2	3285	2000	9	(Valencia & Jørgensen, 1992)
San Francisco, Ecuador	LMCF	-4	-79.1	8.75	-	2375	3089	13.6	(Homeier *et al.*, 2010)
San Francisco, Ecuador	LMCF	-4	-79.1	12.5	-	2450	3254	13.3	(Homeier *et al.*, 2010)
San Francisco, Ecuador	LMCF	-4	-79.1	6.25	-	2540	3452	12.9	(Homeier *et al.*, 2010)
San Francisco, Ecuador	LMCF	-4	-79.1	9	-	2560	3496	12.8	(Homeier *et al.*, 2010)
Loja, Ecuador	LMCF	-4.08	-79.2	15.3	8.7	2900	3000	11	(Madsen & Ollgaard, 1994)
Zamora-	UMCF	-4.47	-79.2	44	39.5	2700	3000	12	(Madsen & Ollgaard,

Site	Forest	Lat	Long	≥5cm	≥10cm	Alt.	Rain	Temp.	Source
Chinchipe									1994)
Piura, Peru	LMCF	-4.59	-79.7	-	45.3	2700	1500	15	(Ledo *et al.*, 2009)
Yanachaga, Peru	LMCF	-10.5	-75.4	15.4	11.2	2385	2162	13	Present Study
Yanachaga, Peru	LMCF	-10.5	-75.4	33.9	32	2430	3670	13.3	Present Study
Yanachaga, Peru	UMCF	-10.5	-75.4	15.3	12.2	2812	4070	10.7	Present Study
Cotapata, Bolivia	UMCF	-16.2	-68.9	-	15	2600	3970	12.8	(Gerold *et al.*, 2008)
Canaima, Venezuela	LMCF	-	-	55.9	51.6	1400	2000	18	(Hernández *et al.*, 2012)
Cordillera Central, DR	UMCF	-	-	-	26.3	2050	1800	11.3	(Martin *et al.*, 2010)
T. Quemado, Bolivia	UMCF	-	-	-	19.4	3412	-	-	(Araujo-Murakami *et al.*, 2005)

Appendix Table 9: Stem density and physical data from known cloud forest sites.

Site	Forest	Lat	Long	≥5cm	≥10cm	Alt.	Rain	Temp.	Source
Xalapa, Mexico	LMCF	19.2	-97	1370	-	1340	2200	17	(Williams-Linera, 2002)
Luquillo, Puerto Rico	UMCF	18.3	-65.8	2664	-	1000	4500	19.5	(Weaver, 2010a)
Luquillo, Puerto Rico	UMCF	18.3	-65.8	-	687	1010	3908	19.5	(Gould *et al.*, 2006)
Volcán Barva, Costa Rica	-	10.4	-84	-	617	2600	3268	10.2	(Heaney & Proctor, 1990)
Volcán Barva, Costa Rica	-	10.4	-84	-	654	2600	3268	10.2	(Lieberman *et al.*, 1996)
Monteverde, Costa Rica	LMCF	10.3	-84.8	1560	-	1320	4400	15.1	(Häger & Dohrenbusch, 2010)
Monteverde, Costa Rica	LMCF	10.3	-84.8	3280	-	1440	3760	15.8	(Häger & Dohrenbusch, 2010)
Monteverde, Costa Rica	LMCF	10.3	-84.8	1340	-	1450	4210	15.8	(Häger & Dohrenbusch, 2010)
Monteverde, Costa Rica	LMCF	10.3	-84.8	1940	-	1500	4310	16.2	(Häger & Dohrenbusch, 2010)
La Damita	LMCF	9.68	-83.9	1660	-	2380	2500	14.1	(Oosterhoorn, 2000)
Talamanca, Costa Rica	UMCF	9.59	-83.7	1197	340	2900	2812	10.9	(Kappelle *et al.*, 1996)
Alto Roble	LMCF	9.56	-83.9	1260	-	2380	2500	14.1	(Oosterhoorn, 2000)
Providencia	LMCF	9.56	-83.8	1240	-	2450	2500	13.7	(Oosterhoorn, 2000)
San Gerardo, Costa Rica	LMCF	9.54	-83.8	1500	-	2710	2500	12.5	(Oosterhoorn, 2000)
La Carbonera, Venezuela	LMCF	8.65	-71.4	-	850	2321	1600	12	(Schwarzkopf *et al.*, 2010)
La Carbonera, Venezuela	LMCF	8.65	-71.4	-	859	2321	1600	12	(Rollet, 1984)
Monte Zerpa, Venezuela	LMCF	8.63	-71.2	-	366	2219	2008	14	(Schwarzkopf *et al.*, 2010)
La Mucuy,	LMCF	8.61	-71	-	723	2588	3100	13	(Schwarzkopf *et al.*,

Site	Forest	Lat	Long	≥5cm	≥10cm	Alt.	Rain	Temp.	Source
Venezuela									2010)
San Francisco, Ecuador	LMCF	4	-79.1	1250	-	2375	3089	13.6	(Homeier *et al.*, 2010)
San Francisco, Ecuador	LMCF	4	-79.1	1700	-	2450	3254	13.3	(Homeier *et al.*, 2010)
San Francisco, Ecuador	LMCF	4	-79.1	1075	-	2540	3452	12.9	(Homeier *et al.*, 2010)
San Francisco, Ecuador	LMCF	4	-79.1	1125	-	2560	3496	12.8	(Homeier *et al.*, 2010)
Guacra Urca, Ecuador	-	-0.42	-77.8	-	494	1710	2165	-	(Grubb *et al.*, 1963)
Pasochoa, Ecuador	-	-0.48	-78.7	1058	715	3285	2000	9	(Valencia & Jørgensen, 1992)
Loja, Ecuador	LMCF	-4.08	-79.2	2090	478	2900	3000	11	(Madsen & Ollgaard, 1994)
Zamora-Chinchipe	UMCF	-4.47	-79.2	2310	1273	2700	3000	12	(Madsen & Ollgaard, 1994)
Piura, Peru	LMCF	-4.59	-79.7	-	1246	2700	1200	15	(Ledo *et al.*, 2009)
Yanachaga, Peru	LMCF	-10.5	-75.4	1344	507	2385	2162	13	Present Study
Yanachaga, Peru	LMCF	-10.5	-75.4	1013	542	2430	3670	13.3	Present Study
Yanachaga, Peru	UMCF	-10.5	-75.4	1187	390	2812	4070	10.7	Present Study
Canaima, Venezuela	LMCF	-	-	-	814	1400	2000	18	(Hernández *et al.*, 2012)
Cordillera Central, DR	UMCF	-	-	-	810	2050	1800	11.3	(Martin *et al.*, 2010)

Appendix Table 10: Average stem height, canopy height and physical data from known cloud forest sites.

Site	Forest	Lat	Long	Av Hei	Can. Hei	Alt.	Rain	Temp	Source
Luquillo, Puerto Rico	UMCF	18.3	-65.8	10	-	1000	4500	19.5	(Weaver, 2010b)
Luquillo, Puerto Rico	UMCF	18.3	-65.8	7.8	-	1000	4500	19.5	(Weaver, 2010a)
Luquillo, Puerto Rico	UMCF	18.3	-65.8	6	-	1010	3908	19.5	(Gould *et al.*, 2006)
Volcán Barva, Costa Rica		10.4	-84	13	28	2600	3268	10.2	(Lieberman *et al.*, 1996)
Volcán Barva, Costa Rica		10.4	-84	-	32	2600	3268	10.2	(Heaney & Proctor, 1990)
Monteverde, Costa Rica	LMCF	10.3	-84.8	14	22	1320	4400	15.1	(Häger & Dohrenbusch, 2010)
Monteverde, Costa Rica	LMCF	10.3	-84.8	6	12	1440	3760	15.8	(Häger & Dohrenbusch, 2010)
Monteverde, Costa Rica	LMCF	10.3	-84.8	18	25	1450	4210	15.8	(Häger & Dohrenbusch, 2010)
Monteverde, Costa Rica	LMCF	10.3	-84.8	10	15	1500	4310	16.2	(Häger & Dohrenbusch, 2010)
La Damita	LMCF	9.68	-83.9	-	42	2380	2500	14.1	(Oosterhoorn, 2000)
Talamanca, Costa Rica	UMCF	9.59	-83.7	-	36	2900	2812	10.9	(Kappelle *et al.*, 1996)
Alto Roble	LMCF	9.56	-83.9	-	33	2380	2500	14.1	(Oosterhoorn, 2000)

Site	Forest	Lat	Long	Av Hei	Can. Hei	Alt.	Rain	Temp	Source
Providencia	LMCF	9.56	-83.8	-	38	2450	2500	13.7	(Oosterhoorn, 2000)
San Gerardo, Costa Rica	LMCF	9.54	-83.8	-	35	2710	2500	12.5	(Oosterhoorn, 2000)
La Carbonera, Venezuela	LMCF	8.65	-71.4	-	26.7	2321	1600	12	(Schwarzkopf *et al.*, 2010)
Monte Zerpa, Venezuela	LMCF	8.63	-71.2	-	23.7	2219	2008	14	(Schwarzkopf *et al.*, 2010)
La Mucuy, Venezuela	LMCF	8.61	-71	-	20.9	2588	3100	13	(Schwarzkopf *et al.*, 2010)
San Francisco, Ecuador	LMCF	4	-79.1	6	-	2375	3089	13.6	(Homeier *et al.*, 2010)
San Francisco, Ecuador	LMCF	4	-79.1	8	-	2450	3254	13.3	(Homeier *et al.*, 2010)
Pasochoa, Ecuador	-	-0.48	-78.7	7.6	21	3285	2000	9	(Valencia & Jørgensen, 1992)
Loja, Ecuador	LMCF	-4.08	-79.2	6.6	12	2900	3000	11	(Madsen & Ollgaard, 1994)
Zamora-Chinchipe	UMCF	-4.47	-79.2	8.2	12	2700	3000	12	(Madsen & Ollgaard, 1994)
Yanachaga, Peru	LMCF	-10.5	-75.4	8.47	17.6	2385	2162	13	Present Study
Yanachaga, Peru	LMCF	-10.5	-75.4	12	32	2430	3670	13.3	Present Study
Yanachaga, Peru	UMCF	-10.5	-75.4	9.78	20.9	2812	4070	10.7	Present Study
Canaima, Venezuela	LMCF	-	-	-	45	1400	2000	18	(Hernández *et al.*, 2012)
Cordillera Central, DR	UMCF	-	-	11	11.3	2050	1800	11.3	(Martin *et al.*, 2010)
TamboQuemado, Bolivia	UMCF	-	-	6.3	20	3412	-	-	(Araujo-Murakami *et al.*, 2005)

Appendix I: Indicator species analysis

Appendix Table 11: Cluster group indicator scores of leeward forest species.

Species Code	Group	Value	Mean	S.Dev	P
Alsophil	1	60.6	38.7	10	0.032
Cy s3	1	57.6	37.9	11.39	0.068
Ne cissi	1	51.4	26.7	13.65	0.066
Eug s4	1	35.4	26.7	12.75	0.137
Mys cori	1	35.4	27.2	13.62	0.149
Or s1	1	33.6	25.5	13.32	0.191
Mys pell	1	28.3	31.8	13.31	0.434
Ax lance	1	27.5	23	12.16	0.477
Pos cori	1	27.5	23.7	13.34	0.485
Mi weber	1	27.5	23.6	12.97	0.491
Mi adina	1	27.1	37.7	11.21	0.784
Alch gra	1	24.3	34.9	12.37	0.804
Be aflat	1	22.2	16.5	13.3	0.277
Pa cf li	1	22.2	17.3	13.19	0.306
Be aftov	1	16.8	20.3	13.47	0.651
Alch s1	1	13.5	22.9	12.56	1
Ax weber	1	13.5	24.2	13.42	1
Mi coele	1	13.5	23.6	12.68	1
Turpinia	1	13.5	23.4	12.24	1
Allophyl	1	6.8	16.7	13.28	1
Cit s2	1	6.8	16.5	12.82	1
Hye andi	1	6.8	16.2	12.58	1
Mycn s2	1	6.8	16.8	12.9	1
Or iodop	1	6.8	16.8	13.24	1
Pa cf ob	1	6.8	16.6	13.13	1
Solanum	1	6.8	16.6	12.92	1
Elaeagia	1	4.9	15.7	12.11	1
Mi afamn	1	4.9	16	12.78	1
Cec s2	2	45.9	33.3	14.1	0.2
Wei s2	2	30	30.1	14.38	0.301
Clu cf e	2	28.6	23.5	12.4	0.402
Fic amer	2	21.4	20.1	13.38	0.42
Cit s1	2	21.4	20.6	14.12	0.424
Cy s2	2	21	29.6	14.21	0.63
Fic giga	2	17.6	26.8	12.76	0.928
Mi barbe	2	16.3	23.4	13.35	0.81
Mys lati	2	14.3	15.4	12	0.549
Myc s1	2	14.3	16.1	12.35	0.567
Pos cf l	2	14.3	16.6	13.6	0.569
Mi carpi	2	14.3	16.7	13.13	0.574
Oc s2 sp	2	14.3	17.4	13.91	0.578
Clu s1	2	14.3	17.7	13.52	0.607
Eug s2	2	14.1	23.1	12.58	0.718
Clu ducu	2	14.1	22.8	11.13	0.744
Cro s1	2	13.2	22.4	11.47	0.809
Cupania	2	8	19.4	12.24	1
Morus in	2	8	19.6	13.66	1
Sym fuli	2	8	20	12.69	1

Species Code	Group	Value	Mean	S.Dev	P
Persea sp01	3	100	15.9	12.65	0.003
Cecropia sp01	3	95.5	19.9	12.68	0.003
Perrottetia sp01	3	91	26.4	13.69	0.005
Cyathea pallescens	3	73.3	26	11.57	0.035
Guarea kunthiana	3	70.6	38.4	10.9	0.002
Eugenia sp05	3	68.1	26.2	12.31	0.031
Wei lech	3	63.4	35.5	13.17	0.053
Mi bangg	3	43.9	31.4	13.82	0.172
Ne retic	3	39.9	20.4	12.66	0.089
Cy s4	3	38.9	20.4	13.36	0.088
Casearia	3	38.9	20	13.93	0.091
Hed anis	3	37.5	23.3	12.95	0.101
Fic afcu	3	36.6	19.6	12.38	0.164
Cedrela	3	36.6	19.2	12.71	0.17
Cle pedi	3	34.6	20.3	13.59	0.226
Mi afpav	3	30.3	24.4	14.34	0.244
Den s1	3	30	19.9	13.08	0.257
Rua pube	3	28.9	22.9	13.27	0.245
Sty cord	3	28.9	23	12.68	0.254
Saurauia	3	28.9	24.2	13.18	0.354
Be s1	3	26.7	23.2	13.55	0.38
Wei pube	3	24.6	26.4	11.97	0.619
Topobea	3	24	26.2	12.6	0.416
Maytenus	3	21	28.1	13.38	0.675

Appendix Table 12: Cluster group indicator scores of ridge forest species.

Species	Group	Value	Mean	S.Dev	P
Mys andi	6	65.6	37.2	7.34	0.001
Ilex hua	6	46.2	21.1	10.91	0.041
Clu alat	6	44.7	33.5	10.15	0.133
Fre s4	6	32.8	29.4	10.53	0.312
Pod olei	6	25.6	21	10.95	0.276
Sch angu	6	23.1	28.1	10.11	0.618
Wei pinn	6	23.1	16.6	9.23	0.192
Pod magn	6	22.2	26	11.13	0.496
Hed domb	6	20	21.1	11.1	0.486
Hed angu	6	15.4	15.4	7.34	0.685
Hye scab	6	15.4	15	7.46	0.649
Mi saltu	6	15.3	22.1	10.81	0.701
Mi apric	5	63	35.8	8.43	0.006
Hed lech	5	61.9	31.3	9.36	0.005
Mi s1	5	54.5	19.7	10.06	0.015
Wei balb	5	52.1	38.3	5.93	0.019
Wei micr	5	27.3	28.7	11.17	0.468
Bacchari	5	19.1	15.2	7.75	0.281
Clu spha	5	19.1	14.6	6.89	0.271
Geonoma	5	19.1	15.3	7.29	0.293
Hed s1	5	15.5	15.1	8.13	0.335
Mi coele	5	13.8	16.5	8.93	0.652
Mi s2	5	13.8	16.5	8.58	0.674

Species	Group	Value	Mean	S.Dev	P
Sym quit	5	13.8	16.9	8.88	0.682
Ilex s3	5	13	18.7	10.26	0.692
Clu elli	4	39.2	31.6	9.78	0.176
Gor s1	4	37.5	20.3	10.4	0.116
Mi carpi	4	25	15	7.19	0.113
Mi lasio	4	25	15.1	7.88	0.131
Ne s1	4	20.7	16.3	8.75	0.277
Mys cori	4	13.4	18.4	9.37	0.626
Mi media	4	9.6	14.7	7.68	0.819
Lic s1	4	7.7	16.7	8.82	1
Cy palle	4	5.6	14.7	7.43	1

Appendix Table 13: Cluster group indicator scores of windward forest species.

Species	Group	Value	Mean	S.Dev	P
Clu schu	9	82.1	41.9	7.39	0.001
Myc s1	9	62.4	36.9	11.89	0.028
Wei auri	9	46.3	34.4	13.25	0.213
Sch pedi	9	37.1	35.3	12.33	0.339
Gor frut	9	35.7	24.5	12.95	0.149
Ne purpu	9	35.7	25.3	13.11	0.158
Sch sp1	9	28.6	22.8	12.72	0.334
Ter s1	9	21.7	29.2	14.26	0.657
Cin hirs	9	21.4	20	13.66	0.408
Ne s1	9	21.4	19.7	13.14	0.412
Oc arnot	9	21.4	20.3	13.86	0.423
Pod s1	9	14.3	17	13.25	0.579
Hye s1	8	87.5	22.4	10.93	0.003
Be latif	8	77.3	24.5	11.84	0.023
Cle revo	8	74.4	27.2	12.57	0.014
Cy carac	8	73.7	39.1	10.28	0.001
Cy delga	8	63	27.4	12.69	0.061
Wei pube	8	48.6	16.1	11.85	0.046
Ilex s2	8	43.7	16.4	12.58	0.098
Sty vilc	8	43.7	16	12.34	0.089
Sch micr	8	40.9	16.1	12.35	0.145
Gor s1	8	38.9	19.5	12.33	0.088
Per areo	8	38.9	19.9	12.23	0.084
Oc calop	8	36.6	20	13.57	0.188
Hed domb	8	34.6	15.9	12.45	0.142
Wei pinn	8	29.9	32.2	12.91	0.443
Panopsis	8	26.7	25	12.82	0.356
Fre s3	8	26.5	23	13.28	0.446
Mi suban	8	24	27.6	12.58	0.385
Clu thur	8	21.6	26.2	13.35	0.641
Fre s1	7	64.2	28.2	14.11	0.05
Ilex ter	7	50.9	26.8	13.69	0.068
Mi nerii	7	22.2	17.3	13.37	0.303
Fre s2	7	20.3	24.6	12.24	0.588
Rua pube	7	19.7	20.5	13.06	0.521

Species	Group	Value	Mean	S.Dev	P
Clu ducu	7	15	20.3	13.47	0.643
Pod olei	7	12	24.7	12.3	1
Ilex s1	7	11.3	24.4	12.91	1
Hye scab	7	8.4	16.7	12.96	0.798
Graffenr	7	6.8	16.7	12.54	1
Guatteri	7	6.8	17.3	14.5	1
Morella	7	6.8	16.6	13.07	1
Sym quit	7	6.8	16.2	12.75	1

Appendix J: Species NMS axis correlations

Appendix Table 14: Pearson's correlation scores between leeward forest species and NMS ordination axes.

Species	*r* Axis 1	*r* Axis 2	*r* Axis 3
Alch gra	0.48	0.18	0.21
Alch s1	0.04	0.27	0.21
Allophyl	-0.08	-0.11	-0.09
Alsophil	-0.01	0.39	0.35
Ax lance	0.09	0.45	0.25
Ax weber	-0.21	-0.20	-0.37
Be aflat	0.06	0.34	0.02
Be aftov	-0.04	0.30	-0.09
Be s1	0.39	0.10	0.22
Casearia	0.14	-0.07	0.32
Cec s1	-0.34	-0.39	0.25
Cec s2	0.76	-0.09	0.22
Cedrela	-0.62	0.04	0.18
Cit s1	-0.37	-0.33	0.02
Cit s2	-0.03	0.09	-0.27
Cle pedi	-0.18	0.12	0.14
Clu cf e	0.10	-0.17	0.33
Clu ducu	0.15	-0.16	0.27
Clu s1	-0.03	-0.25	0.00
Cro s1	0.17	-0.11	-0.10
Cupania	-0.01	0.11	0.00
Cy palle	-0.44	0.02	0.38
Cy s2	-0.15	0.04	-0.34
Cy s3	-0.31	0.68	-0.10
Cy s4	0.23	-0.32	0.01
Den s1	-0.27	0.21	-0.18
Elaeagia	-0.02	0.11	0.27
Eug s2	0.18	0.06	0.20
Eug s4	0.06	0.16	0.13
Eug s5	-0.19	-0.13	-0.10
Fic afcu	-0.27	-0.04	0.30
Fic amer	-0.13	0.06	0.40
Fic giga	0.30	0.06	0.02
Guarea k	-0.02	-0.47	0.58
Hed anis	-0.27	0.22	-0.02
Hye andi	-0.08	0.22	0.03
Maytenus	-0.35	-0.37	-0.09
Mi adina	0.48	0.34	-0.19
Mi afamn	-0.23	0.02	-0.58
Mi afpav	0.32	-0.11	-0.09
Mi bangg	0.36	0.21	0.21
Mi barbe	-0.14	-0.41	-0.11
Mi carpi	0.18	-0.26	-0.57
Mi coele	0.12	0.32	0.13
Mi weber	0.18	0.22	-0.09
Morus in	-0.39	0.08	-0.32
Myc s1	0.02	-0.18	-0.48

Species	*r* Axis 1	*r* Axis 2	*r* Axis 3
Mycn s2	0.15	-0.02	-0.18
Mys cori	0.27	0.56	-0.15
Mys lati	-0.05	0.03	0.28
Mys pell	-0.45	0.17	-0.17
Ne cissi	0.20	0.51	-0.01
Ne retic	-0.30	-0.35	0.05
Oc s2 sp	0.10	-0.12	0.08
Or iodop	-0.10	0.15	-0.02
Or s1	0.18	0.23	-0.22
Pa cf li	-0.03	0.30	-0.31
Pa cf ob	-0.02	-0.24	0.02
Perrotte	-0.34	-0.34	0.24
Per s1	-0.23	-0.26	0.32
Pos cf l	-0.15	-0.21	0.18
Pos cori	0.24	0.29	0.01
Rua pube	-0.26	-0.07	0.37
Saurauia	-0.20	0.17	0.07
Solanum	0.00	0.01	0.08
Sty cord	-0.15	-0.07	-0.24
Sym fuli	0.00	-0.17	0.24
Topobea	0.01	-0.07	-0.33
Turpinia	0.06	0.01	-0.38
Wei lech	-0.34	-0.55	0.10
Wei pube	0.03	0.36	0.06
Wei s2	-0.18	-0.31	-0.59

Appendix Table 15: Pearson's correlation scores between ridge forest species and NMS ordination axes.

Species	*r* Axis 1	*r* Axis 2	*r* Axis 3
Bacchari	-0.02	0.23	0.04
Clu alat	0.37	-0.05	-0.59
Clu elli	-0.61	-0.04	-0.09
Clu spha	-0.09	0.14	0.06
Cy palle	0.15	0.34	-0.08
Fre s4	0.56	-0.10	0.15
Geonoma	0.14	0.05	0.15
Gor s1	-0.19	0.27	-0.12
Hed angu	0.23	0.03	-0.06
Hed domb	0.23	0.29	-0.18
Hed lech	0.33	0.06	0.50
Hed s1	0.02	0.18	0.04
Hye scab	0.33	-0.02	0.41
Ilex hua	0.52	-0.04	0.36
Ilex s3	0.35	0.04	-0.19
Lic s1	-0.02	-0.04	-0.10
Mi apric	-0.36	0.55	0.07
Mi carpi	-0.33	0.12	-0.17

Species	*r* Axis 1	*r* Axis 2	*r* Axis 3
Mi coele	-0.06	0.19	-0.07
Mi lasio	-0.06	0.16	-0.24
Mi media	0.01	0.04	-0.22
Mi saltu	0.32	-0.20	0.48
Mi s1	-0.23	0.51	0.25
Mi s2	-0.15	-0.10	0.26
Mys andi	0.70	-0.19	-0.07
Mys cori	-0.32	0.40	-0.12
Ne s1	-0.17	0.14	-0.27
Pod magn	0.08	0.17	-0.53
Pod olei	0.28	-0.44	-0.23
Sch angu	0.10	0.25	-0.31
Sym quit	-0.17	0.24	-0.12
Wei balb	0.14	0.59	0.01
Wei micr	-0.45	-0.57	0.11
Wei pinn	0.39	-0.32	-0.44

Appendix Table 16: Pearson's correlation scores between windward forest species and NMS ordination axes.

Species	*r* Axis 1	*r* Axis 2
Be latif	-0.42	0.56
Cin hirs	0.40	0.00
Cle revo	-0.57	0.35
Clu ducu	-0.03	0.17
Clu schu	0.77	0.18
Clu thur	-0.12	0.32
Cy carac	-0.69	0.54
Cy delga	-0.49	0.38
Fre s1	-0.40	-0.62
Fre s2	-0.50	-0.12
Fre s3	-0.41	0.25
Gor frut	0.37	0.10
Gor s1	-0.05	0.24
Graffenr	-0.03	0.21
Guatteri	0.14	0.19
Hed domb	-0.42	0.01
Hye scab	-0.18	0.35
Hye s1	-0.17	0.42
Ilex s1	0.19	0.33
Ilex s2	-0.23	0.27
Ilex ter	-0.49	-0.41
Mi nerii	-0.31	-0.18
Mi suban	0.12	-0.03

Species	*r* Axis 1	*r* Axis 2
Morella	-0.08	0.28
Myc s1	0.52	0.42
Ne purpu	0.47	0.03
Ne s1	0.30	0.29
Oc arnot	0.50	-0.05
Oc calop	-0.28	0.33
Panopsis	0.14	-0.30
Per areo	0.00	0.14
Pod olei	-0.07	0.24
Pod s1	0.20	0.09
Rua pube	-0.22	0.43
Sch micr	-0.42	0.41
Sch pedi	0.37	0.39
Sch sp1	0.38	-0.26
Sty vilc	-0.09	0.20
Sym quit	-0.03	0.03
Ter s1	0.13	0.42
Wei auri	0.37	0.09
Wei pinn	-0.23	0.41
Wei pube	-0.36	0.25

Appendix K: Biophysical NMS axis correlations

Appendix Table 17: Pearson's correlation scores between biophysical variables and NMS ordination axes.

Parameter	Code	Leeward NMS			Ridge NMS			Windward NMS		All Forests NMS	
		Ax.1	Ax.2	Ax.3	Ax.1	Ax.2	Ax.3	Ax.1	Ax.2	Ax.1	Ax.2
Floristic Parameters (DBH ≥10cm)											
Stem density	SD	-0.18	0.21	0.23	0.19	0.21	-0.21	-0.48	0.64	0.19	0.33
Species diversity	SP	-0.18	0.15	0.18	0.26	0.22	-0.16	-0.25	0.78	0.57	0.04
Total basal area	BA	-0.27	0.12	0.11	0.01	0.28	-0.36	-0.43	0.53	0.65	0.07
Total crown area	CA	-0.13	0.19	0.18	-0.06	0.31	-0.21	-0.32	0.65	0.53	0.09
Aver. basal area	BAm	-0.32	-0.01	0.00	-0.54	0.33	-0.34	-0.41	0.60	0.71	-0.02
Total crown area	CAm	0.28	-0.24	-0.15	-0.56	0.43	-0.25	-0.68	0.49	0.65	-0.17
Aver. stem height	SH	-0.18	0.04	0.00	-0.55	0.29	-0.13	-0.35	0.72	0.67	-0.11
Aver. stem incline	SI	0.50	-0.03	-0.19	0.23	0.46	-0.14	-0.51	0.03	0.78	-0.07
Slope	Sl	0.24	-0.10	0.28	-0.40	-0.21	-0.01	0.71	0.04	-0.07	-0.13
Environmental Parameters (Taylor, 2008)											
O hor. Al+3	Al3	0.39	0.64	-0.06	0.10	0.10	-0.27	0.28	0.31	-0.82	0.02
A hor. bulk dens.	BD	0.25	-0.13	0.15	-0.34	-0.26	0.01	-0.35	-0.54	0.59	0.10
Bryophyte cover	Br	-0.14	-0.12	0.39	0.67	-0.06	-0.22	0.22	0.24	-0.53	-0.64
O horizon EC	CE	0.07	-0.29	0.25	-0.25	0.07	-0.06	0.19	0.24	0.46	-0.04
Exposed soil cover	ES	0.30	0.13	-0.14	0.13	0.31	0.14	0.15	-0.27	0.53	-0.11
O hor. K content	K	-0.50	-0.06	-0.13	0.56	0.02	0.11	0.51	0.25	-0.39	-0.04
LAI	Lai	-0.21	0.07	-0.41	-0.17	0.15	0.10	-0.21	0.21	0.58	0.07
LAI deviation	LaiD	0.25	-0.02	-0.19	-0.10	-0.36	0.02	-0.23	0.20	0.26	-0.02
Leaf litter cover	Li	0.19	-0.20	0.15	-0.63	0.34	-0.02	0.06	0.27	-0.05	0.31
Below canopy rad.	Mol	0.19	0.18	-0.24	0.34	-0.30	0.07	-0.21	-0.49	-0.54	-0.04
A hor. pH	MpH	-0.31	-0.48	0.06	0.23	-0.08	-0.10	-0.22	-0.36	0.52	0.09
O hor. org. content	OM	-0.30	0.08	-0.26	0.16	0.17	-0.13	0.48	0.26	-0.69	0.05
O hor. pH	OpH	-0.29	-0.42	0.06	0.06	0.29	0.07	-0.42	-0.25	0.64	0.25
O hor. P content	P	-0.59	-0.04	0.08	0.29	0.09	-0.41	0.47	0.12	0.14	-0.18
Root mat height	RmH	-0.18	0.23	0.15	0.33	-0.28	0.03	0.52	0.14	-0.83	-0.18
Visible sky fraction	VS	0.26	0.09	-0.17	0.41	-0.27	-0.01	-0.05	-0.40	-0.60	0.03
Woody debris cover	WD	-0.19	0.08	-0.21	-0.23	-0.06	0.11	-0.40	-0.40	0.25	0.14

Very strong correlation (r > 0.8)	Strong correlation (r > 0.6 – 0.8)	Moderate correlation (r > 0.4 – 0.6)

Appendix L: Stem dispersion of leeward forest species

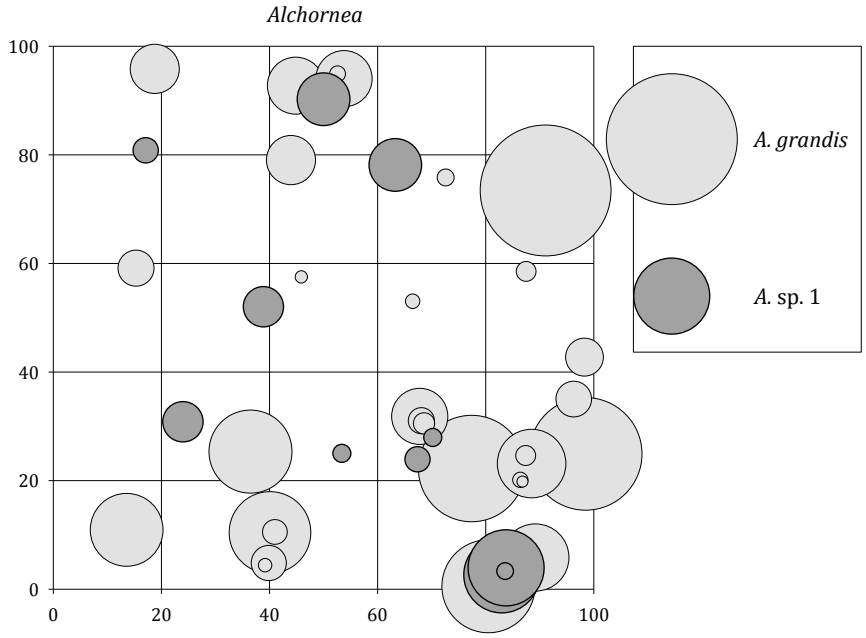

Appendix Figure 9: Dispersion of *Alchornea* species in the leeward forest plot. .

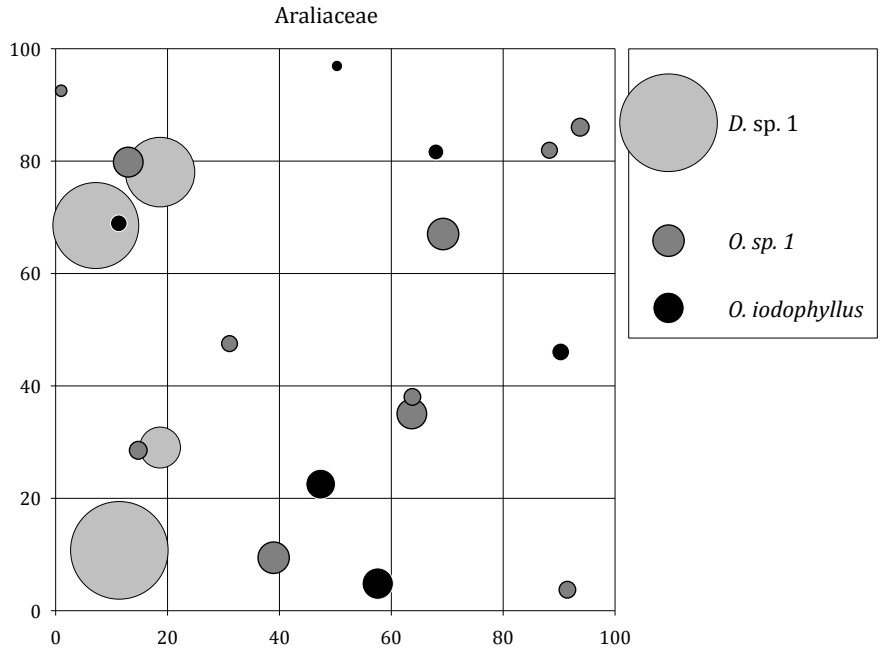

Appendix Figure 10: Dispersion of *Dendropanax* and *Oreopanax* species in the leeward forest plot. Circle sizes are relative to the maximum DBH indicated in the legend.

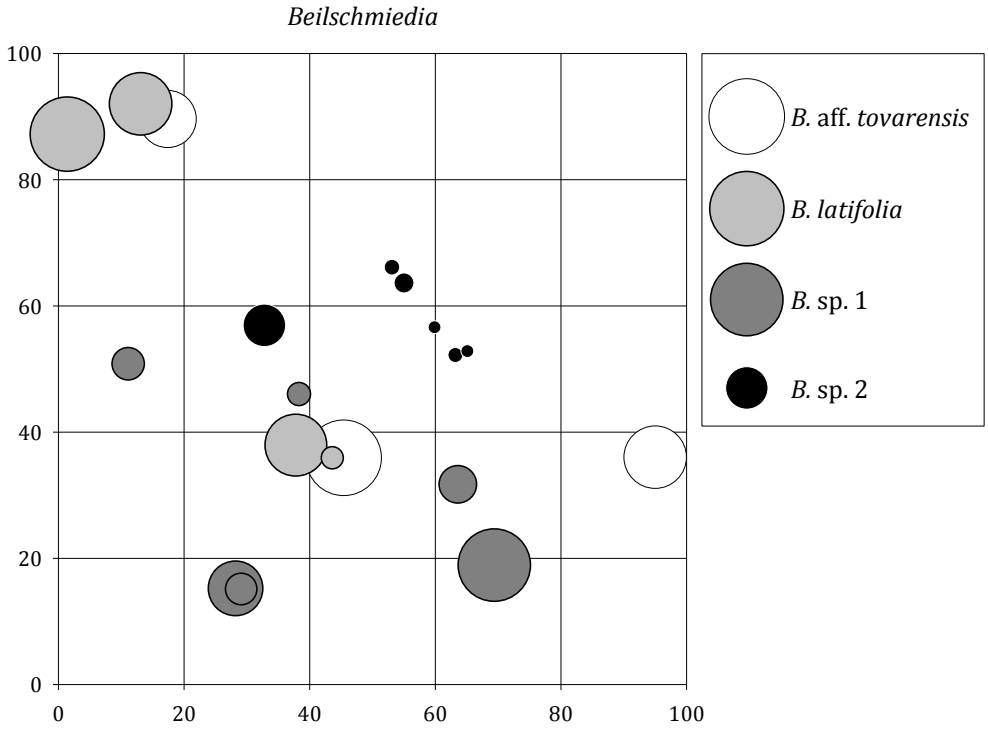

Appendix Figure 11: Dispersion of *Beilschmiedia* species in the leeward forest plot. Circle sizes are relative to the maximum DBH indicated in the legend.

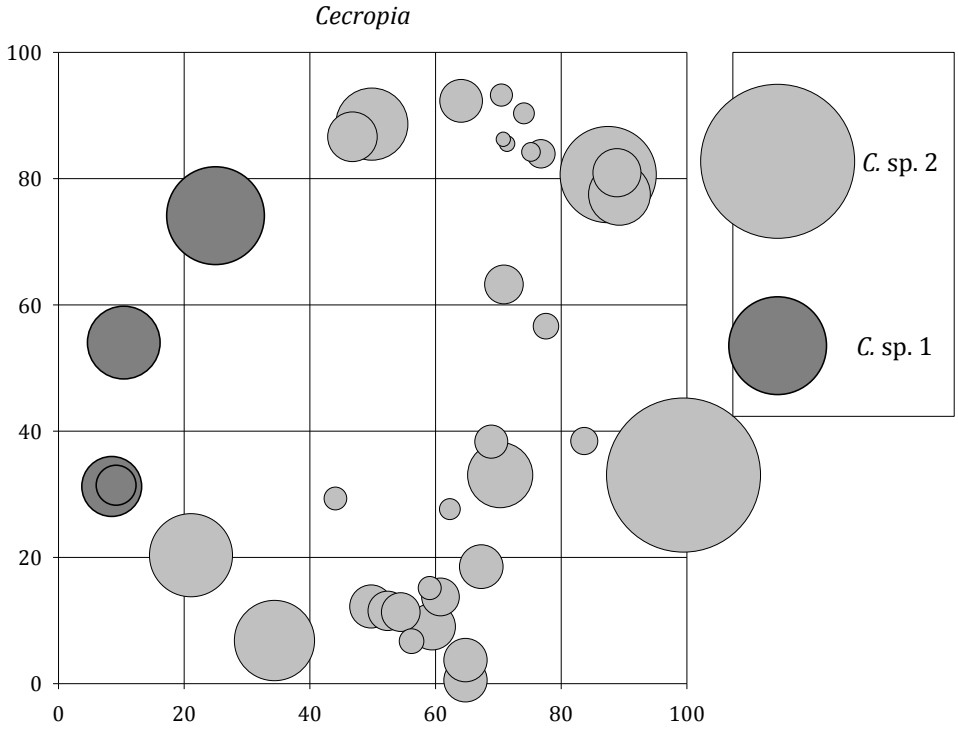

Appendix Figure 12: Dispersion of *Cecropia* species in the leeward forest plot. Circle sizes are relative to the maximum DBH indicated in the legend.

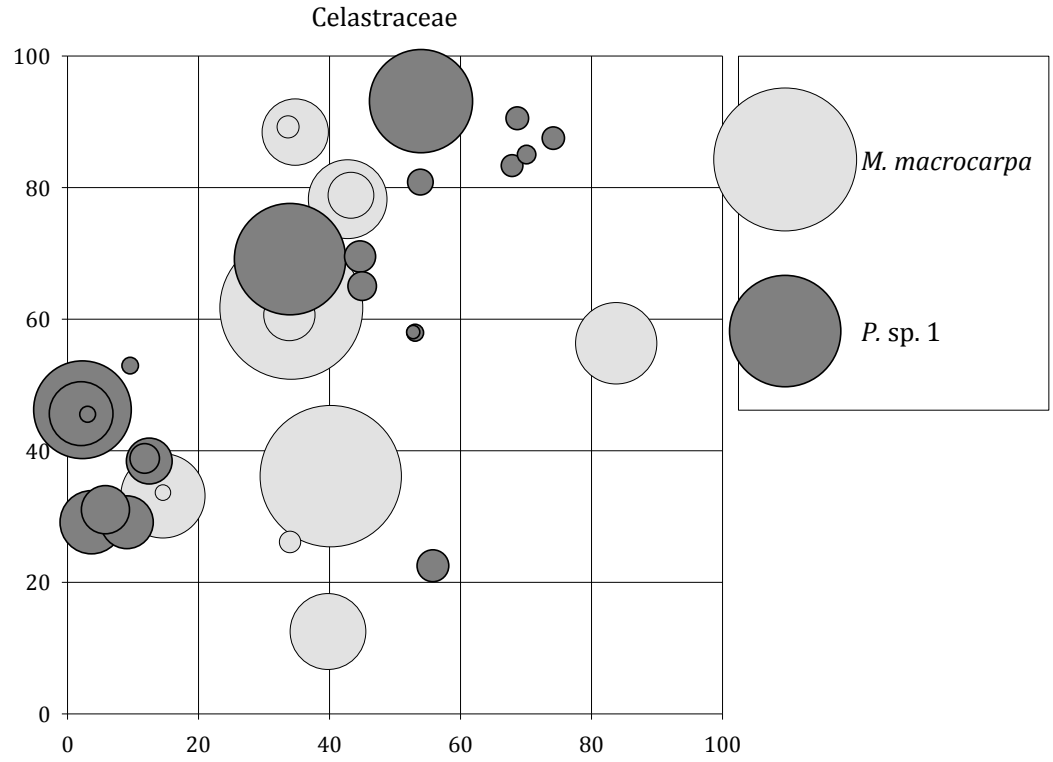

Appendix Figure 13: Dispersion of Celastraceae species in the leeward forest plot. Circle sizes are relative to the maximum DBH indicated in the legend.

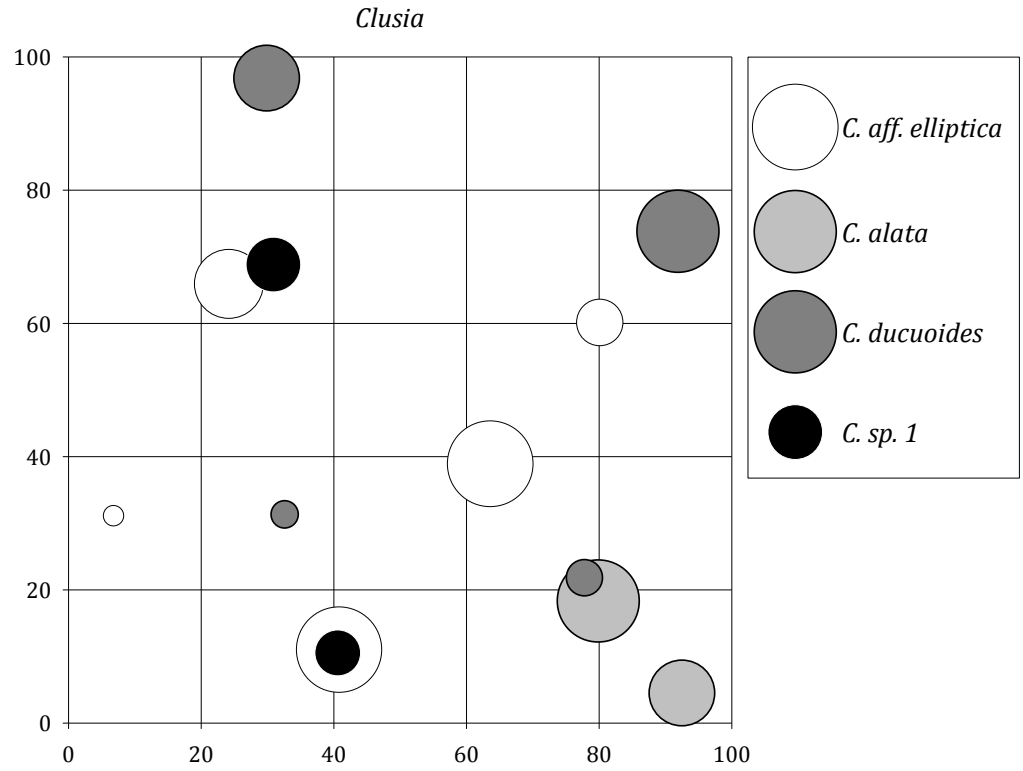

Appendix Figure 14: Dispersion of *Clusia* species in the leeward forest plot. Circle sizes are relative to the maximum DBH indicated in the legend.

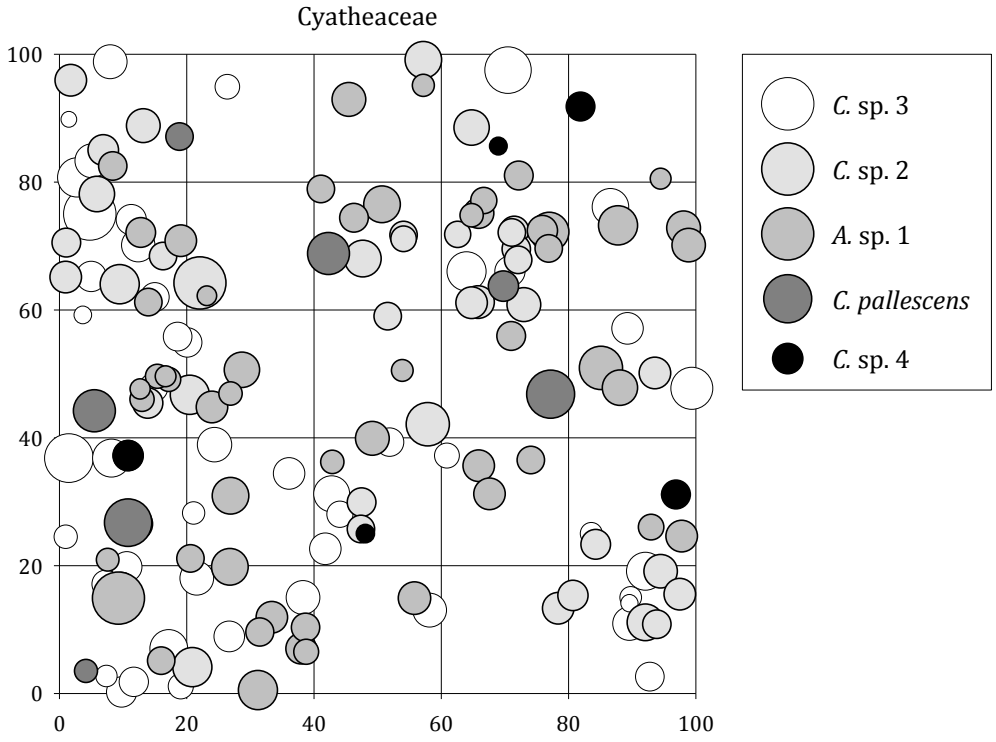

Appendix Figure 15: Dispersion of *Cyathea* and *Alsophila* species in the leeward forest plot. Circle sizes are relative to the maximum DBH indicated in the legend.

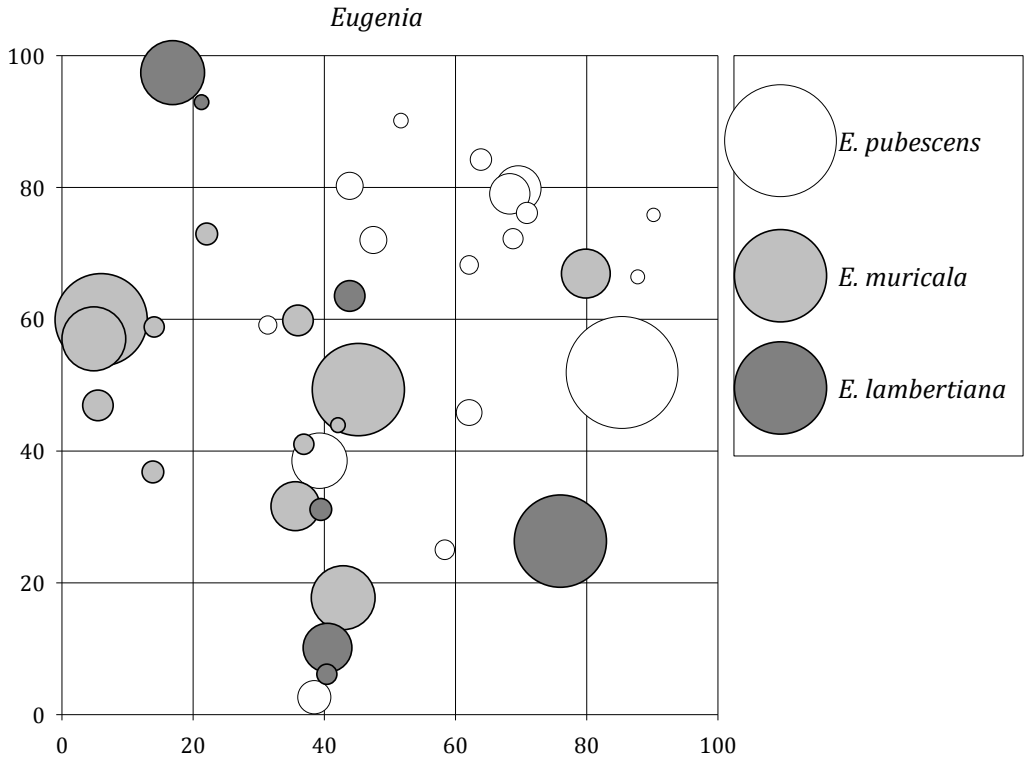

Appendix Figure 16: Dispersion of *Eugenia* species in the leeward forest plot. Circle sizes are relative to the maximum DBH indicated in the legend.

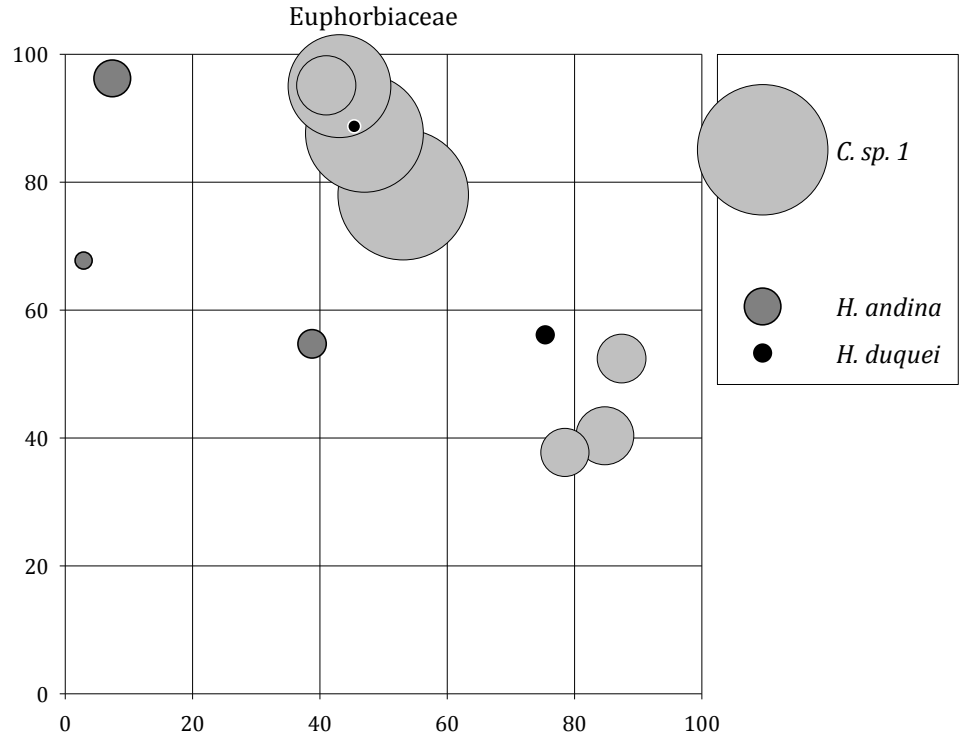

Appendix Figure 17: Dispersion of Euphorbiaceae species in the leeward forest plot. Circle sizes are relative to the maximum DBH indicated in the legend.

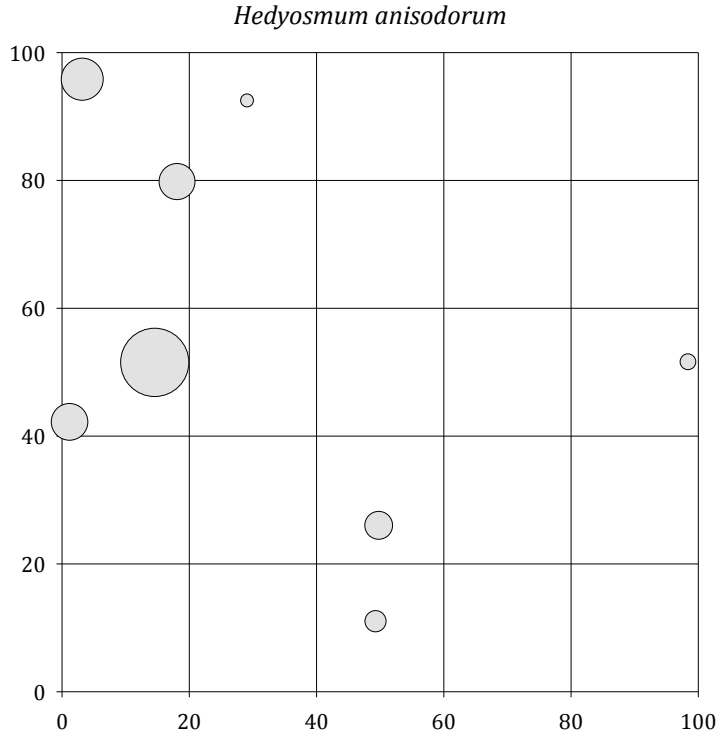

Appendix Figure 18: Dispersion of *Hedyosmum* species in the leeward forest plot. Circle sizes are relative to the maximum DBH indicated in the legend.

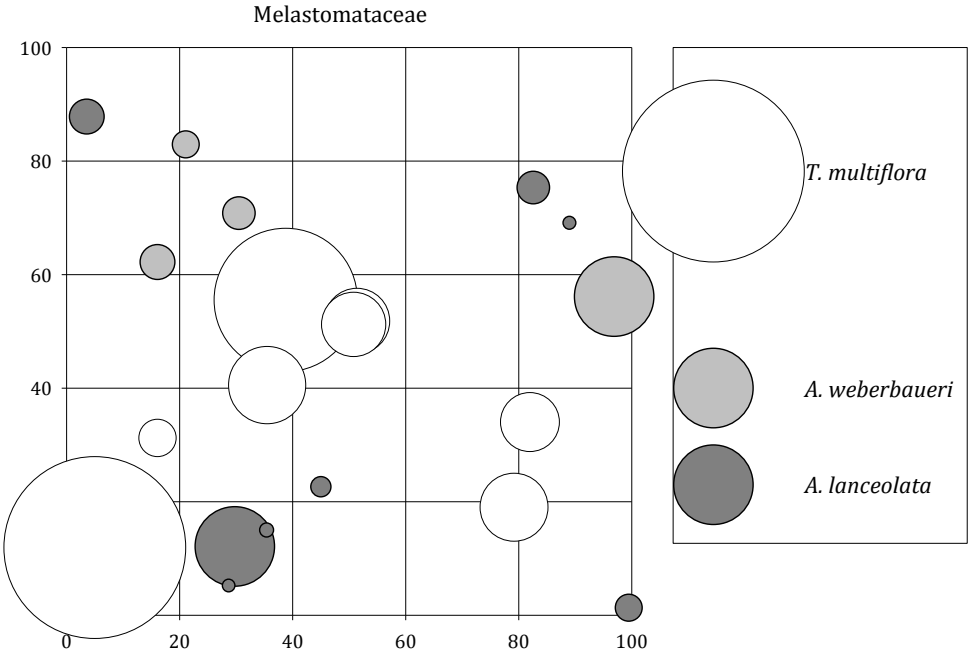

Appendix Figure 19: Dispersion of *Topobea* and *Axinaea* species in the leeward forest plot. Circle sizes are relative to the maximum DBH indicated in the legend.

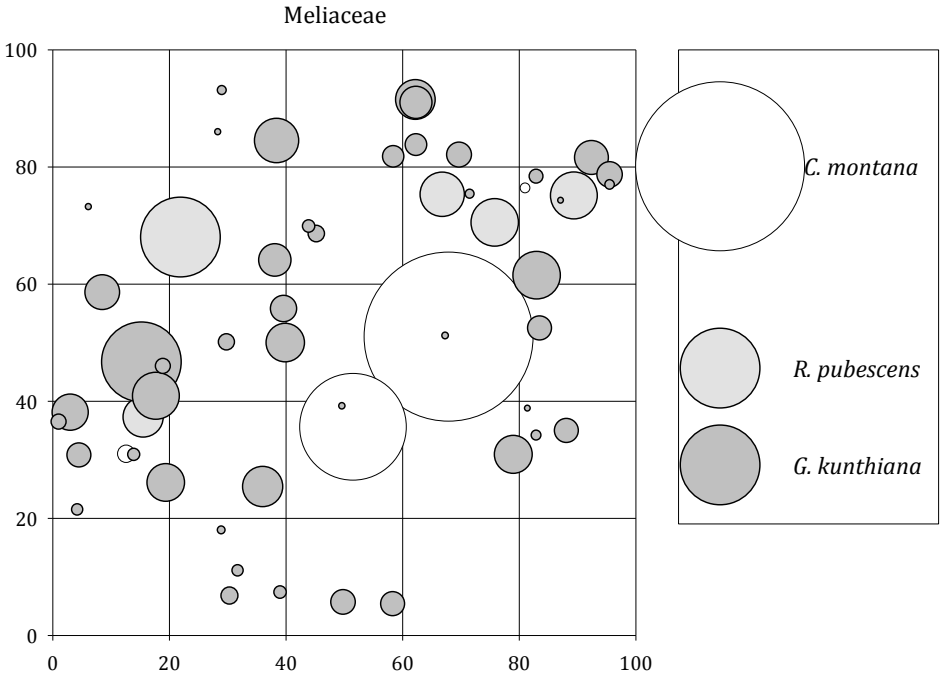

Appendix Figure 20: Dispersion of *Cedrela*, *Ruagea* and *Guarea* species in the leeward forest plot. Circle sizes are relative to the maximum DBH indicated in the legend.

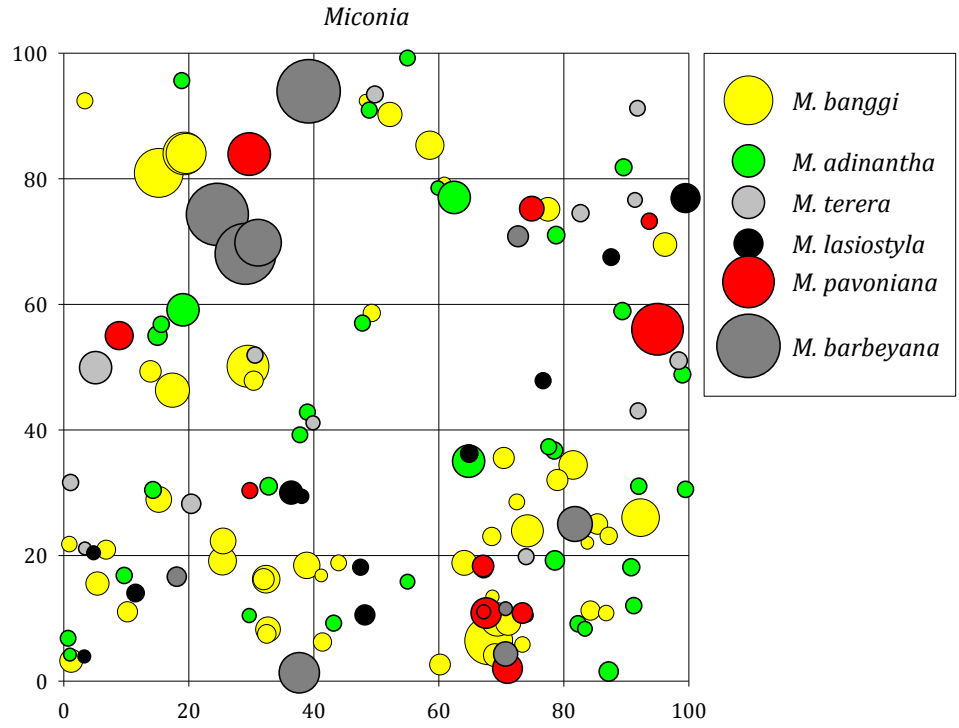

Appendix Figure 21: Dispersion of *Miconia* species in the leeward forest plot. Circle sizes are relative to the maximum DBH indicated in the legend.

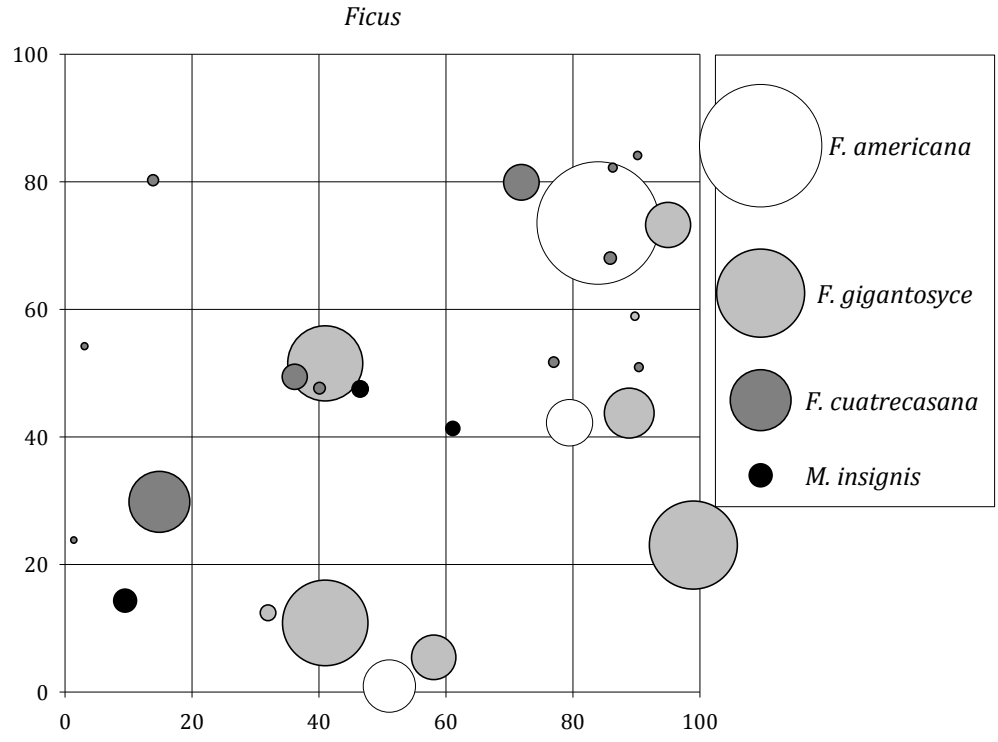

Appendix Figure 22: Dispersion of *Ficus and Moralis* species in the leeward forest plot. Circle sizes are relative to the maximum DBH indicated in the legend.

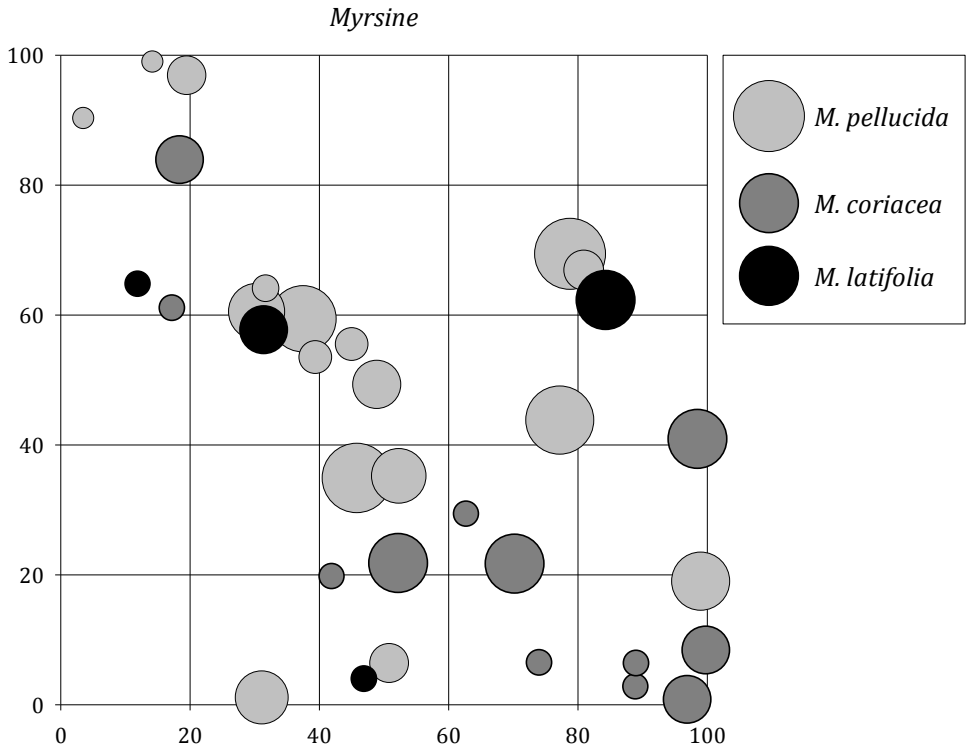

Appendix Figure 23: Dispersion of *Myrsine* species in the leeward forest plot. Circle sizes are relative to the maximum DBH indicated in the legend.

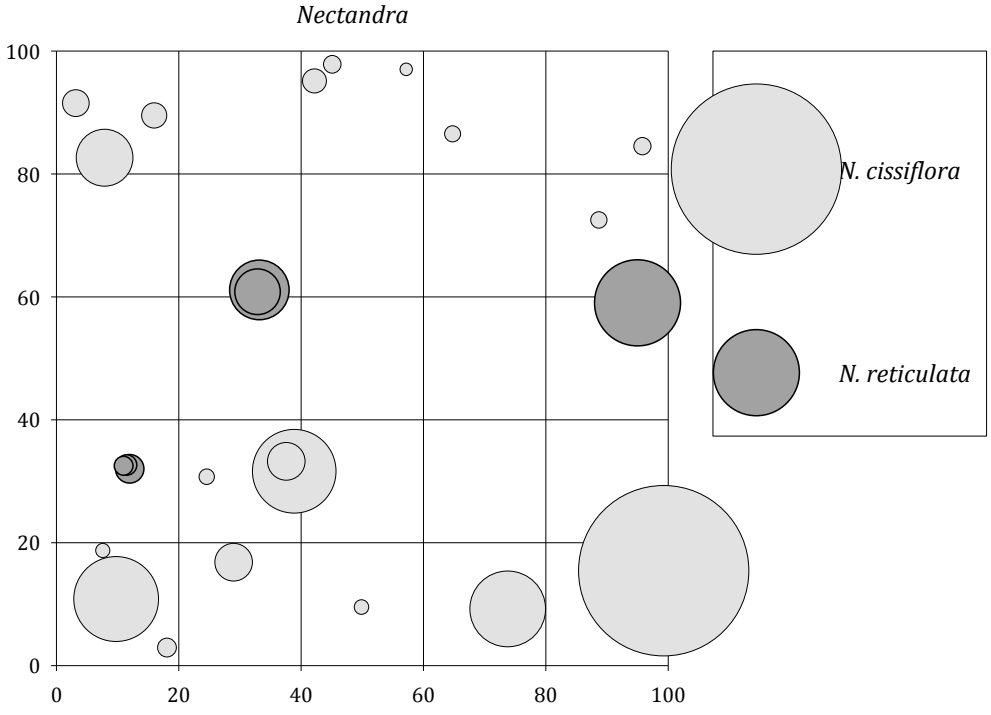

Appendix Figure 24: Dispersion of *Nectandra* species in the leeward forest plot. Circle sizes are relative to the maximum DBH indicated in the legend.

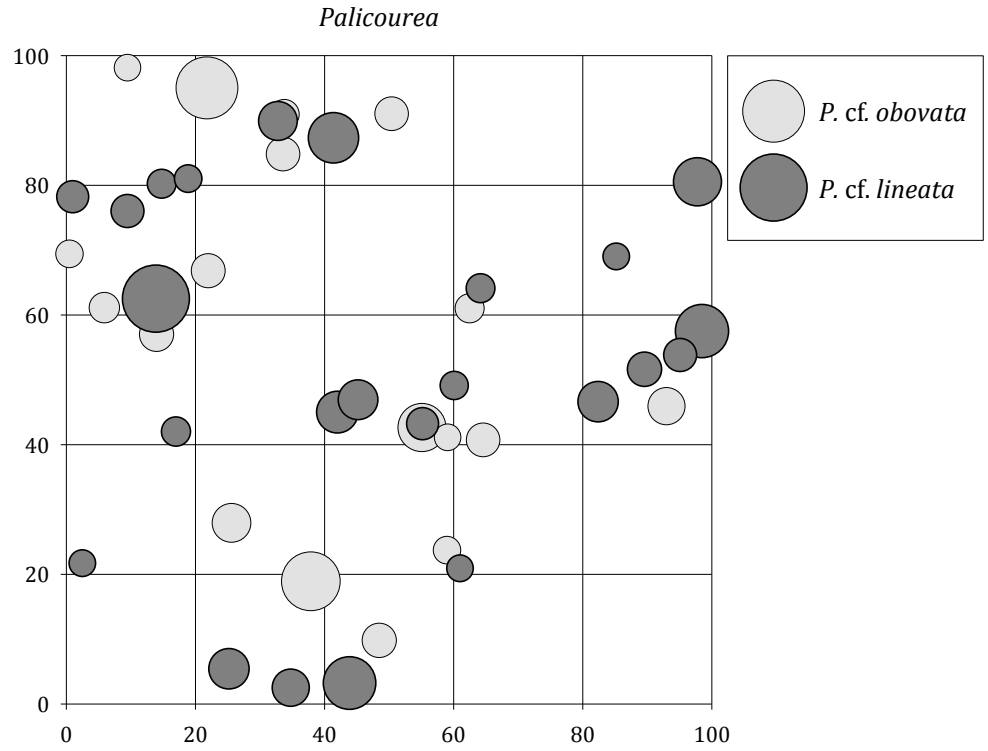

Appendix Figure 25: Dispersion of *Palicorea* species in the leeward forest plot. Circle sizes are relative to the maximum DBH indicated in the legend.

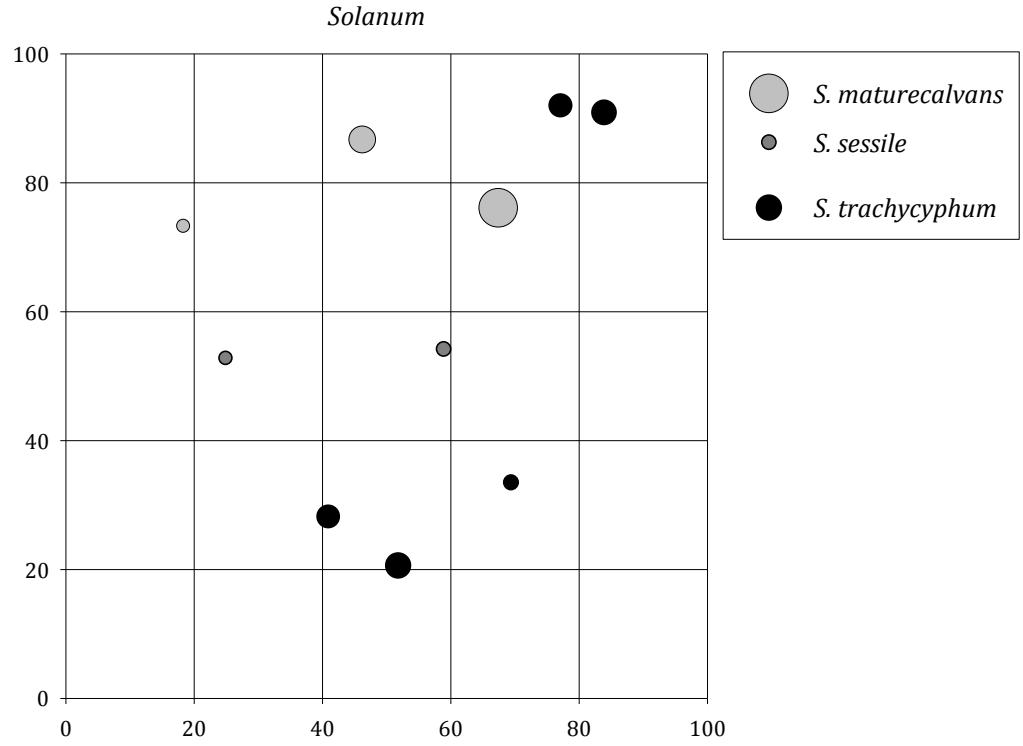

Appendix Figure 26: Dispersion of *Solanum* species in the leeward forest plot. Circle sizes are relative to the maximum DBH indicated in the legend.

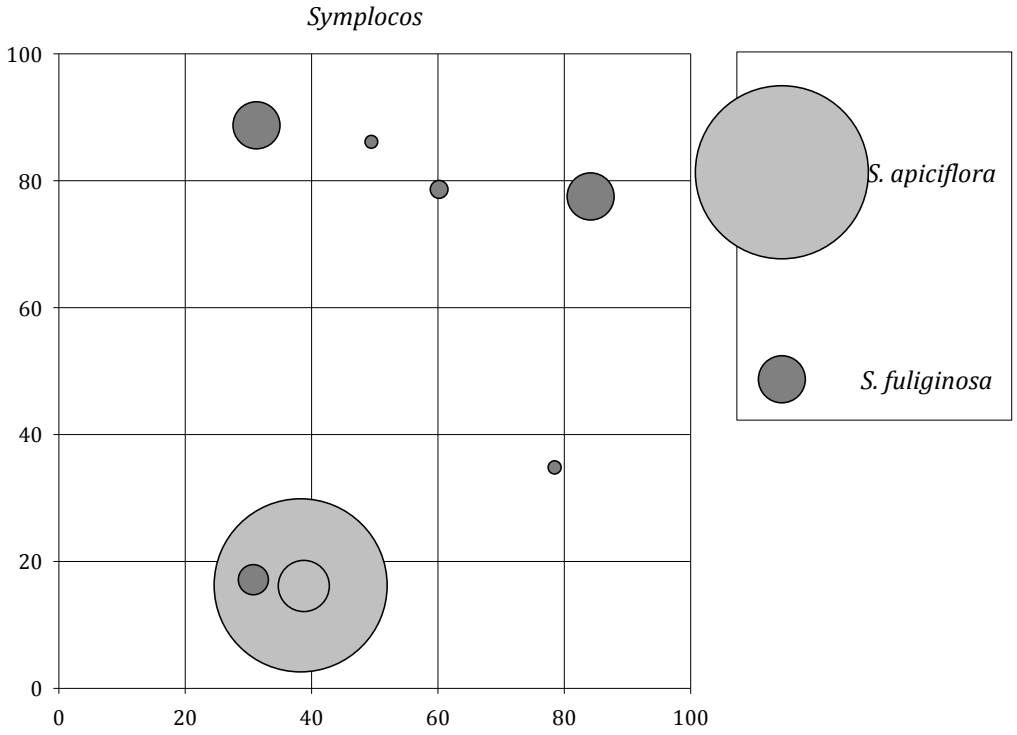

Appendix Figure 27: Dispersion of *Symplocos* species in the leeward forest plot. Circle sizes are relative to the maximum DBH indicated in the legend.

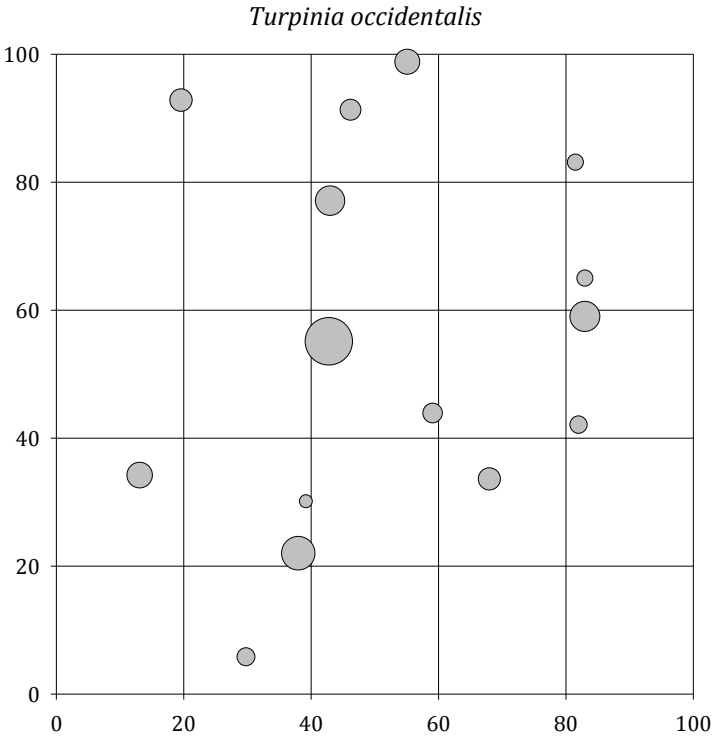

Appendix Figure 28: Dispersion of *Turpinia occidentalis* in the leeward forest plot. Circle sizes are relative to the maximum DBH indicated in the legend.

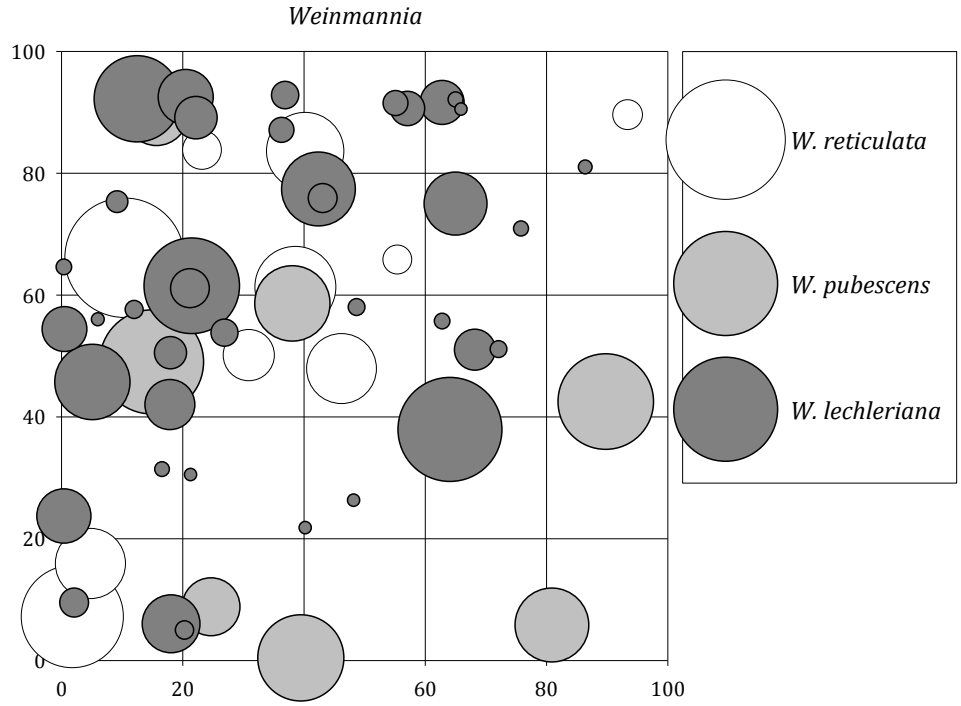

Appendix Figure 29: Dispersion of *Weinmannia* species in the leeward forest plot. Circle sizes are relative to the maximum DBH indicated in the legend.

Appendix M: Stem dispersion of ridge forest species

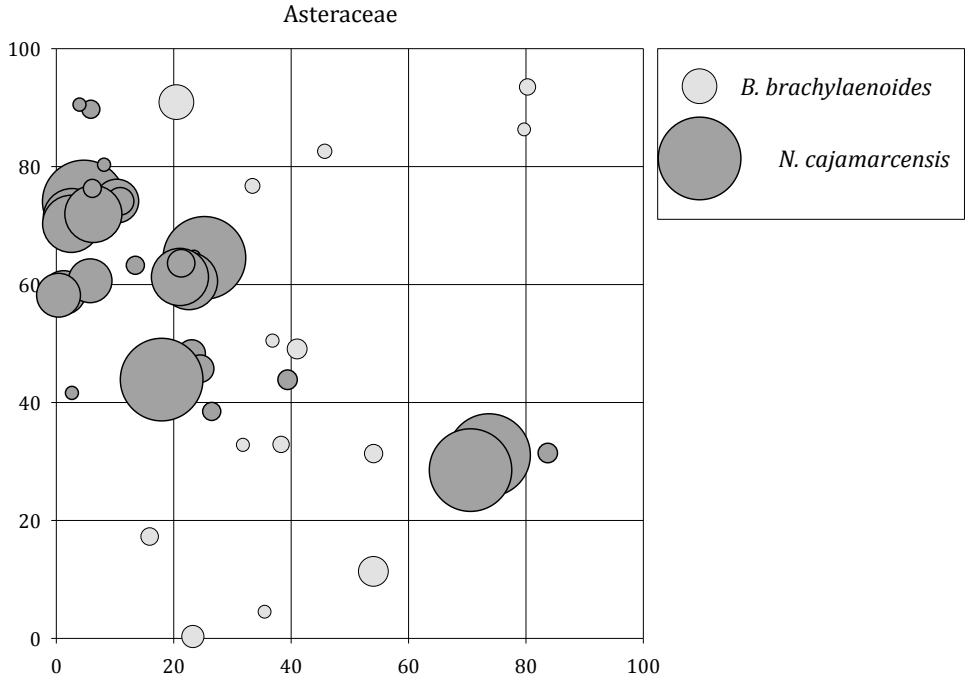

Appendix Figure 30: Dispersion of Asteraceae species in the ridge forest plot. Circle sizes are relative to the maximum DBH indicated in the legend.

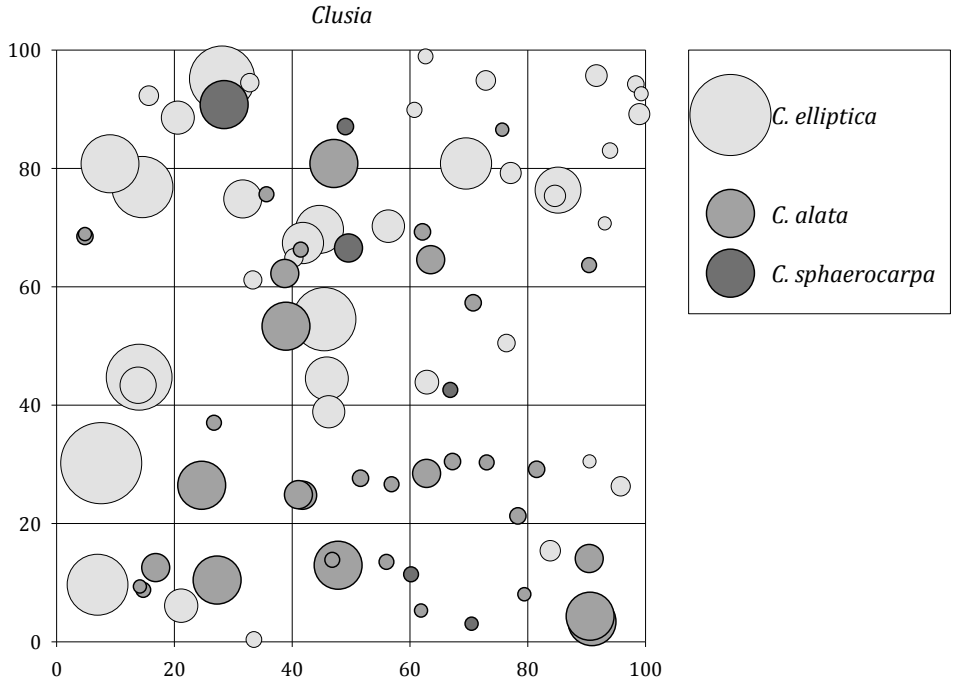

Appendix Figure 31: Dispersion of *Clusia* species in the ridge forest plot. Circle sizes are relative to the maximum DBH indicated in the legend.

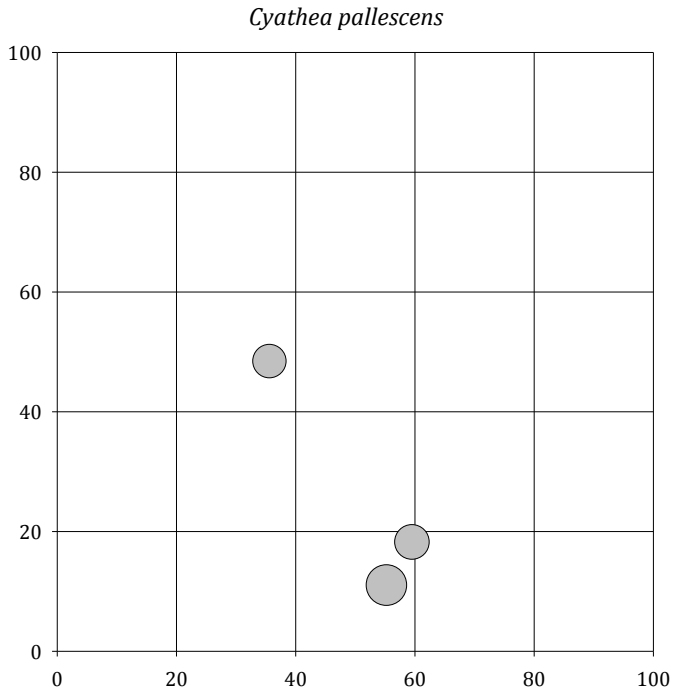

Appendix Figure 32: Dispersion of *Cyathea pallescens* in the ridge forest plot. Circle sizes are relative to the maximum DBH.

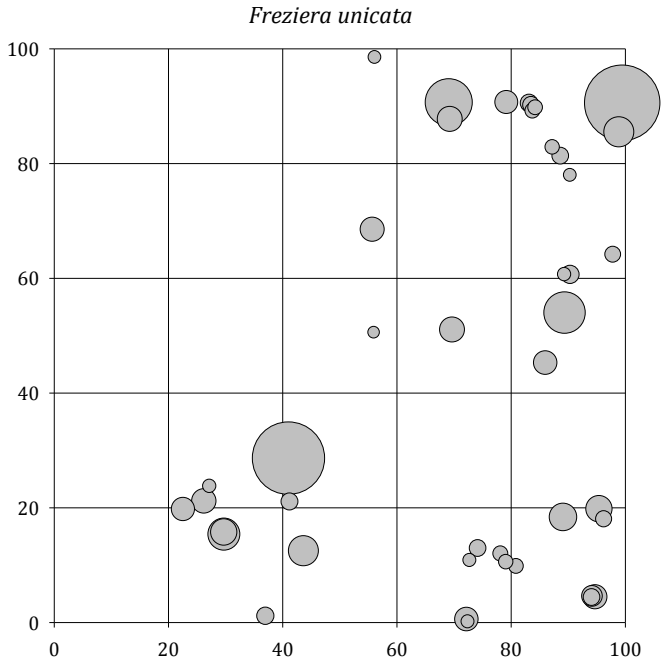

Appendix Figure 33: Dispersion of *Freziera unicata* in the ridge forest plot. Circle sizes are relative to the maximum DBH. Circle sizes are relative to the maximum DBH.

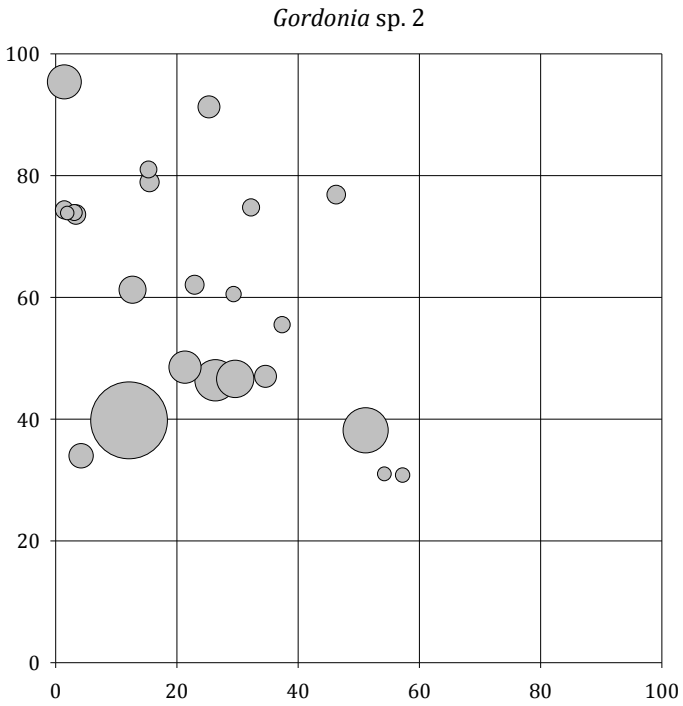

Appendix Figure 34: Dispersion of *Gordonia* sp. 2 in the ridge forest plot. Circle sizes are relative to the maximum DBH.

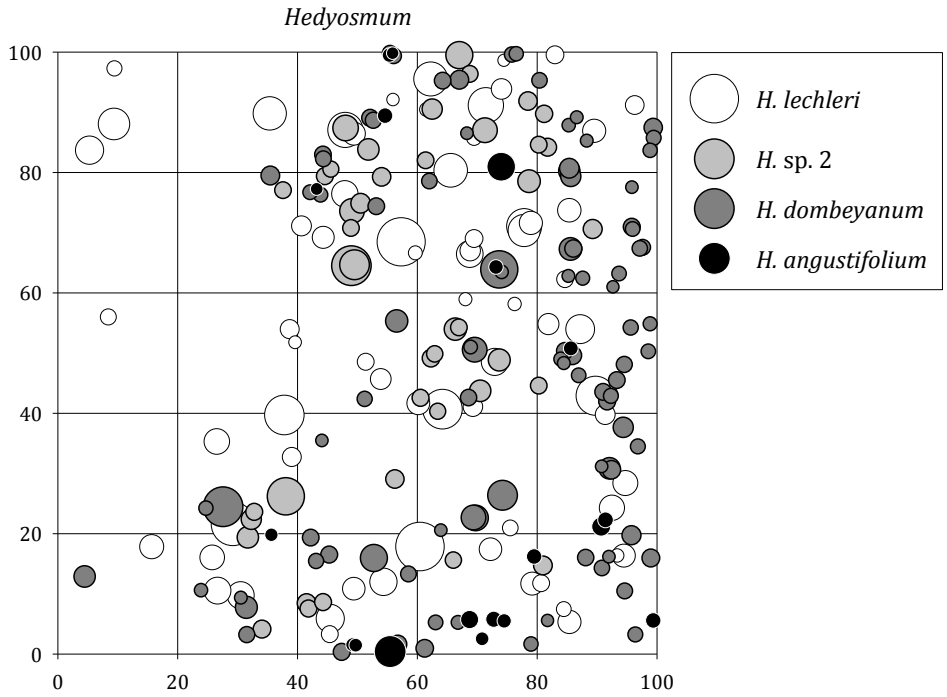

Appendix Figure 35: Dispersion of *Hedyosmum* species in the ridge forest plot. Circle sizes are relative to the maximum DBH.

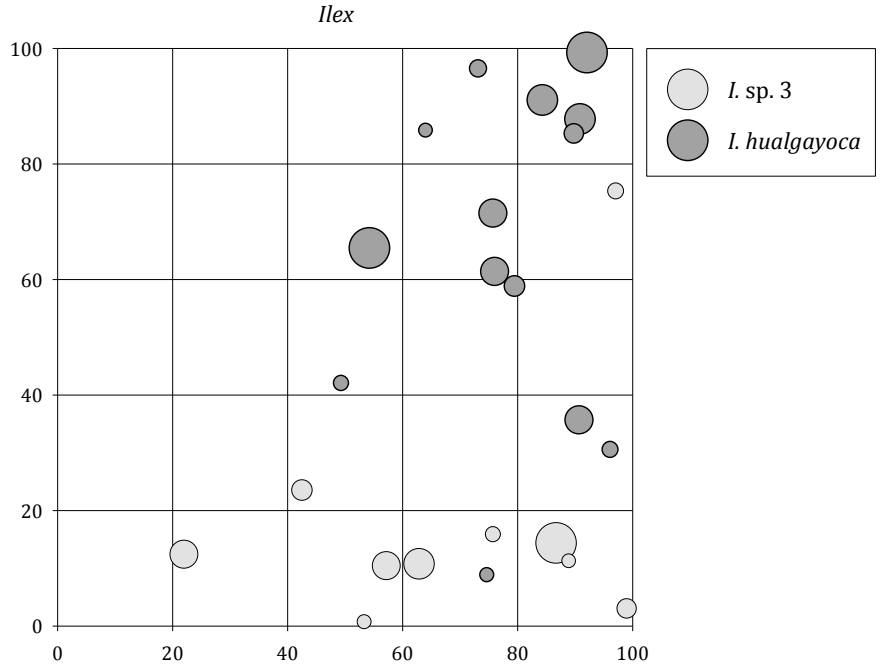

Appendix Figure 36: Dispersion of *Hedyosmum* species in the ridge forest plot. Circle sizes are relative to the maximum DBH.

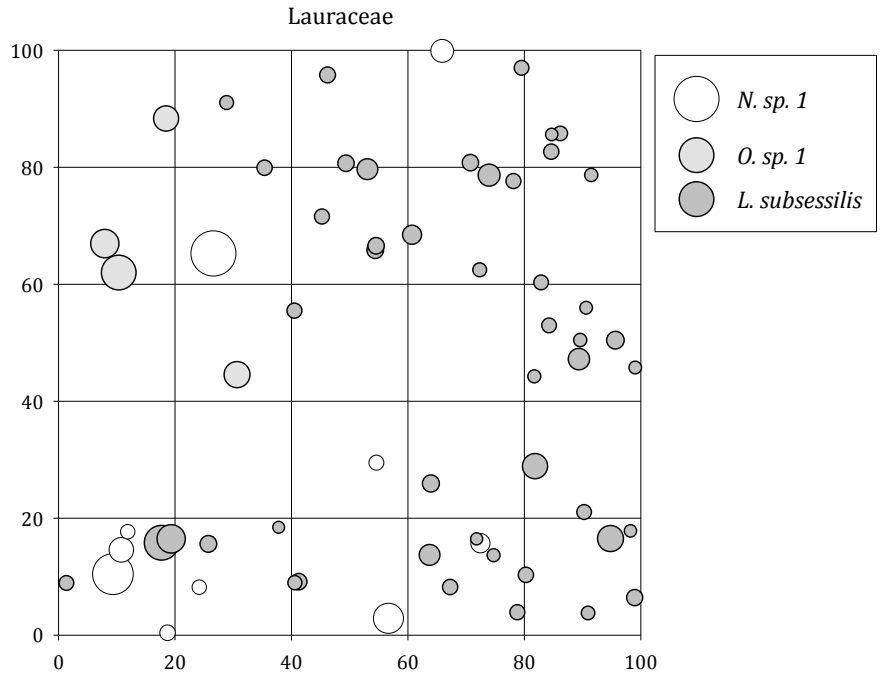

Appendix Figure 37: Dispersion of Lauraceae species in the ridge forest plot. Circle sizes are relative to the maximum DBH.

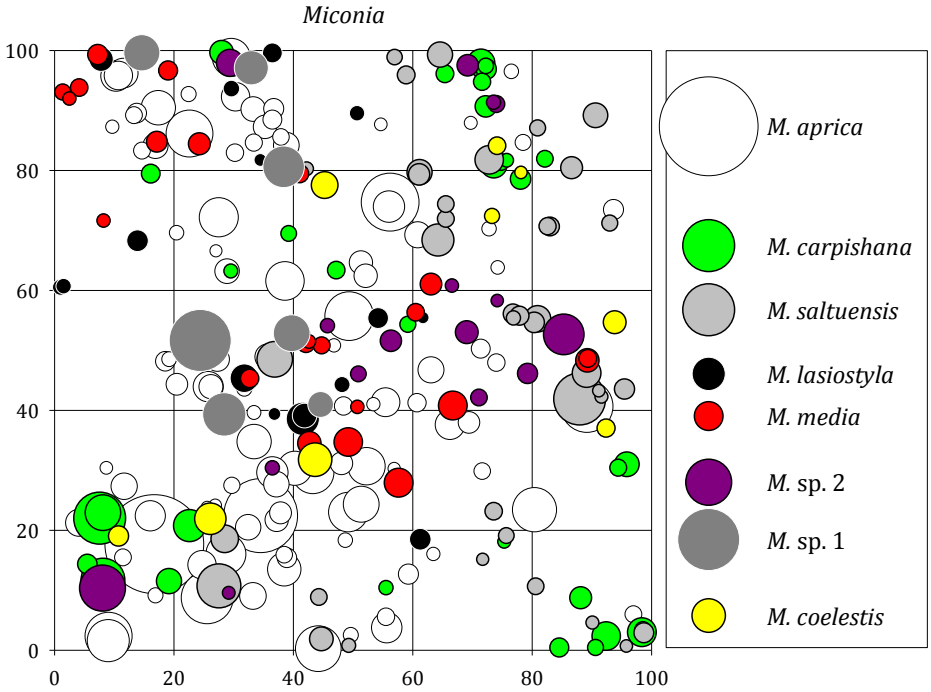

Appendix Figure 38: Dispersion of *Miconia* species in the ridge forest plot. Circle sizes are relative to the maximum DBH.

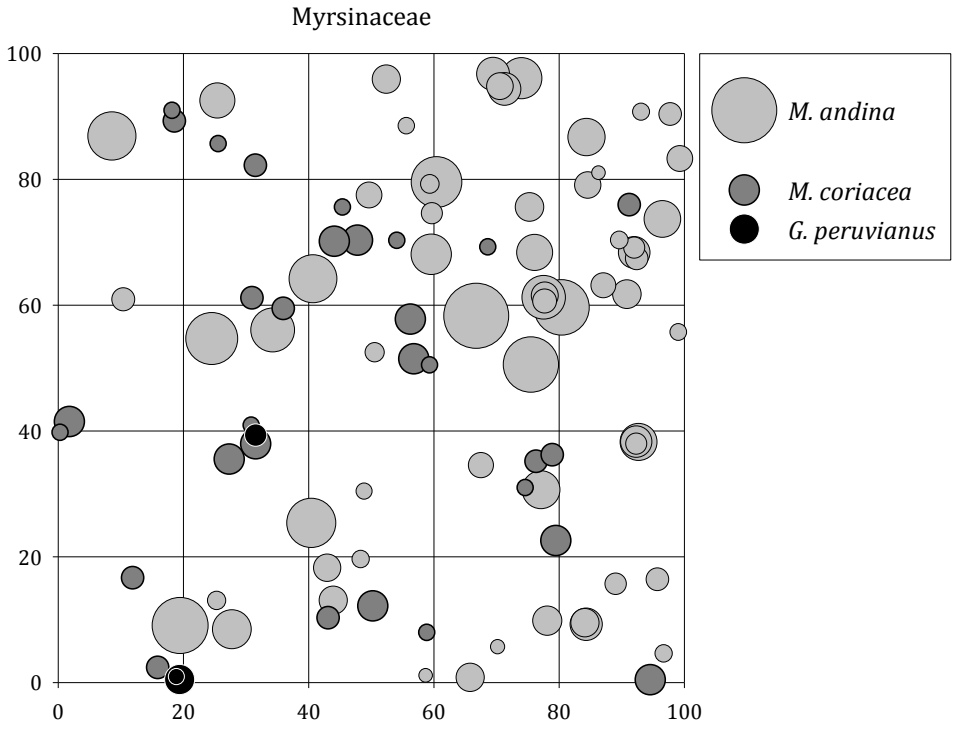

Appendix Figure 39: Dispersion of Myrsineaceae species in the ridge forest plot. Circle sizes are relative to the maximum DBH.

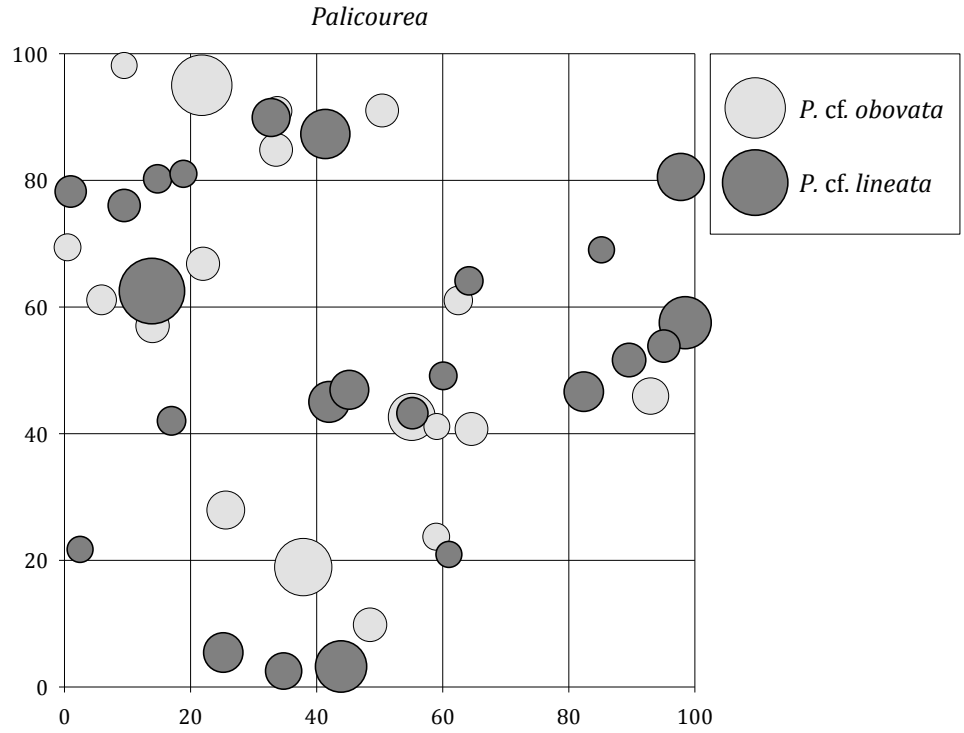

Appendix Figure 40: Dispersion of *Palicorea* species in the ridge forest plot. Circle sizes are relative to the maximum DBH.

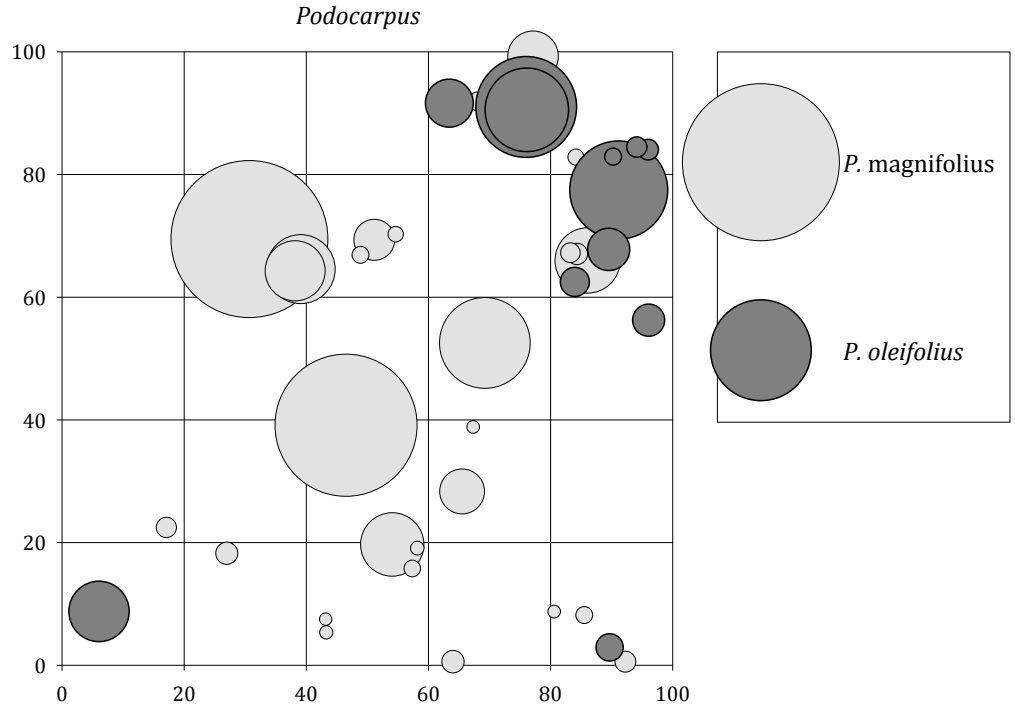

Appendix Figure 41: Dispersion of *Podocarpus* species in the ridge forest plot. Circle sizes are relative to the maximum DBH.

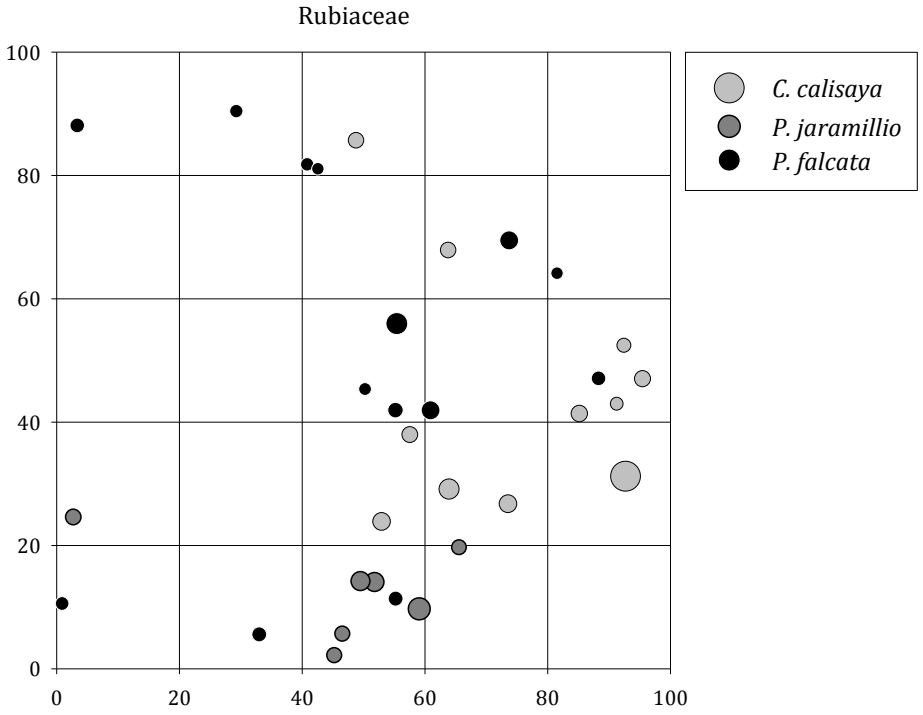

Appendix Figure 42: Dispersion of Rubiaceae species in the ridge forest plot. Circle sizes are relative to the maximum DBH.

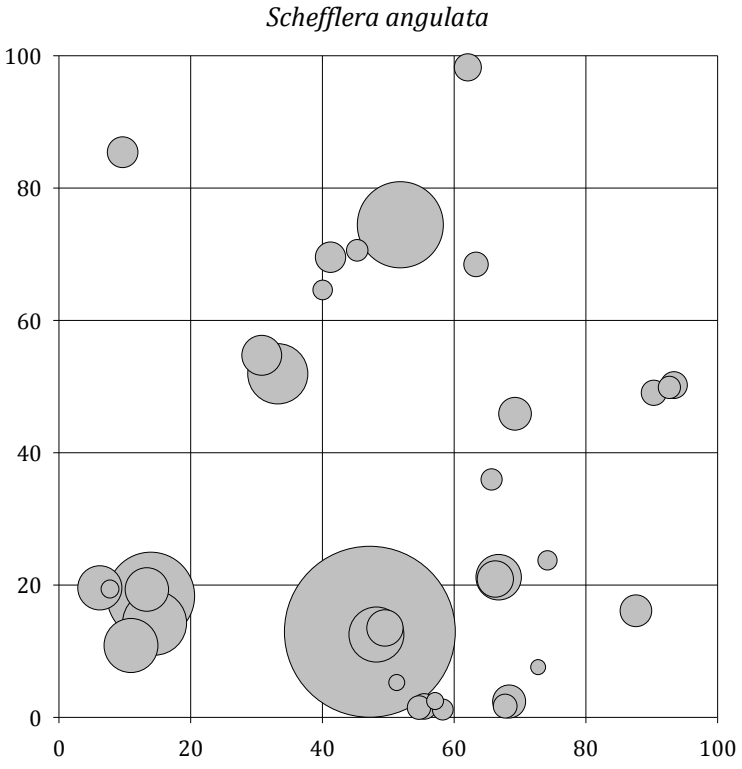

Appendix Figure 43: Dispersion of *Schefflera angulata* in the ridge forest plot. Circle sizes are relative to the maximum DBH.

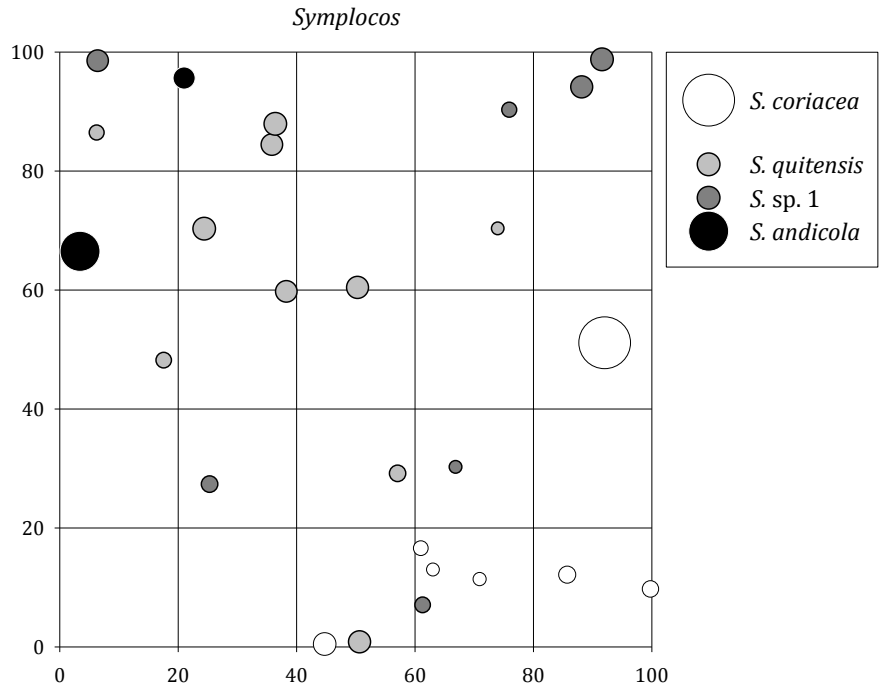

Appendix Figure 44: Dispersion of *Symplocos* species in the ridge forest plot. Circle sizes are relative to the maximum DBH.

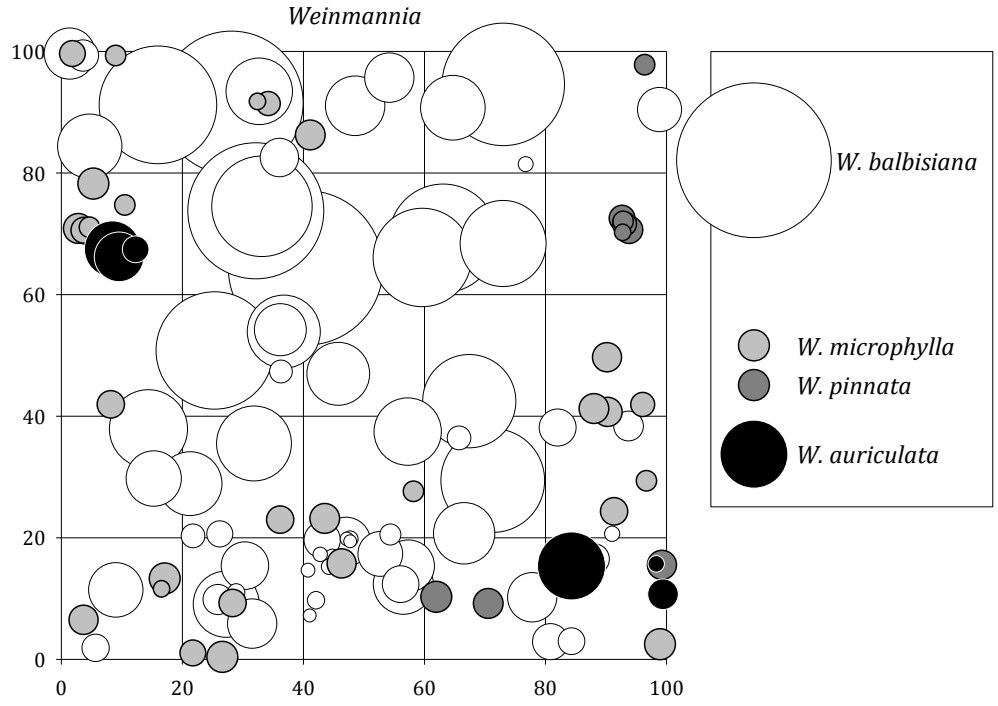

Appendix Figure 45: Dispersion of *Weinmannia* species in the ridge forest plot. Circle sizes are relative to the maximum DBH.

Appendix N: Stem dispersion of windward forest species

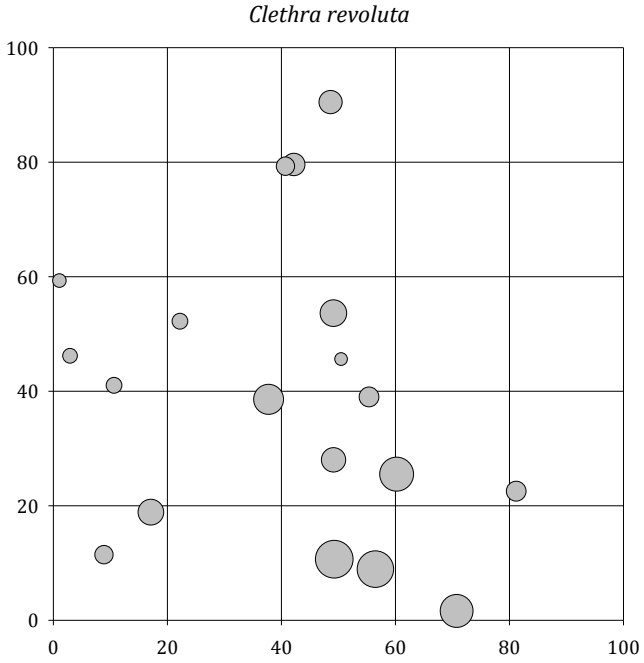

Appendix Figure 46: Dispersion of *Clethra revoluta* in the windward forest plot. Circle sizes are relative to the maximum DBH.

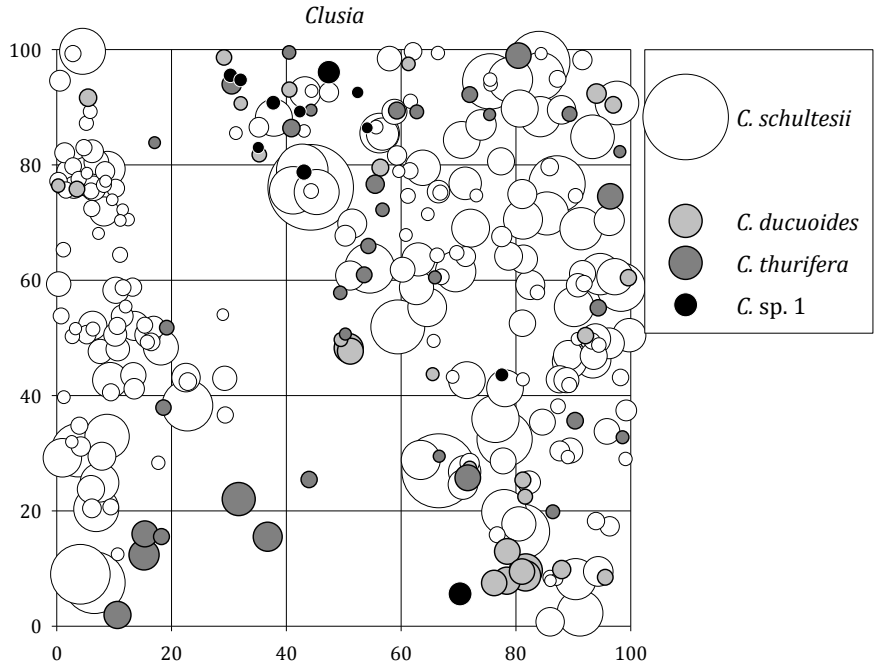

Appendix Figure 47: Dispersion of *Clusia* species in the windward forest plot. Circle sizes are relative to the maximum DBH.

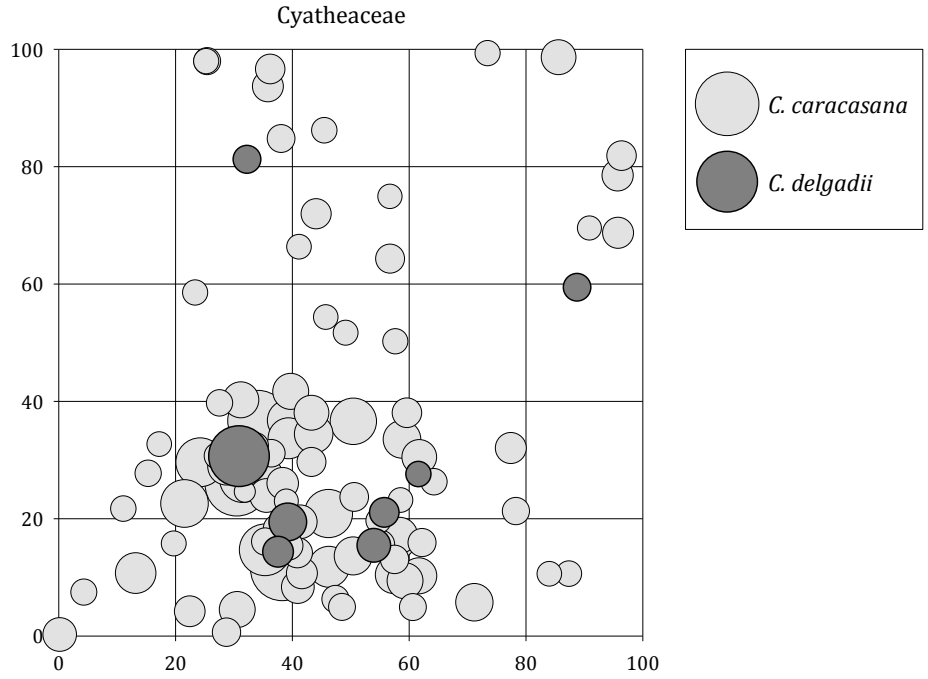

Appendix Figure 48: Dispersion of *Cyathea* species in the windward forest plot. Circle sizes are relative to the maximum DBH.

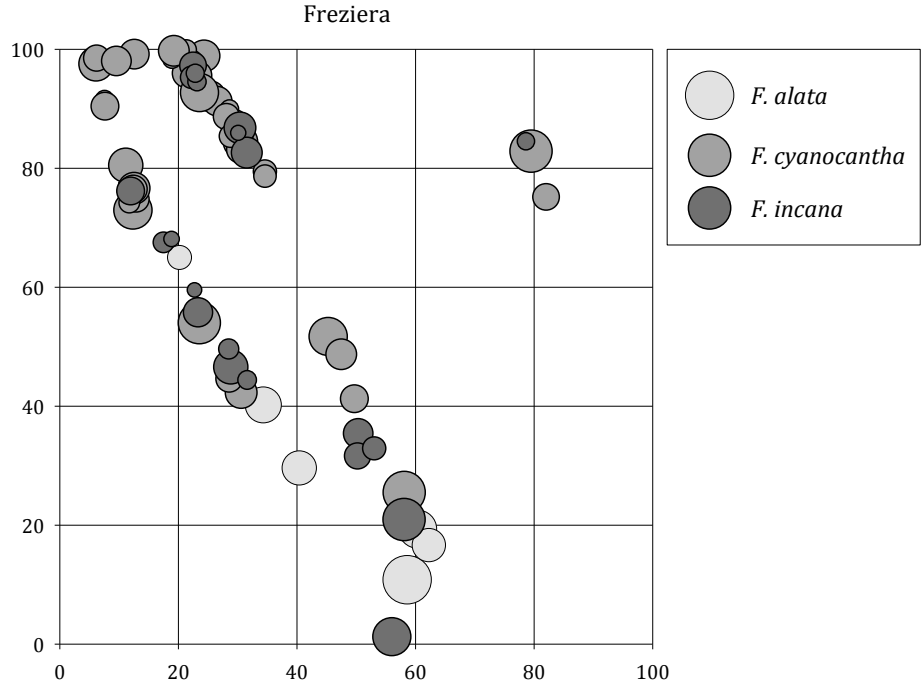

Appendix Figure 49: Dispersion of *Freziera* species in the windward forest plot. Circle sizes are relative to the maximum DBH.

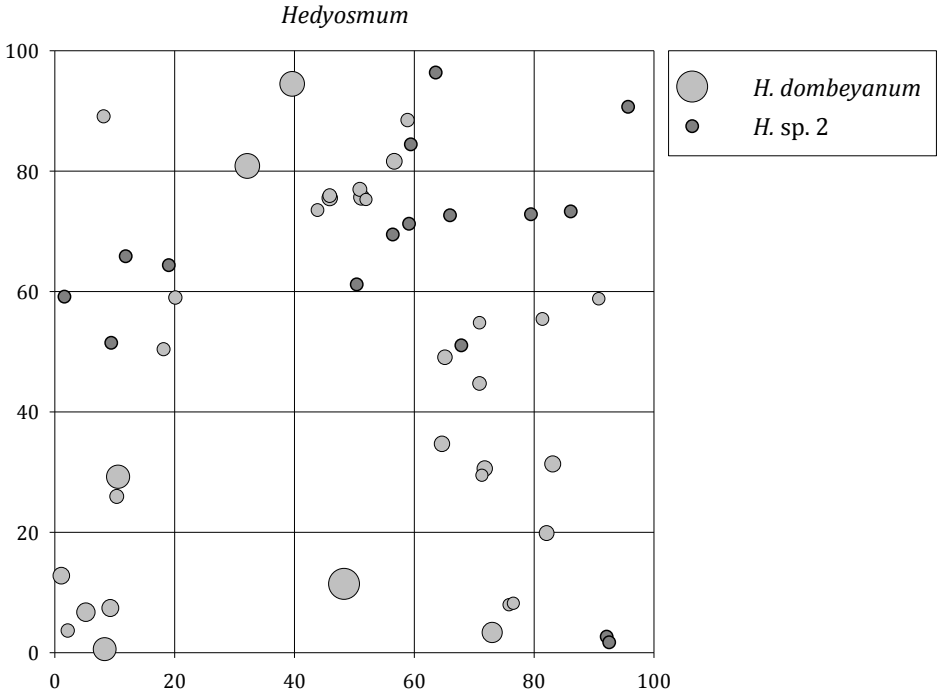

Appendix Figure 50: Dispersion of *Hedyosmum* species in the windward forest plot. Circle sizes are relative to the maximum DBH.

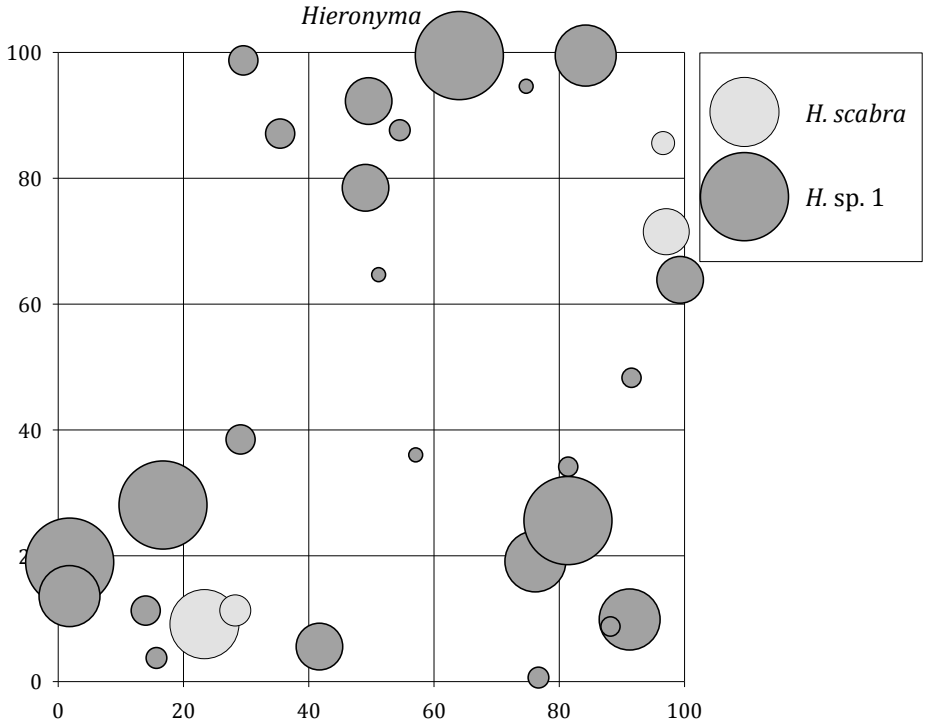

Appendix Figure 51: Dispersion of *Hieronyma* species in the windward forest plot. Circle sizes are relative to the maximum DBH.

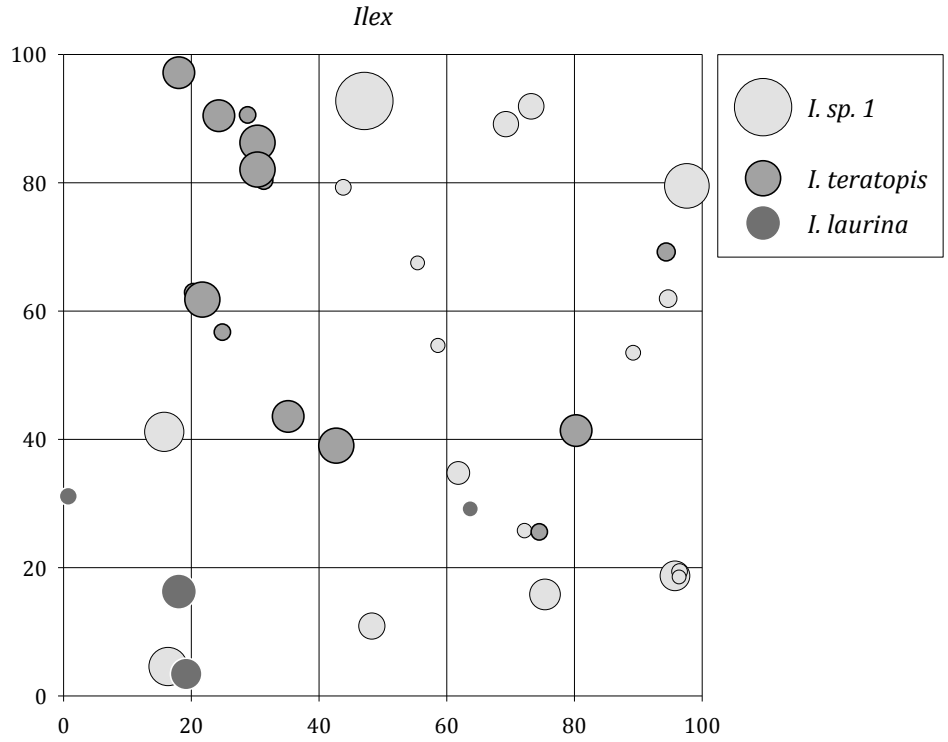

Appendix Figure 52: Dispersion of *Ilex* species in the windward forest plot. Circle sizes are relative to the maximum DBH.

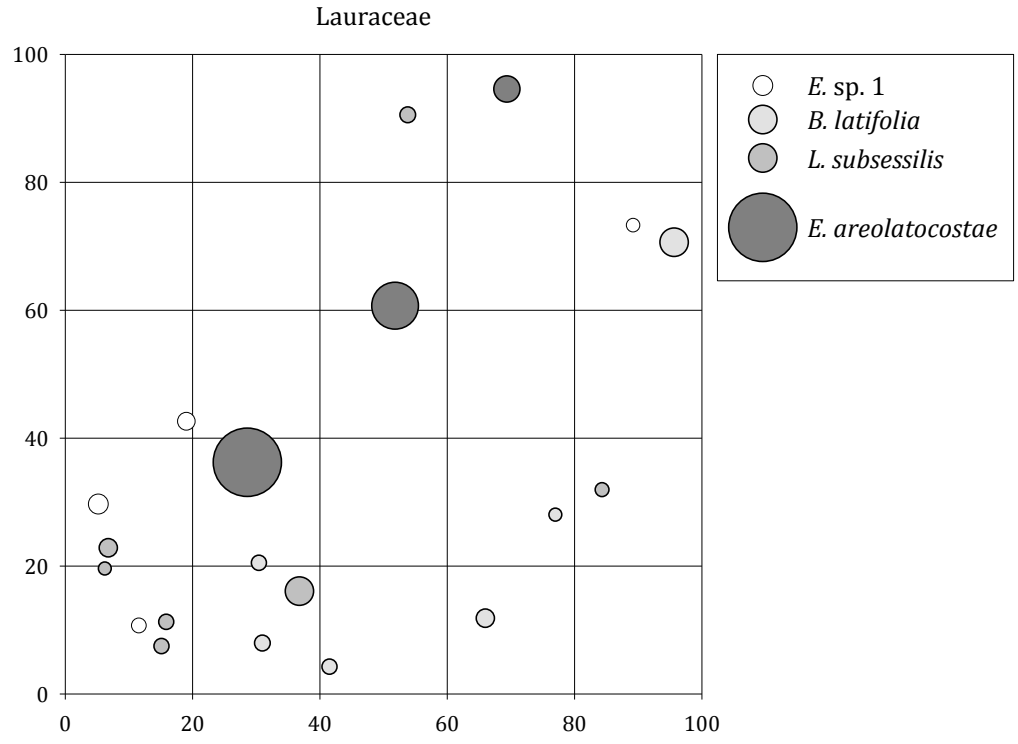

Appendix Figure 53: Dispersion of Lauraceae species in the windward forest plot. Circle sizes are relative to the maximum DBH.

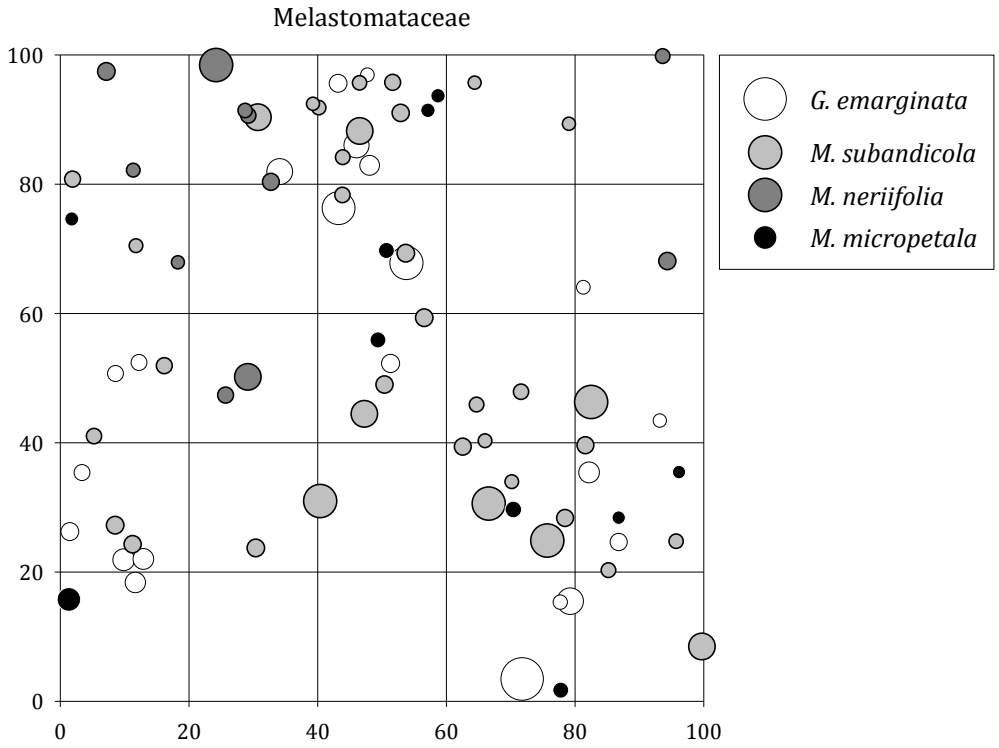

Appendix Figure 54: Dispersion of Melastomataceae species in the windward forest plot. Circle sizes are relative to the maximum DBH.

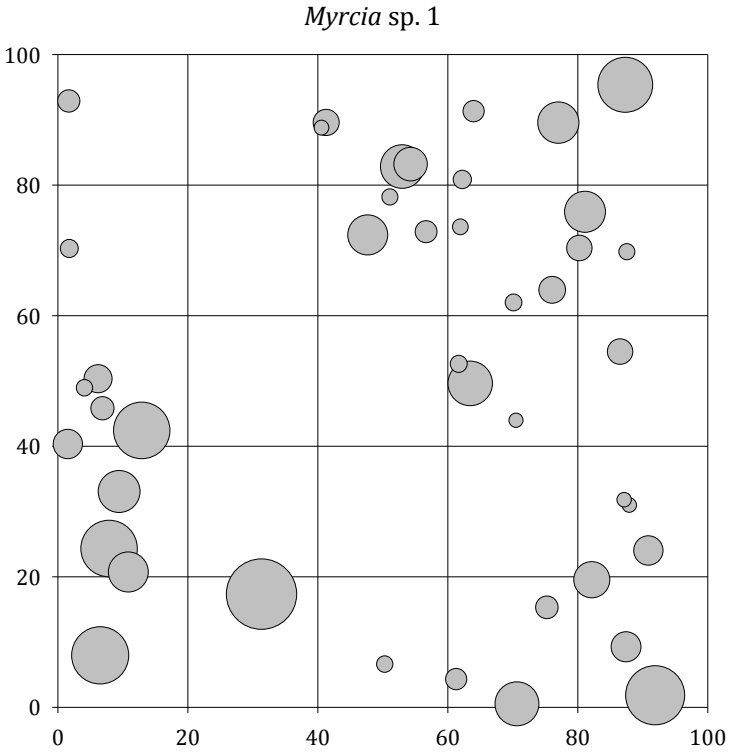

Appendix Figure 55: Dispersion of *Myrcia* sp. 1 in the windward forest plot. Circle sizes are relative to the maximum DBH.

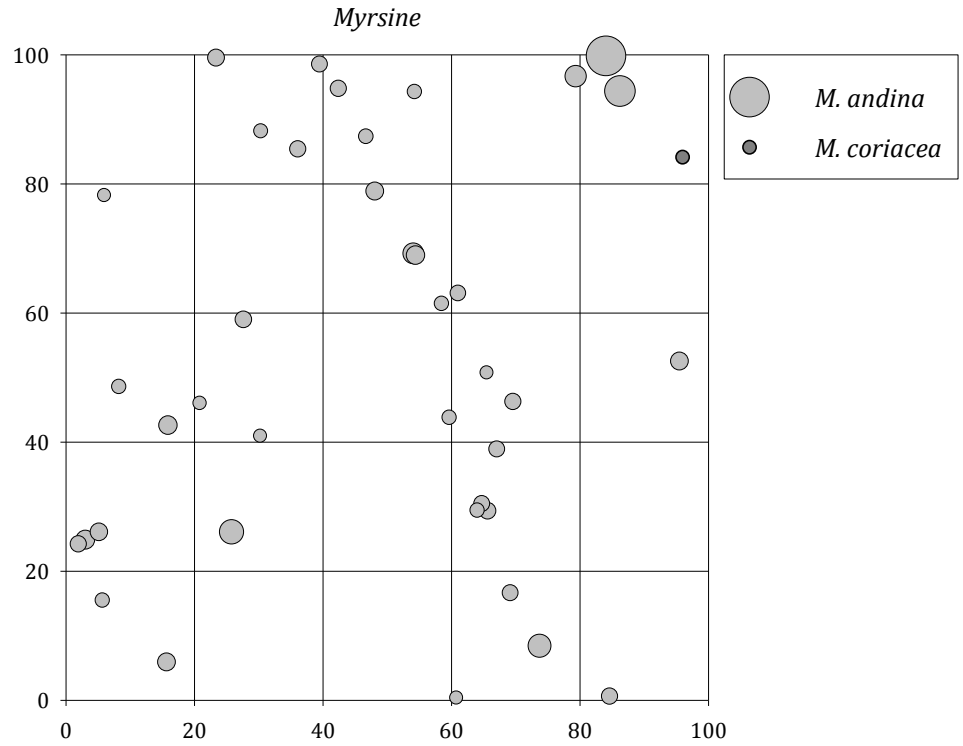

Appendix Figure 56: Dispersion of *Myrsine* species in the windward forest plot. Circle sizes are relative to the maximum DBH.

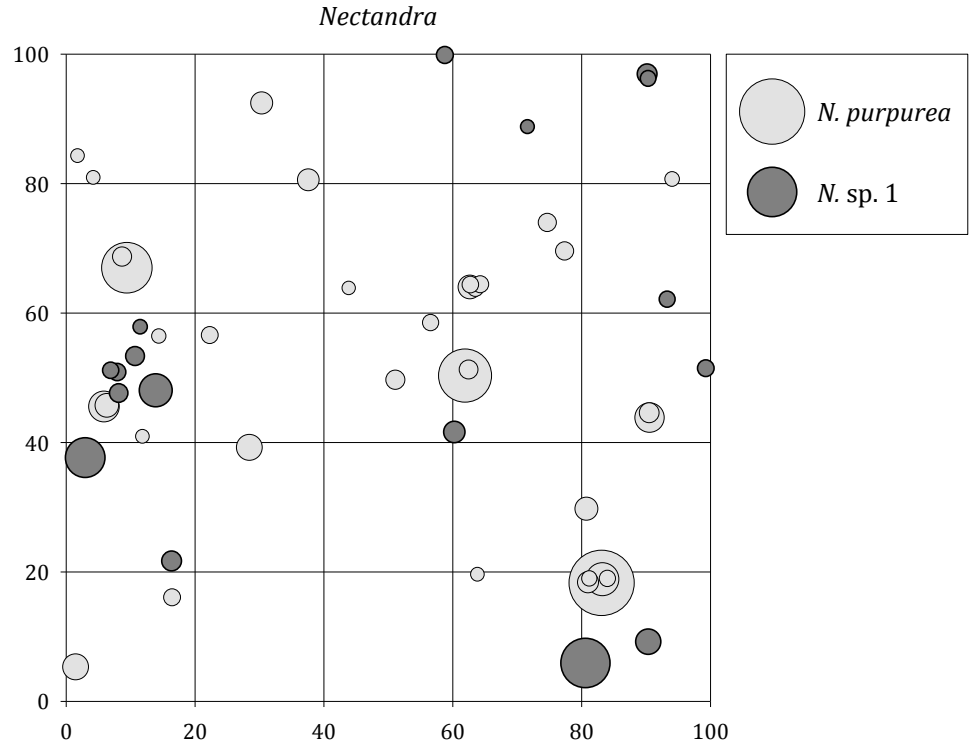

Appendix Figure 57: Dispersion of *Nectandra* species in the windward forest plot. Circle sizes are relative to the maximum DBH.

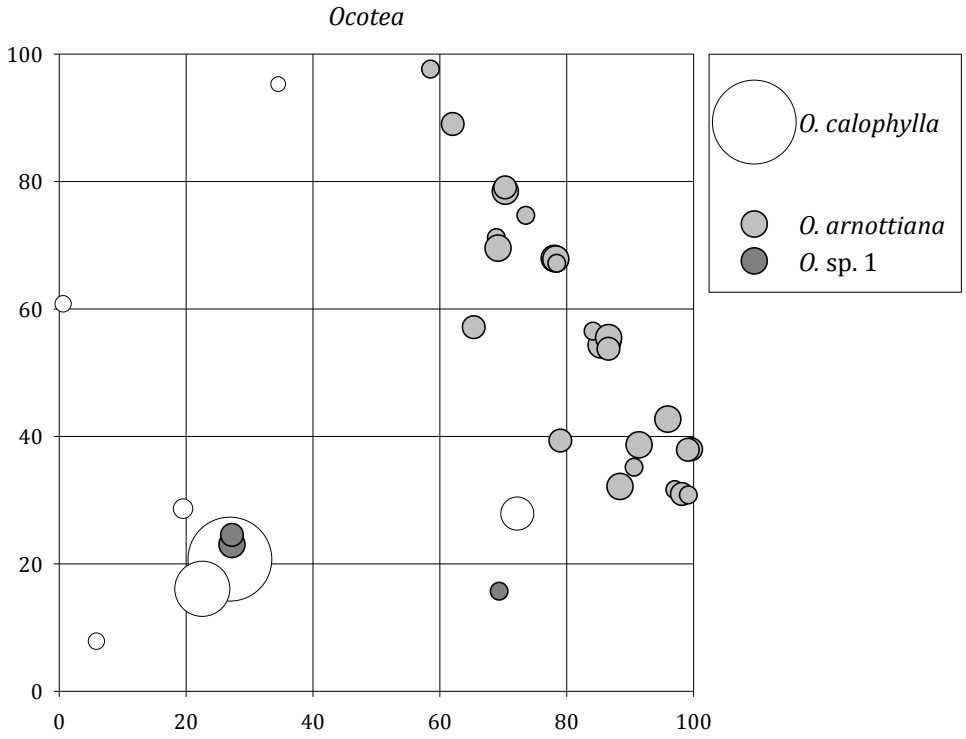

Appendix Figure 58: Dispersion of *Ocotea* species in the windward forest plot. Circle sizes are relative to the maximum DBH.

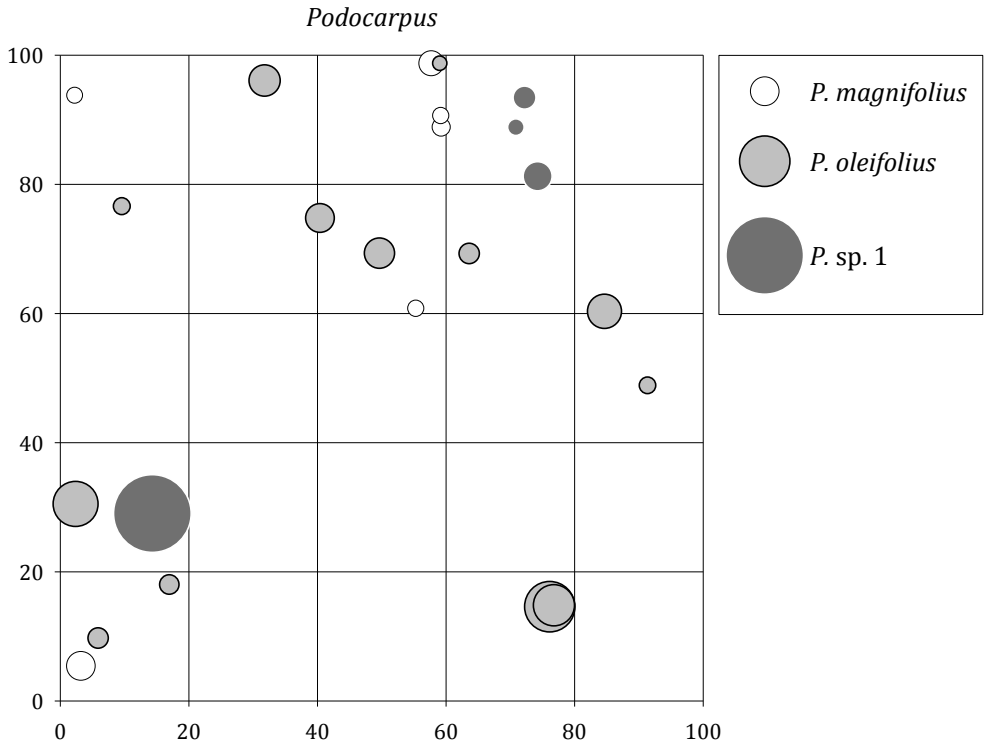

Appendix Figure 59: Dispersion of *Podocarpus* species in the windward forest plot. Circle sizes are relative to the maximum DBH.

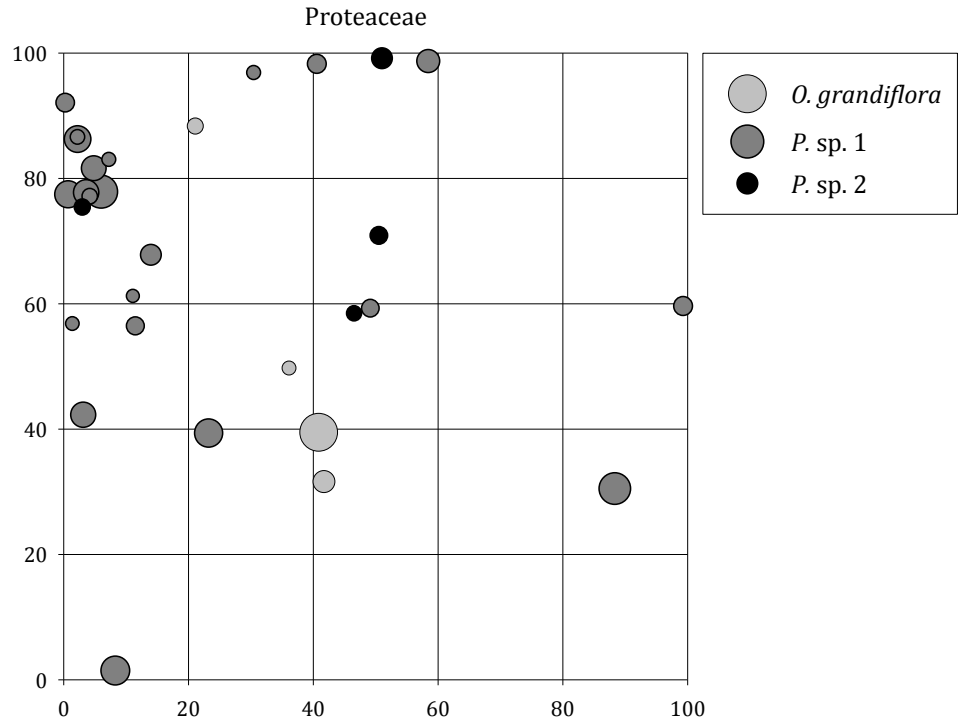

Appendix Figure 60: Dispersion of Proteaceae species in the windward forest plot. Circle sizes are relative to the maximum DBH.

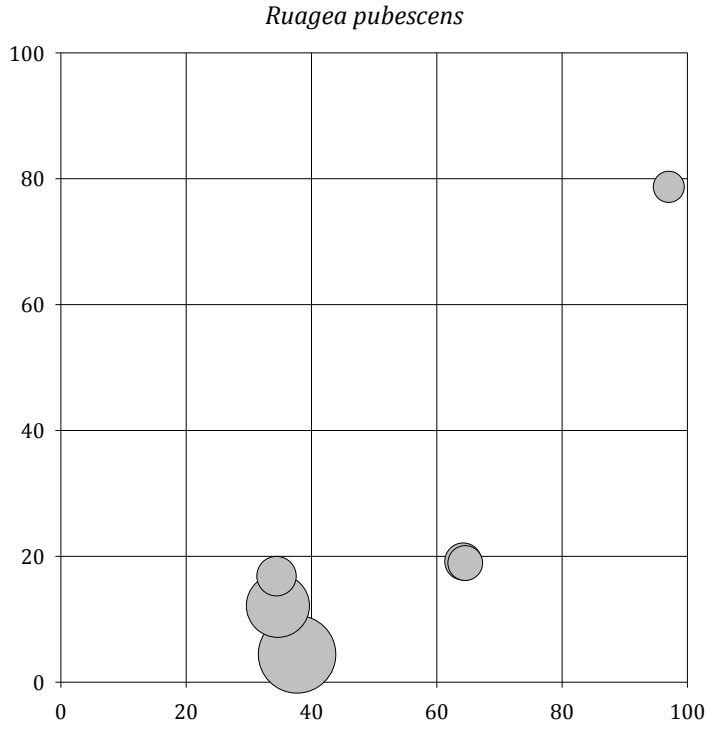

Appendix Figure 61: Dispersion of *Ruagea pubescens* in the windward forest plot. Circle sizes are relative to the maximum DBH.

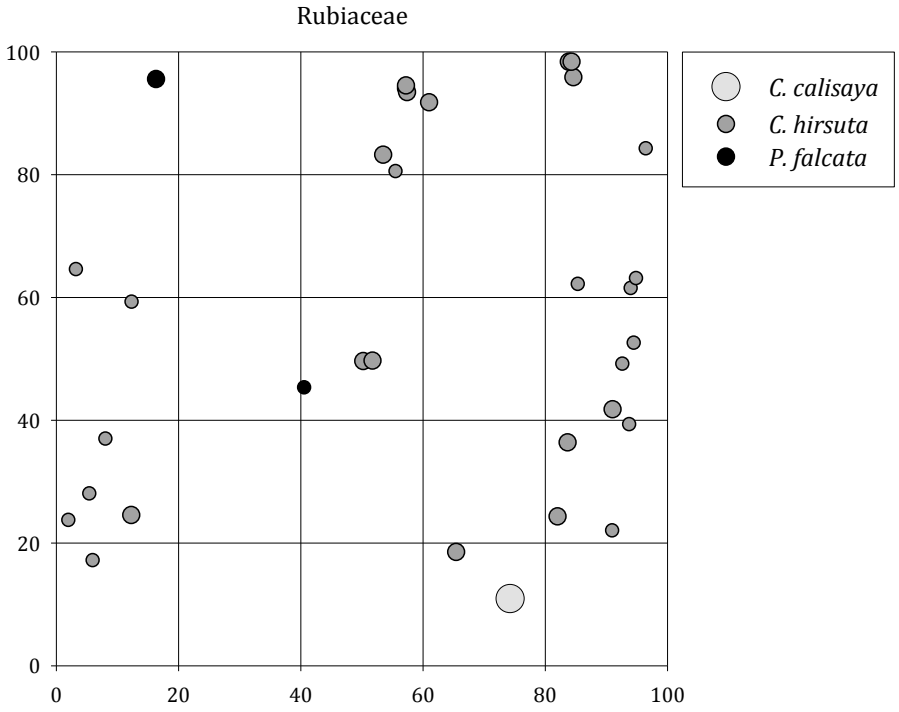

Appendix Figure 62: Dispersion of Rubiaceae species in the windward forest plot. Circle sizes are relative to the maximum DBH.

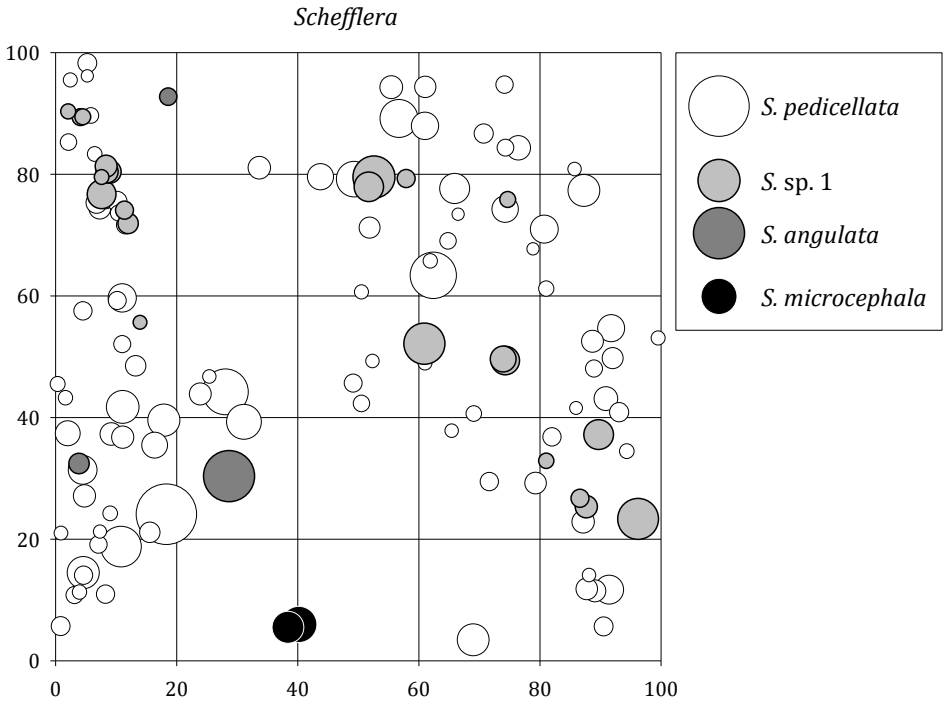

Appendix Figure 63: Dispersion of *Schefflera* species in the windward forest plot. Circle sizes are relative to the maximum DBH.

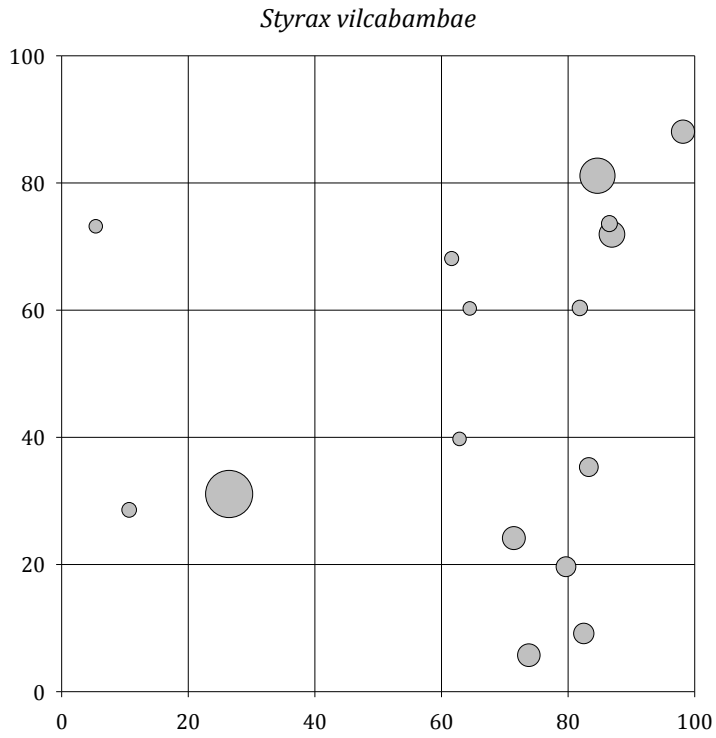

Appendix Figure 64: Dispersion of *Styrax vilcabambae* in the windward forest plot. Circle sizes are relative to the maximum DBH.

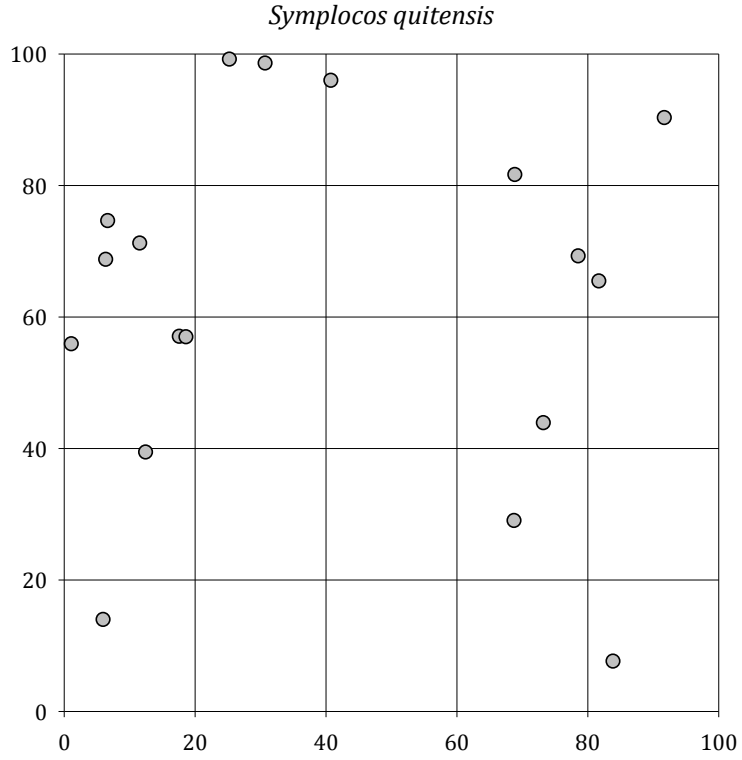

Appendix Figure 65: Dispersion of *Symplocos quitensis* in the windward forest plot. Circle sizes are relative to the maximum DBH.

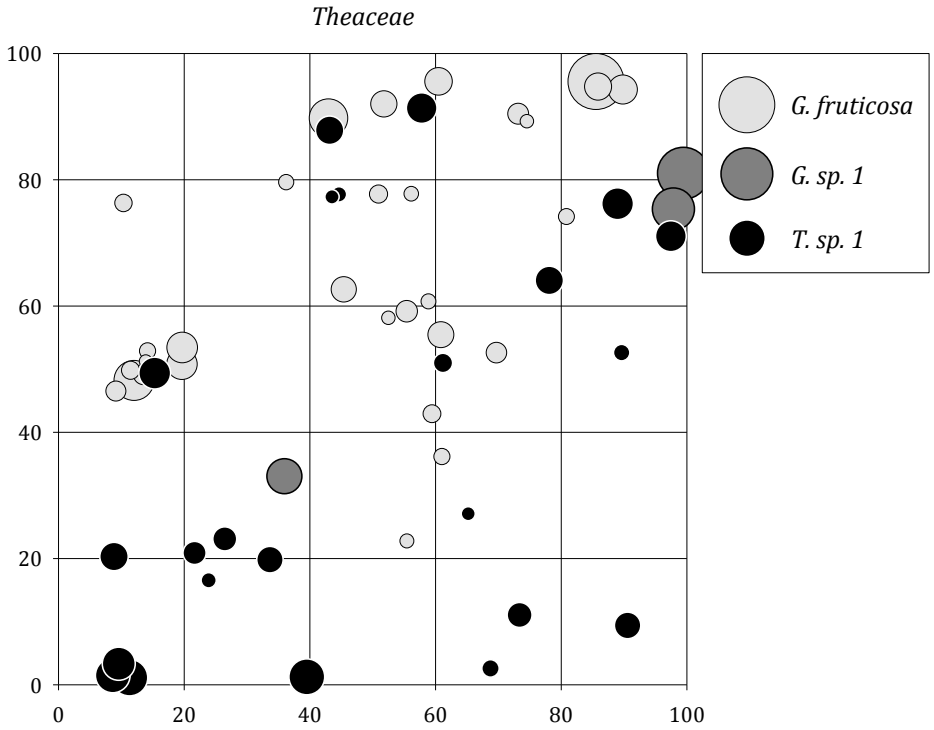

Appendix Figure 66: Dispersion of Theaceae species in the windward forest plot. Circle sizes are relative to the maximum DBH.

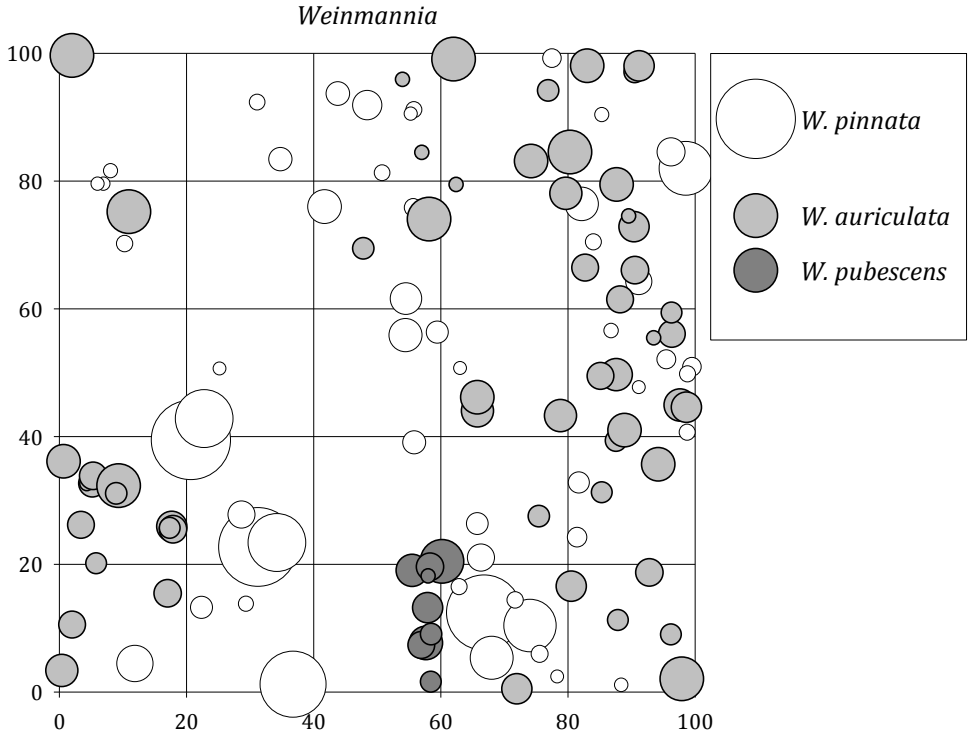

Appendix Figure 67: Dispersion of *Weinmannia* species in the windward forest plot. Circle sizes are relative to the maximum DBH

Appendix O: Probability Plots

The following figures show the distribution within parameter datasets and P-values of Anderson-Darling normality tests ($P < 0.05$ = normal distribution).

Wet Season Diurnal Parameter Datasets

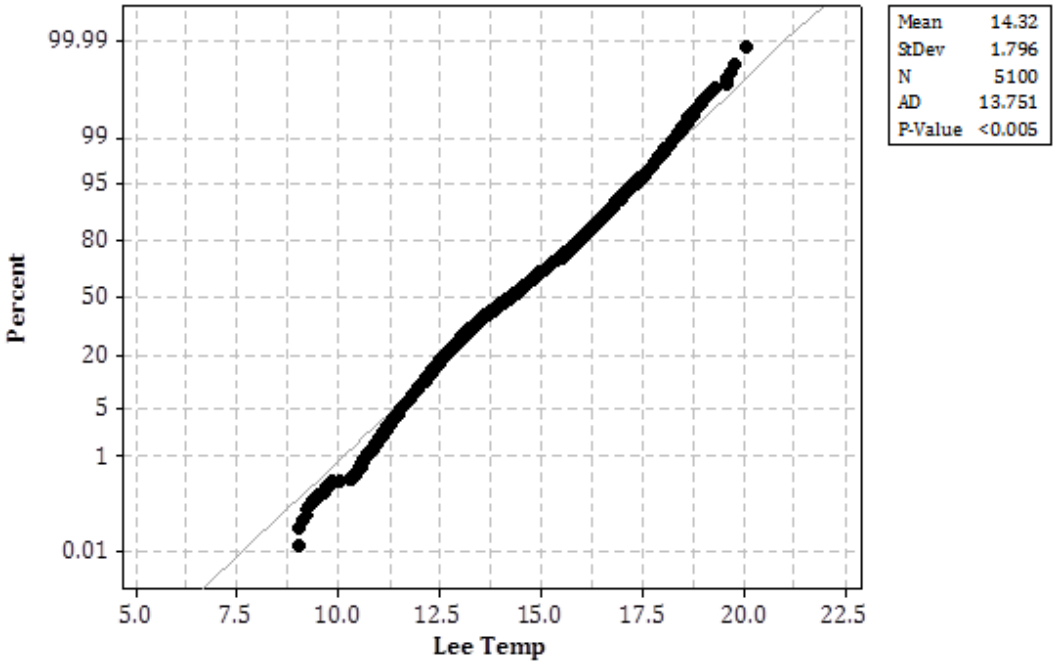

Appendix Figure 68: Probability Plot of wet season diurnal temperature data at the leeward forest plot (2007 – 2008).

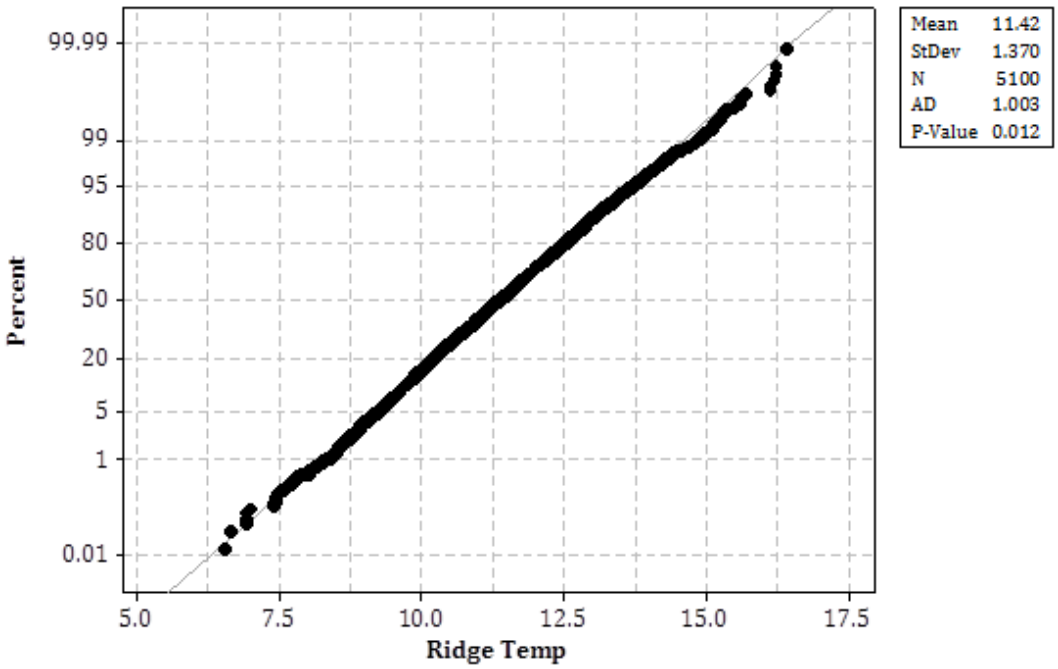

Appendix Figure 69: Probability Plot of wet season diurnal temperature data at the ridge forest plot (2007 – 2008).

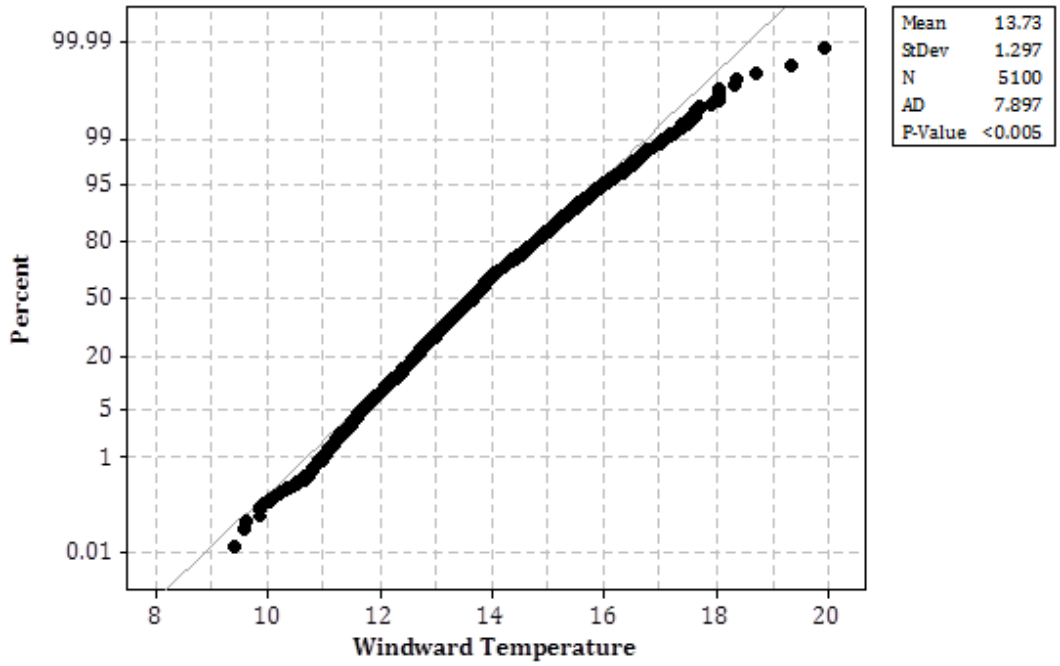

Appendix Figure 70: Probability Plot of wet season diurnal temperature data at the windward forest plot (2007 – 2008).

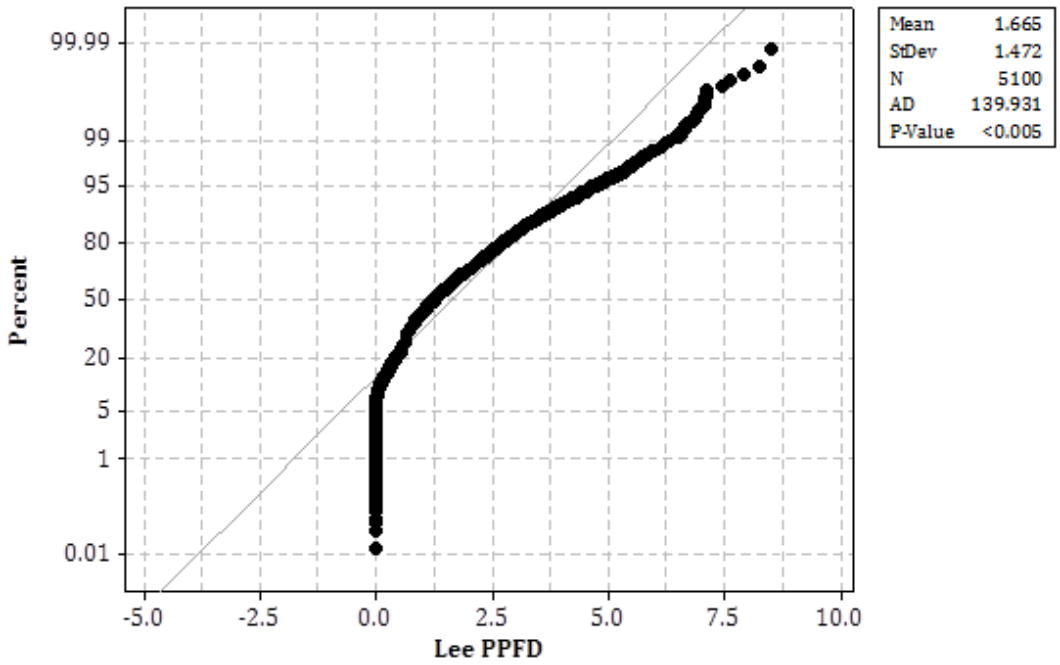

Appendix Figure 71: Probability Plot of wet season diurnal PPFD data at the leeward forest plot (2007 – 2008).

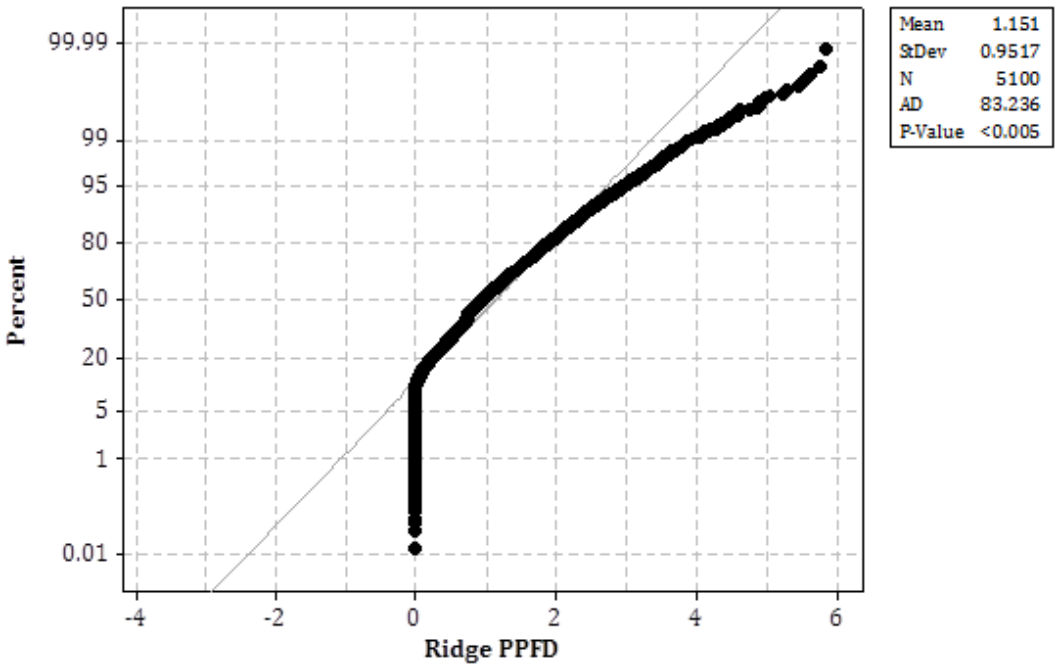

Appendix Figure 72: Probability Plot of wet season diurnal PPFD data at the ridge forest plot (2007 – 2008).

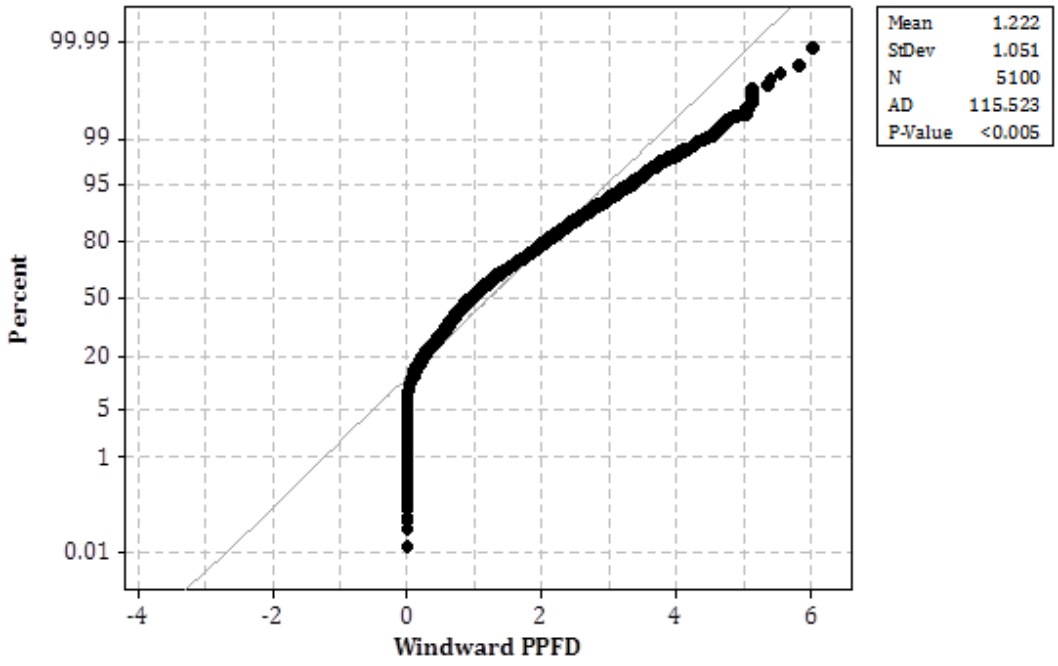

Appendix Figure 73: Probability Plot of wet season diurnal PPFD data at the windward forest plot (2007 – 2008).

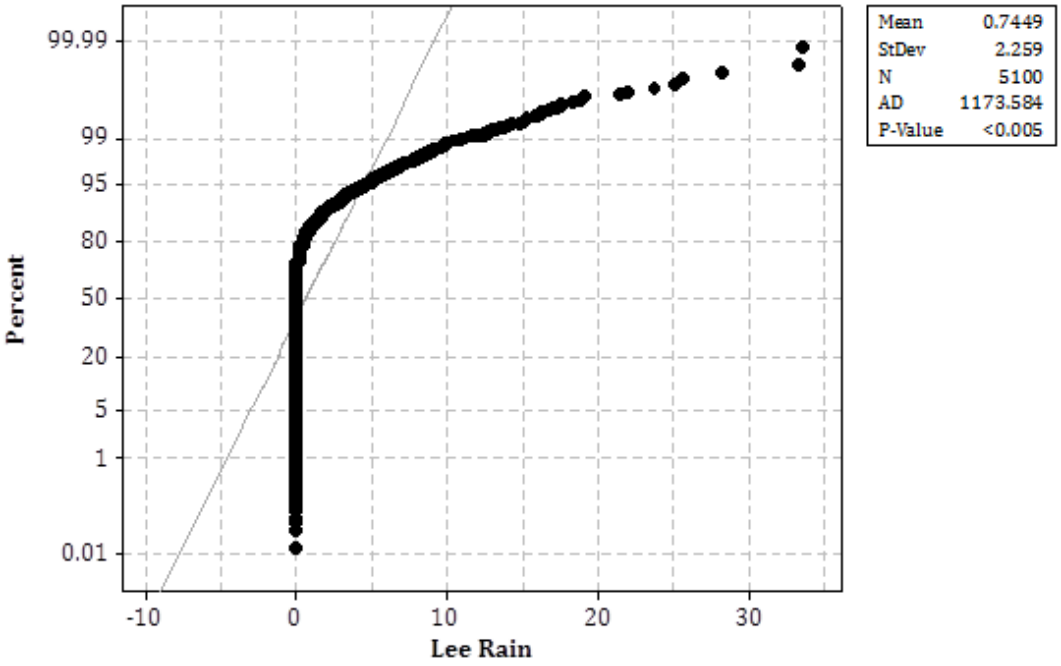

Appendix Figure 74: Probability Plot of wet season diurnal rainfall data at the leeward forest plot (2007 – 2008).

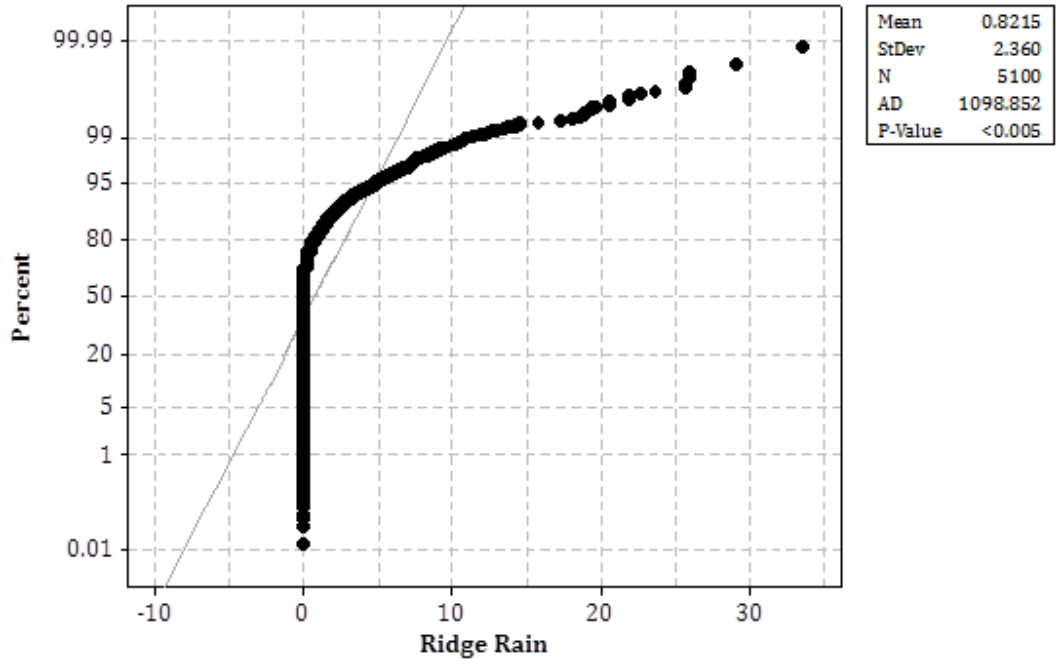

Appendix Figure 75: Probability Plot of wet season diurnal rainfall data at the ridge forest plot (2007 – 2008).

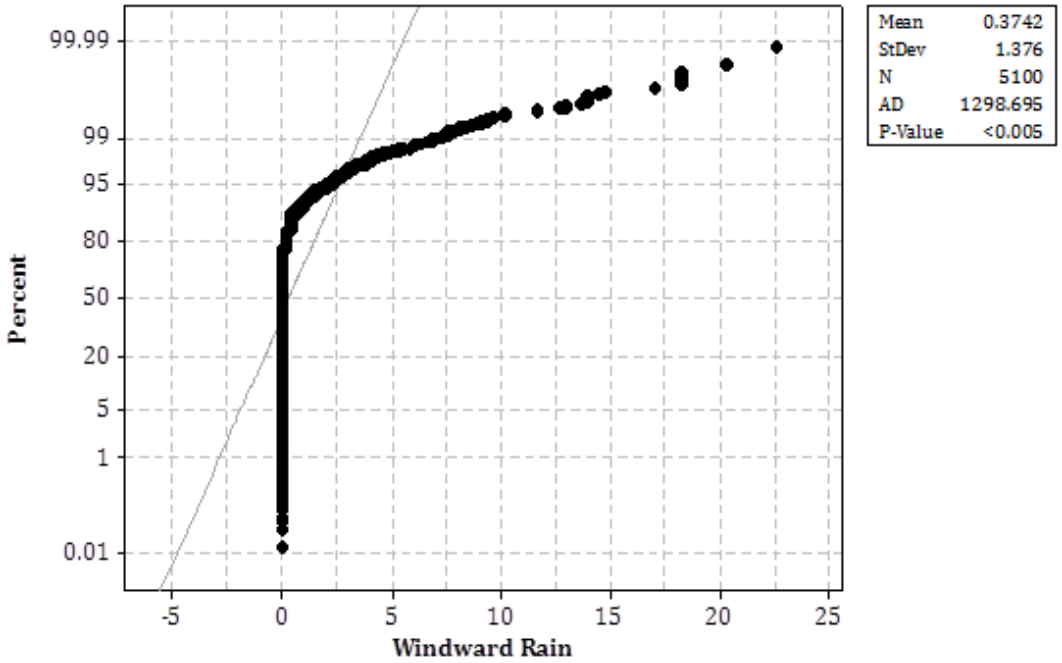

Appendix Figure 76: Probability Plot of wet season diurnal rainfall data at the windward forest plot (2007 – 2008).

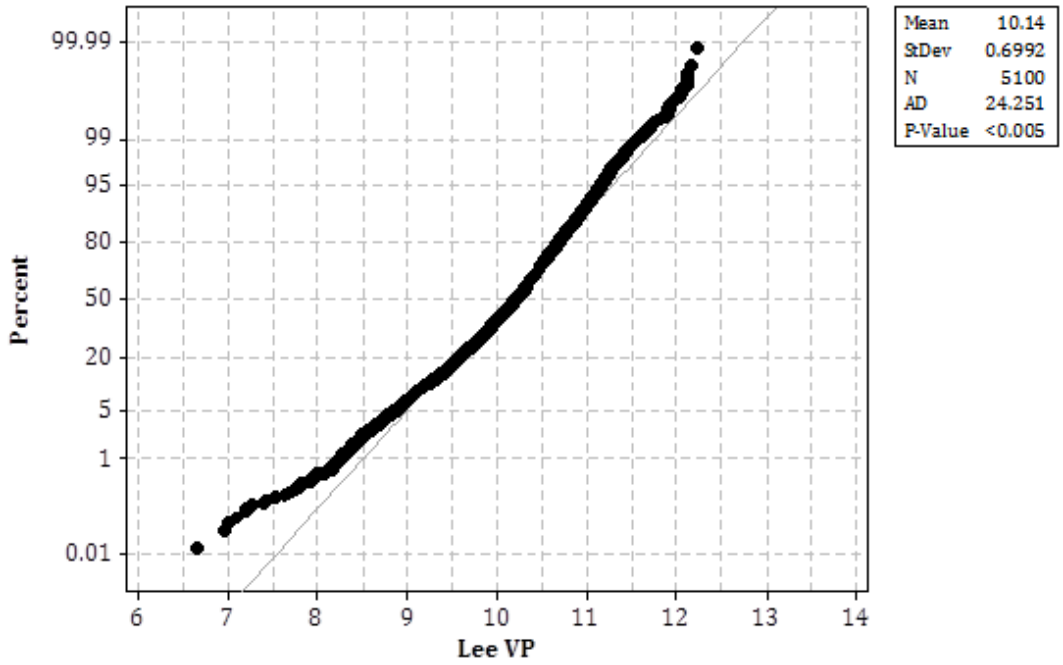

Appendix Figure 77: Probability Plot of wet season diurnal vapour pressure data at the leeward forest plot (2007 – 2008).

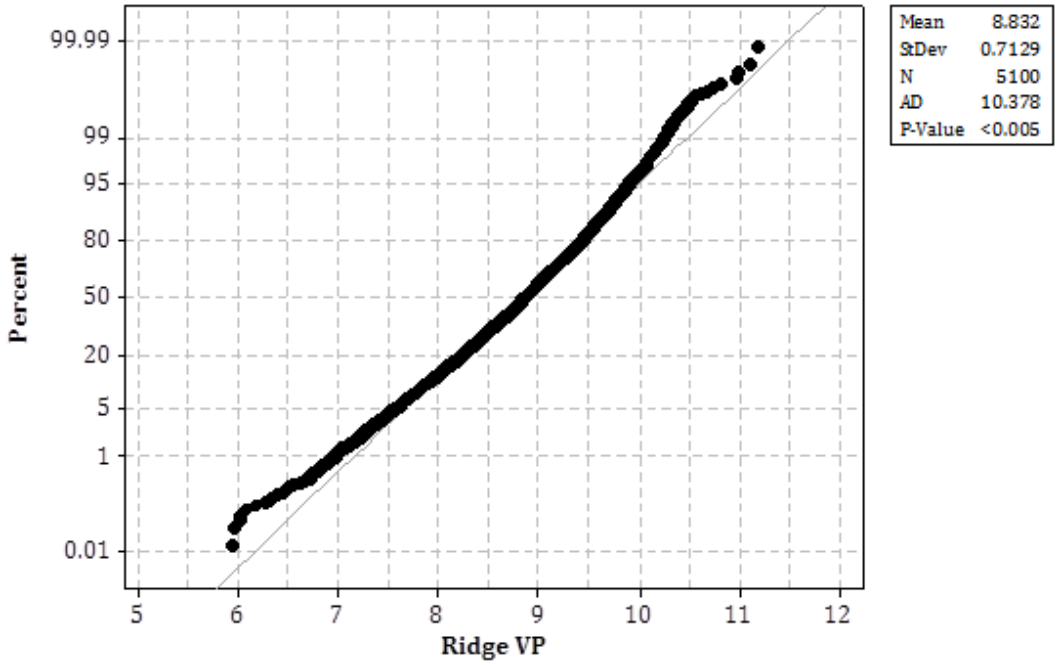

Appendix Figure 78: Probability Plot of wet season diurnal vapour pressure data at the ridge forest plot (2007 – 2008).

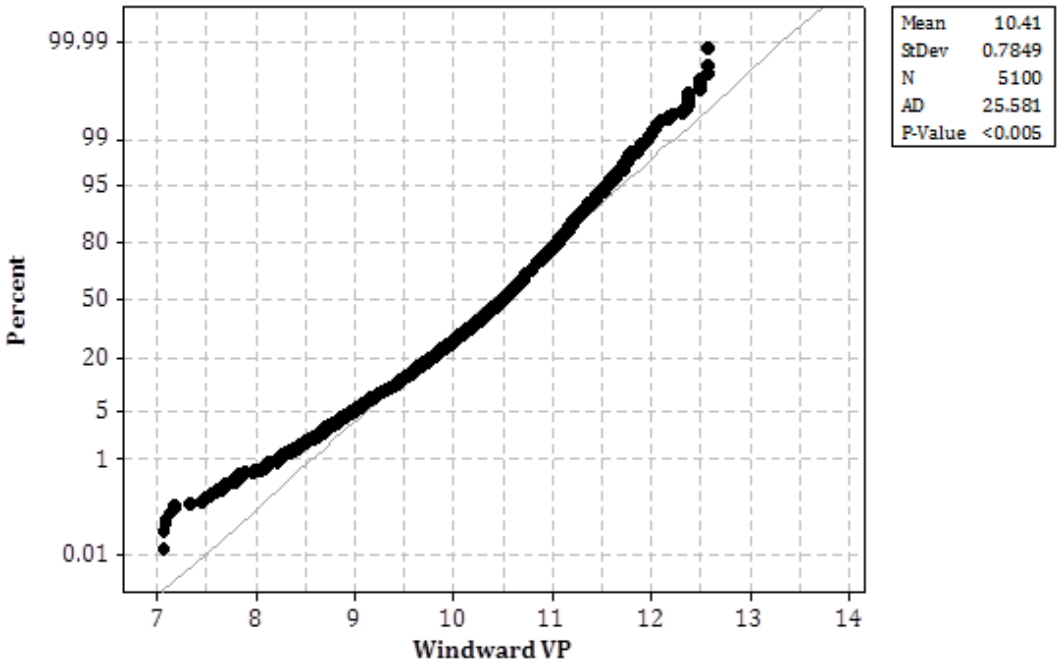

Appendix Figure 79: Probability Plot of wet season diurnal vapour pressure data at the windward forest plot (2007 – 2008).

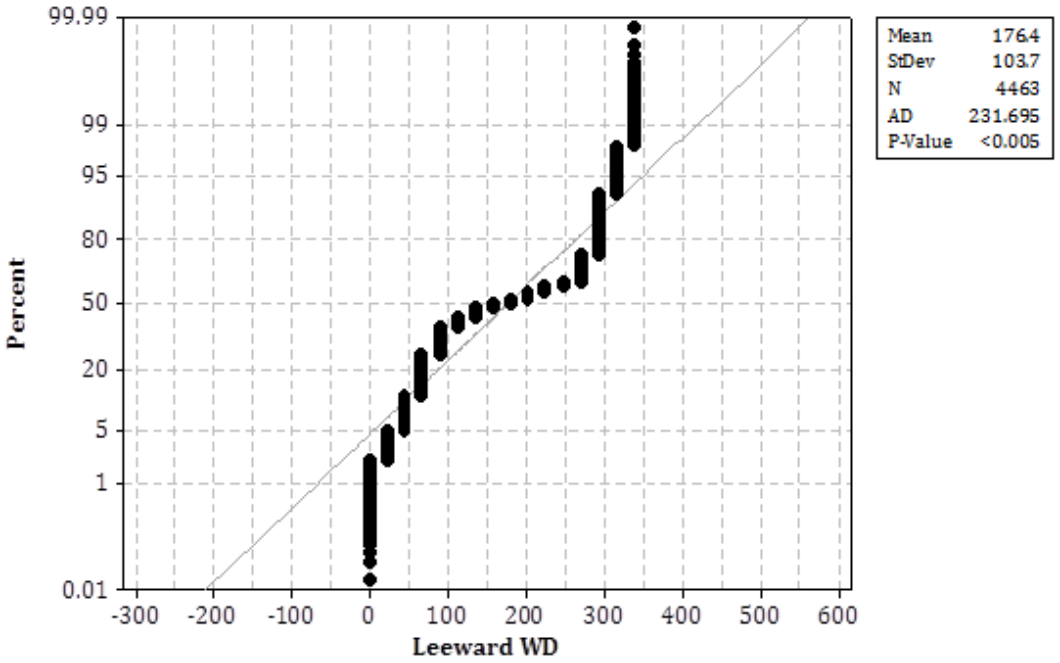

Appendix Figure 80: Probability Plot of wet season diurnal wind direction data at the leeward forest plot (2007 – 2008).

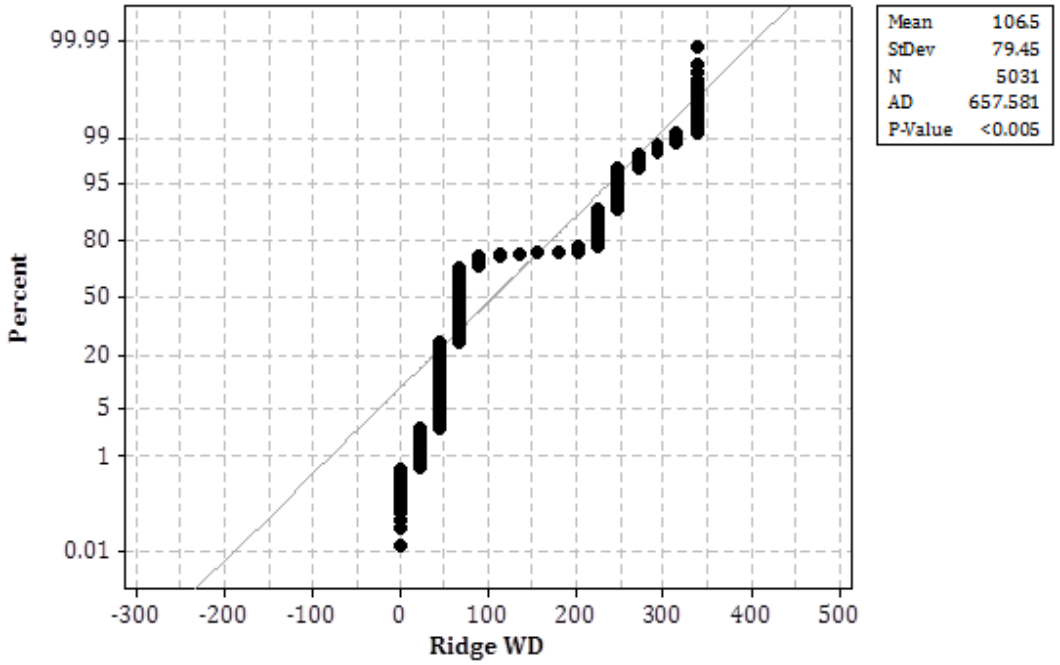

Appendix Figure 81: Probability Plot of wet season diurnal wind direction data at the ridge forest plot (2007 – 2008).

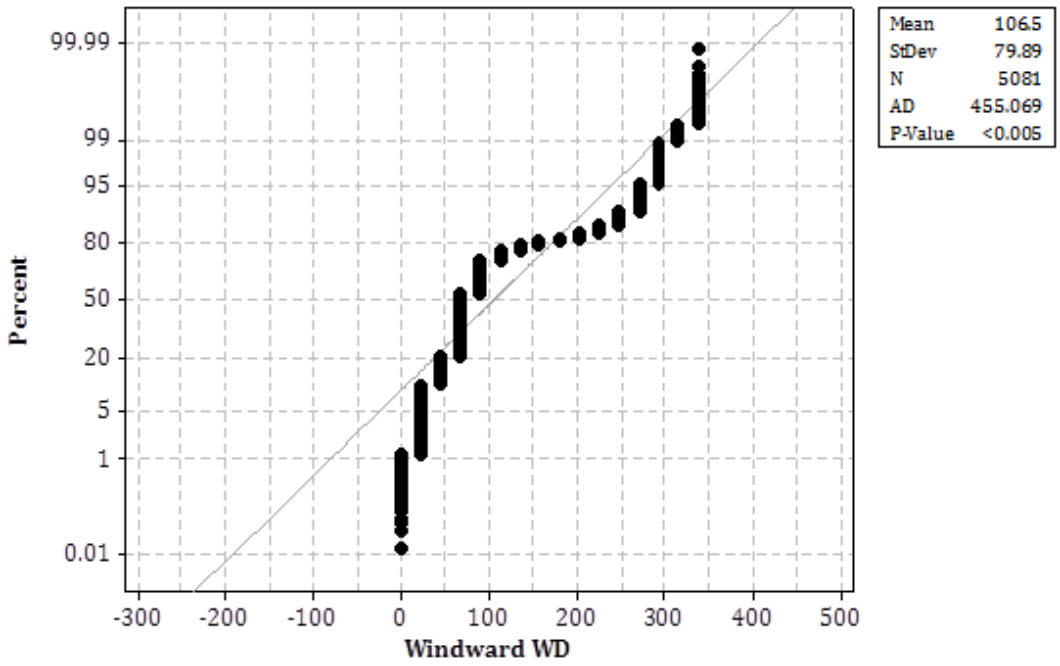

Appendix Figure 82: Probability Plot of wet season diurnal wind direction data at the windward forest plot (2007 – 2008).

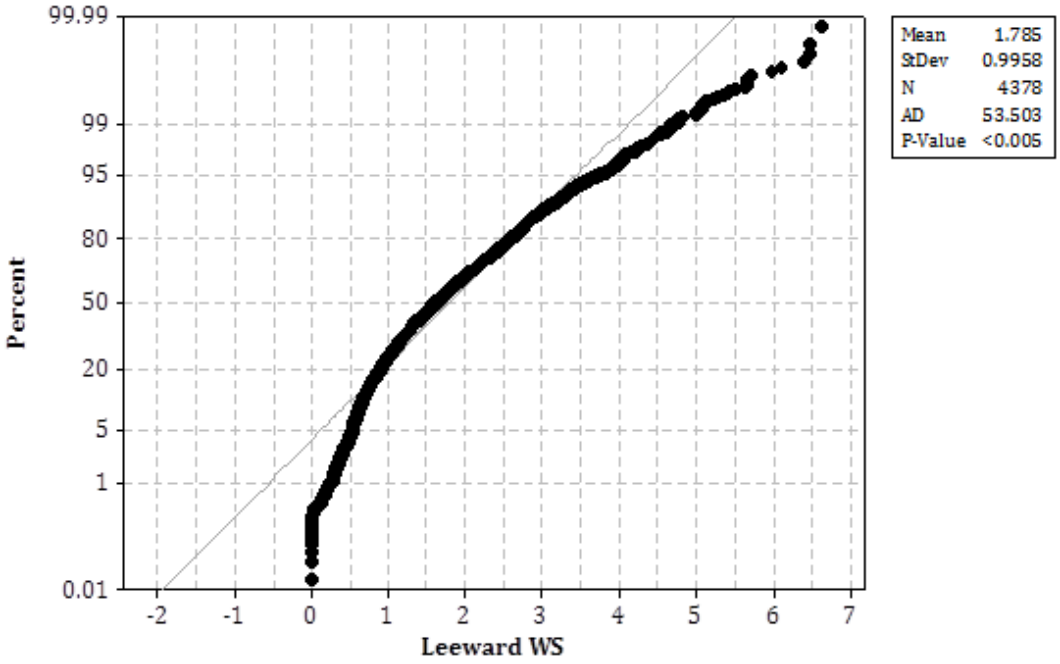

Appendix Figure 83: Probability Plot of wet season diurnal wind speed data at the leeward forest plot (2007 – 2008).

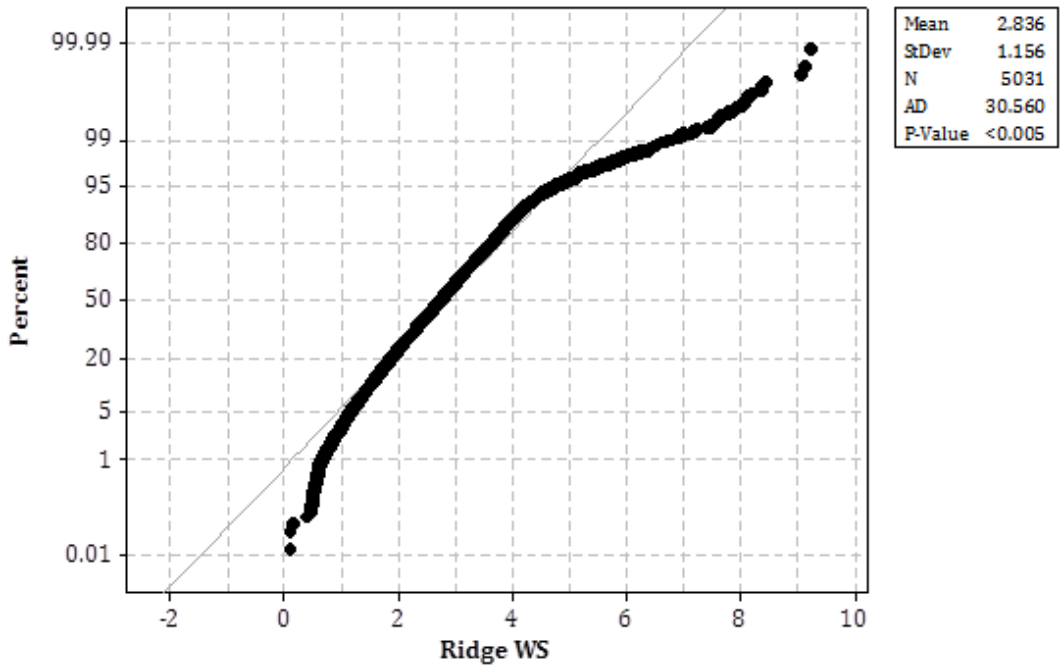

Appendix Figure 84: Probability Plot of wet season diurnal wind speed data at the ridge forest plot (2007 – 2008).

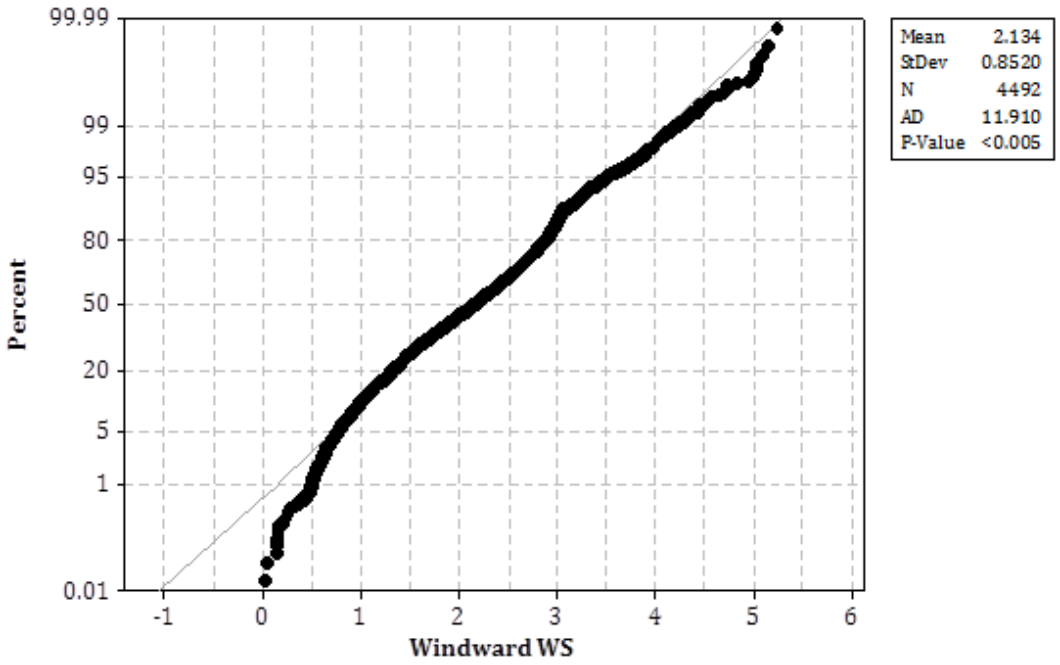

Appendix Figure 85: Probability Plot of wet season diurnal wind speed data at the windward forest plot (2007 – 2008).

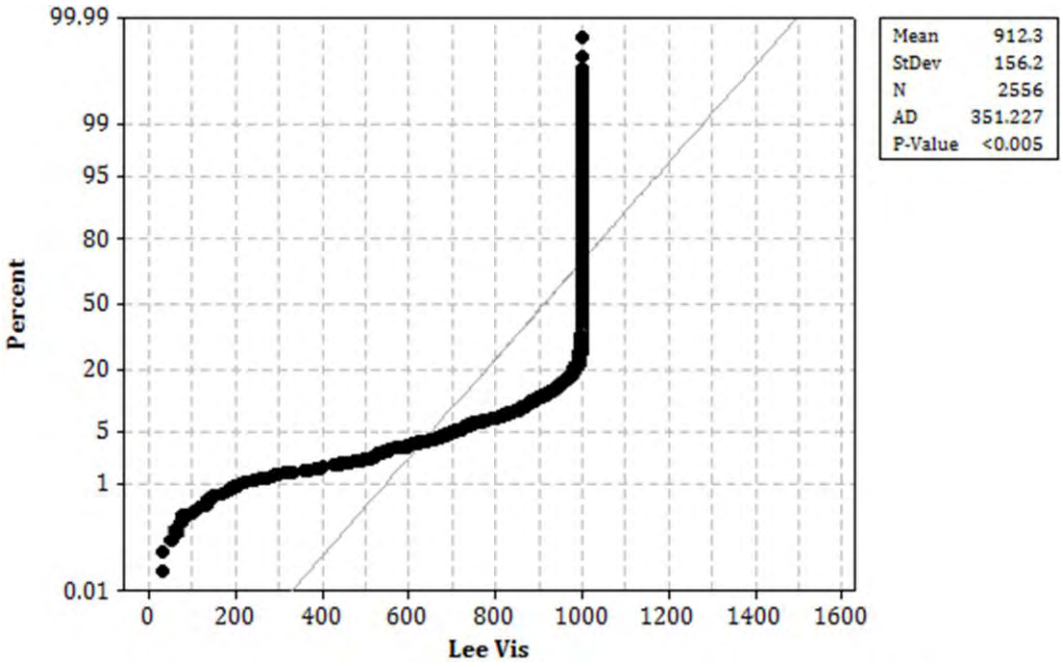

Appendix Figure 86: Probability Plot of wet season diurnal visibility data at the leeward forest plot (2008).

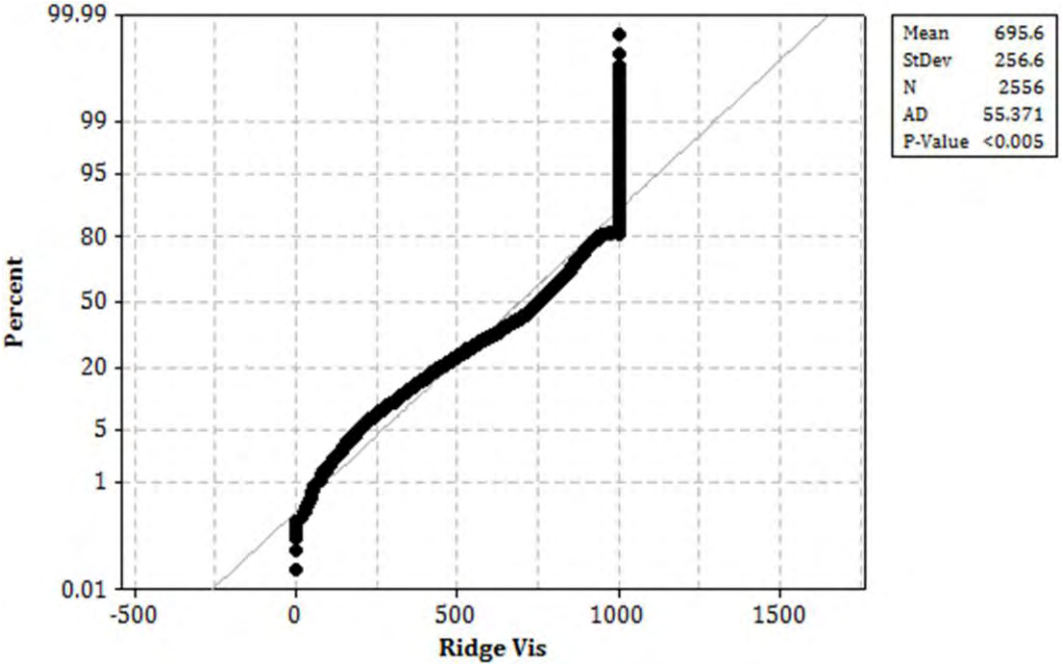

Appendix Figure 87: Probability Plot of wet season diurnal visibility data at the ridge forest plot (2008).

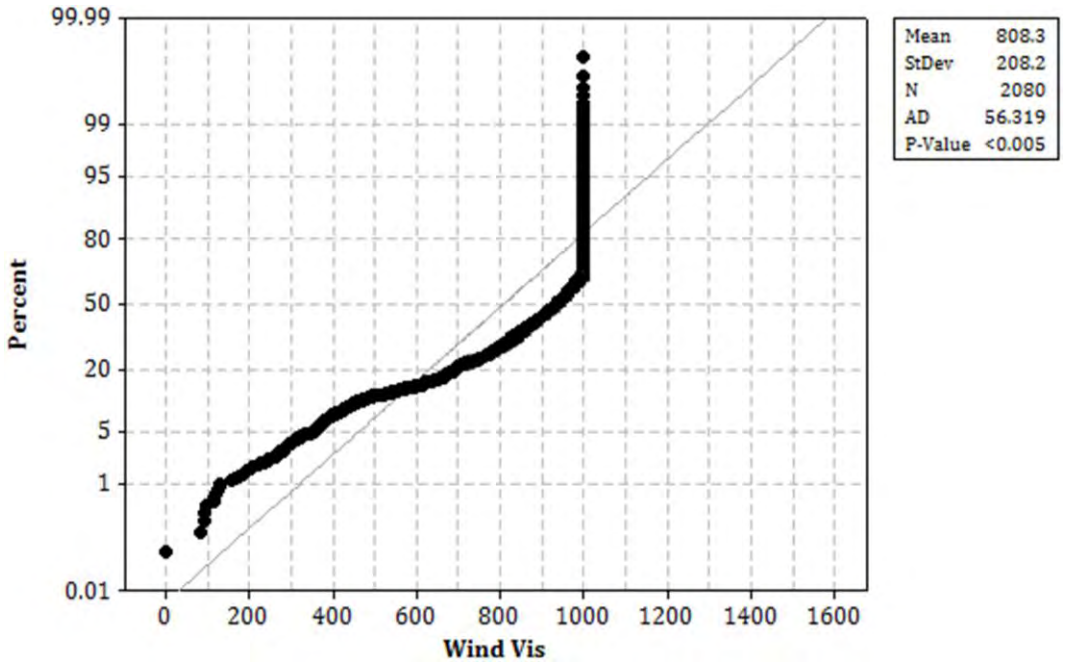

Appendix Figure 88: Probability Plot of wet season diurnal visibility data at the windward forest plot (2008).

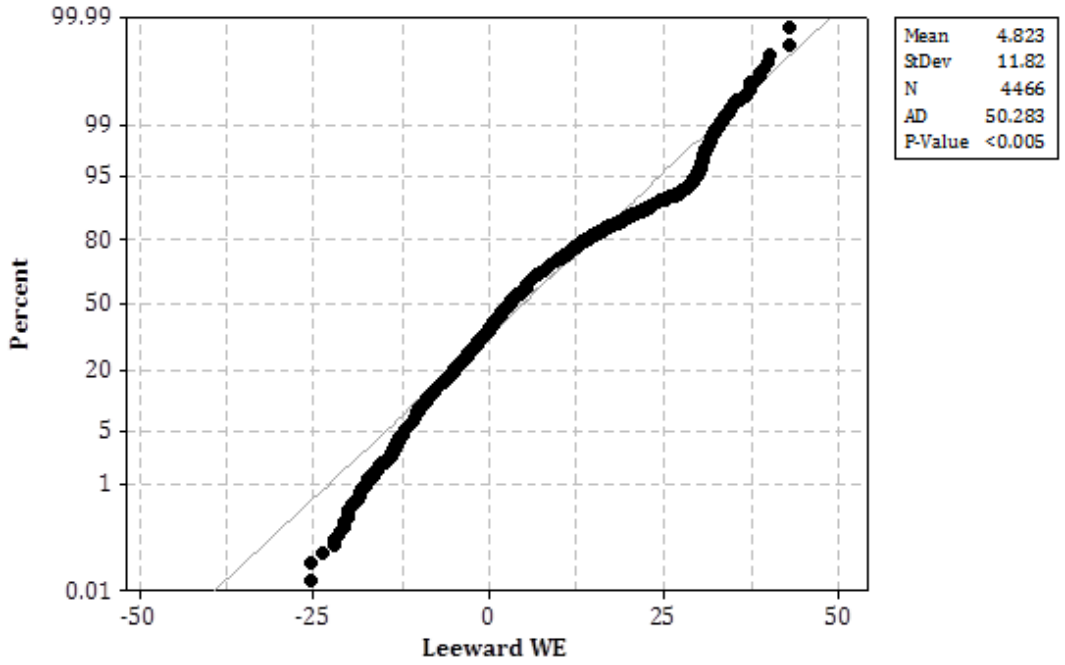

Appendix Figure 89: Probability Plot of wet season diurnal wind elevation data at the leeward forest plot (2007-2008).

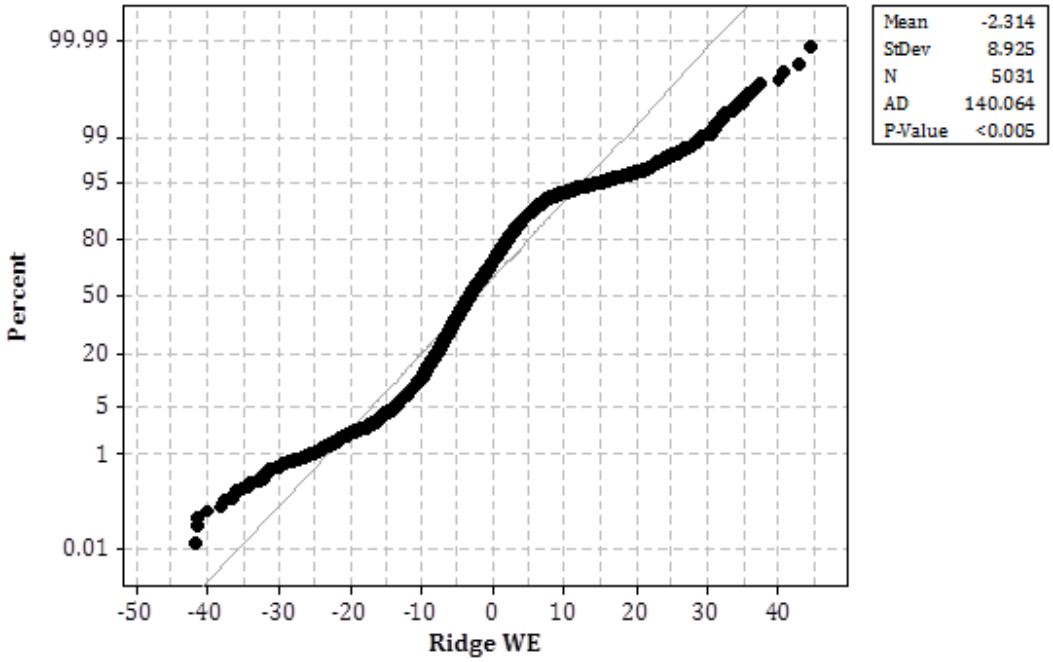

Appendix Figure 90: Probability Plot of wet season diurnal wind elevation data at the ridge forest plot (2007-2008).

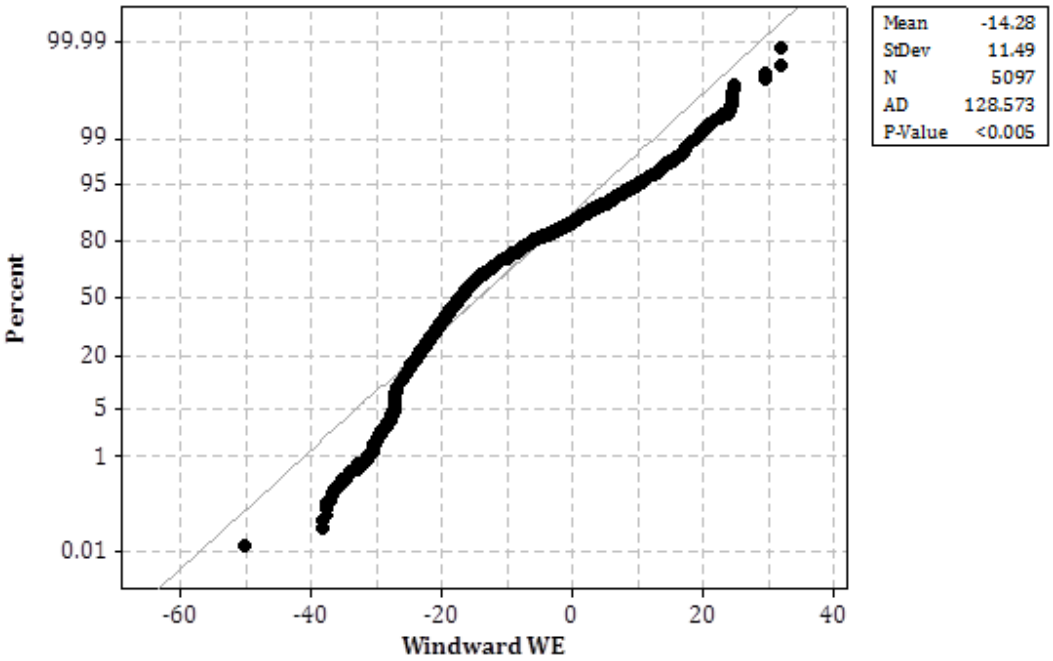

Appendix Figure 91: Probability Plot of wet season diurnal wind elevation data at the windward forest plot (2007-2008).

Dry Season Diurnal Parameter Datasets

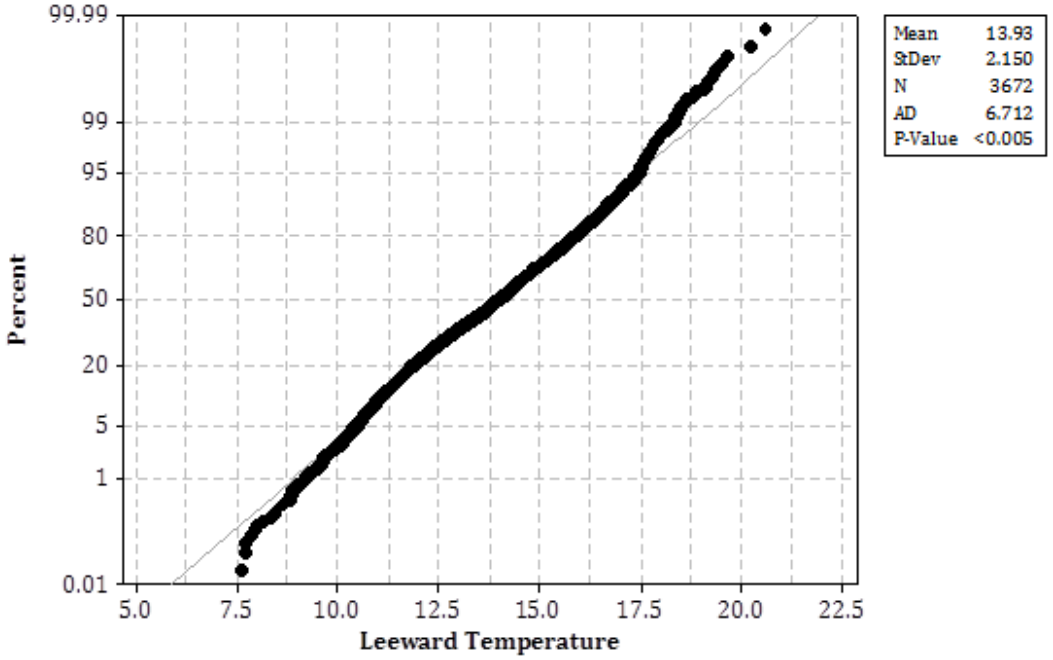

Appendix Figure 92: Probability Plot of dry season diurnal temperature data at the leeward forest plot (2007 – 2008).

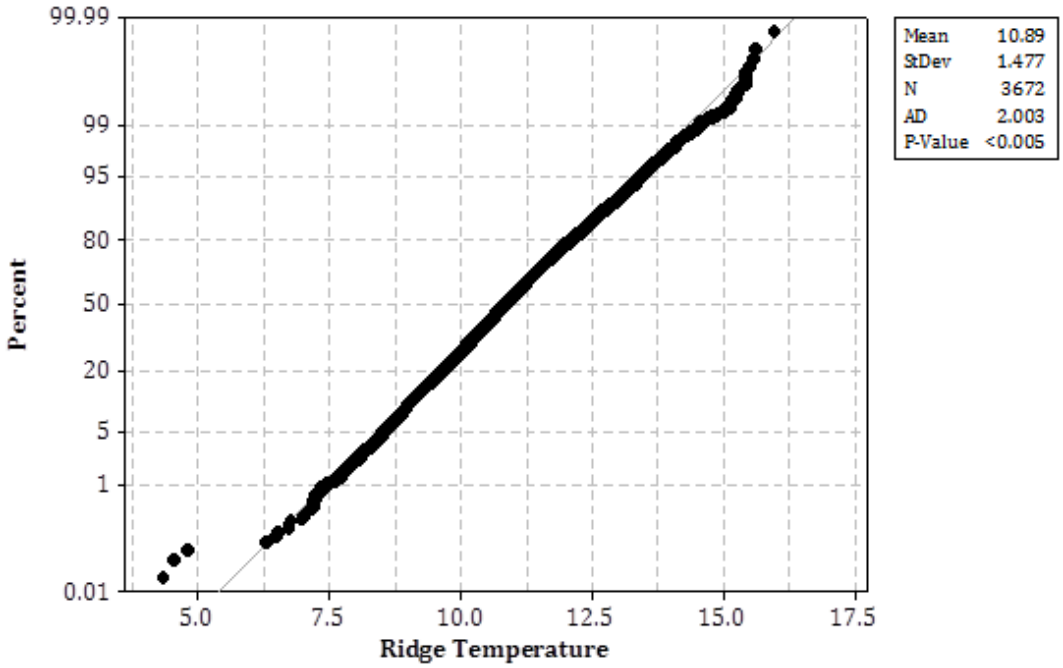

Appendix Figure 93: Probability Plot of dry season diurnal temperature data at the ridge forest plot (2007 – 2008).

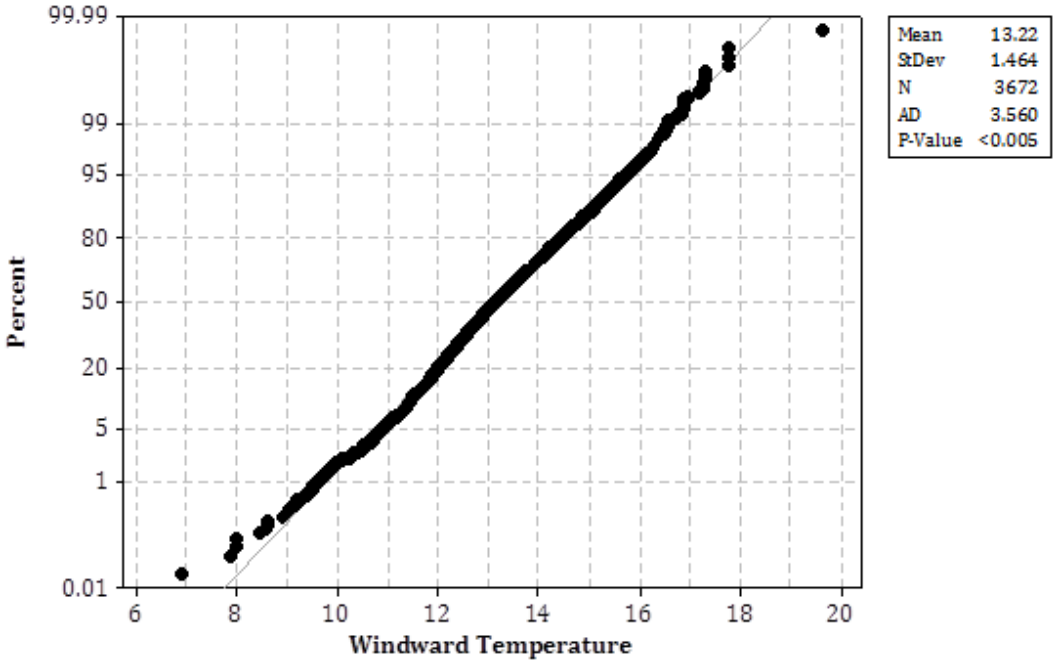

Appendix Figure 94: Probability Plot of dry season diurnal temperature data at the windward forest plot (2007 – 2008).

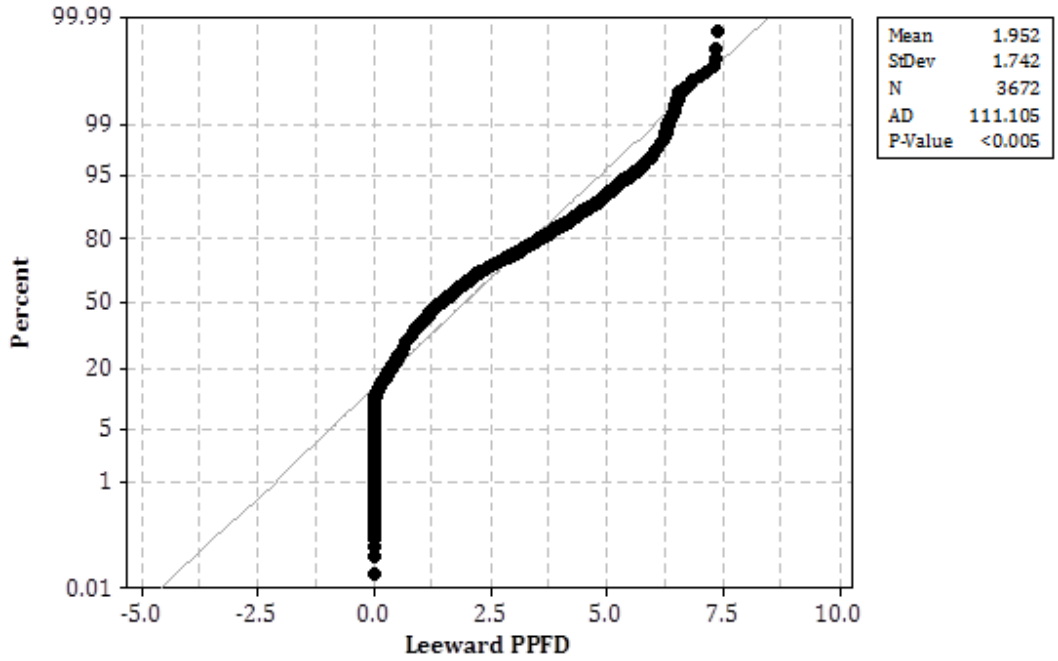

Appendix Figure 95: Probability Plot of dry season diurnal PPFD data at the leeward forest plot (2007 – 2008).

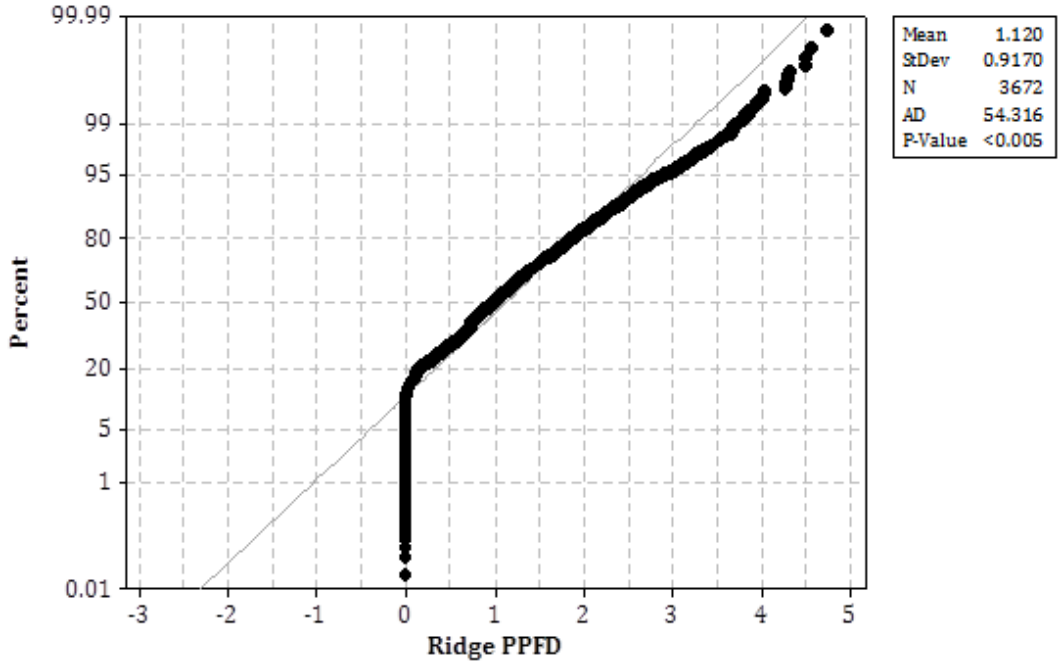

Appendix Figure 96: Probability Plot of dry season diurnal PPFD data at the ridge forest plot (2007 – 2008).

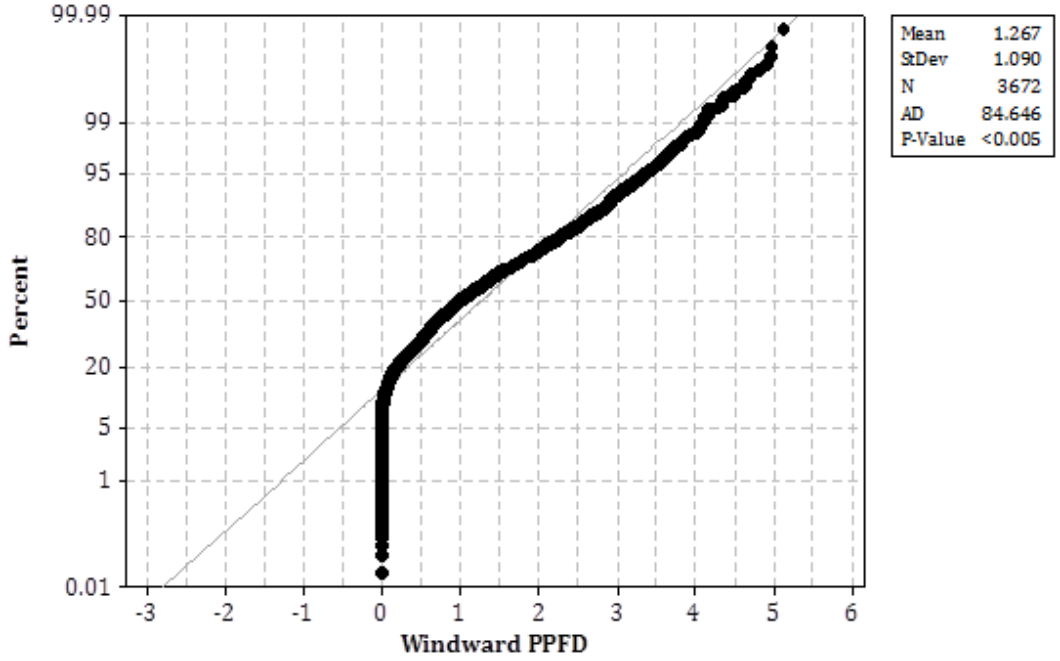

Appendix Figure 97: Probability Plot of dry season diurnal PPFD data at the windward forest plot (2007 – 2008).

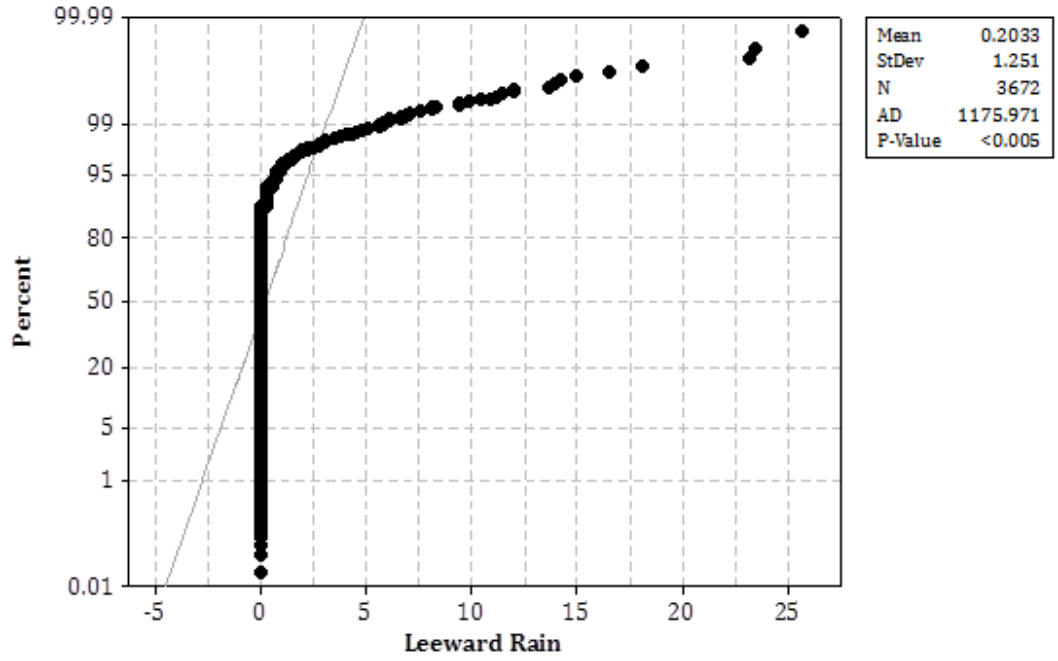

Appendix Figure 98: Probability Plot of dry season diurnal rainfall data at the leeward forest plot (2007 – 2008).

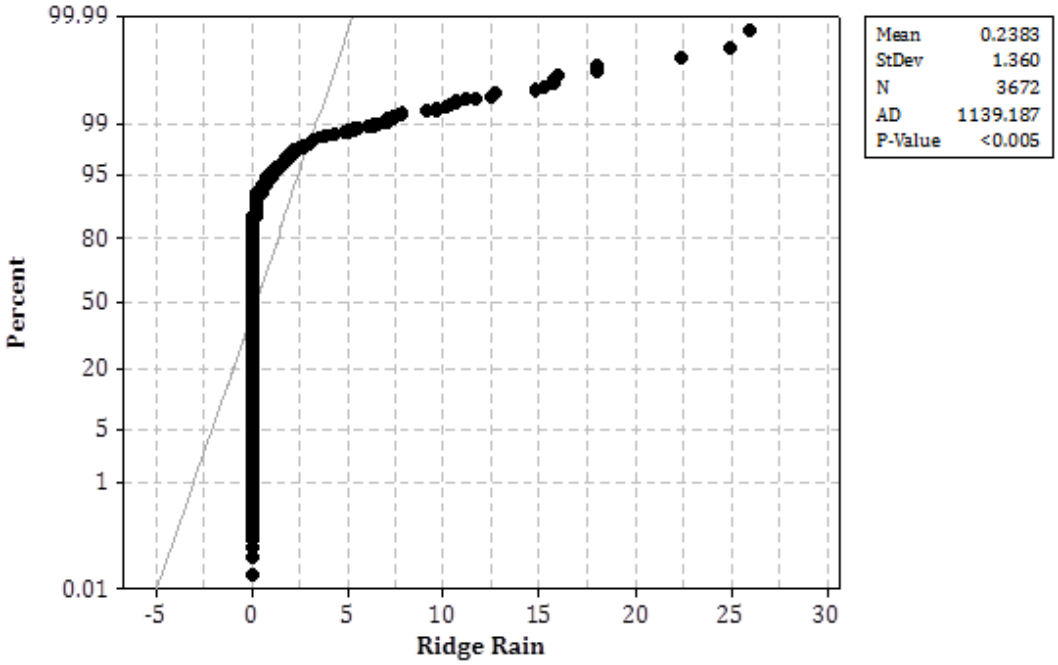

Appendix Figure 99: Probability Plot of dry season diurnal rainfall data at the ridge forest plot (2007 – 2008).

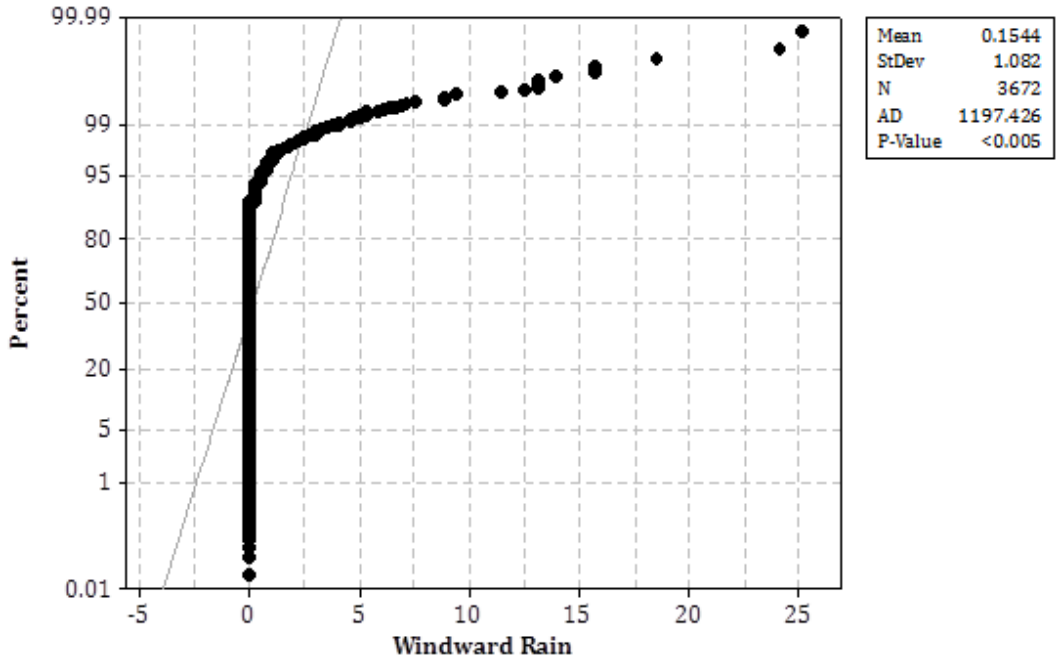

Appendix Figure 100: Probability Plot of dry season diurnal rainfall data at the windward forest plot (2007 – 2008).

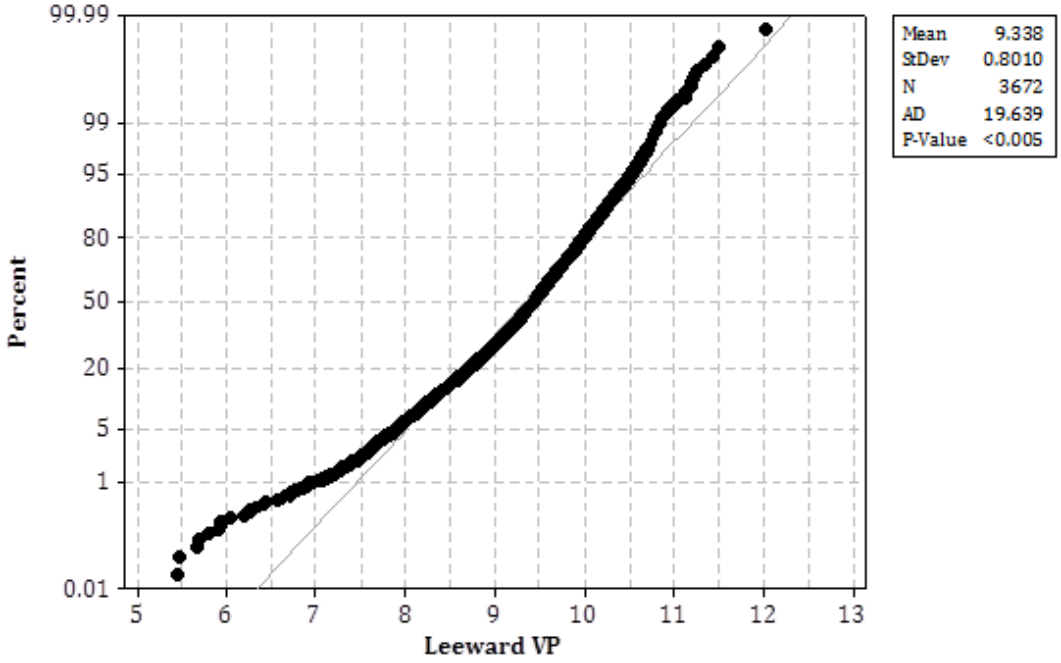

Appendix Figure 101: Probability Plot of dry season diurnal vapour pressure data at the leeward forest plot (2007 – 2008).

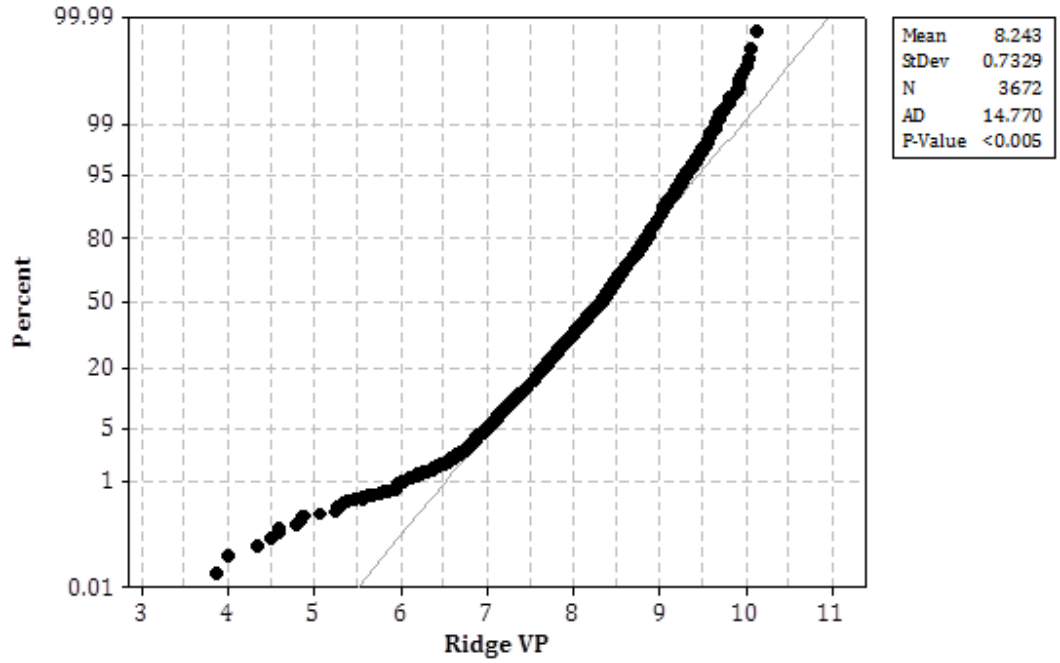

Appendix Figure 102: Probability Plot of dry season diurnal vapour pressure data at the ridge forest plot (2007 – 2008).

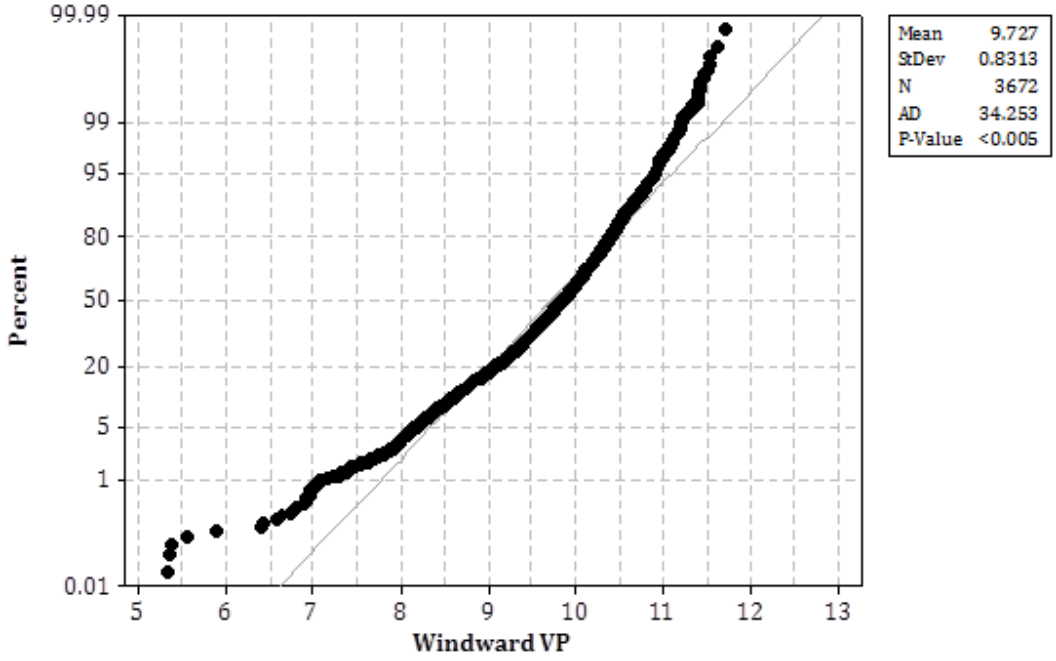

Appendix Figure 103: Probability Plot of dry season diurnal vapour pressure data at the windward forest plot (2007 – 2008).

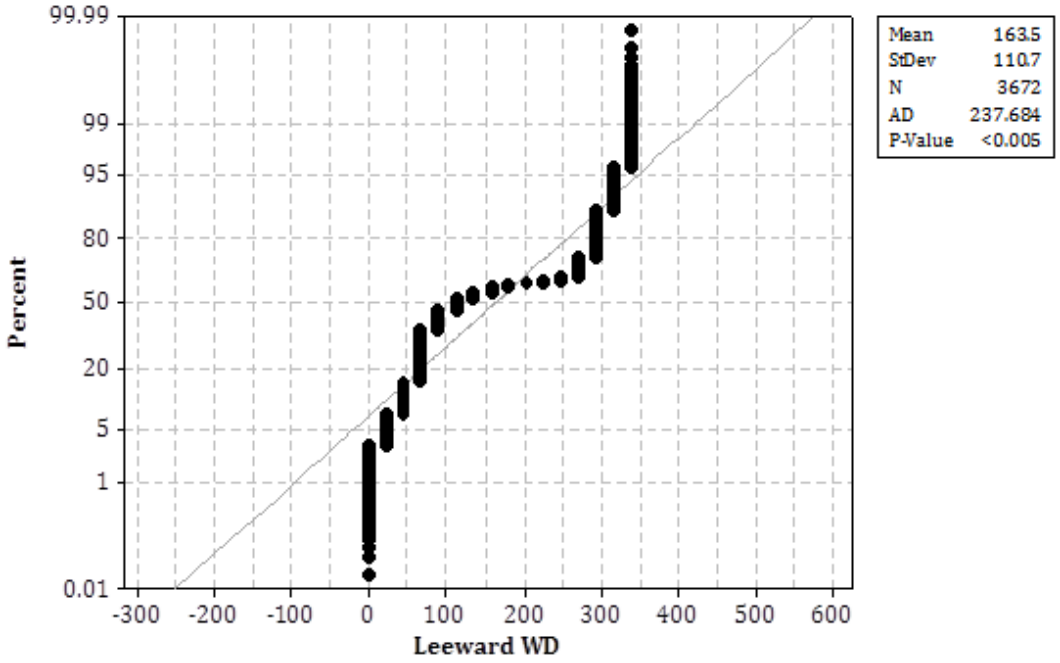

Appendix Figure 104: Probability Plot of dry season diurnal wind direction data at the leeward forest plot (2007 – 2008).

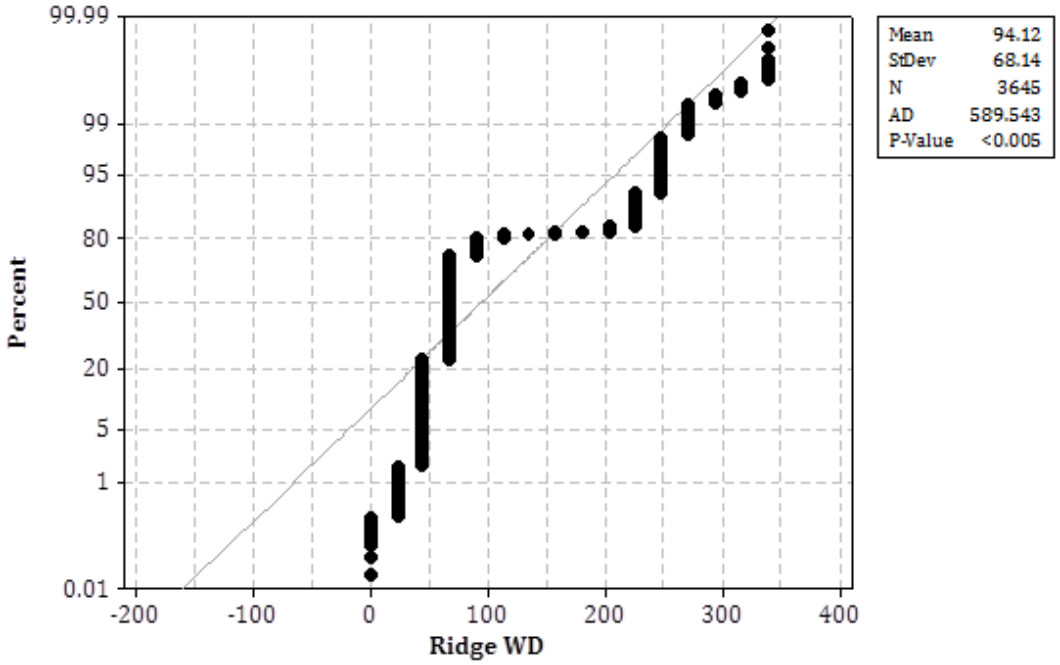

Appendix Figure 105: Probability Plot of dry season diurnal wind direction data at the ridge forest plot (2007 – 2008).

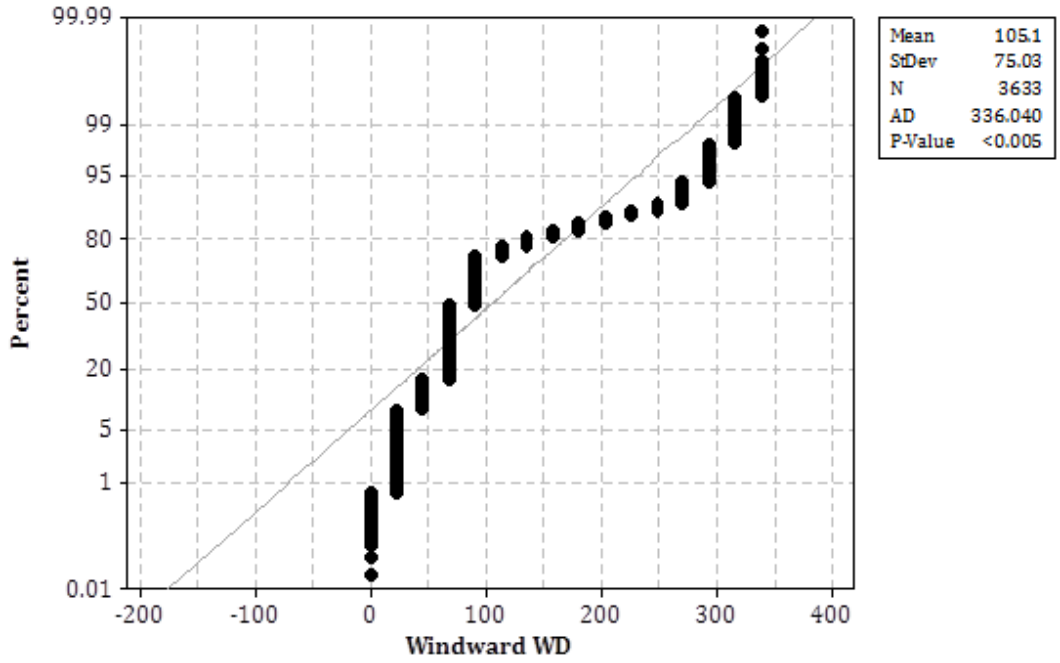

Appendix Figure 106: Probability Plot of dry season diurnal wind direction data at the windward forest plot (2007 – 2008).

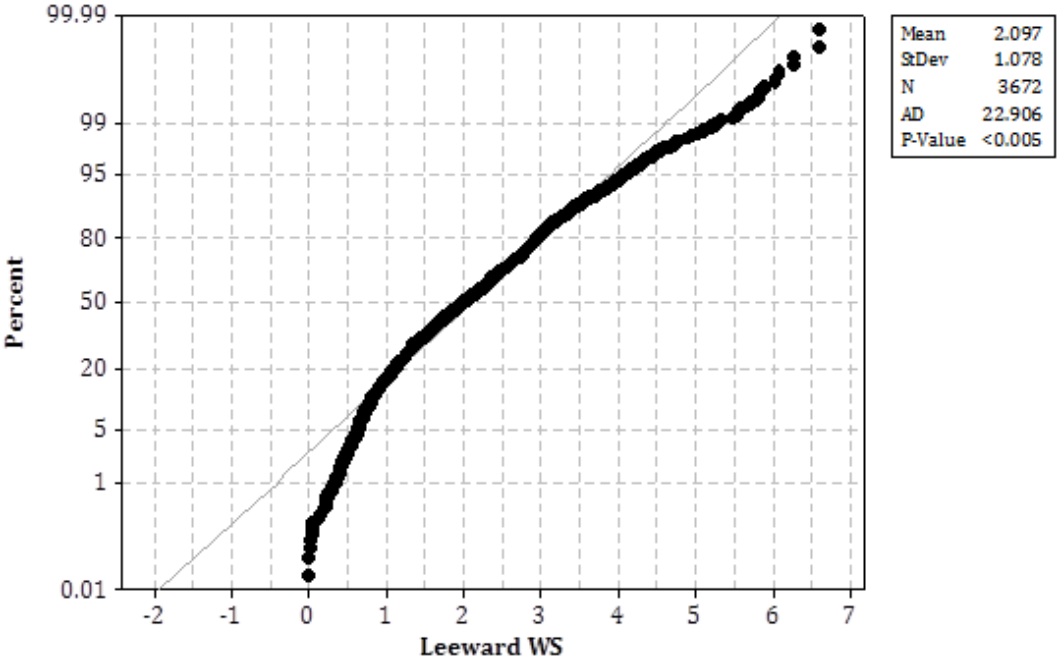

Appendix Figure 107: Probability Plot of dry season diurnal wind speed data at the leeward forest plot (2007 – 2008).

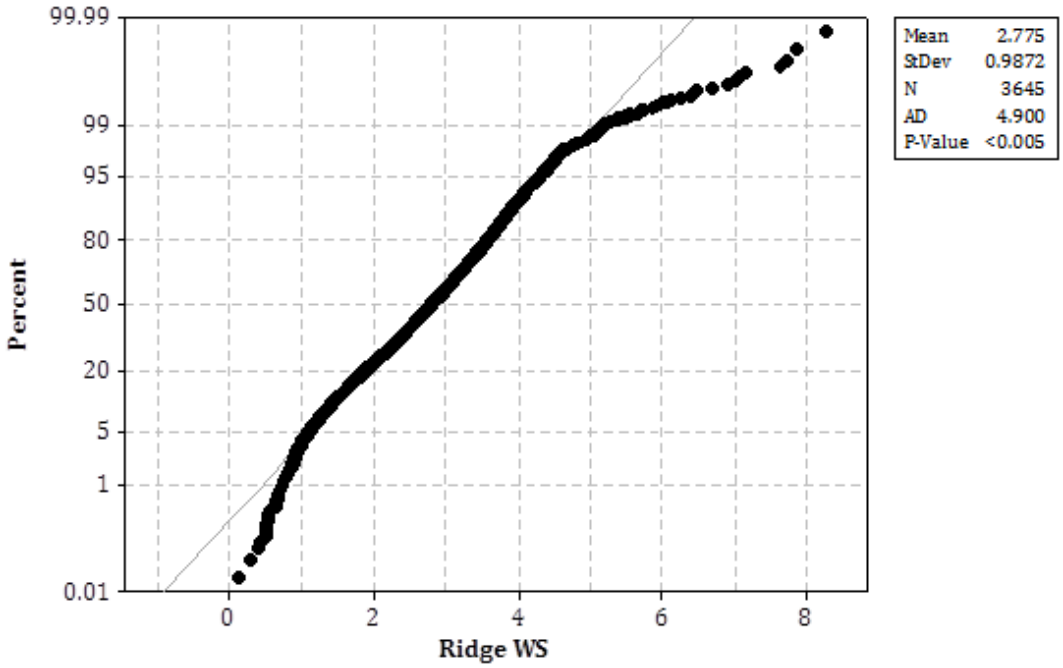

Appendix Figure 108: Probability Plot of dry season diurnal wind speed data at the ridge forest plot (2007 – 2008).

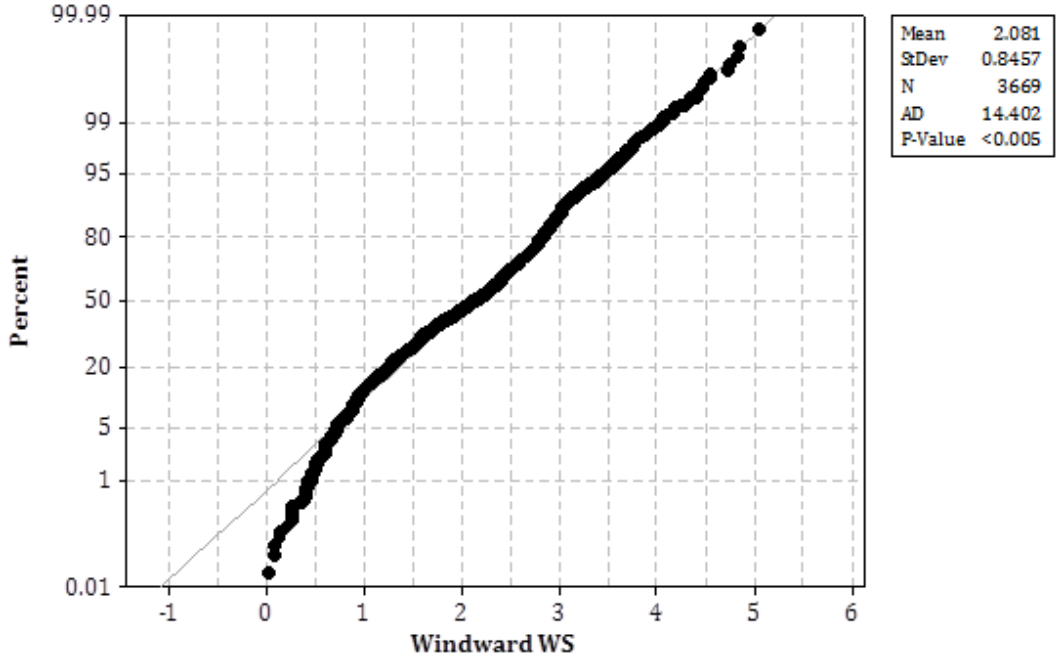

Appendix Figure 109: Probability Plot of dry season diurnal wind speed data at the windward forest plot (2007 – 2008).

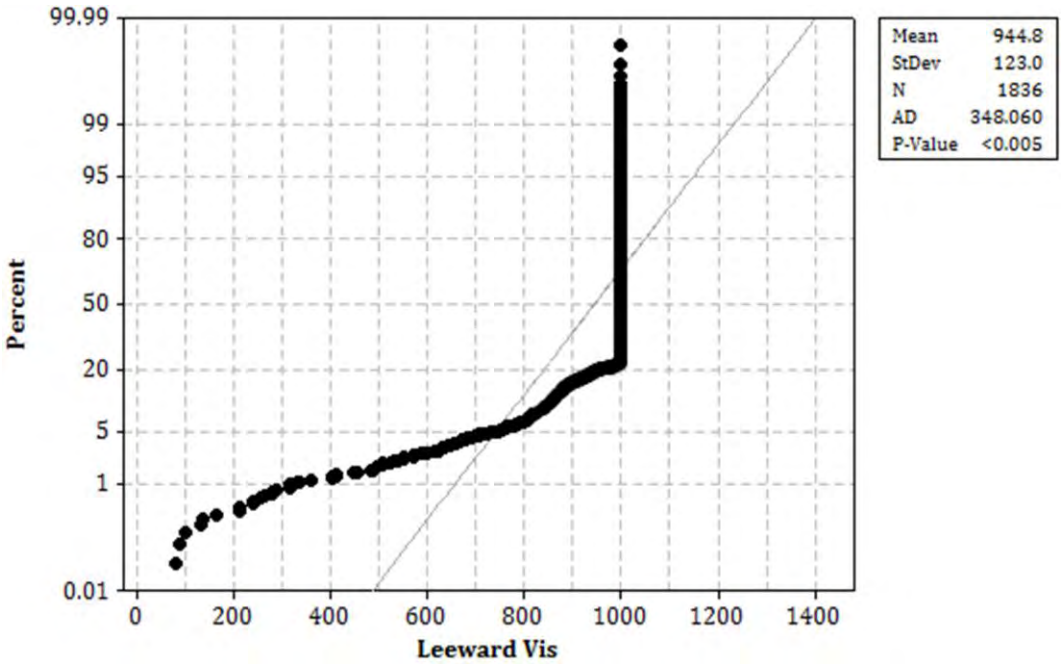

Appendix Figure 110: Probability Plot of dry season diurnal visibility data at the leeward forest plot (2008).

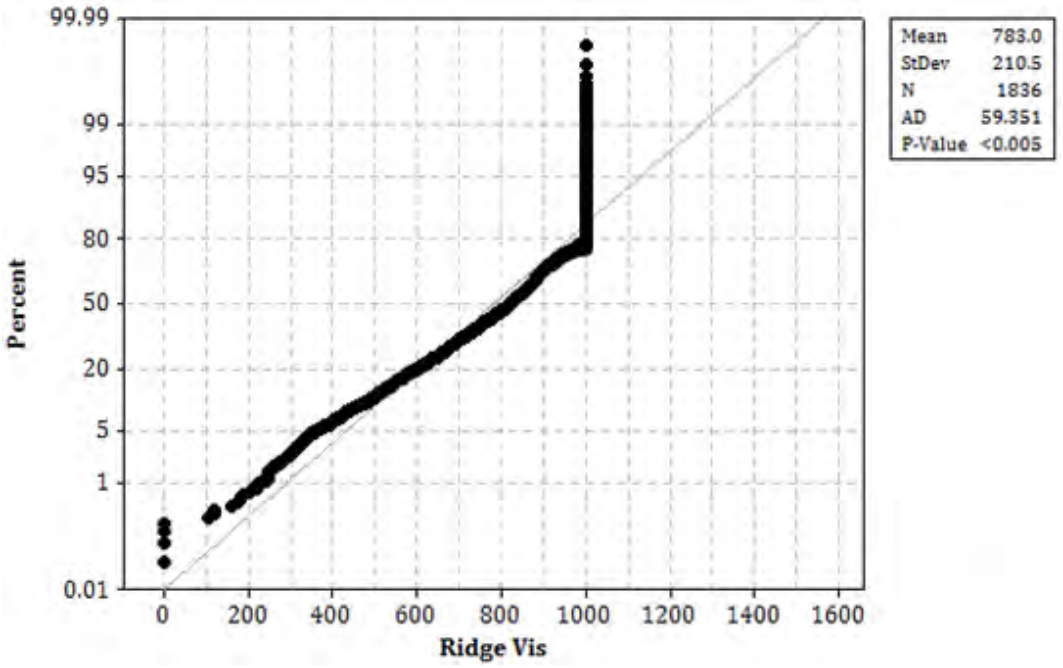

Appendix Figure 111: Probability Plot of dry season diurnal visibility data at the ridge forest plot (2008).

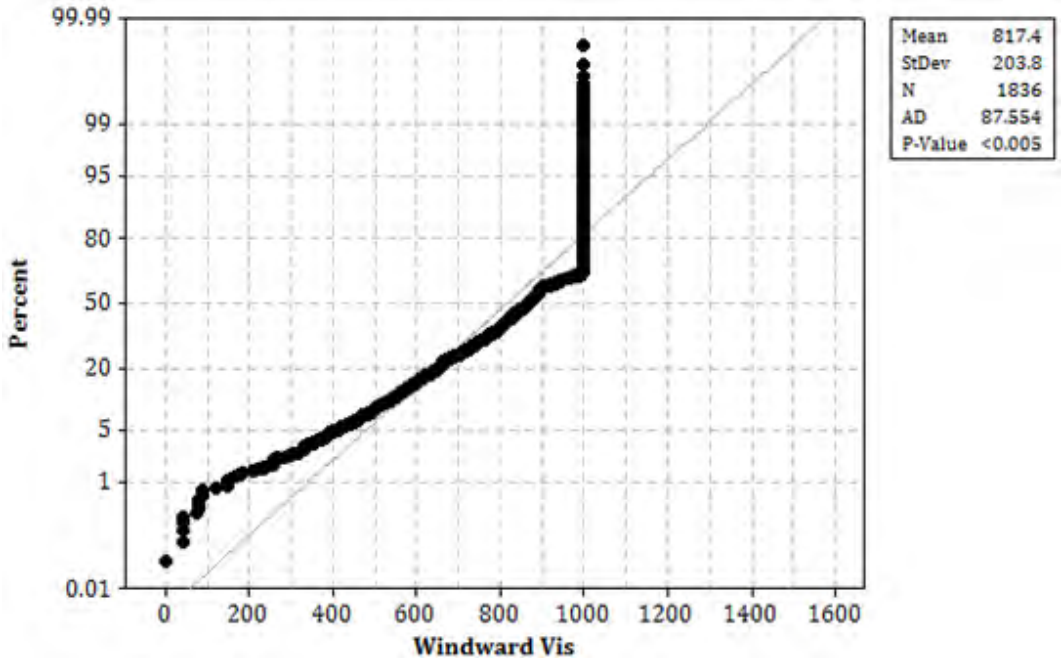

Appendix Figure 112: Probability Plot of dry season diurnal visibility data at the windward forest plot (2008).

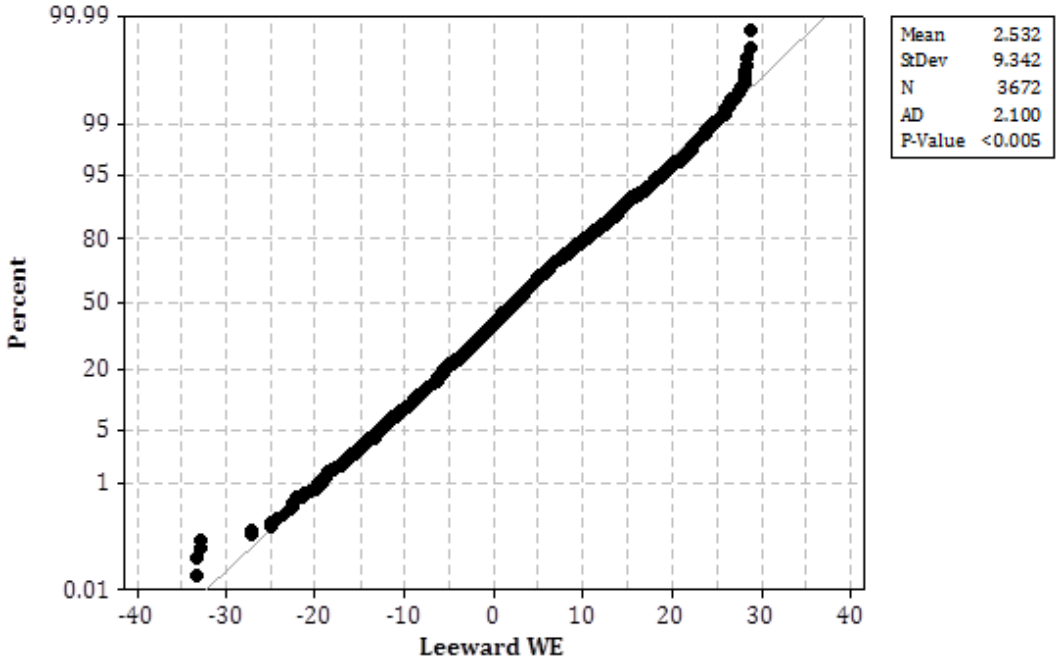

Appendix Figure 113: Probability Plot of dry season diurnal wind elevation data at the leeward forest plot (2007-2008).

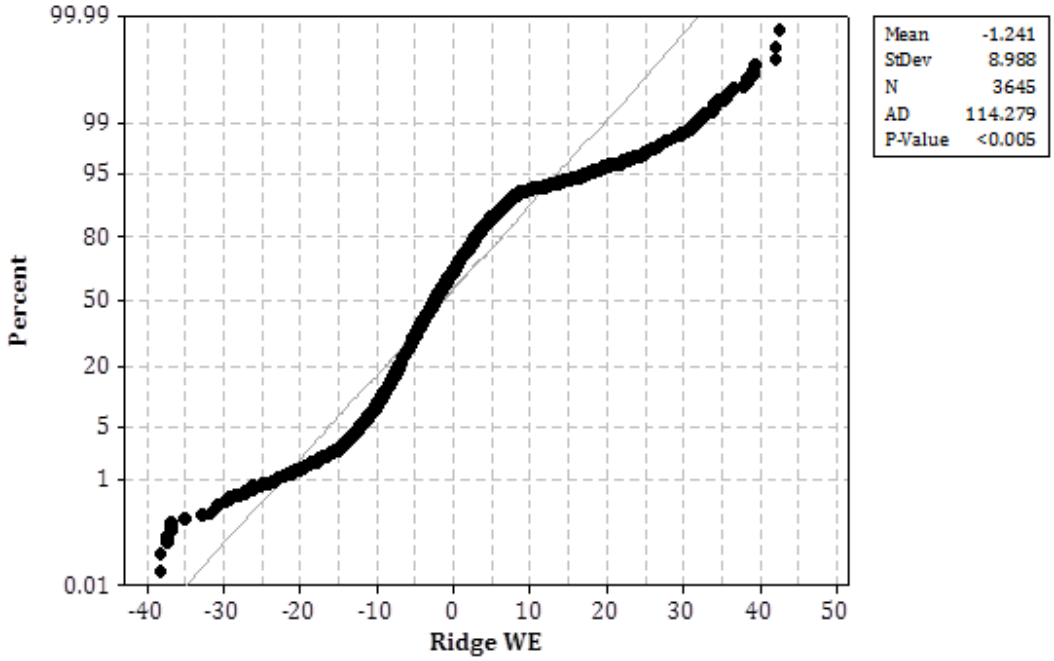

Appendix Figure 114: Probability Plot of dry season diurnal wind elevation data at the ridge forest plot (2007-2008).

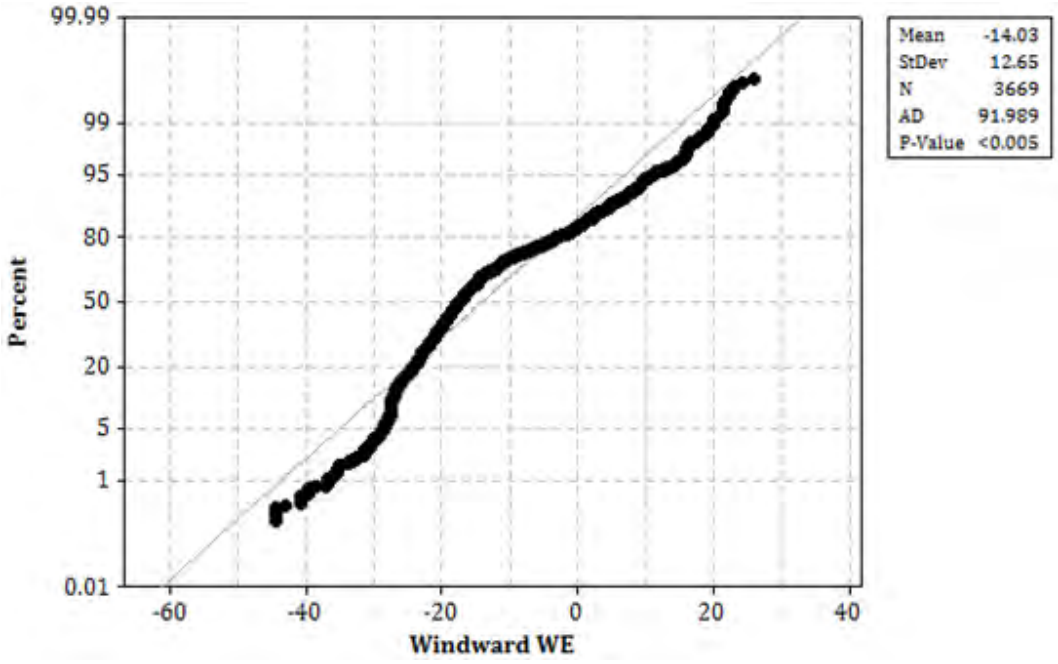

Appendix Figure 115: Probability Plot of dry season diurnal wind elevation data at the windward forest plot (2007-2008).

Wet Season Nocturnal Parameter Datasets

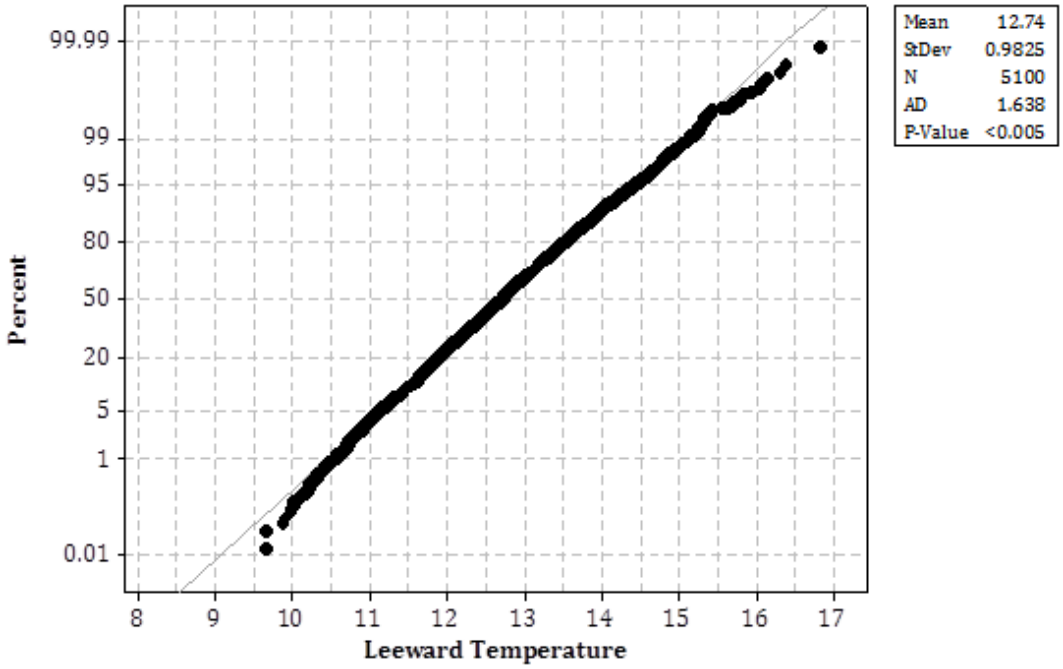

Appendix Figure 116: Probability Plot of wet season nocturnal temperature data at the leeward forest plot (2007 – 2008).

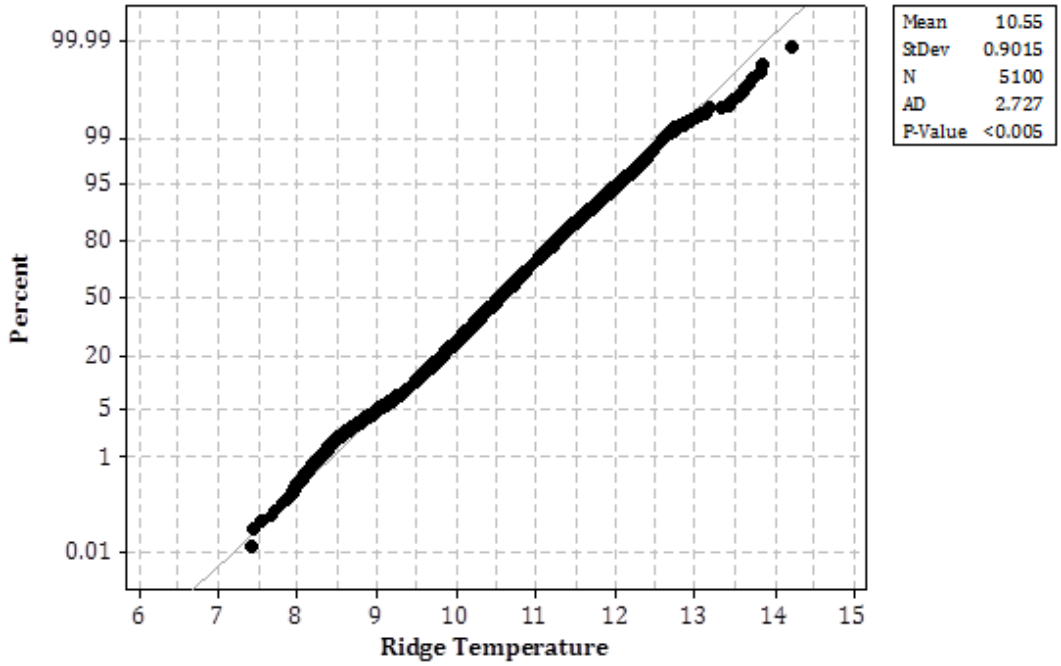

Appendix Figure 117: Probability Plot of wet season nocturnal temperature data at the ridge forest plot (2007 – 2008).

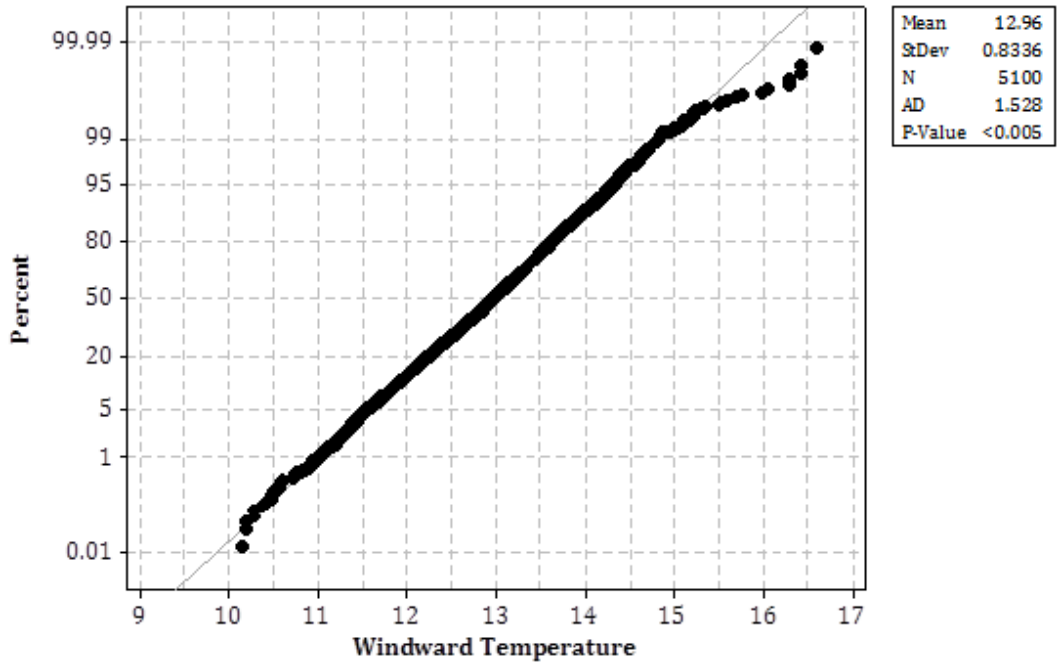

Appendix Figure 118: Probability Plot of wet season nocturnal temperature data at the windward forest plot (2007 – 2008).

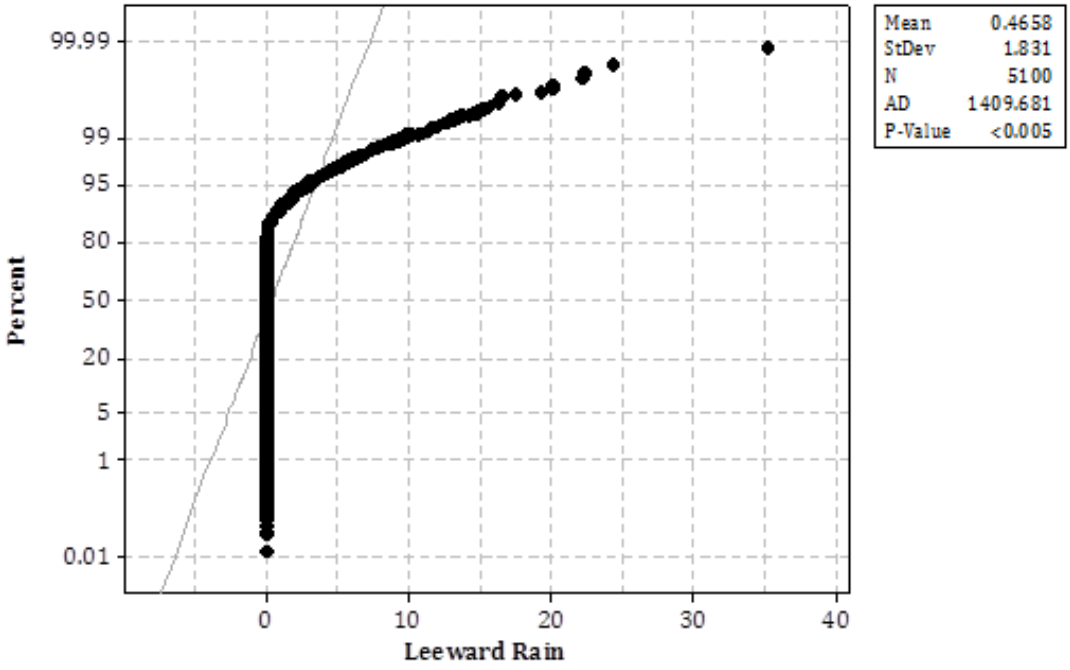

Appendix Figure 119: Probability Plot of wet season nocturnal rainfall data at the leeward forest plot (2007 – 2008).

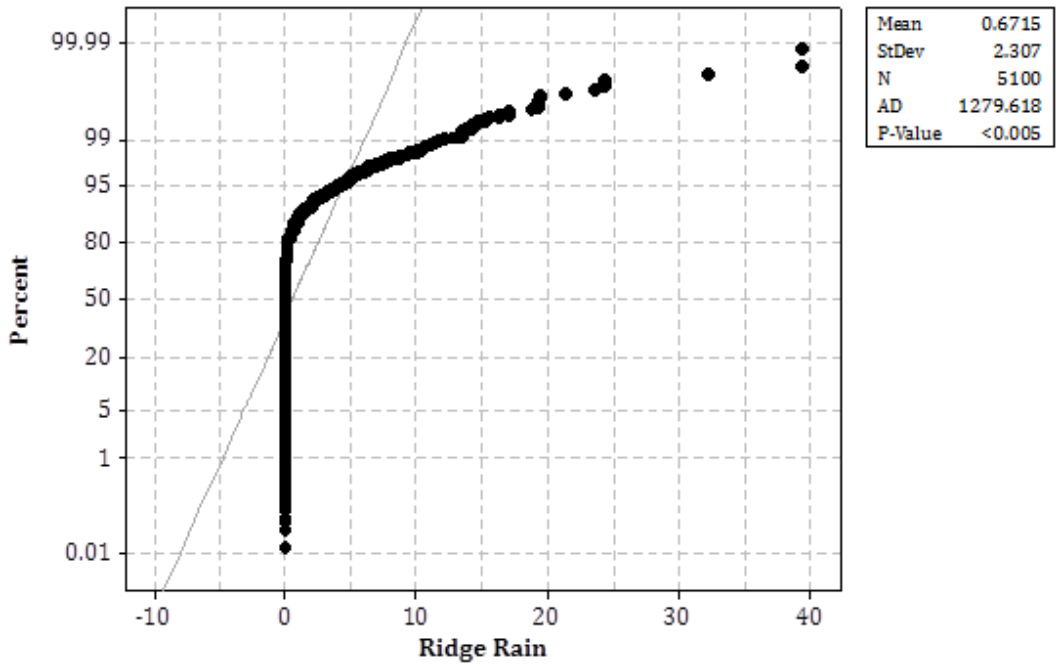

Appendix Figure 120: Probability Plot of wet season nocturnal rainfall data at the ridge forest plot (2007 – 2008).

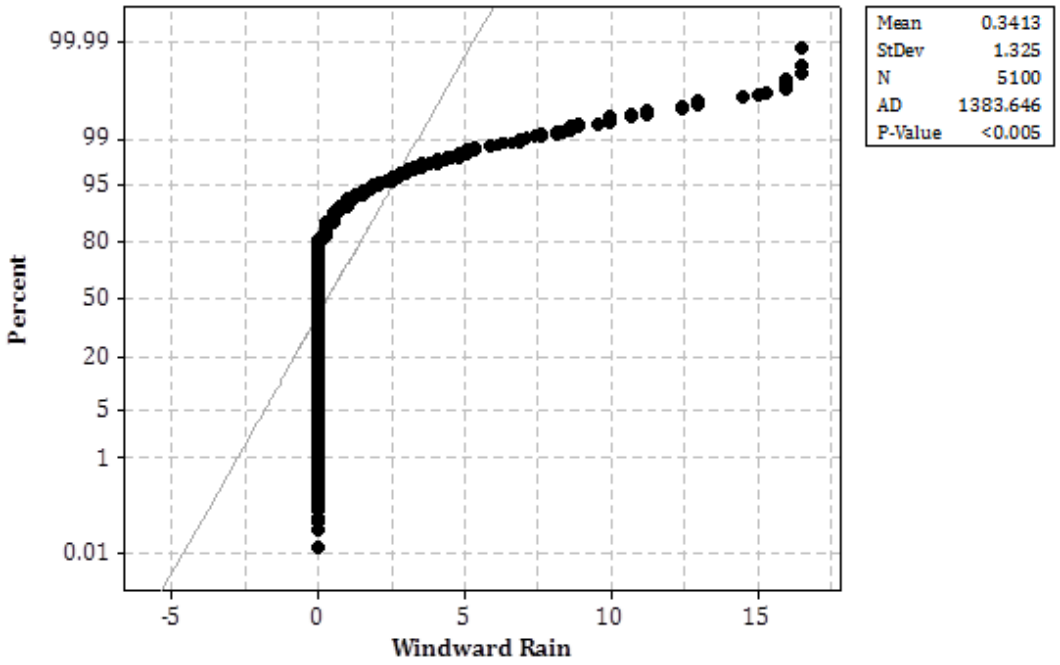

Appendix Figure 121: Probability Plot of wet season nocturnal rainfall data at the windward forest plot (2007 – 2008).

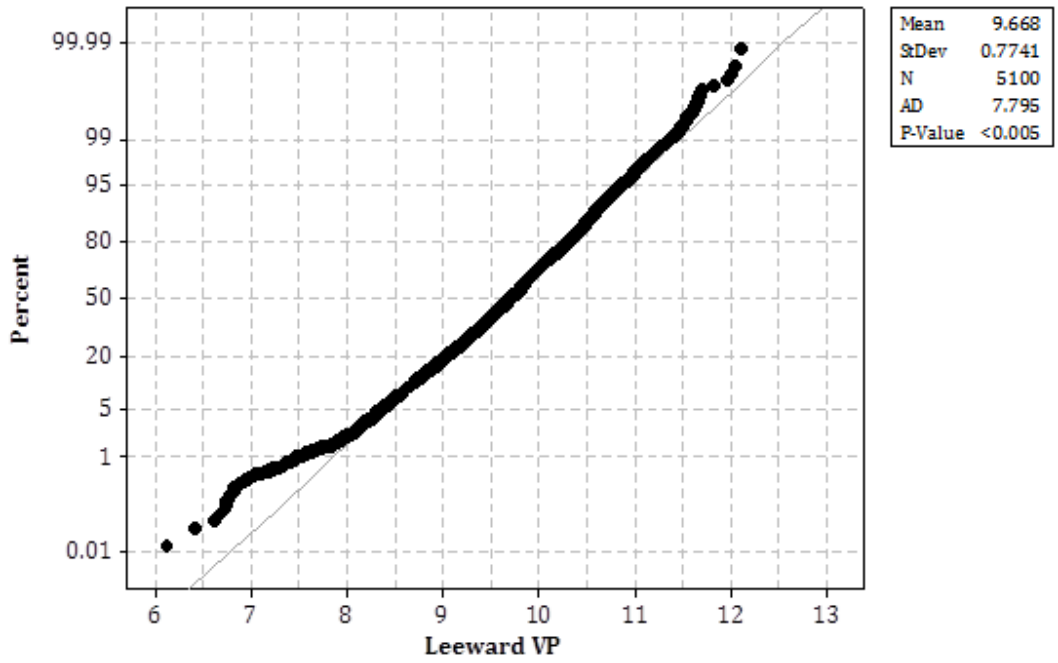

Appendix Figure 122: Probability Plot of wet season nocturnal vapour pressure data at the leeward forest plot (2007 – 2008).

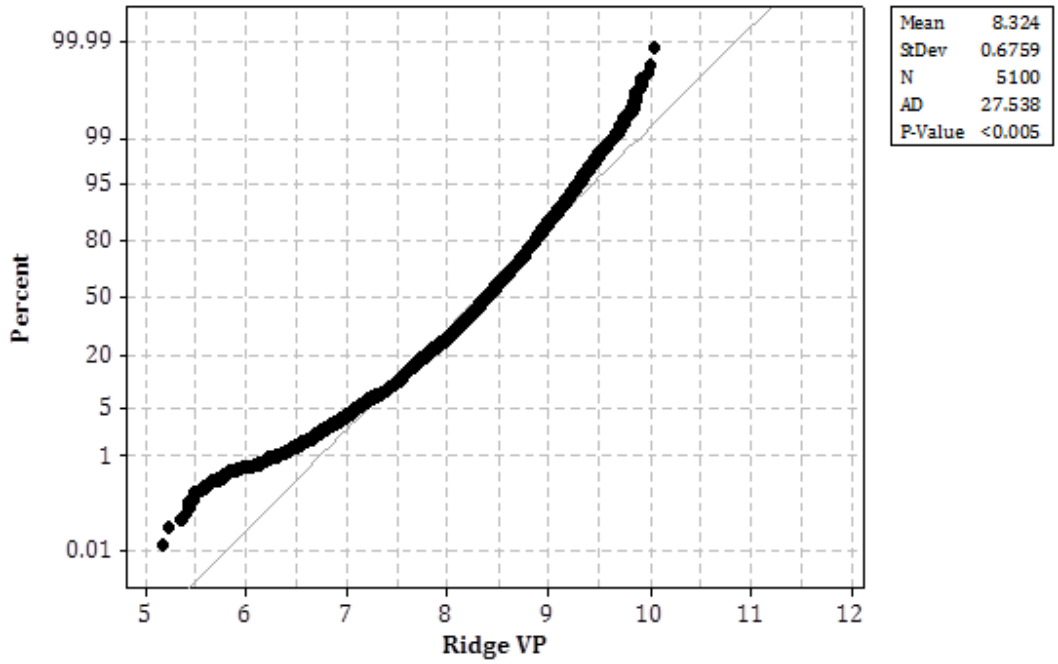

Appendix Figure 123: Probability Plot of wet season nocturnal vapour pressure data at the ridge forest plot (2007 – 2008).

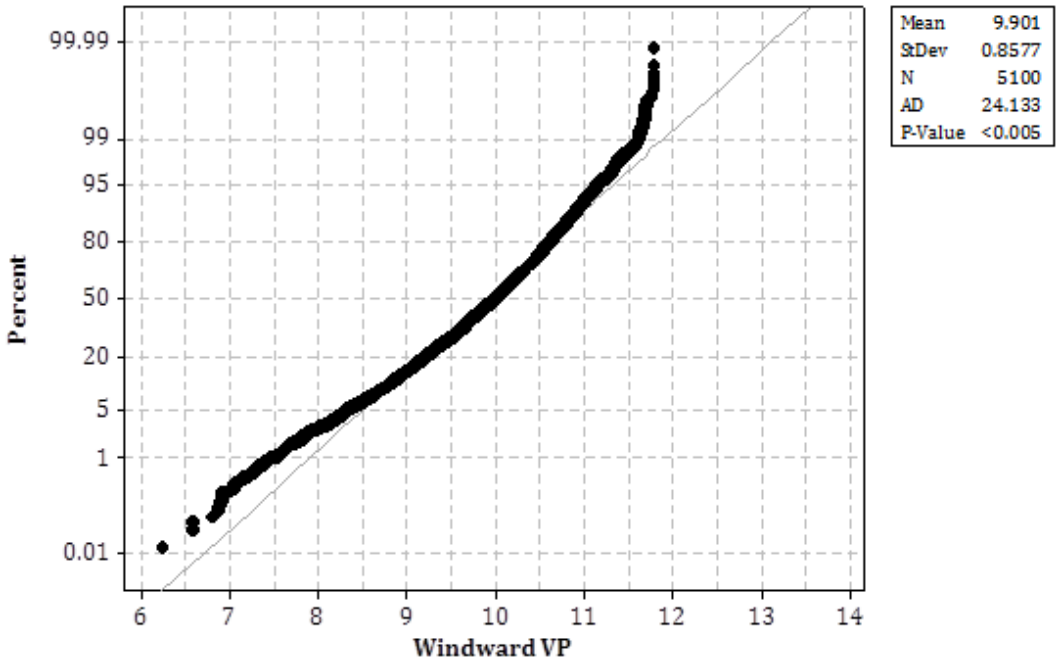

Appendix Figure 124: Probability Plot of wet season nocturnal vapour pressure data at the windward forest plot (2007 – 2008).

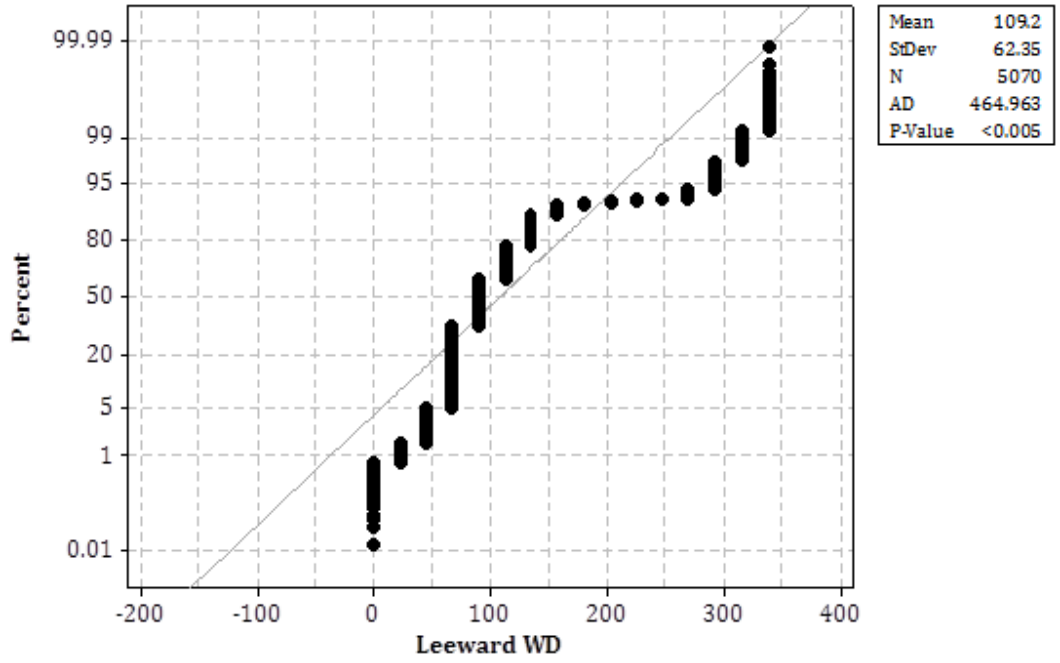

Appendix Figure 125: Probability Plot of wet season nocturnal wind direction data at the leeward forest plot (2007 – 2008).

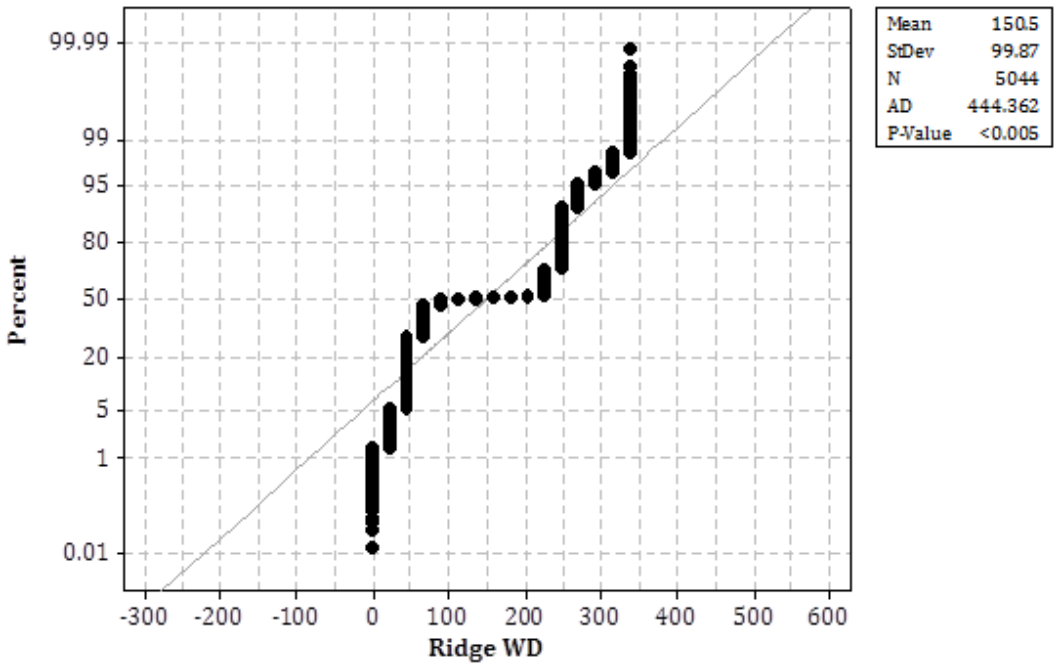

Appendix Figure 126: Probability Plot of wet season nocturnal wind direction data at the ridge forest plot (2007 – 2008).

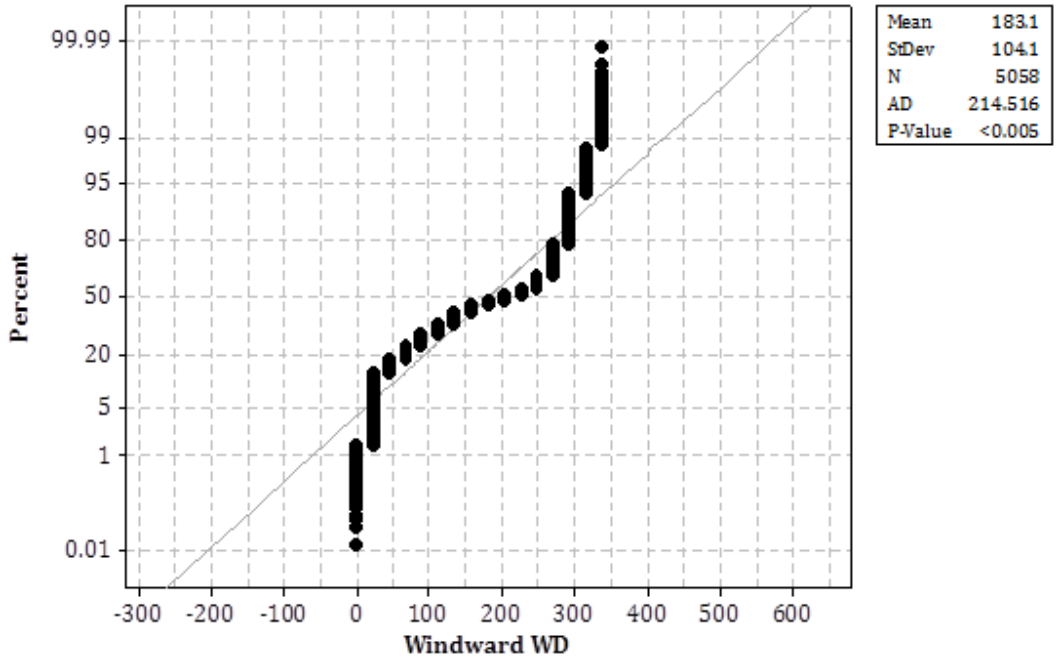

Appendix Figure 127: Probability Plot of wet season nocturnal wind direction data at the windward forest plot (2007 – 2008).

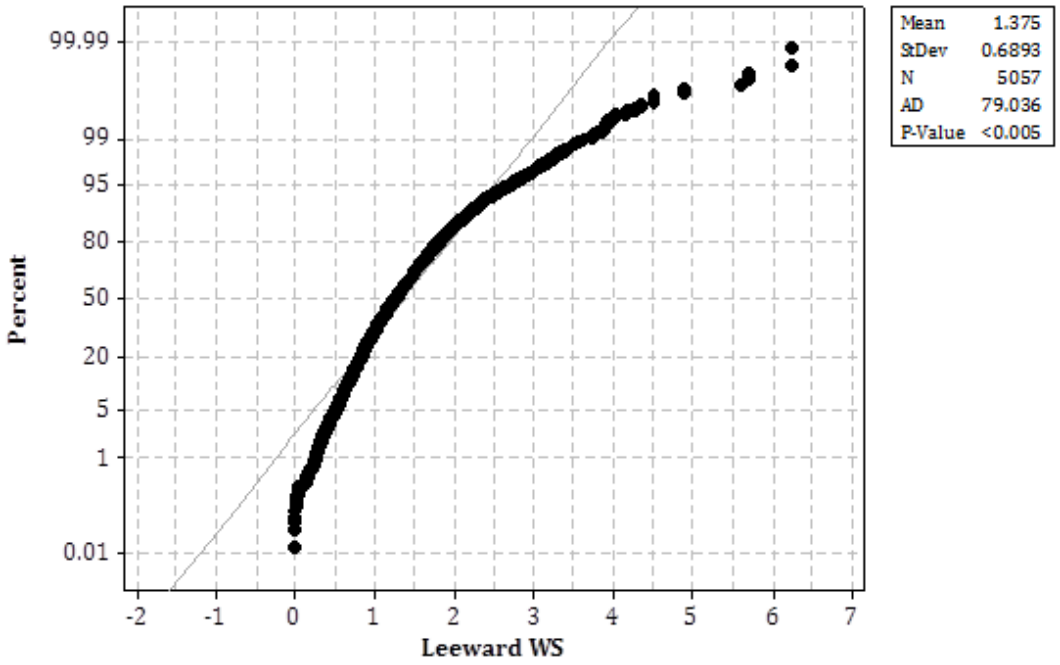

Appendix Figure 128: Probability Plot of wet season nocturnal wind speed data at the leeward forest plot (2007 – 2008).

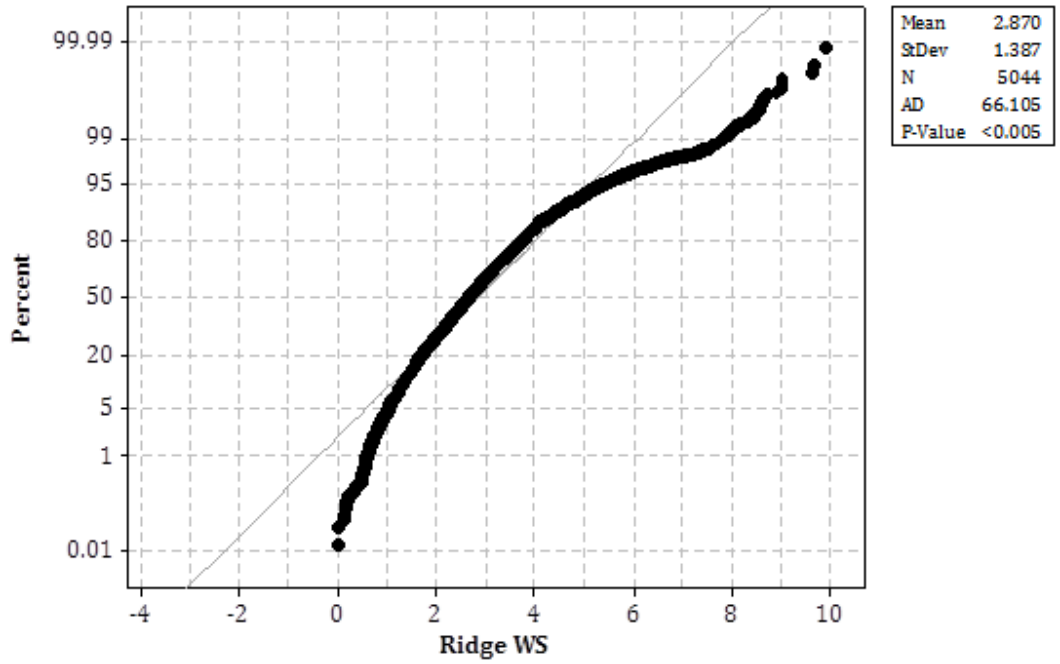

Appendix Figure 129: Probability Plot of wet season nocturnal wind speed data at the ridge forest plot (2007 – 2008).

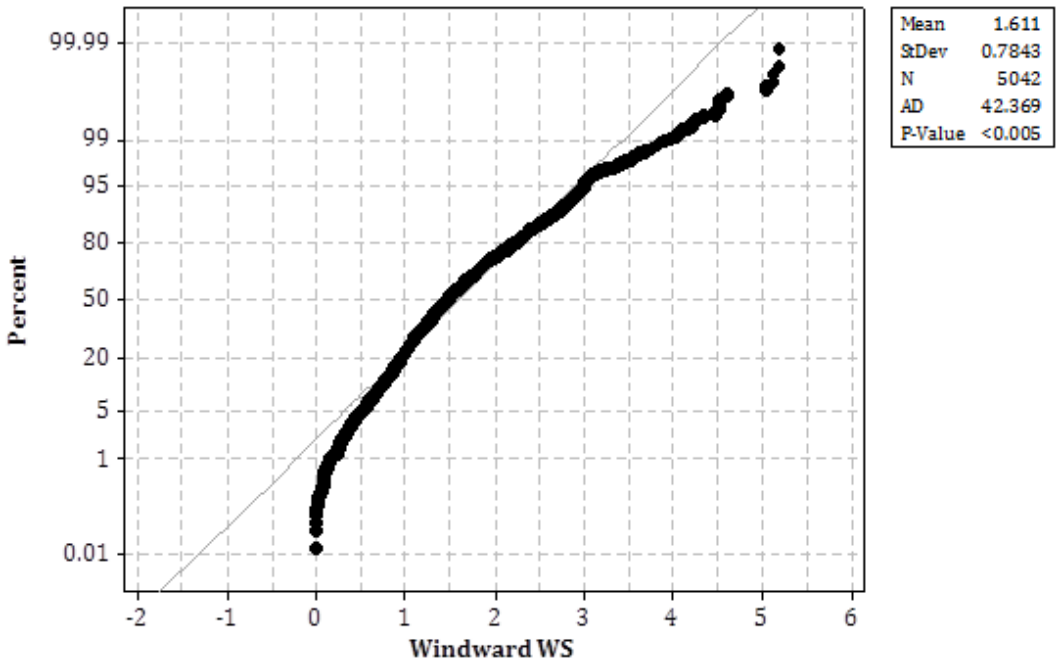

Appendix Figure 130: Probability Plot of wet season nocturnal wind speed data at the windward forest plot (2007 – 2008).

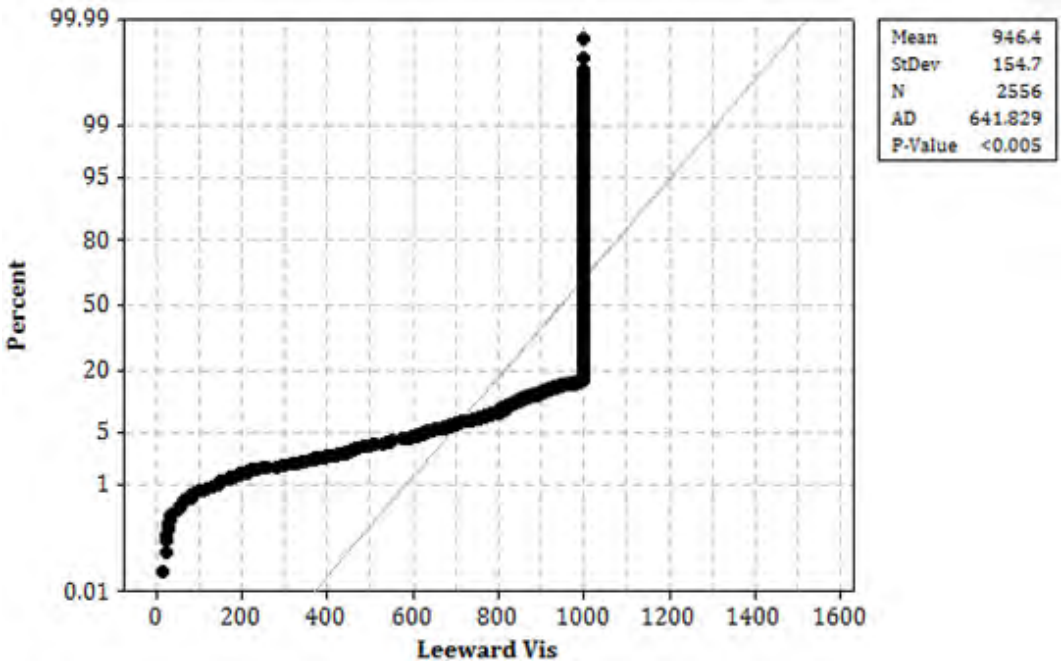

Appendix Figure 131: Probability Plot of wet season nocturnal visibility data at the leeward forest plot (2008).

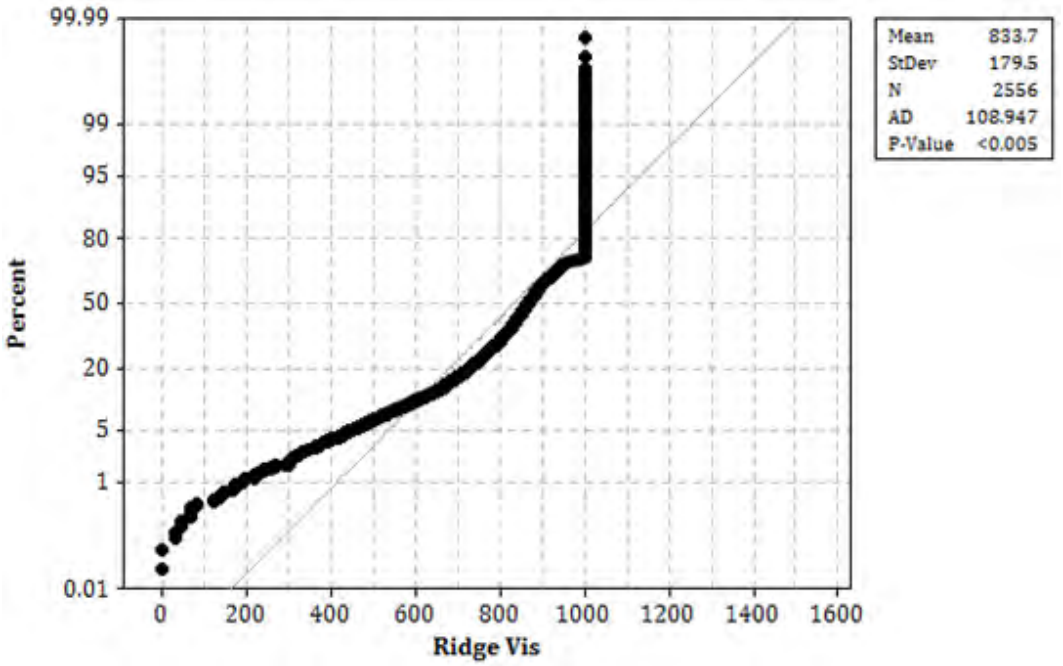

Appendix Figure 132: Probability Plot of wet season nocturnal visibility data at the ridge forest plot (2008).

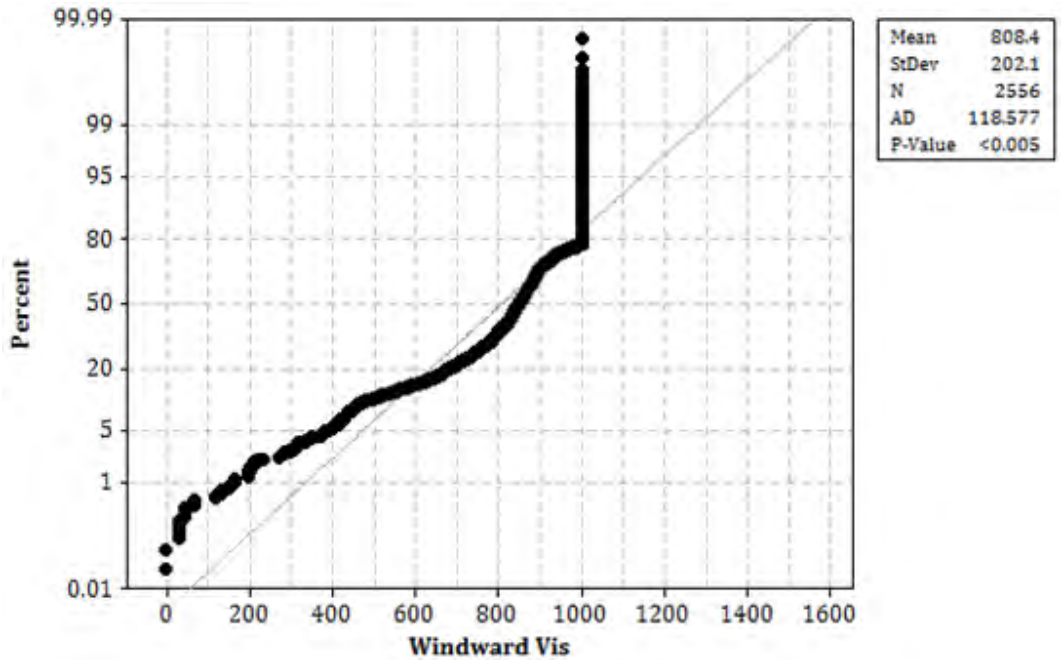

Appendix Figure 133: Probability Plot of wet season nocturnal visibility data at the windward forest plot (2008).

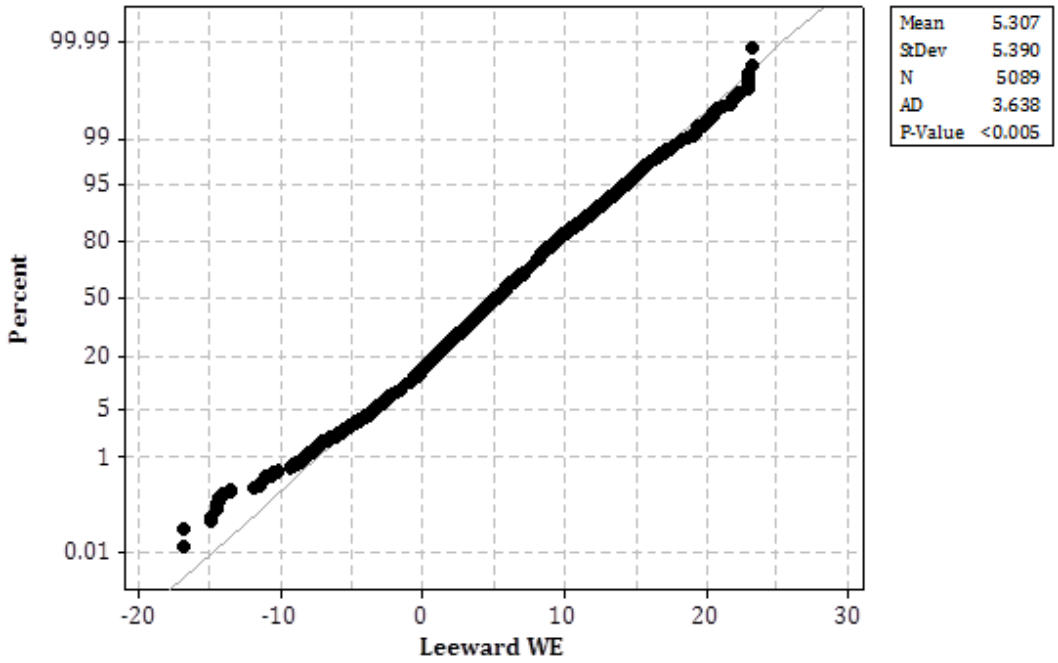

Appendix Figure 134: Probability Plot of wet season nocturnal wind elevation data at the leeward forest plot (2007-2008).

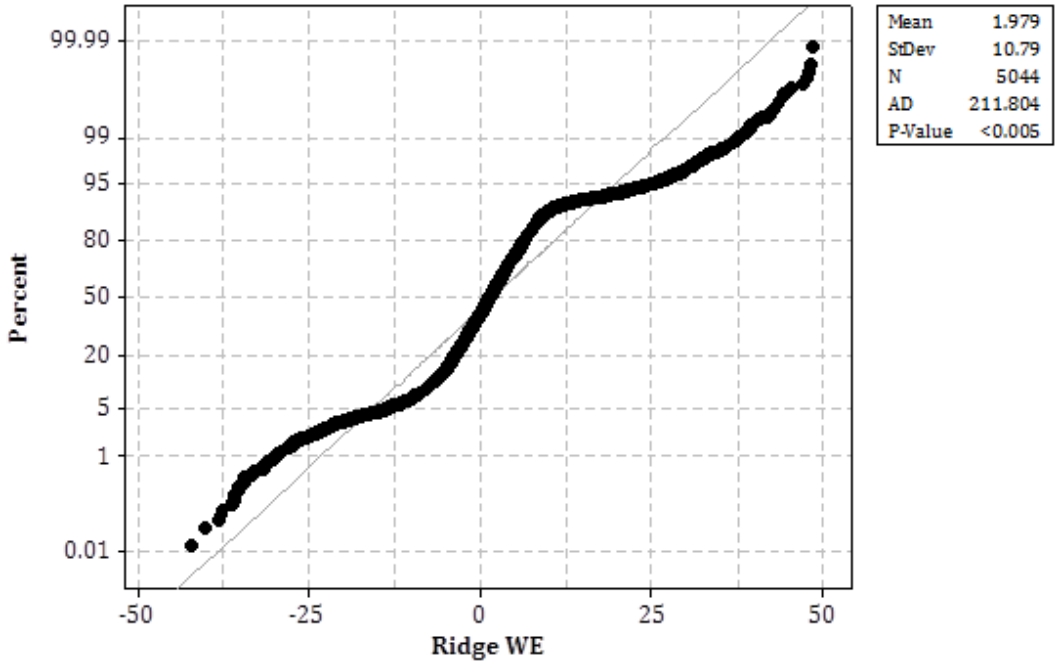

Appendix Figure 135: Probability Plot of wet season nocturnal wind elevation data at the ridge forest plot (2007-2008).

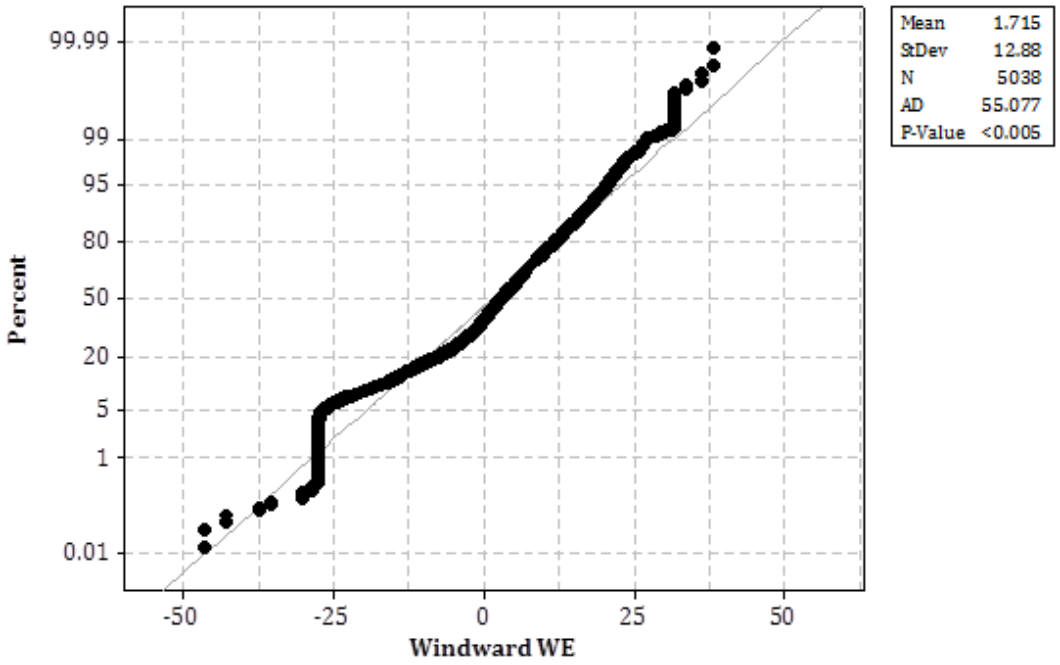

Appendix Figure 136: Probability Plot of wet season nocturnal wind elevation data at the windward forest plot (2007-2008).

Dry season Nocturnal Parameter Datasets

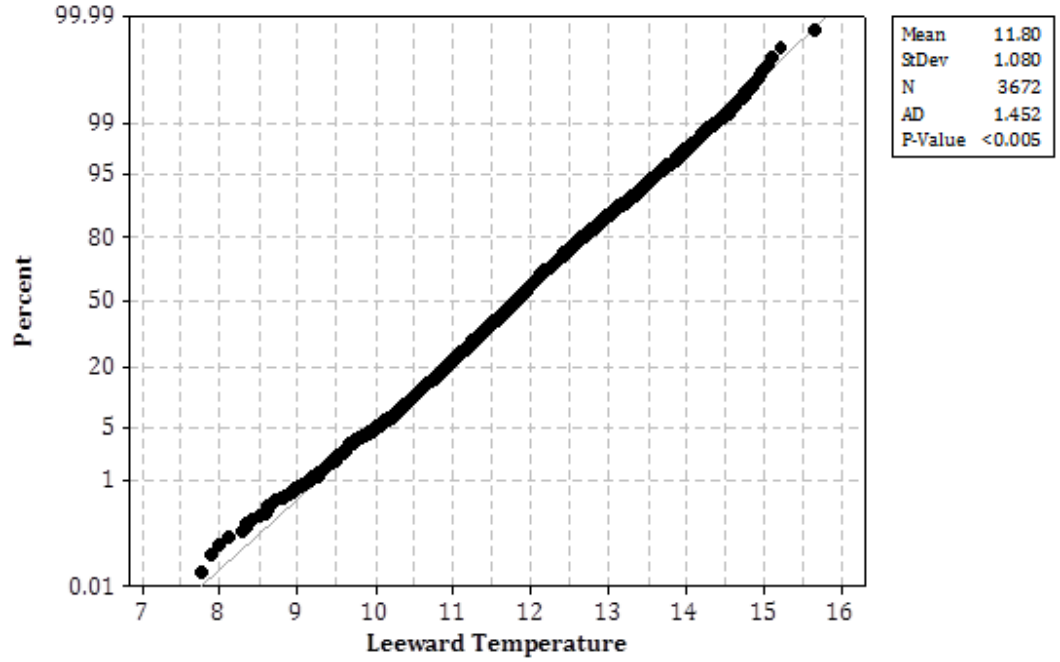

Appendix Figure 137: Probability Plot of dry season nocturnal temperature data at the leeward forest plot (2007 – 2008).

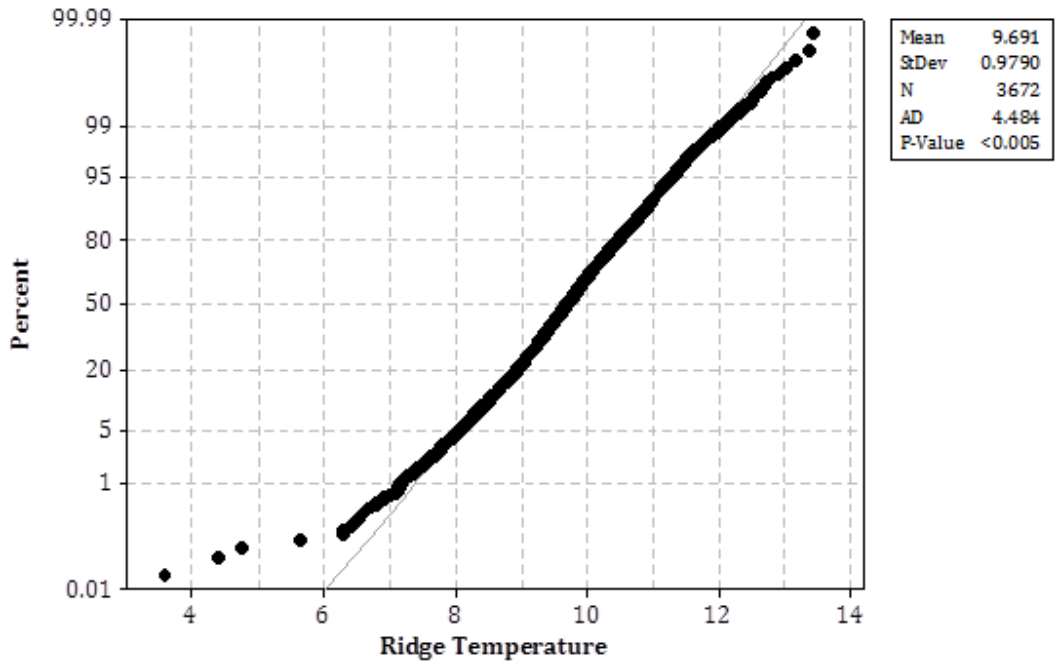

Appendix Figure 138: Probability Plot of dry season nocturnal temperature data at the ridge forest plot (2007 – 2008).

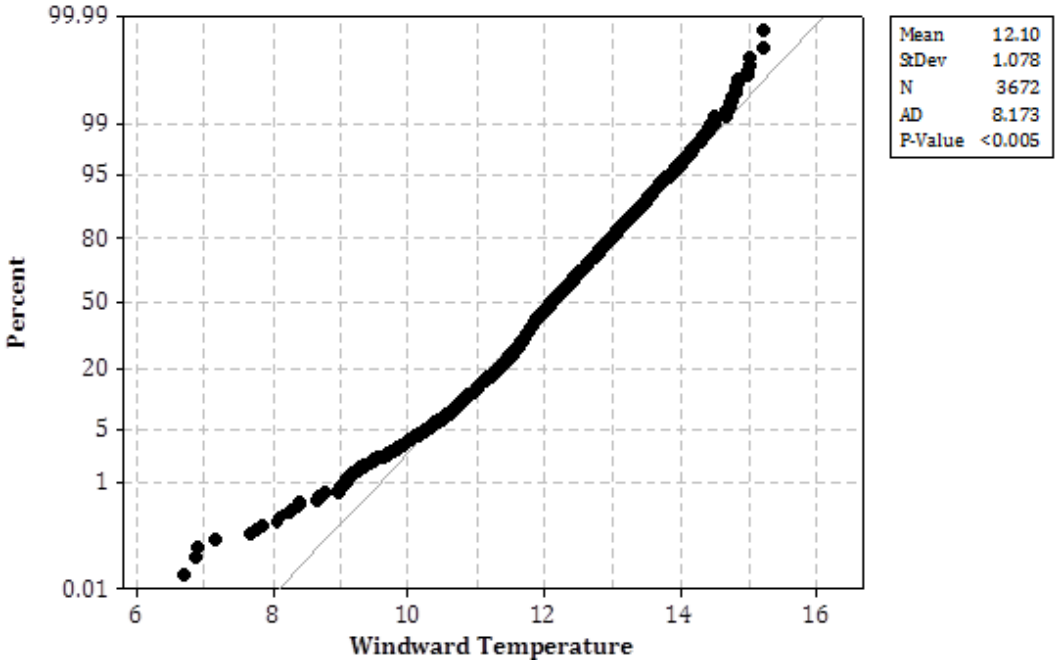

Appendix Figure 139: Probability Plot of dry season nocturnal temperature data at the windward forest plot (2007 – 2008).

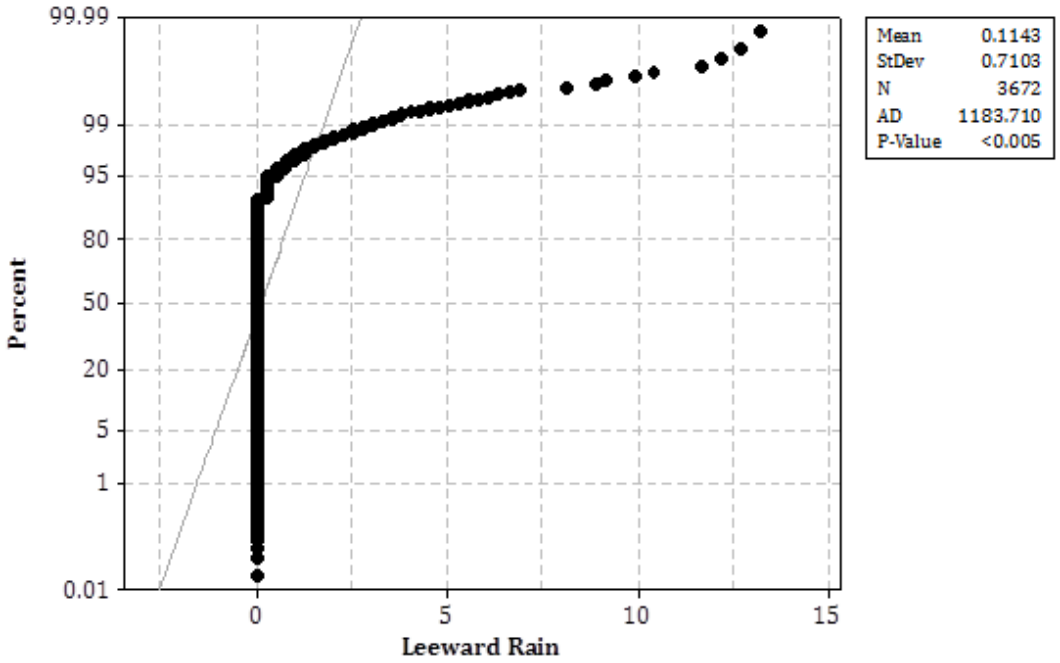

Appendix Figure 140: Probability Plot of dry season nocturnal rainfall data at the leeward forest plot (2007 – 2008).

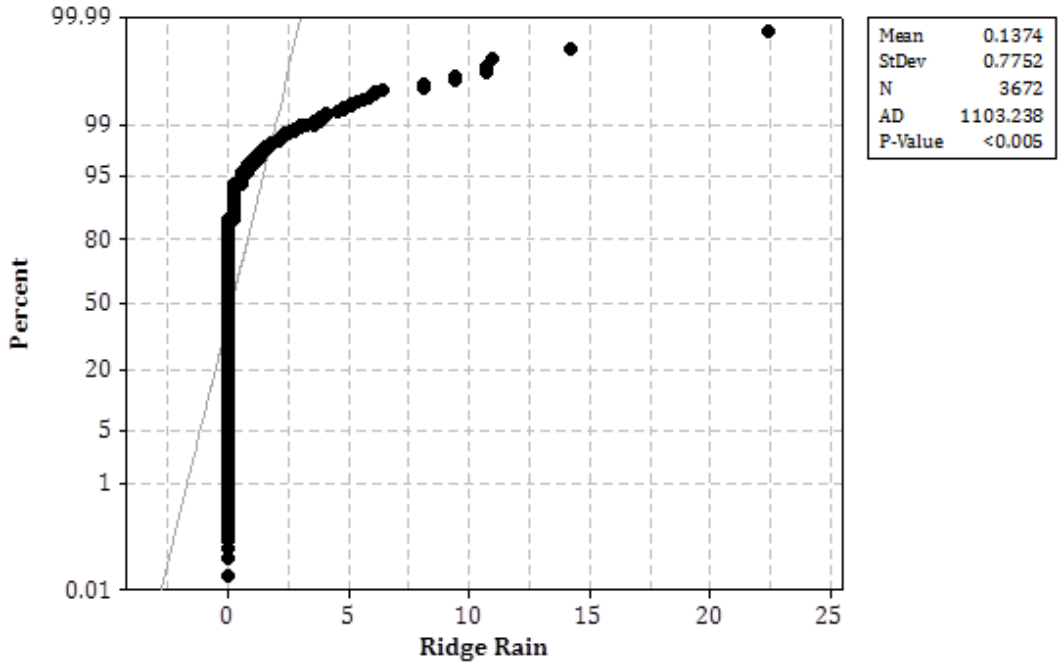

Appendix Figure 141: Probability Plot of dry season nocturnal rainfall data at the ridge forest plot (2007 – 2008).

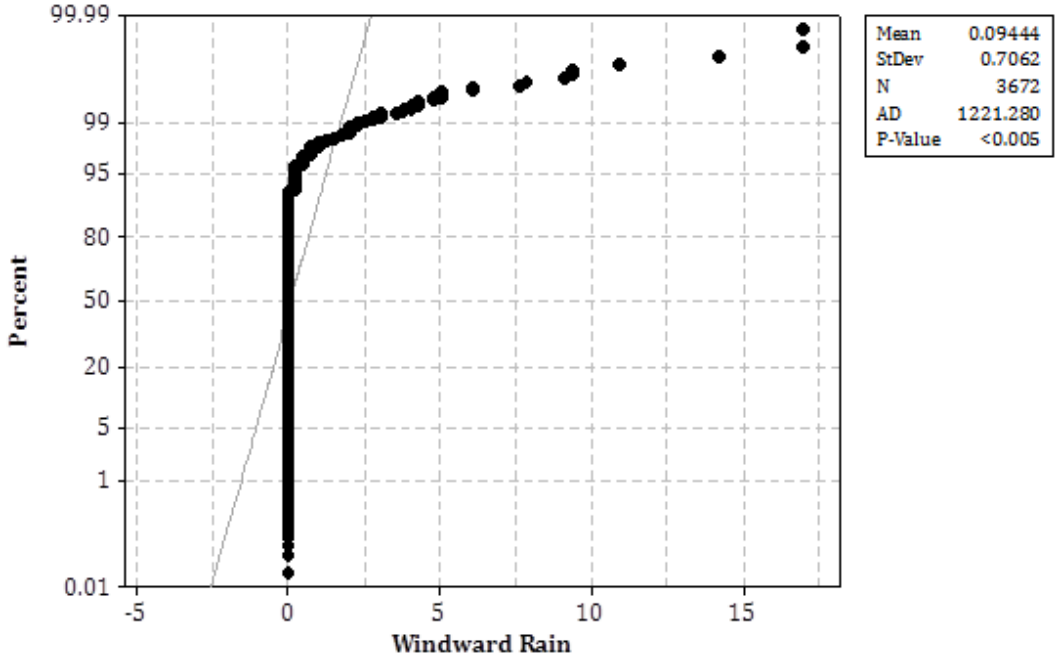

Appendix Figure 142: Probability Plot of dry season nocturnal rainfall data at the windward forest plot (2007 – 2008).

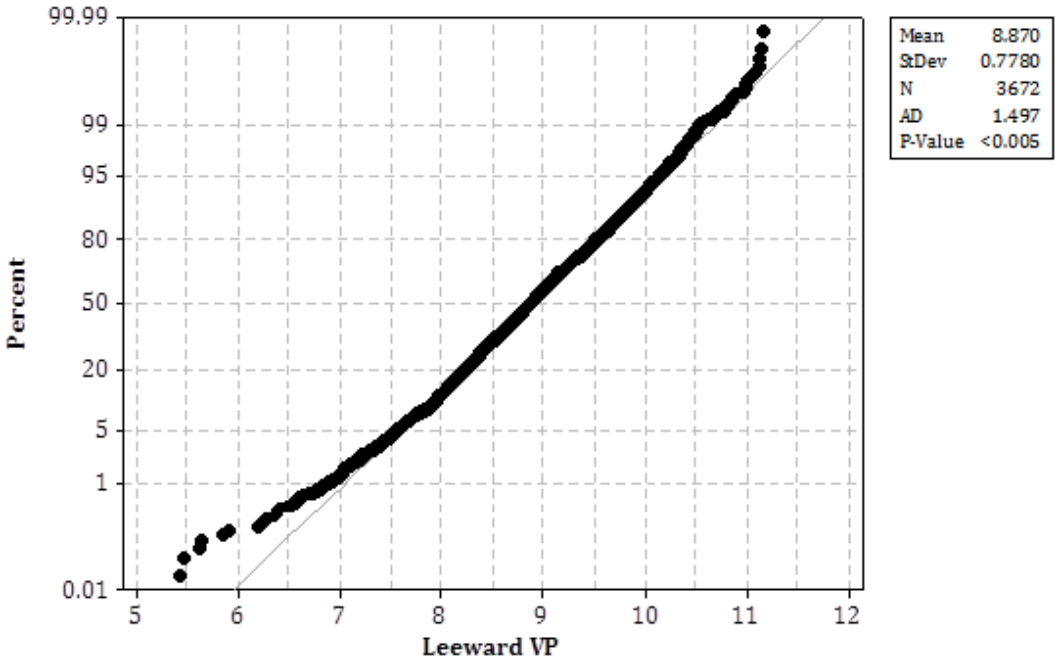

Appendix Figure 143: Probability Plot of dry season nocturnal vapour pressure data at the leeward forest plot (2007 – 2008).

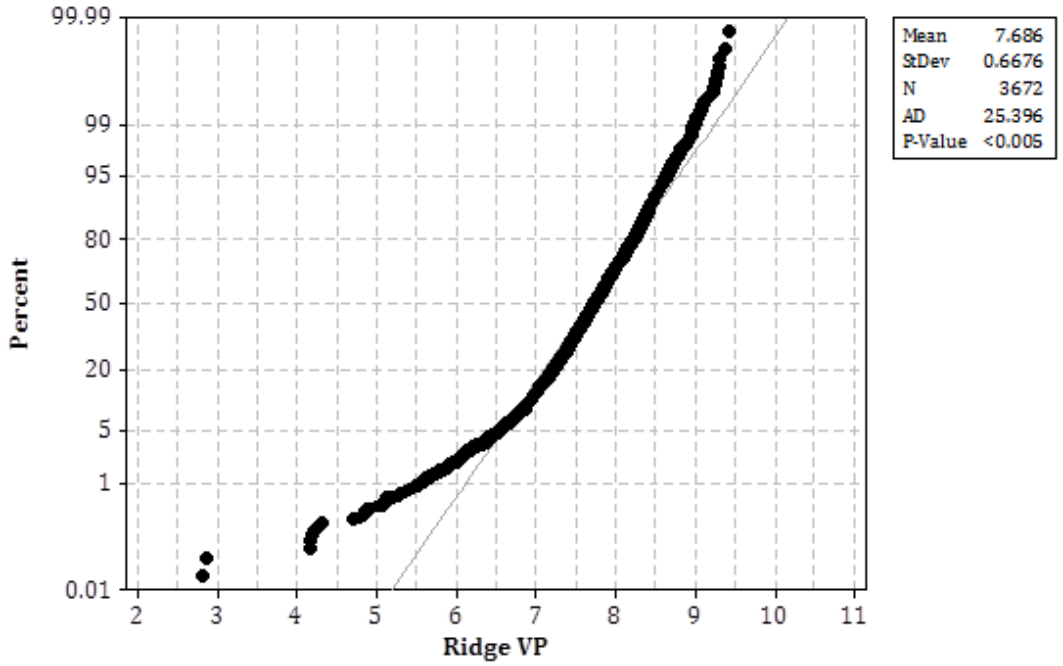

Appendix Figure 144: Probability Plot of dry season nocturnal vapour pressure data at the ridge forest plot (2007 – 2008).

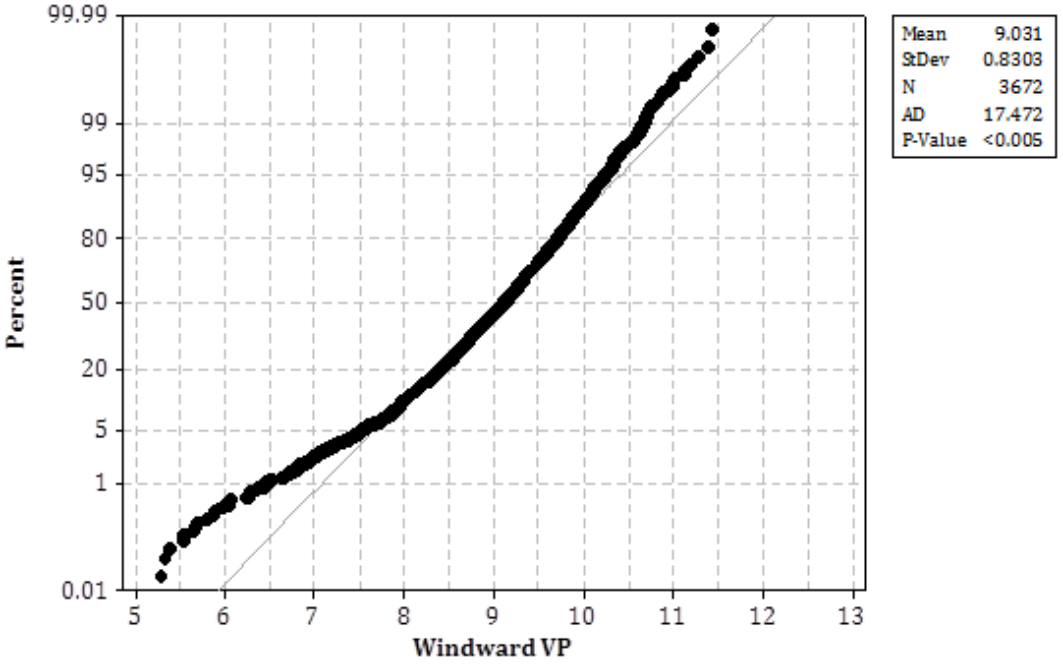

Appendix Figure 145: Probability Plot of dry season nocturnal vapour pressure data at the windward forest plot (2007 – 2008).

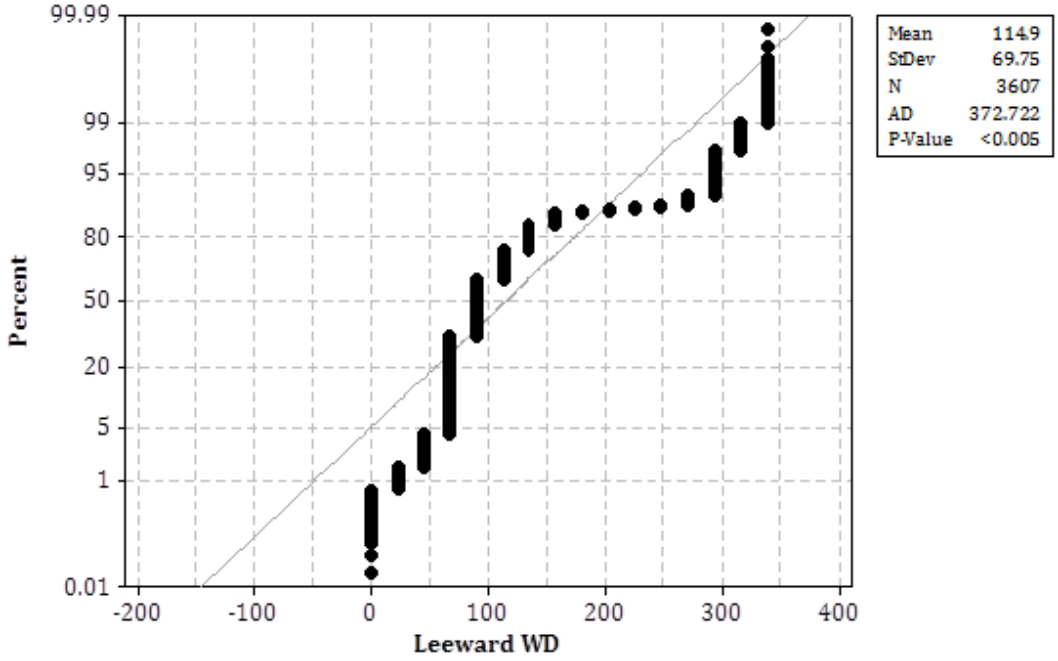

Appendix Figure 146: Probability Plot of dry season nocturnal wind direction data at the leeward forest plot (2007 – 2008).

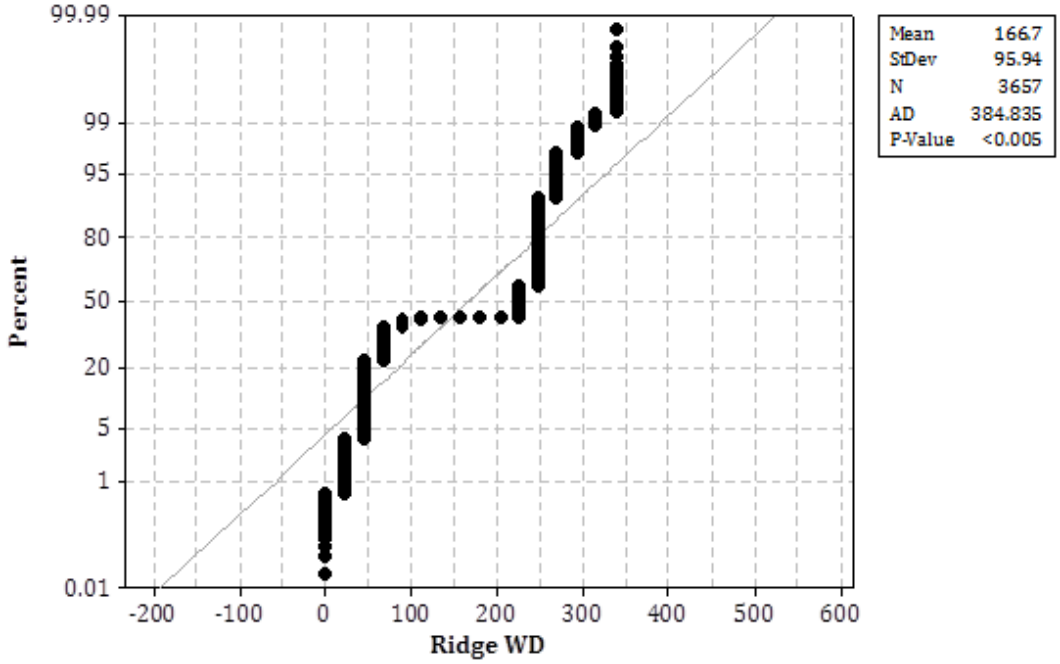

Appendix Figure 147: Probability Plot of dry season nocturnal wind direction data at the ridge forest plot (2007 – 2008).

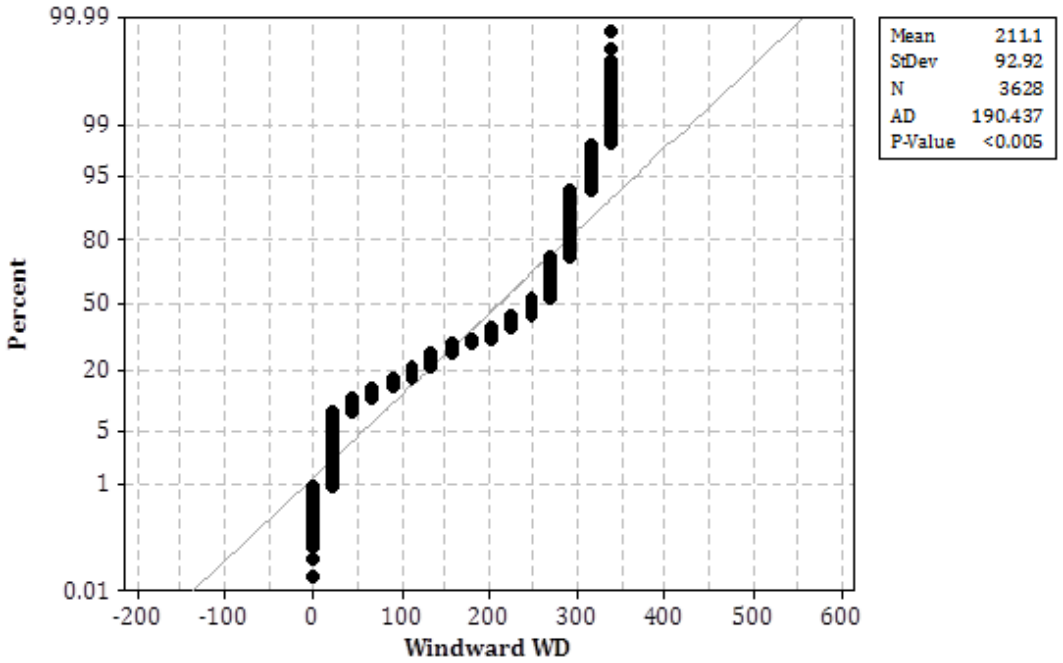

Appendix Figure 148: Probability Plot of dry season nocturnal wind direction data at the windward forest plot (2007 – 2008).

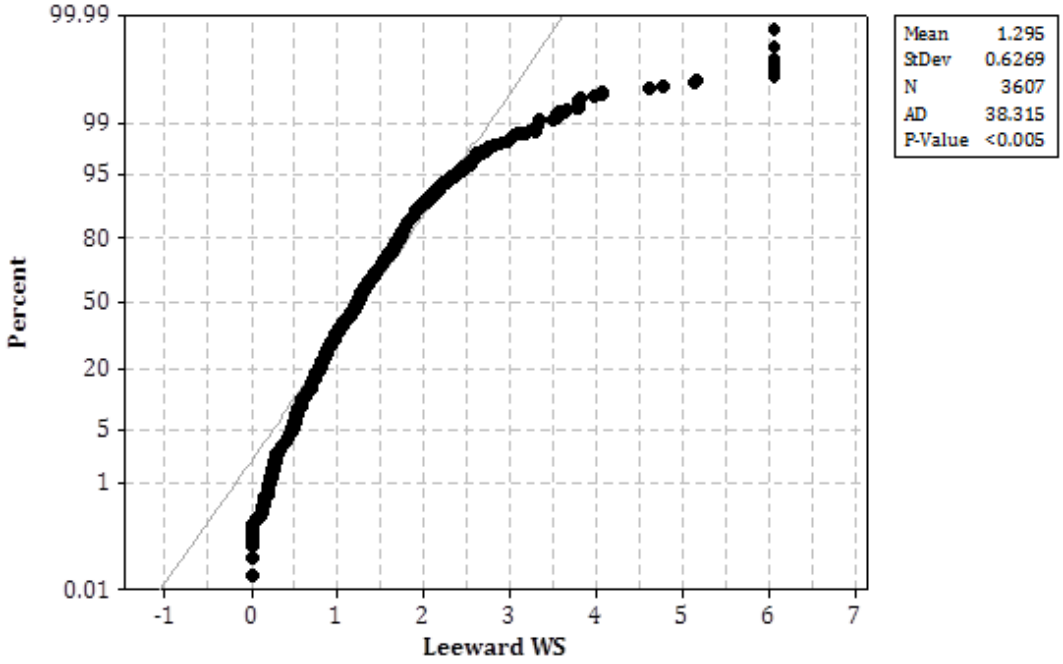

Appendix Figure 149: Probability Plot of dry season nocturnal wind speed data at the leeward forest plot (2007 – 2008).

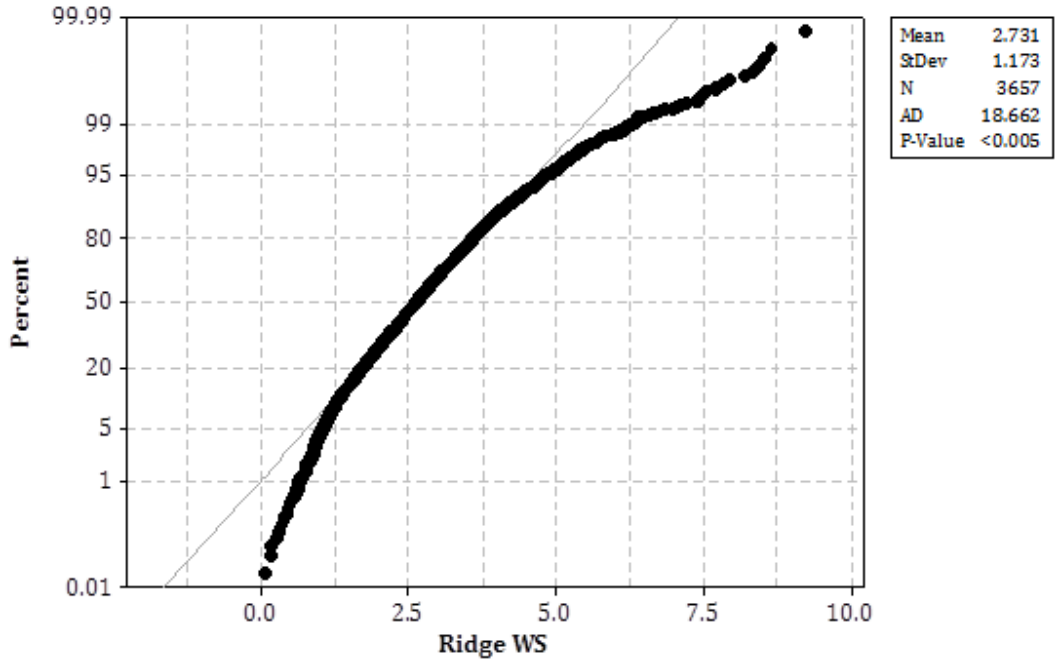

Appendix Figure 150: Probability Plot of dry season nocturnal wind speed data at the ridge forest plot (2007 – 2008).

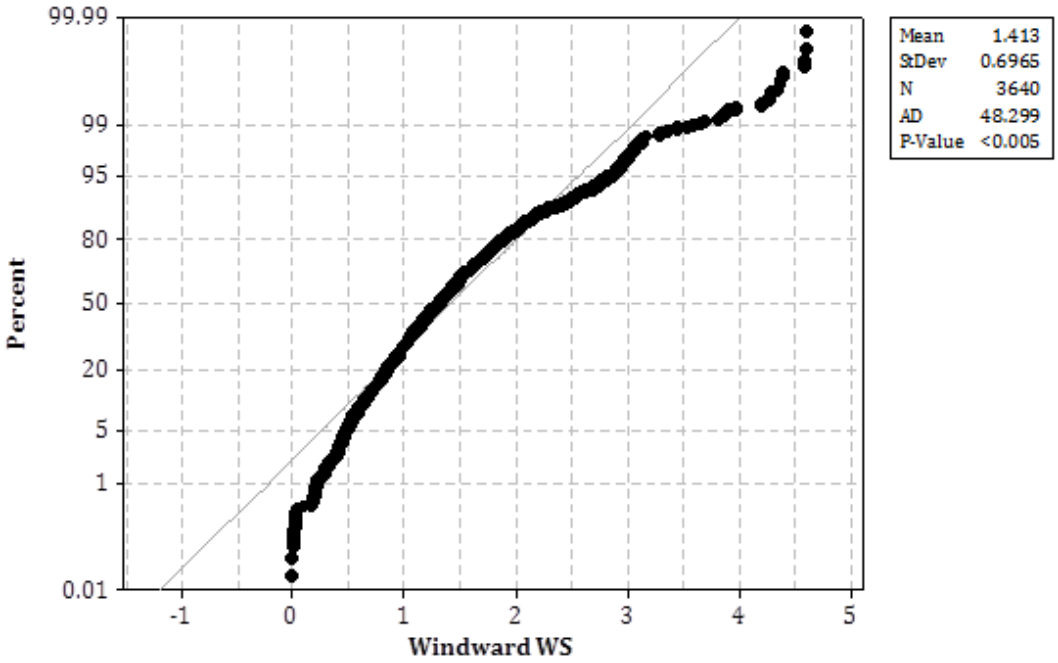

Appendix Figure 151: Probability Plot of dry season nocturnal wind speed data at the windward forest plot (2007 – 2008).

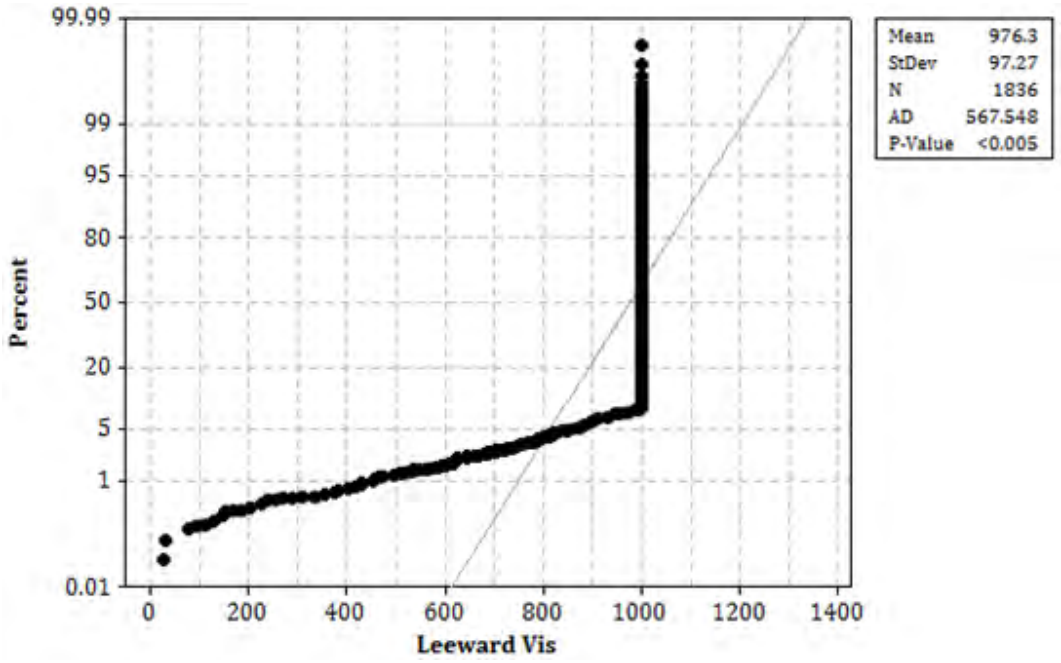

Appendix Figure 152: Probability Plot of dry season nocturnal visibility data at the leeward forest plot (2008).

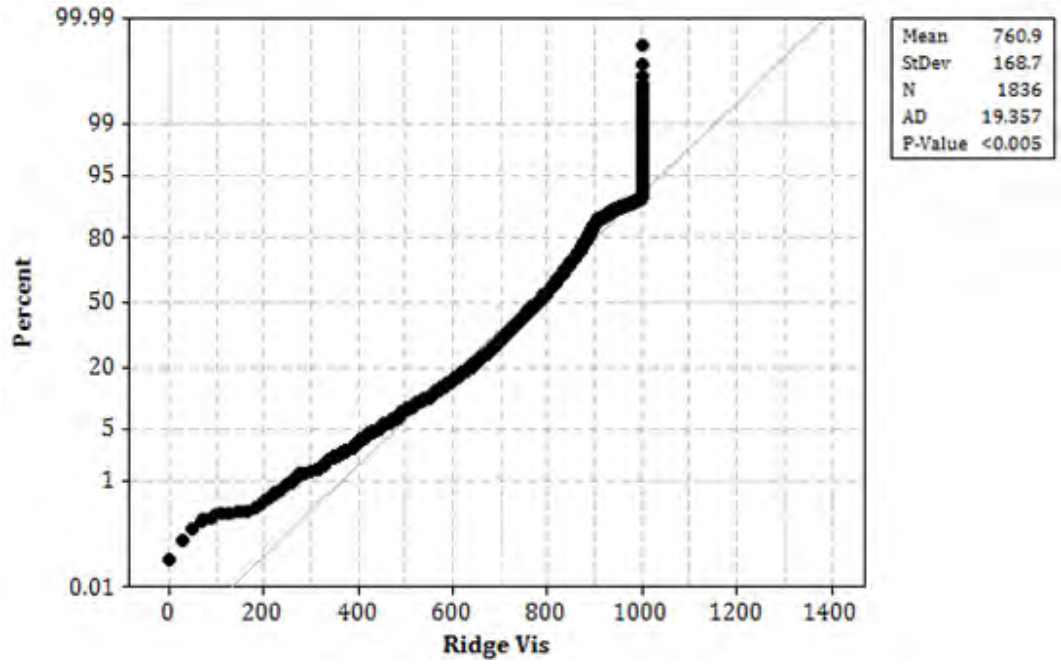

Appendix Figure 153: Probability Plot of dry season nocturnal visibility data at the ridge forest plot (2008).

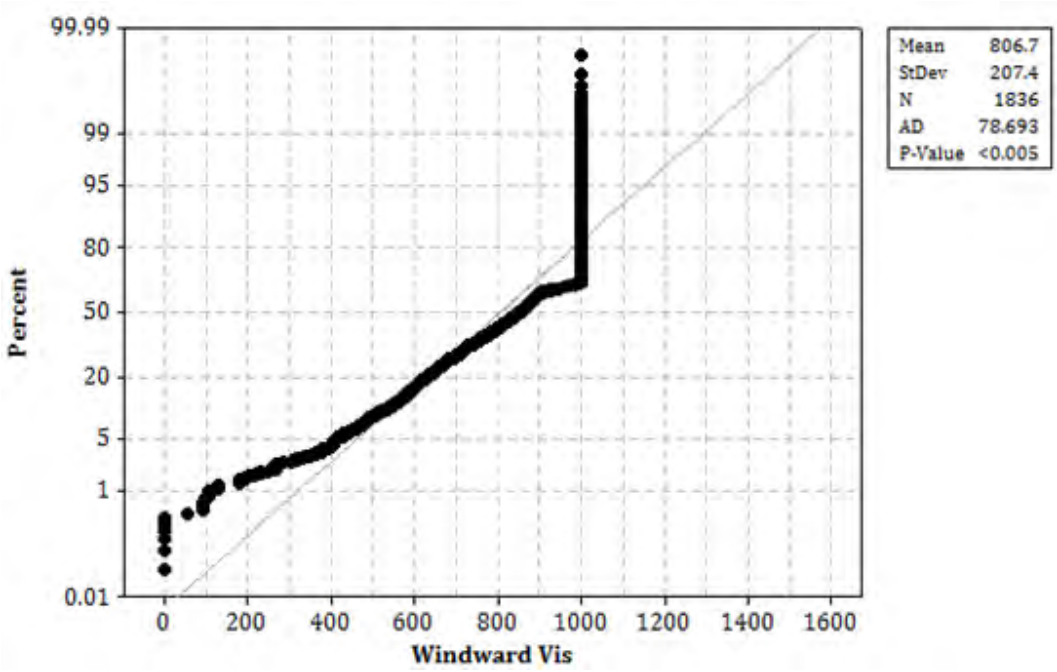

Appendix Figure 154: Probability Plot of dry season nocturnal visibility data at the windward forest plot (2008).

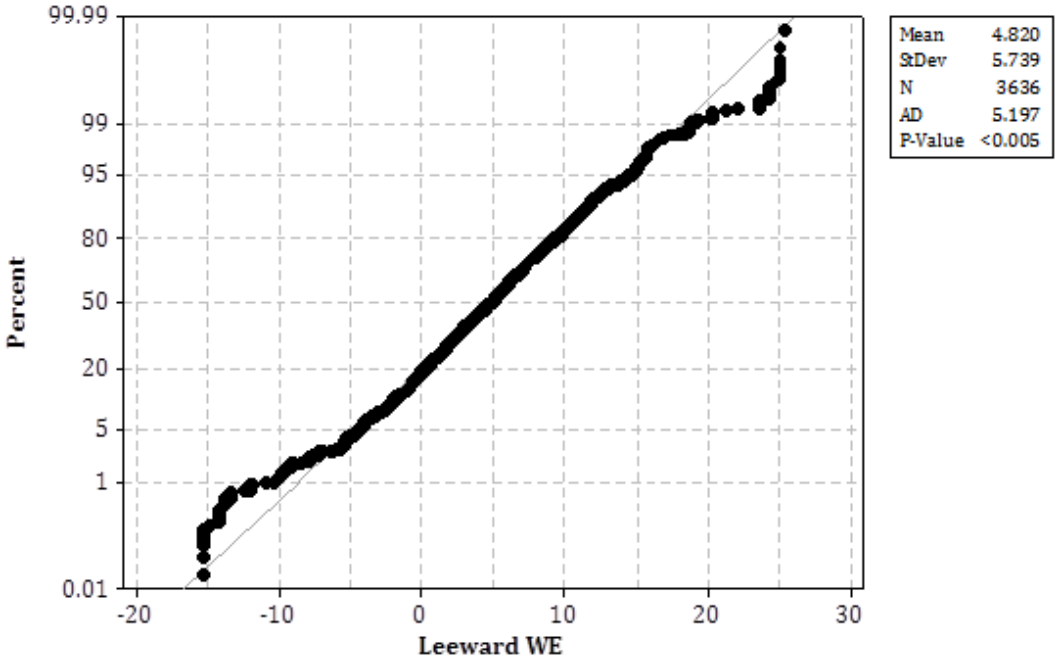

Appendix Figure 155: Probability Plot of dry season nocturnal wind elevation data at the leeward forest plot (2007-2008).

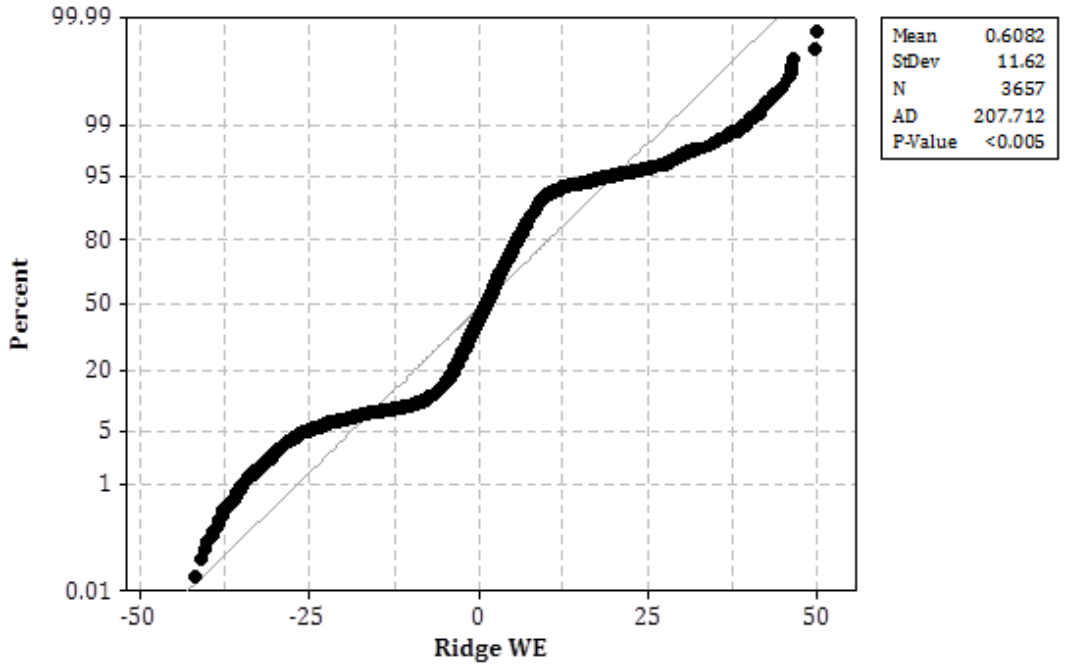

Appendix Figure 156: Probability Plot of dry season nocturnal wind elevation data at the ridge forest plot (2007-2008).

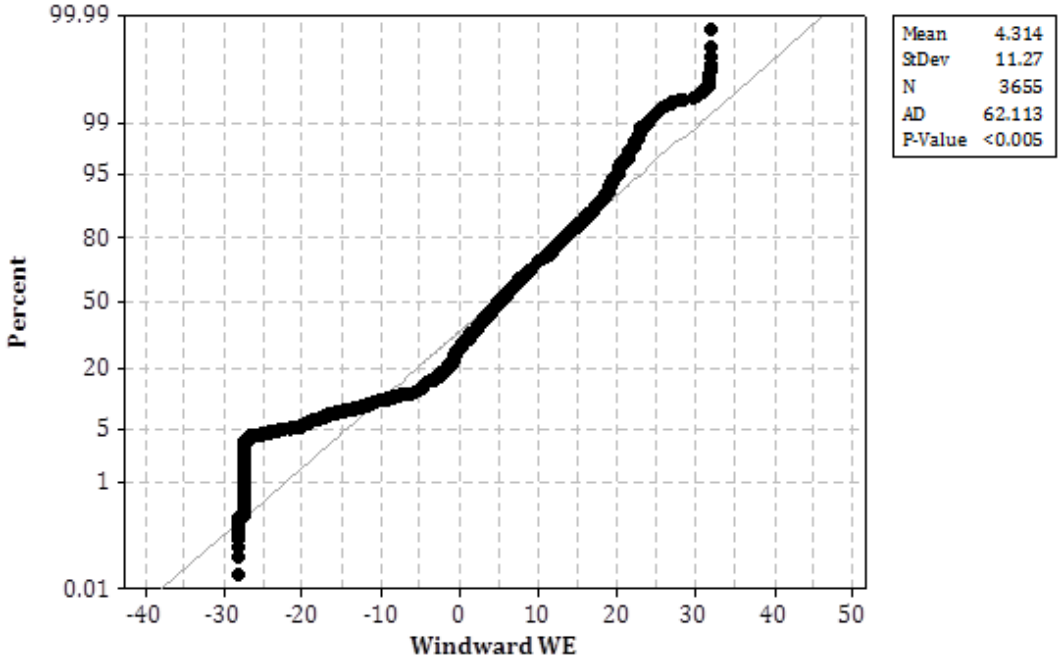

Appendix Figure 157: Probability Plot of dry season nocturnal wind elevation data at the windward forest plot (2007-2008).